Contract FP6-IST 508009

ACE

Antenna Centre of Excellence

Instrument: Network of Excellence

Thematic Priority: IST - Information Society Technologies
Mobile and wireless systems beyond 3G

Deliverable A1.1D2
Software Benchmark and Results for typical Test-Cases Report

Due date of deliverable: December 2005
Actual submission date: December 2005

Start date of project: 1/1/2004 Duration: 24 months

Organisation name of lead contractor for this deliverable: IETR

Revision 1

Project co-funded by the European Commission within the Sixth Framework Programme (2002-2006)		
Dissemination Level		
PU	Public	x
PP	Restricted to other programme participants (including the Commission Services)	
RE	Restricted to a group specified by the consortium (including the Commission Services)	
CO	Confidential, only for members of the consortium (including the Commission Services)	

Document Number: FP6-IST-508009-A1.1D2

Workpackage: WP1.1-2

Estimated Person Months: 39

Dissemination level (PU,PP,RE,CO): PU

Nature (R, P, D, O): R

Version: 1

Total Number of Pages: 338

File name: ACE_A11_D2

Editors: IETR, CNRS-LEAT, UPM, UNISI, FT R&D

Participants: IETR, CNRS-LEAT, UPM, UNISI, FT R&D, KUL, EPFL, UPV, LIVUNI, IDS, UNIBRIS, IMST, SAPIENZA, FOI, CHALMERS, THALES, ICCS-NTUA, UPC, UNIFI, POLITO

Abstract

This document presents the results of the work-package dedicated to the assessment of antenna software.

It sums up the different tasks that have been achieved during the last 18 months in order to create a framework for benchmarking.

At the end of the document, a large section presents a detailed description of the test-cases that have been selected and the simulation results that have been obtained.

Keyword List

Antenna software, benchmark, on-line service

Document Evolution

Revision	Date	Reason of change
Rev. 1.0 Draft A	15/12/05	Draft Edition
Rev. 1.0		First Edition

Table of contents

1. Introduction

Antenna design definitively relies on the availability of user-friendly and powerful antenna software. The assessment of these software tools is essential for antenna designers. CAD tools must be seen as heavy investments that cannot be done without due consideration. They are often very expensive to purchase and to support. They also require costly training sessions and long-term experience. Only experienced engineers can extract the best performances that these software tools can yield. Even when a freeware CAD tool can be downloaded instantaneously from the web, it is not acceptable to waste a couple of weeks before discovering that it cannot correctly handle the antenna structure to be studied!
Unfortunately, the assessment process is not an easy task due to several factors. First, there are many software packages, both commercial or home-made, with very different features and performances. Even if we limit the investigations to a single analysis method (FDTD for instance), many different tools can be found whose differences could sometimes appear to be very subtle for non-specialists. Indeed, there is no real overview anywhere concerning the actual capabilities of all these codes. Some of them are obviously premature. Others exhibit good performances but are limited to very specific configurations. None of them can of course be regarded as the universal solution for antenna simulation. When different codes yield different results, there is no way of determining which one has to be preferred. Moreover, it is very likely that the optimal CAD tool for a given job depends on the specific antenna topology under consideration. The recent emergence of new types of algorithms (wavelet-based compression techniques and other fast solvers) has sometimes significantly extended the performances of classical methods. This makes the global vision even more difficult as the traditional references have changed. In most cases, only the people who have developed the software know precisely its actual capabilities.
There is another reason why the assessment of software is complex. The needs of the users themselves can vary from one to another. Some of them are only interested in the accuracy of results while others are also considering computer requirements (CPU time and memory storage), user-friendly GUI or any other secondary features. What is expected from a given code also depends on the particular application for which it is utilized. Moreover, the needs evolve very rapidly because of the constant improvements of antenna technologies and systems : complex environments must now be accounted when optimising antenna systems and, at the same time, many new technological details (such as MEMS) have to be considered.

The main objective of this work-package was to define a set of benchmarking structures in order to assess the antenna software. As a result, it provides standards for the evaluation of existing and future antenna software. It also improves communication between software developers and antenna designers, by clarifying the actual challenges in antenna modelling (from both the expressed needs and the expected scientific capabilities). Finally, it facilitates the convergence to future research programs in antenna modelling by concentrating the effort on a set of agreed problems.

2. Work-package overview

The software benchmark was a 18 months work-package that has been initiated within the ACE software activity.

The benchmarking task started at the beginning of June 2004 in Gothenburg, after that a global overview of available antenna software has been obtained thanks to the "Antenna Software Inventory" (WP1.1-1). A first questionnaire (Benchmarking Form) has then been elaborated and agreed and a first call for proposals has been organized to collect candidate structures for the benchmarking process. The questionnaire was distributed among work-package participants. As this task also summarizes and co-ordinates intermediary benchmarking activities initiated in the Joint research program for the specific types of antennas considered there, the questionnaire was also disseminated within vertical activities.
As a result, 30 different structures have been proposed from 14 different institutions or companies.

During the 2nd meeting in Leuven (September 2004), the proposed structures have then been analysed and categorized. Three working groups (microstrip elements, 3D antennas, arrays and periodic structures) have been created to perform the selection, and to this purpose, following criteria have been established:

- Representativeness of structures with regards to real-life configurations
- Large coverage of present modelling challenges
- Large coverage of new applications and technologies
- Identification of salient parameters to be benchmarked
- Availability of well-accepted reference results (either experimental or analytical)
- Independence of any particular method

A special attention has also been paid to the realization of the benchmarking structures which are considered for the measurements. As a result, eleven structures have been pre-selected.

For these pre-selected structures, a detailed "Structure Description Form" has been elaborated, so that all information about the structures is made available to all under a common format.
A third meeting took place in November 2004 in Nice. Its main objective was the organisation of the first benchmarking run. This first run considered a few test-cases (from the pre-selected structures) for which many participants could provide simulation results. A poll was organized to identify the pertinent test-cases. At the same time, a "Result Form" was agreed for a clear and coherent presentation of benchmarking results. A general scheme for the first run process has also been elaborated (see figure1). All the forms developed within this work-package have also been transferred to other work-packages with more specific benchmarking activities so that a global and coherent view could be achieved at the end.
During the fifth meeting in Rome, February 2005, five test-cases were definitively fixed for the "First Run" by analysing the results of the poll. The benchmark was then officially open internally to ACE. The main objective of this internal "First Run" was to obtain first simulation results and to experiment the established process. At the same time, the main steps were identified in order to open the benchmark outside the ACE network. To do so, the development of an "On-Line Benchmark Service" in VCE was initiated. This service, called SoftLAB (Software on-Line Antenna Benchmark), was thought as an actual service for the antenna community providing all usual information for people wishing to participate in the benchmark. More precisely, SoftLAB aims at presenting the five selected test-cases and allowing access to the corresponding description files. SoftLAB also provides a convenient and easy way of uploading all simulation results.

During the sixth meeting in Leuven, June 2005, the results of the "First Run" were analysed and the final requirements for SoftLAB were agreed. SoftLAB was developed by IDS during summer 2005 and the first version was presented at Dubrovnik during the seventh meeting, October 2005. The

benchmark was then officially opened to external participants and an invitation to participate in the benchmark was sent to 13 identified software vendors.

3. Benchmark achievements

The main achievements within this work-package during the last 18 months are the following:

- Collection of candidate test-cases among ACE participants
- Selection of 5 typical test-cases
- Organization of a complete process for benchmarking antenna software (standardized files and procedures)
- Development of an "on-line service" (SoftLAB) using VCE facilities
- First benchmark run (within ACE participants)
- Opening of the benchmark run to the ACE community (using SoftLAB)

As a result, an actual framework for antenna software assessment has been established, on-line services have been opened to the whole antenna community and a large amount of data has been collected for a few test-cases.

Less than one year after the benchmark has been opened, 36 simulations have already been realized. 14 different participants took part to this benchmark and 18 different software tools (11 in-house and 7 commercial) have been used.

4. Benchmark process

The benchmark process is summarized in figure 1. First, "submitting institutions" (among work-package participants) propose test-cases and provide all useful information using standardized files. All the documents, including measured data, are uploaded in the private section of VCE so that any participant in the work-package can analyse the proposed structure. When a sufficient number of participants have expressed their interest for a given structure, it is considered for benchmarking. To do so, the SoftLAB manager creates a new test-case in SoftLAB by transferring all the uploaded files to the public section of VCE. The test-case is then visible for anyone among the ACE community. Anyone wishing to provide simulation results ("testing institution") is invited to proceed. However, a few conditions must be satisfied before uploading simulation results. Firstly, the used software tool must be declared in the European Antenna Software Inventory (this can be achieved interactively using VCE facilities). This guaranties that enough information about the software tool is available. Secondly, all provided information must comply with the standardized file requirements. This guaranties that all the simulation results look similar in order to make the comparisons easier. Finally, the testing institution should provide data in tabular form, in addition to the standardized "result file", in order to permit anyone to make its own comparisons.

All uploaded simulation results are visible for anyone within the ACE community. This really offers the capability for anyone to analyse the performance of different software tools for different antenna structures. SoftLAB also allows anyone to demonstrate the capabilities of its software tool for simulating particular antenna configurations.

It must be pointed out that SoftLAB only publishes hard simulation results and comments from the testing institutions. No particular ranking nor comparison is achieved within SoftLAB. Indeed, the chosen strategy is

definitively to provide all material so that anyone can make all the necessary comparisons himself. This should prevent SoftLAB from any biased opinions.

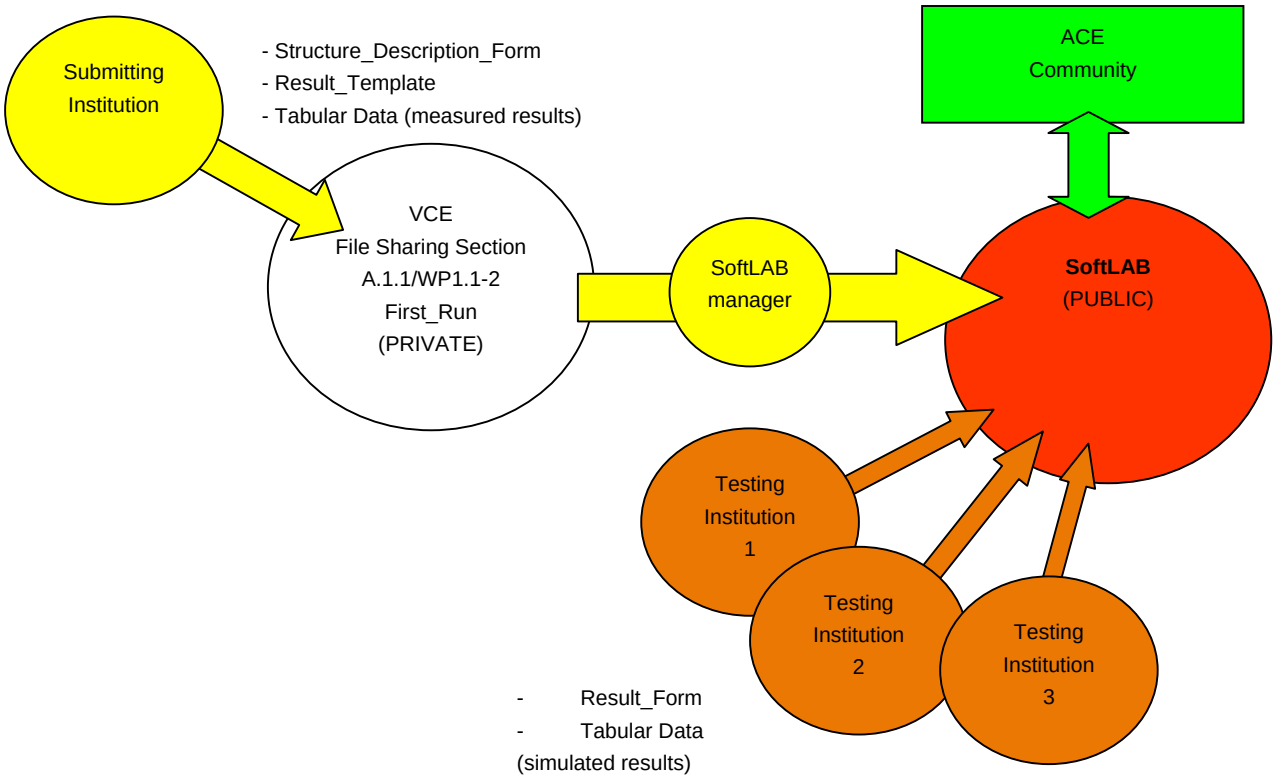

Figure 1 : Scheme of the benchmark process

Figure 2 gives a view of the SoftLAB interface, the WEB service for On-Line benchmark.

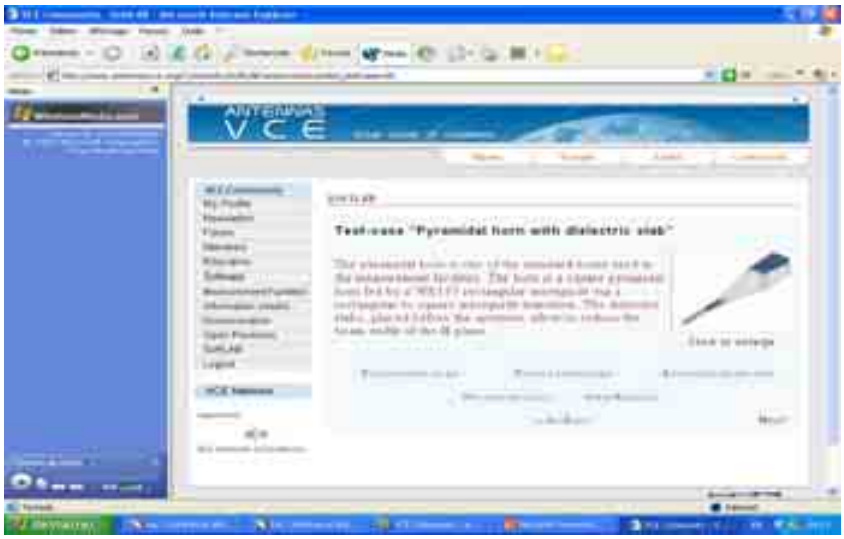

Figure 2 : SoftLAB interface

5. Benchmark conclusions

The large amount of simulation data obtained and the large number of tested codes demonstrate that numerous CAD tools are available within European universities and companies. In-house software tools have demonstrated very good performance compared to commercial tools. Although they are usually less general and not as easy to use as commercial software, they often overcome the accuracy or the speed of their commercial counterpart for specific configurations. On the other side, some tools also appear to be very general but they require large memory storage and CPU time.

As could be expected, there is a real software offer to simulate planar radiating elements. Many codes exist, usually based on the resolution of integral equations, with different combinations of meshes and basis functions. This is demonstrated by the large number of simulated results that were obtained for such planar structures as the ones proposed by IETR and UNISI. However, the performances of these software tools are still limited when the number of unknowns increases. For instance, no large array has been selected for the first run. This issue will be addressed in ACE-2 : advanced and fast solvers with multi-resolution capabilities will be assessed. A few modelling points could also be improved : the finite dimensions of the ground plane and of the substrates are usually not taken into account which results in bad predictions for large angles. Also, the modelling of the excitation is usually a weak point. This can explain why most simulators do not provide the radiation efficiency. Finally, it must be pointed out that no conformal planar antennas have been chosen so far for test-cases although a few ones were proposed : this is due to the small number of simulators that can really deal with such structures.

When the planar structure includes vertical metallizations or other specific features, like the structures from UPM and CNRS-LEAT, the number of candidate software tools also decreases. For the second structure (CNRS-LEAT), it is interesting to notice that no software tool was really able to provide accurate results for the first frequency band. This demonstrates that present simulators partly fail in analyzing more complex but realistic antennas. New configurations where circuit elements (like for instance MEMS switches or active devices) are integrated in antennas should also be considered in the future.

The situation is somewhat different for non planar 3D structures (FT R&D structure). All results have been obtained with industrial / commercial software tools. It seems that a few well accepted tools give satisfactory results and that the research activity is not so active in this domain. The same could be said for reflector antennas as no such test-cases were submitted during the call for proposals.

At the moment, the benchmark can be seen as a first level benchmark : both the number of tested structures and their complexity are still limited. This results from the limited time since the kick-off of the activity. This was also due to the necessity to involve as many participants as possible since the beginning, by selecting general purpose structures (that can be simulated by many software tools). This was seen as an essential issue for a large acceptance of the benchmarking among the European antenna community.

The benchmark must be a continuous activity which permanently updates the panorama of new software capabilities. As an example, the new capabilities brought by the development of a standard Electromagnetic Data Interface (EDI) should be evaluated. Moreover, ACE-2 will offer the possibility to extend the assessment work to more challenging structures and problems. This is actually required in order to benefit from the large effort that has been provided during the first phase (ACE-1) : all the procedure and tools are now operational which permits to concentrate on the assessment itself.

Benchmark results

This last section presents the selected test-cases together with the associated simulation results.

The five selected test-cases are:

- a microstrip antenna whose shape has been optimised using genetic algorithms
- a linear microstrip array of aperture-coupled patches
- a cavity-backed microstrip antenna with dual coaxial probe feed
- a dual wideband radiating element for mobile handsets
- a pyramidal horn with dielectric slabs.

For each of this structure, the presentation is organized as follows:

- description of the structure
- presentation of the measured results
- presentation of each simulation result
- synthesis

The benchmark is a continuous process that will continue in ACE2. New results are still expected for these five test-cases and some have already been uploaded (from IMST for instance) after this report was completed. An up-to-date view can be obtained at any time by using SoftLAB service in VCE.

BENCHMARKING ACTIVITY

(WP1.1-2)

Microstrip Patch Antenna Optimized Using Genetic Algorithms

Proposed by
Institut d'Electronique et de Télécommunications de Rennes
- IETR -

1. STRUCTURE DESCRIPTION

1. Entity

IETR
IETR/INSA, 20 avenue des Buttes de Coëmes
35043 Rennes cedex
Tel : + 33 2 23 23 87 00
Email : delia.cormos@insa-rennes.fr , raphael.gillard@insa-rennes.fr

2. Name of the structure

GAOptimPatch : Patch antenna optimized by a Genetic Algorithm.

3. Generalities

The proposed structure is a microstrip patch antenna having an unconventional shape. It has been optimized using a genetic algorithm in order to obtain an improved bandwidth (compared to a classical rectangular patch) and a linear polarization. The unconventional shape results from the progressive removal of small rectangular cells in an original rectangular metallization. The proposed antenna is fed by a microstrip line and works in the [9,9.3] GHz frequency band.

4. Structure Description

Two structures are considered for the benchmark:

4.1. The first one is a simple rectangular patch antenna with an inset microstrip line; it can be seen as a reference antenna.

4.2. The second is the unconventional patch antenna resulting from the GA optimization process; it directly derives from the reference antenna.

Both antennas have been fabricated and measured within the same conditions. Only the shape of the radiating patch differs.

The antennas are printed on PTFE dielectric substrate. The substrate is mounted on an metallic aluminium fixture.

Material Table

Name (in Figure)	Reference	Material	Characteristics
Substrate	METCLAD (MY2)	Woven glass PTFE	Dielectric Constant εr=2.2 Loss tangent 0.0009

			Substrate thickness hs=762 µm Metallization (copper) thickness 18 µm Metallization conductivity 5.76e7 S/m
Fixture	Non Applicable	Aluminium	Conductivity 3.96e7 S/m

Both patch antennas are centred on the substrate and the fixture. The antennas are fed with microstrip line through a SMA connector which is centred on the microstrip line.

The structures are symmetrical with respect to the (xoy) plane (see following figures).

4a – Simple rectangular patch antenna

Figure 1 presents the first considered patch antenna placed on the fixture.
As can be seen in figure 1(a), the patch has two identical notches for matching purpose.
Figure 1 (b) presents a side view of the antenna.

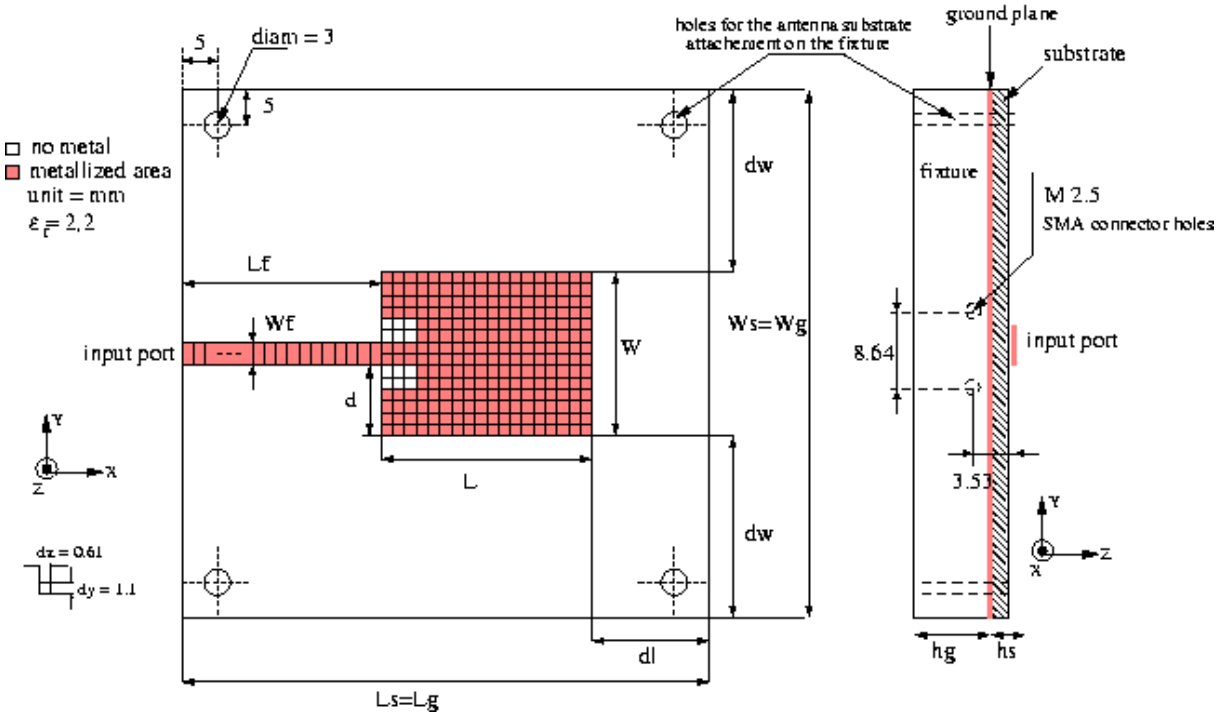

a) top view b) side view

Figure 1 : Classical Patch Antenna placed with grounded substrate and fixture.

Dimensions Table (mm)

L	*W*	*Lf*	*Wf*	*dx*	*dy*	*d*	*dl*	*dw*	*Ls*	*Lg*	*Ws*	*Wg*
11	*15.4*	*32.5*	*2.2*	*0.61*	*1.1*	*6.6*	*32.5*	*30.3*	*76*	*76*	*76*	*76*

N.B : Intermediate dimensions (as the notch dimension) can be deduced from the elementary cell size (dx and dy). Note that the width of the microstrip line is twice the cell width on the patch.

4b – GA optimized patch antenna

Figure 2 presents the second considered patch antenna placed on the fixture. As can be seen in figure 2(a), some rectangular cells have been removed from the patch metallization. Figure 2 (b) presents a side view of the antenna.

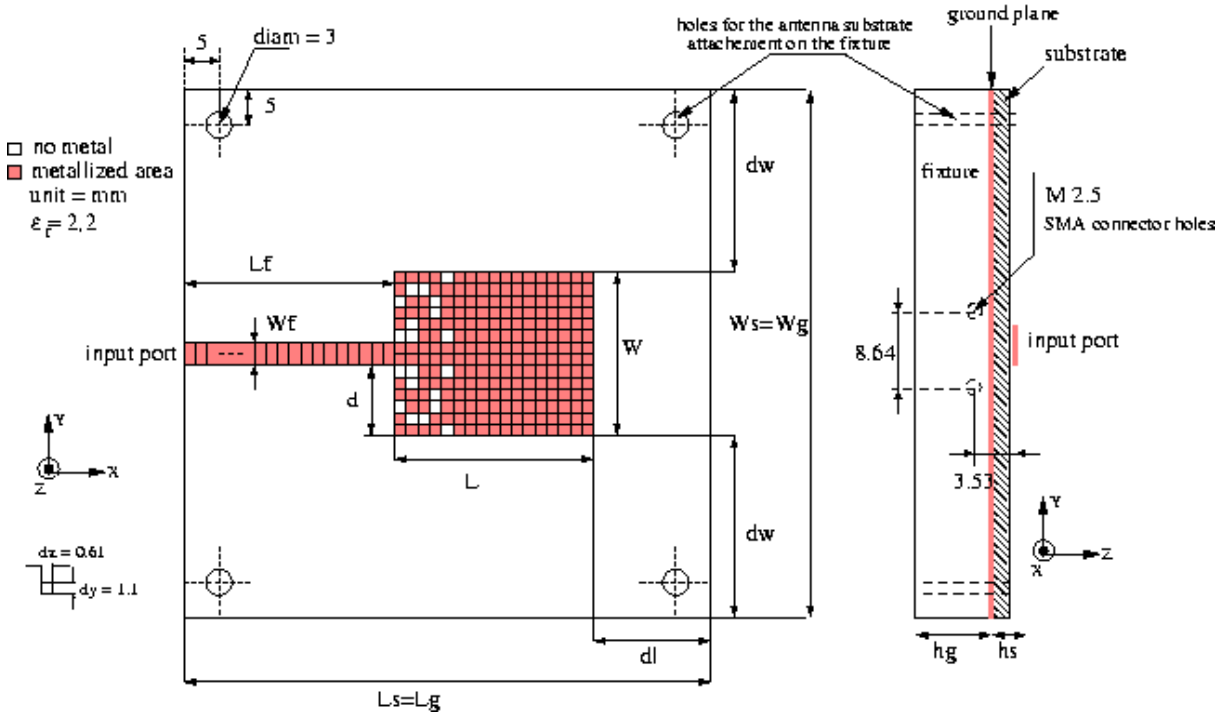

Figure 2 : GA optimized Patch Antenna on grounded substrate and fixture.

Dimensions Table (mm)

L	*W*	*Lf*	*Wf*	*dx*	*dy*	*d*	*dl*	*dw*	*Ls*	*Lg*	*Ws*	*Wg*
10.39	*15.4*	*32.8*	*2.2*	*0.61*	*1.1*	*6.6*	*32.8*	*30.3*	*76*	*76*	*76*	*76*

N.B : Intermediate dimensions can be deduced from the elementary cell size (dx and dy). Note that the width of the microstrip line is twice the cell width on the patch.

5. Computed results

The results that should be computed are :

- the reflection coefficient (magnitude and phase) with the following constraints

5.1.1. the reference plane is in the entrance of the line (referred to as input port in figure 1 and 2)

5.1.2. the reference impedance is 50Ω
5.1.3. the frequency range is [8.9-9.4] GHz

5.2. the far fields (E_θ, E_φ) with the following constraints
5.2.1. the cut planes are φ=0° and φ=90°, as presented in figure 3
5.2.2. the frequency for calculation is 9.12 GHz for the simple rectangular patch antenna and 9.35 GHz for the GA optimized antenna.

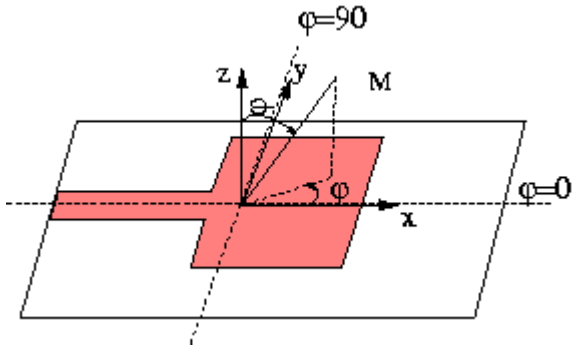

Figure 3 : Cut planes.

6- References

Measurements have been done by IETR.

2- STRUCTURE MEASUREMENTS

Entity

IETR

Contact persons:
Raphaël GILLARD
Phone: +33 (0)2 23 23 86 61
email: Raphael.gillard@insa-rennes.fr

1. **Description of measurement tools**

   - Input impedance and Voltage Standing Wave Ratio measurements have been realised in IETR using a Wiltron vector network analyser. SMA connectors were used and a standard SOLT was involved. No phase measurement were realised.
   - Radiation pattern measurements are realised in IETR using a conventional anechoic chamber. Only front radiation was measured.

2. **Generalities about measurement tools**

3. **Measurements Set-up**

4. Measurement results

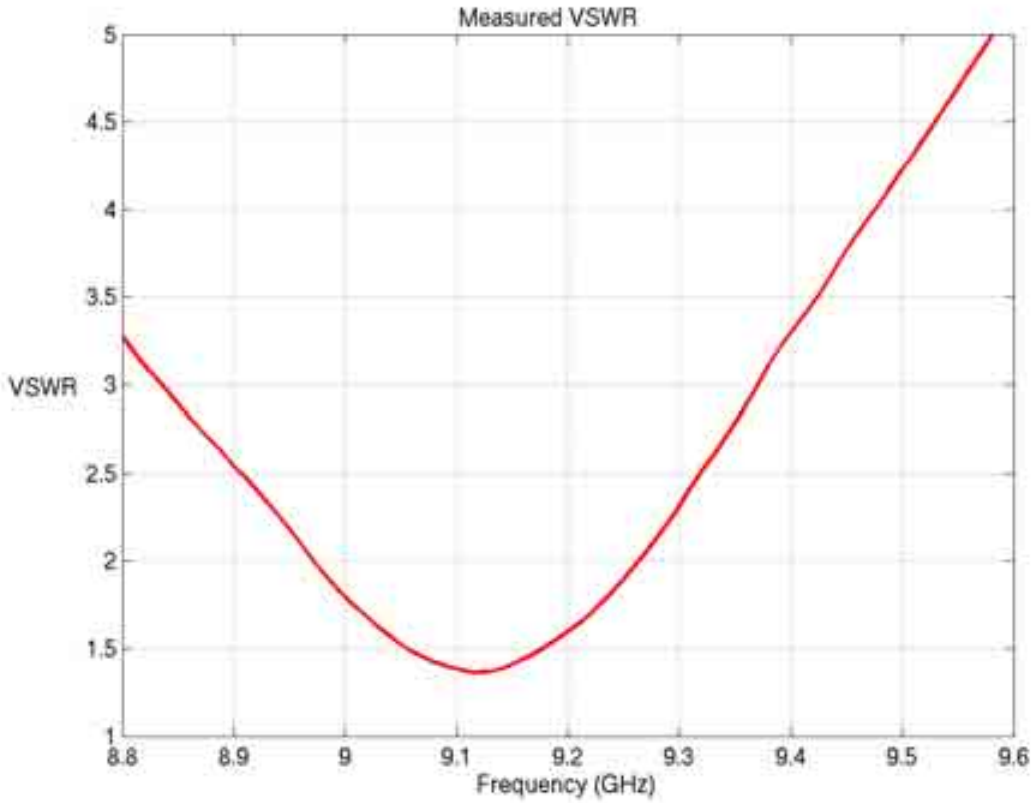

Figure 1 : VSWR versus frequency for the Classical Patch antenna.

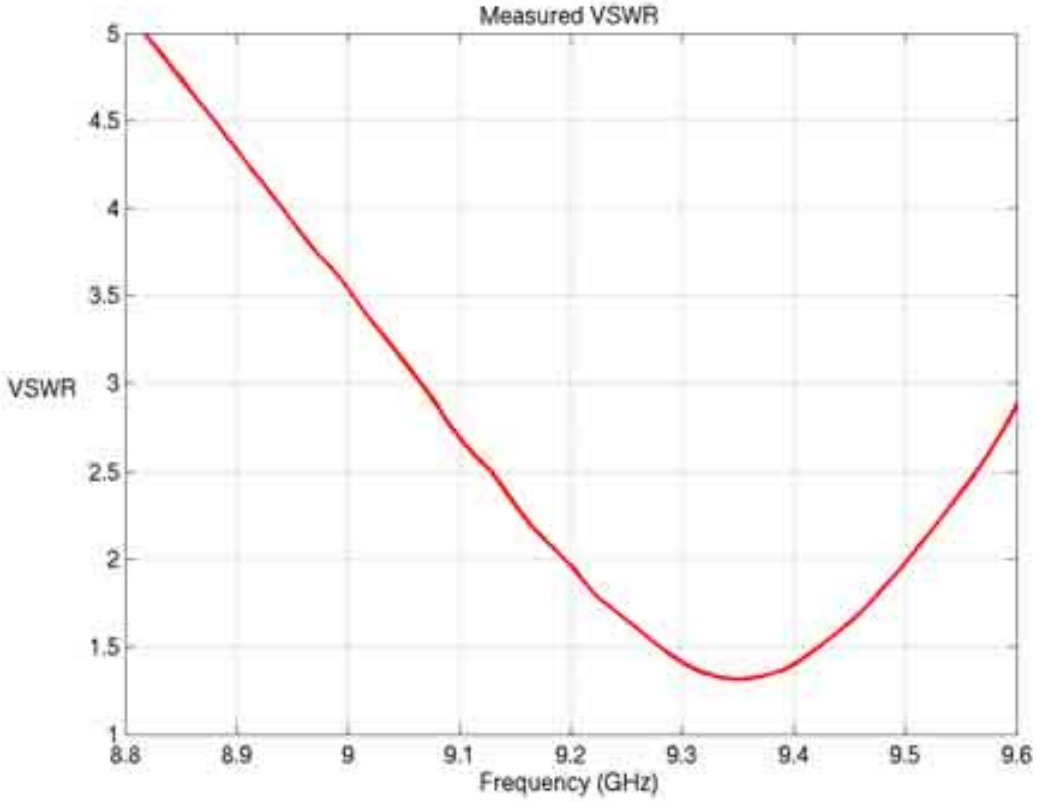

Figure 2 : VSWR versus frequency for the GA optimized antenna.

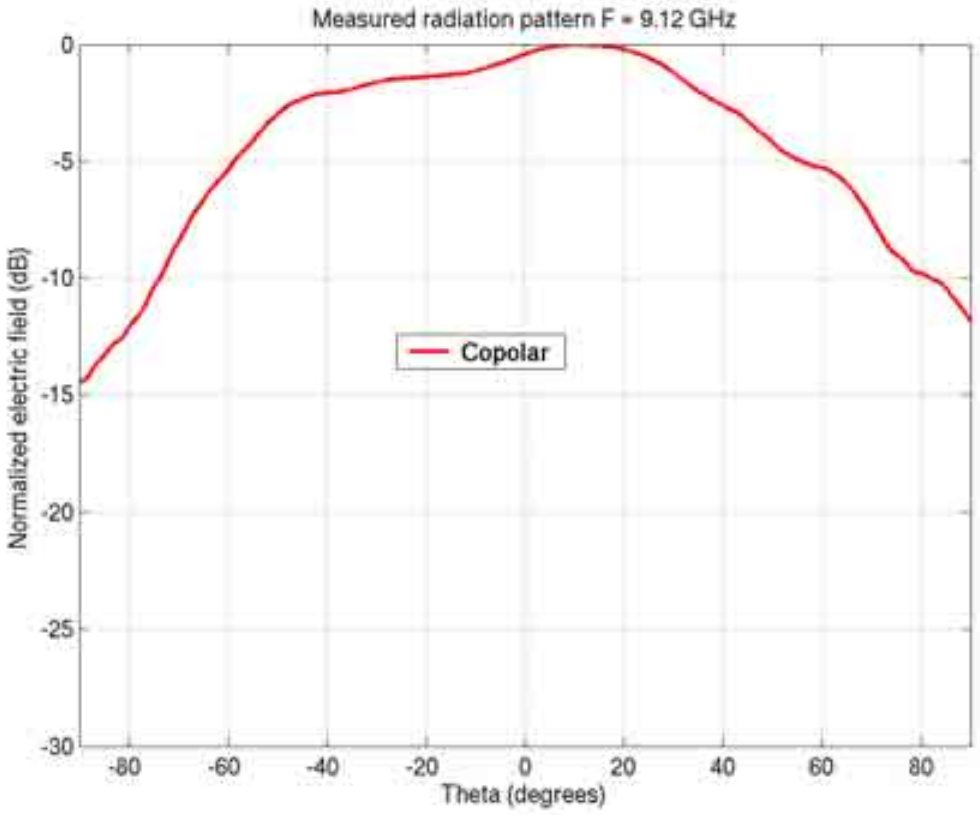

Figure 3 : E-plane radiation pattern versus theta for the Classical Patch antenna (f=9.12 GHz).

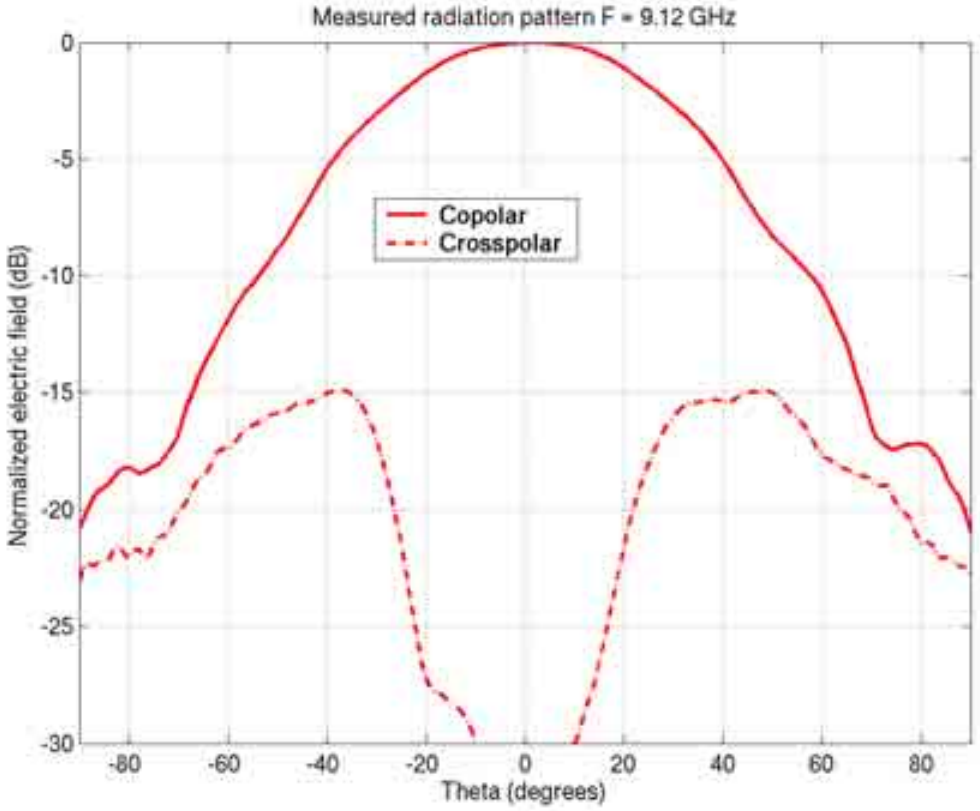

Figure 4 : H-plane radiation pattern versus theta for the Classical Patch antenna (f=9.12 GHz).

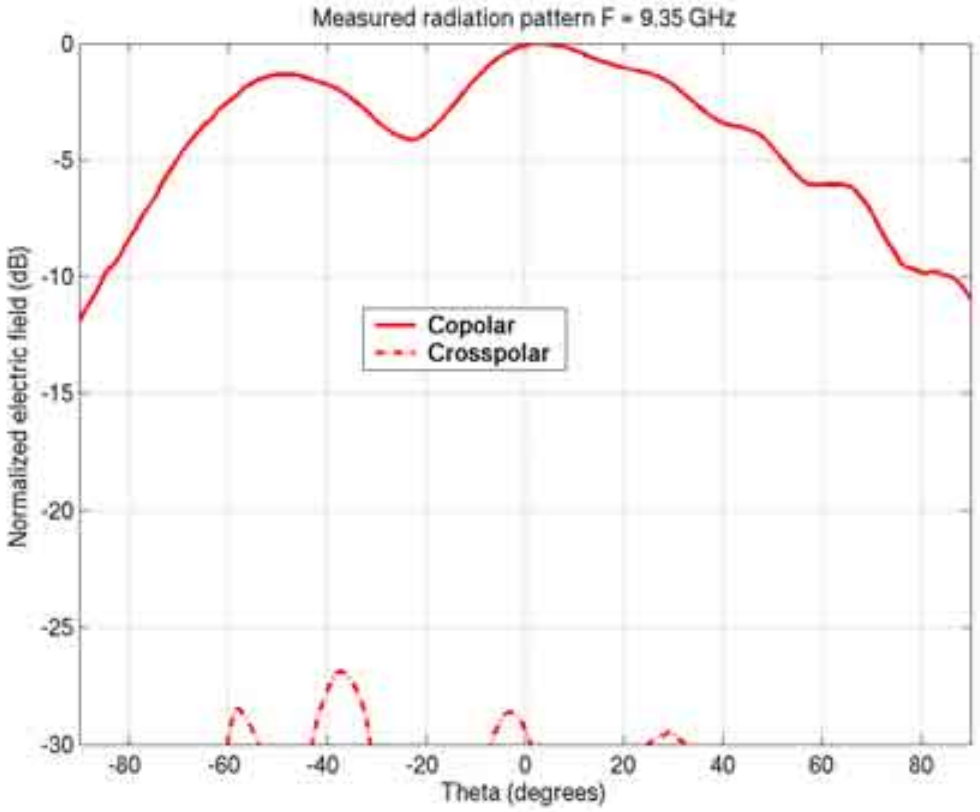

Figure 5 : E-plane radiation pattern versus theta for the GA optimized antenna (f=9.35 GHz).

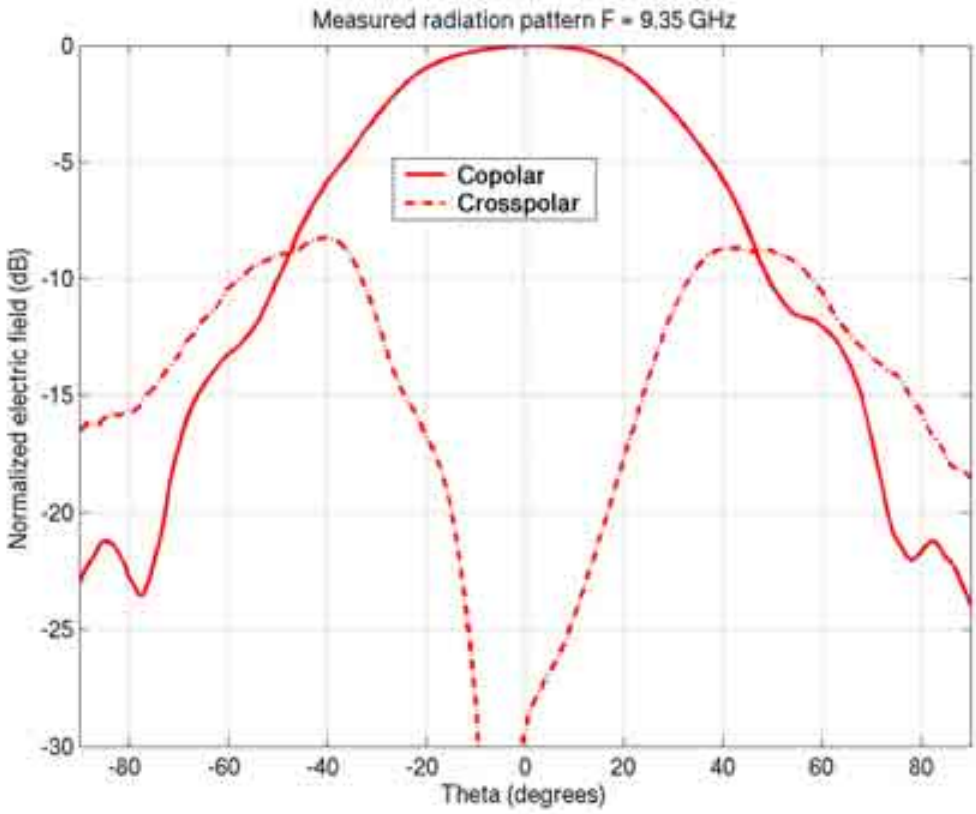

Figure 6 : H-plane radiation pattern versus theta for the GA optimized antenna (f=9.35 GHz).
Note : for each plane (E, H) the far field is normalized with the maximum value of the considered cut plane

3- SIMULATION RESULTS

From IETR

1- Entity

IETR/INSA, 20 avenue des Buttes de Coëmes
35043 Rennes cedex
Tel : + 33 2 23 23 87 00
Email : raphael.gillard@insa-rennes.fr, delia.cormos@insa-rennes.fr

2- Name of the simulation tool

SAPHIR

3- Generalities about the simulation tool

SAPHIR uses the Method of Moments (MoM) to solve the Mixed Potential Integral Equations (MPIE) in multilayered printed structures (air + 2 dielectric substrates + 1 ground plane). It relies on the computation of exact Green Functions and uses rooftop basis functions and test segments. SAPHIR can handle both 2D horizontal metallizations (divided in rectangular cells) and 1D vertical metallizations (either wires or strips). Both microstrip lines and coaxial feeds can be involved for excitation.

4- Simulation Set-up (Geometry set-up, GUI, mesh, boundary conditions, excitation)

The geometrical structure is described (metallizations, substrates, excitation,…) in a text file. The meshing operation is defined manually. The metallized structure is divided into different parts, each of which involving a regular mesh. Here, two different parts are considered : the microstrip line only uses a 1D mesh (only one cell transversally to the line) as the basis functions already include the singular transversal dependency of the longitudinal current densities. The length of the line should be long enough so that at least a $\lambda g/4$ "quiet" section is available for the determination of the return loss. In the present example, no additional line section is required as the physical length itself is sufficient. The second part is the microstrip patch. It is first described as a simple rectangular patch and meshed using a regular grid. Cells are then removed from the meshed structure to account for the non intuitive shape of the surface (removed cells are simply defined by a "0" bit in the text file while remaining cells are defined by a "1" bit).

The excitation is achieved by impressing an excitation current at the entrance of the line. This technique (which requires a special basis function for the feed point) prevents from the

excitation of higher order modes and usually permits to use a smaller line (compared to a classical delta gap voltage generator).
An infinite transversal substrate and an infinite ground plane are considered for the computation of Green functions.

The analysis is performed in the frequency domain (one new computation for any new frequency point).

The frequency range is [8.8-9.6] GHz and the maximum frequency step is 50 MHz.

The geometry is compatible with the software constraints which makes it possible to simulate the exact shape.
The only assumptions are:

a. infinite substrate and ground plane,
b. zero thick metallization.

The mesh size for the line is 0.305 mm along x and 2.2 mm along y.
The mesh size for the patch is 0.305 mm along x and 0.55 mm along y.

The maximum simulation time is 20 mn for a frequency.

5- Simulation results

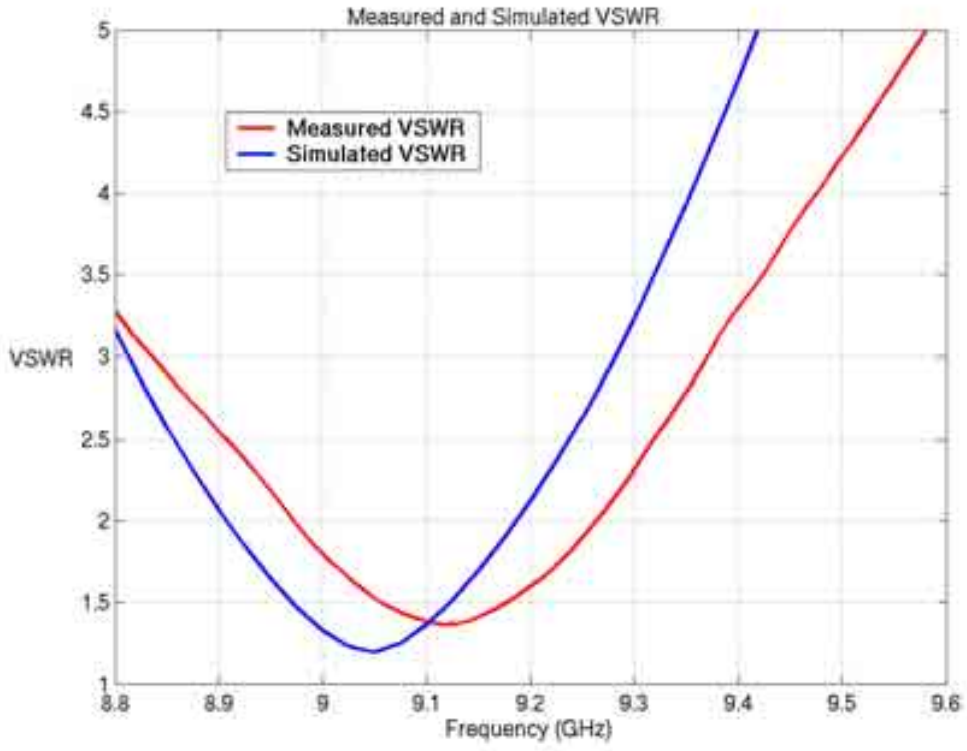

Note :

Simulation results are in blue

Figure 1 : VSWR versus frequency for the Classical Patch antenna.

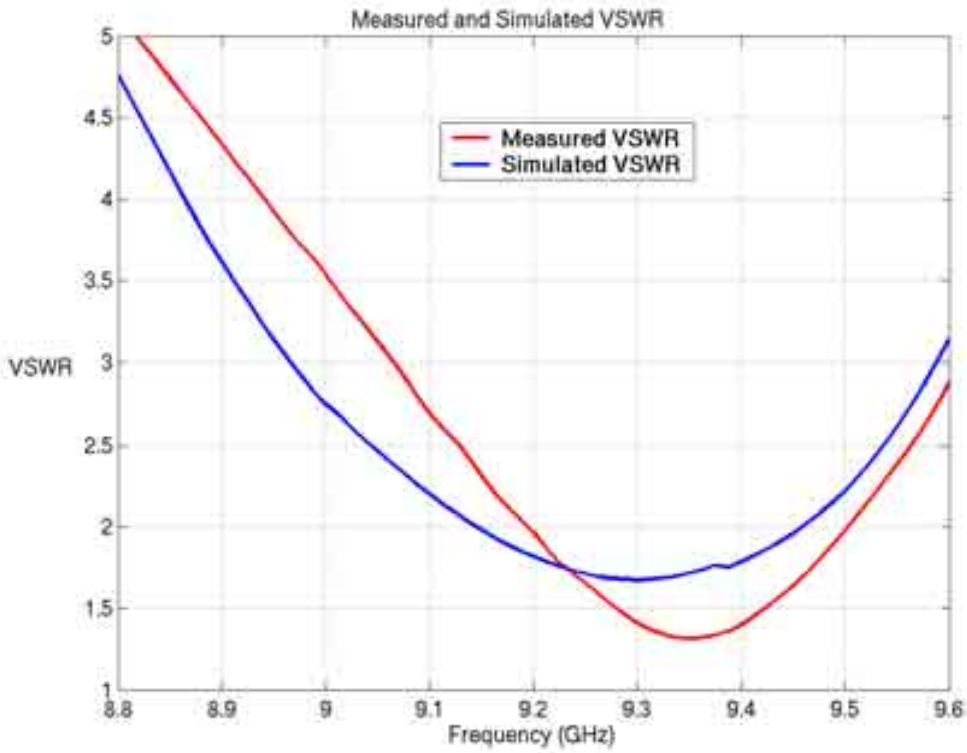

Figure 2 : VSWR versus frequency for the GA optimized antenna.

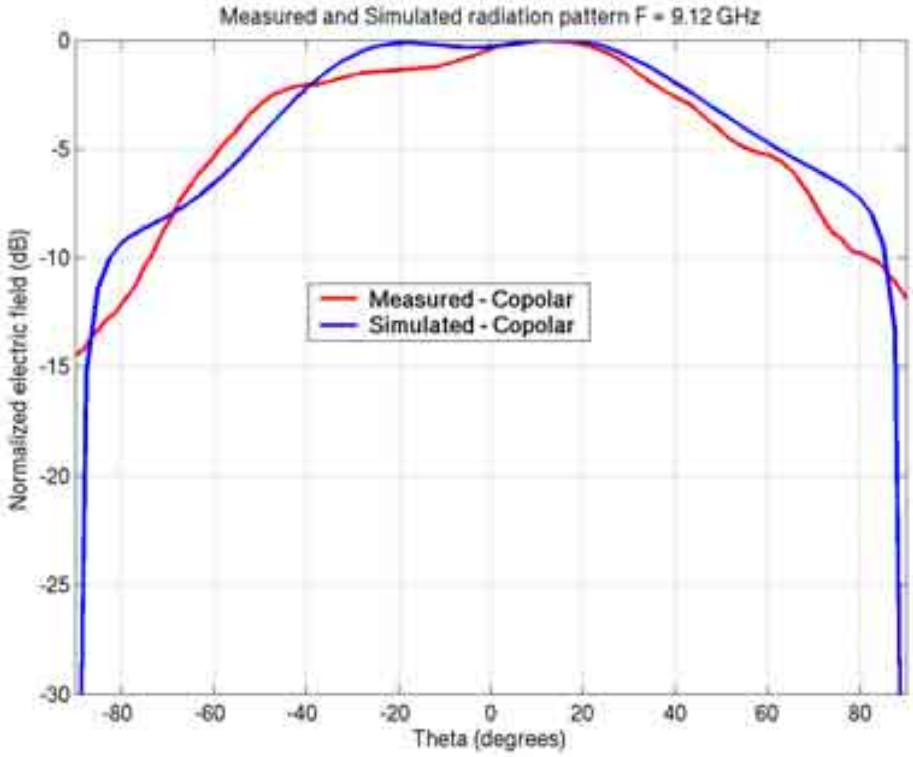

Figure 3 : E-plane radiation pattern versus theta for the Classical Patch antenna (f=9.12 GHz).

Note :

Simulation results are in blue

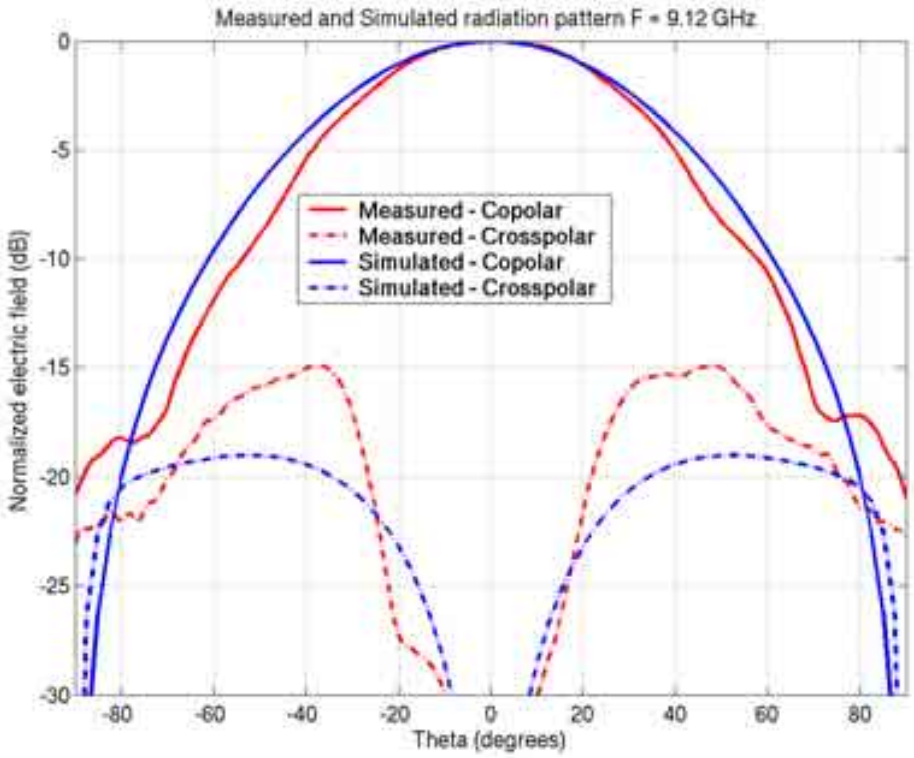

Figure 4 : H-plane radiation pattern versus theta for the Classical Patch antenna (f=9.12 GHz).

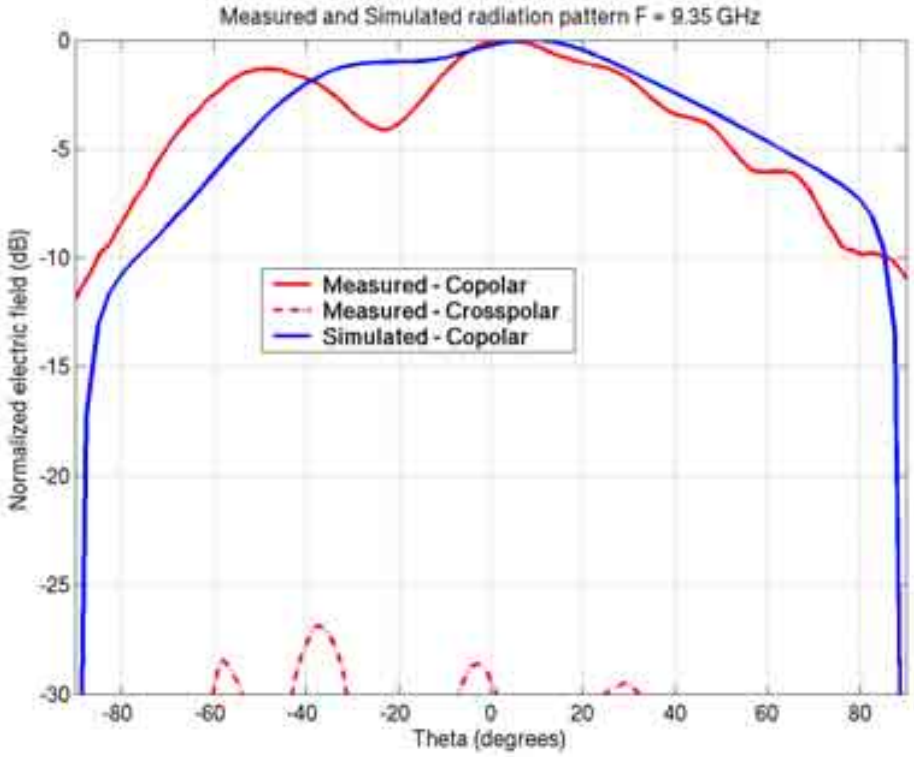

Note :

Simulation results should be in blue

Figure 5 : E-plane radiation pattern versus theta for the GA optimized antenna (f=9.35 GHz).

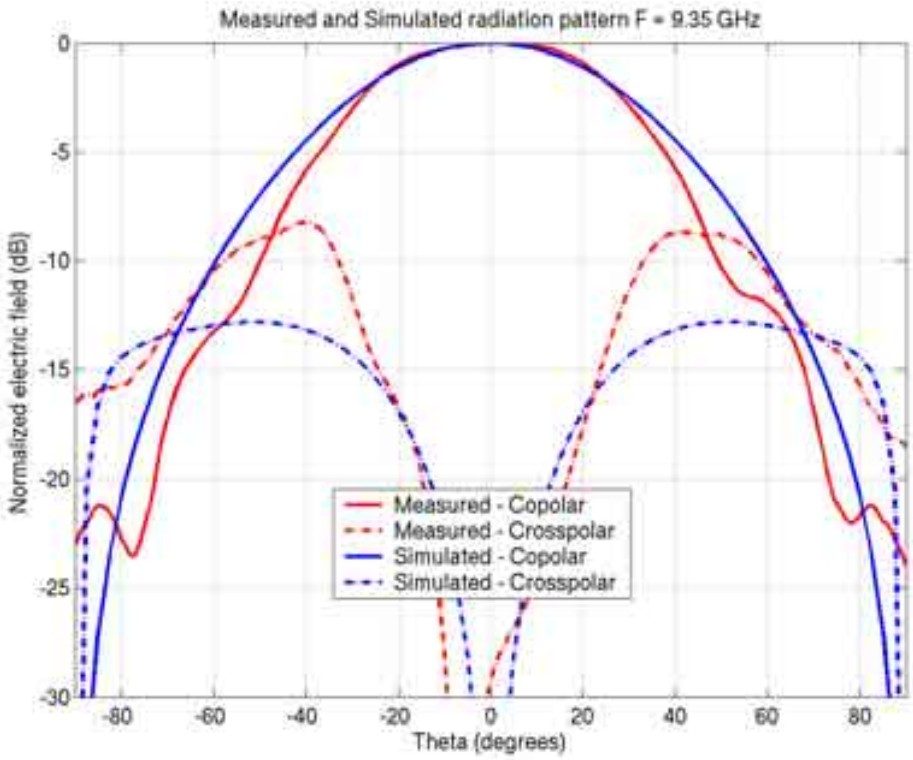

Figure 6 : H-plane radiation pattern versus theta for the GA optimized antenna (f=9.35 GHz).
Note : for each plane (E, H) the far field is normalized with the maximum value of the considered cut plane

6- Computation resources

The simulation has been performed on a PC with 2 processors(1.67GHz CPU speed), 2Gb memory.
The computation time for one frequency point was:

	CPU time (s)
Classical antenna	57.7
GA optimized antenna	42.9

7- Discussion

The first simulation results were obtained for a coarser mesh (the coarse mesh is defined by dx=0.610 mm and dy =1.1 mm). The final fine mesh is obtained by dividing the coarse mesh by 2 in both directions.
The agreement between the measured results and the simulated ones was not very good. So, we performed several test simulations with different mesh size. This numerical convergence study points out that GA optimized antenna is more sensible to the mesh size than the classical antenna.

Therefore, for a more rigorous analysis we consider only the results obtained for a fine mesh.

For the VSWR, a good agreement between the measured results and the simulated results with a fine mesh (see section 5) is obtained.

For the far field, there are some differences especially for the H-plane cross-polar. Compared to the simulation it is about 5 dB higher in measure for both antennas. Note that due to the longitudinal meshing of the line, no cross-polar can be accounted for this line.

8- Additional comments

4- SIMULATION RESULTS

From LEMA EPFL

1- Entity

Electromagnetics and Acoustics Laboratory (LEMA)
Ecole Polytechnique Fédérale de Lausanne (EPFL)
EPFL STI-iTOP-LEMA ELB
Station 11
CH-1015 Lausanne, Switzerland

Contact person
Ivica Stevanovic
Phone +41 21 693 4637
Fax +41 21 6932673
E-mail ivica.stevanovic@epfl.ch

2- Name of the simulation tool

POLARIS

3- Generalities about the simulation tool

POLARIS is an IE-MoM based solver for modeling planar multilayered structures with dielectrics supporting slotted ground planes and feeding printed lines. Slotted ground planes can have a sizable thickness, the structure can be backed by rectangular cavities and the arrays can be obtained by periodical repetition of basic radiating elements.

4- **Simulation Set-up (Geometry set-up, GUI, mesh, boundary conditions, excitation)**

The geometry is defined using the GUI of the software. The software assumes laterally unbounded dielectric layers and ground planes. The metallic parts are discretized using rectangular basis functions. The discretization is done using the GUI, which contains a structured mesher. The mesh has been produced at 10GHz with 50% of cell density leading to 1272 and 1178 RWG basis functions for the classical and the GA optimized patch antenna, respectively. The analysis is performed in the frequency domain. A discrete frequency sweep has been used (41 points in frequency). The excitation is modeled as a delta-gap generator located at the edge of the microstrip feeding line. Approximate time to set-up the geometry and simulation parameters was about 10 min.

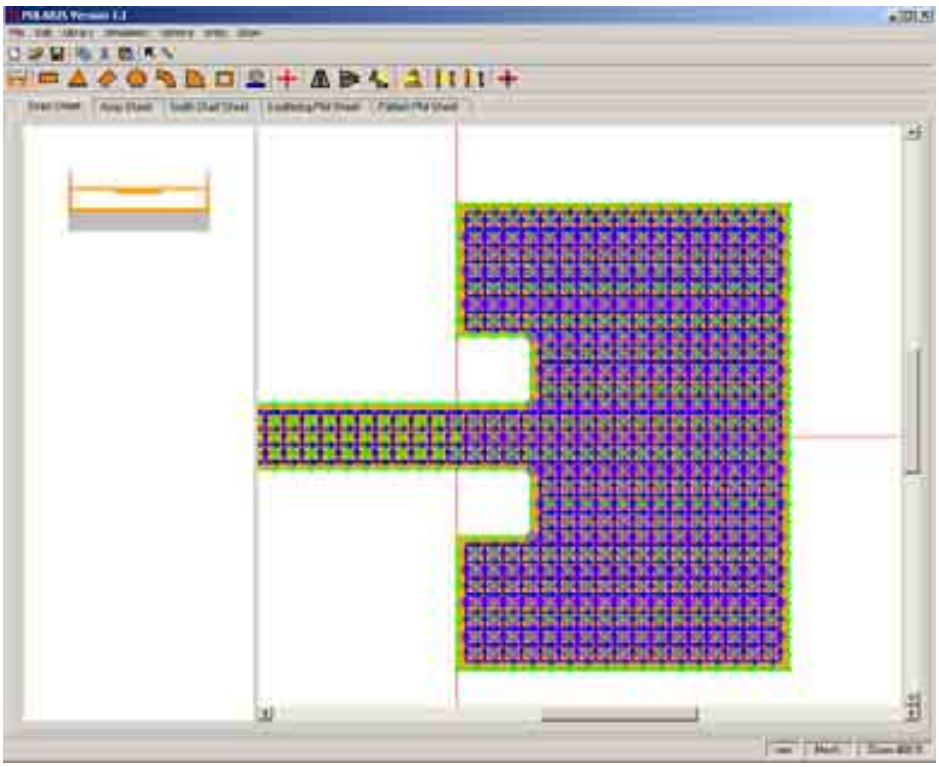

Fig. 1: Snapshot of the classical patch antenna geometry inside the POLARIS GUI.

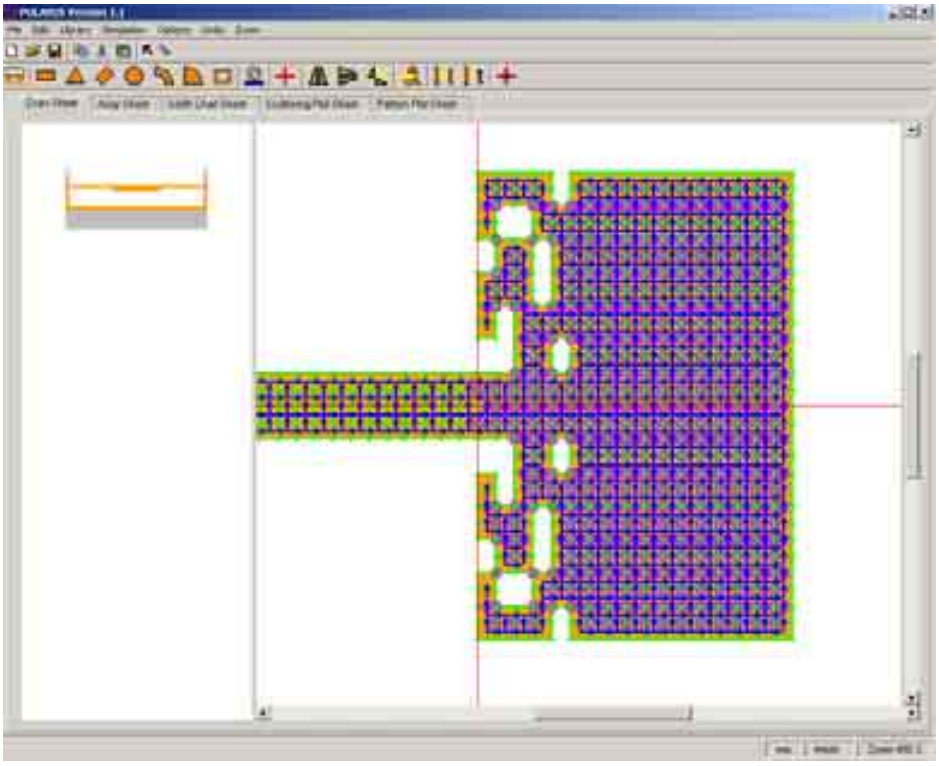

Fig. 2: Snapshot of the GA optimized patch antenna geometry inside the POLARIS GUI.

5- Simulation results

The results that have been computed are:

- Input port parameters (VSWR)
- Radiation patterns in both E and H planes

The input port parameters are computed at the input port, with a normalization impedance of 50Ω. Results for the VSWR are shown in Fig. 3 (classical patch) and in Fig. 4 (GA optimized patch). The blue lines represent the results obtained with POLARIS and the red ones the measurements.

E- and H-planes radiation patterns are shown in Fig. 5 and Fig. 6, respectively, for the classical patch antenna. The same radiation pattern plots are presented in Fig. 7 and Fig. 8 for the GA optimized patch antenna.

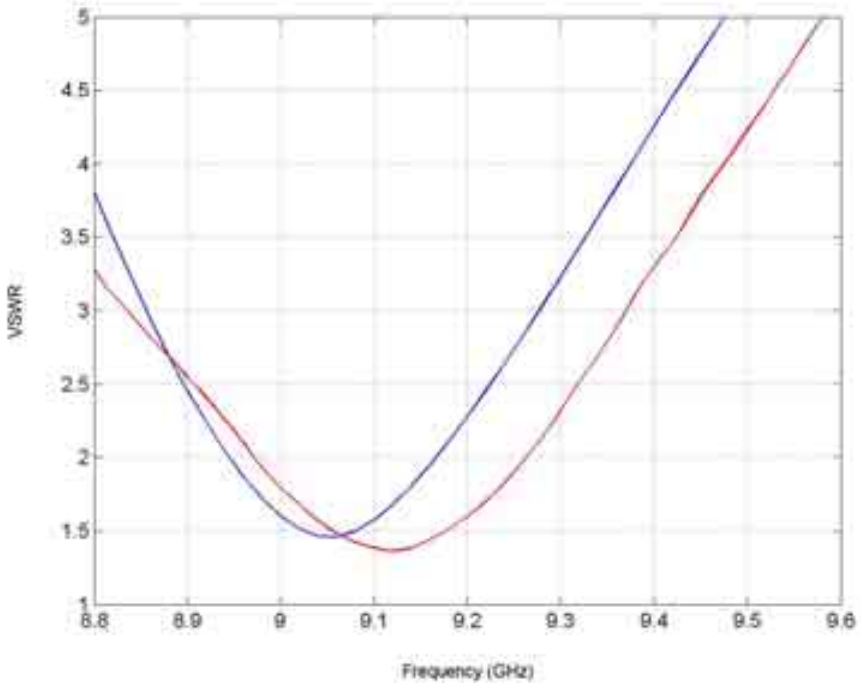

Fig. 3: VSWR versus frequency for the Classical Patch antenna.
Blue: Simulation results, red: measurements.

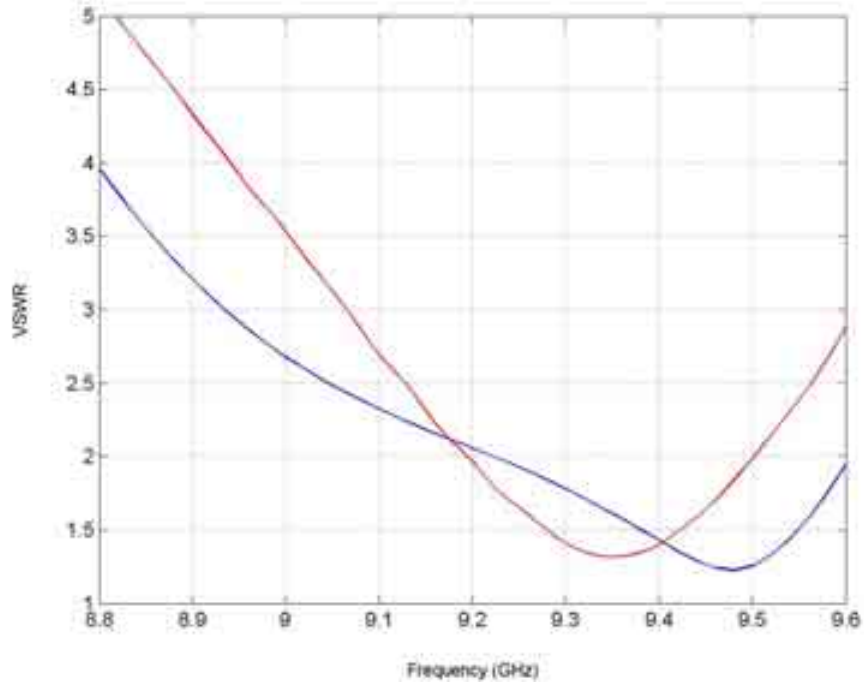

Fig. 4: VSWR versus frequency for the GA optimized patch antenna. Blue: Simulation results, red: measurements.

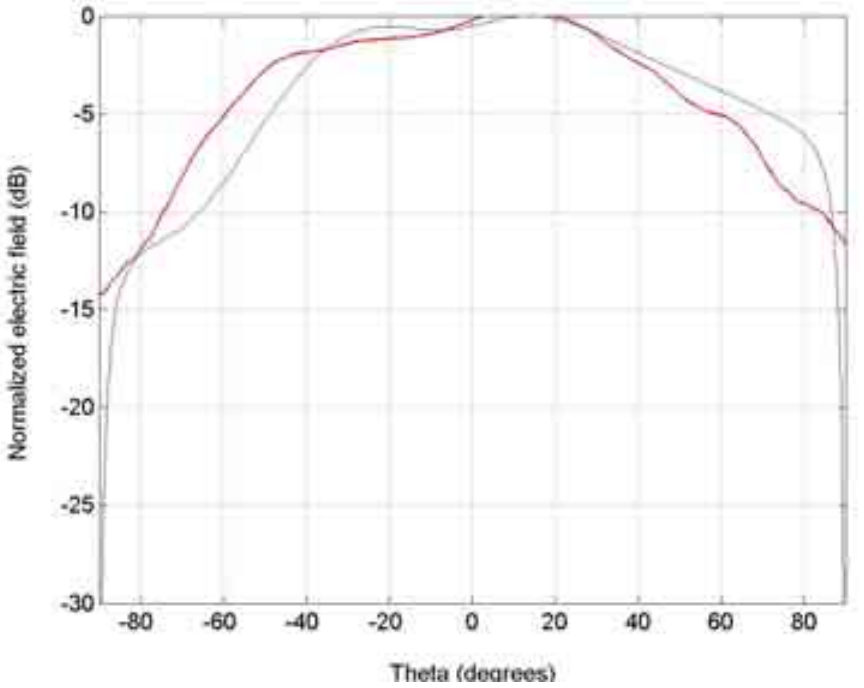

Fig. 5: : E-plane radiation pattern versus theta for the Classical Patch antenna (f=9.12 GHz). Blue: Simulation results, red: measurements.

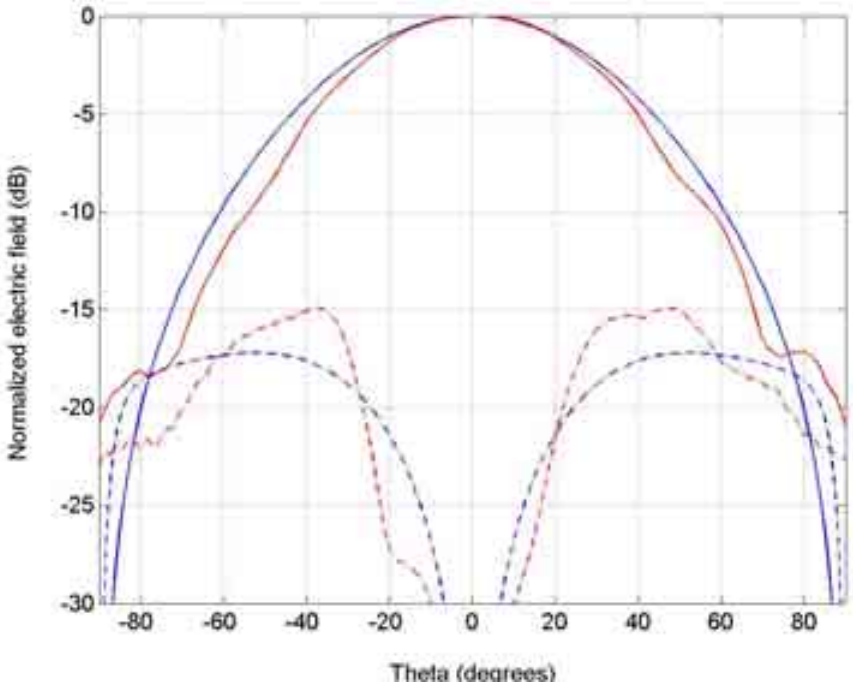

Fig. 6: H-plane radiation pattern versus theta for the Classical Patch antenna (f=9.12 GHz).
Blue: Simulation results, red: measurements.

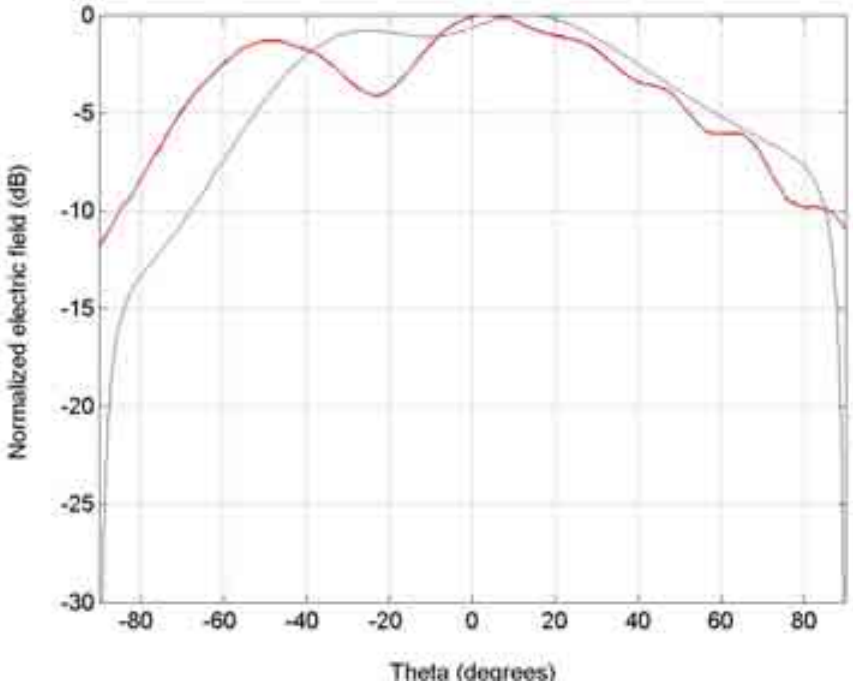

Fig. 7: E-plane radiation pattern versus theta for the GA optimized antenna (f=9.35 GHz).
Blue: Simulation results, red: measurements.

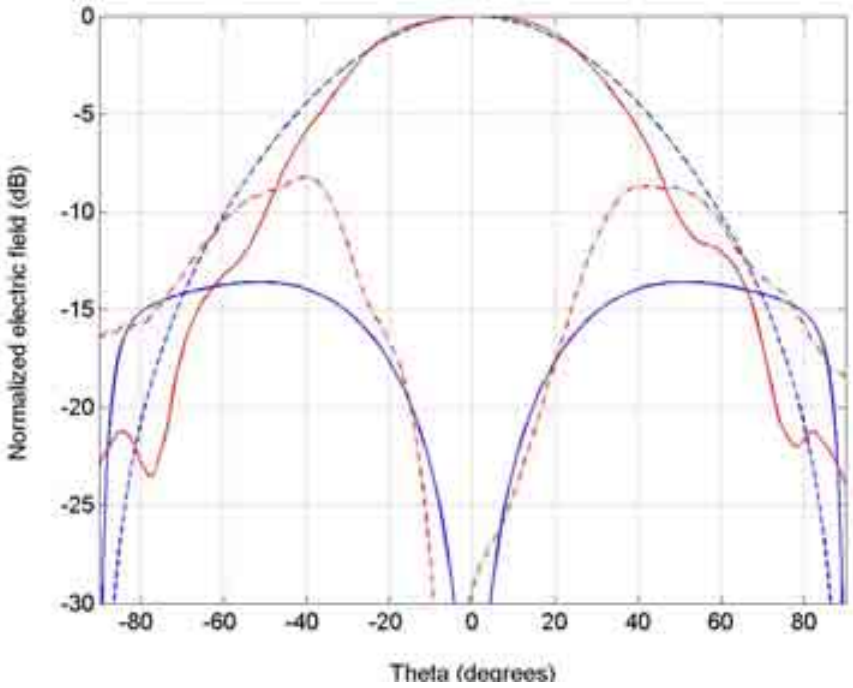

Fig. 8: H-plane radiation pattern versus theta for the GA optimized antenna (f=9.35 GHz). Blue: Simulation results, red: measurements.

6- Computation resources

The simulation has been performed on a PC with 1 AMD processor at 1.4 GHz and 512 MB of available memory. The operating system was Redhat Linux.

The data relevant to the two computers are reported in the following table.

Table 1 Properties of the PC used for the simulation

Type of machine	Desktop PC
Number of CPUs	1 AMD
CPU Speed	1.4 GHz
RAM	512 MB
OS	Linux, RedHat

The simulation is performed over 41 discrete points in frequency (in the range 5.5 – 6.0 GHz). Data relevant to the simulation are listed in the following table.

Table 2 Simulation requirements for the PC

	classical patch	GA optimized
Average CPU time per frequency point	2 min 34 sec	1 min 36 sec
Max. required RAM	50 MB	43 MB
Number of unknowns	1272	1178

7- Discussion

Both structures simulated here are easy to set up and are not computationally difficult for POLARIS. The test simulations were performed after obtaining the measurements results shown above. Two different mesh densities were used (30% and 50% as defined in POLARIS GUI) and both gave very close results, showing that the procedure numerically converged.
The mismatch in VSWR and cross-polar radiation patterns for both classical and GA optimized patch antennas can be attributed to the finite ground plane that was not taken into account in the simulations.
The new feature that should be added to the simulator, concerning this example is the finite ground plane.

8- Additional comments

None.

5- SIMULATION RESULTS

From CNRS LEAT

1- Entity

Laboratoire d'Electronique, Antennes et Télécommunications (LEAT)
CNRS UMR 6071
250 rue Albert Einstein, Bât. 4, 06560 Valbonne, France

Contact persons:
Jean-Lou Dubard
Phone: +33 (0)4 92 94 28 07
Fax: +33 (0)4 92 94 28 12
Email : jean-lou.dubard@unice.fr

2- Name of the simulation tool

FP-TLM

3- Generalities about the simulation tool

The Transmission Line Matrix (TLM) method is a finite-difference-time-domain technique. Although it is very similar to the FDTD method, it allows computing the six electromagnetic field components at the same location. As TLM simulation is performed in time domain, analysis in a wide frequency band is obtained with only one run by using a Fourier Transform. In FP-TLM code, the FFT operation is replaced by a Prony-Pisarenko method which performs accurate spectral analysis even with short time response. FP-TLM includes PML layers for modeling free space and is implemented on parallel computers.

4- Simulation Set-up (Geometry set-up, GUI, mesh, boundary conditions, excitation)

Since no GUI is available, the input of the geometrical structure into FP-TLM software was done manually. Also, a variable hexaedric meshing was manually performed. Perfectly matched layers (PMLs) were used to simulate free space surrounding the antenna. For excitation, a lumped matched generator occupying a volume of $1\Delta x.1\Delta y.3\Delta z$ at the beginning of the microstrip feed-line (yellow cell on the snapshots) with a gaussian pulse was used. About six hours were needed to draw the geometry and to set up the rest of the simulation.

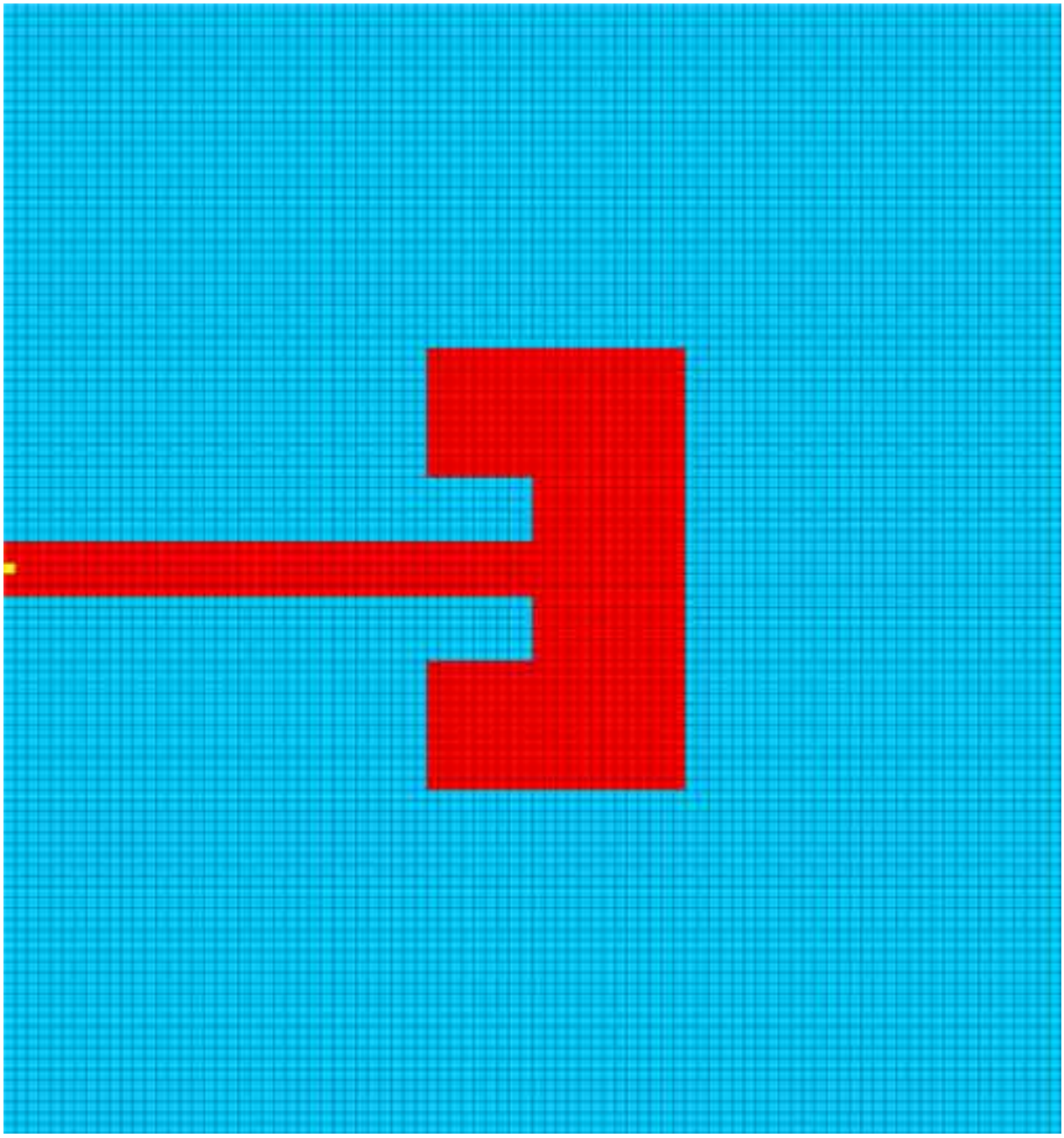

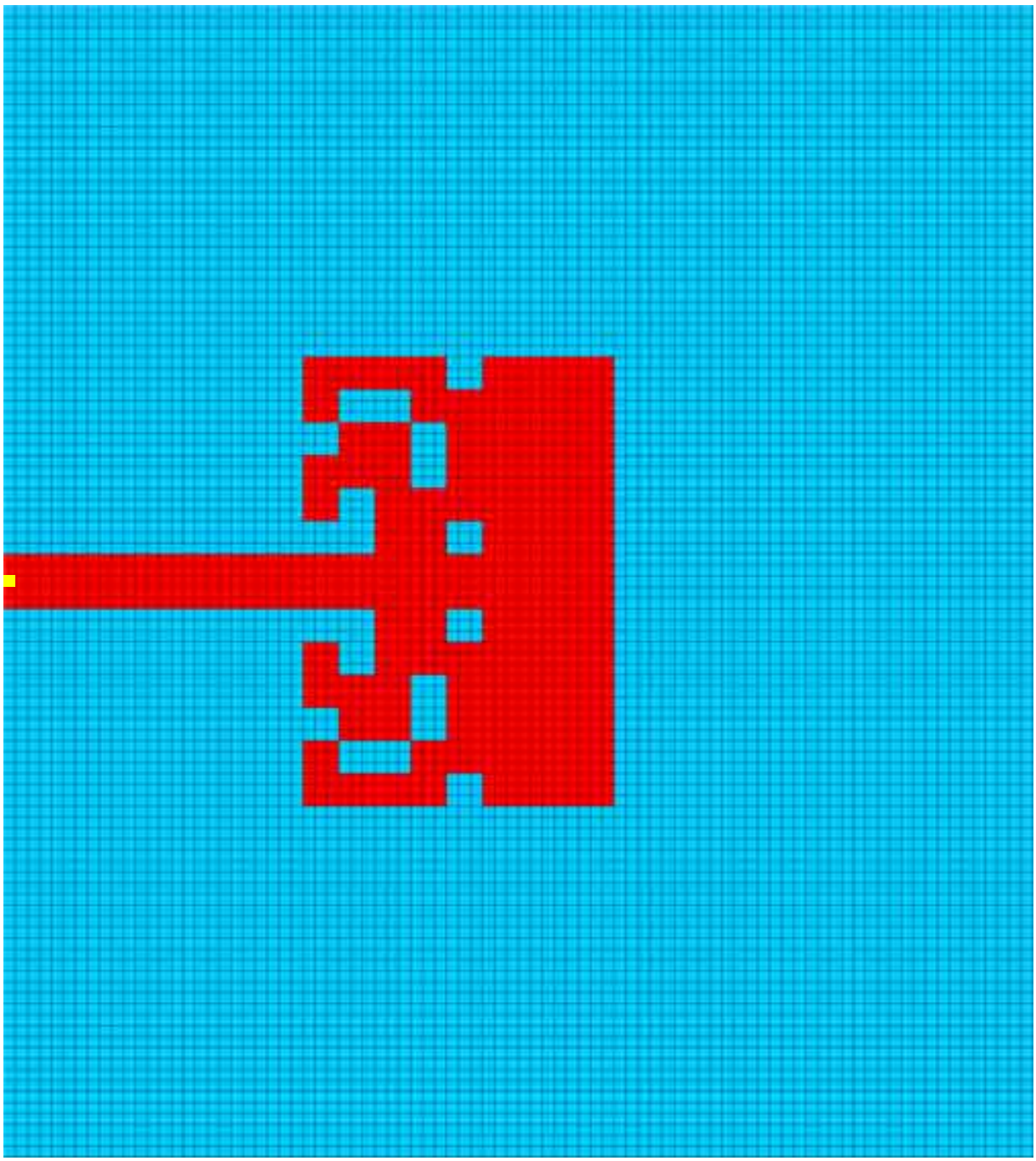

These snapshots show only the mesh density used in the TLM simulations for modeling the radiating patch and the finite ground plane. The apparent uniform size step corresponds to the smallest size step over the mesh. The real dimensions are taken into account in the FP-TLM code by multiplying this smallest size step with an appropriate factor for each cell.

5- Simulation results

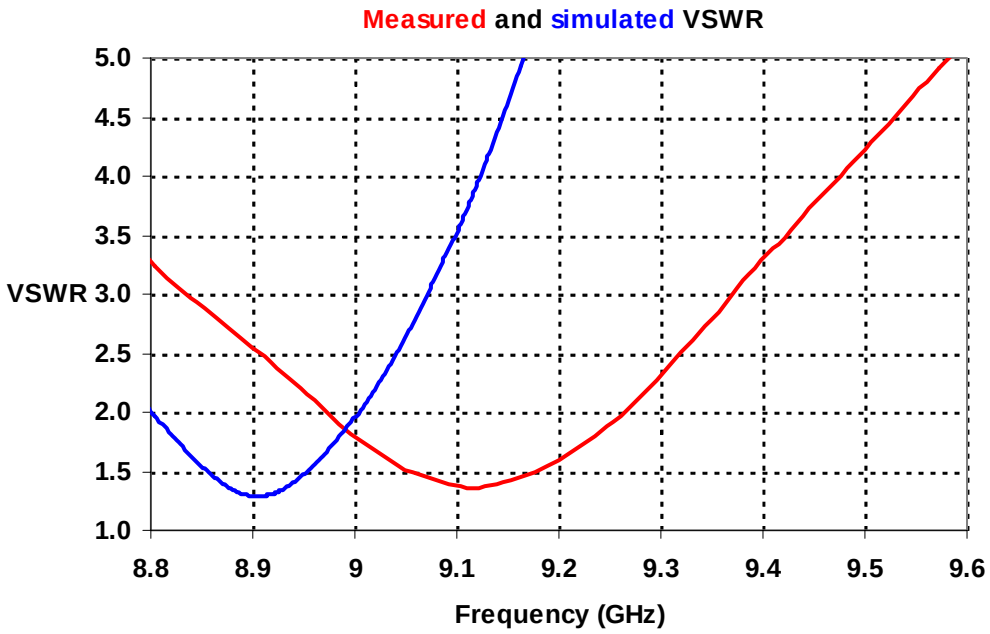

Figure 1: VSWR versus frequency for the Classical Patch antenna.

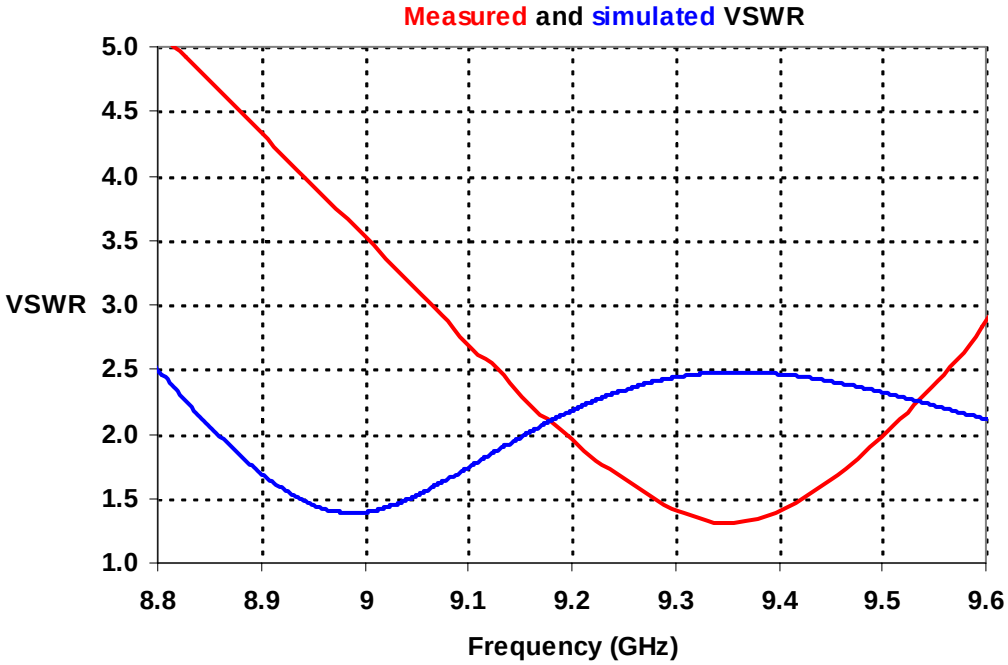

Figure 2: VSWR versus frequency for the GA optimized antenna.

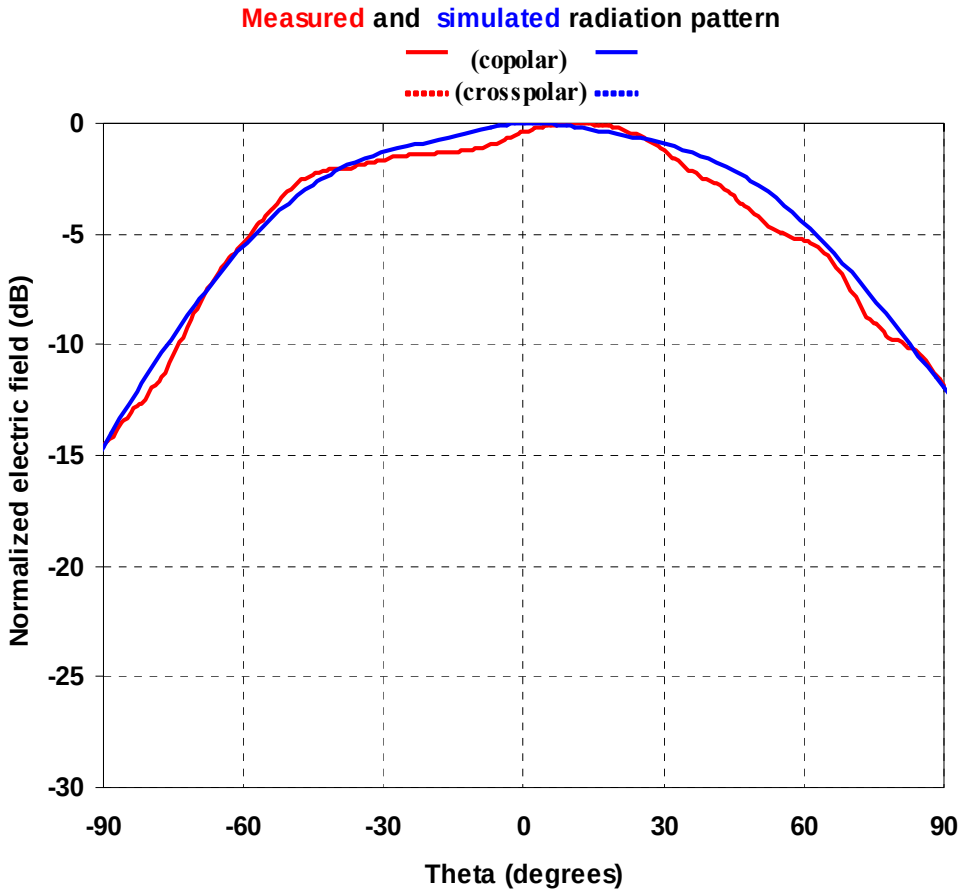

Figure 3 : E-plane radiation pattern versus theta for the Classical Patch antenna (f=9.12 GHz).

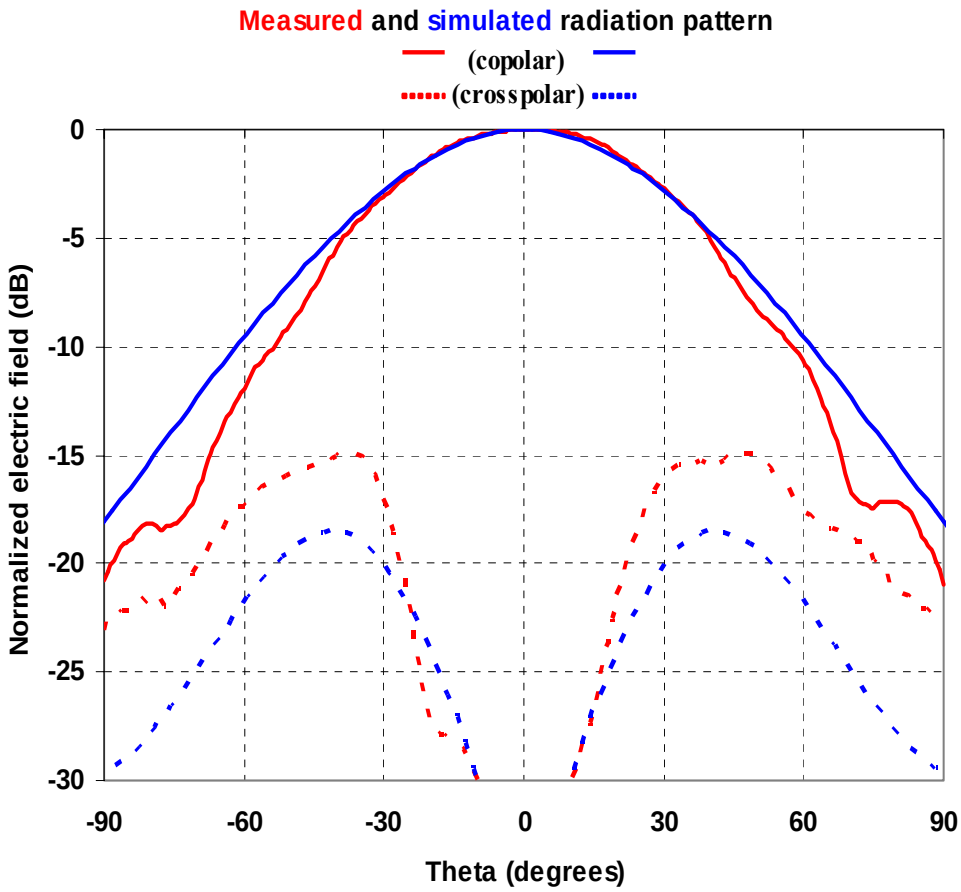

Figure 4: H-plane radiation pattern versus theta for the Classical Patch antenna (f=9.12 GHz).

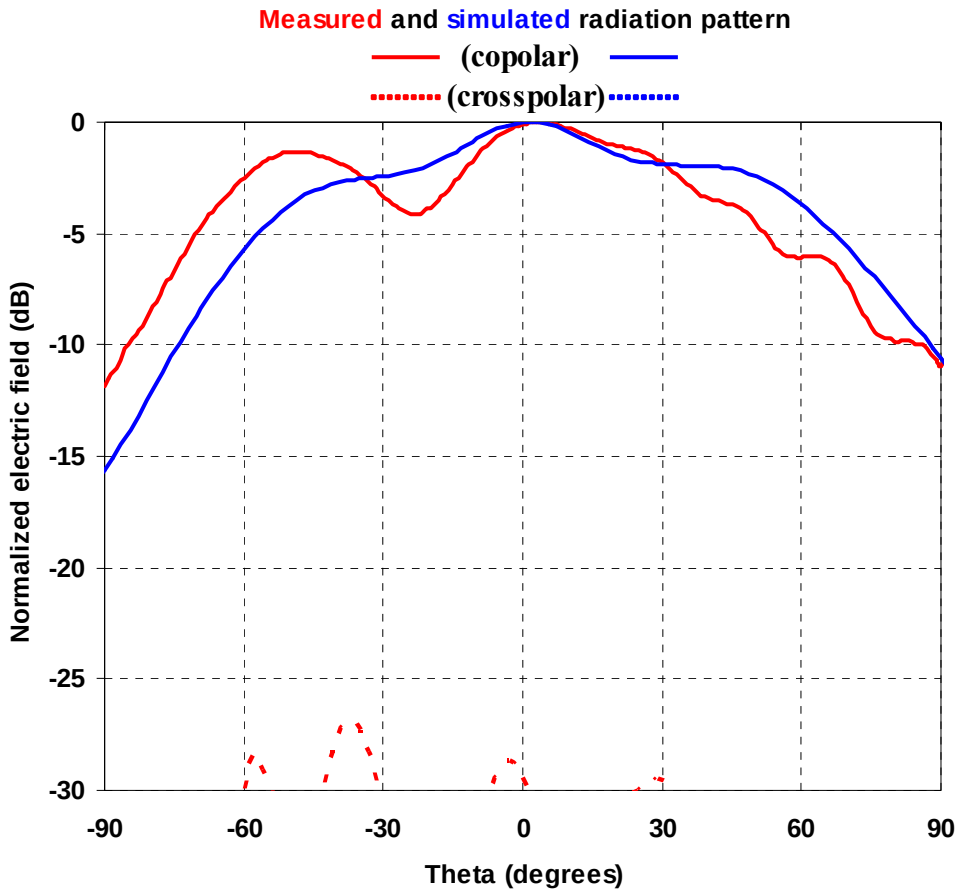

Figure 5: E-plane radiation pattern versus theta for the GA optimized antenna (f=9.35 GHz).

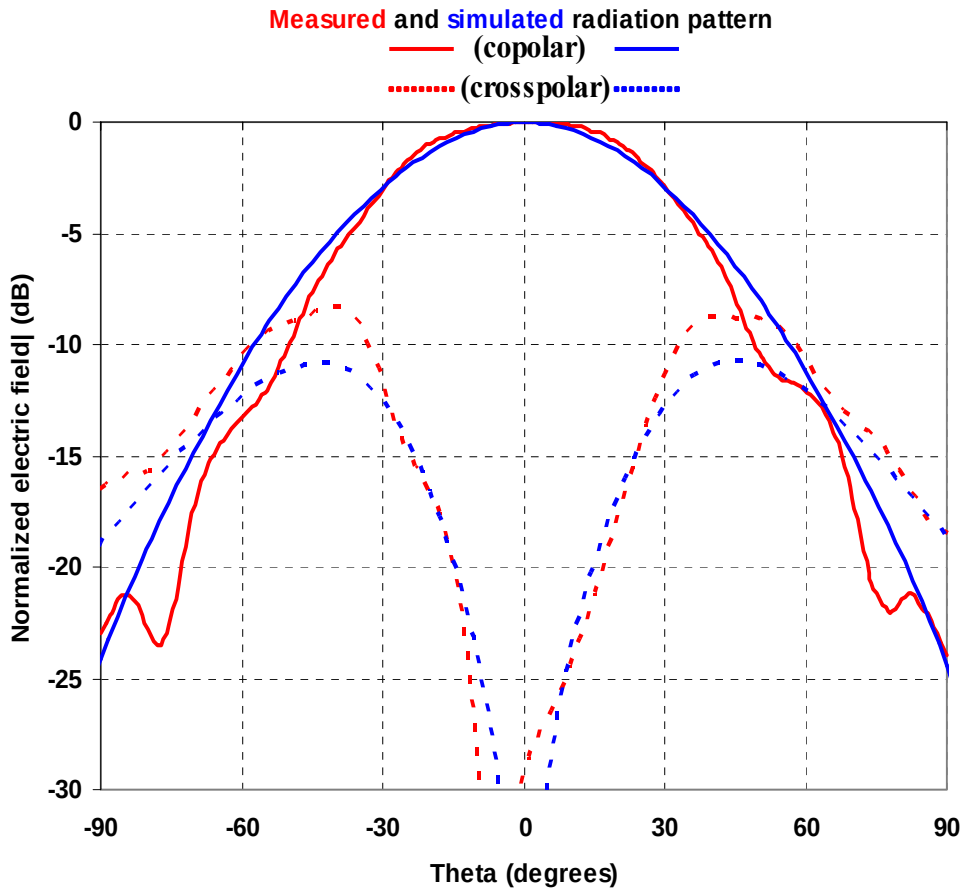

Figure 6: H-plane radiation pattern versus theta for the GA optimized antenna (f=9.35 GHz).

Note : for each plane (E, H) the far field is normalized with the maximum value of the considered cut plane.

6- Computation resources

- *Type of machine (PC, Workstation, …),*
  parallel computer IBM SP4
- *Number of processors,*
  16 processors
- *Maximum available memory,*
  2Gbytes/processor
- *Memory used for simulation,*
  426Mbytes/processor
- *CPU speed, ….*
  1,3GHz/processor
- *computation time*
  CPU time/proc=600s

7- Discussion

There are no difficulties to set up the simulation and to obtain results. However, the drawing of this structure is not easy and is time consuming (no GUI).
Usually, a size step lower than $\lambda_{min}/20$ and at least 3 size steps for modelling the finest details are required in TLM simulations to obtain reliable results. For this antenna, zero thickness perfect metallic part was considered and the smallest rectangular hole in the patch was modelled using $3\Delta x.3\Delta z$. Then, the entire computational domain was modelled using $123\Delta x.23\Delta y.115\Delta z$.

We observe a good agreement between simulation and measurements for the radiation pattern. The VSWR results are slightly different (shift in frequency of 2.4% for the classical patch and 3.9% for the GA optimized antenna).

8- Additional comments

FP-TLM software is based on the HSCN (Hybrid Symmetrical Condensed Node) implementation. Comparatively to the classical SCN, the HSCN allows the time step to be independent of the ratio between the maximum and minimum size step of the non uniform mesh. This leads to lower time step and shorter time simulation. In counterpart, HSCN exhibits more dispersion error. Then, I have also performed the same simulations with a version of FP-TLM software including the SCN. As expected, the VSWR results obtained are more accurate than those given above (shift in frequency of 1.2% for the classical patch). However, the CPU time is increased by a factor 6.

6- SIMULATION RESULTS

From KUL

1- Entity

Katholieke Universiteit Leuven (KUL)
ESAT-TELEMIC
B-3001, Leuven
Belgium

Contact persons

Guy Vandenbosch
Phone +32 16 321110
Fax +32 16 321986
E-mail guy.vandenbosch@esat.kuleuven.ac.be

Vladimir Volski
Phone +32 16 321874
Email vladimir.volski@esat.kuleuven.ac.be

2- Name of the simulation tool

MAGMAS (**M**odel for the **A**nalysis of **G**eneral **M**ultilayered **A**ntenna **S**tructures).

3- Generalities about the simulation tool

MAGMAS is a software framework developed for the analysis of general planar structures. MAGMAS uses the method of moments to solve integral equations.

4- **Simulation Set-up (Geometry set-up, GUI, mesh, boundary conditions, excitation)**

The geometry is defined using the GUI of the software.

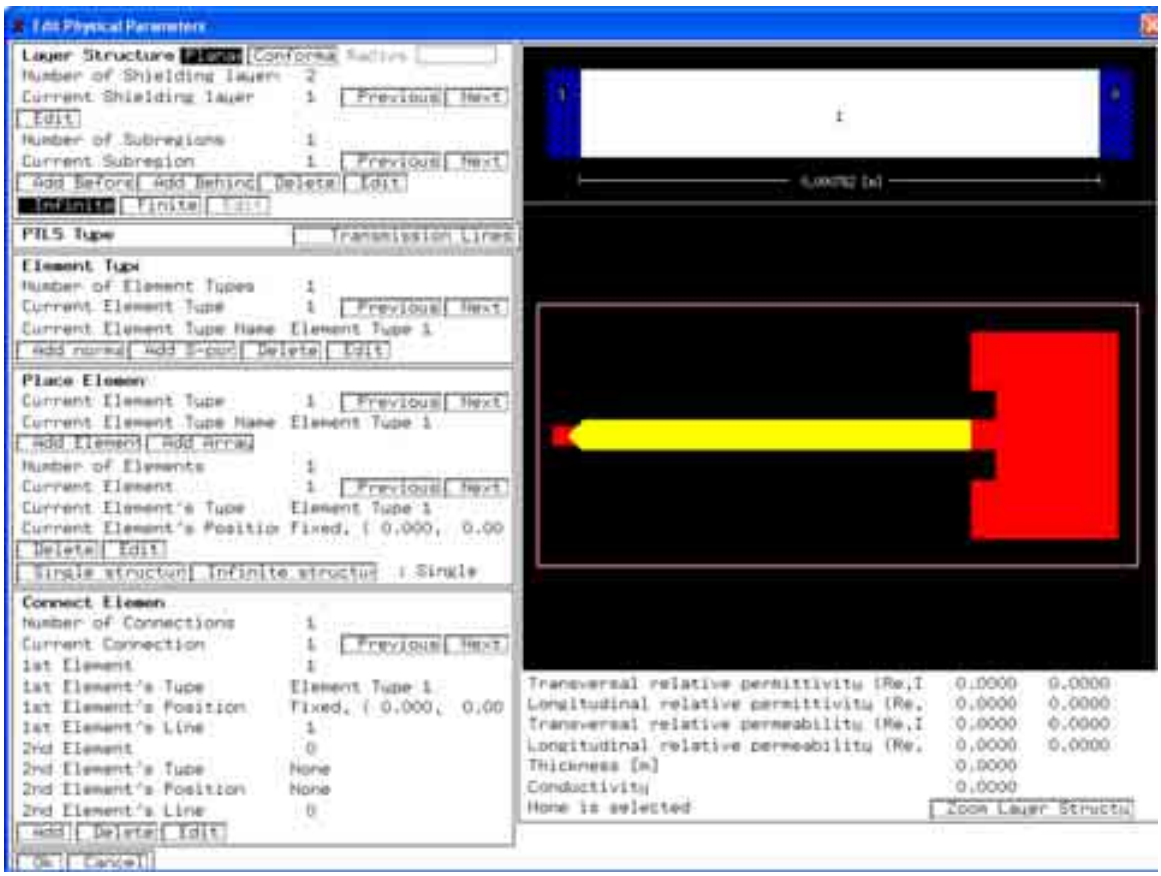

Fig. 9 Snapshot of the classical patch antenna geometry inside the MAGMAS GUI.

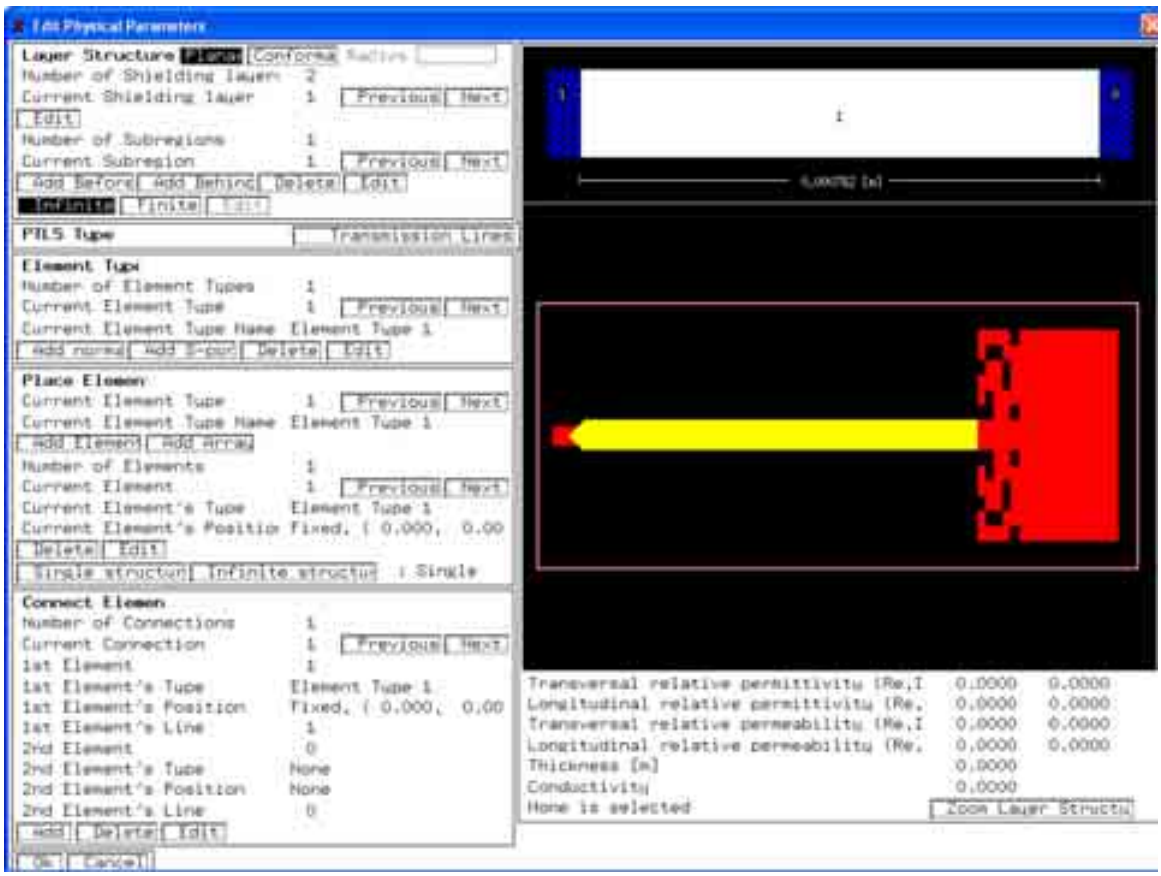

Fig. 10 Snapshot of the GA optimized patch antenna geometry inside the MAGMAS GUI.

5- Simulation results

The results that have been computed are:

- Input port parameters (VSWR)
- Radiation patterns in both E and H planes for finite and infinite ground planes.

Computed radiation patterns for the patches on the infinite ground plane are plotted in Fig. 5, 6, 9, 10 and patterns for the patches on a finite ground plane are plotted in Fig. 7, 8, 11, 12.

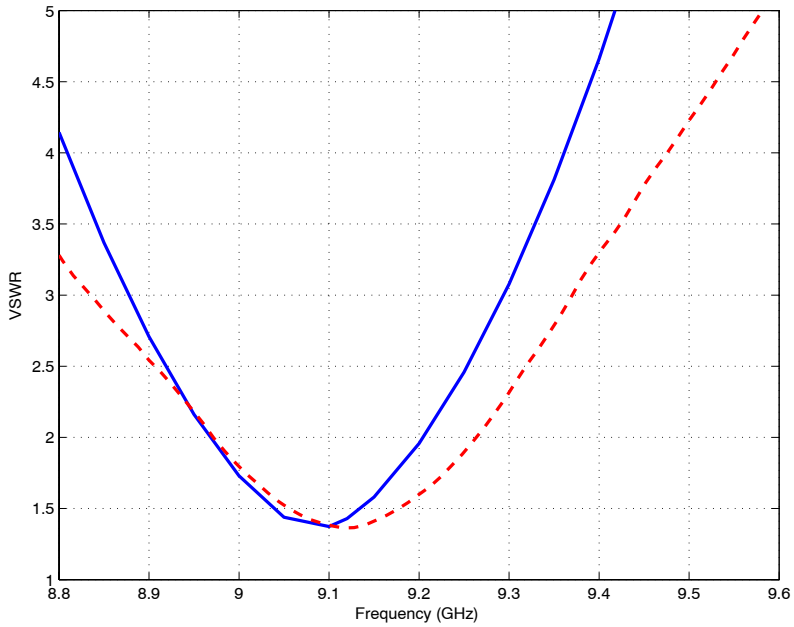

Fig. 11 VSWR versus frequency for the Classical Patch antenna.
Blue: simulation results, red: measurements.

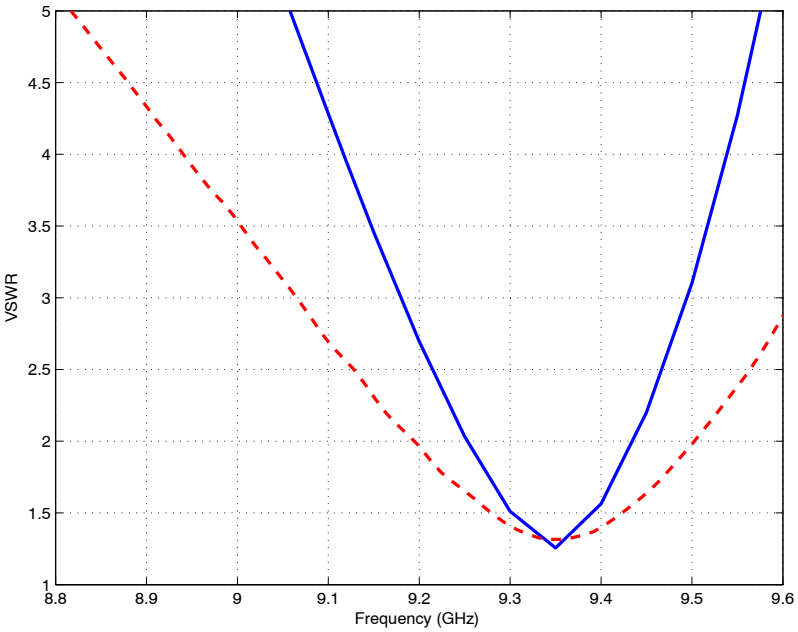

Fig. 12 VSWR versus frequency for the GA optimized patch antenna.
Blue: simulation results, red: measurements.

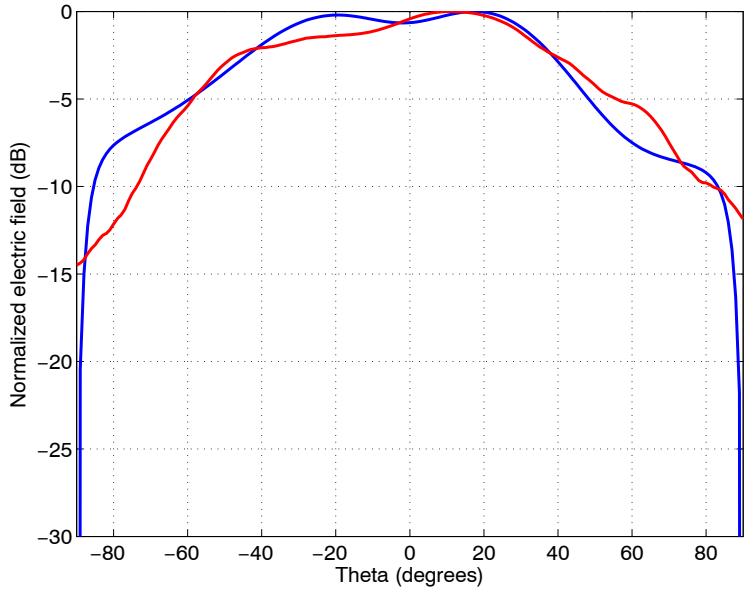

Fig. 13 E-plane radiation pattern versus theta for the Classical Patch antenna (infinite ground plane, f=9.12 GHz).
Blue: simulation results, red: measurements.

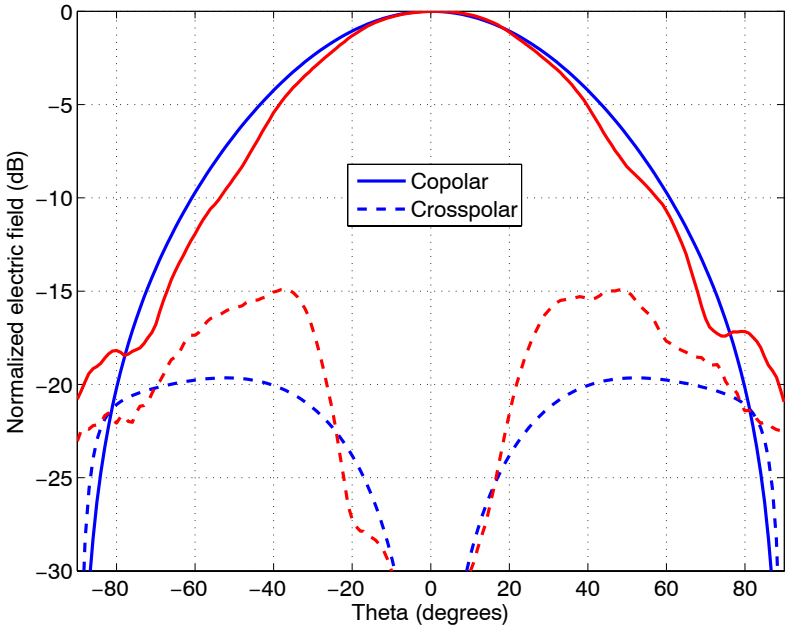

Fig. 14 H-plane radiation pattern versus theta for the Classical Patch antenna (infinite ground plane, f=9.12 GHz).
Blue: simulation results, red: measurements.

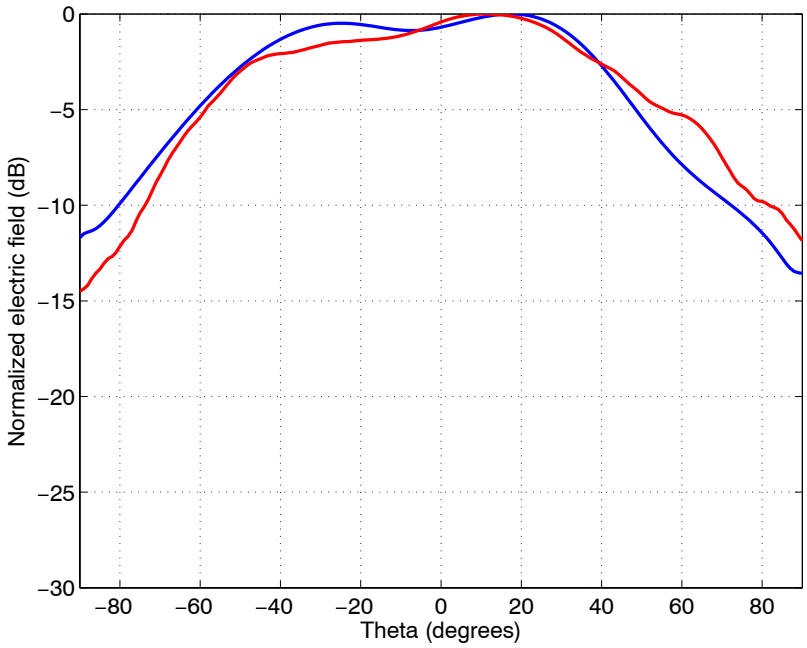

Fig. 7 E-plane radiation pattern versus theta for the Classical Patch antenna (finite ground plane, f=9.12 GHz).
Blue: simulation results, red: measurements.

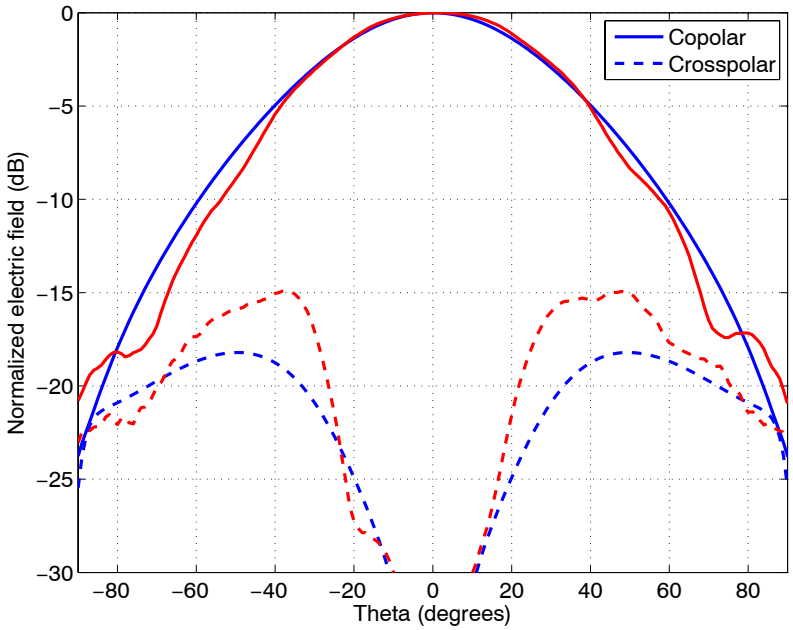

Fig. 8 H-plane radiation pattern versus theta for the Classical Patch antenna (finite ground plane, f=9.12 GHz).
Blue: simulation results, red: measurements.

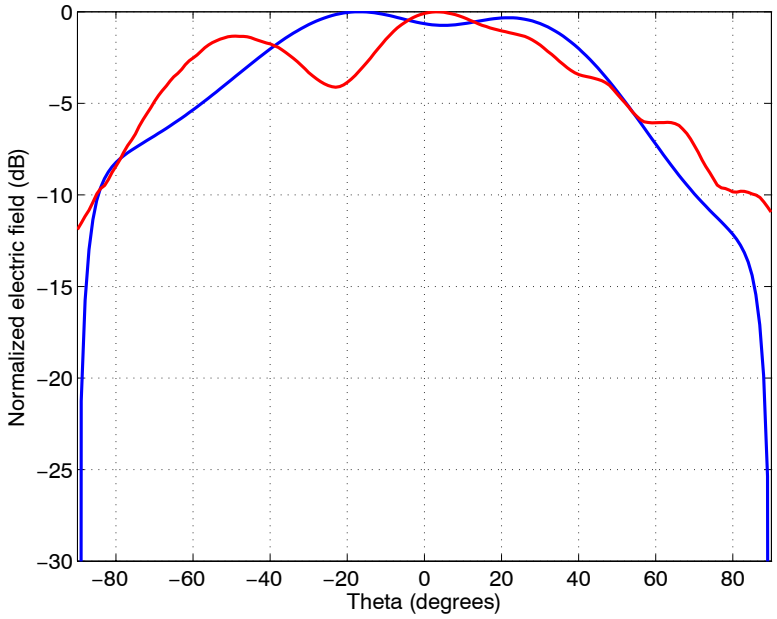

Fig. 9 E-plane radiation pattern versus theta for the GA optimized antenna (infinite ground plane *f*=9.35 GHz).
Blue: simulation results, red: measurements.

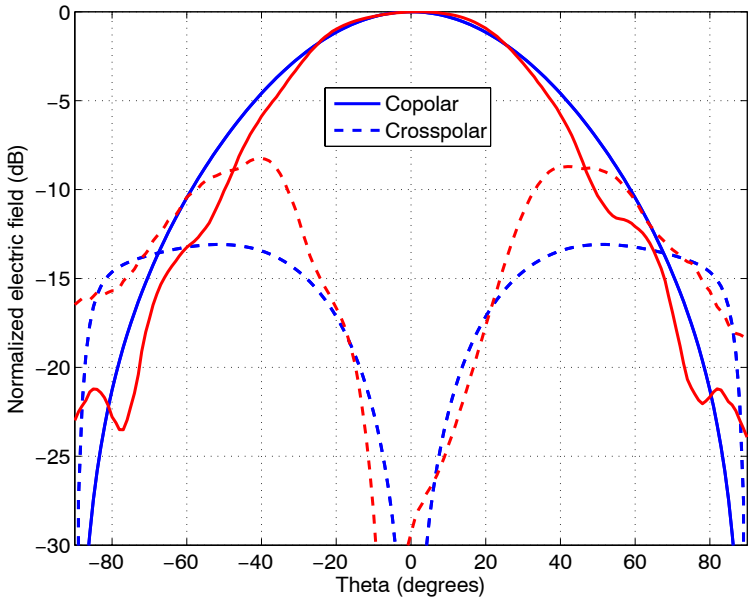

Fig. 10 H-plane radiation pattern versus theta for the GA optimized antenna (infinite ground plane, *f*=9.35 GHz).
Blue: simulation results, red: measurements.

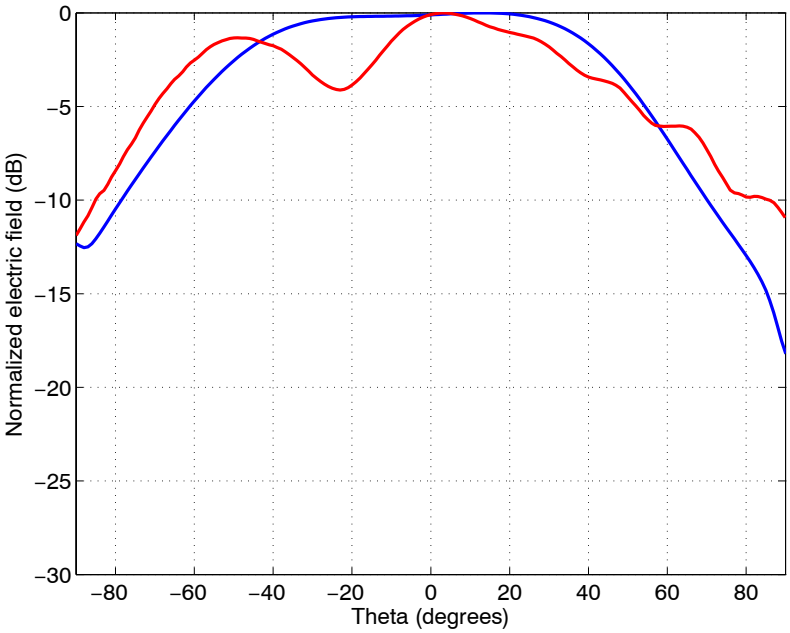

Fig. 11 E-plane radiation pattern versus theta for the GA optimized antenna (finite ground plane, *f*=9.35 GHz).
Blue: simulation results, red: measurements.

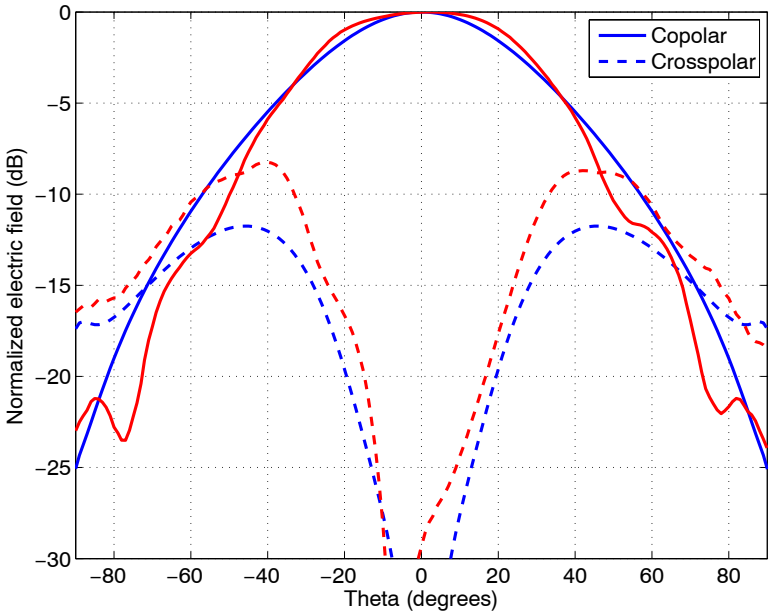

Fig. 12 H-plane radiation pattern versus theta for the GA optimized antenna (finite ground plane, *f*=9.35 GHz).
Blue: simulation results, red: measurements.

6- Computation resources

Table 3 Properties of the WorkStation used for the simulation

Type of machine	HP 9000/785/J6000

Number of CPUs	2
CPU Speed	552 MHz
RAM	2 GB
OS	HP_UX 11.00A

7- Discussion

The finiteness of a ground plane is taken into account using the physical optics method [1].

[1] V. Volski and G.A.E. Vandenbosch, "Efficient physical optics approximation for the calculation of radiation patterns of planar antennas located on a finite ground plane", IEEE AP, 53 (1): 460-465 Part 2, JAN 2005

8- Additional comments

None

7- SIMULATION RESULTS

From LIVUNI

1- Entity

Department of Electrical Engineering and Electronics
The University of Liverpool
Liverpool, L69 3GJ
United Kingdom

Contact person

Greepol Niyomjan
E-mail: G.Niyomjan@liverpool.ac.uk

2- Name of the simulation tool

Ansoft™ HFSS™ version 9 [1]

3- Generalities about the simulation tool

HFSS (High Frequency Structure Simulator) is a full-wave electromagnetic (EM) field simulator for arbitrary 2D and 3D passive device modelling. It integrates simulation, visualization, solid modelling, and automation in an easy-to-use environment where solutions to the 3D EM problems are quickly and accurately obtained. HFSS employs the Finite Element Method (FEM), adaptive meshing, and brilliant graphics to all of the 3D EM problems. Ansoft HFSS can be used to calculate parameters such as S-Parameters, Resonant Frequency, and Fields.

4- Simulation Set-up (Geometry set-up, GUI, mesh, boundary conditions, excitation)

The geometry of antenna was created by using the 3D Modeller of HFSS. The mesh is in the form of tetrahedral except at the excitation port where the mesh is in the form of triangle. Adaptive meshing was used to make sure that changes of fields in any areas of the antenna structure were covered. HFSS reduces the mesh size at the critical areas after each simulation. The adaptive growth is controlled by refinement. The adaptive process repeats until the difference between S-parameters of two consecutive passes is less than a specific value, Max delta S (for example 0.01). The adaptive process is terminated when the delta S is achieved its target value or the number of requested passes is reached (30 passes in our case). GUI is similar to the GUI of Microsoft Windows which is easy to use. The analysis is performed in the frequency domain. A discrete frequency sweep has been used to simulate this structure. (Step size equals to 0.01 GHz). For our simulation, an air box was used for the radiation boundary. Lumped port (50 ohms) was used to excite at the edge of the main microstrip line feed. Estimated time to completely set up both of these antenna structures was about 3 hours. Geometry of antenna structures for both conventional and GA optimized are illustrated in Figure 1.

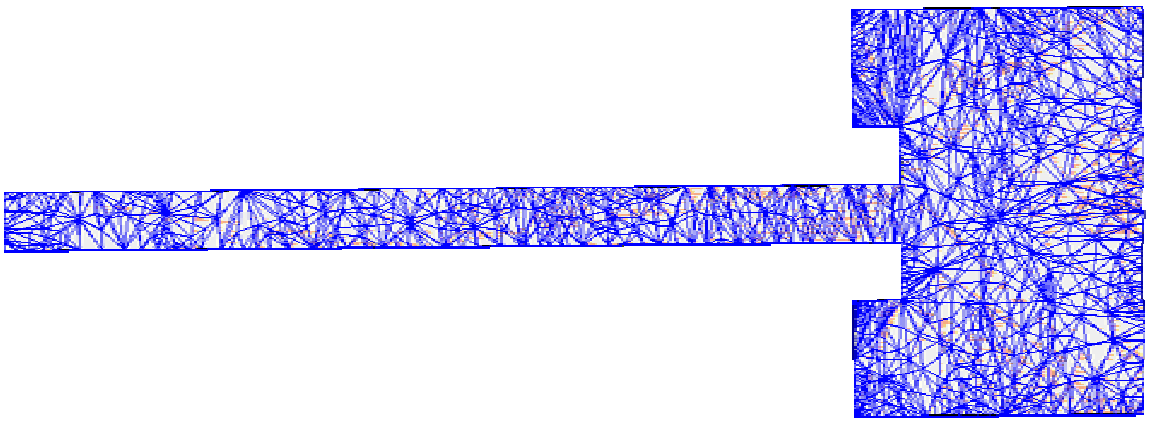

Figure 15a: Snapshot of the conventional patch geometry from Ansoft HFSS.

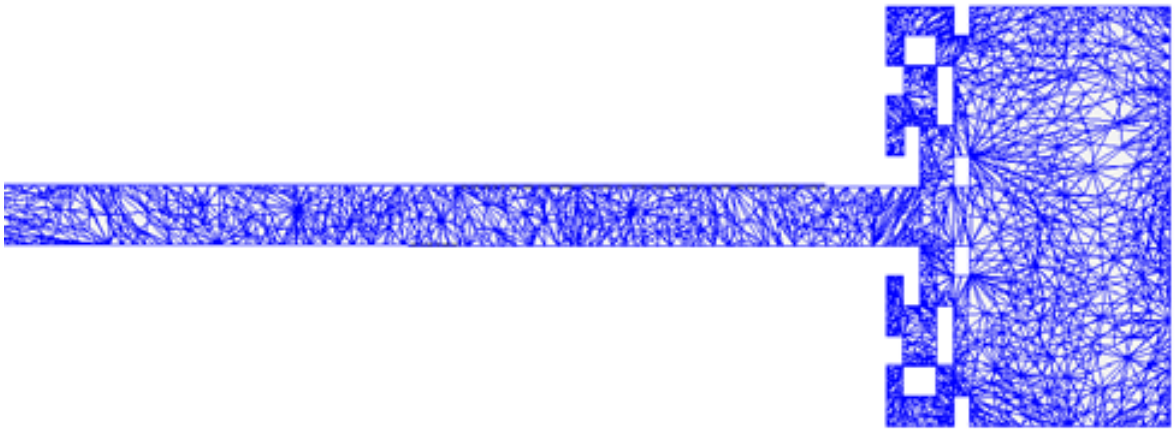

Figure 16b: Snapshot of the GA Optimized patch geometry from Ansoft HFSS.

Figure 1:Snapshot of conventional patch and GA Optimized patch antennas.

5- Simulation results

The results that have been computed are:

- Voltage Standing Wave Ratio (VSWR)
- Radiation Patterns (Normalized E field)

Values of VSWR at the input port for both structures are plotted as shown in Figures 2-3. Values of Normalized Electric field in dB are plotted against the theta angles from -90 to 90 degree as shown in Figures 4 – 7.

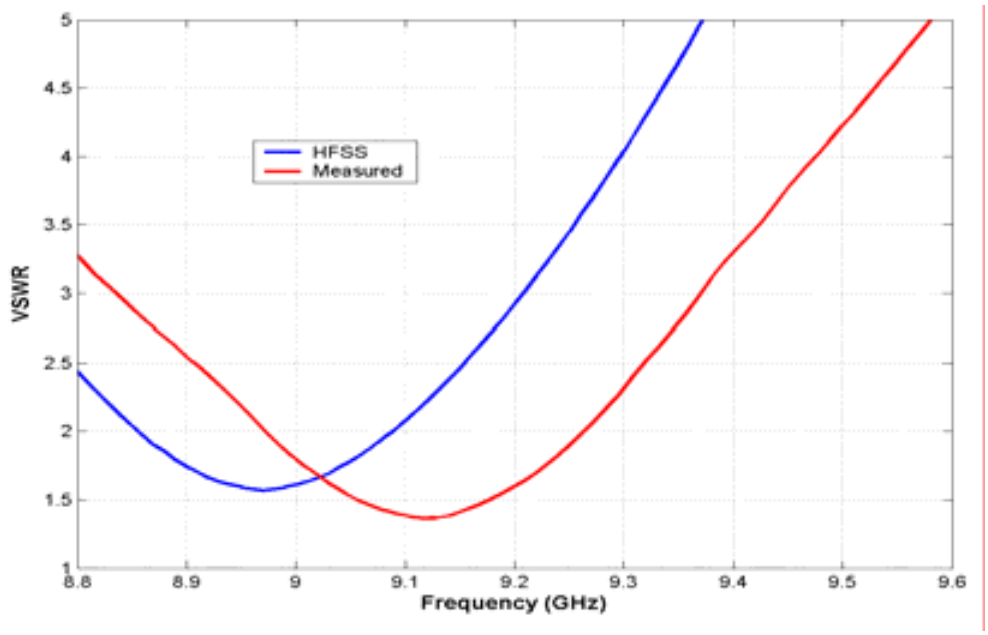

Figure 2: VSWR versus frequency for Conventional Patch in frequency range 8.8-9.6 GHz.

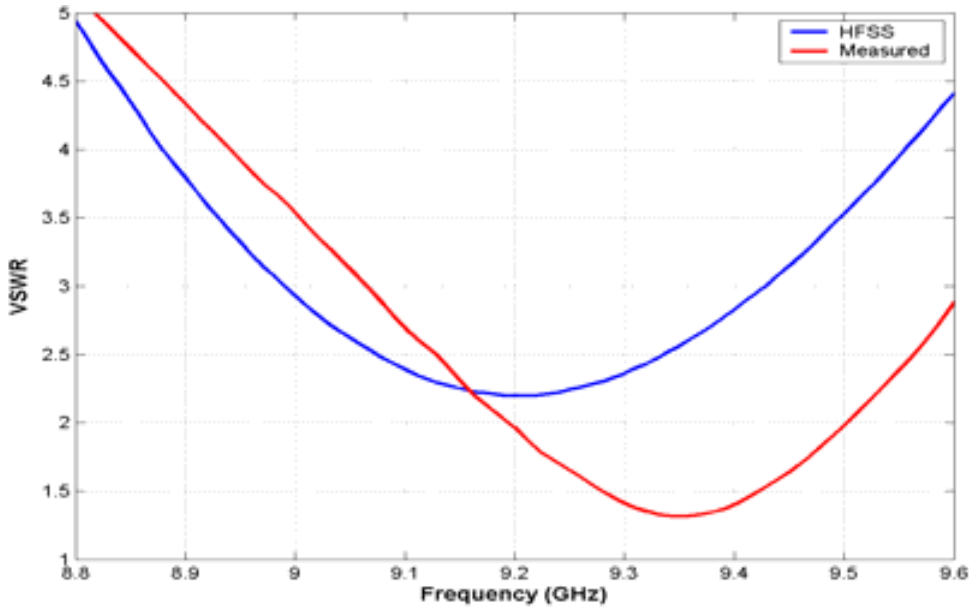

Figure 3: VSWR versus frequency for GA Optimized Patch in frequency range 8.8-9.6 GHz.

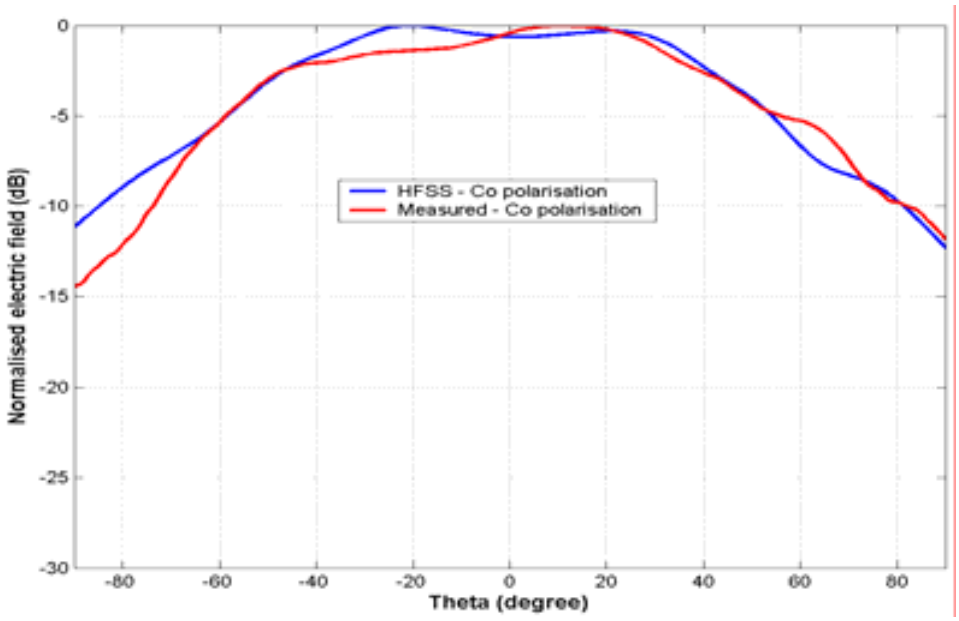

Figure 4: E-field pattern in the E-plane (φ = 0°) for Conventional Patch, computed at the frequency f = 9.12 GHz.

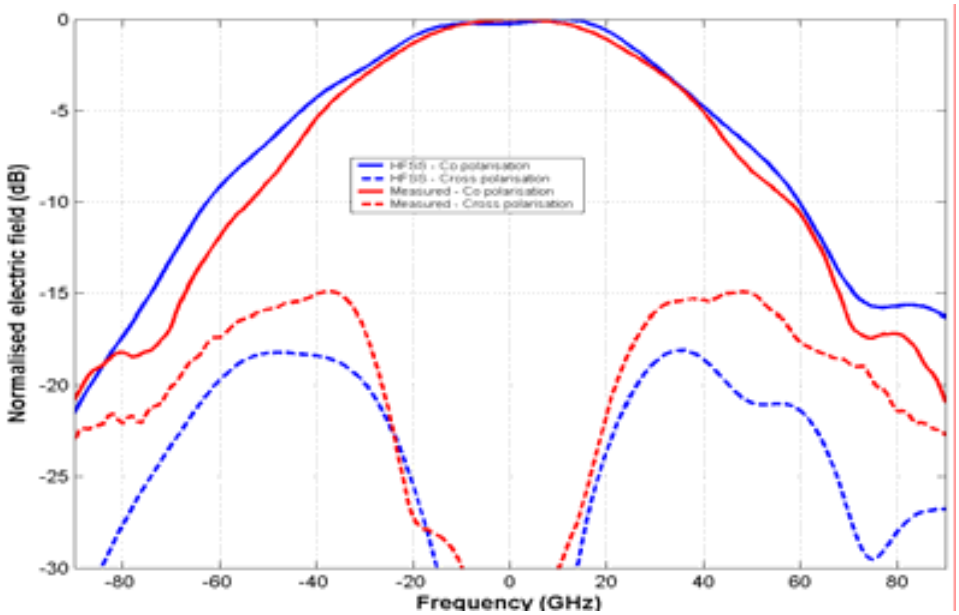

Figure 5: E-field patterns for in the H-plane (φ = 90°) for Conventional Patch, computed at the frequency f = 9.12 GHz.

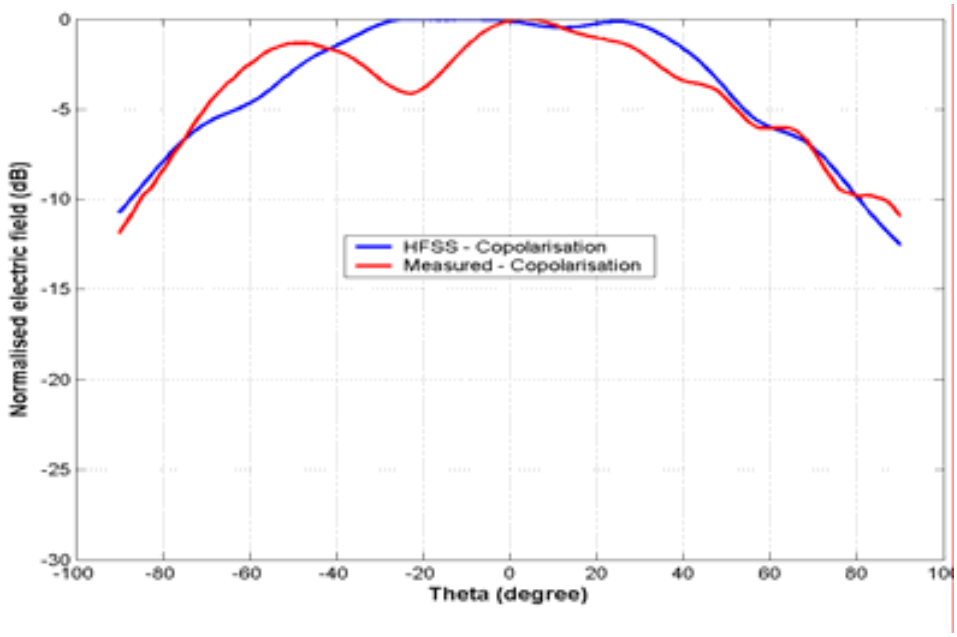

Figure 6: E-field patterns for in the E-plane (φ = 0°) for GA Optimized Patch, computed at the frequency f = 9.35 GHz.

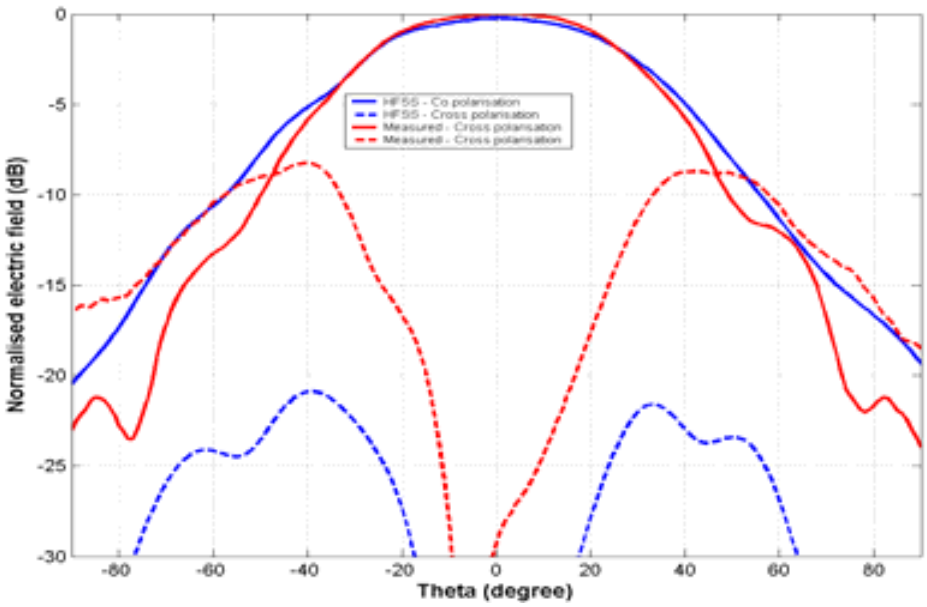

Figure 7: E-field patterns for in the H-plane (φ = 90°) for GA Optimized Patch, computed at the frequency f = 9.35 GHz.

6- Computation resources

PC desktop with specifications shown in Table 1 was used to simulate the Conventional and GA optimized patch antennas. The total times spent on these simulations are shown in Table 2.

Table 1: Specification of the desktop used for HFSS simulation

Type of machine	Desktop PC
Number of CPUs	1 Intel Pentium 4
CPU Speed	2.4 GHz
RAM	512 MB
OS	Win XP Home Sp2

Table 2: Simulation time for HFSS

Total real time	Conventional Patch	17 hrs, 52 mins, 11 secs
	GA Optimized Patch	17 hrs, 24 mins, 47 secs
Total CPU time	Conventional Patch	8 hrs, 48 mins, 56 secs
	GA Optimized Patch	2 hrs, 20 mins, 45 secs

7- Discussion

The results of VSWR and Normalized E-field patterns for conventional patch obtained from HFSS are comparable to the VSWR and Normalized E-field patterns obtained from measurement [2]. VSWR for GA Optimized patch obtained from HFSS shows good agreement with measured VSWR for GA optimized patch except at frequency range higher than 9.2 GHz. This is due to the effect of the two additional rectangular thin copper layers that were added in to the patch layer in order to overcome the non manifold edges problem seen by ACIS kernel of 3D modeler of HFSS. This effect becomes more imminent as the frequency gets higher. Nevertheless the Normalized E-field radiation patterns for GA Optimized patch antenna obtained from HFSS show close agreement with the measured Normalized E-field radiation patterns obtained from measurement. However the value of cross polarized pattern for GA optimization patch obtained from HFSS is observed to be lower than the measured cross polarized pattern. This might be due to the radiation effect from the feed connector added to the resulted radiation pattern of the actual antenna structure. Normalized E-field radiation patterns obtained from HFSS are not symmetric due to the way HFSS generates the size and number of mesh to cover the whole antenna structure as shown in Figures 1a – 1b. These processes are done randomly. From the simulation time in table 2, it is obvious to see that HFSS is an accurate but time consuming simulation tool.

Reference:

[1] http://www.ansoft.com.

[2] Institut National des Sciences Appliquées de Rennes (IETR).

8- SIMULATION RESULTS

From UOB

1- Entity

Computational Electromagnetics Group, Centre for Communications Research,
Department of Electrical & Electronic Engineering, Merchant Venturers Building,
Woodland Road, University of Bristol (UOB), Bristol BS8 1UB, United Kingdom

Dominique Lynda Paul
Tel. +44 117 954 51 23
email: d.l.paul@bristol.ac.uk

2- Name of the simulation tool

FDTD32

3- Generalities about the simulation tool

FDTD32 is an in-house 3D full-wave solver based on the Finite-Difference Time-Domain (FDTD) method. In this simulation, perfect metal conductors and lossless dielectric substrates were considered. The ground plane was modelled as infinite. MAMPS correction factors [1] were applied in order to take account of field singularities near the edges of the patch. However, this technique is valid for an edge (classical patch) but not really for the small holes of the GA optimized patch antenna.

4- Simulation Set-up (Geometry set-up, GUI, mesh, boundary conditions, excitation)

The geometry was specified using our GUI Gema as displayed in Figures 1 to 3 and a dense graded mesh was created manually. A 4-cells PML layer was employed to terminate the FDTD box and simulate an open structure. A raised cosine waveform of width 120ps was applied to the microstrip feed.

Two different meshes were utilised for the simulations: for the radiation patterns, the graded meshes of Figures 1-3 were utilized for both antennas. However, for the VSWR results, which tend to be more sensitive, the dense mesh (cells sizes of 0.1mm) was maintained throughout the whole FDTD space. The size of the computational volumes was 709x40x462 cells for the dense uniform mesh and 181x25x226 cells for the graded

mesh. A transient response of 3,000ps was required to allow the fields to decay in the feedline.

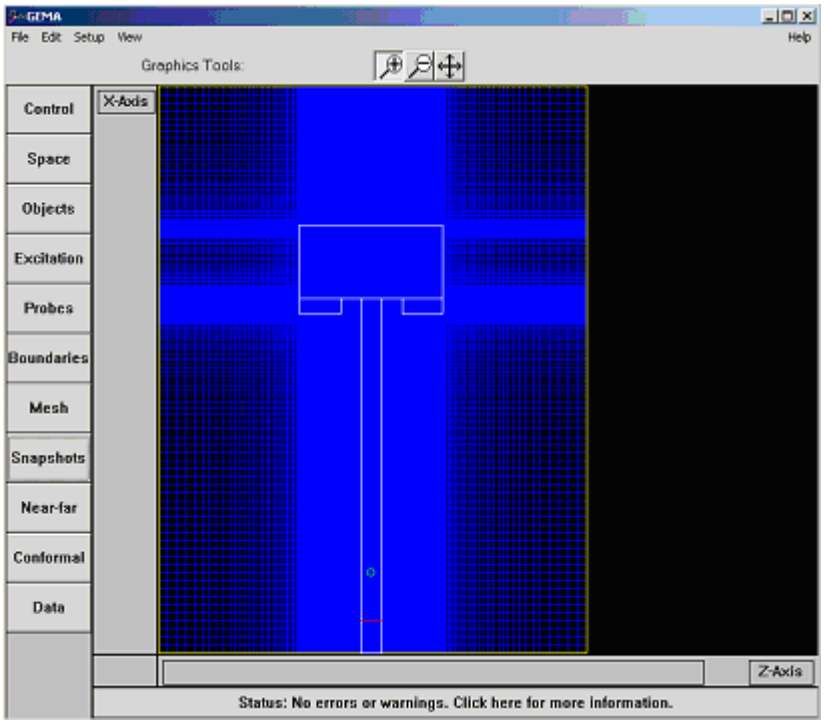

Figure 1. Classical Patch antenna model in Gema GUI

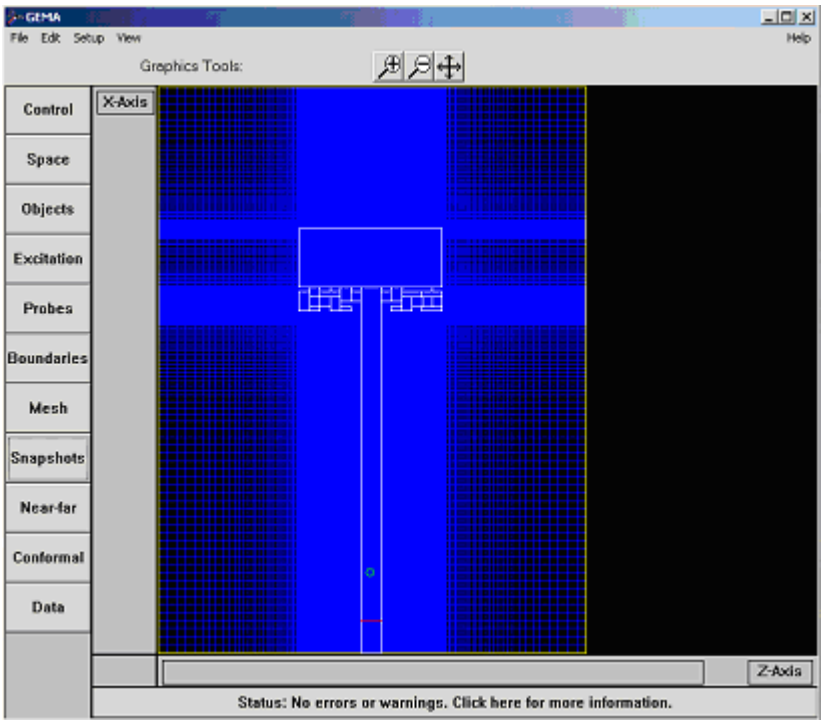

Figure 2. GA optimized antenna model in Gema GUI

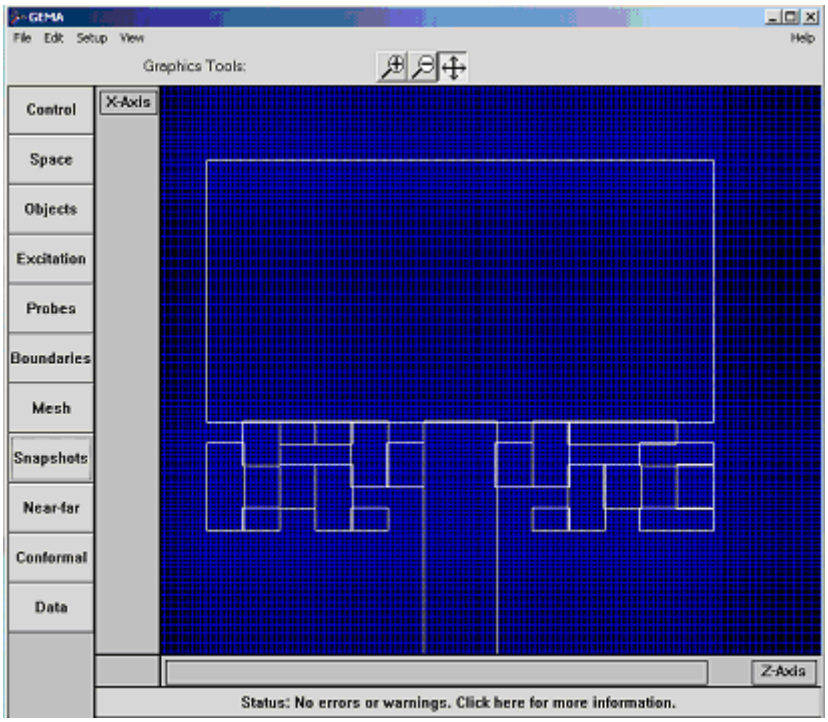

Figure 3. Zoom of Figure 2 to show the mesh density used for the model

5- Simulated and measured results

- **VSWR results.**

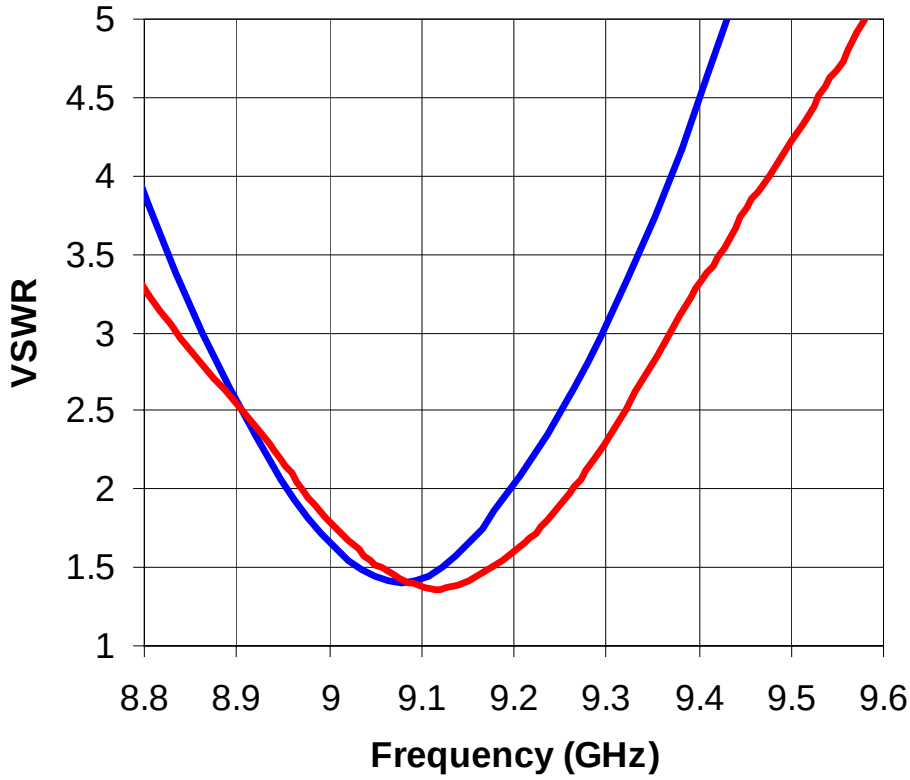

Figure 4: VSWR versus frequency for the Classical Patch antenna

Measured VSWR **Simulated VSWR**

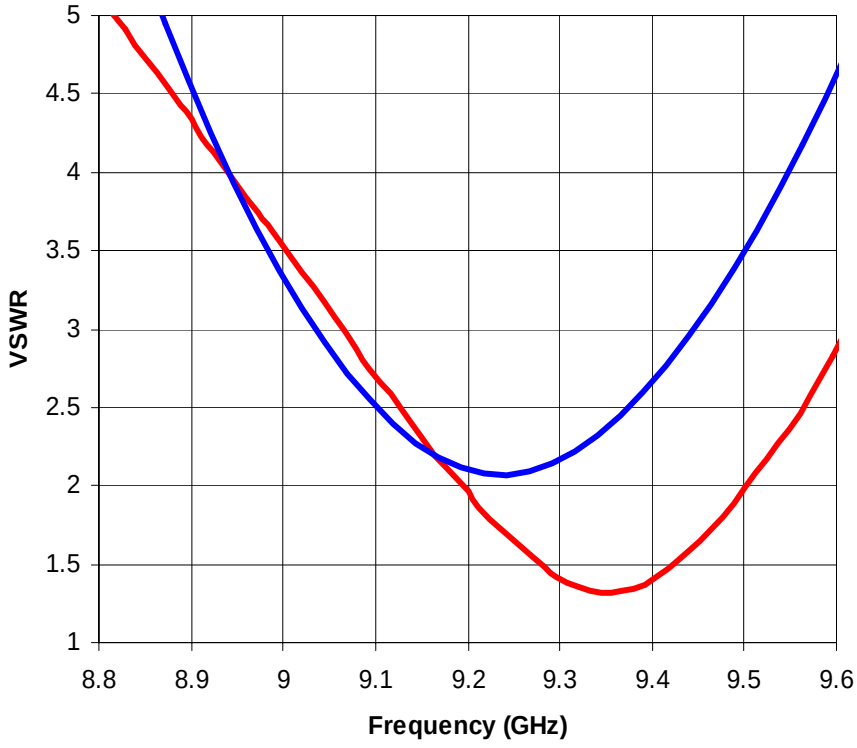

Figure 5: VSWR versus frequency for the GA optimized antenna

Measured VSWR **Simulated VSWR**

● **Far-field radiation patterns.**

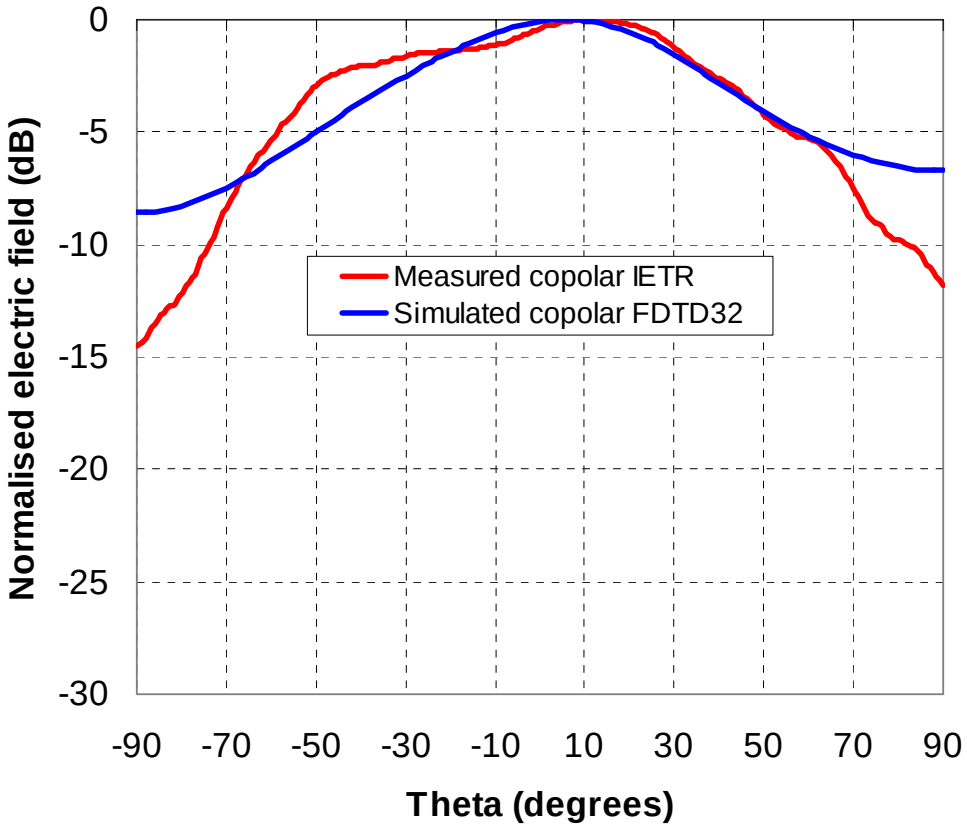

Figure 6: E-plane radiation pattern versus theta for the Classical patch antenna (F=9.12GHz)

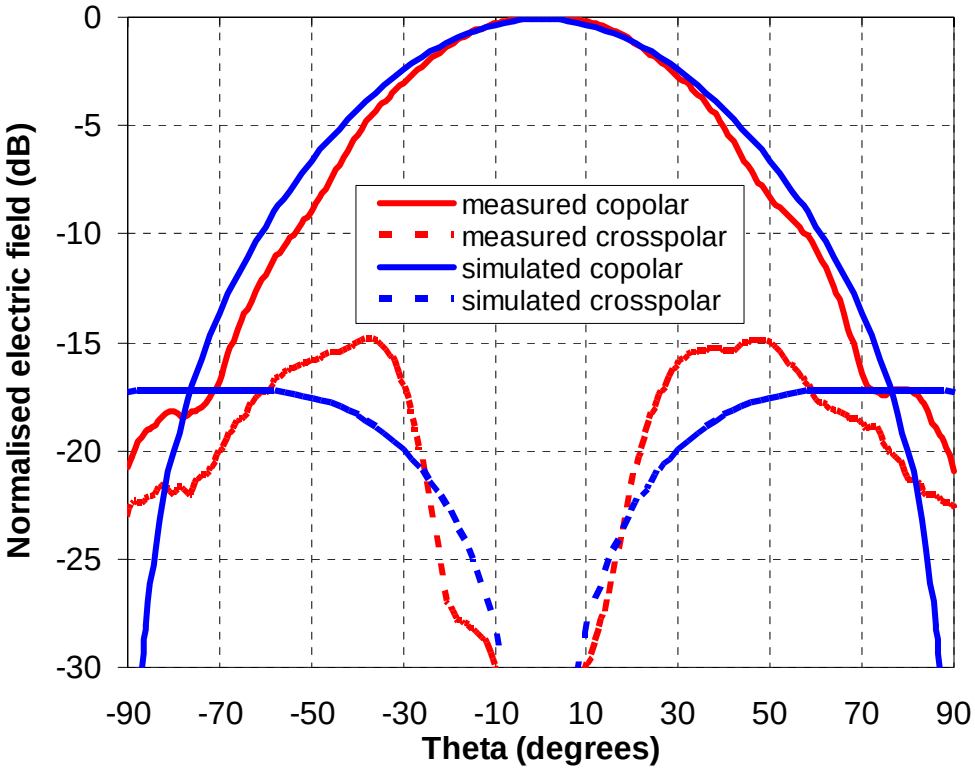

Figure 7: H-plane radiation pattern versus theta for the Classical patch antenna (F=9.12GHz)

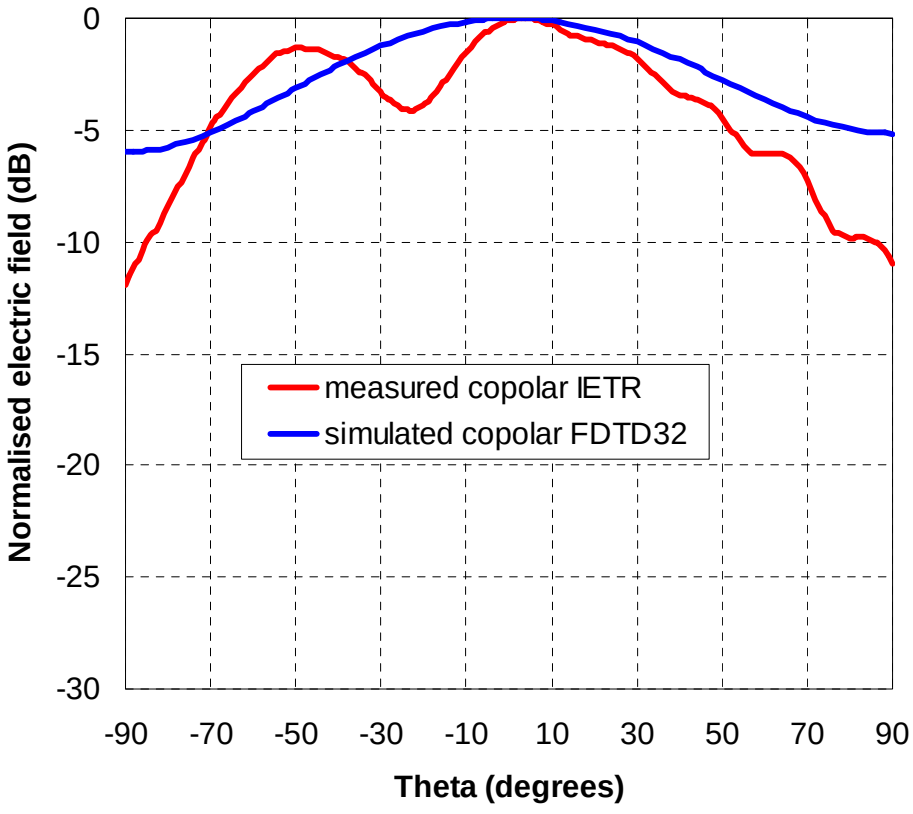

Figure 8: E-plane radiation pattern versus theta for the GA Optimized patch antenna (F=9.35GHz)

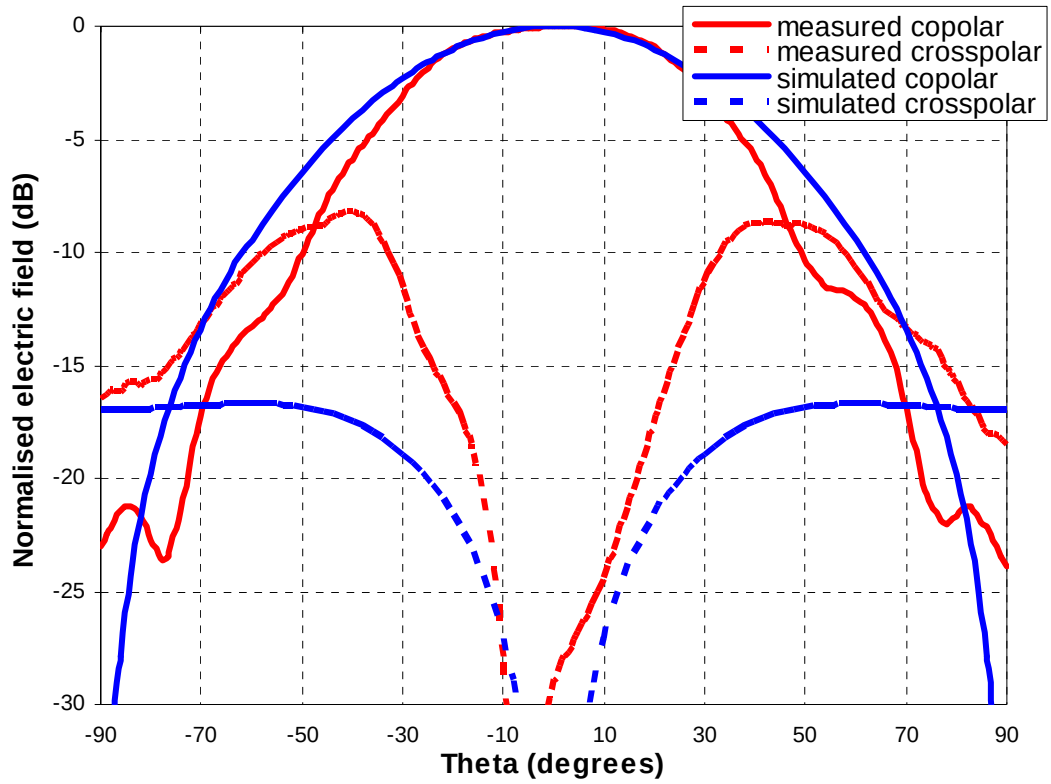

Figure 9: H-plane radiation pattern versus theta for the GA Optimized patch antenna (F=9.35GHz)

6- Computation resources

The simulation was performed on a Viglen PC (3.2GHz, 2 GBytes RAM available). The simulation time was about 12 hours with 806 Mbytes RAM for the dense uniform mesh (VSWR) and less than 2 hours with 190 Mbytes RAM for the graded mesh (radiation patterns).

7- Discussion

As shown in Figure 4, there is a good agreement between measured and simulated VSWR results for the patch antenna, the resonant frequency found by simulation being only 0.6% lower than the one obtained by measurements. The match levels are very similar at resonance but the simulation tends to produce a slightly narrower bandwidth. Many more uniform coarser meshes were actually tried for this antenna but all failed to achieve this accuracy as the response was always underestimated and it was only by using this level of mesh refinement together with the application of MAMPs that this agreement was achieved. I

would not say that it is a converged result yet but it was not possible to densify the mesh even further because of the large computing requirements.

Figure 5 shows the VSWR results for the GA optimized patch. The simulated response is shifted up compared to the one for the patch antenna. However it is slightly lower in frequency compared to measurements. Also the match is not as good.

In terms of radiation patterns, the E-plane characteristic for the patch antenna is shown in Figure 6 and the H-plane in Figure 7. In the E-plane, we obtain a much smoother curve than the wobbly curve obtained by measurements. Also, like in the measured data, it is a bit asymmetrical. Differences occur at endfire due to the fact that our ground plane is infinite. In the H-plane, the agreement is quite good except again at endfire for the same reason. The cross-polar level is lower by a few dBs but has about the same shape, the place of the trough in particular being very well predicted.

For the GA optimized patch, the E- and H-plane radiations patterns are displayed in Figures 8 and 9 respectively. Basically the same conclusions as for the patch antenna can be drawn. The cross-polar in the H-plane however only increases marginally compared to the patch (only a few dBs) and we do not observe as much an increase as in the measurements.

Overall, these results are rather satisfactory. This technique is well suited for the analysis of a patch antenna. However, due to the very small features involved in the GA optimized patch antenna, the technique is not ideal at all and the results we obtain are almost surprisingly good. A more rigorous treatment of small holes in the FDTD technique to take account of field singularities would be required to improve this result.

8- References:

[1] C.J. Railton, D.L. Paul, I.J. Craddock and G.S. Hilton, “The treatment of Geometrically Small Structures in FDTD by the Modification of Assigned Material Parameters”, submitted for publication in IEEE Antennas and Propagation

9- SIMULATION RESULTS

From UPV

1- Entity

Universidad Politécnica de Valencia
U.P.V.
I.T.E.A.M.
Edificio 8G
Camino de Vera S/N
Valencia 46022
Spain
Tel: 963879585

2- Name of the simulation tool

IE3D

3- Generalities about the simulation tool

IE3D is a full-wave, method-of-moments based electromagnetic simulator solving the current distribution on 3D and multilayer structures of general shape. It has been widely used in the design of MMICs, RFICs, LTCC circuits, microwave/millimeter-wave circuits, IC interconnects and packages, HTS circuits, patch antennas, wire antennas, and other RF/wireless antennas.

4- Simulation Set-up (Geometry set-up, GUI, mesh, boundary conditions, excitation)

The structure has been redrawn using the GUI available is the IE3D software, called MGrid, which allows to introduce this type of planar structures easily. A rectangular uniform meshing is performed automatically by the software in the classic patch antenna, while an adaptive rectangular and triangular meshing was automatically applied in the optimized patch antenna. In both cases, the criterion used was to impose at least 30 cells per wavelength at 10 GHz. This criterion was chosen to provide great accuracy in the simulation, as the computational requirements were still low (790 unknowns for the classic patch antenna and 897 for the GA Optimized antenna) as long as the infinite ground plane approximation is used.

All the simulations have been performed with an infinite dielectric and infinite ground plane. This approximation allows the software to mesh the conductor material only, and therefore the computation requirements are greatly reduced.

The excitation has been performed using the software "Extension ports", which can simulate a 50 Ohm microstrip line as the one used for this structure. Note that this type of excitation may not be exactly the one used during the measurements, where probably a coaxial connector was used, but it would be the one used once this antenna is integrated, and it is the best approach that can be taken.

Once the structure was introduced a frequency domain simulation was performed at 80 frequency points from 8.7 GHz to 9.7 GHz, that is, in the same frequency range used during the measurements. For each frequency point, the S parameters, the current distribution, and the radiation pattern in 37 planes with 215 points per plane were calculated.

Figures 1 and 2 show the snapshot of the classic patch antenna and the optimized patch antenna as introduced in IE3D:

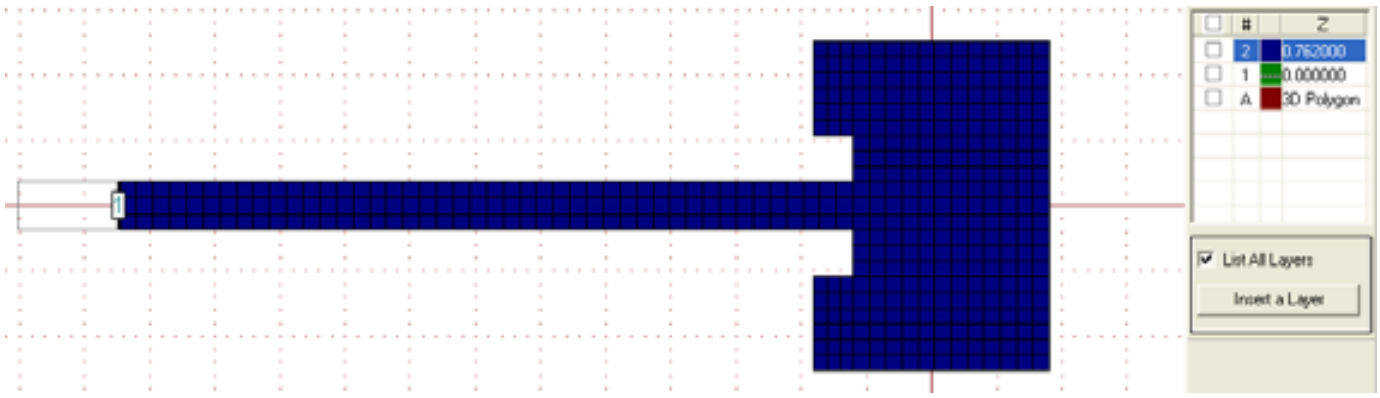

Figure 1 Classic patch antenna

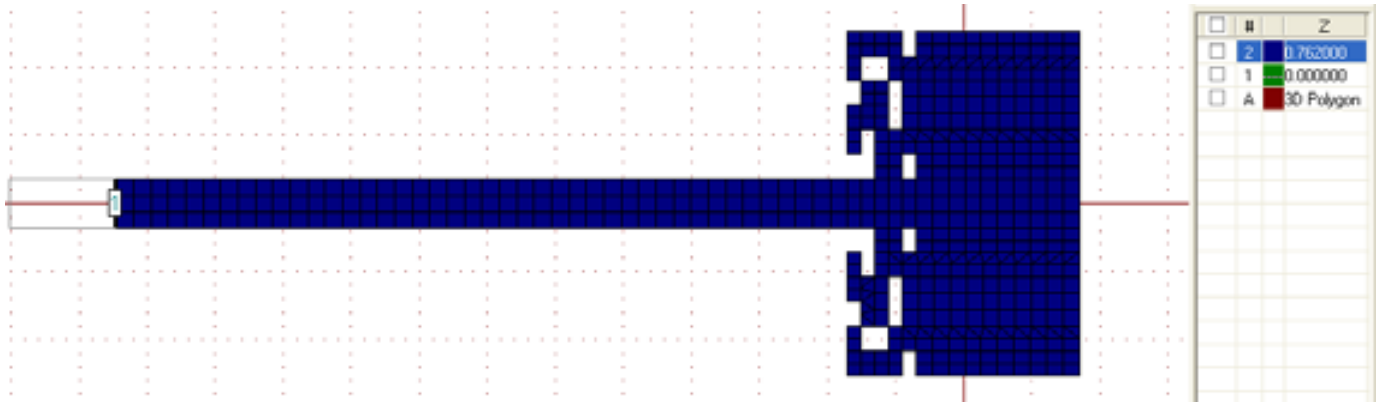

Figure 2 GA Optimized patch antenna

The IE3D GUI (MGrid) is extremely well suited for this type of structures. The classic patch antenna can be introduced in less than 5 minutes, and the simulation setup is immediate. The optimized patch antenna requires a little bit more of previous work, but once all the coordinates of the holes have been calculated, it can be introduced in less than 10 minutes.

5- Simulation results

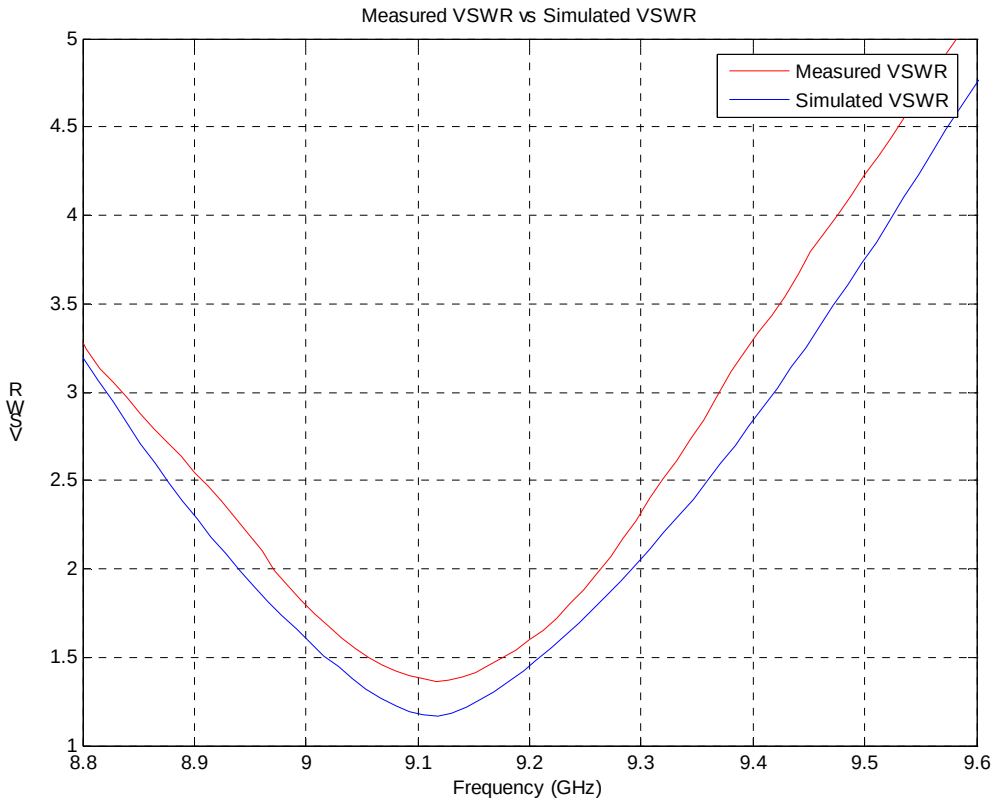

Figure 3 : VSWR versus frequency for the Classical Patch antenna.

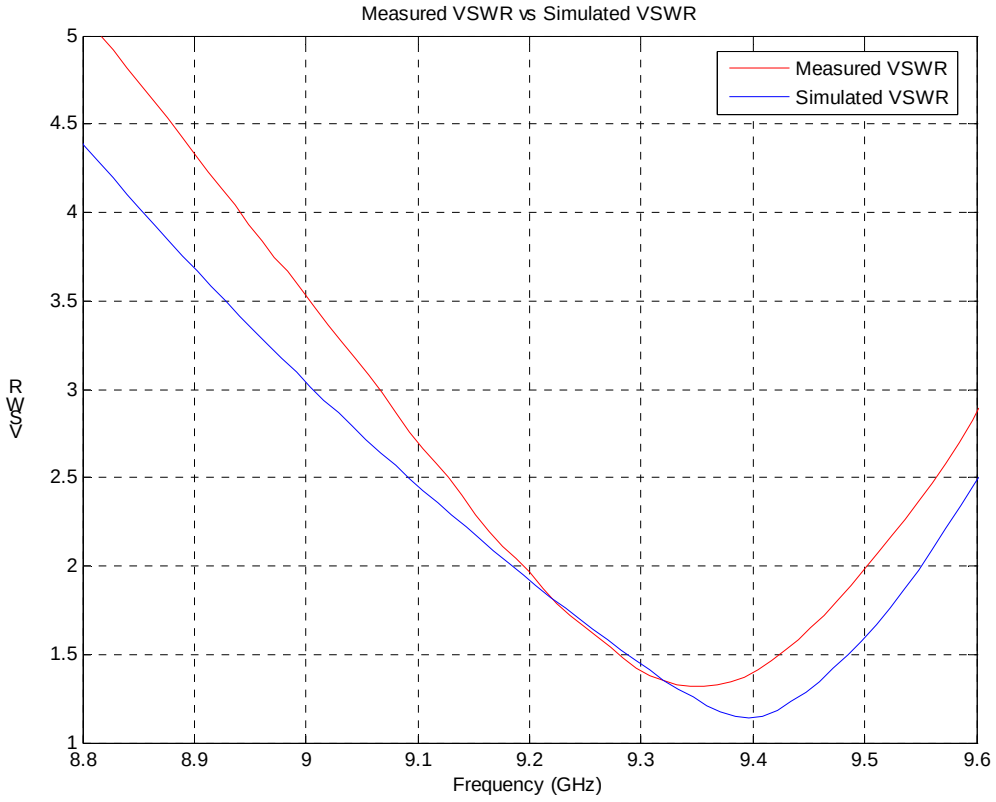

Figure 4 : VSWR versus frequency for the GA optimized antenna.

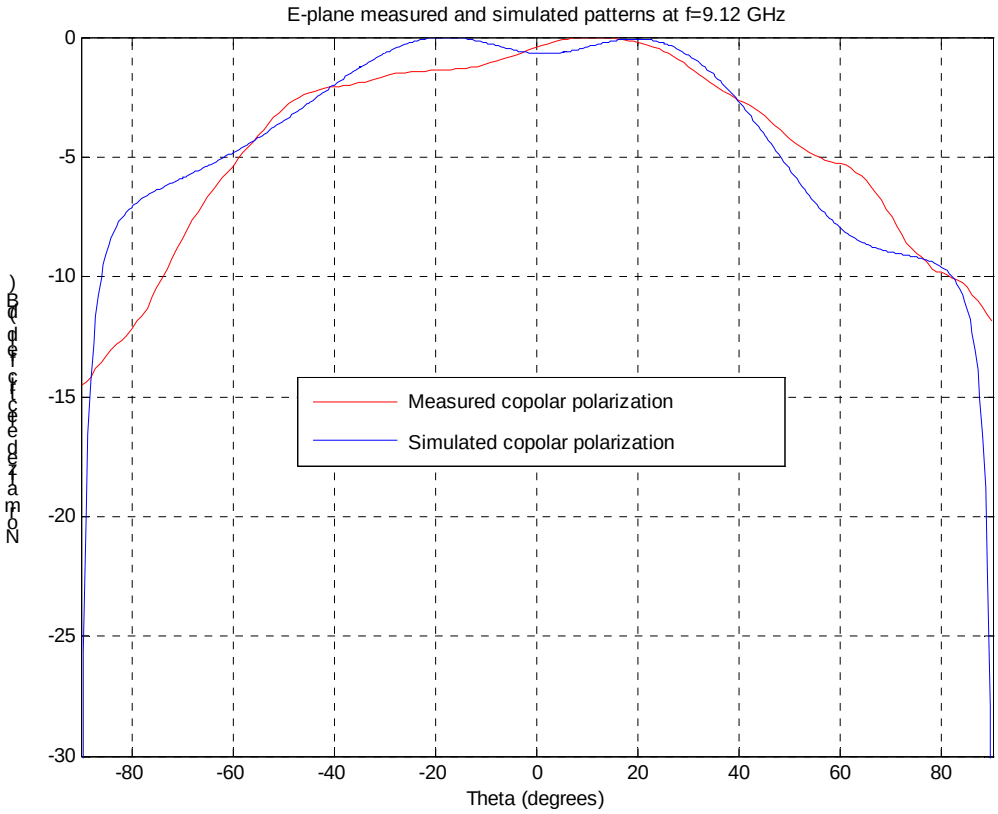

Figure 5 : E-plane radiation pattern versus theta for the Classical Patch antenna (f=9.12 GHz).

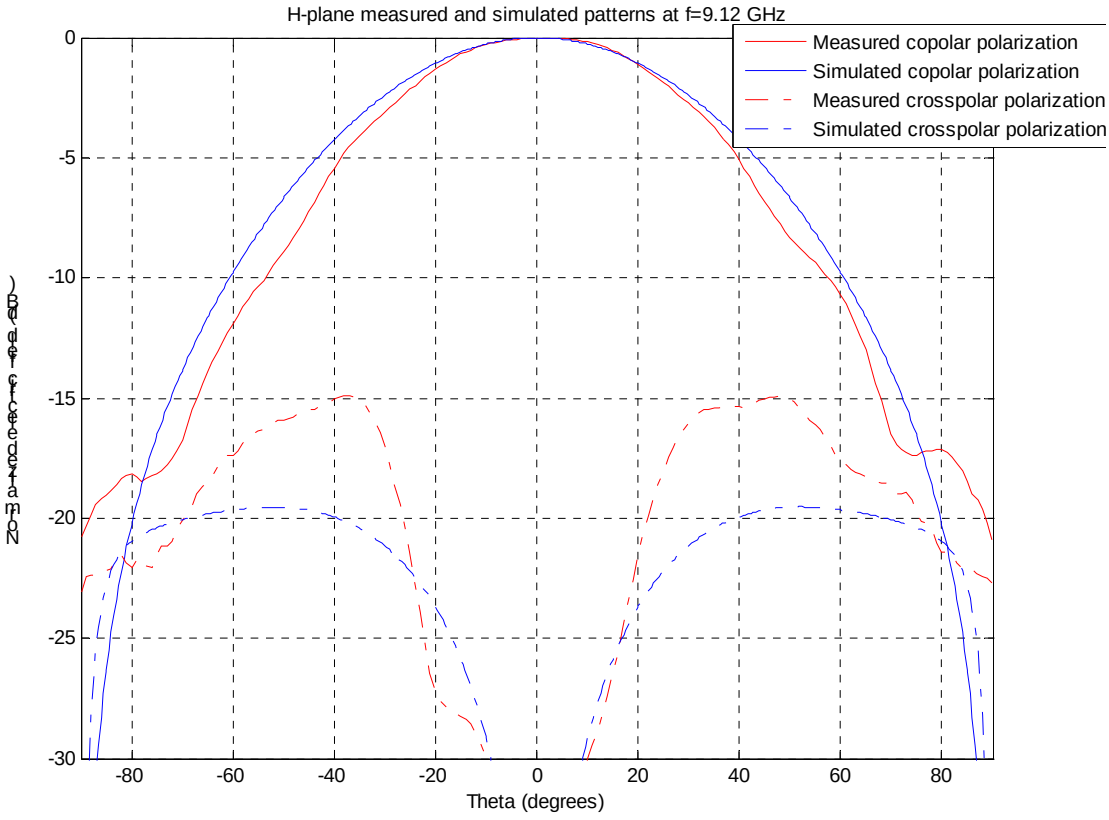

Figure 6 : H-plane radiation pattern versus theta for the Classical Patch antenna (f=9.12 GHz).

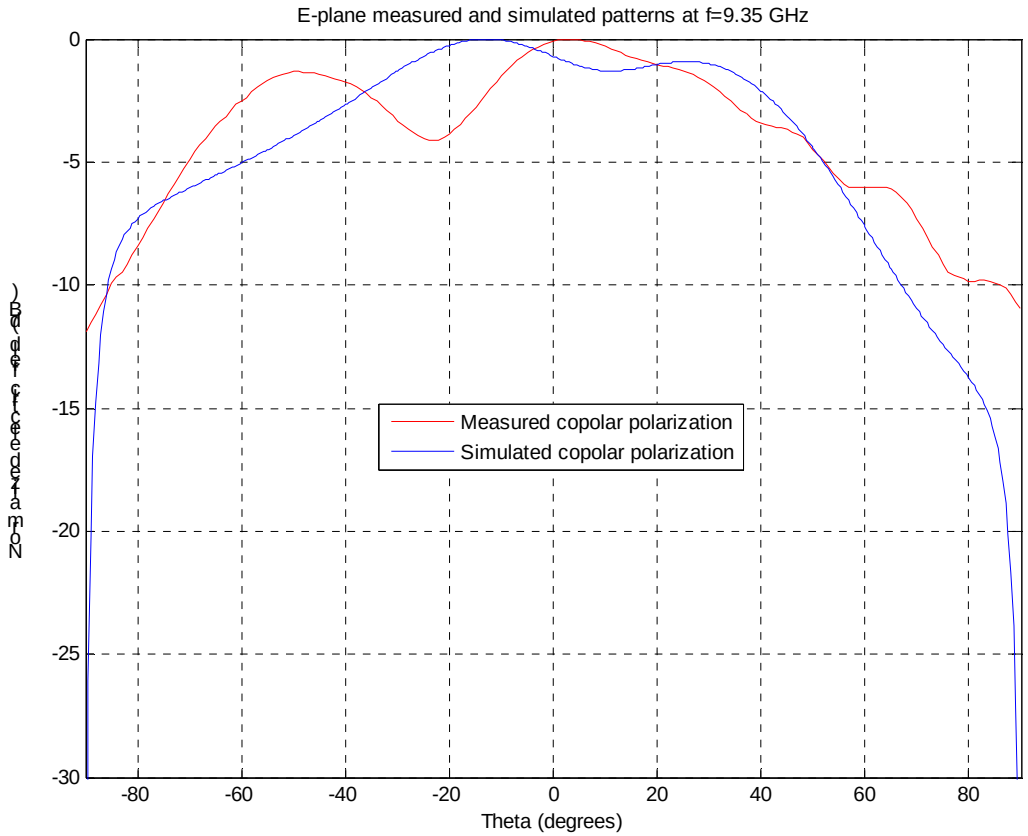

Figure 7 : E-plane radiation pattern versus theta for the GA optimized antenna (f=9.35 GHz).

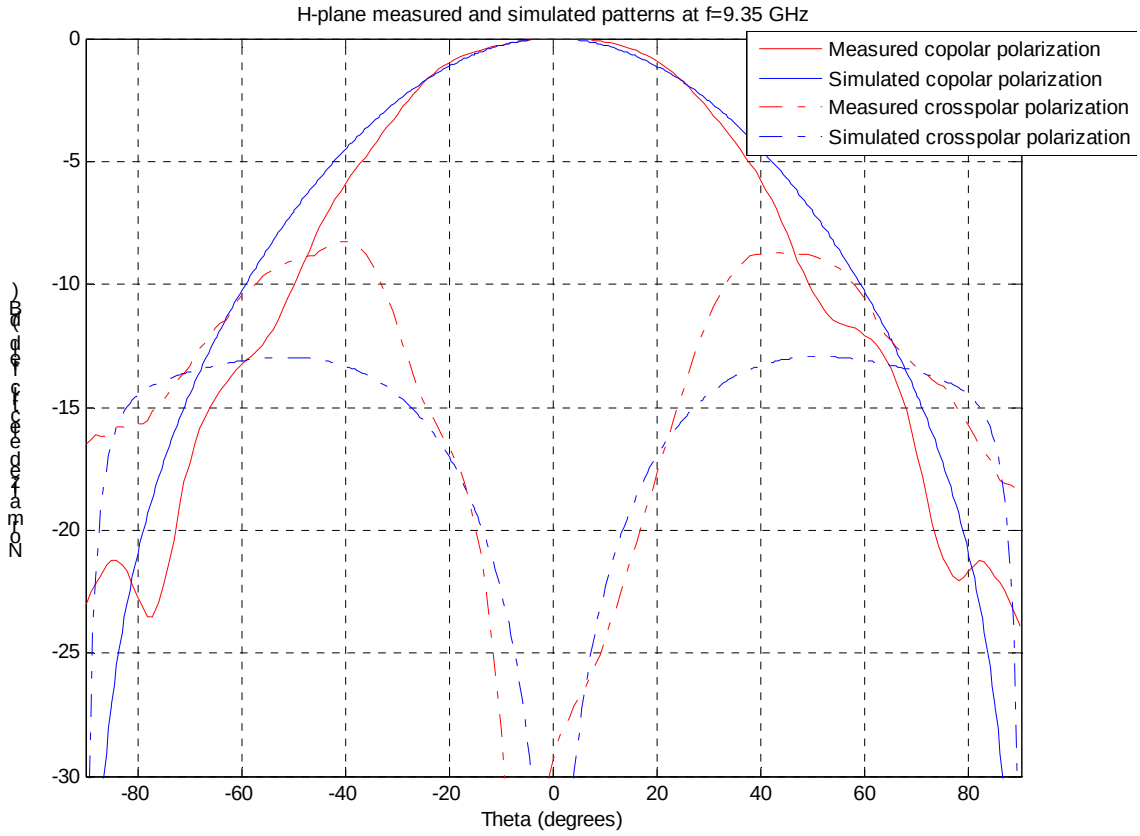

Figure 8 : H-plane radiation pattern versus theta for the GA optimized antenna (f=9.35 GHz).

6- Computation resources

The simulation was performed in a desktop PC. This machine has two Pentium 4 3 GHz processors; however, only one was used for the computation. The available memory in the PC is 1 GB, but much less is needed for this simulation.

For the classic antenna simulation it took 258 seconds to complete the calculus of the current distribution and S parameters at all the frequency points, while it took 2160 seconds to calculate all the antenna patterns at the different frequency points. It must be noted that the antenna pattern was calculated at 37 different planes with 215 points per plane for each frequency point, so it was very time-consuming. The complete program occupied 50 MB in memory, however, according to the program information just 5 MB was needed for the matrix solver.

For the optimized antenna simulation it took 130 seconds to complete the calculus of the current distribution and S parameters at all the frequency points, while it took 2600 seconds to calculate all the antenna patterns at the different frequency points. Again, it must be pointed out that the antenna pattern calculus took so long because it was calculated in 37 planes with 215 points per plane for each frequency point. The complete program occupied 50 MB in memory, however, according to the program information just 6 MB was needed for the matrix solver.

	Time		**Memory**	
	Current distribution	**Antenna pattern**	**Matrix solver**	**Whole program**
Classical patch antenna	258 s	2160 s	5 MB	50 MB
GA Optimized patch antenna	361 s	2600 s	6 MB	50 MB

If a finite ground plane is used instead of the infinite ground plane approximation the computation requirements are much bigger. These simulations have been started with the GA optimized patch antenna with a finite ground plane, but none has been finished:

- With the 30 cells per wavelength criterion the system has 24821 unknowns, and IE3D has not been able to launch the simulation due to memory problems.
- With the 24 cells per wavelength the system has 15528 unknowns, and the memory requirements are around 2GB of RAM memory. The available machines could not make this simulation.
- With the 20 cells per wavelength criterion the system had 10950 unknowns, and the memory requirements were slightly over 1 GB.

For all these simulations the time requirements are simply not acceptable, as they may last even weeks.

7- Discussion

The IE3D has proved to be a very powerful tool to analyze any type of patch antennas when the infinite ground approximation is good enough for the application. This program allows the designer to easily introduce the structure under study using its own GUI, and the simulation setup is almost immediate, as very few parameters must be changed.

As long as an infinite ground plane is supposed, the computation requirements are very low, so the simulation can be carried out with rather old machines within an hour or two.

However, if a finite ground plane is introduced, the computation requirements are simply not acceptable. This is due to the fact that all the volume must be meshed, and not just the planar metallic strip, so the number of unknowns in the system is multiplied by more than 20.

For this reason, the infinite ground plane approximation has been used, and this explains the differences in the antenna patterns for θ angles near 90º. For angles near the maximum of the antenna pattern, the differences are much smaller, below 2 dB, and it can be considered that they are due to the combination of both the measurement uncertainty and finite ground plane effect.

The simulated VSWR shows very good agreement with the measured values. Differences are below 0.5 for all the measured points, and the antenna bandwidth difference between the measurements and the simulation is below 15%. These differences may be due to the simulated excitation, which is a perfect strip with 50 Ohm impedance, while during the measurements, a real line, or maybe a coaxial connector was used. The finite ground plane may modify the simulation results too.

It is the author's opinion that this tool is very well suited for the simulation of most patch antennas, as it provides very useful information for the antenna designer, with very little effort to introduce the structure, very low computation requirements and an straightforward simulation setup where most of the options can be let in their nominal values.

10- SIMULATION RESULTS

From UPV

1- Entity

Universidad Politécnica de Valencia
U.P.V.
I.T.E.A.M.
Edificio 8G
Camino de Vera S/N
Valencia 46022
Spain
Tel: 963879585

2- Name of the simulation tool

Owner software on Matlab.

3- Generalities about the simulation tool

The implemented software is a full-wave, method-of-moments based electromagnetic simulator solving the current distribution on microstrip structures of general shape. The CG-FFT method is used to solve the matrix equation.

4- Simulation Set-up (Geometry set-up, GUI, mesh, boundary conditions, excitation)

The structure has been drawn using the GUI tool of the owner software, which allows us to introduce planar structures composed by a grounded dielectric slab and arbitrarily shaped metallic patches above the same.

A uniform squared mesh is employed to define rooftop base currents above a squared region which integrates the metallic patches. This meshing has the advantage of allowing us to use the CG-FFT method as the resultant matrix is a block Toeplitz matrix, and thus a great computational cost and memory saving is achieved. In spite of defining currents above a more extensive surface than the surface of the metallic patches, the computational cost and memory saving is enormous giving rise to a fast tool to analyze microstrip structures.

However, the shape of patches has to be adjusted to the grid, which supposes some limitation on the simulation time for structures of given dimensions.

We have taken a squared mesh of 40 × 40 cells of size 44mm × 44mm for the classical patch antenna, where each cell has dimensions of 1.1mm × 1.1mm. In electrical terms, that is 30 cells per wavelength at 9.12GHz. The figure 1 shows the defined structure on the GUI interface as well as the mesh employed for the classical patch antenna. The axes X and Y indicate the number of cells in each direction.

In all the simulations, an infinite layer of dielectric material as well as an infinite ground plane have been considered. This approximation allows us only to mesh the squared surface which are located inside the metallic patches, and therefore the computation requirements are greatly reduced. As a result, 3120 unknowns were needed to simulate the total squared mesh in our case, of which only 326 are real unknowns and the rest are fictitious unknowns whose value have been forced to zero in the Conjugate Gradient iterative algorithm.

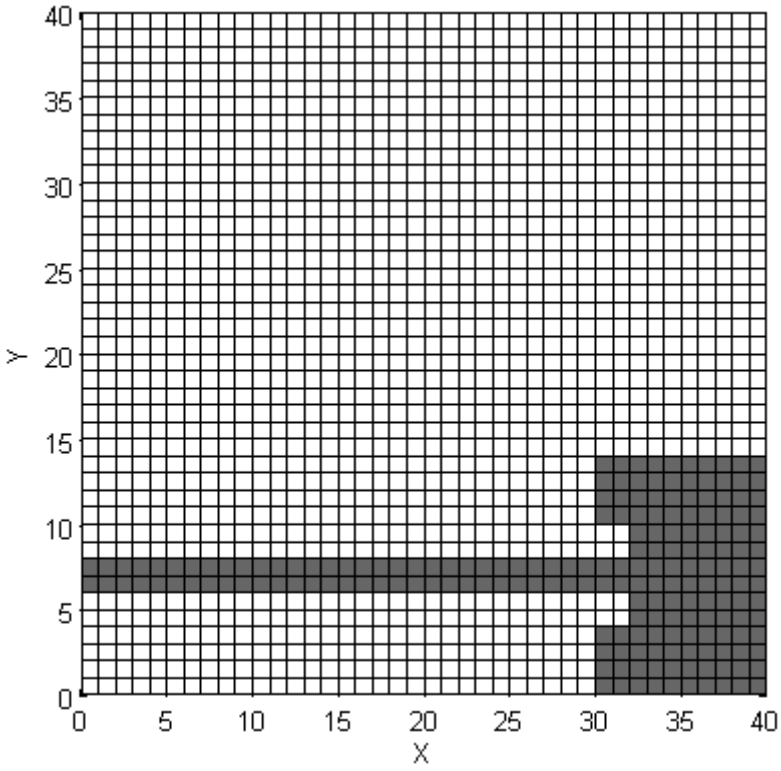

Figure 1: Meshed structure of Classical Patch antenna

As a consequence of the limitation imposed by the meshing, the simulated structure has not the exact dimensions provided by IETR. The dimensions are shown in the following table. Intermediate dimensions can be deduced from the elementary cell size (dx and dy).

Dimensions Table of Classical Patch antenna (mm)

L	*W*	*Lf*	*Wf*	*dx*	*dy*	*d*
11	*15.4*	*33*	*2.2*	*1.1*	*1.1*	*6.6*

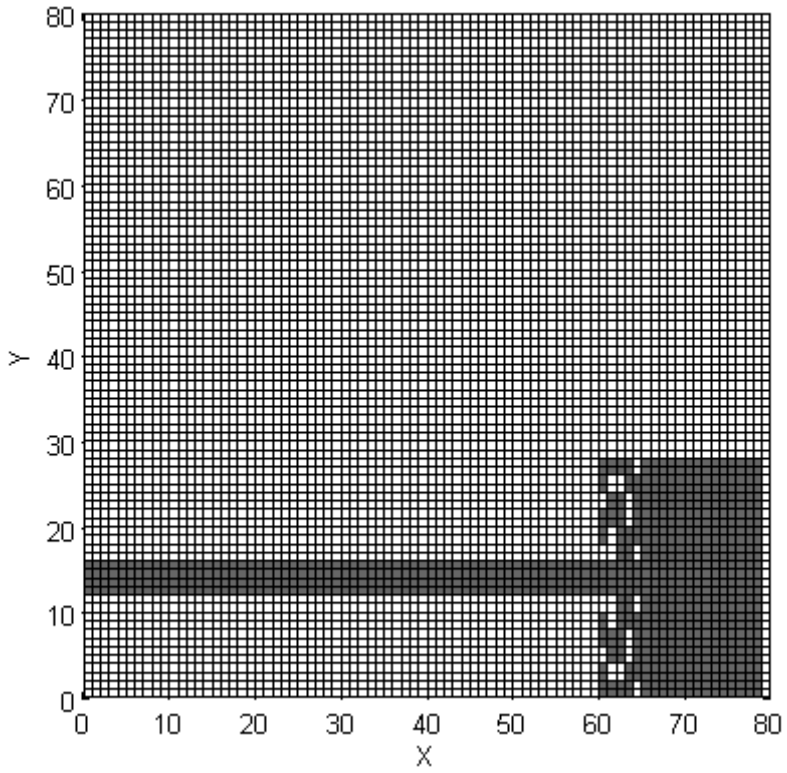

Figure 2: Meshed structure of GA Optimized Patch antenna

For the GA optimized patch antenna we have taken a squared mesh of 80 × 80 cells of size 44mm × 44mm for the GA optimized patch antenna, where each cell has dimensions of 0.55mm × 0.55mm. In electrical terms, that is approximately 60 cells per wavelength at 9.35GHz. The figure 2 shows the defined structure on the GUI interface as well as the mesh employed in this case. The required unknown number was 12640, of which only 1319 are real unknowns.

In this case, the simulated structure does neither have the exact dimensions provided by IETR. The dimensions are shown in the following table. Intermediate dimensions can be deduced from the elementary cell size (dx and dy).

Dimensions Table of GA Optimized Patch antenna (mm)

L	*W*	*Lf*	*Wf*	*dx*	*dy*	*d*
10.45	*15.4*	*33*	*2.2*	*0.55*	*0.55*	*6.6*

An impressed-current excitation model equivalent to a delta-gap voltage excitation model has been considered. The excitation has been modelled by introducing half rooftop currents in the edge of the microstrip line.

The owner software shows to be extremely well suited for microstrip structures, patches or patch arrays on an infinite grounded dielectric slab. The classical patch can be introduced in no more than 1 minute time and the optimized patch is drawn in less than 2 minutes. The main limitation at the moment is in the uniform squared meshing, which forces us to approximate the patch structure to adjust to the grid.

5- Simulation results

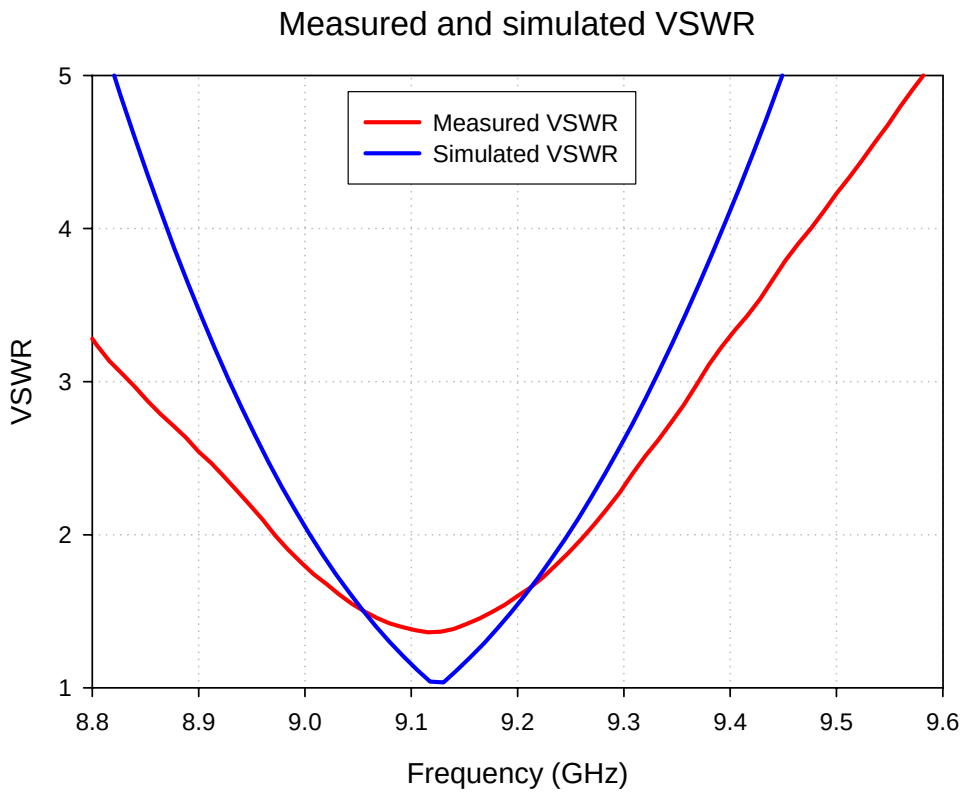

Figure 3 : VSWR versus frequency for the Classical Patch antenna.

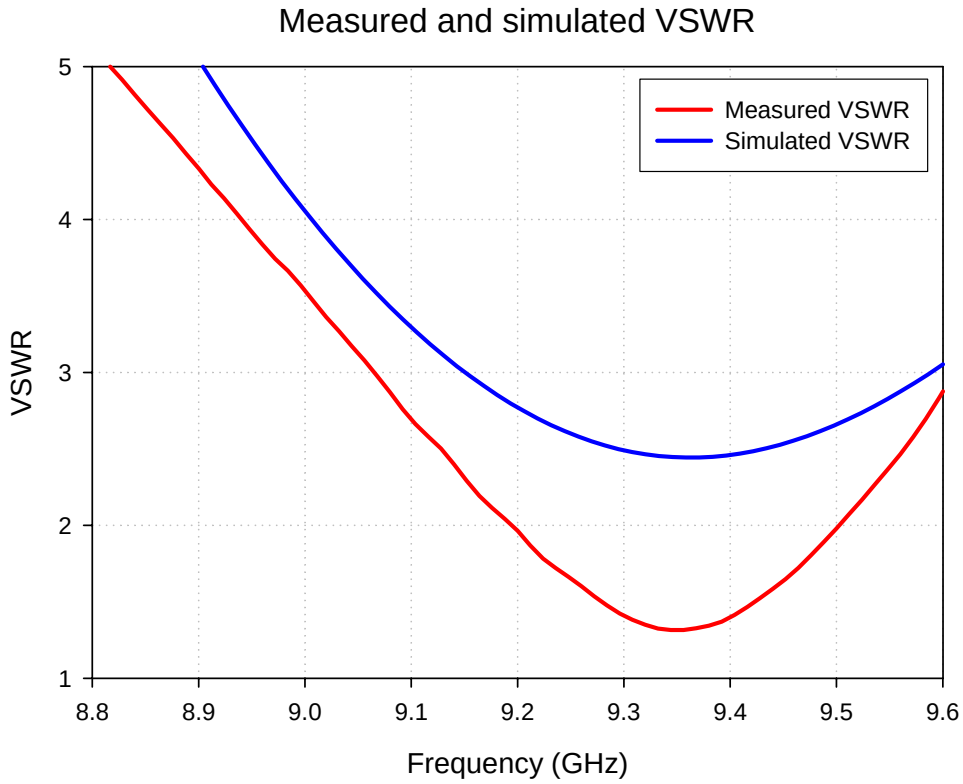

Figure 4 : VSWR versus frequency for the GA optimized antenna.

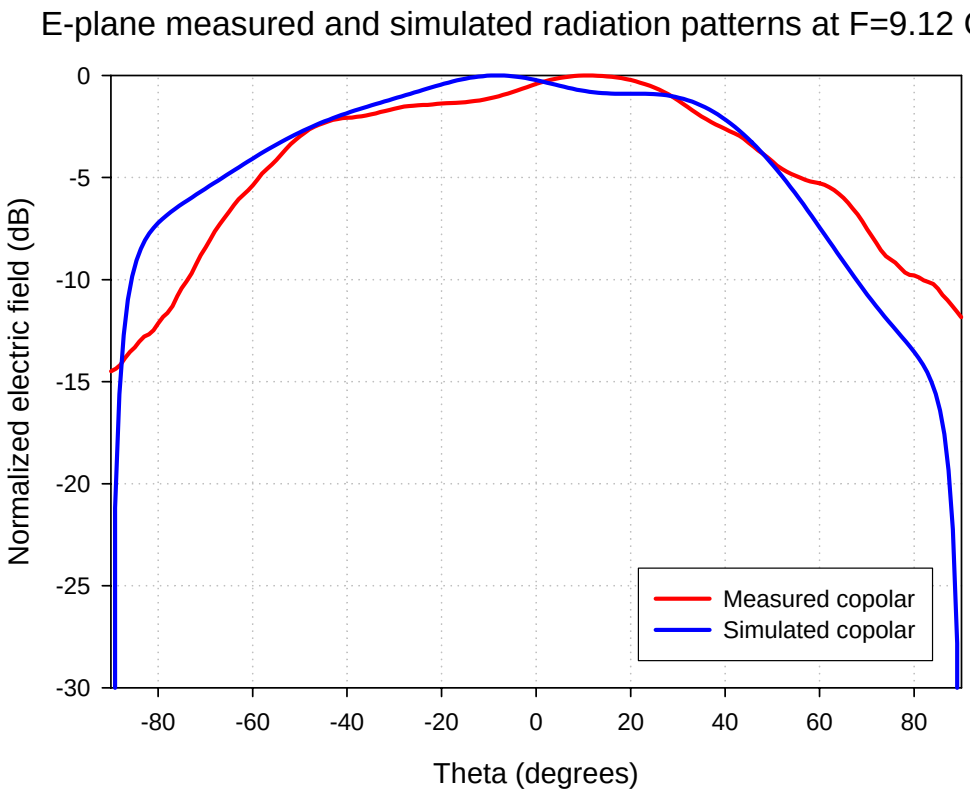

Figure 5 : E-plane radiation pattern versus theta for the Classical Patch antenna (f=9.12 GHz).

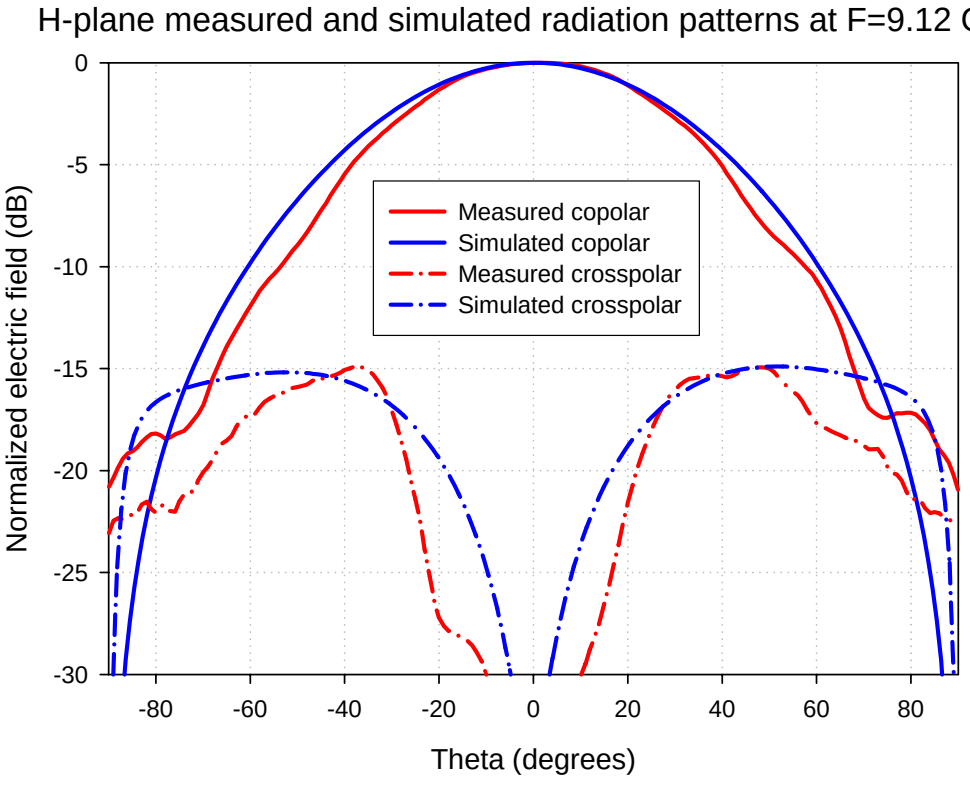

Figure 6 : H-plane radiation pattern versus theta for the Classical Patch antenna (f=9.12 GHz).

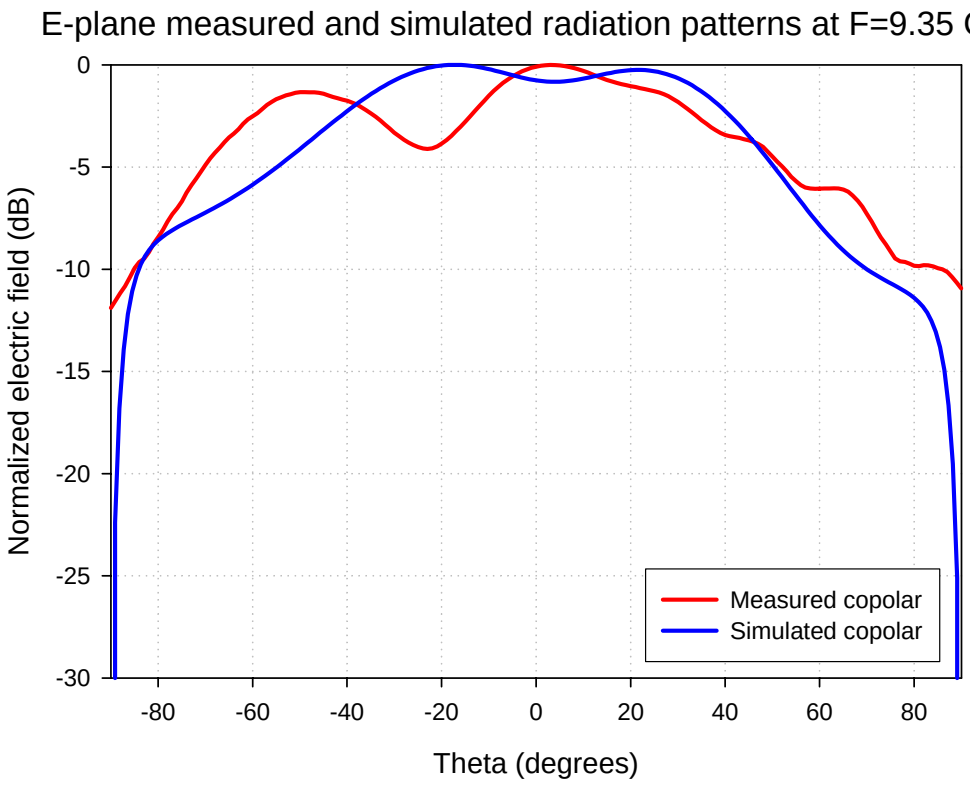

Figure 7 : E-plane radiation pattern versus theta for the GA optimized antenna (f=9.35 GHz).

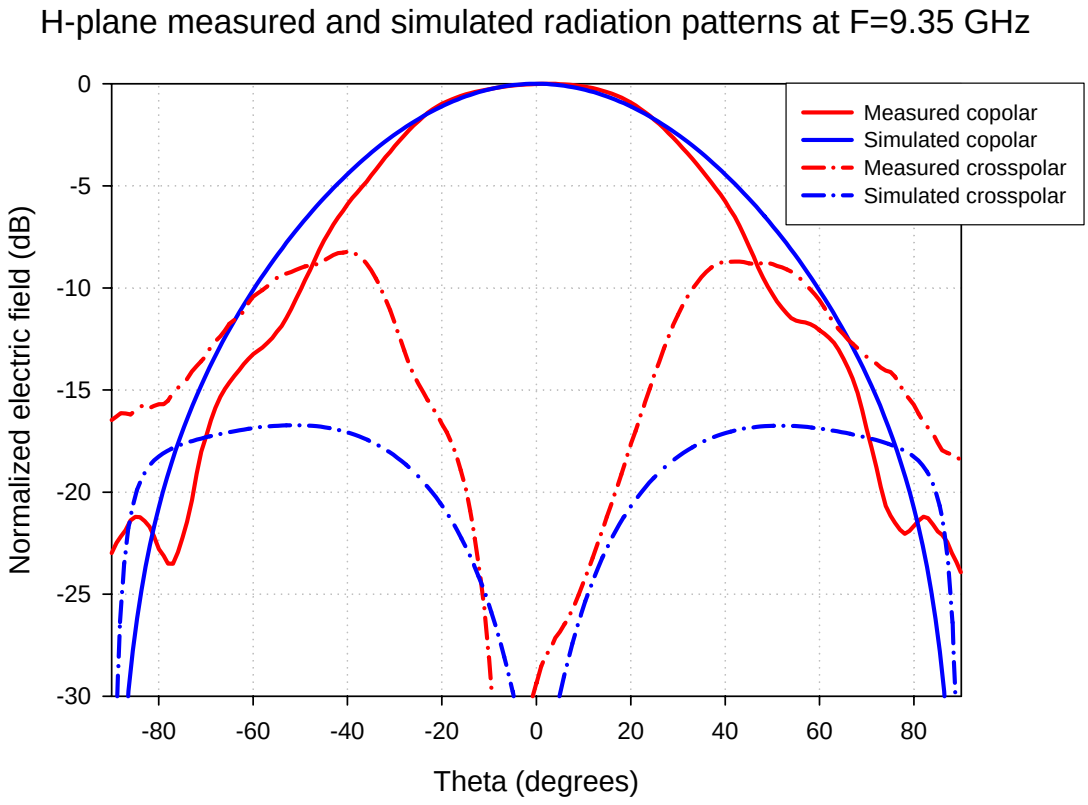

Figure 8 : H-plane radiation pattern versus theta for the GA optimized antenna (f=9.35 GHz).

6- Computation resources

The simulation was performed on a desktop PC. This machine has a Pentium 4 - 3 GHz processor with an available RAM memory of 1 GB.

The simulation has been run for 80 frequencies ranging from 8.7GHz to 9.7GHz for both patches. The E-plane and H-plane antenna pattern were calculated at 200 points per plane at the frequency 9.12 GHz for the classical patch antenna and at 9.35 GHz for the GA optimized patch antenna.

For the classical antenna simulation it took 390 seconds to complete the computation of the current distribution and S parameters at all the frequency points. An amount less than 500 KB of memory was needed for the matrix solver.

For the optimized antenna simulation it took 42 minutes to complete the calculus of the current distribution and S parameters at all the frequency points. An amount less than 1.3 MB of memory was needed for the matrix solver.

Finally, note that finite dielectrics and/or ground plane have not been considered in order to reduce the computation time.

7- Discussion

This tool is very fast and efficient to analyze arbitrarily shaped microstrip antennas. Also, we intend to use it to analyze scattering from periodic microstrip structures, as hard/soft surfaces, EBG surfaces, FSS and reflectarrays. As long as infinite layers are supposed, the computation requirements are very low.

Due to high computational cost that implies to consider a finite dielectric layer and a finite ground plane, in the simulations infinite layers have been considered. For this reason, the results show more significant differences in the antenna pattern for θ angles near 90º. For angles near the maximum of the antenna pattern, the differences are much smaller, and it can be considered that they are due to the combination of both the measurement uncertainty and finite ground plane effect.

For the classical patch simulation, the VSWR presents greater differences with regards to the values measured when you move away of the frequency of resonance, therefore differences between the measured and simulated bandwidths exist. However, the resonance frequency coincides with the measured values. These differences respect to bandwidth may be due to the dimensions of the patch which has slightly been changed. The finite ground plane may modify the simulation results too.

For the GA optimized patch simulation, the VSWR shows good agreement with the measured values with an average difference about 1, but it is observed that the antenna is not well adapted at the resonance frequency. These differences which may be due to slot dimensions are not exactly the same.

In general, we can say the obtained results are good enough. But we expect to introduce future improvements to achieve a more powerful tool.

11- SIMULATION RESULTS

From IDS

1- Entity

IDS - Ingegneria Dei Sistemi S.p.A.
Via Livornese, 1019
56010 Pisa
Italy
Web-site: www.ids-spa.it

Contact person
Massimiliano Marrone
E-mail: m.marrone@ids-spa.it
Phone: +39.050.3124.264
Fax: +39.050.3124.201

2- Name of the simulation tool

ADF (Antenna Design Framework)

3- Generalities about the simulation tool

ADF is a framework which contains many tools for antenna analysis, placement and design. For the present simulation, we have utilized a full-wave MOM solver (MPIE formulation, RWG basis functions) modeling infinite multilayered dielectrics and ground planes employing suitable Green functions.

4- Simulation Set-up (Geometry set-up, GUI, mesh, boundary conditions, excitation)

The set up of the geometry is performed by a CAD tool (Bentley Microstation) available in ADF.

The mesh is a triangular one, and it is created automatically by a proprietary 2D mesher tool, available in ADF. The meshing is performed directly on the geometry drawn by the CAD tool, the average step-size of the mesh being decided by the user. The mesher allows also to perform a local refinement of the mesh in any location.
In the present case we have utilized a mesh with a step-size of about $\lambda/30$-$\lambda/40$.

Both an infinite ground plane and infinite dielectric layer have been employed to model the antennas. The feed line is excited at the entrance using a voltage generator.

The analysis is performed in the frequency domain, one simulation per frequency. In particular the main analysis, called “internal model calculation”, and involving the calculation of the modal currents, is performed at each frequency of the specified range. The far field pattern and the VSWR are calculated, after that the internal model calculation has been performed, at some or at all the frequencies within the specified range.
The frequency range for the Classical patch antenna case is [8.8-9.6] GHz with a frequency step of 0.02 GHz (41 frequency points).
The frequency range for the GA optimized patch antenna case is [8.8-9.6] GHz with a frequency step of 0.025 GHz (33 frequency points).

Both an infinite ground plane and an infinite dielectric layer have been employed to model the antennas. The meshes are conformal to the geometry shapes. The patches were assumed to be lossless and with zero thickness.

Mesh
Triangles: 1362

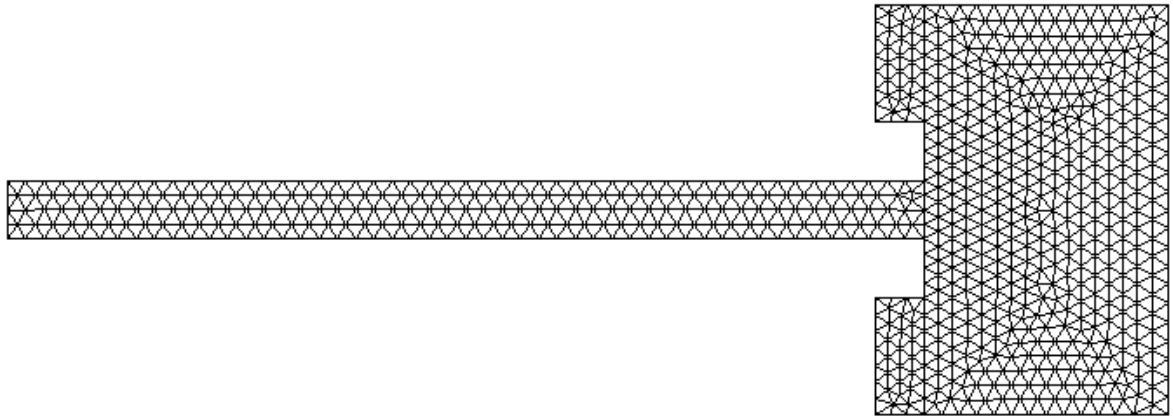

Figure 1 : Classical patch antenna mesh.

Mesh
Triangles: 1134

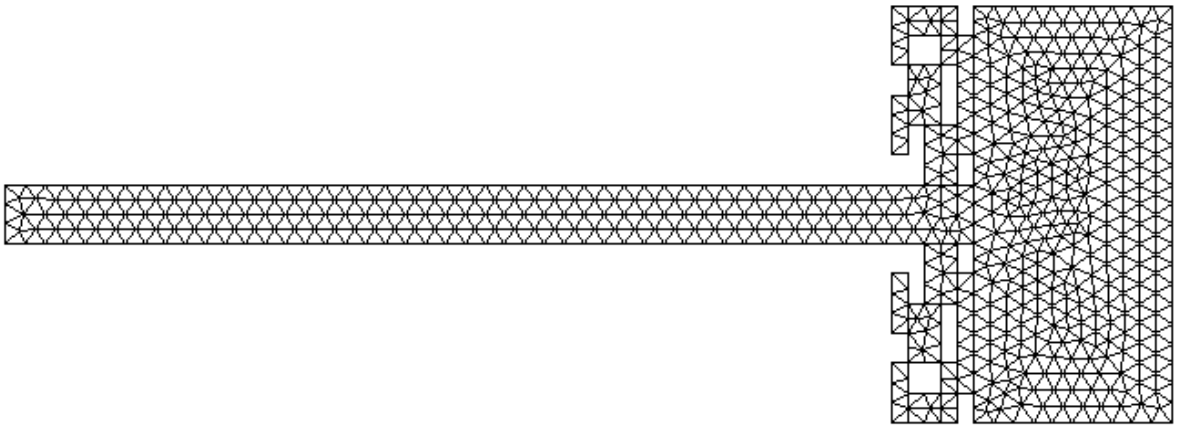

Figure 2 : GA Optimized patch antenna mesh.

In order to redraw the geometry by the CAD, it takes about 20 minutes for the simple patch and 30-40 minutes for the GA optimized patch. In order to set up the rest of the simulation, it takes about 10 minutes.

5- Simulation results

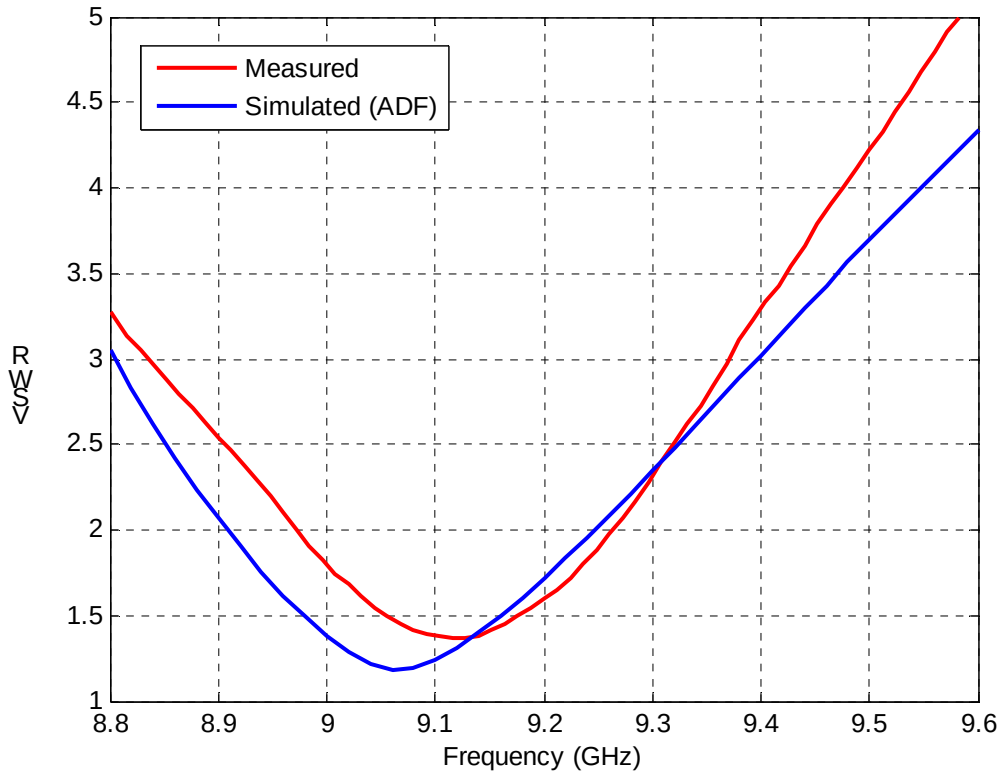

Figure 3 : VSWR versus frequency for the Classical Patch Antenna.

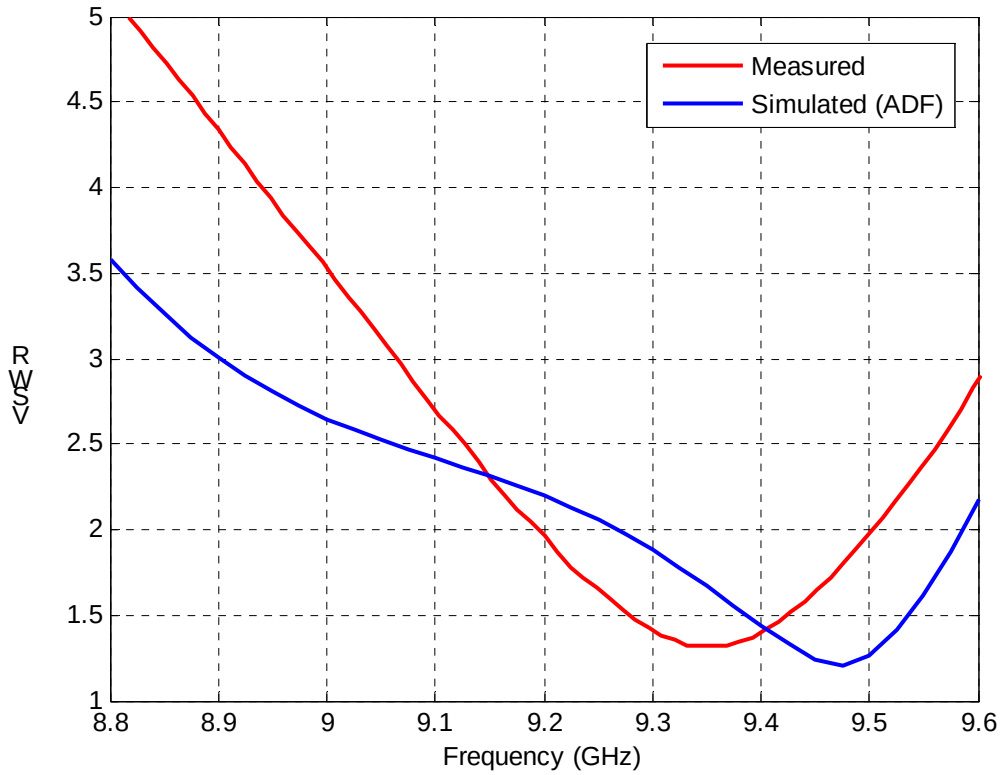

Figure 4 : VSWR versus frequency for the GA Optimized Patch Antenna (f=9.35 GHz).

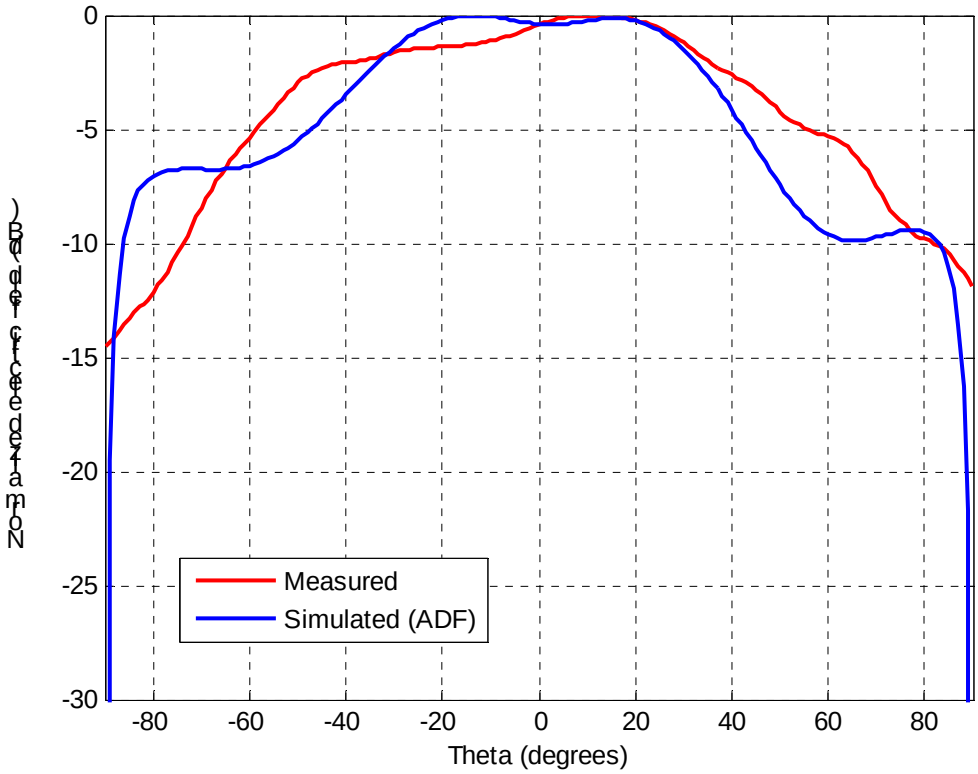

Figure 5 : E-plane radiation pattern versus theta for the Classical Patch Antenna (f=9.12 GHz).

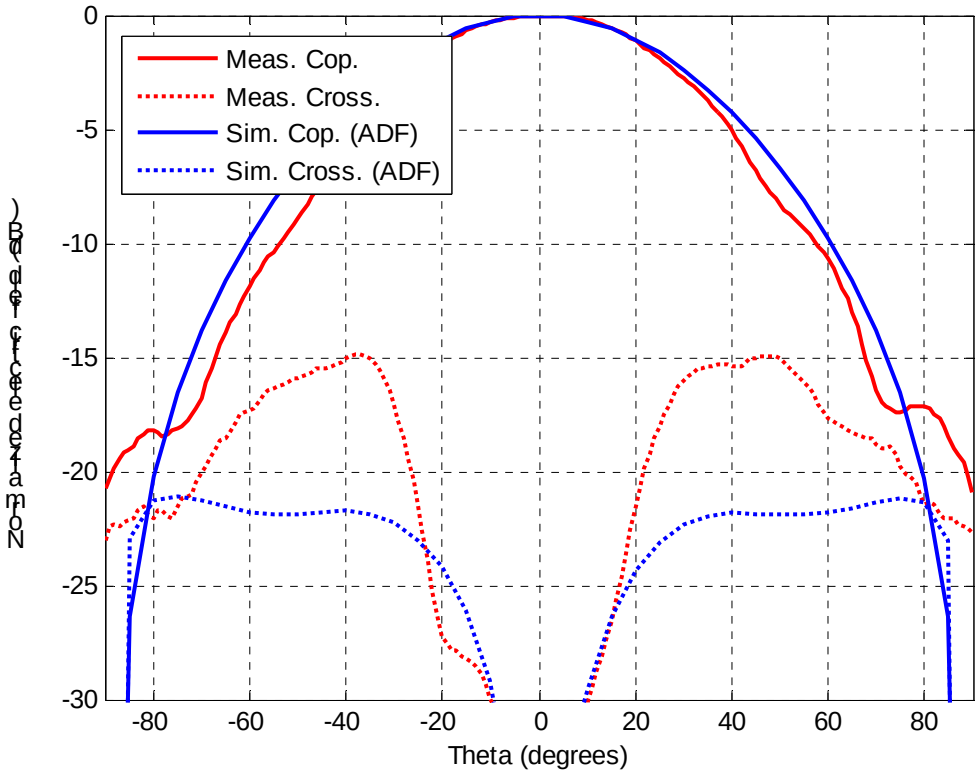

Figure 6 : H-plane radiation pattern versus theta for the Classical Patch Antenna (f=9.12 GHz).

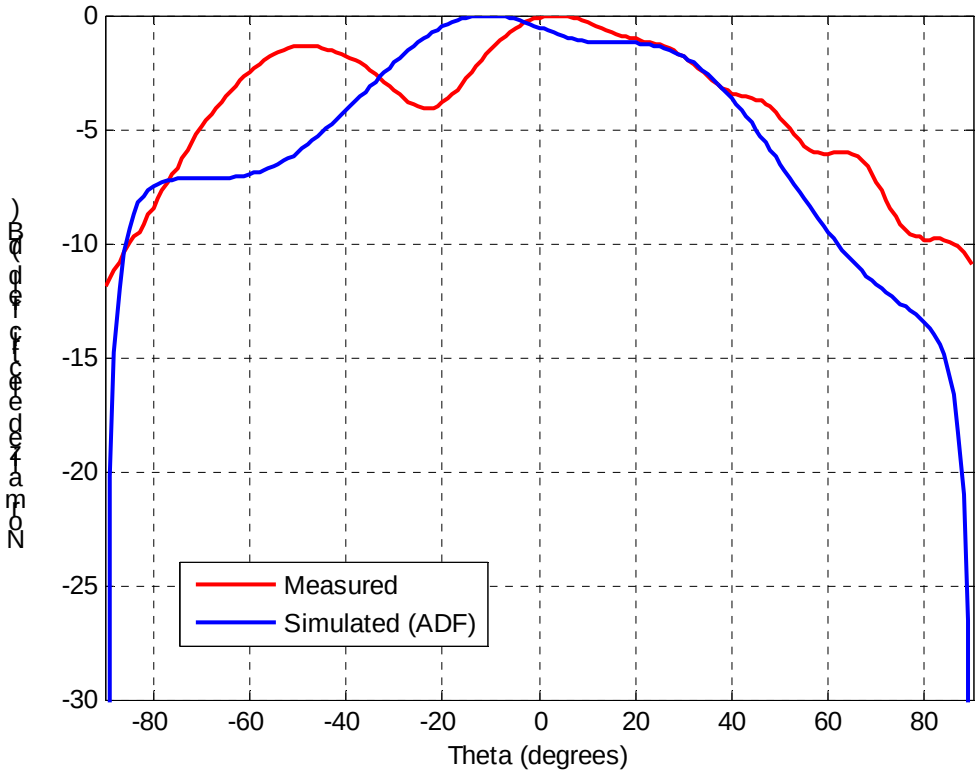

Figure 7 : E-plane radiation pattern versus theta for the GA Optimized Patch Antenna (f=9.35 GHz).

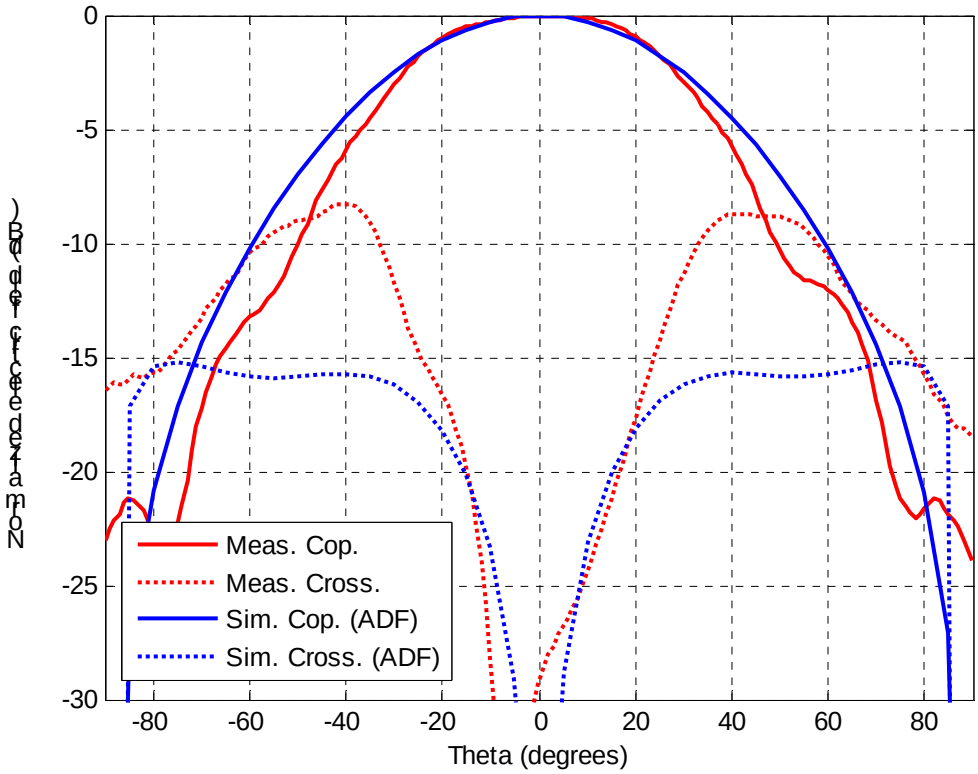

Figure 8 : H-plane radiation pattern versus theta for the GA Optimized Patch Antenna (f=9.35 GHz).

6- Computation resources

The simulation has been performed on a PC-server with 2 XEON processors running at 3.2 GHz, and with 4 GB of available memory. The operating system was Windows Server 2003.

	Simple patch antenna	GA optimized
Number of unknowns	1953	1588
CPU time x frequency point	22 sec	15 sec
Max required RAM	32 MB	20 MB

7- Discussion

Both structures are not difficult to set up since in the CAD environment there are a lot of tools available to help the user in the geometry input process.
Moreover the integration of a proprietary meshing tool in the CAD environment speed up considerably the meshing process up, and the availability of many tools for managing the mesh allows the user to refine it locally and to improve either manually or semi-automatically the quality of the mesh.
The computations were performed first using a coarse mesh and then a fine mesh. The results obtained, whose only those ones related to the fine mesh are displayed, were pretty close to each other, showing their convergence.
The differences in the VSWR results are probably due to the excitation model employed (a voltage generator at the input edge of the feed line) that does not accurately model the experimental set up (feeding through the SMA connector).
For the far field pattern there is a good agreement with the H-plane co-polar, whereas there is a mismatch with the E-plane and H-plane cross-polar.
The differences in the radiation patterns are probably attributed to the infinite ground plane employed instead of the finite one.

8- Additional comments

12- SIMULATION RESULTS

From LIVUNI

1- Entity

Department of Electrical Engineering and Electronics
The University of Liverpool
Liverpool, L69 3GJ
United Kingdom
Contact person
Greepol Niyomjan
E-mail: G.Niyomjan@liverpool.ac.uk

2- Name of the simulation tool

CST Microwave Studio (MWS) 5.0.0 [1].

3- Generalities about the simulation tool

CST MWS5 is a simulation tool for High Frequency simulations. It offers Transient, Eigenmode and Frequency Domain solvers and uses a Finite Integration (FI) method with perfect boundary approximation (PBA).

4- Simulation Set-up (Geometry set-up, GUI, mesh, boundary conditions, excitation)

The model is defined using the GUI of the software. Everything is made using primitives and Boolean subtraction. The GA patch is traced point by point and then extruded to a given thickness before Boolean subtracting the inner holes. The Mesh is automatically generated at 10 lines/wavelength and run through the adaptive mesh update three times giving a total number of mesh cells of 290000 (increased from ~50000). The transient

solver was used to simulate the structure which is a time domain based method. The excitation was a 1-10 GHz Gaussian pulse applied to a discrete port (connected between the microstrip feed point and ground plane). The port and simulation were both normalized to 50 ohm with a -30dB accuracy limit imposed to determine simulation time. Monitors for specific frequencies were setup to obtain the far-field parameters at those frequencies. Geometry of antenna structures for both conventional and GA optimized are illustrated in Figure 1.

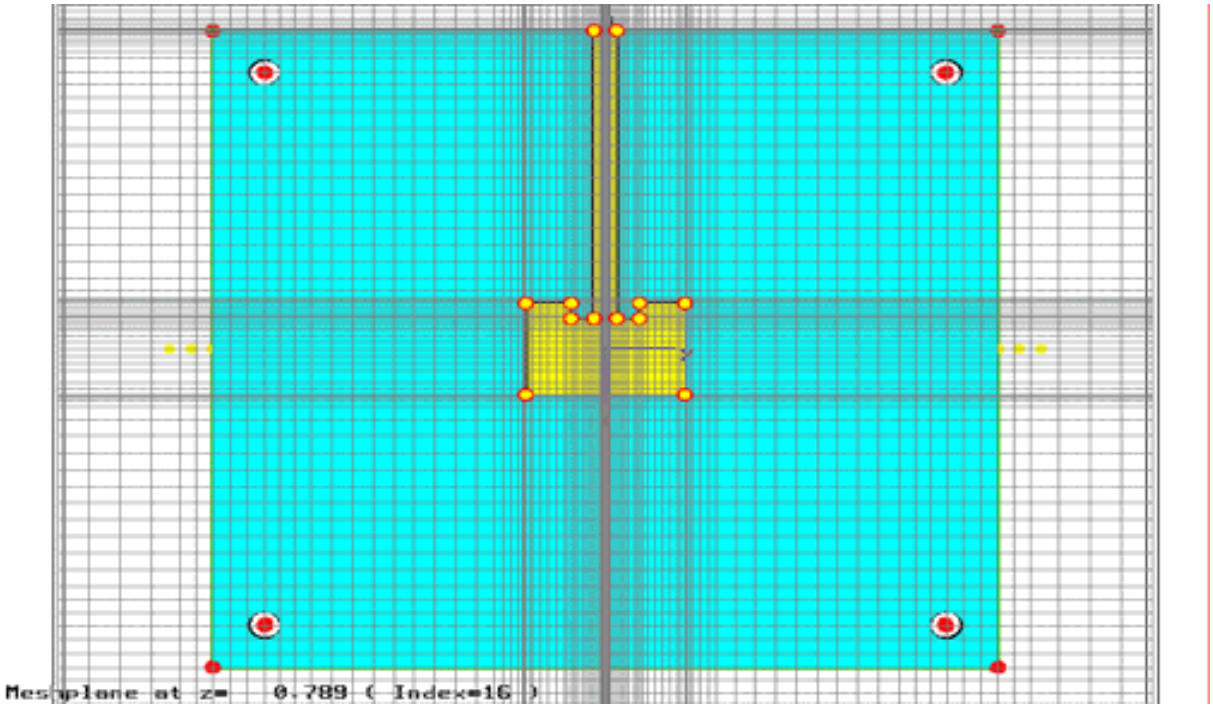

Figure 17a: Snapshot of the conventional patch geometry from CST.

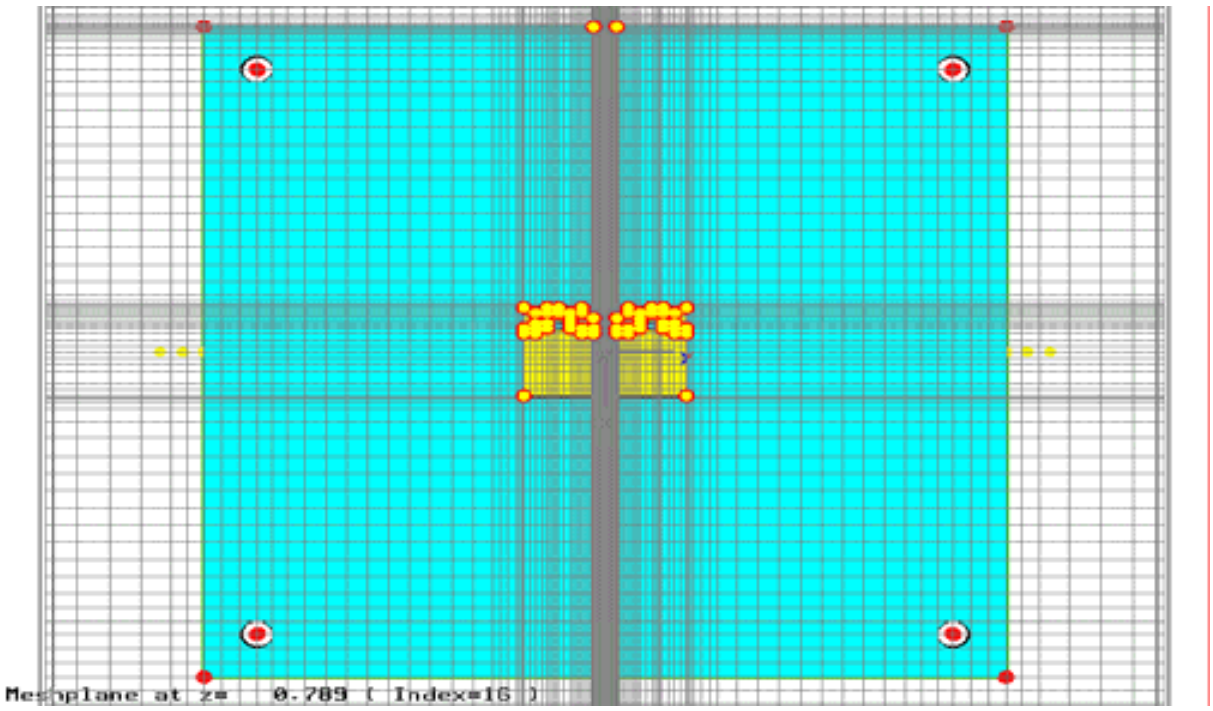

Figure 18b: Snapshot of the GA Optimized patch geometry from CST.

Figure 1:Snapshot of conventional patch and GA Optimized patch antennas.

5- Simulation results

The results that have been computed are:

- Voltage Standing Wave Ratio (VSWR)
- Radiation Patterns (Normalized E field)

Values of VSWR at the input port for both structures are plotted as shown in Figures 2-3. Values of Normalized Electric field in dB are plotted against the theta angles from -90 to 90 degree as shown in Figures 4 – 7.

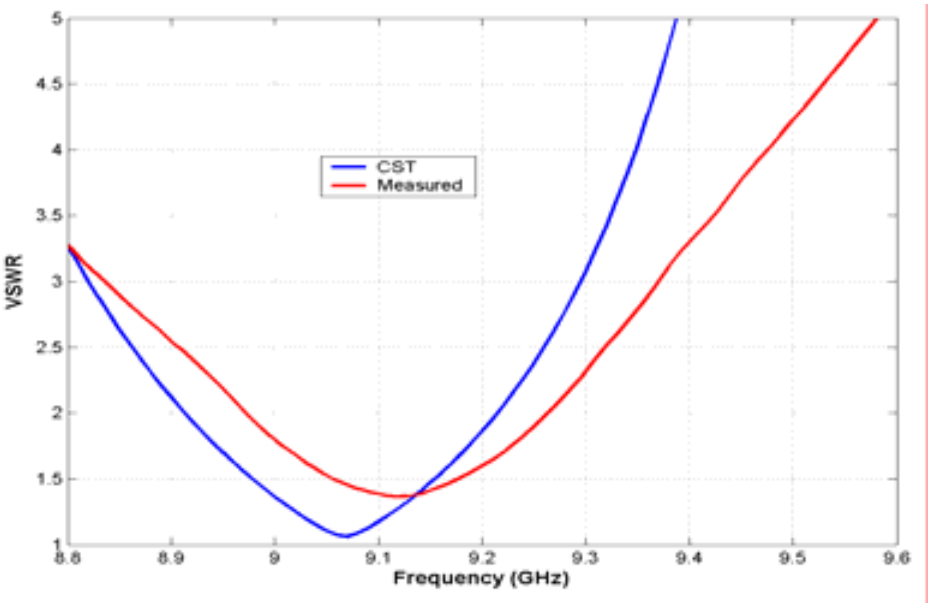

Figure 2: VSWR versus frequency for Conventional Patch in frequency range 8.8-9.6 GHz.

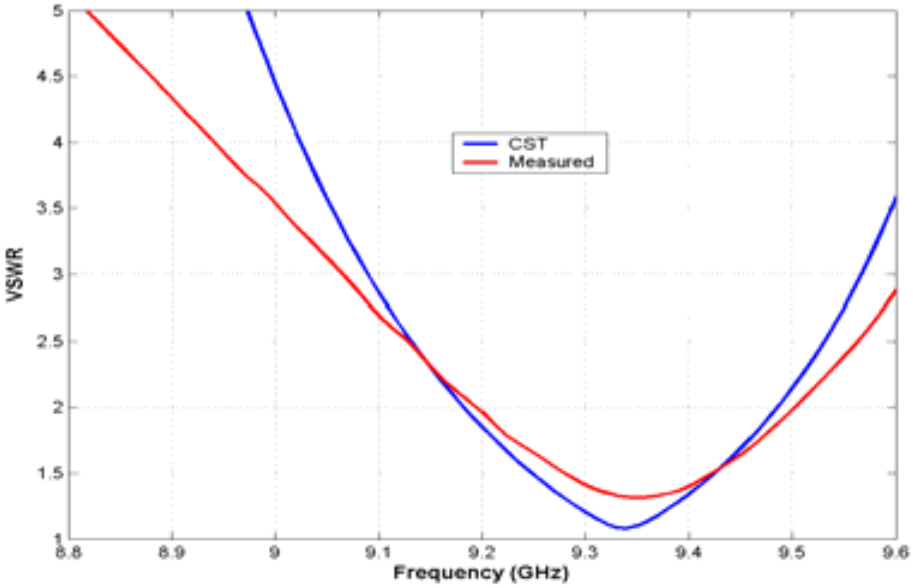

Figure 3: VSWR versus frequency for GA Optimized Patch in frequency range 8.8-9.6 GHz.

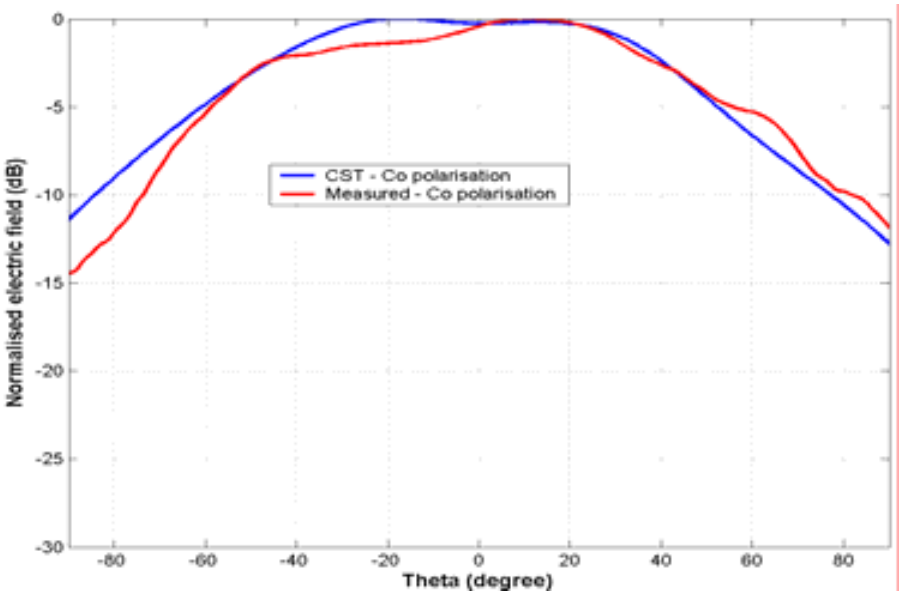

Figure 4: E-field pattern in the E-plane (φ = 0°) for Conventional Patch, computed at the frequency f = 9.12 GHz.

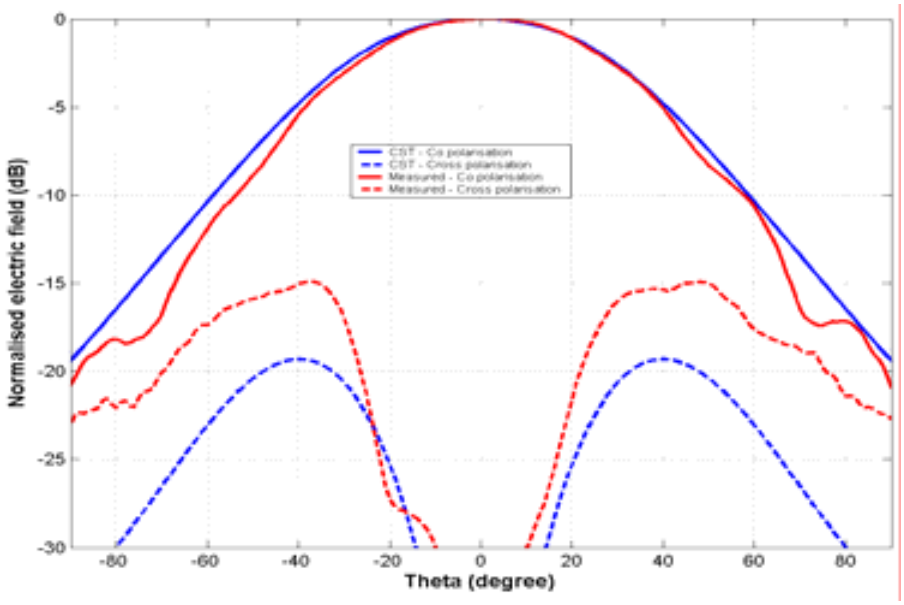

Figure 5: E-field patterns for in the H-plane (φ = 90°) for Conventional Patch, computed at the frequency f = 9.12 GHz.

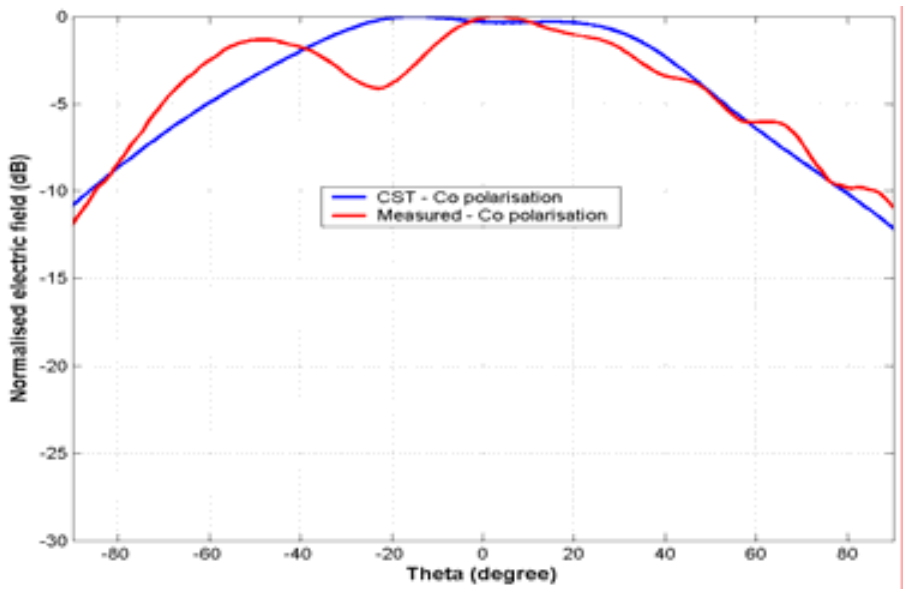

Figure 6: E-field pattern for in the E-plane (φ = 0°) for GA Optimized Patch, computed at the frequency f = 9.35 GHz.

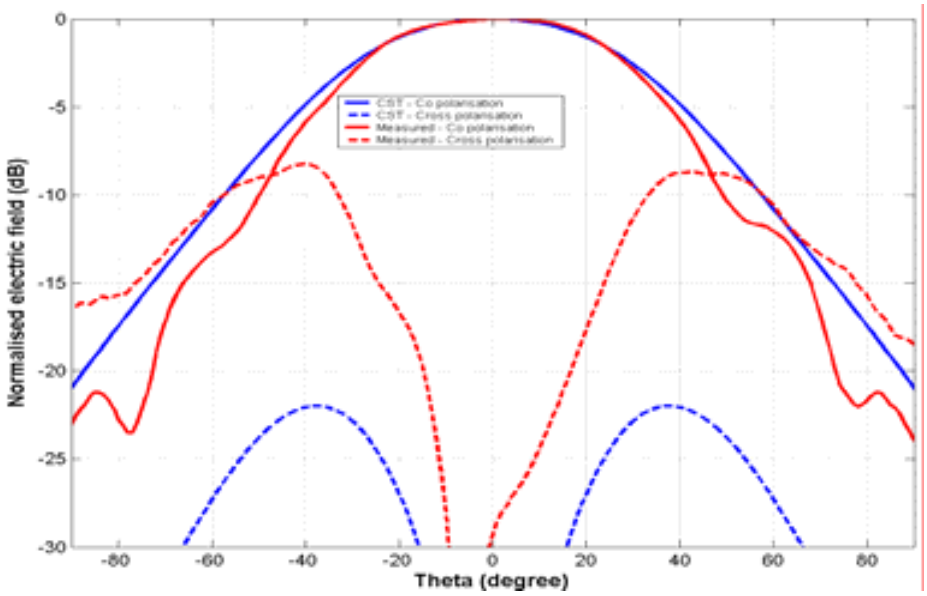

Figure 7: E-field patterns for in the H-plane (φ = 90°) for GA Optimized Patch, computed at the frequency f = 9.35 GHz.

6- Computation resources

PC desktop with specifications shown in Table 1 was used to simulate the Conventional and GA optimized patch antennas. The total times spent on these simulations are shown in Table 2.

Table 1: Specification of the desktop used for CST simulation

Type of machine	Desktop PC
Number of CPUs	1 Intel Pentium 4
CPU Speed	1.7 GHz
RAM	1 GB
OS	Win XP Home Sp2

Table 2: Simulation time for CST

Total time	Conventional Patch	1 hr 10 min
	GA Optimized Patch	1 hr, 20 min

7- Discussion

The VSWR for conventional patch obtained from CST is comparable to the VSWR obtained from measurement [2] except at the frequency range from 9.4 to 9.6 GHz where values of VSWR obtained from CST are relatively high compared to the VSWR results obtained from measurement. However VSWR for GA Optimized patch obtained from CST shows good agreement with the measured VSWR for GA Optimized patch. Normalized E-field radiation patterns for both convention patch and GA Optimized patch obtained from CST show close agreement with the Normalized E-field radiation patterns obtained from measurement. However cross polarized pattern for GA optimization patch obtained from CST appears to be lower than the measured pattern. This might be due to the radiation effect of the feed connector added to resulted radiation pattern of antenna structure. From the simulation time in table 2, it is obvious to see that CST is one of the efficient simulation tools which offers both speed and accuracy.

Reference:

[1] www.cst.com

[2] Institut National des Sciences Appliquées de Rennes (IETR).

13- SIMULATION RESULTS

From UPC

1- Entity

Universitat Politècnica de Catalunya
Department of Signal Theory and Communications (TSC)
Electromagnetic and Photonic Engineering Group (EEF)
Campus Nord UPC, Edifici D-3
Jordi Girona, 1-3
08034 - Barcelona
Spain

Contact person:
Juan Manuel Rius Casals
Phone: 34-93-4017219
Fax: 34-93-4017232
e-mail: rius@tsc.upc.edu

2- Name of the simulation tool

FIESTA-3D (Fast Integral Equation Solver for scaTTerers and Antennas in 3D)

3- Generalities about the simulation tool

FIESTA uses MoM discretization of EFIE, MFIE or CFIE in RWG triangles. Fast iterative solvers accelerated by MLFMA or MLMDA can be used.
For this benchmark, the multilayer Green's function is calculated using Sommerfeld integrals. The number of integration points when computing the impedance matrix elements is 4 per source triangle times 4 per testing triangle. It can be reduced to 1 point in source and testing triangles when the distance between them is larger than a threshold (Rinteg).

4- Simulation Set-up (Geometry set-up, GUI, mesh, boundary conditions, excitation)

The structures were modelled and automatically meshed using GiD[1] software. The classical patch antenna was meshed in 475 triangle elements of size 1mm and 300 nodes, and the GA optimized patch antenna was meshed with 479 triangle elements of the same size and 316 nodes. The number of RWG unknowns is respectively 653 and 639.
Both meshed structures were exported to a *.msh format recognized by FIESTA.

[1] GID is a software created by the International Center of Numerical Methods in Engineering (CIMNE) at UPC (http://gid.cimne.upc.es)

All the simulations have been performed with an infinite multilayer Green's function.
The excitation is a delta-gap on the RWG testing functions that have an edge in the x = 0 plane (marked with red colour in Fig. 1 and Fig. 2).
Once the structure was introduced on FIESTA, a multifrequency computation was performed at 80 frequency points from 8.8 GHz to 9.6 GHz, that is, at the same frequency range used during the measurements.

For each frequency point, the current distribution, the radiation pattern, the input impedance (real and imaginary) and the reflection coefficient were calculated by FIESTA. The radiation pattern was calculated for $\Delta\theta$ and $\Delta\phi$ increments of 0.8, so for a 180º plane we had 225 computed points.

Figures 1 and 2 show a snapshot of the classic patch antenna and the optimized patch antenna as exported to FIESTA from GiD.

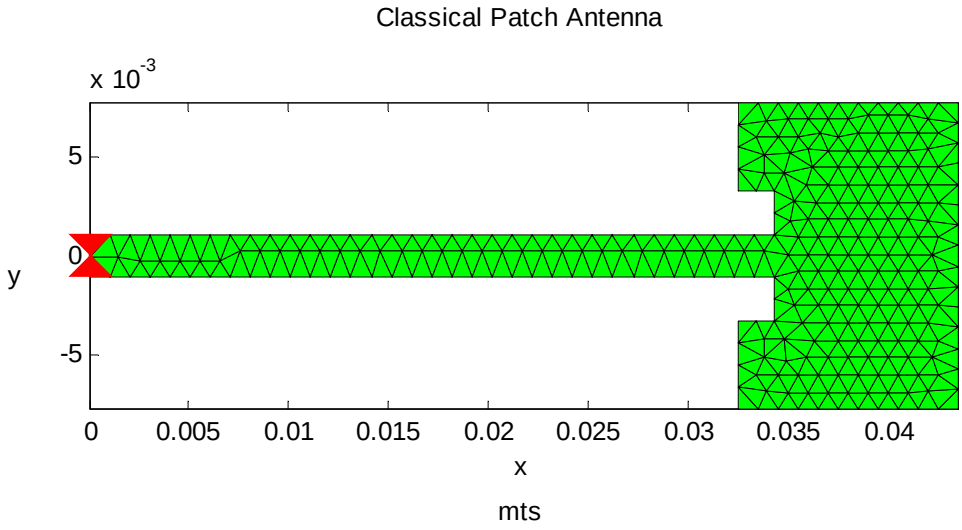

Fig. 1. Classic patch antenna

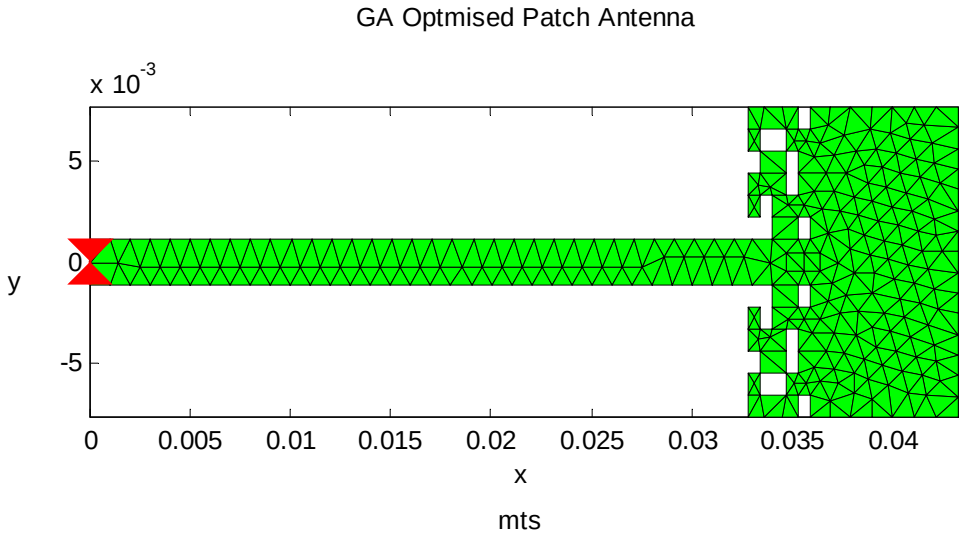

Fig. 2. GA Optimized patch antenna

The classical patch antenna can be modelled and meshed in GiD by approximately 5 minutes, while setting up the simulation in FIESTA is immediate. The optimized patch antenna can be modelled and meshed in GiD by approximately 10 minutes.

Figure 3 and 4 show the density of current distribution over the surface of the object in three dimensions, the plots show vector arrows representing current direction.

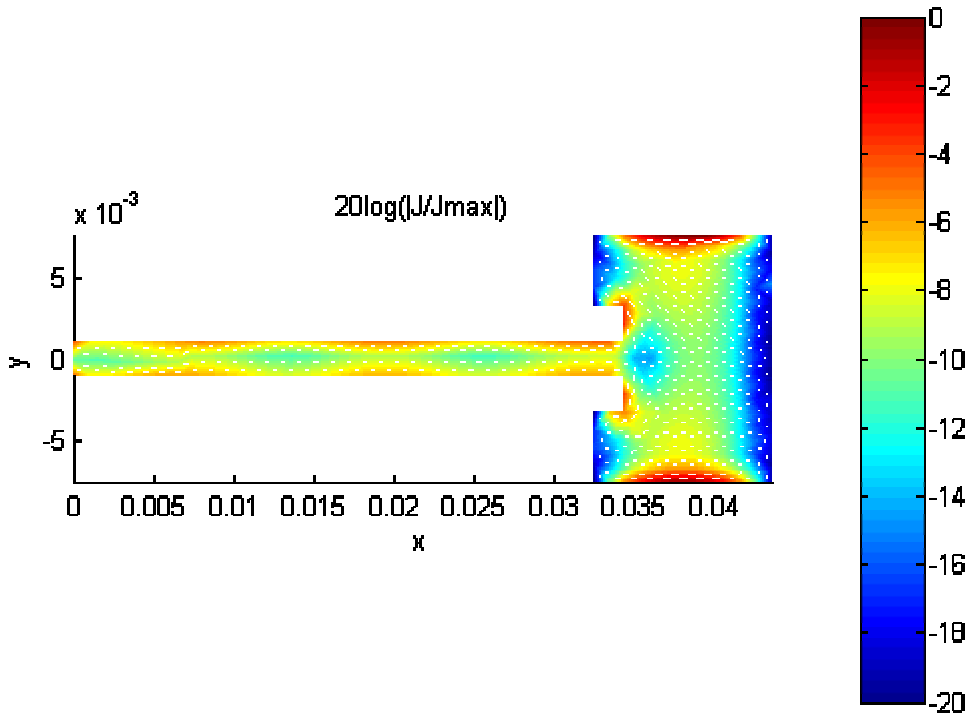

Fig. 3. Density of current distribution for the Classical Patch antenna (f = 9.12GHz).

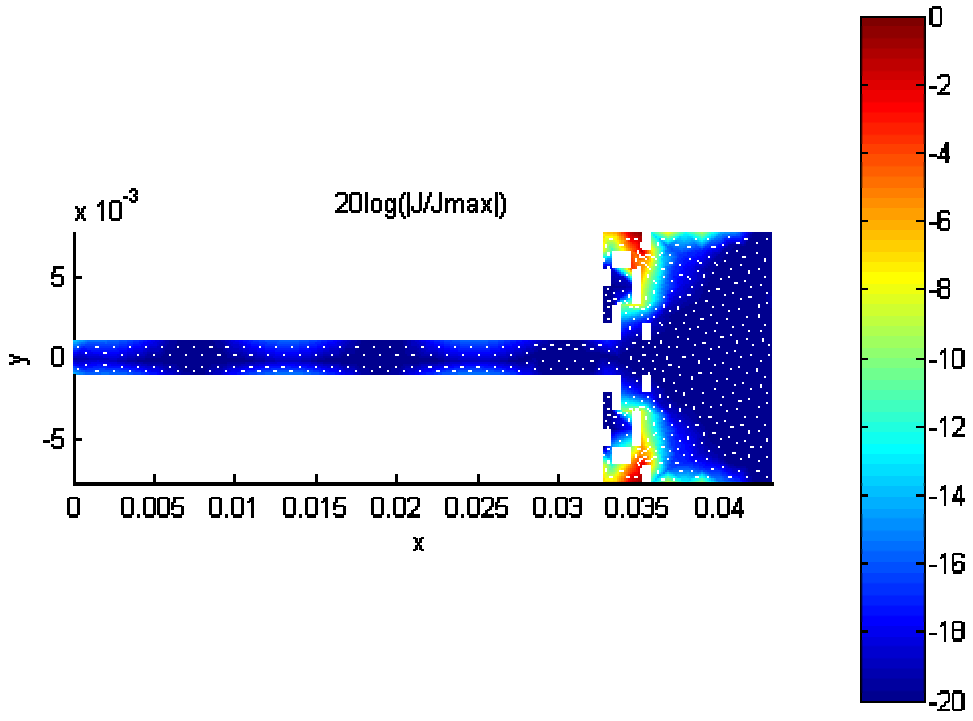

Fig. 4. Density of current distribution for the GA Optimized Patch antenna (f = 9.35GHz).

5- Simulation results

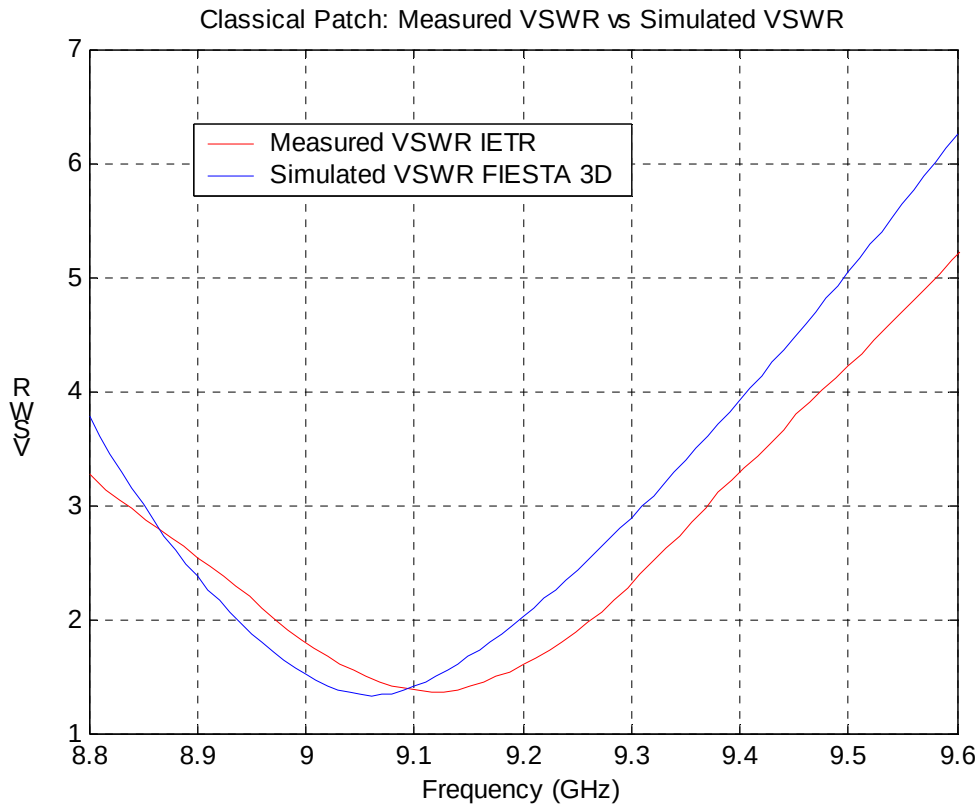

Fig. 5. VSWR versus frequency for the Classical Patch antenna.

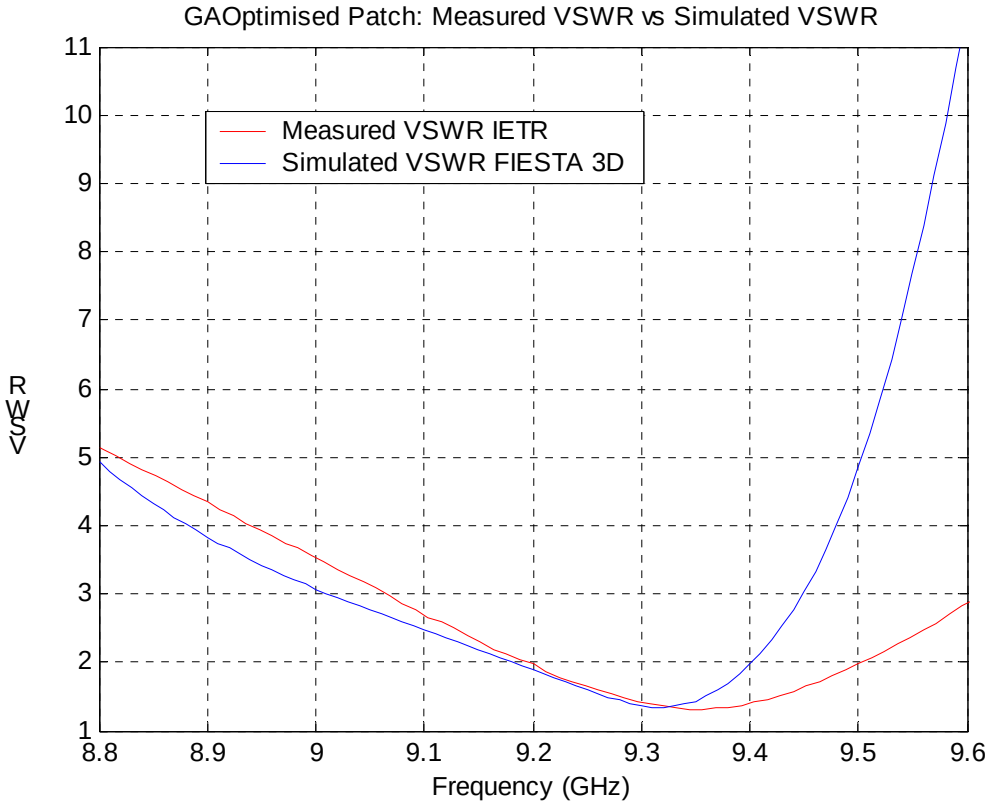

Fig. 6. VSWR versus frequency for the GA optimized antenna.

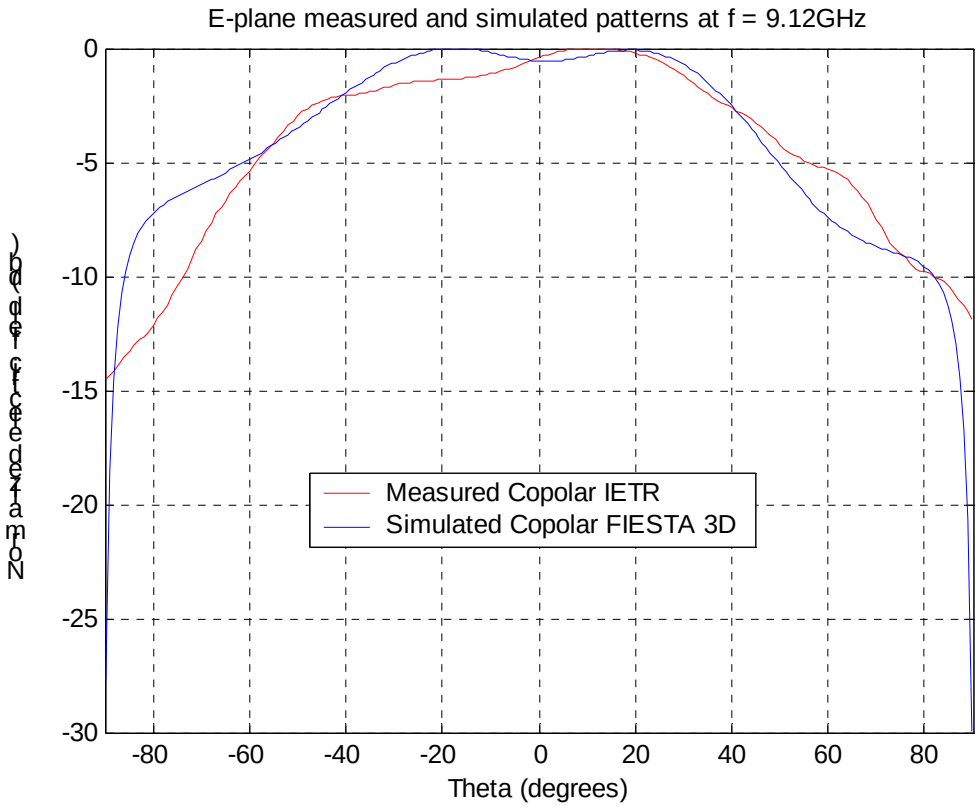

Fig. 7. E-plane radiation pattern versus theta for the Classical Patch antenna (f=9.12 GHz).

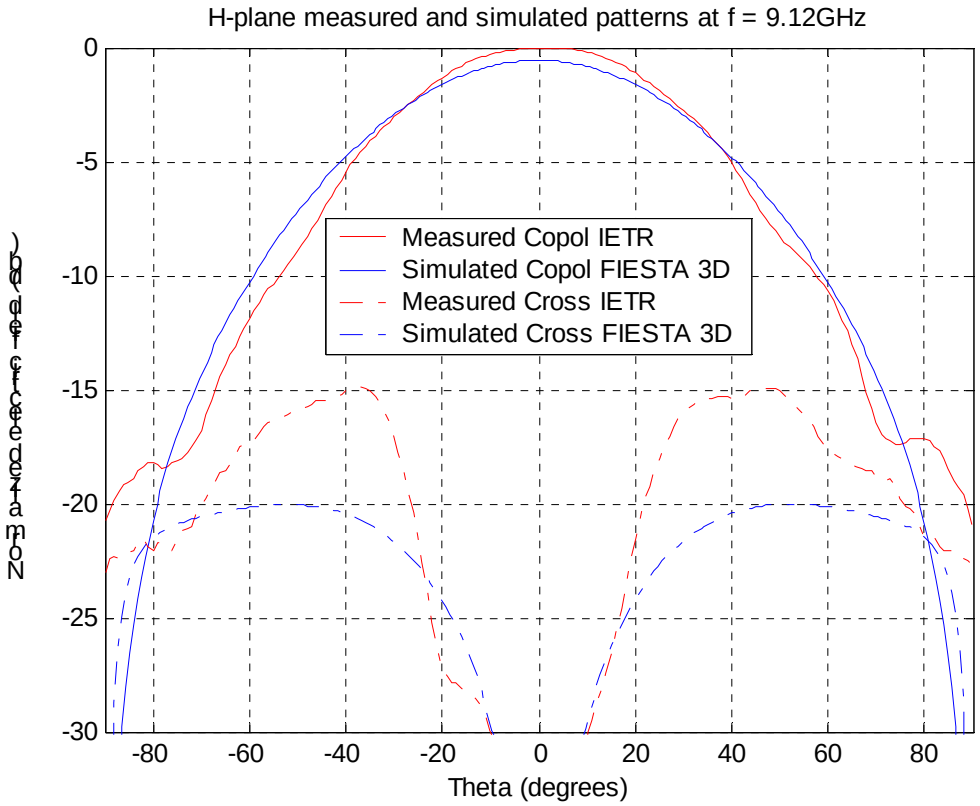

Fig. 8. H-plane radiation pattern versus theta for the Classical Patch antenna (f=9.12 GHz).

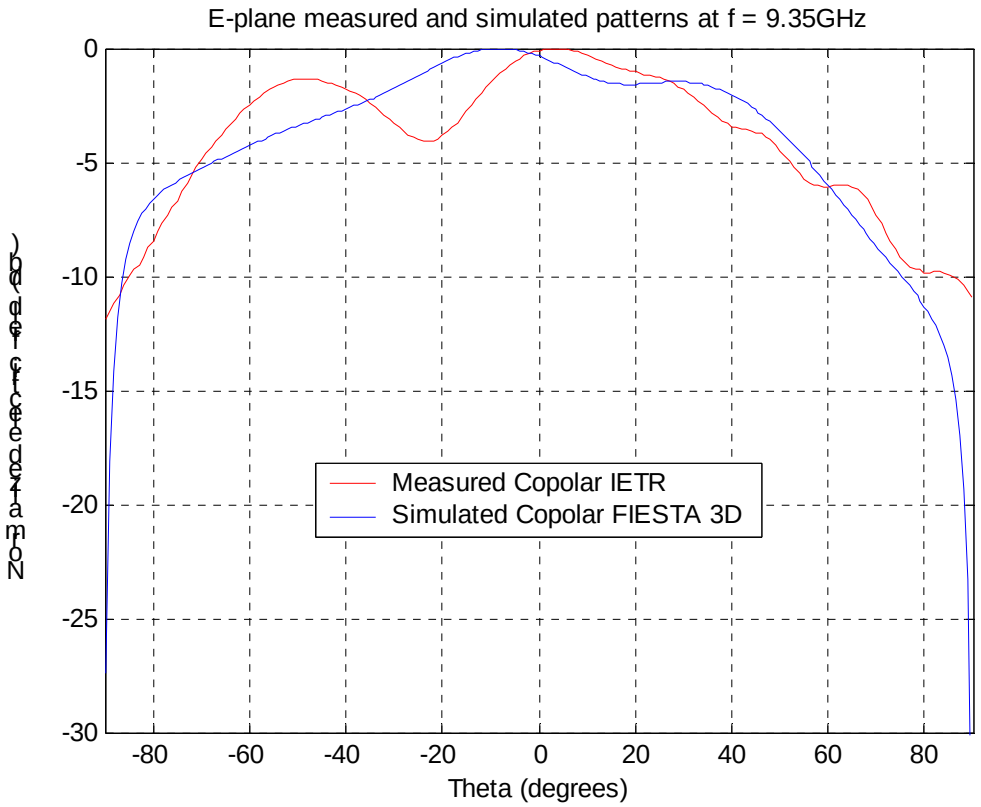

Fig. 9. E-plane radiation pattern versus theta for the GA optimized antenna (f=9.35 GHz).

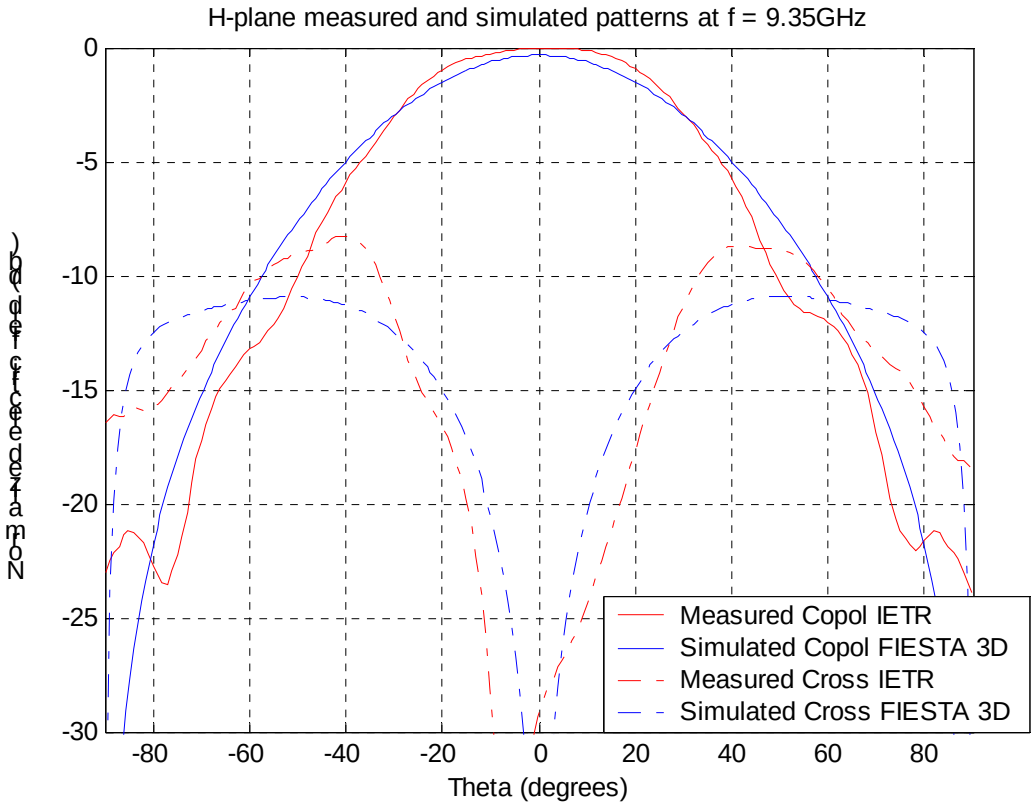

Fig. 10. H-plane radiation pattern versus theta for the GA optimized antenna (f=9.35 GHz).

6- Computation resources

The simulation has been performed on a PC with the following characteristics (table 1):

Type of machine	Desktop PC
Number of CPUs	1 AMD Athlon FX55
CPU Speed	2.6GHz
RAM	4 GB
OS	Windows XP

Table 4 Properties of the PC used for the simulation

For the classical patch antenna, the simulation at f = 9.12GHz took 0.33s to complete the calculus of the current distribution, 1.22s to compute the impedance matrix Z, and 1.87s to compute the radiation pattern.
For the whole frequency range, we considered 80 points from 8.8 GHz to 9.6GHz and the simulation took 4min to complete the calculus of the reflection coefficient.

For the Optimized patch antenna, the simulation at f = 9.35GHz took 0.33s to complete the calculus of the current distribution, 1.22s to compute the impedance matrix Z, and 1.87s to compute the radiation pattern.
For the same frequency range, the simulation took 4min to complete the calculus of the reflection coefficient.

The Z was computed with 4 integration points per source and 4 per testing triangles when the distance between the centroids of source and field triangles is less than 2mm, otherwise only 1 integration point was used. The threshold Rinteg = 2mm is automatically computed by FIESTA based on the average and the maximum side of the mesh triangles.

Data relevant to the simulation are listed in the following table 2:

	Classical Patch Antenna	**GA Optimized Patch Antenna**
Number of unknowns	475 triangle elements	479 triangle elements
Computation of Green function tables	1.36 seg	1.36 seg
Computation of impedance matrix Z	1.22 seg	1.22 seg
Computation of Current distribution	0.33 seg	0.33 seg
Average CPU time per frequency point	2.91 seg	2.91 seg
Computation of Antenna Pattern	1.87 seg	1.87 seg
Memory of Matrix solver	$16 * N^2$ bytes = 6.5 MB **	$16 * N^2$ bytes = 6.5 MB **
Max. required RAM	7 MB Aprox.	7 MB Aprox.

** N = 653 unknowns for the classical patch and 639 for the optimized patch.

Table 5 Simulation requirements for the PC

7- Discussion

As explained above, both antennas were modelled and meshed using GiD software, which is a very user-friendly program and it was not difficult to design the antennas and to discretize them.

The simulations of section 5 proved that FIESTA is an efficient tool for analyzing patch antennas with a very low cost computation.

The level of agreement between the measurements and simulations was good. The finite grounded plane was not possible to implement by FIESTA, and due to the fact that we used an infinite ground approximation, the antenna pattern and the reflection coefficient showed some differences.

In the classical antenna, the reflection coefficient, the E-plane radiation pattern, and the H-plane co-polar pattern showed a good agreement. The H-plane cross-polar pattern was 5db below the measured one.

For the optimized antenna, the reflection coefficient showed differences specifically after 9.4GHz, and the radiation pattern differed between both results less than 3db at any angle. In both cases, the co-polar H-plane results agreed between measured and simulated.
The E-plane cross-polar pattern was 60db below the co-polar maximum.

The simulations were obtained by FIESTA with very low computation requirements, the antenna dimensions were not redefined and all simulation parameters were set to the values suggested by IETR.

The results presented here were obtained in a first run, without previous test simulations.
After that first run, we checked that computing [Z] with 4 integration points per all source triangles and 4 per all test triangles produced the same result as the first run, that was obtained by the default FIESTA parameter Rinteg = 2mm.

14- SYNTHESIS OF RESULTS

Participants and simulations tools

-. The structure proposed by IETR has been simulated by **9 participants** for a **total of 11 simulation results** (2 participants provided 2 different results).

- 7 results were obtained with in-house tools and 4 with commercial tools:

- **IETR** (Institut d'Electronique et Télécommunications de Rennes) :
  Method : **SAPHIR** (Integral Equation Formulation and method of moments)
- **EPFL** (Ecole Polytechnique Fédérale de Lausanne) :
  Method : **POLARIS** (Integral Equation Formulation and method of moments)
- **CNRS-LEAT** (Laboratoire d'Electronique, Antennes et Télécommunications)
  Method: **FP-TLM** (Transmission Line Matrix method)
- **KUL** (Katholieke Universiteit Leuven):
  Method: **MAGMAS** (Integral Equation Formulation and method of moments)
- **LIVUNI** (University of Liverpool)
  Method: **ANSOFT HFSS** (Finite Element commercial software)
- **UNIBRIS** (University of Bristol):
  Method : **FDTD32** (Finite- Difference Time Domain).
- **UPV** (Universidad Politécnica de Valencia)
  Method: **IE3D** (Method of moments, commercial software)
- **UPV** (Universidad Politécnica de Valencia)
  Method: **In-house Software** (Fast method of moments)
- **IDS** (Ingegneria Dei Sistemi S.p.A)
  Method: **ADF** (Integral Equation Formulation and method of moments)
- **LIVUNI** (University of Liverpool)
  Method: **CST Microwave Studio** (Transient Finite Integration)
- **UPC** (Universidad Politécnica de Catalunya)
  Method: **FIESTA 3D** (Fast method of moments)

Main comments

7 results over 11 have been obtained using MoM based software tools (both in-house and commercial) which demonstrates such a method is particularly mature for the analysis of purely planar antennas.
For all these frequency domain solvers, the typical CPU time per frequency point is less than 1 minute and can be only a few seconds for methods with accelerating routines.

The 4 other results have been obtained with 3D solvers using time domain methods (except HFSS which is a 3D frequency domain method). The total CPU time is usually much larger since these methods are not particularly optimized for the analysis of planar structures. It must also be pointed out that the structure exhibits a narrow bandwidth which does not permit to fully benefit from the advantage of TD methods.

The agreement is usually good for return losses. Slight frequency shifts can be observed when the mesh density is released. This parameter appears as a very important one, especially for the GA optimized structure whose shape is irregular. It seems TD methods require a finer mesh than FD methods.

The agreement for radiated fields is not so good : simulated cross-polar is usually much lower than measured one. Most tested tools (especially MoM-based codes) predict the increase of the cross-polar level that is observed for the GA-optimized patch. However, a few ones predict an opposite behaviour. It must be pointed out that the agreement for radiated field is improved when the finite dimensions of the ground plane are taken into account (see KUL simulations).

None of the tested codes include the modelling of the connector in its simulation. This can also explains discrepancy with measured results.

To sum up, all the tested codes give acceptable results but the best agreement is not obtained with the same tool for VSWR and radiated patterns. MoM-based codes appear particularly efficient for such planar structures. More general 3D methods can also be applied but usually require a larger CPU time. The modelling of the excitation and the ability to account for finite dimensions (ground plane and substrates) are two major issues. Fine meshes are required when irregular geometries are involved (GA optimized structure).

BENCHMARKING ACTIVITY

(WP1.1-2)

Linear microstrip array of aperture-coupled patches

Proposed by
University of Siena
- UNISI -

1. STRUCTURE DESCRIPTION

1- Entity

Department of Information Engineering
University of Siena
Via Roma 56
53100 Siena (Italy)

Contact person
Alessio Cucini
Phone +39 0577 46124
Fax +39 0577 233609
E-mail cucini@dii.unisi.it

2- Name of the structure

Microstrip linear array antenna

3- Generalities

The linear array is composed by 4 microstrip rectangular patches with an aperture-coupled excitation. It operates in the IMS band (5.725-5.85) GHz, with linear vertical polarization.

4- Structure Description

The antenna is composed by a linear array of 4 (four) rectangular patches printed on a dielectric support. Each patch is aperture-coupled to the microstrip line. A common ground plane separates the radiating part from the microstrip feeding network. The network is composed by 3 inline power dividers: the first divider is symmetric, while the other two are asymmetric 1:049 dividers. Consequently the excitation amplitudes are 0.7,1,1,0.7. The elements are in phase. The microstrip line is fed by a port.
The dielectric stratification is shown in Fig. 1. The parameters of the various layers (material, dielectric constant, loss tangent, and thickness) are reported in Table 1.
Next, in Fig. 2, a three-dimensional view of the structure is presented, showing the dielectric stratification and the antenna. A top view of the array antenna is shown in Fig. 3, with the radiating patches, the coupling apertures on the ground plane and the microstrip feeding network . In the figure the feeding point is shown. The excitation is provided by means of a gap source at the input port. Only one (dominant) mode is allowed at the input port.
Each layer is presented next, together with a table containing the dimensions (in millimetres) of the geometrical parameters of the structure. In particular, the radiating

patches are described in Fig. 4 and in Table 2, the coupling apertures are described in Fig. 5 and in Table 3, and the microstrip network is described in Fig. 6 and in Table 4.
The layers files are available in DXF data format.

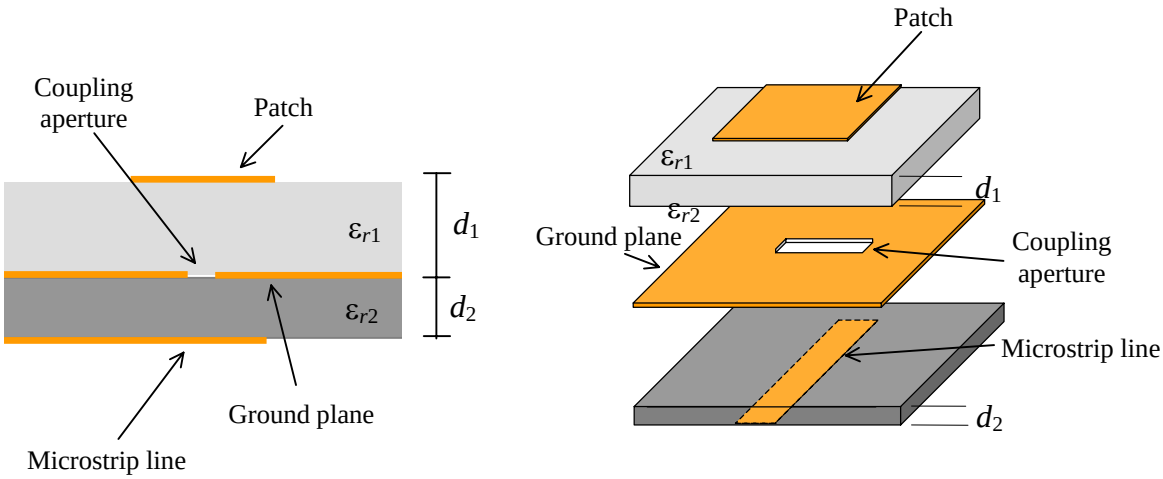

Fig. 1 Dielectric stratification (left) and exploded view of the structure (right). The copper metallization is assumed to have zero thickness.

Table 1 Material table of the dielectric layers: dielectric constant, loss tangent, thickness.

	Material	Dielectric constant @ 10 GHz	tgδ @ 10 GHz	Thickness (mm)
1	Taconic TLY5	2.18	0.0009	2.339
2	GIL GML1000	3.2	0.004	0.762

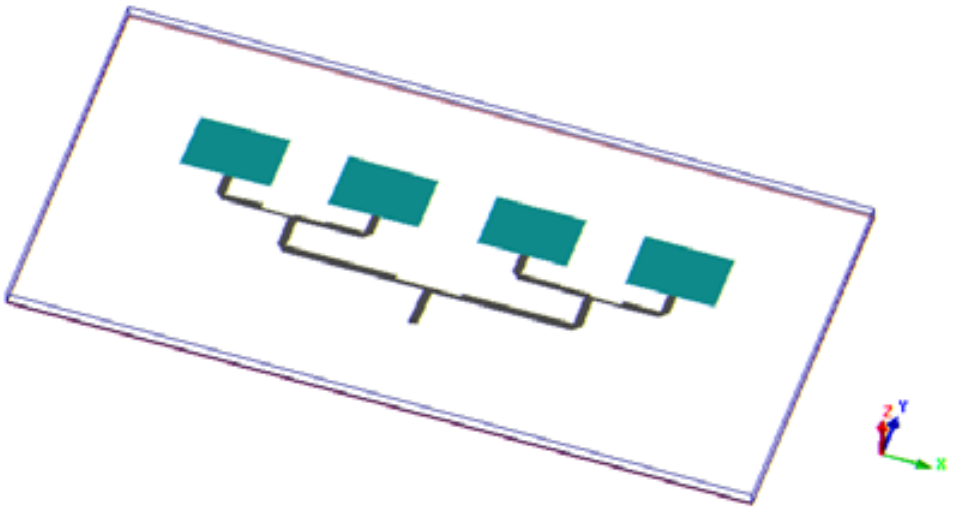

Fig. 2 3D view of the microstrip array structure.

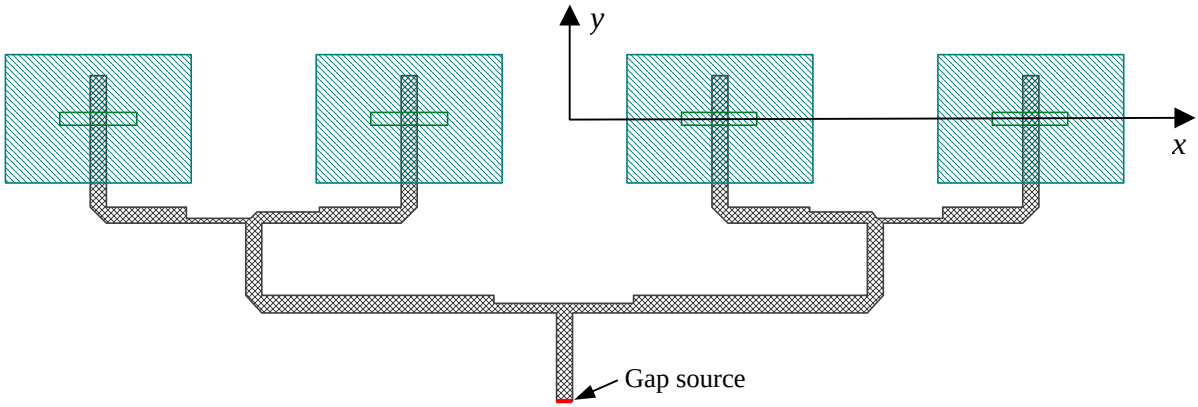

Fig. 3 Top view of the microstrip array structure: patches, apertures and microstrip network.

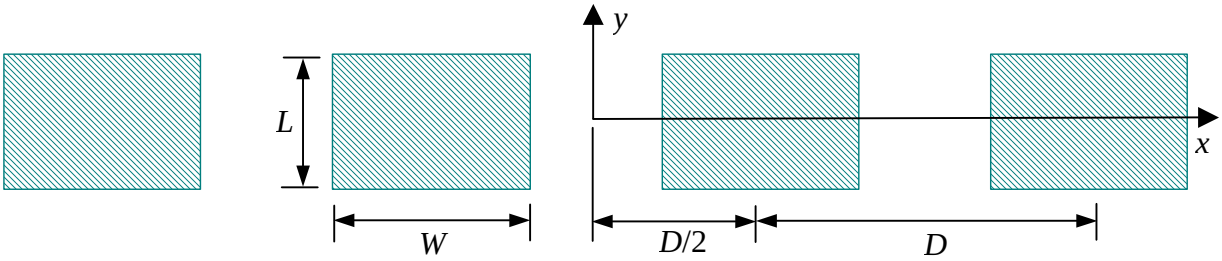

Fig. 4 Top view of the array of radiating patches

Table 2 Dimension table: radiating patches

Parameter	Dimension (mm)
L	14.4
W	21
D	35.145

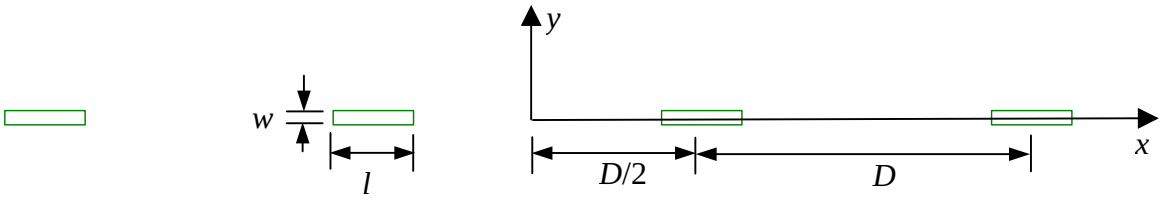

Fig. 5 Top view of the apertures on the round plane

Table 3 Dimension table: apertures on ground plane

Parameter	Dimension (mm)
l	8.57
w	1.5

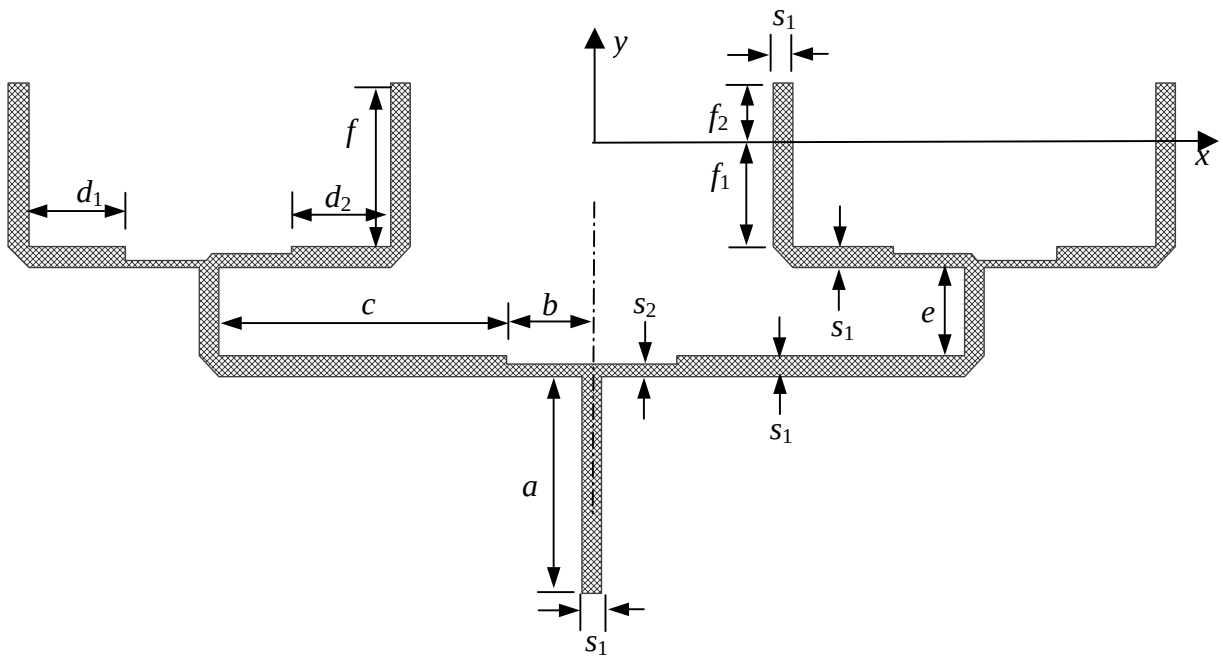

Fig. 6 Top view of the microstrip feeling network.

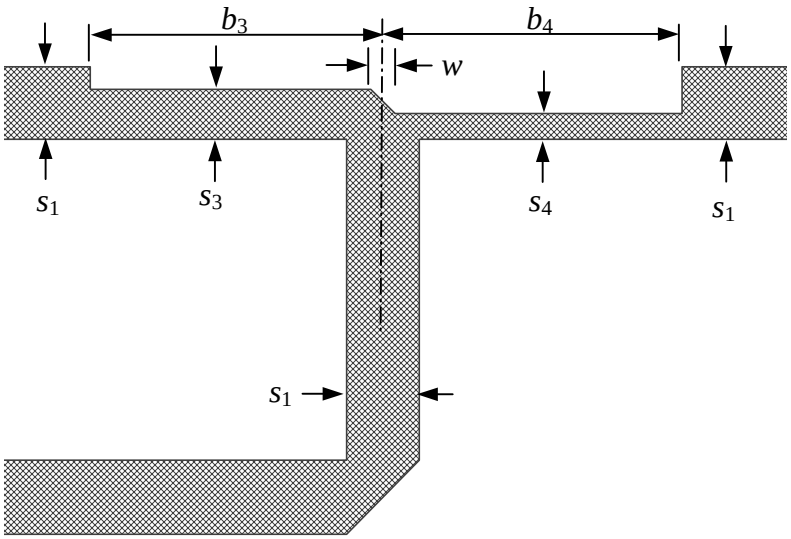

Fig. 7 Top view of the microstrip asymmetric 1:049 power divider.

Table 4 Dimension table: microstrip feeding network

Parameter	Dimension (mm)
s_1	1.855
s_2	1.03
s_3	1.28
s_4	0.645
a	20
b	7.86
c	26.3575
d_1	8.975
d_2	9.125
e	8.145
f	15
f_1	10
f_2	5
b_3	7.67
b_4	7.52
w	0.58

A prototype antenna has been realized on a finite rectangular multilayer substrate (Fig. 8). The dimensions of the rectangular substrate are reported in Table 5..

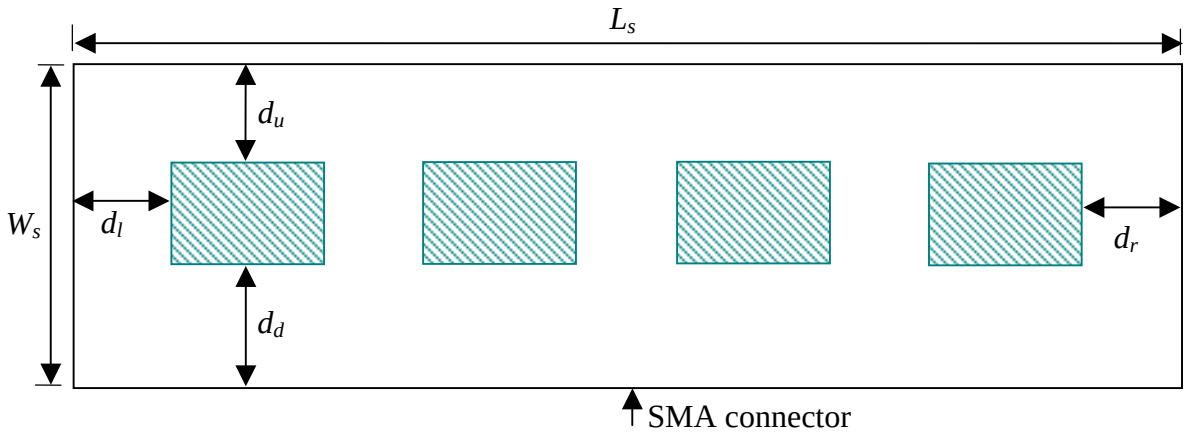

Fig. 8 Top view of the microstrip array antenna, with the finite substrate.

Table 5 Dimension table: finite substrate

Parameter	Dimension (mm)
L_s	186.435
W_s	78.9
d_u	30.0
d_d	34.5
d_l	30.0
d_r	30.0

5- Computed results

Numerical simulations have been performed using the software Ansoft™ Designer v 1.0, based on the Method of Moments.
The results that have been computed are:

- S-parameters (reflection coefficient)
- Far field (H-plane normalized pattern, maximum gain)

6- References

Experimental results will be available.

7- Additional comments

2. STRUCTURE MEASUREMENTS

Entity

1- Description of measurement tools

A prototype of the antenna has been manufactured at the Laboratory of Applied Electromagnetics of the Department of Information Engineering of the University of Siena. The prototype antenna has been measured. Radiation pattern and gain measurements have been performed at the Polytechnic University of Madrid in the framework of the workpackage WP 1.2.3 (Facility sharing) [1]. Reflection coefficient measurements have been performed at the University of Siena.

[1] M. S. Castañer, Measurement of the Linear Microstrip Array Antenna of University of Siena at UPM, July 2005.

2- Generalities about measurement tools

The antenna pattern and gain have been measured in the antenna measurement facilities of the Technical University of Madrid. These facilities include three anechoic chambers with several antenna measurement systems installed. The first one is a spherical system with a distance between antenna source and AUT equal to 5.3 meters, and rotary joints until 20 GHz. The second chamber has a length of 15.5 meters, and two antenna systems are installed: a Gregorian compact range system, to measure large antennas from 6 GHz and a planar-spherical-cylindrical system to measure from 1 to 40 GHz. This antenna has been measured in the Spherical field system. The measured parameters have been: radiation pattern and gain. The gain is measured by the substitution technique (with a Standard Gain Horn) and the directivity can be obtained from the radiation pattern measurement (by integrating the pattern).
The reflection coefficient measurements have been performed in the electromagnetic laboratory facilities of the University of Siena. The reflection coefficient and VSWR have been measured using a HP 8720D Network Analyzer.

***3*- Measurements results**

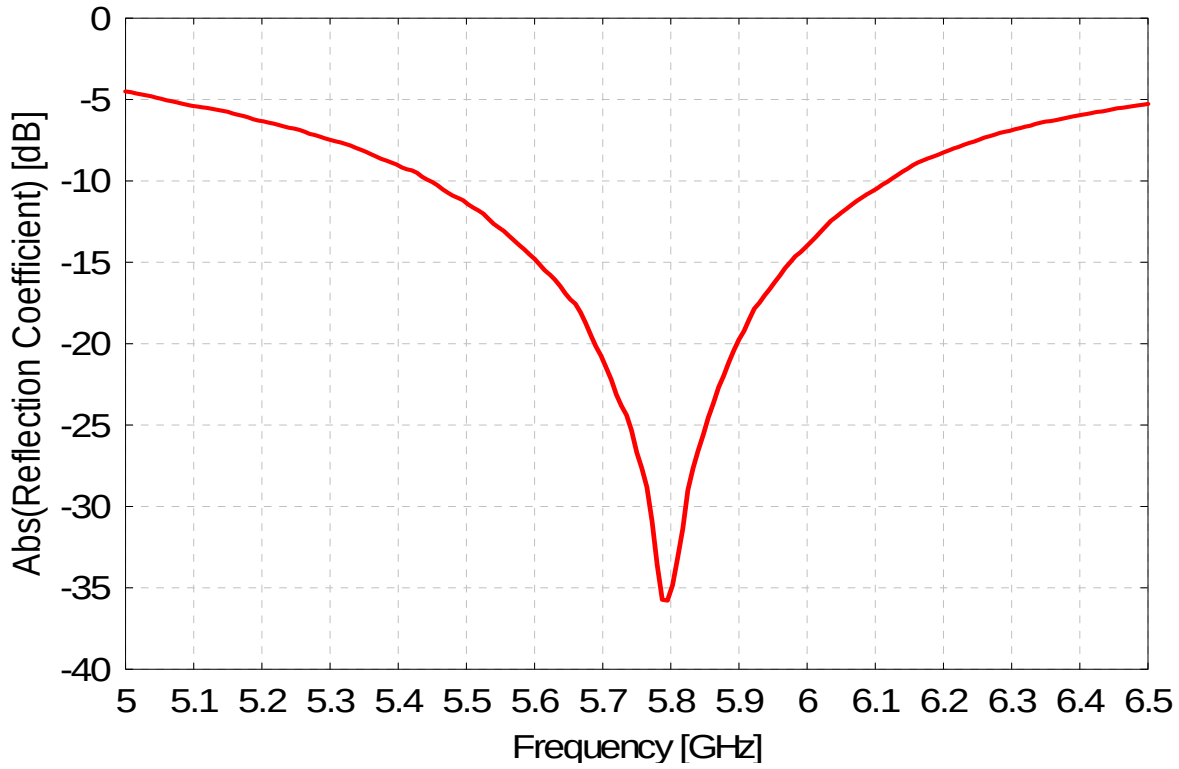

Fig. 9 Reflection coefficient (in dB) at the input port in the frequency range (5.0-6.5) GHz. The reflection coefficient is referred to a 50 Ω port impedance.

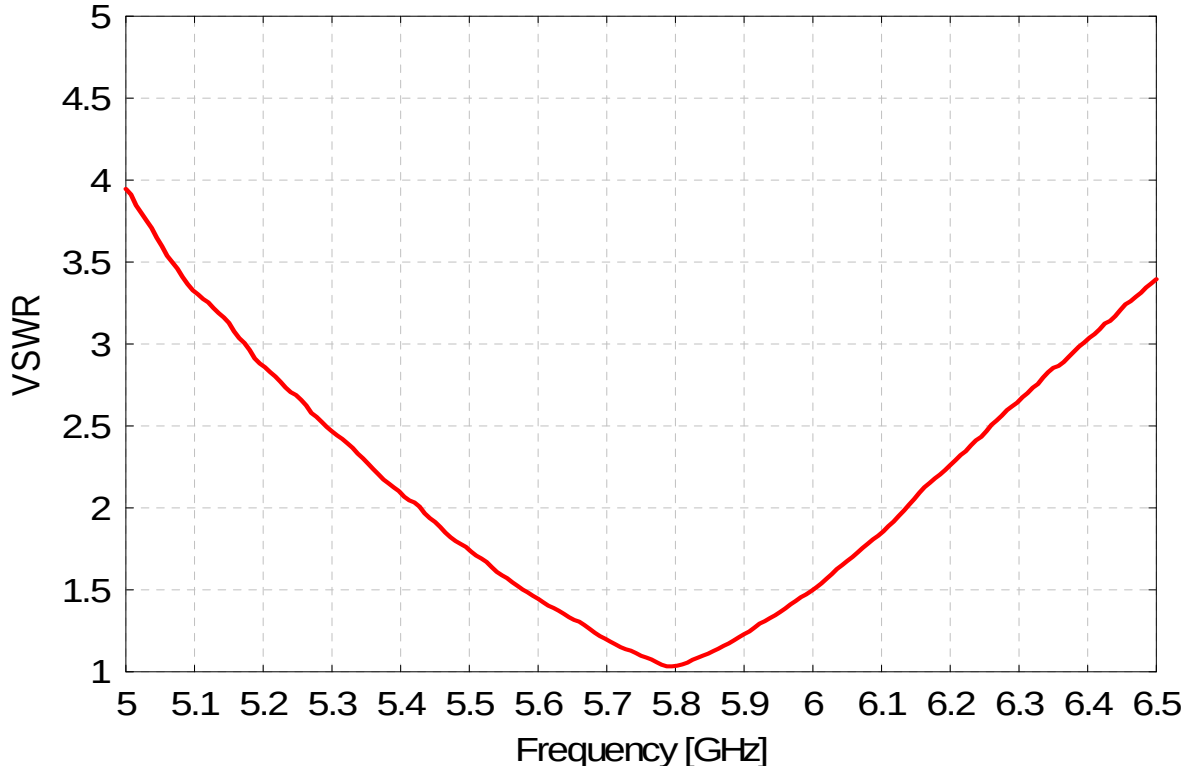

Fig. 10 Voltage standing wave ration (VSWR) at the input port in the frequency range (5.0-6.5) GHz.

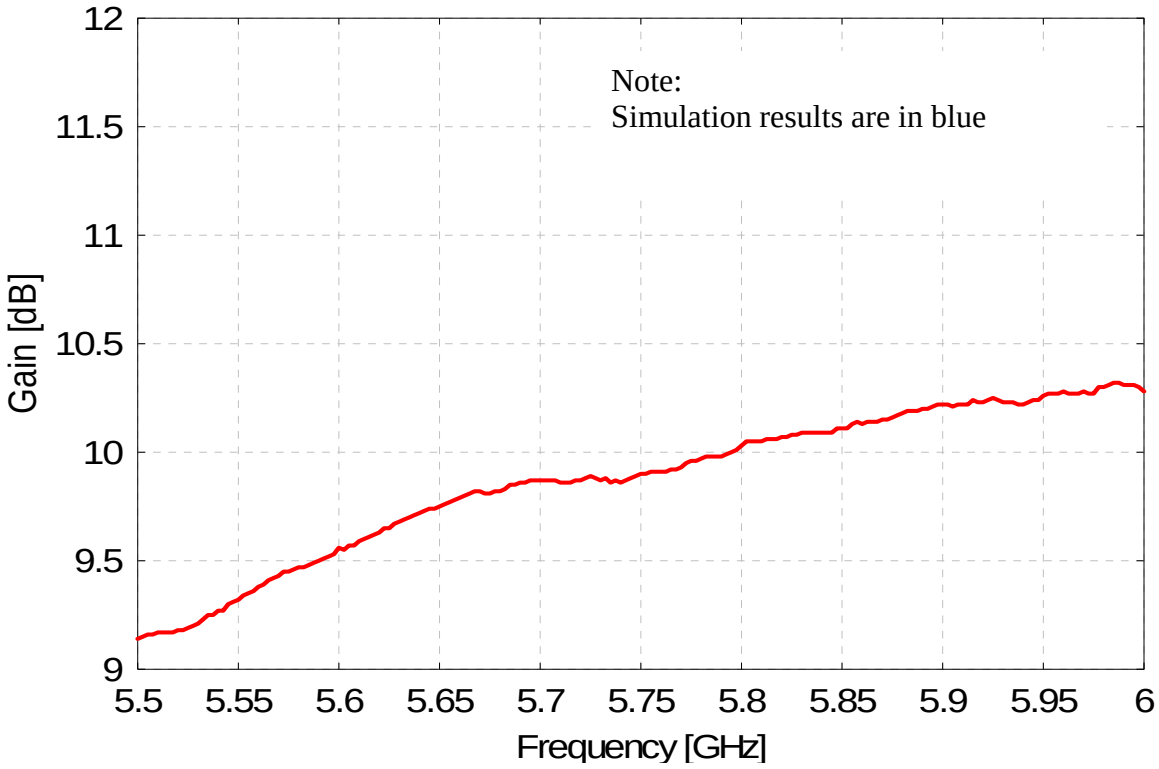

Fig. 9 Maximum gain (in dB) in the frequency range (5.6-6.0) GHz.

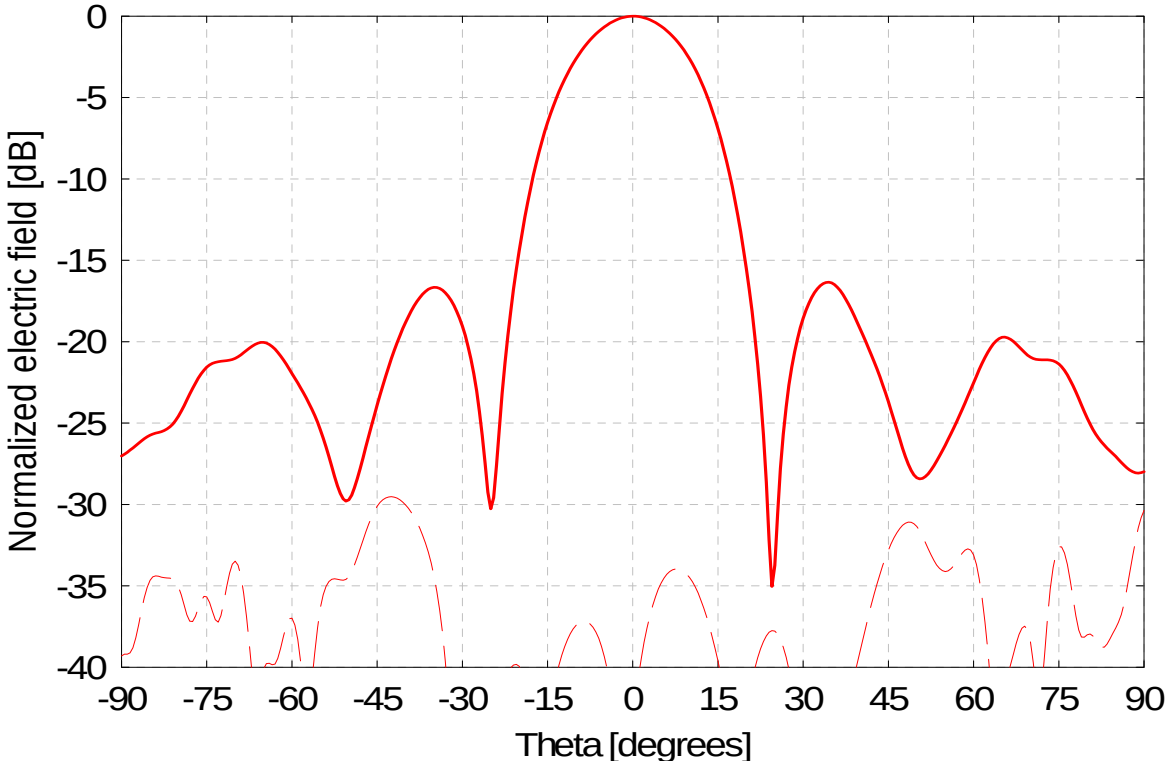

Fig. 10 Normalized electric field in the H-plane ($\varphi = 0°$), computed at the frequency $f = 5.600$ GHz. Co-pol: continuous line; X-pol: dashed line.

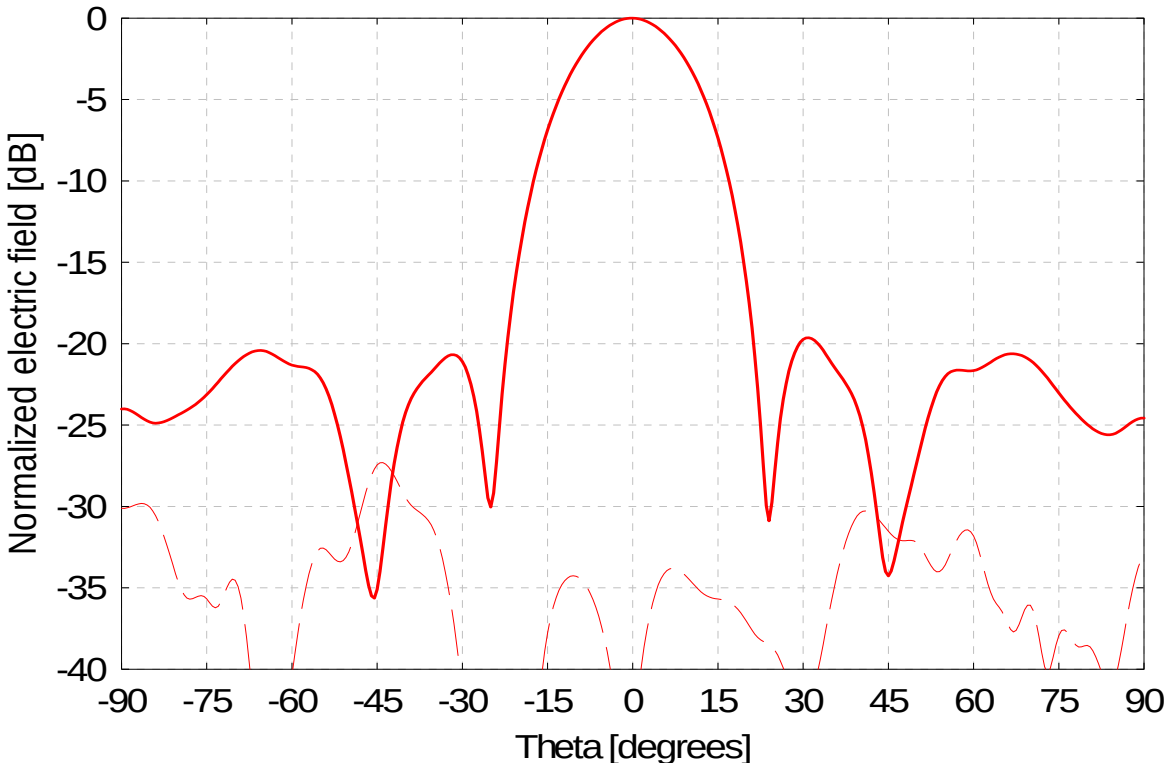

Fig. 11 Normalized electric field in the H-plane (φ = 0°), computed at the frequency *f* = 5.800 GHz. Co-pol: continuous line; X-pol: dashed line.

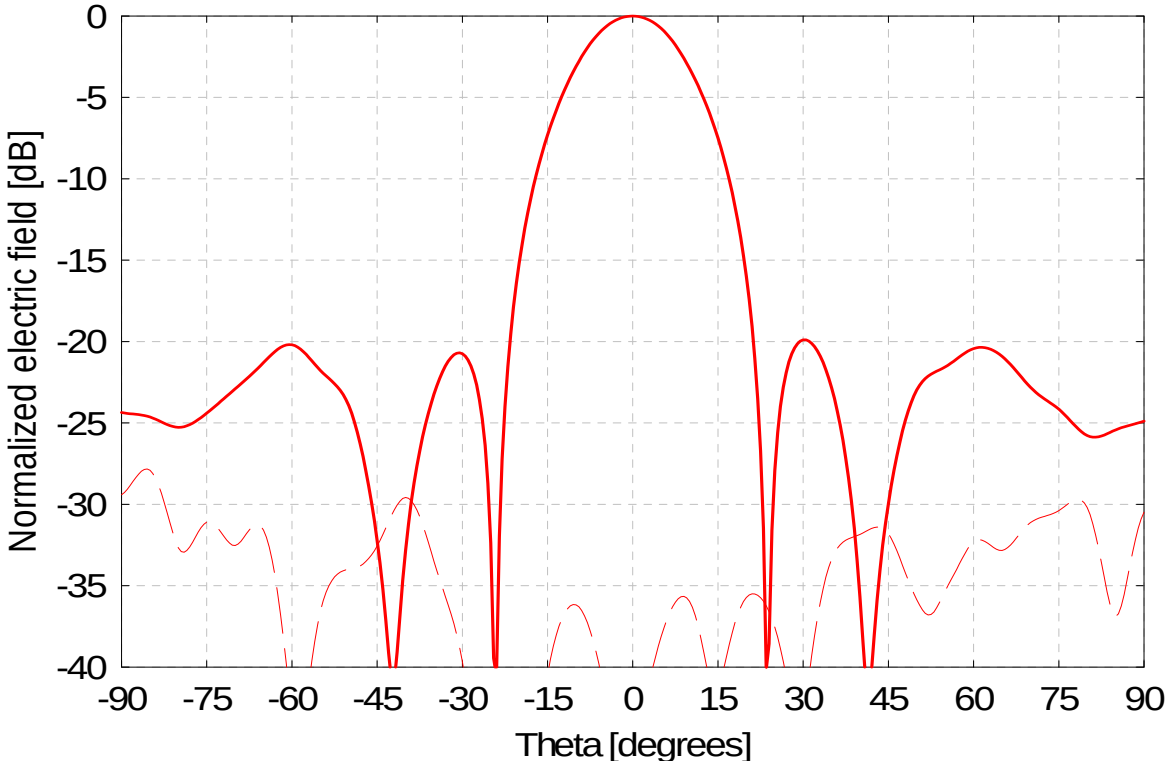

Fig. 12 Normalized electric field in the H-plane (φ = 0°), computed at the frequency *f* = 6.000 GHz. Co-pol: continuous line; X-pol: dashed line.

3. SIMULATION RESULTS
From UNISI

1- Entity

Department of Information Engineering
University of Siena
Via Roma 56
53100 Siena (Italy)

Contact person
Alessio Cucini
Phone +39 0577 46124
Fax +39 0577 233609
E-mail cucini@dii.unisi.it

2- Name of the simulation tool

Ansoft™ Designer™.

3- Generalities about the simulation tool

The design of the antenna has been performed using Ansoft Designer. This commercial software is based on the Method of Moments in the frequency domain. The software is devoted to the analysis of planar stratified structures.

4- Simulation Set-up (Geometry set-up, GUI, mesh, boundary conditions, excitation)

The geometry is defined using the CAD of the software.
The software assumes that the dielectric stratification is infinite along the transverse direction.
The metallic parts and the apertures in the infinite ground are meshed into triangles. The mesh has been done at higher frequency of the band (6.5 GHz).
RWG basis functions are used to expand the unknown electric and magnetic current.
The analysis is performed in the frequency domain. A discrete frequency sweep has been used (61 points in frequency). Also, the currents on the structure are computed.

5- Simulation results

The results that have been computed are:

- Input port parameters (input reflection coefficient, VSWR)
- Gain

The input port parameters are computed at the input port, with a normalization impedance of 50Ω. Results are shown in Fig. 13 (magnitude of the reflection coefficient in dB) and in Fig. 14 (voltage standing wave ratio, VSWR), computed in the frequency band (5.0-6.5) GHz.

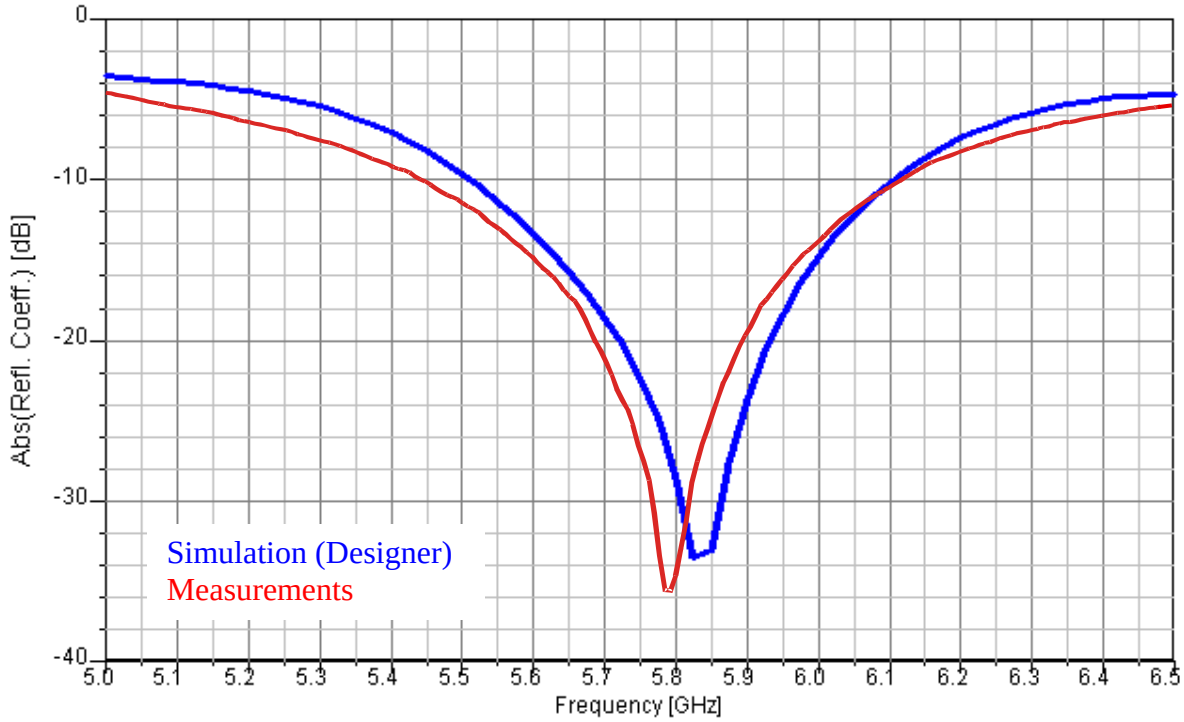

Fig. 13 Reflection coefficient (in dB) at the input port in the frequency range (5.5-6.0) GHz.

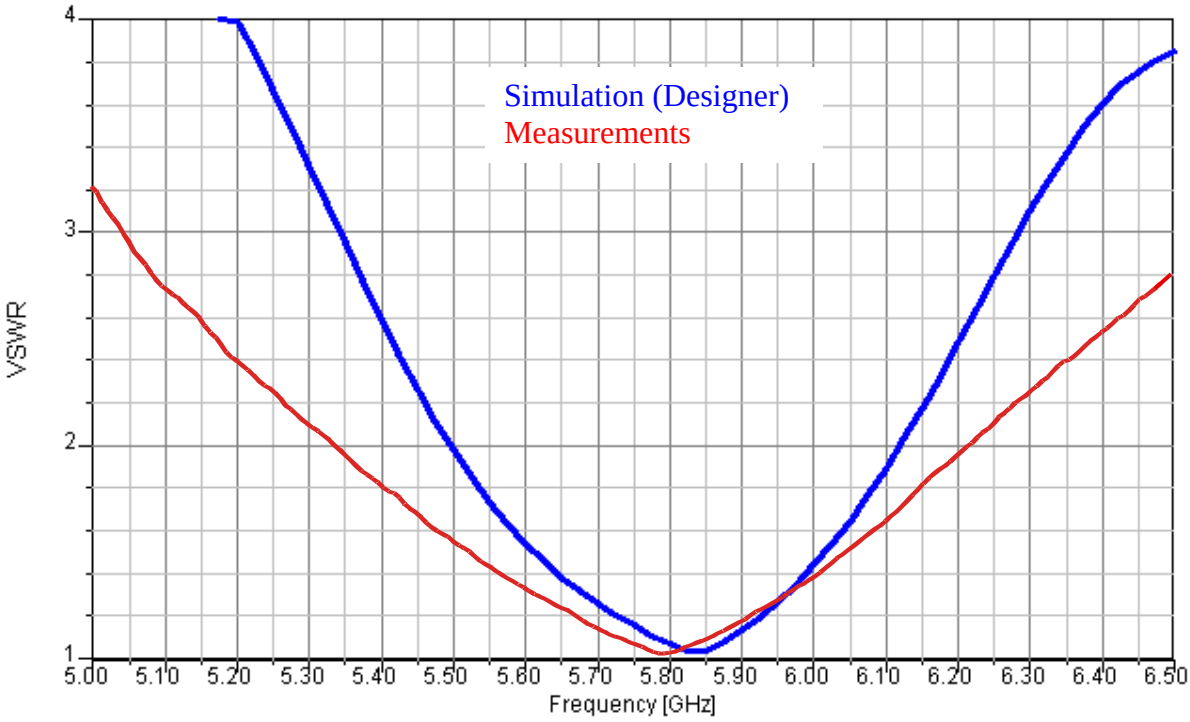

Fig. 14 Voltage standing wave ratio (VSWR) at the input port in the frequency range (5.5-6.0) GHz.

The following figures show results relevant to the computer gain. In Fig. 9, the maximum gain (computed at the angle $\theta = 0°$) is shown, for the frequency band (5.5-6.0) GHz. In Fig. 10-Fig. 18, the gain on the plane $\varphi = 0°$ (H-plane) is shown, at the frequencies of 5.600, 5.800, and 6.000 GHz, respectively.

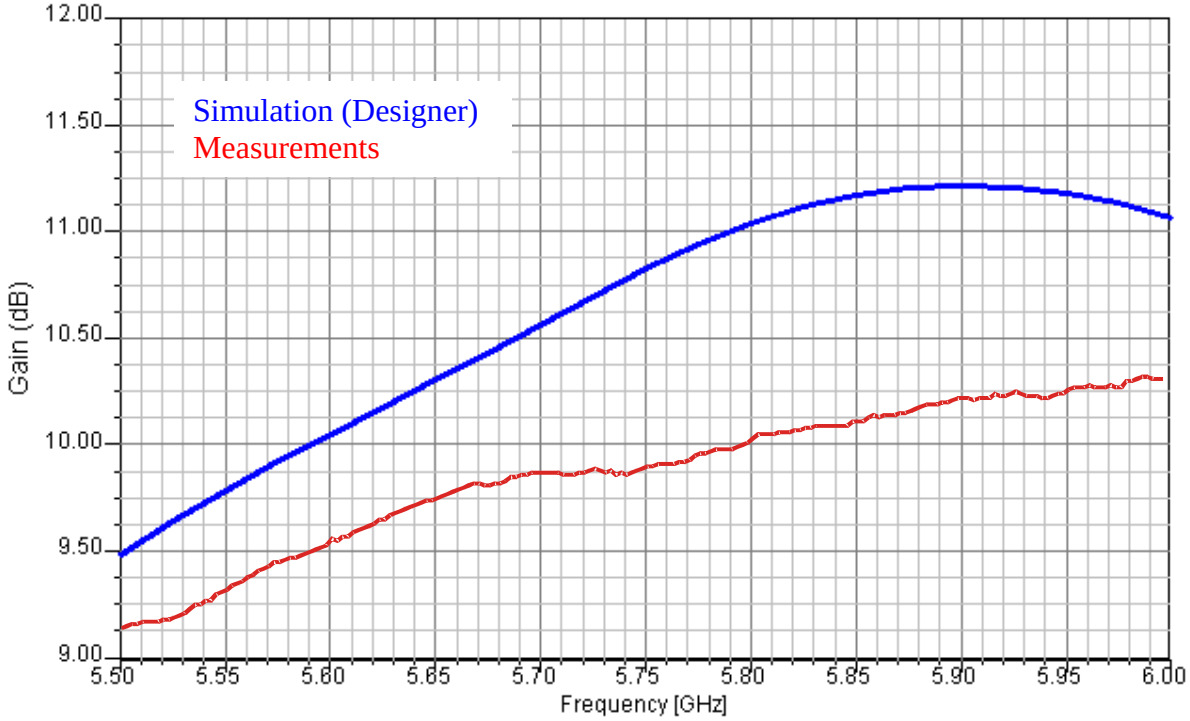

Fig. 15 Maximum gain (in dB) in the frequency range (5.5-6.0) GHz.

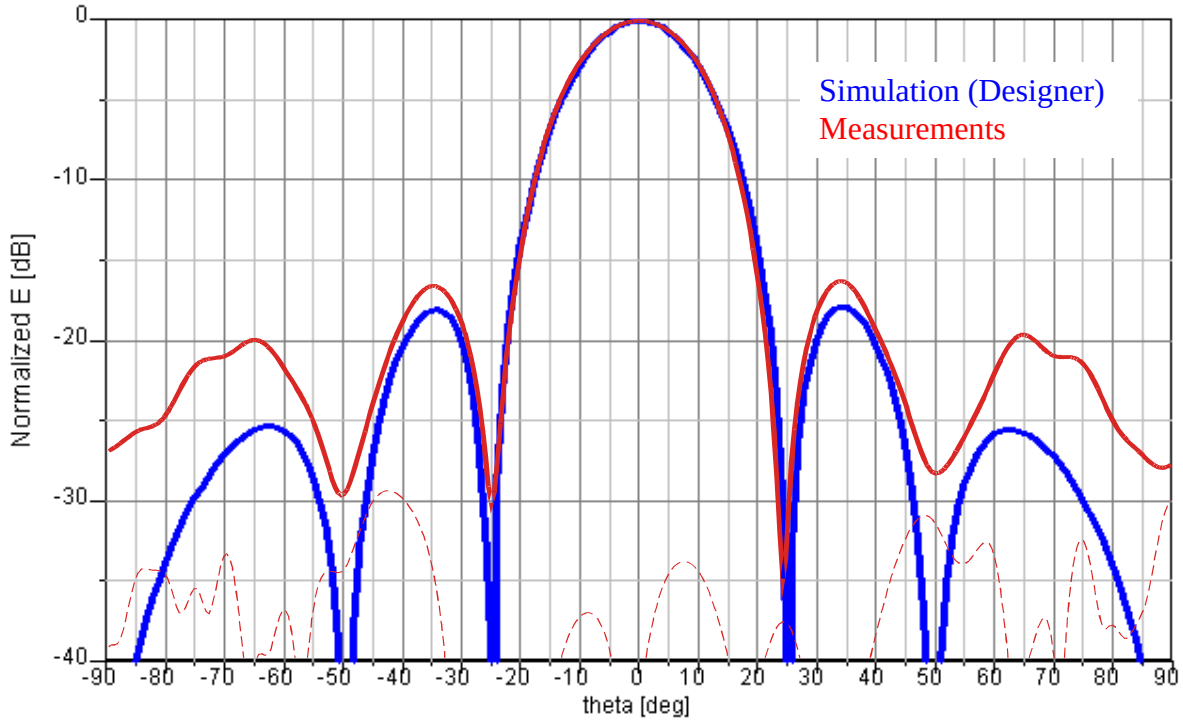

Fig. 16 Gain in the H-plane (φ = 0°), computed at the frequency *f* = 5.600 GHz.

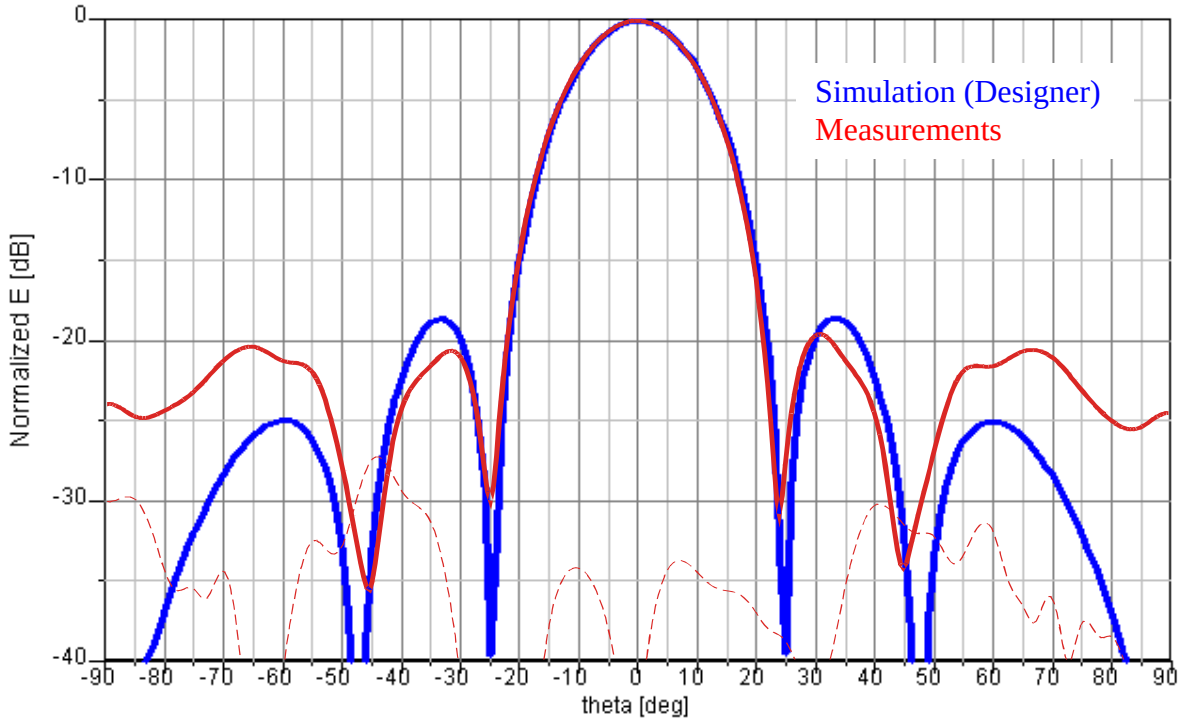

Fig. 17 Gain in the H-plane (φ = 0°), computed at the frequency *f* = 5.800 GHz.

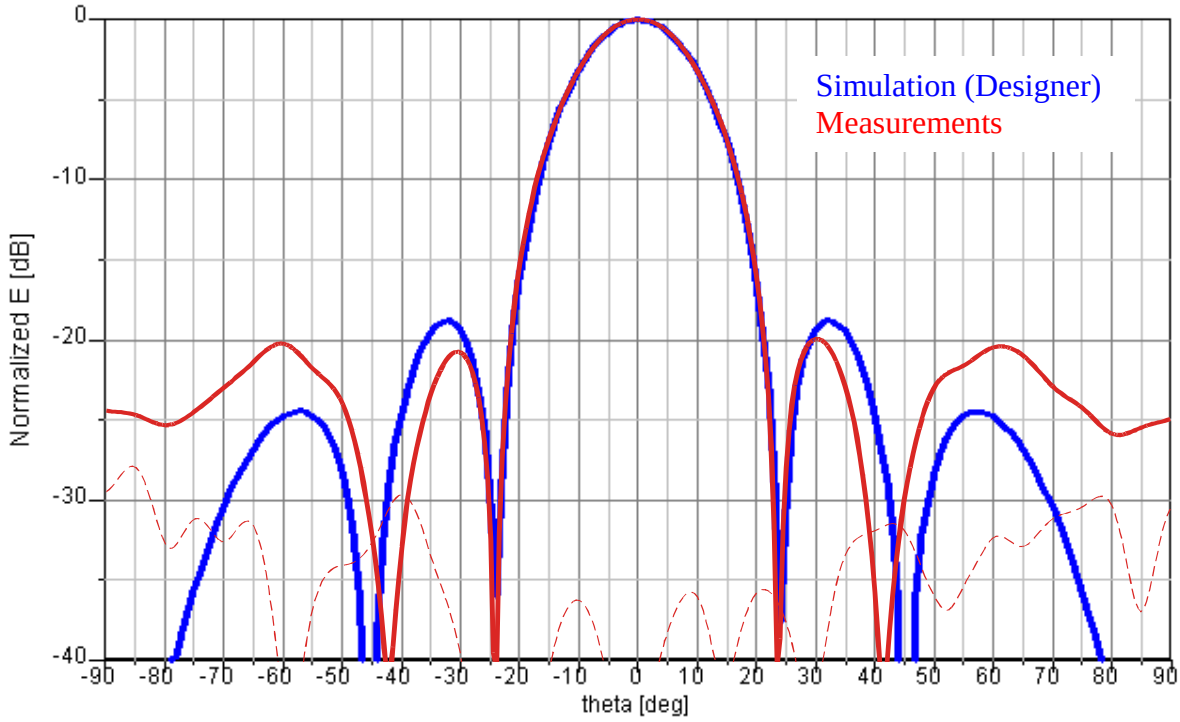

Fig. 18 Gain in the H-plane (φ = 0°), computed at the frequency *f* = 6.000 GHz.

6- Computation resources

The simulation has been performed on two different computers, a laptop and a desktop. The data relevant to the two computers are reported in the following tables.

Table 6 Properties of the *laptop* used for the simulation

Type of machine	Laptop PC
Number of CPUs	1 Intel Pentium 4
CPU Speed	3.2 GHz
RAM	512 MB
OS	Win XP Home

Table 7 Properties of the *desktop* used for the simulation

Type of machine	Desktop PC
Number of CPUs	1 Intel Pentium 4
CPU Speed	3.4 GHz
RAM	1 GB
OS	Win XP Pro

The simulation is performed over 61 discrete points in frequency (in the range 5.0 – 6.5 GHz). Data relevant to the simulation are listed in the following tables, for the laptop and for the desktop, respectively.

Table 8 Simulation requirements for the *laptop* PC

Total CPU time	1h 04’ 03’’
Average CPU time per frequency point	1’ 03’’
Max. required RAM	105992 K
Number of unknowns	2420
Number of triangles	1737

Table 9 Simulation requirements for the *desktop* PC

Total CPU time	43’ 23’’
Average CPU time per frequency point	43’’
Max. required RAM	107562 K
Number of unknowns	2420
Number of triangles	1737

7- Discussion

8- Additional comments

4. SIMULATION RESULTS
From IETR (IMELSI)

1- **Entity**

Institut d'Electronique et Télécommunications de Rennes (IETR)

CNRS UMR 6164

Université de Rennes 1, ***Campus de Beaulieu, Bât 11 D***

263, av. du Général Leclerc

35042 Rennes Cedex, France

Contact persons :
Sylvain Collardey
Phone : +33(0)2 23 23 56 69
Fax : +33(0)2 23 23 69 63
Email : sylvain.collardey@univ-rennes1.fr

2- **Name of the simulation tool**

IMELSI IMpulsionnal ELectromagnetic SImulator (FDTD)

3- **Generalities about the simulation tool**

IMELSI employs the finite difference in time domain method in order to generate an electromagnetic field solution. The FDTD method divides the full problem space into thousands of smaller cubic regions.

4- **Simulation Set-up (Geometry set-up, GUI, mesh, boundary conditions, excitation)**

Describe shortly how the geometrical structure was input into your software:

- I have drawn the structure using the GUI available with your tool

Describe shortly how the meshing operation is performed in your code:

- The mesh is manual and fixed for each simulation
- Give the mesh type: uniform cubic mesh.

Describe shortly the type of boundary conditions and excitation that were used:

Perfectly matched layers (PMLs) are available and are used to simulate open problems that allow waves to radiate infinitely far into space, such as antenna designs.
For the metallic part, I have used perfect metallic material without metallic losses.
For excitation, a lumped port (localised voltage source) associated to a metallic via is used.

Give snapshots, if available, showing the structure and its main features as described in your code, the mesh used for simulation, ...

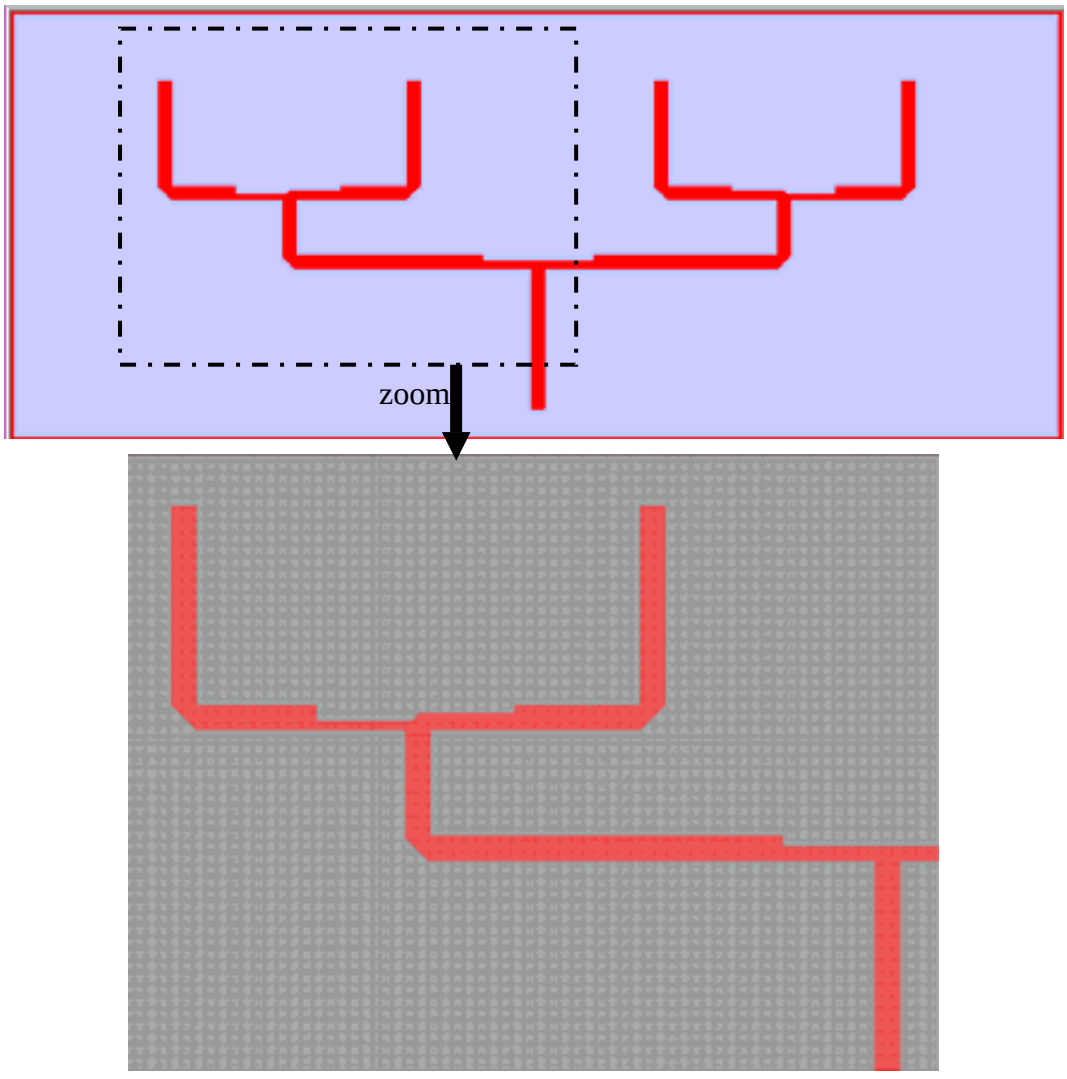

xOy plane (view of feed network)

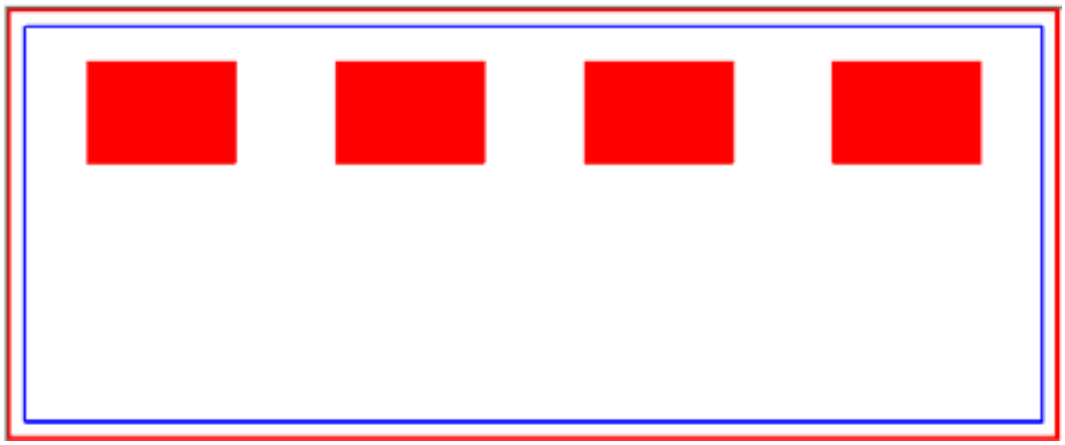

xOy plane (view of antenna array)

How long (approximately) did it take to input the geometry? To set up the rest of the simulation?

About one hour to draw the geometry

And about 5 min to set up the rest of the simulation.

5- Simulation results

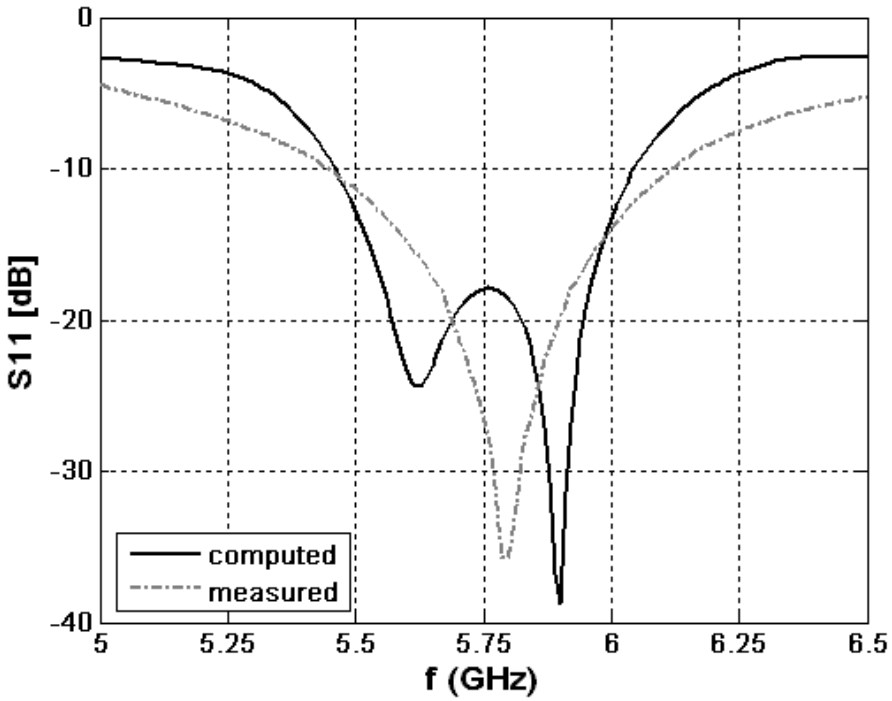

Fig. 19 Reflection coefficient (in dB) at the input port in the frequency range (5.0-6.5) GHz. The reflection coefficient is referred to a 50 Ω port impedance.

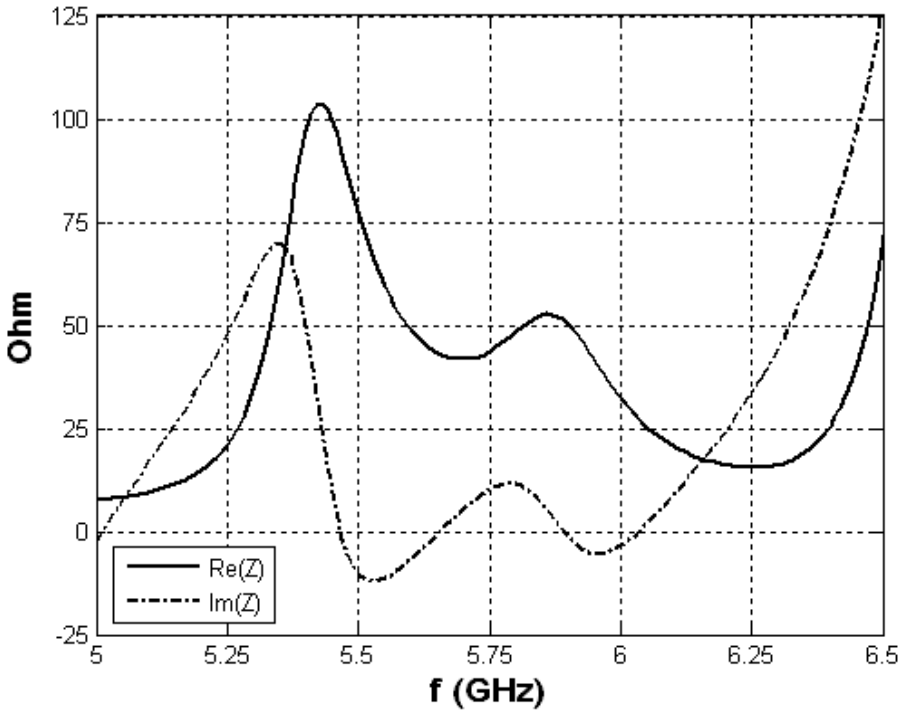

Fig. 20 Computed Real and imaginary part of the input impedance in the frequency range (5.0-6.5GHz).

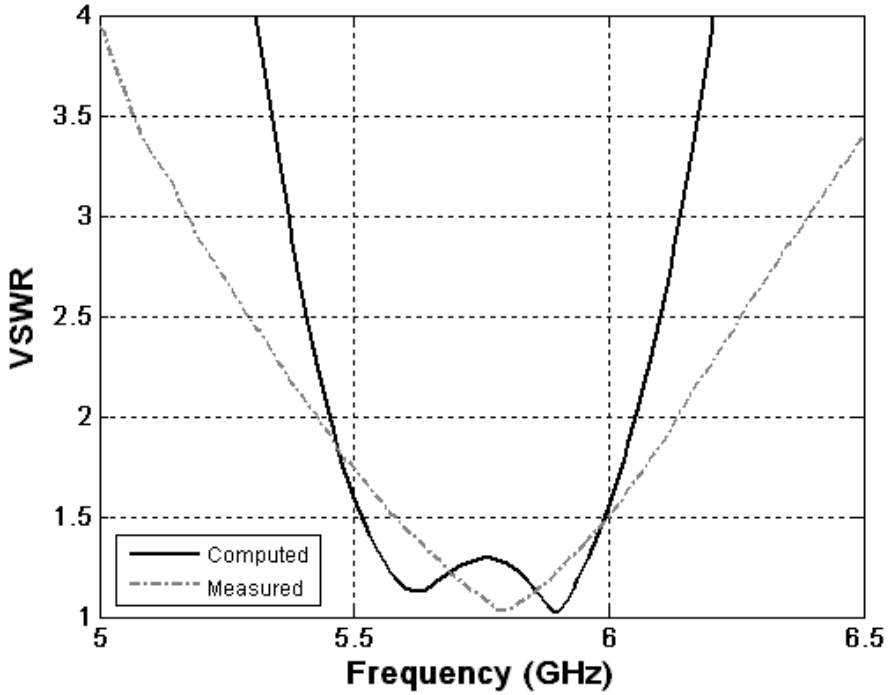

Fig. 21 VSWR in the frequency range (5.0-6.5GHz).

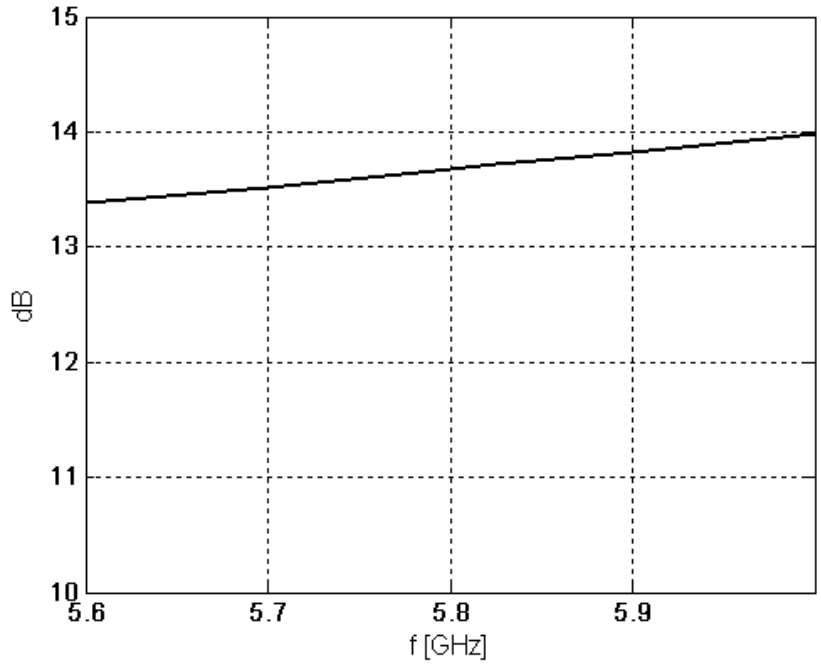

Fig. 22 Directivity (in dB) in the frequency range (5.6-6.0) GHz.

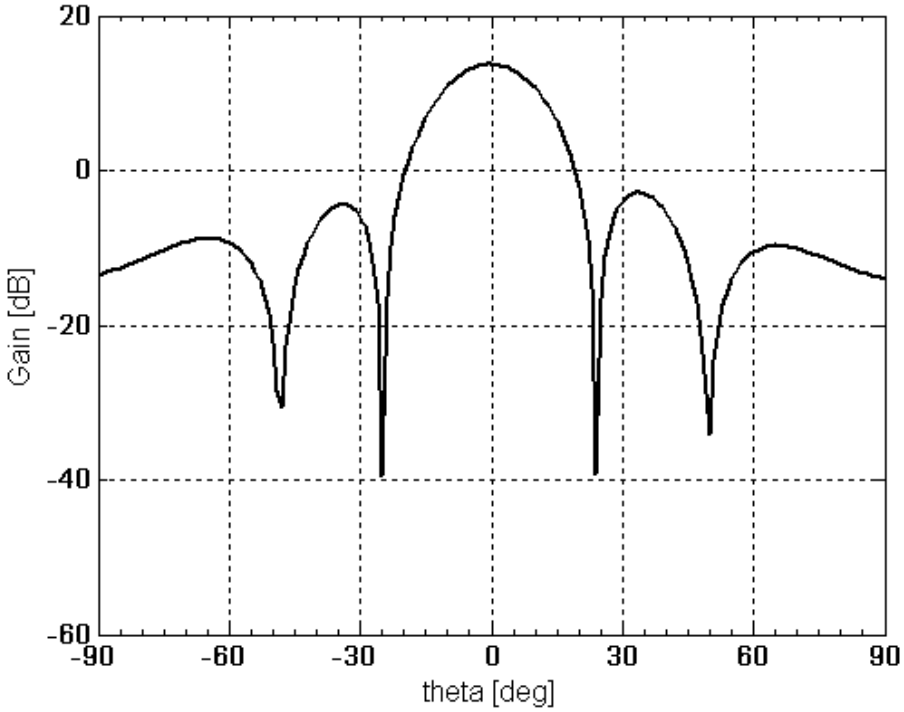

Fig. 23 Directivity in the H-plane ($\varphi = 0°$), computed at the frequency $f = 5.825$ GHz.

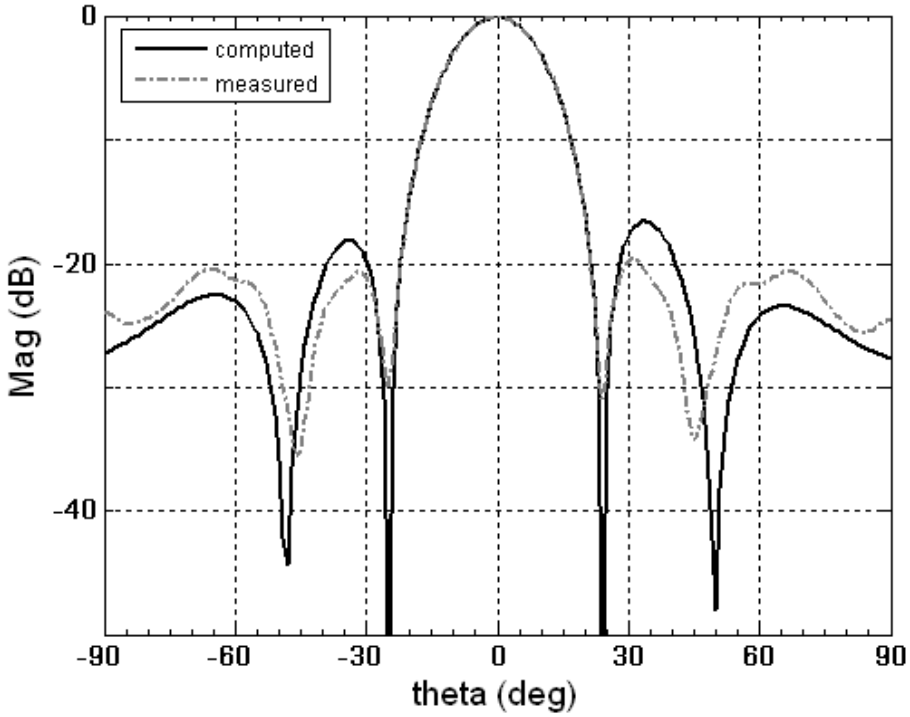

Fig. 24 Normalized pattern in the H-plane (φ = 0°), computed at the frequency *f* = 5.825 GHz.

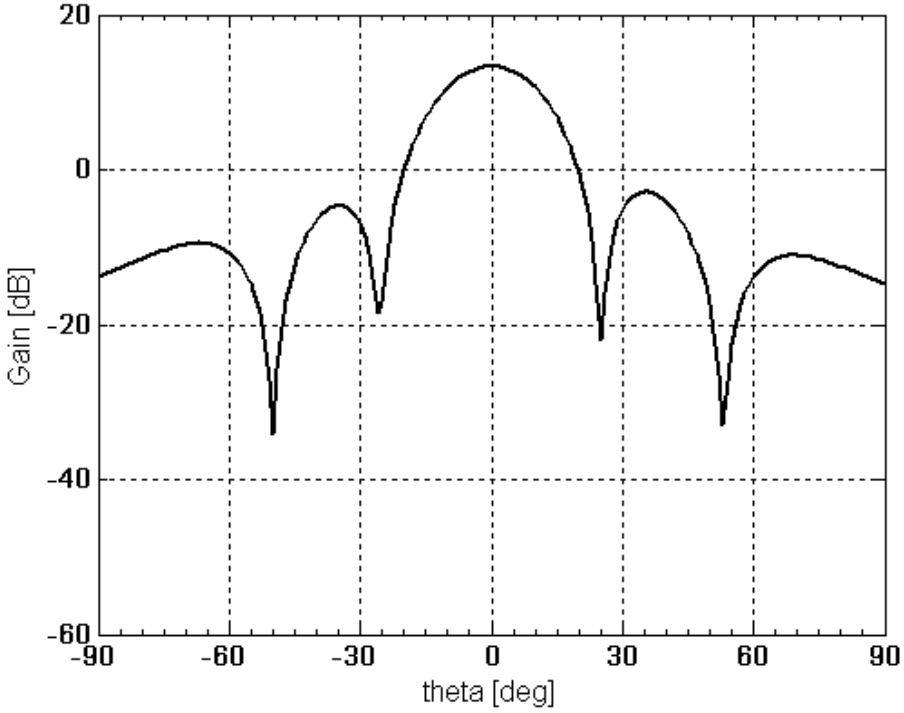

Fig. 25 Directivity in the H-plane (φ = 0°), computed at the frequency *f* = 5.600GHz.

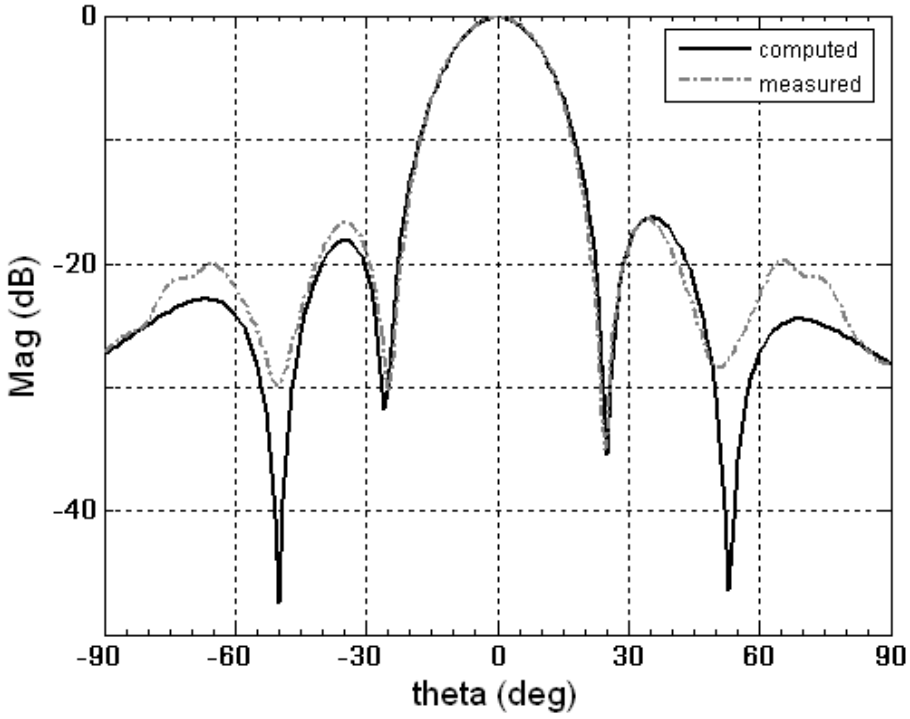

Fig. 26 Normalized pattern in the H-plane (φ = 0°), computed at the frequency *f* = 5.600GHz.

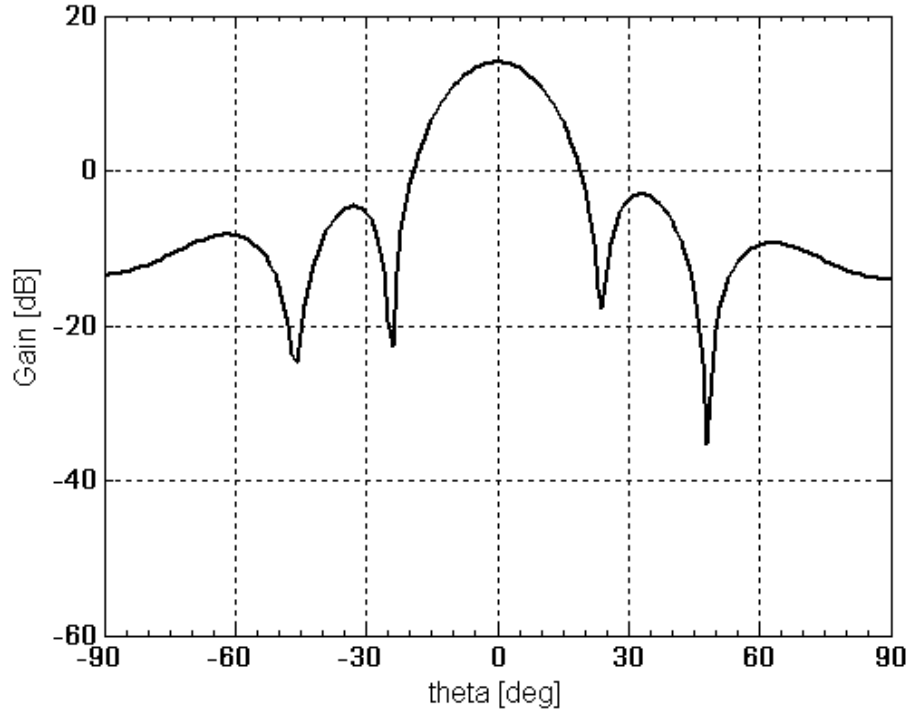

Fig. 27 Directivity in the H-plane (φ = 0°), computed at the frequency *f* = 6.000 GHz.

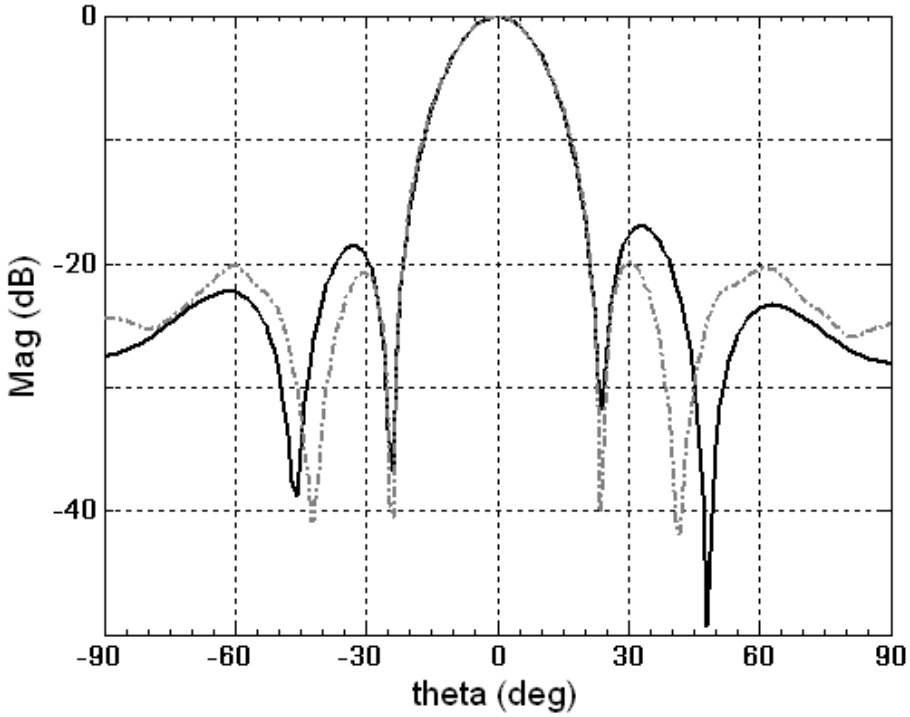

Fig. 28 Normalized pattern in the H-plane ($\varphi = 0°$), computed at the frequency f = 6.000 GHz.

6- Computation resources

The simulations have been performed on PC with one processor at 3GHz and 2Go of memory. The data relevant to the simulation are listed in the following table.

Simulation requirements	Antenna Array
Number of cells	300x740x50
Real Time per simulation	≈ 13h
Memory requirements	1.2Go

7- Discussion

In our case, the antenna array is computed with an infinite ground plane.

8- Additional comments

5. SIMULATION RESULTS
From IETR (MR-FDTD)

1- Entity

Institut d'Electronique et Télécommunications de Rennes (IETR)

CNRS UMR 6164
INSA de Rennes,
20 Avenue des Buttes de Coësmes
35043 Rennes Cedex, France

Contact person :
Romain Pascaud
Phone : +33(0)2 23 23 87 00
Fax : +33(0)2 23 23 84 39

E-mail : romain.pascaud@ens.insa-rennes.fr

2- Name of the simulation tool

MR/FDTD : Multi Region / FDTD

3- Generalities about the simulation tool

The MR/FDTD employs the finite difference in the time domain to generate an electromagnetic field solution. The FDTD method divides the full problem space into thousands of smaller cubic regions.

4- Simulation Set-up (Geometry set-up, GUI, mesh, boundary conditions, excitation)

The structure has been described into a text file that is required by the FDTD software. It has taken about 3 hours to give a correct representation of the array since there is no GUI.

The structure has been automatically meshed while respecting the required size of cells in the three directions (dx = 0.29 mm, dy = 0.32 mm and dz = 0.762). As a consequence, the parameters of the time analysis are dt = 6.6e-13 sec (time step) and Tobs = 5e-09 sec (observation time).

PMLs have been implemented in order to make the simulation of this open problem possible. The metallic part has been designed using perfect metallic material without metallic losses. An infinite ground plane has been taken. Consequently, the Huygens surface for far fields computation only uses 5 faces. The impedance of the source has been chosen to be 50 Ω. Finally, to evaluate the input impedance as well as the return loss, a field probe has been implemented.

The following pictures represent the mesh of the feed network. The first picture is the overall network, whereas the second one presents a small part including the description of the bends.

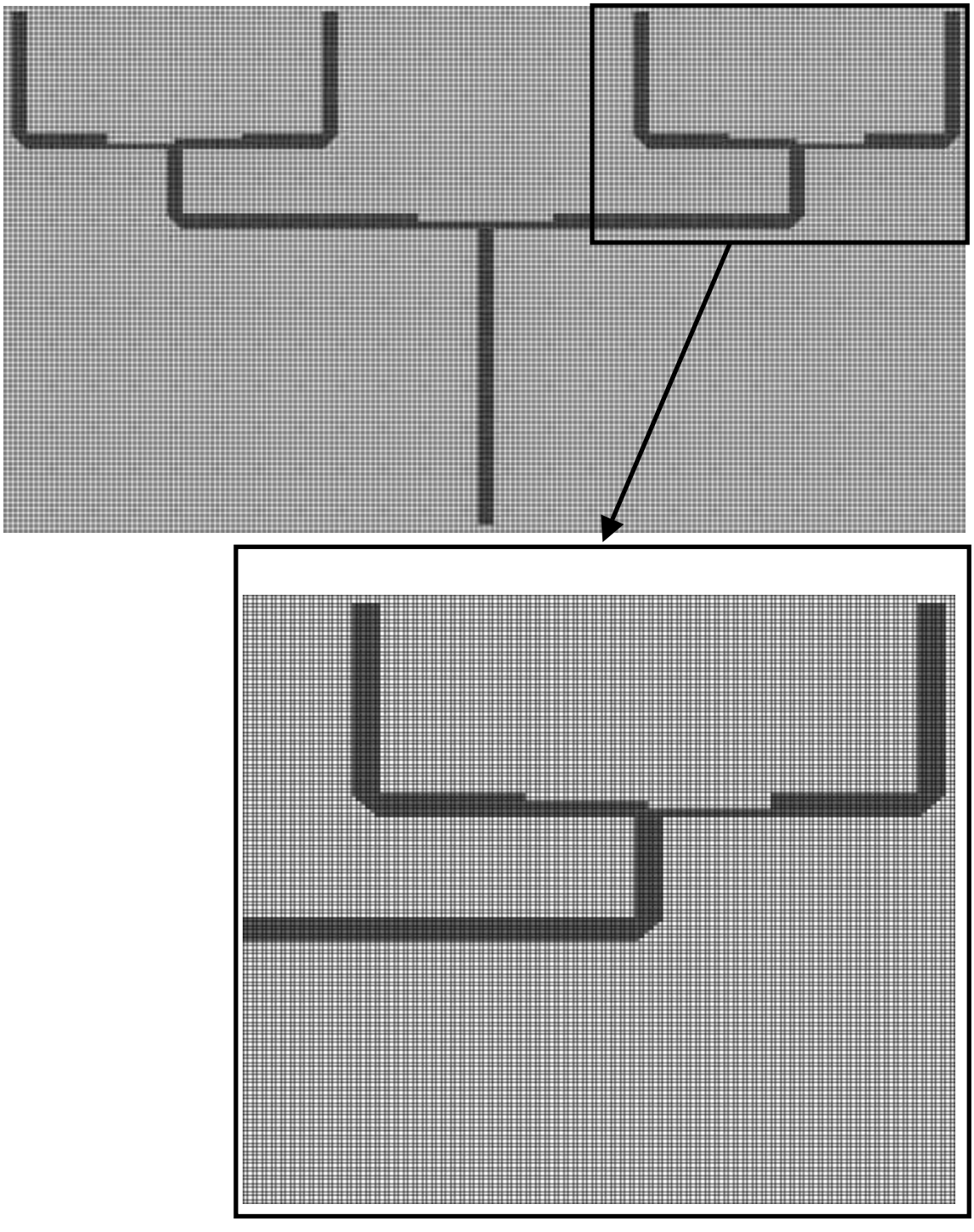

5- Simulation results

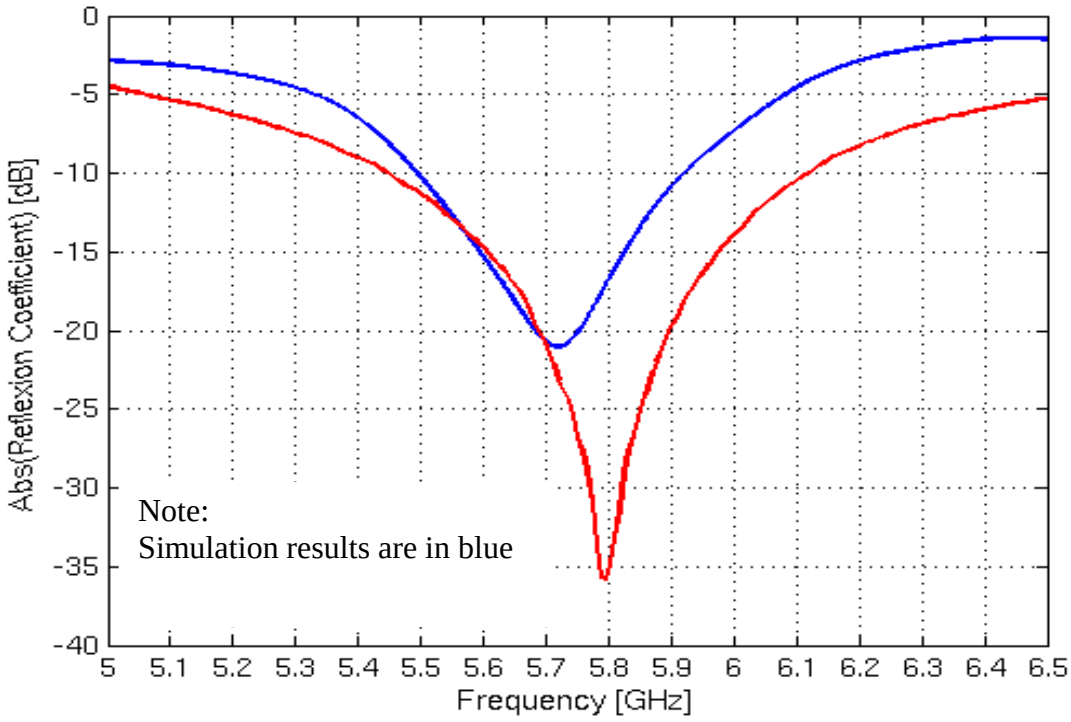

Fig. 29 Reflection coefficient (in dB) at the input port in the frequency range (5.0-6.5) GHz. The reflection coefficient is referred to a 50 Ω port impedance.

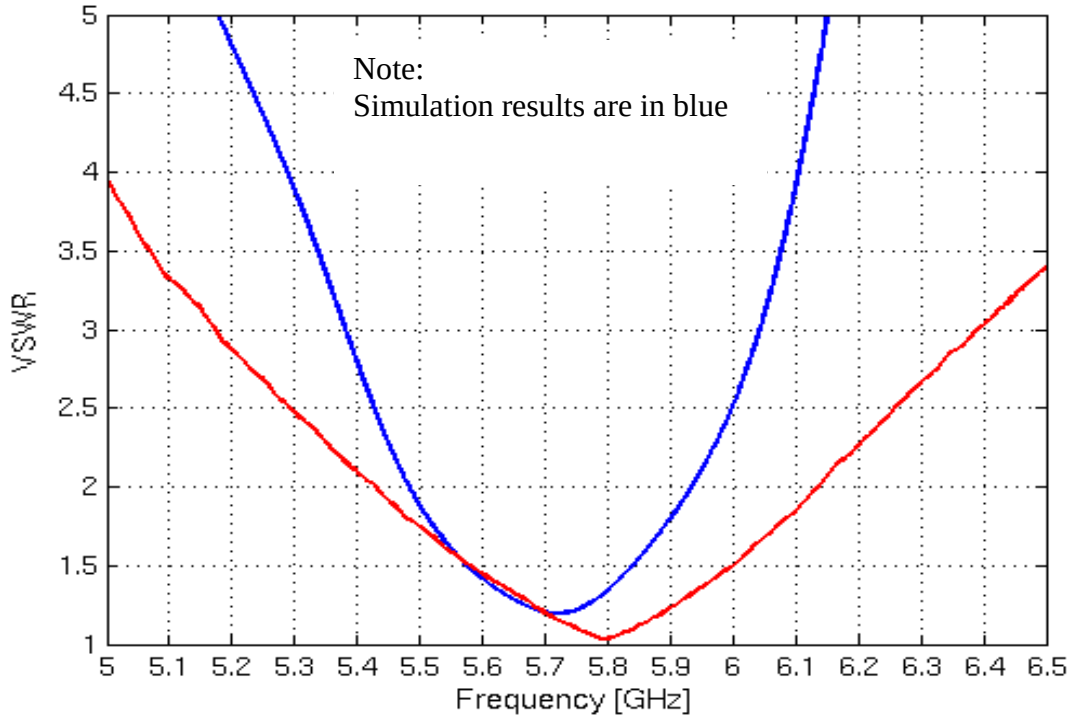

Fig. 30 Voltage standing wave ration (VSWR) at the input port in the frequency range (5.0-6.5) GHz.

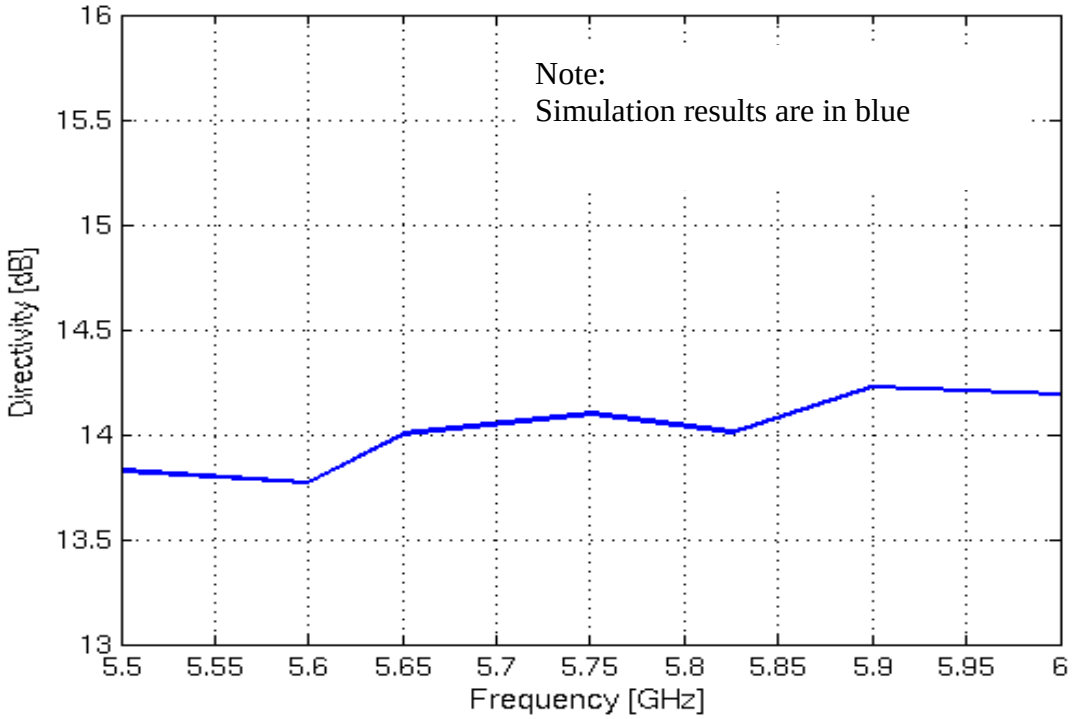

Fig. 31 Maximum directivity (in dB) in the frequency range (5.5-6.0) GHz.

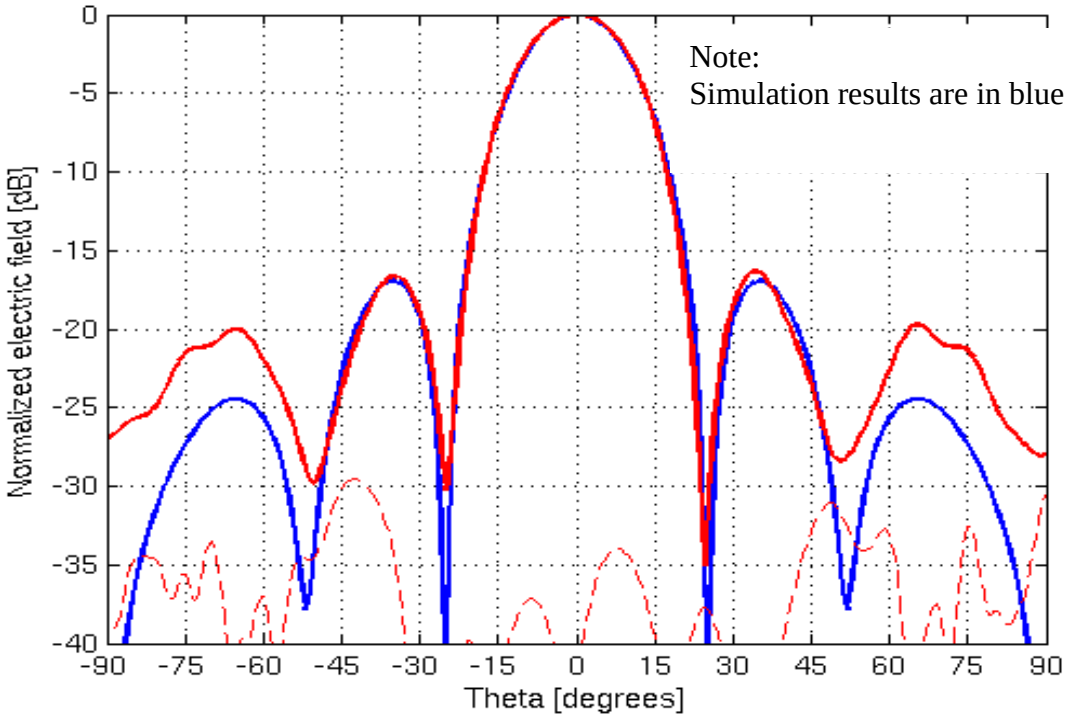

Fig. 32 Normalized electric field in the H-plane (φ = 0°), computed at the frequency *f* = 5.600 GHz. Co-pol: continuous line; X-pol: dashed line.

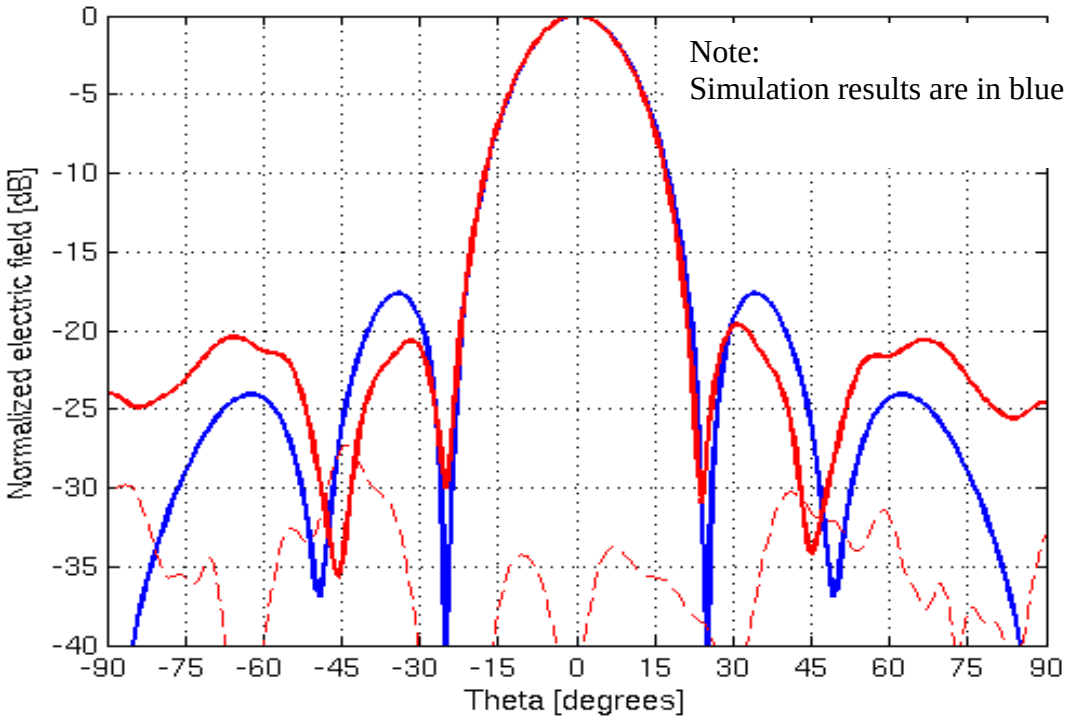

Fig. 33 Normalized electric field in the H-plane (φ = 0°), computed at the frequency *f* = 5.800 GHz. Co-pol: continuous line; X-pol: dashed line.

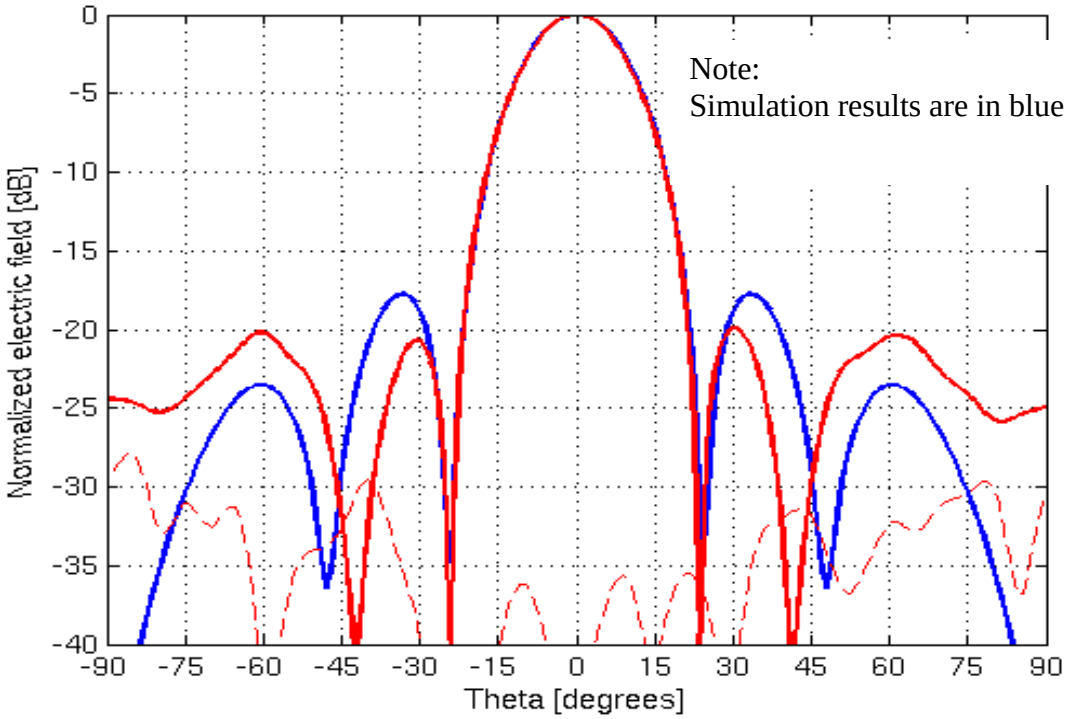

Fig. 34 Normalized electric field in the H-plane (φ = 0°), computed at the frequency *f* = 6.000 GHz. Co-pol: continuous line; X-pol: dashed line.

6- Computation ressources

All the simulations have been carried out on a PC equipped with one Athlon AMD 3500+ processor with 2 Go of RAM. The real time for the FDTD simulation has been 3 h and 42 min. During the simulation, the memory requirements have been 370 Mo. Concerning the post-treatment, it has taken about 30 sec per frequency point for the radiated field computation.

7- Discussion

8- Additional comments

6. SIMULATION RESULTS
From KUL

1- Entity

Katholieke Universiteit Leuven (KUL)
ESAT-TELEMIC
B-3001, Leuven
Belgium

Contact persons

Guy Vandenbosch
Phone +32 16 321110
Fax +32 16 321986
E-mail guy.vandenbosch@esat.kuleuven.ac.be

Vladimir Volski
Phone +32 16 321874
Email vladimir.volski@esat.kuleuven.ac.be

2- Name of the simulation tool

***MAGMAS** (**M**odel for the **A**nalysis of **G**eneral **M**ultilayered **A**ntenna **S**tructures).*

3- Generalities about the simulation tool

MAGMAS is a software framework developed for the analysis of general planar structures. MAGMAS uses the method of moments to solve integral equations.

4- Simulation Set-up (Geometry set-up, GUI, mesh, boundary conditions, excitation)

The geometry is defined using the GUI of the software. The structure is split in several small patches and apertures which are introduced consecutively. Each element is discretized using rectangular and triangular basis functions. The excitation is modeled by an additional microstrip feeding line and the reflection coefficient is calculated using a special deembeding procedure.

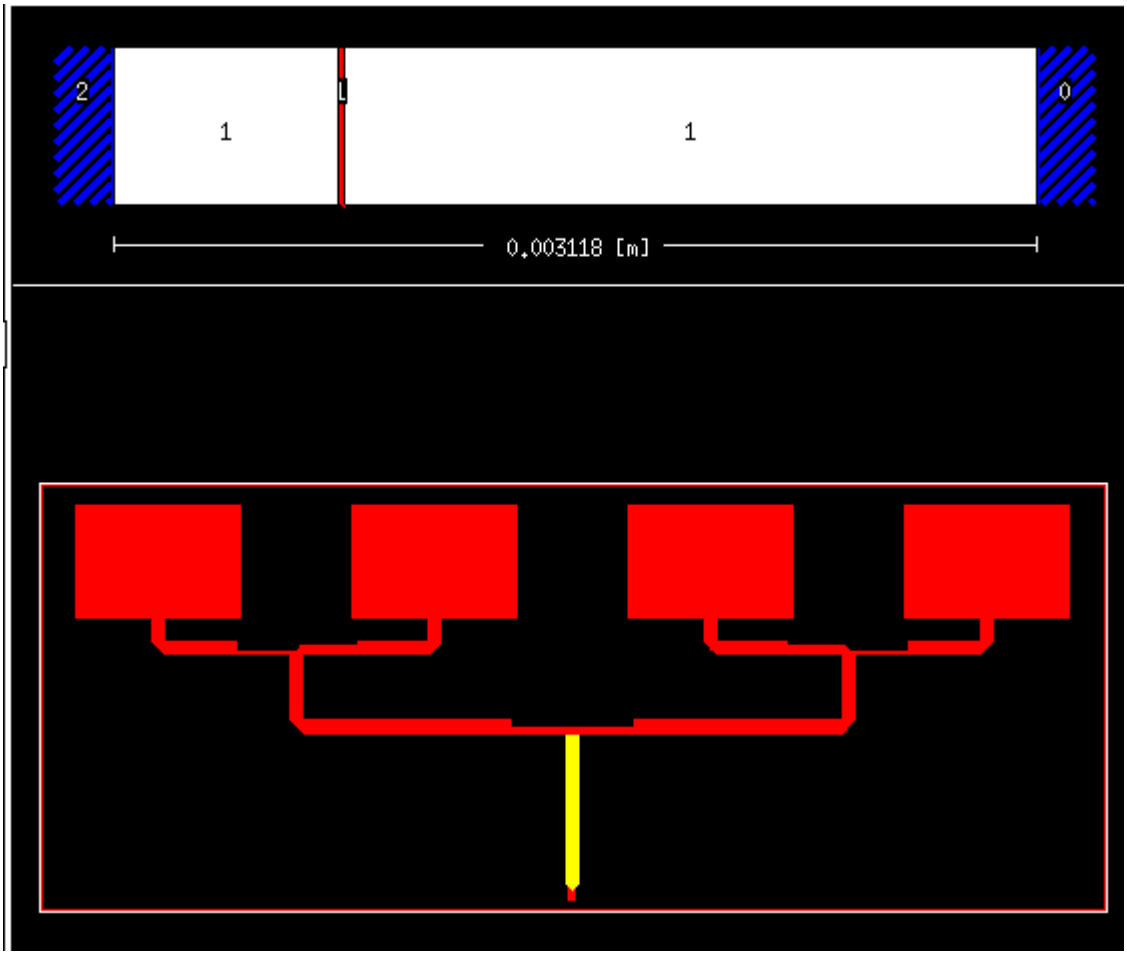

Fig. 35: Snapshot of the linear microstrip array geometry inside the MAGMAS GUI.

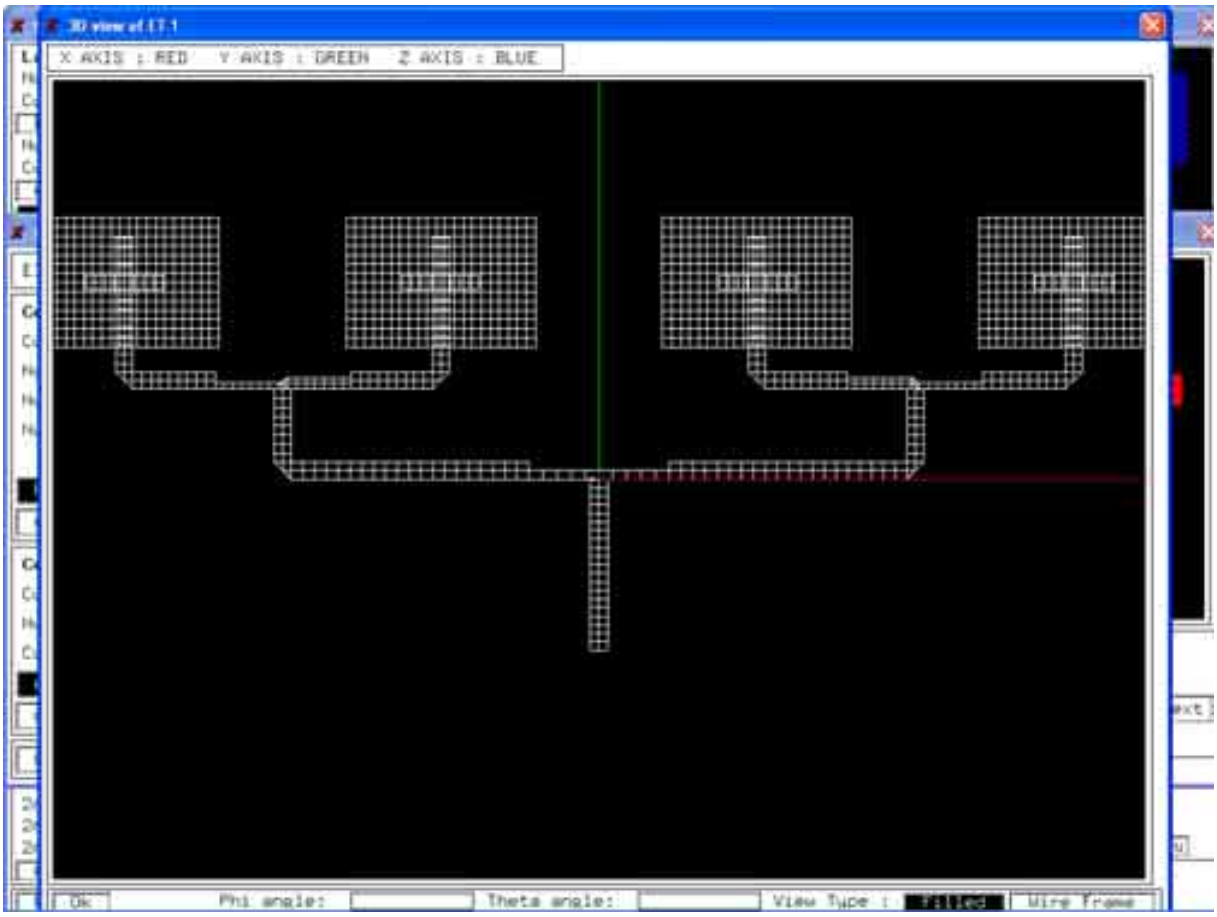

Fig. 2: Snapshot of the mesh inside the MAGMAS GUI.

5- Simulation results

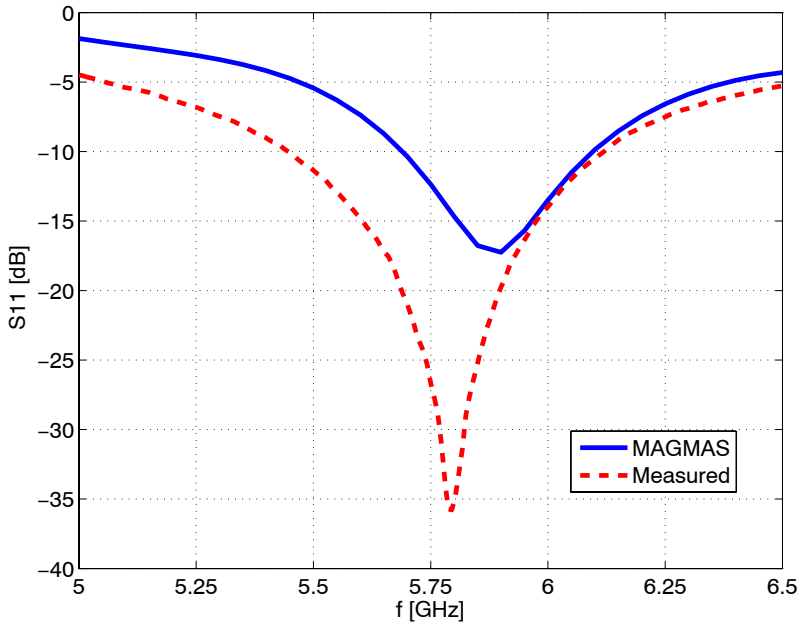

Fig. 3 Reflection coefficient (in dB) at the input port in the frequency range (5.0-6.5) GHz.

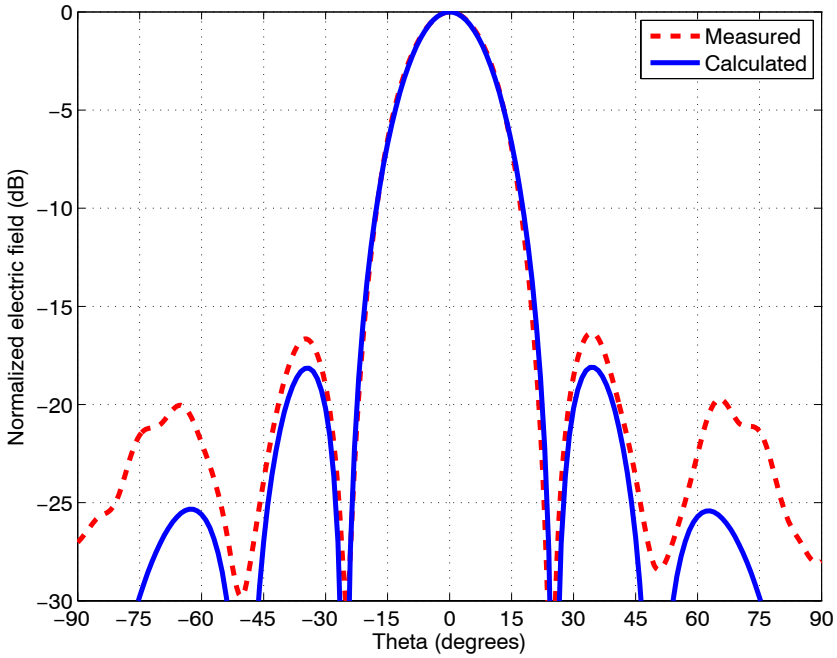

Fig. 4 Directivity in the H-plane ($\varphi = 0°$), computed at the frequency $f = 5.6$ GHz.

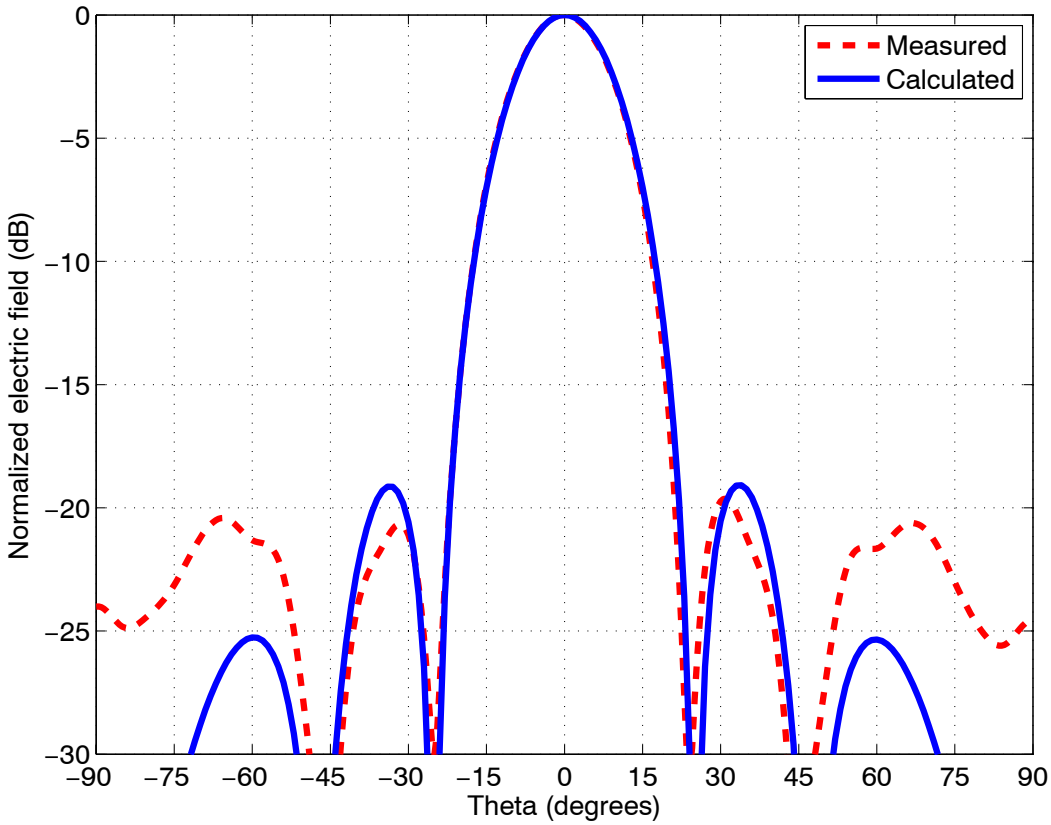

Fig. 5 Directivity in the H-plane (φ = 0°), computed at the frequency f = 5.8 GHz

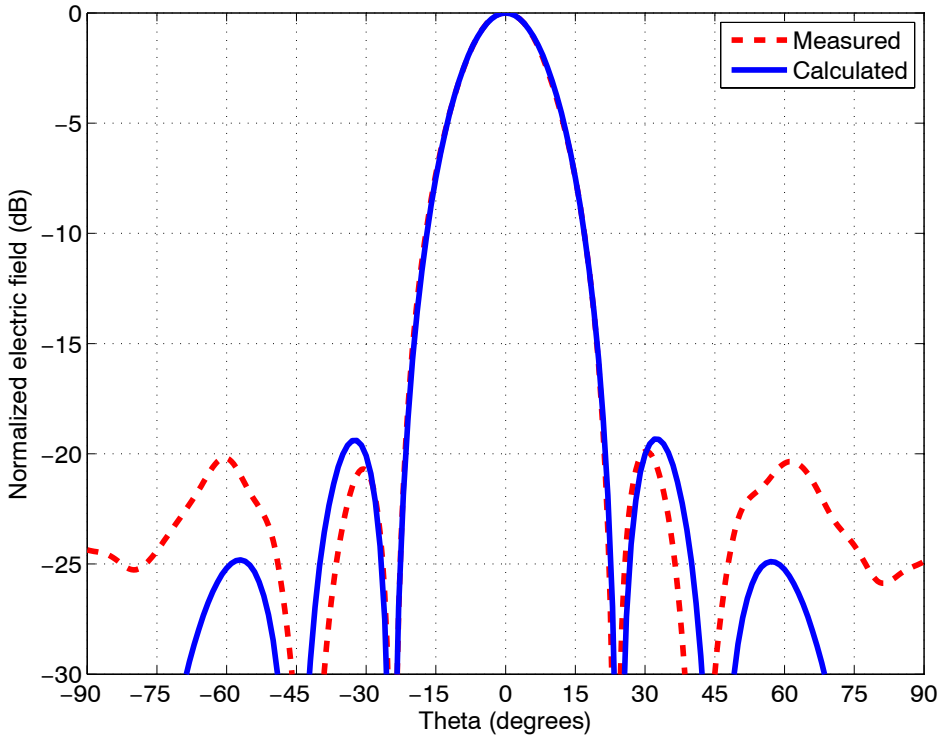

Fig. 6 Normalized pattern in the H-plane (φ = 0°), computed at the frequency f = 6 GHz.

6- Computation resources

Table 10 Properties of the WorkStation used for the simulation

Type of machine	HP 9000/785/J6000
Number of CPUs	2
CPU Speed	552 MHz
RAM	2 GB
OS	HP_UX 11.00A

7- Discussion

The antenna array is computed with an infinite ground plane.

8- Additional comments

None

7. SIMULATION RESULTS
From LEMA_EPFL

1- Entity

Electromagnetics and Acoustics Laboratory (LEMA)
Ecole Polytechnique Fédérale de Lausanne (EPFL)
EPFL STI-iTOP-LEMA ELB
Station 11
CH-1015 Lausanne, Switzerland

Contact person
Ivica Stevanovic
Phone +41 21 693 4637
Fax +41 21 6932673
E-mail ivica.stevanovic@epfl.ch

2- Name of the simulation tool

POLARIS

3- Generalities about the simulation tool

POLARIS is an IE-MoM based solver for modeling planar multilayered structures with dielectrics supporting slotted ground planes and feeding printed lines. Slotted ground planes can have a sizable thickness, the structure can be backed by rectangular cavities and the arrays can be obtained by periodical repetition of basic radiating elements.

4- **Simulation Set-up (Geometry set-up, GUI, mesh, boundary conditions, excitation)**

The geometry is defined using the GUI of the software. The software assumes laterally unbounded dielectric layers and ground planes. The metallic parts (feeding lines, slots and radiation patches) are discretized using rectangular and triangular basis functions. The discretization is done using the GUI, which contains a structured mesher. The mesh has been produced at 10GHz with 15% of cell density leading to 1910 basis functions. The analysis is performed in the frequency domain. A discrete frequency sweep has been used (41 points in frequency). The excitation is modeled as a delta-gap generator put at the edge of the microstrip feeding line. Approximate time to set-up the geometry and simulation parameters was about 10 min.

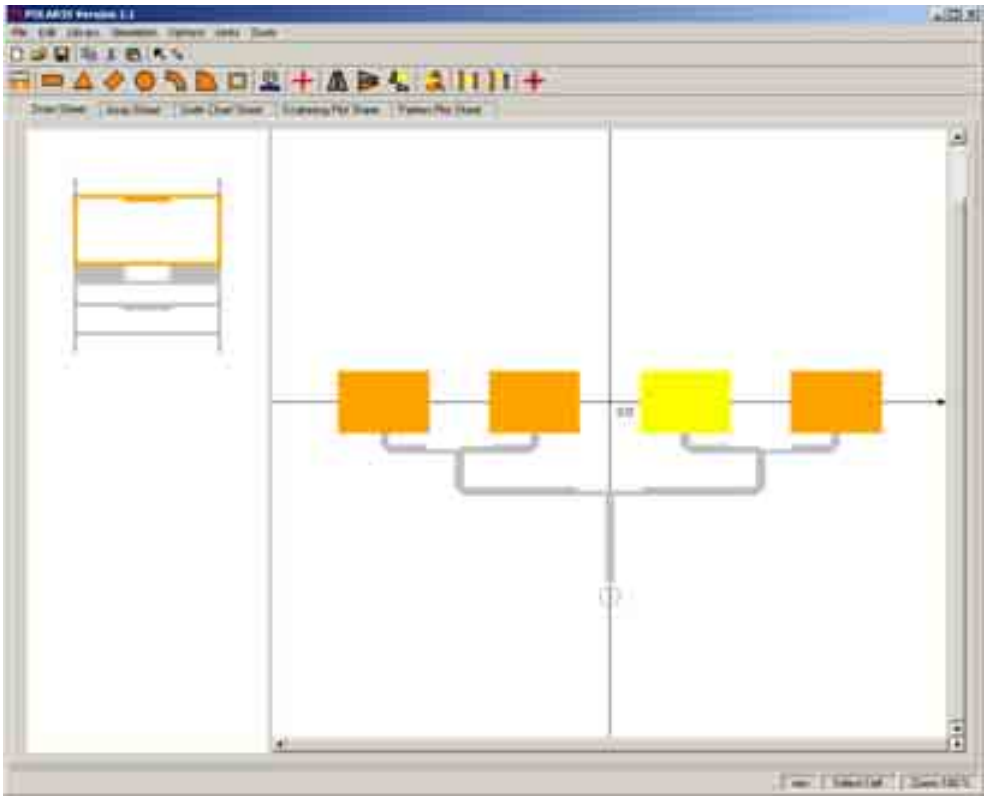

Fig. 36: Snapshot of the linear microstrip array geometry inside the POLARIS GUI.

5- Simulation results

The results that have been computed are:

- Input port parameters (reflection coefficient and VSWR)
- Radiation patterns in H plane

The input port parameters are computed at the input port, with a normalization impedance of 50Ω. Results for the reflection coefficient are shown in Fig. and in Fig. 38 input impedance of the array. The blue lines represent the results obtained in POLARIS and the red ones, the reference results. The relative difference of 0.8% in predicted resonance frequency can be observed.

H-planes radiation patterns at several frequencies are shown in Fig. 39-Fig. 41. The pattern is compared to the reference results obtained using Ansoft Designer (red line). Since POLARIS does not have a possibility of computing the gain, the radiation patterns are compared taking the maximum value as the reference level. Very good agreement with the reference results can be observed.

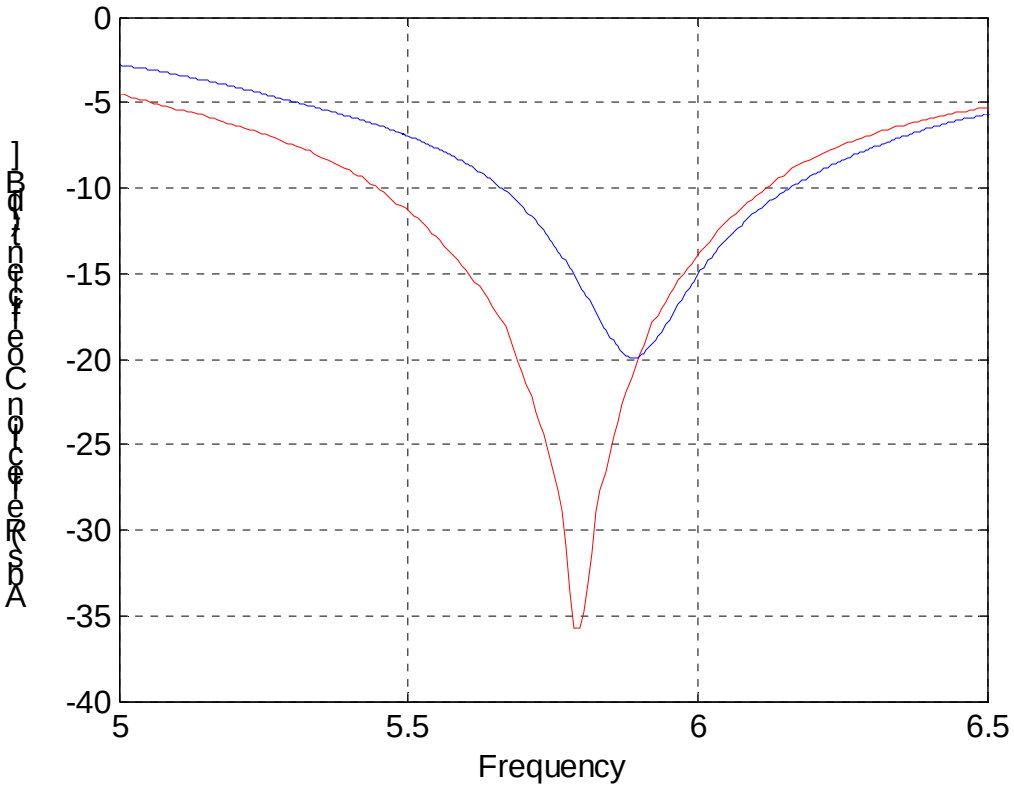

Fig. 37: Reflection coefficient (in dB) at the input port in the frequency range (5.0-6.5) GHz. The reflection coefficient is referred to a 50 Ω port impedance. Polaris (blue line), measurements (red line).

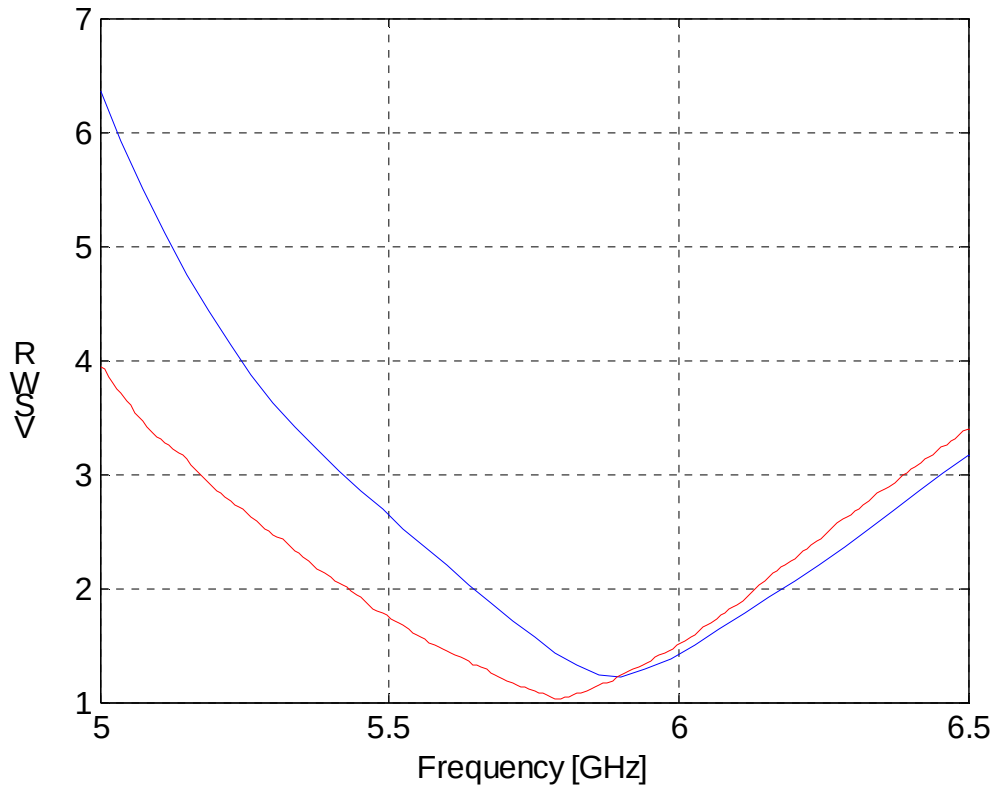

Fig. 38: Voltage standing wave ratio at the input port in the frequency range (5.0-6.5) GHz. POLARIS (blue line), measurements (red line).

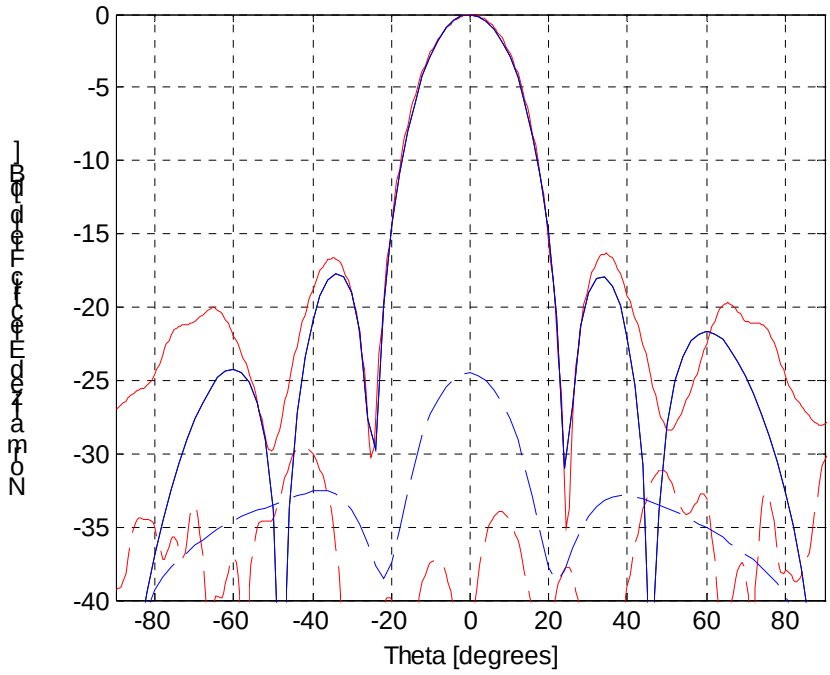

Fig. 39: Normalized electric field in the H-plane (φ = 0°), computed at the frequency *f* = 5.600 GHz. Co-pol: continuous line; X-pol: dashed line. POLARIS (blue lines), measurements (red lines).

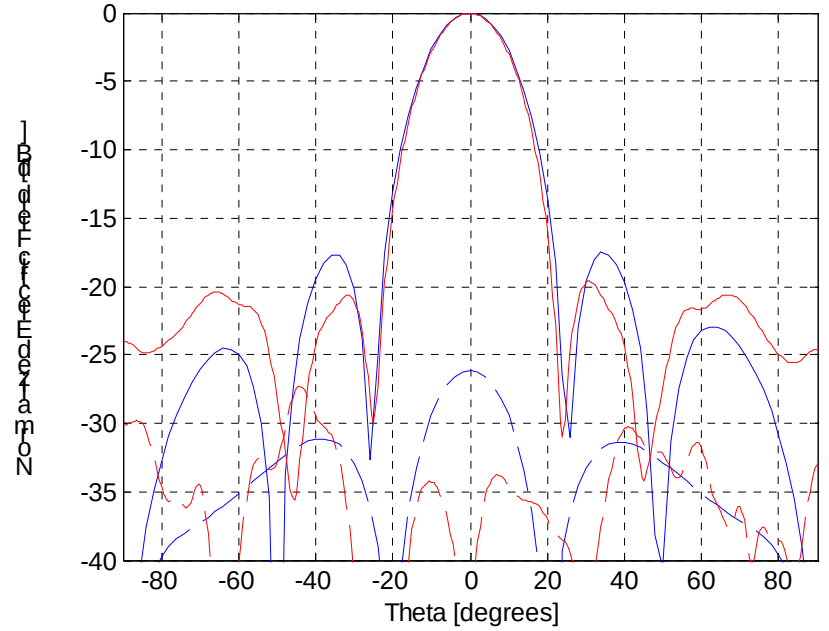

Fig. 40: Normalized electric field in the H-plane (φ = 0°), computed at the frequency *f* = 5.800 GHz. Co-pol: continuous line; X-pol: dashed line. POLARIS (blue lines), measurements (red lines).

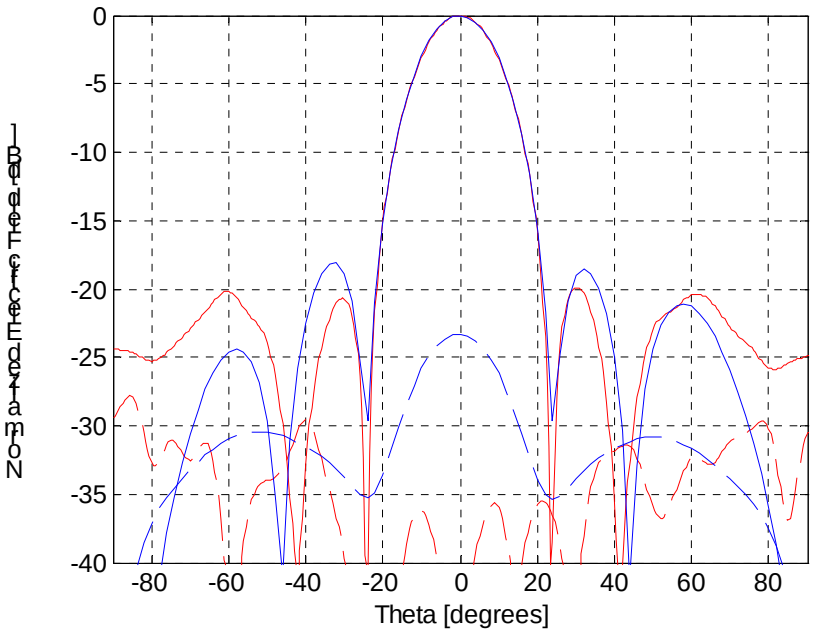

Fig. 41: Normalized electric field in the H-plane (φ = 0°), computed at the frequency *f* = 6.000 GHz. Co-pol: continuous line; X-pol: dashed line. POLARIS (blue lines), measurements (red lines).

6- Computation resources

The simulation has been performed on a PC with 1 AMD processor at 1.4 GHz and 512 MB of available memory. The operating system was Redhat Linux.

The data relevant to the two computers are reported in the following table.

Table 11 Properties of the PC used for the simulation

Type of machine	Desktop PC
Number of CPUs	1 AMD
CPU Speed	1.4 GHz
RAM	512 MB
OS	Linux, RedHat

The simulation is performed over 41 discrete points in frequency (in the range 5.0 – 6.5 GHz). Data relevant to the simulation are listed in the following table.

Table 12 Simulation requirements for the PC

-	Linear Array
Average CPU time per frequency point	12 min 25 sec
Max. required RAM	113 MB
Number of unknowns	1910

7- Discussion

The simulated structure is easy to set up, thanks to the LEGO-like oriented GUI, and it is not computationally difficult for POLARIS. The test simulations were performed after obtaining the reference results.

The new feature that should be added to the simulator is calculation of the gain.

8- Additional comments

None.

8. SIMULATION RESULTS

From LIVUNI (CST)

1- Entity

Department of Electrical Engineering and Electronics
University of Liverpool
Liverpool
United Kingdom

Contact person

Greepol Niyomjan
E-mail: G.Niyomjan@liverpool.ac.uk

2- Name of the simulation tool

CST Microwave Studio 5.0.0 [1].

3- Generalities about the simulation tool

CST MWS5 is a simulation tool for High Frequency simulations. It offers Transient, Eigenmode and Frequency Domain solvers. It uses a Finite Integration (FI) method with perfect boundary approximation (PBA).

4- Simulation Set-up (Geometry set-up, GUI, mesh, boundary conditions, excitation)

The model is defined using the GUI of the software. Everything except the microstrip lines are made using primatives and boolean subtraction. The microstrip lines are traced point by point and then extruded to a given thickness. Metal parts must have thickness to simulate (Ground plane, patches and microstrip, all set to 0.05mm thickness). The Mesh is automatically generated at 10 lines/wavelength and run through the adaptive mesh update once giving a total number of meshcells of 288750 (increased from ~170000).

The transient solver was used to simulate the structure which is a time domain based method. The excitation was a 5-6.5GHz gaussian pulse applied to a discrete port (connected between the microstrip feed point and ground plane). The port and simulation were both normalised to 50 ohm with a -50dB accuracy limit imposed to determine simulation time. Monitors for specific frequencies were setup to obtain the farfield parameters at those frequencies. Geometry of antenna structure is illustrated in Figure1.

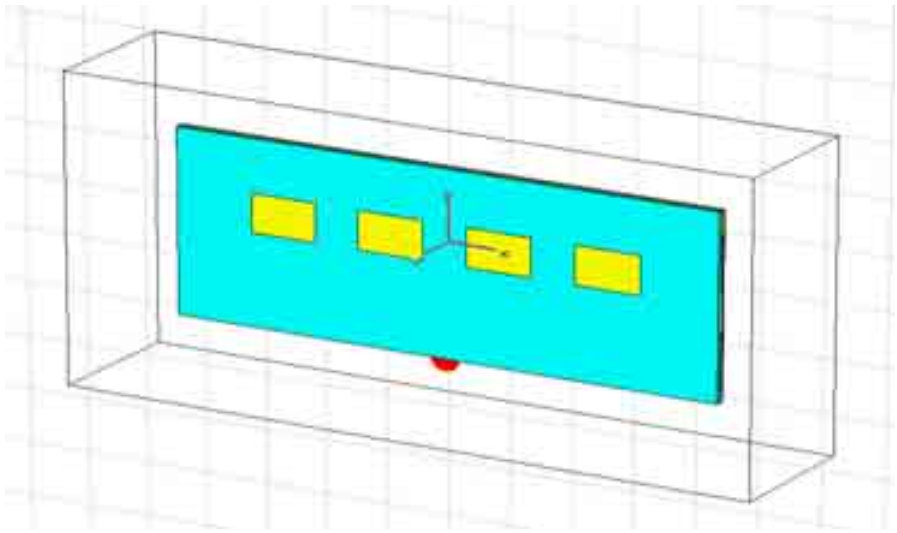

a) Normal view.

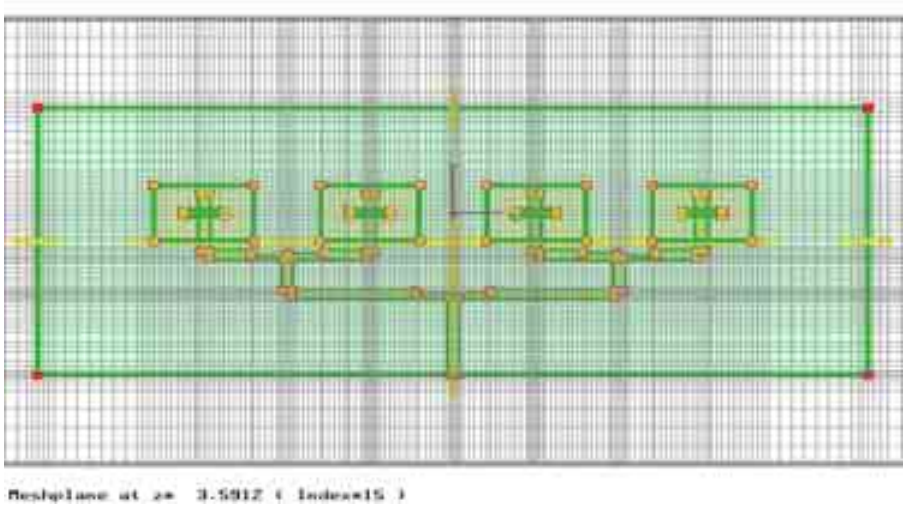

b) Mesh view.

Figure 42: Snapshot of the linear microstrip array geometry from CST Microwave Studio.

5- Simulation results

The results that have been computed are:

- Input Reflection Coefficient (Return Loss)
- Voltage Standing Wave Ratio (VSWR)
- Radiation Pattern (Gain)

Input reflection coefficient (Return loss) values are calculated at the input port. Values of Return Loss and VSWR at the input port are plotted as shown in Figures 2 – 3 respectively. Values of normalised gain are plotted against the theta angles from -90 to 90 degree as shown in Figures 4 – 6.

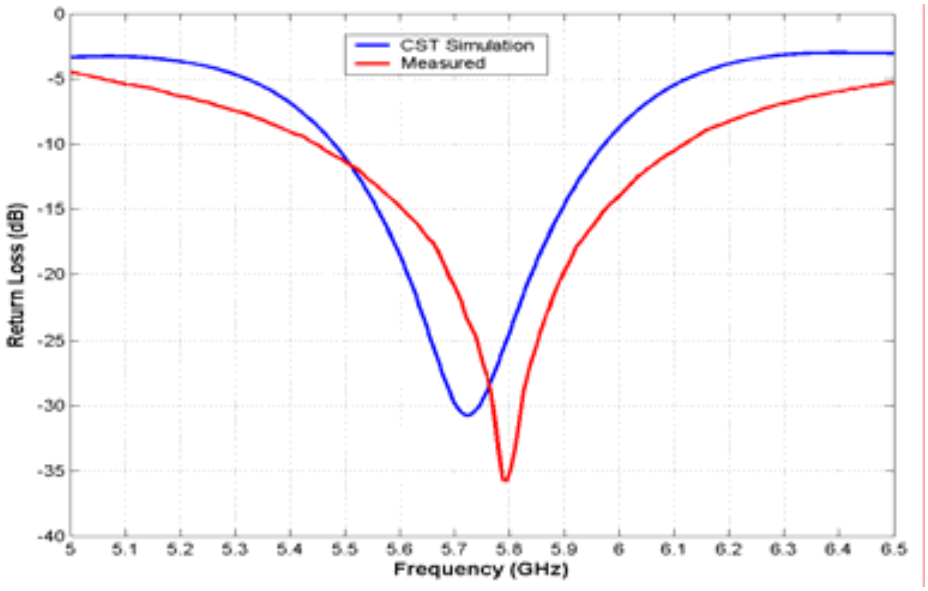

Figure 2: Return loss at the input port in the frequency range 5-6.5 GHz.

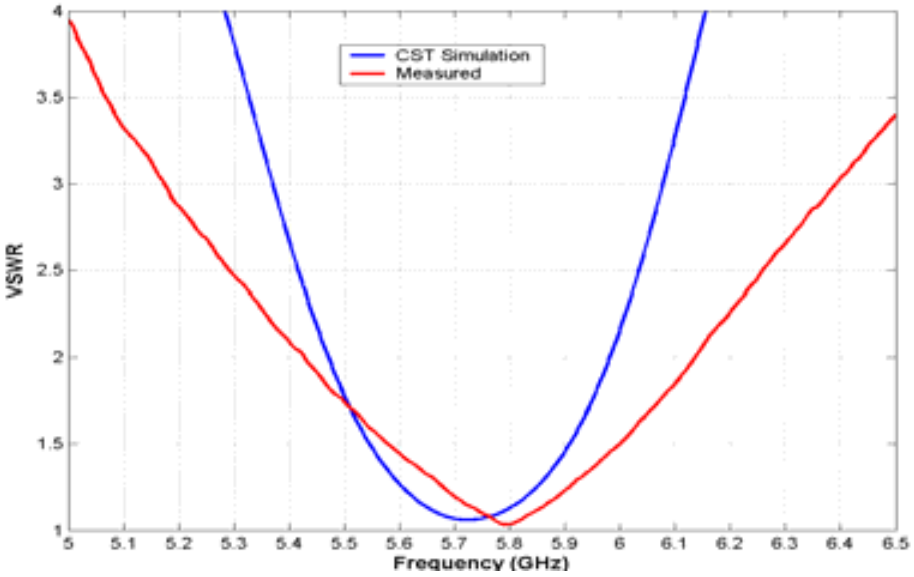

Figure 3: Voltage standing wave ratio at the input port in the frequency range 5-6.5 GHz.

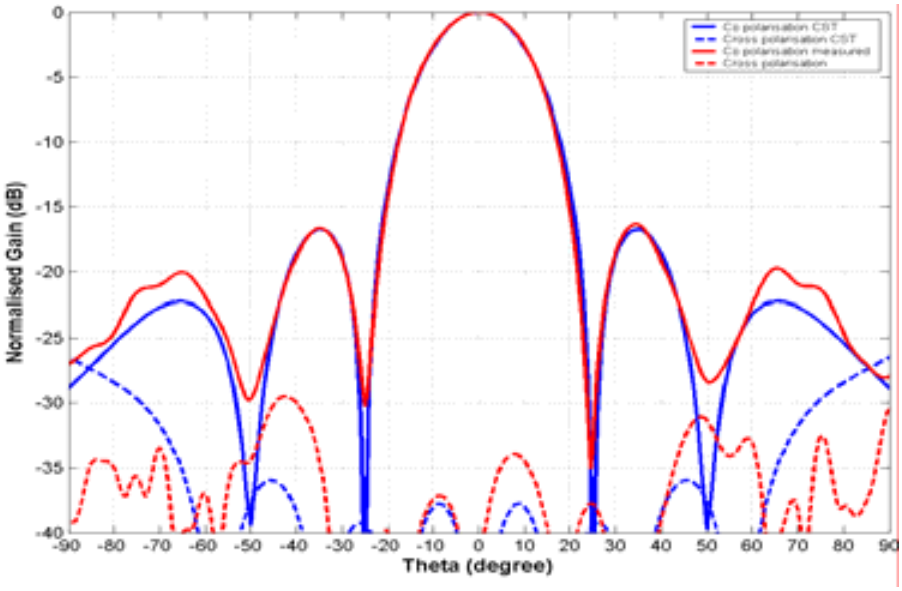

Figure 4: Gain in the H-plane (φ = 0°), computed at the frequency f = 5.6 GHz.

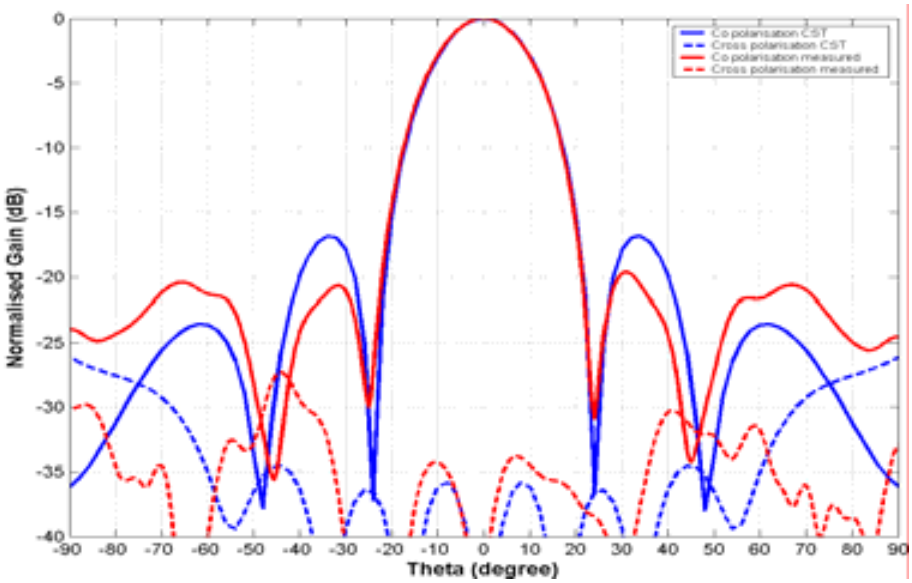

Figure 5: Gain in the H-plane (φ = 0°), computed at the frequency f = 5.8 GHz.

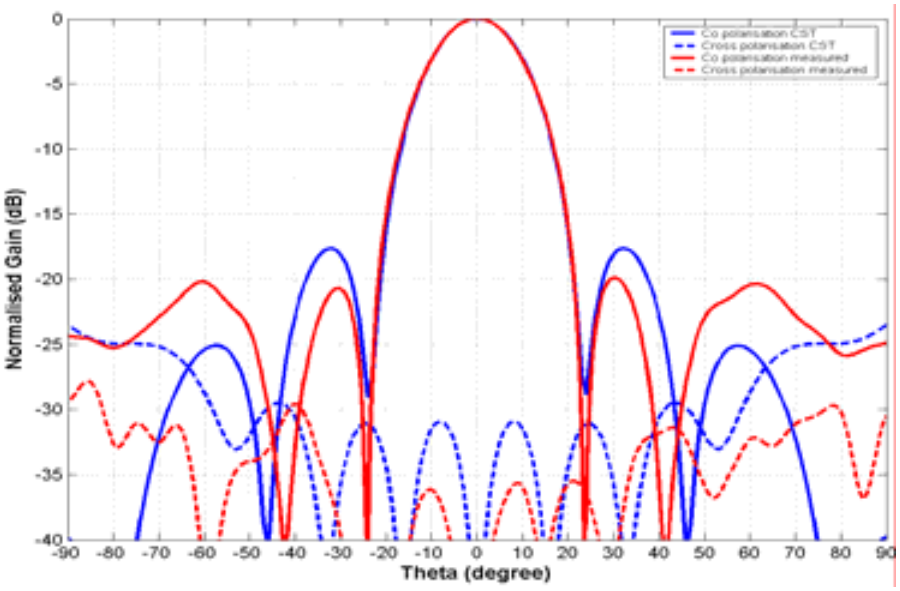

Figure 6: Gain in the H-plane (φ = 0°), computed at the frequency f = 5.8 GHz.

6- Computation resources

A PC desktop with specifications shown in Table 1 was used to simulate the Linear Microstrip Array. The total time spent on this simulation is shown in Table 2.

Table 1: Specification of the desktop used for the simulation

Type of machine	Desktop PC
Number of CPUs	1 Intel Pentium 4
CPU Speed	1.7 GHz
RAM	1 GB
OS	Win XP Home Sp2

Table 2: Simulation requirements for the desktop PC

Total time	1 hr and 45 mins

7- Discussion

From Figures 2 - 3, return loss and VSWR values obtained from CST simulation and measurement [2] are in good agreement. As seen in Figures 4 – 6, normalised gain values for co-polarisation obtained from both HFSS and measurement are in good agreement especially at the main lobe where they are completely overlapped. However the normalised gain values for cross-polarisation obtained from both CST and measurement are in good agreement only within the main lobe region. CST has proved to be one of the most efficient simulation tools due to its accuracy to predict performances of the antenna and its simulating speed.

8- Additional comments

Reference:

[1] http://www.cst.com.
[2] Department of Information Engineering, University of Siena, Italy.

9. SIMULATION RESULTS

From LIVUNI (HFSS)

1- Entity

Department of Electrical Engineering and Electronics
University of Liverpool
Liverpool
United Kingdom

Contact person

Greepol Niyomjan
E-mail: G.Niyomjan@liverpool.ac.uk

2- Name of the simulation tool

Ansoft™ HFSS™ version 9 [1].

3- Generalities about the simulation tool

HFSS (High Frequency Structure Simulator) is a high-performance full-wave electromagnetic (EM) field simulator for arbitrary 2D and 3D passive device modelings. It integrates simulation, visualization, solid modeling, and automation in an easy-to-use environment where solutions to the 3D EM problems are quickly and accurately obtained. HFSS employs the Finite Element Method (FEM), adaptive meshing, and brilliant graphics to all of the 3D EM problems. Ansoft HFSS can be used to calculate parameters such as S-Parameters, Resonant Frequency, and Fields.

4- Simulation Set-up (Geometry set-up, GUI, mesh, boundary conditions, excitation)

The geometry of antenna was created by using the 3D Modeller of HFSS.

Mesh is in the form of tetrahedral except at the excitation port where the mesh is in the form of triangle. Adaptive mesh was used to make sure that changes of fields in any areas of the antenna structure were covered. HFSS reduces the mesh size at the critical areas after each simulation. The adaptive growth is controlled by Refinement. The adaptive process repeats until the difference between S-parameters of two consecutive passes is less than a specific number, Max delta S (0.01).The adaptive process can also be terminated when the number of requested passes is reached (30 passes). GUI is similar to the GUI of Microsoft Windows which is easy to use. The analysis is performed in the frequency domain. A discrete frequency sweep has been used to simulate this structure (Step size equals to 0.01 GHz). Air box was used for the radiation boundary. Conductor (copper) thickness is assumed to be 0.1 mm. Lumped port (50 ohms) was used to excite at the edge of the main microstrip line feed. Geometry of antenna structure is illustrated in Figure1.

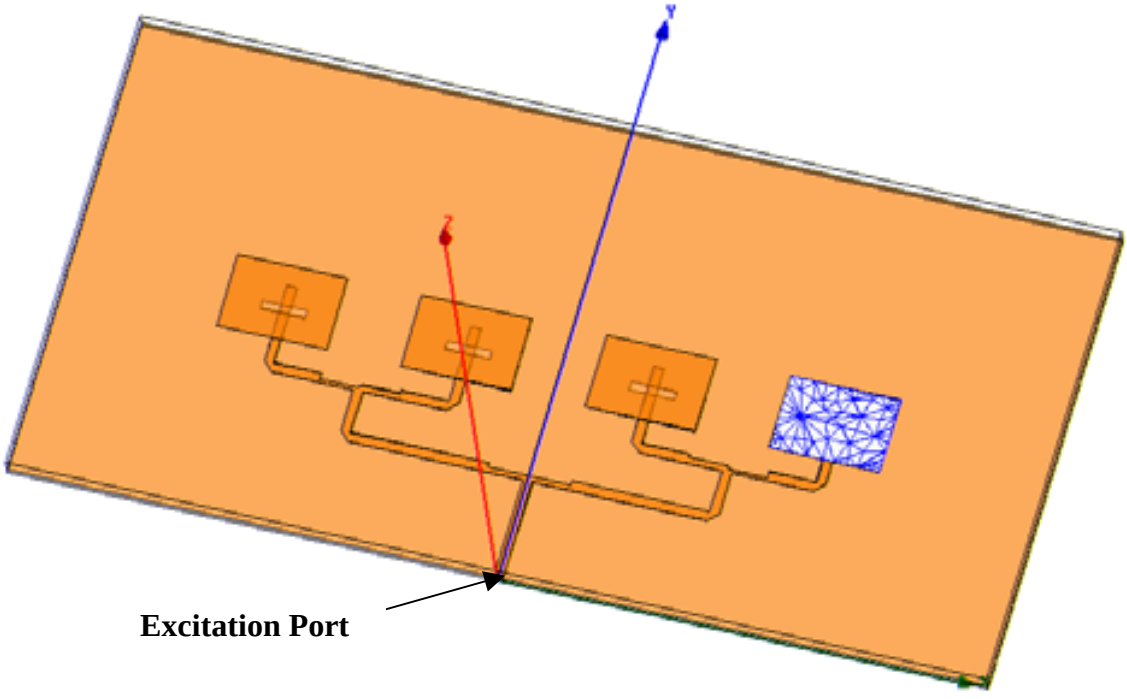

Figure 43: Snapshot of the linear microstrip array geometry from Ansoft HFSS.

5- Simulation results

The results that have been computed are:

- Return Loss (dB)
- Voltage Standing Wave Ratio (VSWR)
- Gain
- Radiation Pattern (Gain)

Input reflection coefficient (Return loss) values are calculated at the input port. Values of Return Loss, VSWR and Gain are plotted as shown in Figures 2 – 4 respectively. Values of Normalised Gain pattern at frequencies 5.6, 5.8 and 6 GHz are plotted against the theta angles from -90 to 90 degree as shown in Figures 5 – 7.

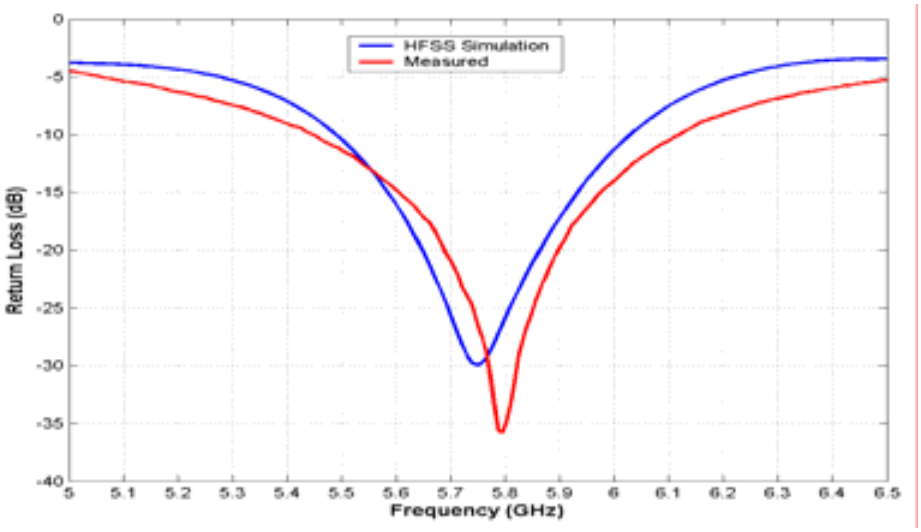

Figure 2: Return loss at input port in the frequency range 5 - 6.5 GHz.

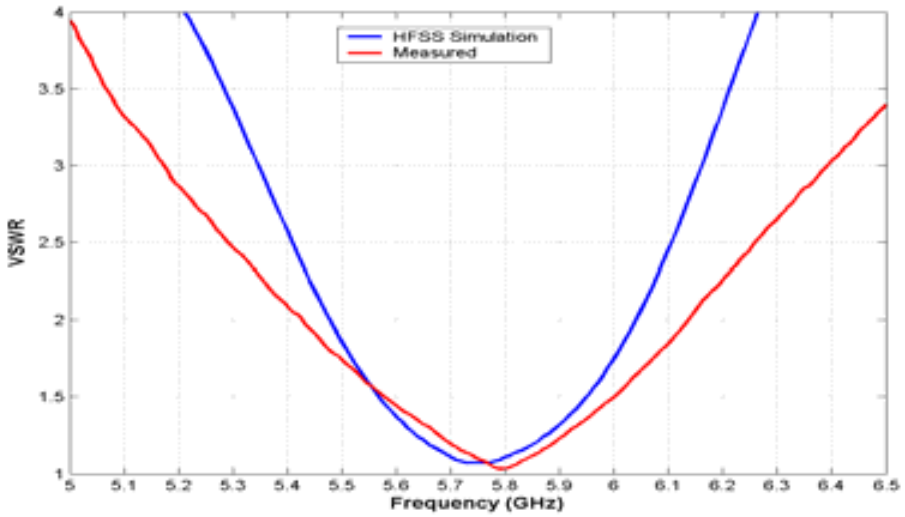

Figure 3: Voltage standing wave ratio at the input port in the frequency range 5 - 6.5 GHz

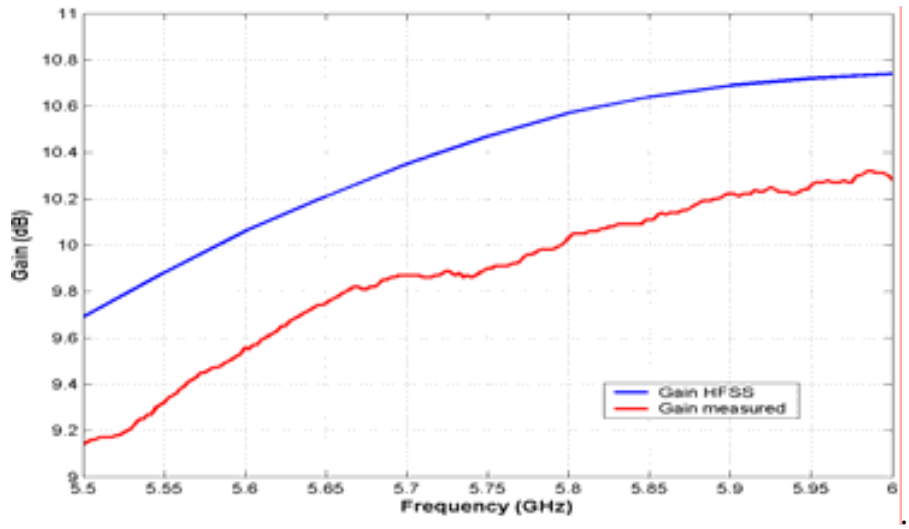

Figure 4: Total Gain in the frequency range 5.5 - 6 GHz.

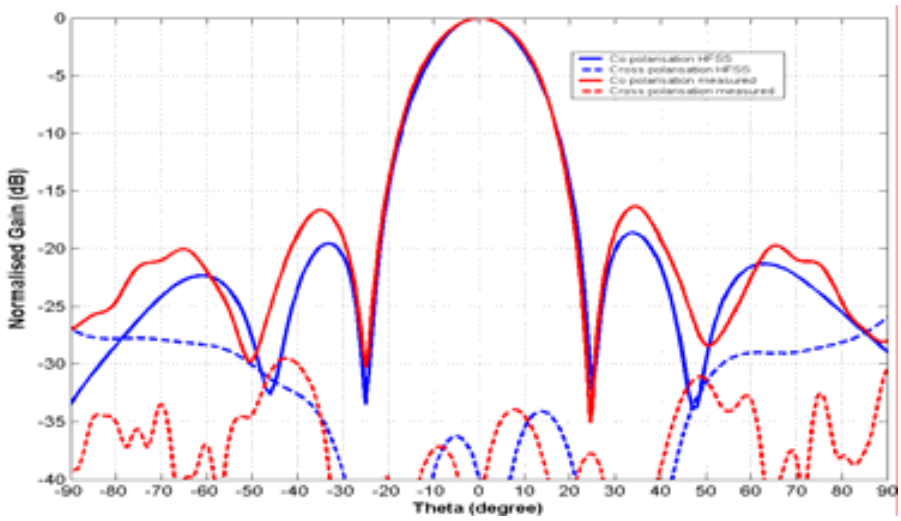

Figure 5: Gain in the H-plane (φ = 0°), computed at the frequency f = 5.6 GHz.

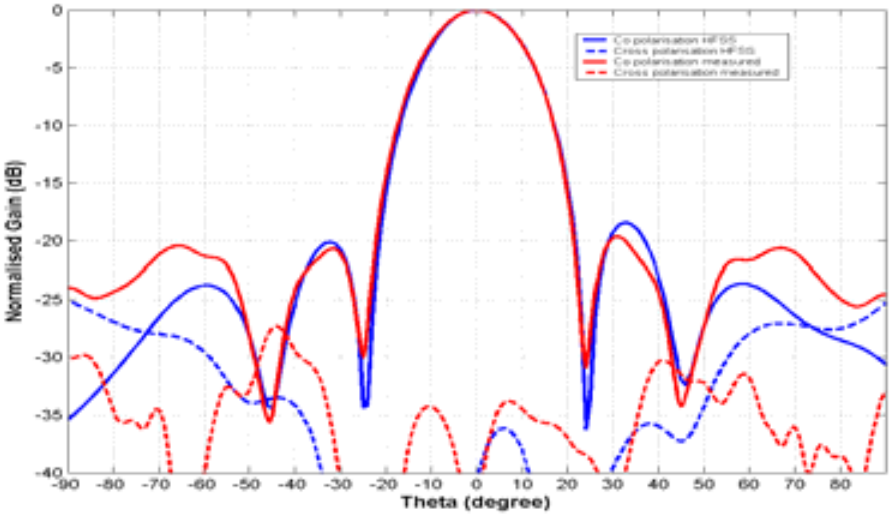

Figure 6: Gain in the H-plane (φ = 0°), computed at the frequency f = 5.8 GHz.

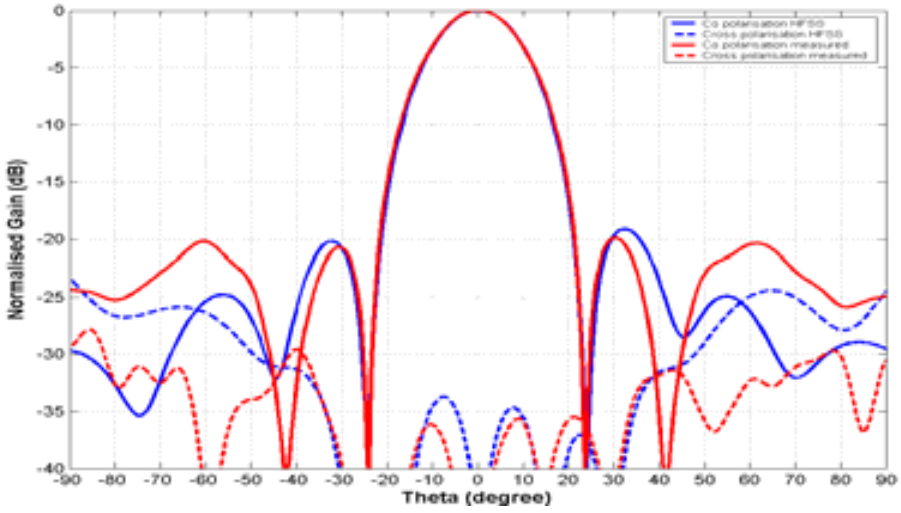

Figure 7: Gain in the H-plane (φ = 0°), computed at the frequency f = 6 GHz.

6- Computation resources

A PC desktop with specifications shown in Table 1 was used to simulate the Linear Microstrip Array. The total time spent on this simulation is shown in Table 2.

Table 1: Specification of the desktop used for the simulation

Type of machine	Desktop PC
Number of CPUs	1 Intel Pentium 4
CPU Speed	2.4 GHz
RAM	512 MB
OS	Win XP Home Sp2

Table 2: Simulation requirements for the desktop PC

Total real time	84 hrs, 12 mins, 16 secs
Total CPU time	31 hrs, 19 mins, 19 secs

7- Discussion

From Figures 2 - 4, return loss, VSWR and gain values obtained from HFSS simulation and measurement [2] are in good agreement. As seen in Figures 5 – 7, normalised gain values for co-polarisation obtained from both HFSS and measurement are in good agreement especially at the main lobe where they are completely overlapped. However the normalised gain values for cross-polarisation obtained from both HFSS and measurement are in good agreement within the region of the main lobe only. Overall HFSS has proved to be one of the most accurate simulation tools to predict the performances for this kind of antenna structure. A few drawbacks for using this simulation tool are time consuming and heavy memory usage.

8- Additional comments

Reference:

[1] http://www.ansoft.com.
[2] Department of Information Engineering, University of Siena, Italy.

10. SIMULATION RESULTS

From UPV (FEKO)

1- Entity

Universidad Politécnica de Valencia
U.P.V.
I.T.E.A.M.
Edificio 8G
Camino de Vera S/N
Valencia 46022
Spain
Tel: 963879585

2- Name of the simulation tool

FEKO

3- Generalities about the simulation tool

The program FEKO is based on the Method-of-Moments (MoM). Electromagnetic Fields are obtained by first calculating the electric surface currents on conducting and equivalent electric and magnetic surface currents on the surface of a dielectric solid. Electrically large problems are usually solved with either the physical optics (PO) approximation and its extensions or the Uniform Theory of Diffraction (UTD), in FEKO, these formulations are hybridised with the MoM at the level of the interaction matrix.

4- Simulation Set-up (Geometry set-up, GUI, mesh, boundary conditions, excitation)

The structure has been drawn using AutoCAD software. The AutoCAD geometry file (.dxf), can be imported with the IN card which allows us to import arbitrary surface easily.

The meshing is performed automatically by the program PREFEKO, but some rules have to be adhered to, which results in a triangular uniform pattern for the surfaces. Alternatively, the software employs a more refined triangular meshing for curved structures.

The edge length of triangular elements should be shorter than ($\lambda/5$). According to the geometry and the need for accuracy, more triangles may be needed.

In our case, the value for maximum edge length was selected as ($\lambda/8$) at the upper frequency of the band (6.5GHz), due to memory constraints.
The following figures show the defined structure on the AutoCAD software as well as the mesh employed by FEKO.

Geometry definition is shown in Figures 1, 2, and figure 3 shows the meshed structure with FEKO.

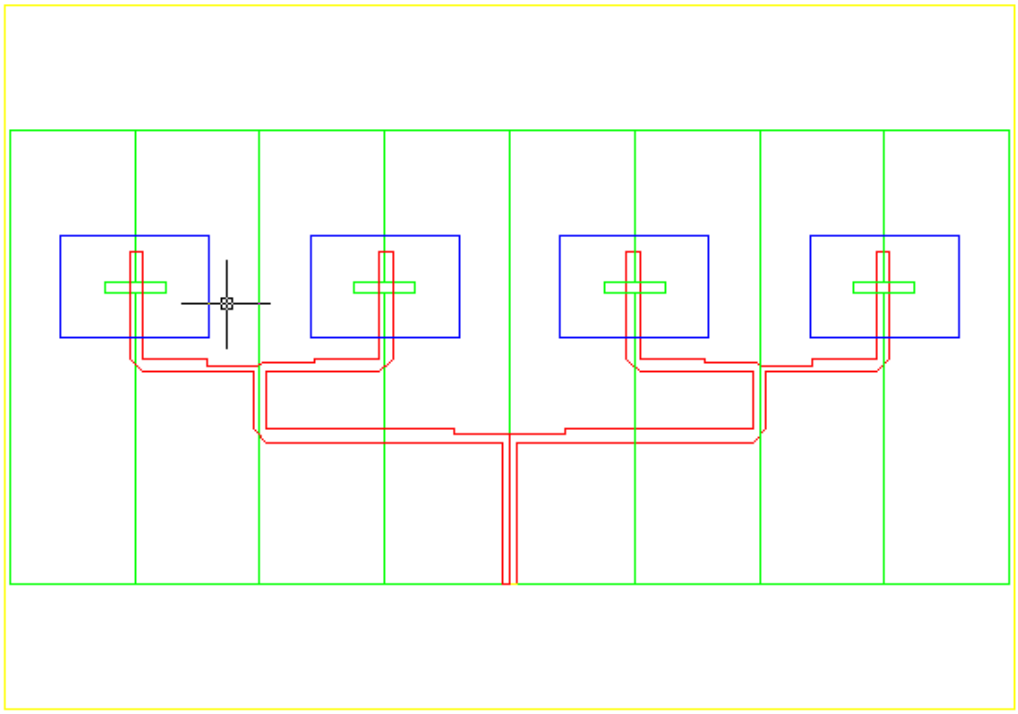

Figure 1: Structure of Linear Patch Array in AutoCAD

Figure 2: Front view

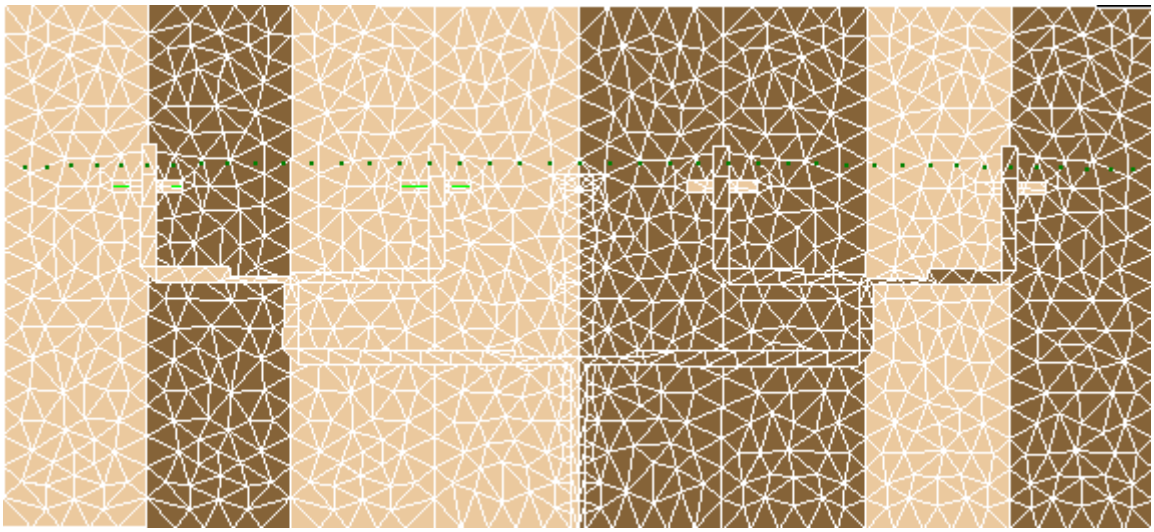

Figure 3: Meshed structure in FEKO

In all the simulations infinite layers of dielectric materials and a finite ground plane have been considered. The dimensions of the ground plane are 140.58x64mm^2

The excitation has been modelled by using the AE card (Edge voltage source between labels), which can simulate a 50 Ohm microstrip lines as the one used in this case.

The AutoCAD software shows to be extremely well suited for planar structures, even for the ones which include slots on a finite ground plane. The patch array and the feeding slots can be introduced in no more than 10 minutes time. However, the definition of the complicated microstrip line divisor requires a longer time due to its corners and oblique edges. Moreover, the numerous editing tools that support AutoCAD help the user to reduce drastically the structure definition time.

5- Simulation results

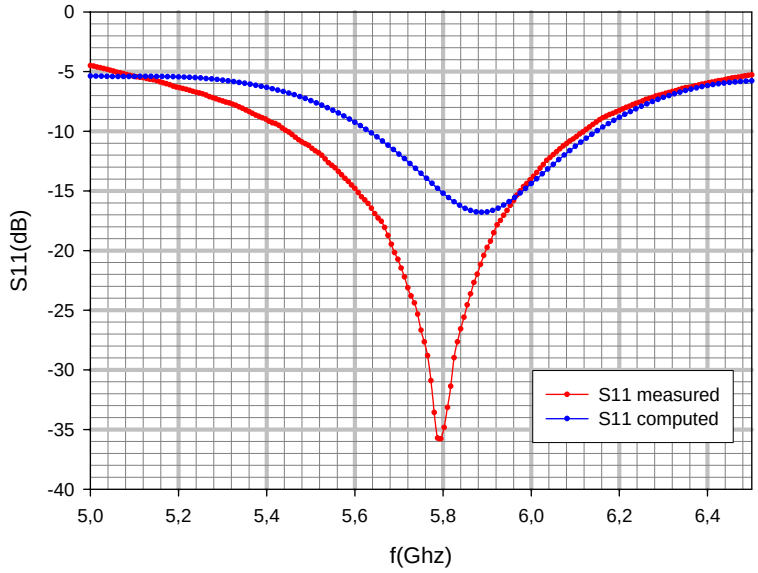

Fig.4.Reflection coefficient (in dB) at the input port in the frequency range (5.0-6.5) GHz. The reflection coefficient is referred to a 50 Ω port

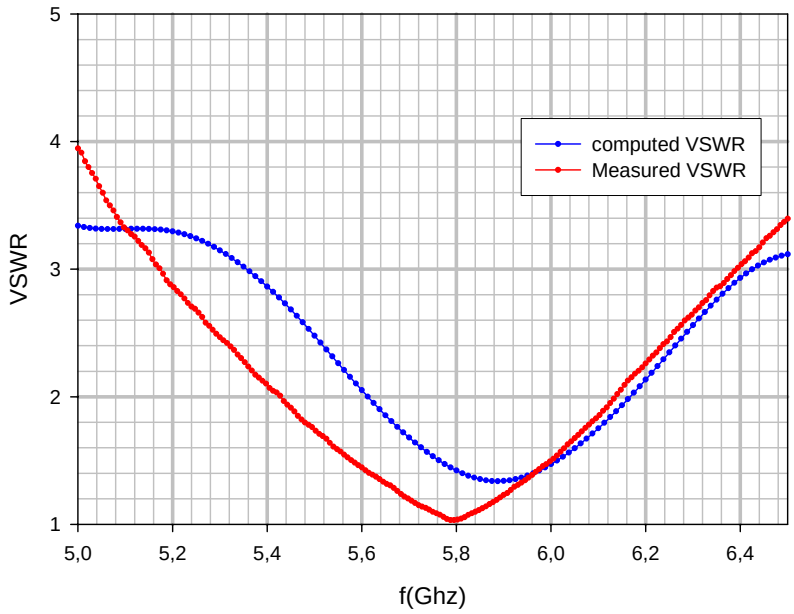

Fig.5. VSWR at the input port in the frequency range (5.0-6.5) GHz, computed and measured.

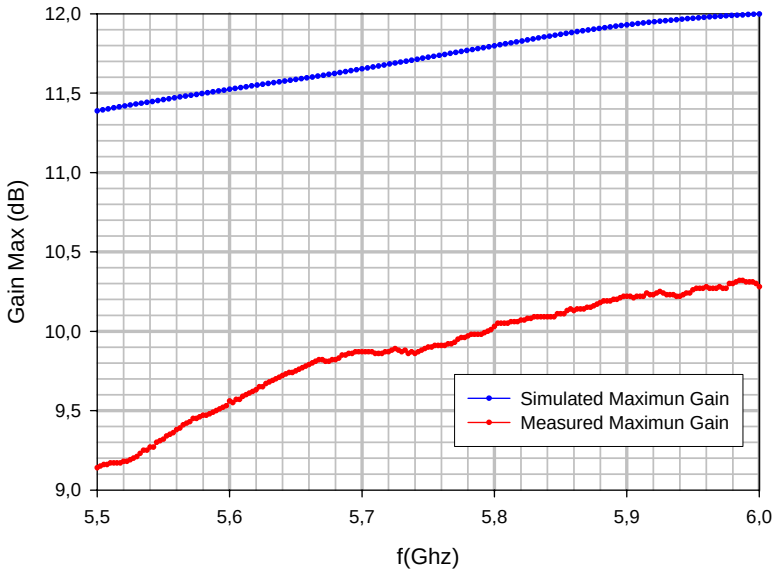

Fig. 6. Maximum Gain in dB in the frequency range (5.5-6.0) GHz.

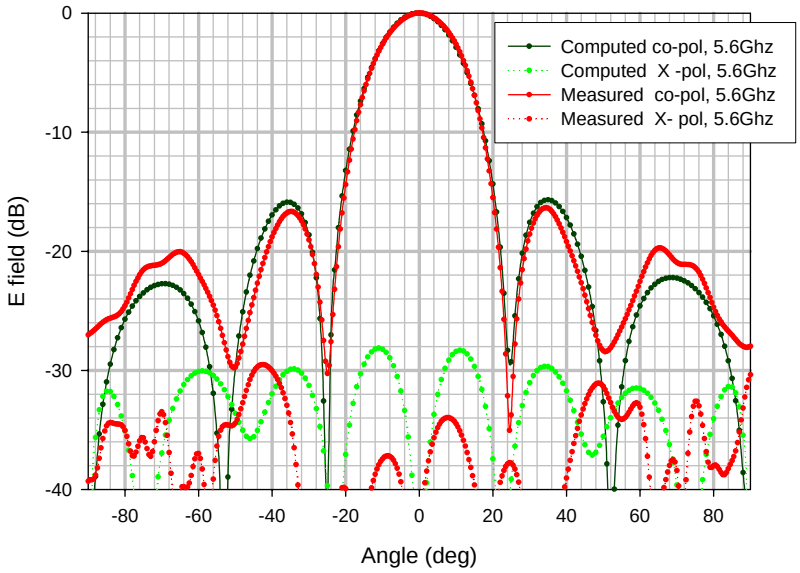

Fig. 7. E field in the H and V-planes (φ = 0°), computed and measured at the frequency *f* = 5.6 GHz.

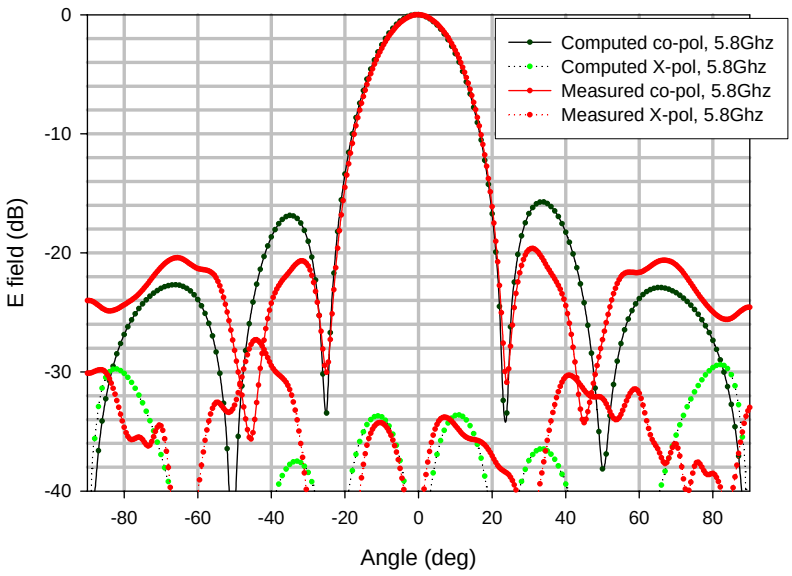

Fig. 8. E field in the H and V-planes (φ = 0°), computed and measured at the frequency f = 5.8 GHz.

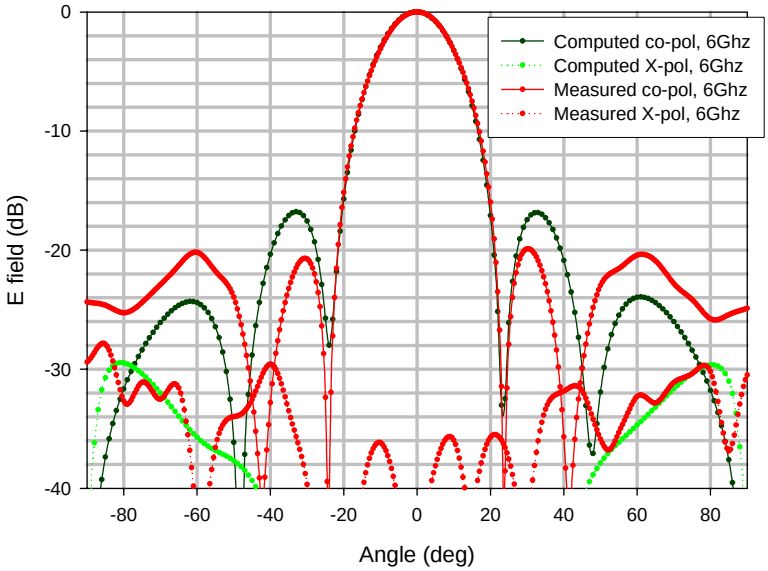

Fig. 9. E field in the H and V-planes (φ = 0°), computed and measured at the frequency f = 6.0 GHz.

6- Computation resources

The simulation was performed on a desktop PC. This machine has a Pentium 4 - 3 GHz processor with an available RAM memory of 1 GB.

The simulation has been run for 29 frequencies ranging from 5GHz to 6.5GHz. The software took 5479.915 seconds to complete the computation of the current distribution and S parameters at all the frequency points. It must be noted that the antenna pattern was calculated at 181 different thetas, so it was very time-consuming. The Peak memory usage during the whole solution was: 143.075 MByte. 3026 unknowns were needed for the matrix solver.

7- Discussion

FEKO has proved to be a powerful and efficient software to analyze any type of multilayer antennas, including geometries with slots in a finite ground plane. As long as infinite dielectric layers are supposed, the computation requirements are low.

This program allows the designer to easily introduce the structure under study using its own EDITFEKO, and the simulation setup is almost immediate, in view of the fact that a considerable number of parameters must be changed, the common edition tools makes the definition of the structure a difficult and unfriendly task due to complicated geometry. Nevertheless, using the AutoCAD tool or its own CADFEKO, the definition of the structure is an easy and friendly task.

The Reflection coefficient (S11) and VSWR frequency performance (figures 4 and 5) shows a visual disagreement, due to finite ground plane considerations and meshing procedure, nevertheless these results could be improved considering the appropriate meshing procedure during the simulation process.

On the other hand, with respect to the simulation results for the radiation pattern, a global good agreement is observed. The radiation patterns (Figures 7-9) fit similarly with the measured results provided by UNISI in every shown plane.

The Maximum Gain (figure 6) does not match to the results provided by the submitting entity, and exhibit a value difference of +1.8dB. In contrast, the frequency evolution of this parameter is in agreement with the provided results. With FEKO, the Green's function approach does not allow the determination of the losses inside the dielectric directly due to the fact that a current distribution must be known to do that. But our substrate is not lossless, so losses can exist. In order to solve this problem, we can compare the far field gain of this antenna in main-beam direction with and without losses in the substrate to determine the lack of efficiency.

It is the author's opinion that this tool is very well suited for the simulation of most patch antennas consisting of multilayer structures, as it provides very useful information for the antenna designer, with very little effort to introduce the structure, very low computation requirements and an straightforward simulation setup where most of the options can be kept in their default values.

11. SIMULATION RESULTS

From UPV (IE3D)

1- Entity

Universidad Politécnica de Valencia
U.P.V.
I.T.E.A.M.
Edificio 8G
Camino de Vera S/N
Valencia 46022
Spain
Tel: 963879585

2- Name of the simulation tool

IE3D

3- Generalities about the simulation tool

IE3D is a full-wave, method-of-moments based electromagnetic simulator solving the current distribution on 3D and multilayer structures of general shape. It has been widely used in the design of MMICs, RFICs, LTCC circuits, microwave/millimeter-wave circuits, IC interconnects and packages, HTS circuits, patch antennas, wire antennas, and other RF/wireless antennas.

4- Simulation Set-up (Geometry set-up, GUI, mesh, boundary conditions, excitation)

The structure has been drawn using the GUI tool of the IE3D software, called MGrid, which allows us to introduce any kind of planar structure easily by defining the layers and the metallizations above each one.

The mesh is generated automatically by the IE3D software, which results in a rectangular uniform pattern for the patches, slots, and straight sections of the microstrip line. Alternatively, the software employs a more refined triangular meshing for corners and discontinuities of the feed microstrip structure. The Automatic Edge Cell feature of the software has demonstrated to be very efficient and useful for novice users.

With respect to the cell size, a value of 15 cells per wavelength at the upper frequency of the band (6.5GHz) was found to be enough for the required accuracy. The following figures show the defined structure on the GUI interface as well as the mesh employed.

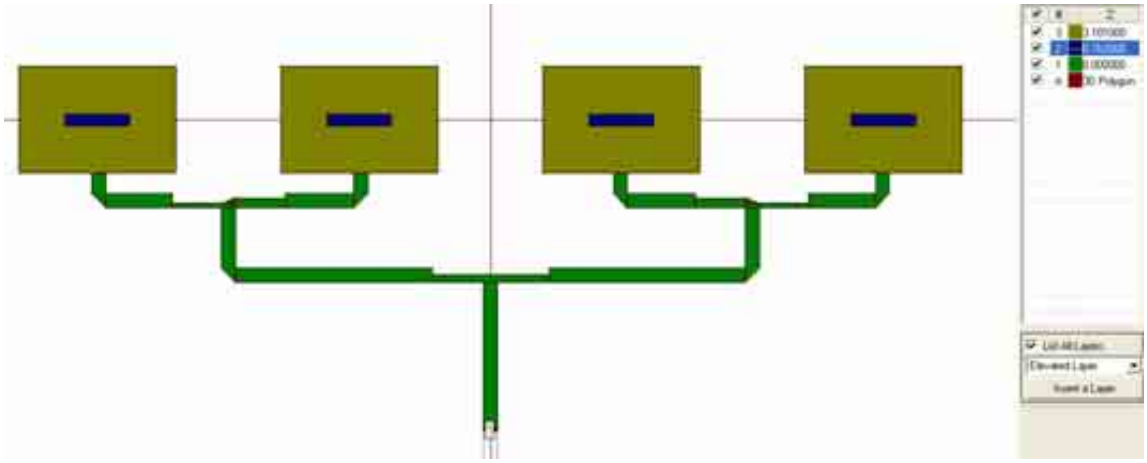

Figure 1: Structure of Linear Patch Array in IE3D

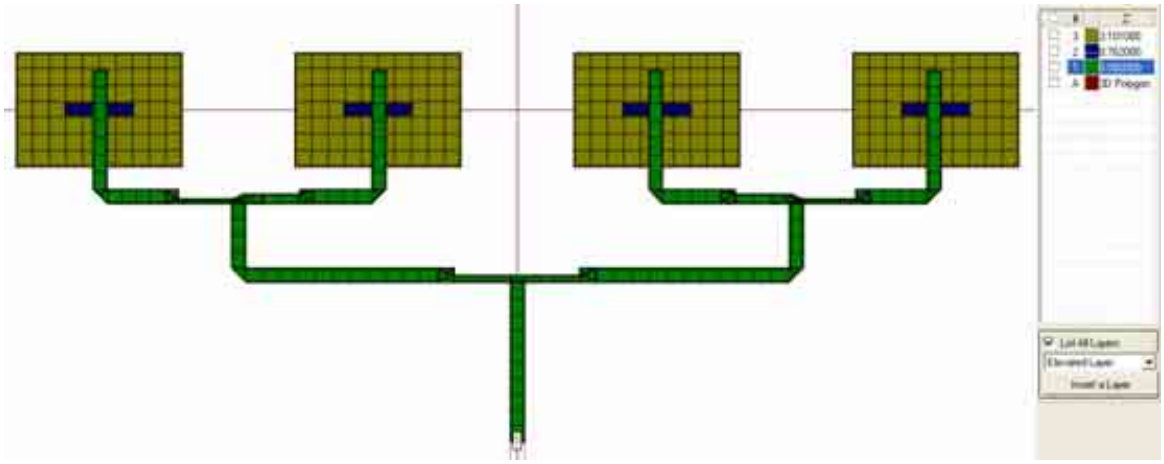

Figure 2: Meshed structure

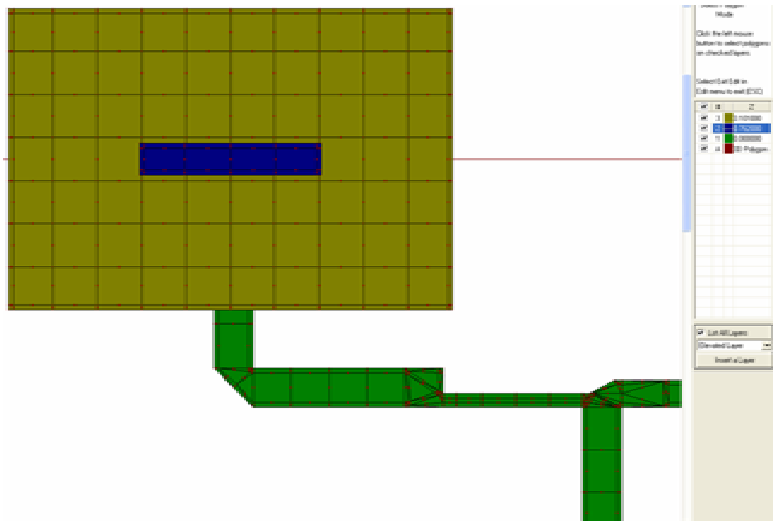

Figure 3: Detail of the mesh

In all the simulations, infinite layers of dielectric materials as well as an infinite ground plane have been considered. In this way, the slots are modelled by introducing artificial magnetic currents on their surface, and thus avoiding the mesh of the whole ground plane. This approximation allows the software to mesh the surfaces where are located the equivalent electric/magnetic currents only, and therefore the computation requirements are greatly reduced. As a result, 1896 unknowns were needed to simulate the total array structure in this case. The figures above illustrate the meshed structure formed by the patches, the slots and the microstrip feed line.

The excitation has been modelled by using the IE3D feature “Extension ports”, which can simulate a 50 Ohm microstrip lines as the one used in this case. In order to obtain a better emulation of the real feeding port (probably a SMA connector), the approach “Extension for MMIC” defined by the IE3D software is employed throughout all the simulations.

The IE3D GUI (MGrid) shows to be extremely well suited for planar of structures, even for the ones which include slots on an infinite ground plane. The patch array and the feeding slots can be introduced in no more than 15 minutes time. However, the definition of the complicated microstrip line divisor requires a longer time due to its corners and oblique edges. Moreover, the numerous editing tools that supports IE3D such as copy&paste, reflection, displacement, and so on, help the user to reduce drastically the structure definition time. On the other hand, the simulation setup is immediate, and most of the options can be kept at their default value.

5- Simulation results

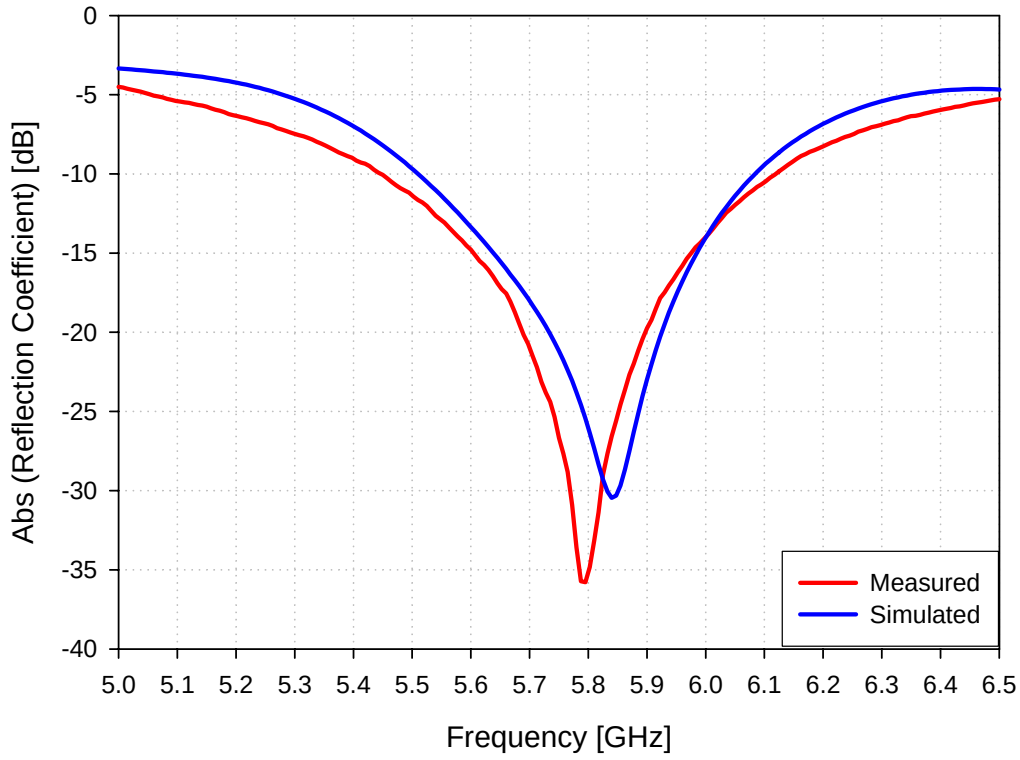

Fig. 4 Reflection coefficient (in dB) at the input port in the frequency range (5.0-6.5) GHz. The reflection coefficient is referred to a 50 Ω port impedance.

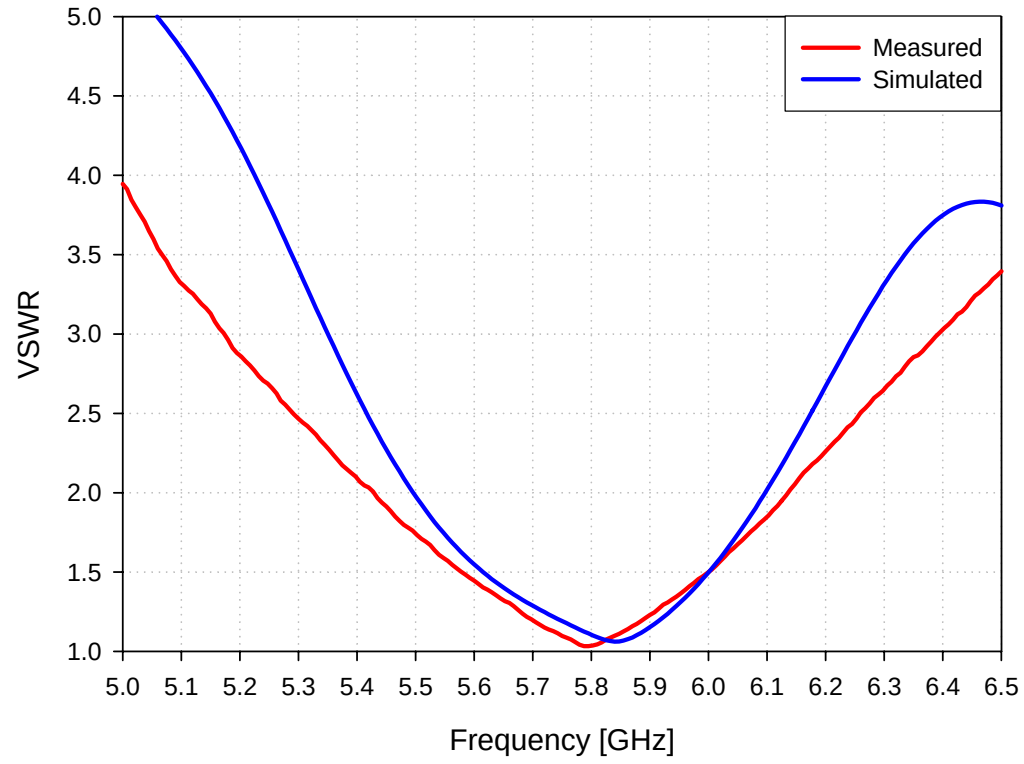

Fig. 44 Voltage standing wave ratio (VSWR) at the input port in the frequency range (5.0-6.5) GHz.

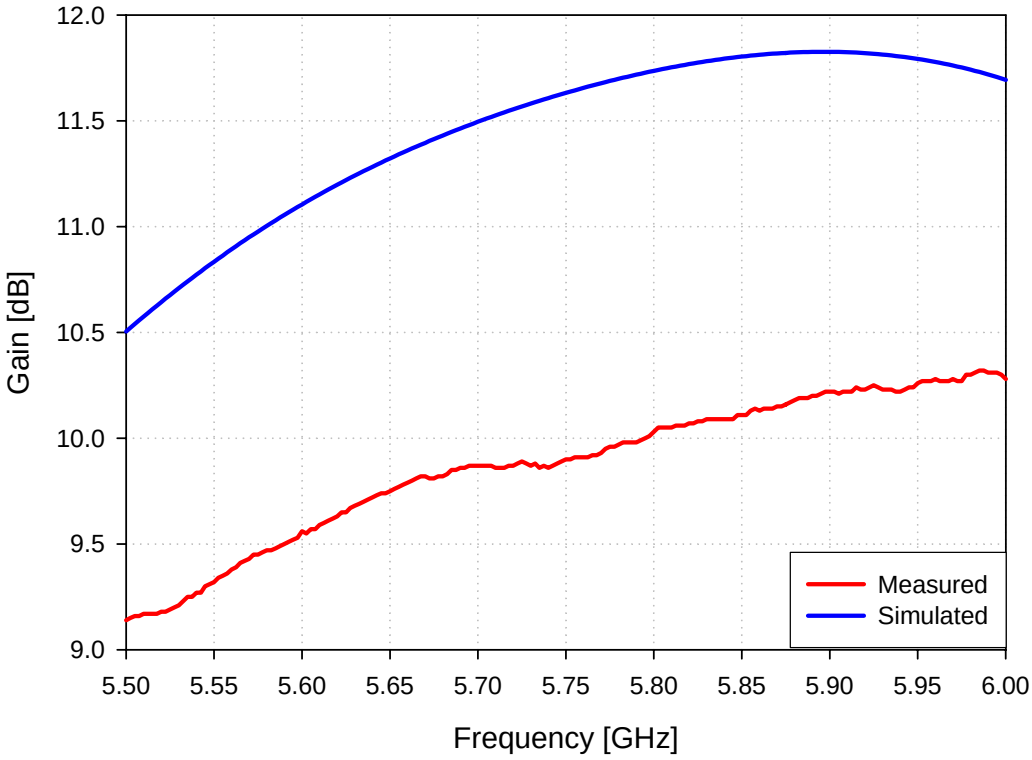

Fig. 45 Maximum gain (in dB) in the frequency range (5.6-6.0) GHz.

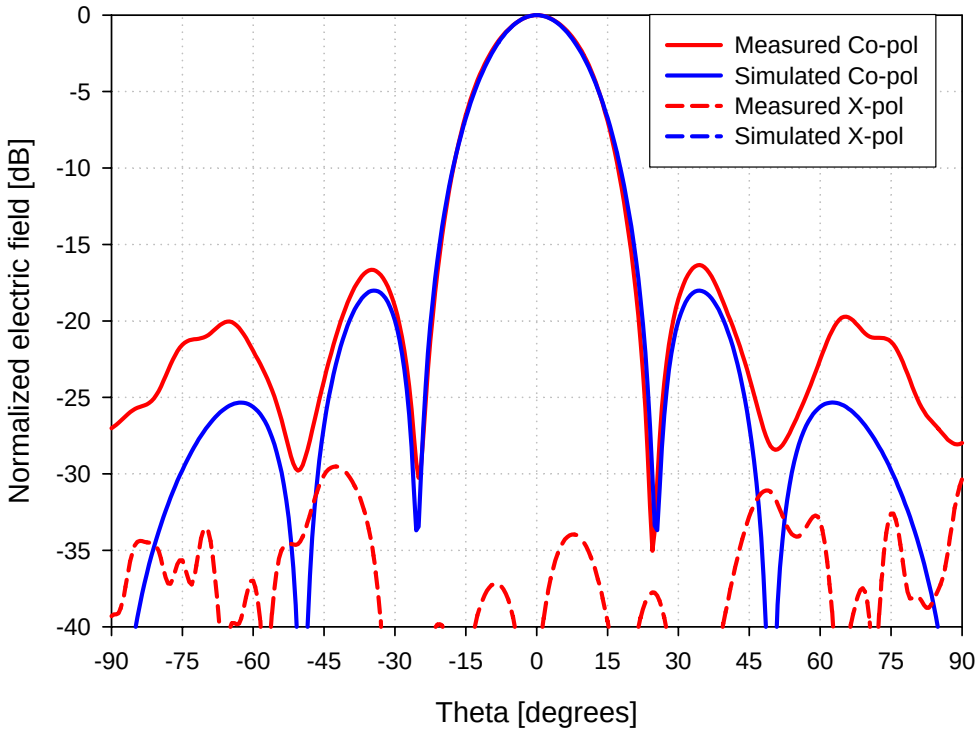

Fig. 46 Normalized electric field in the H-plane (φ = 0°), computed at the frequency *f* = 5.600 GHz. Co-pol: continuous line; X-pol: dashed line.

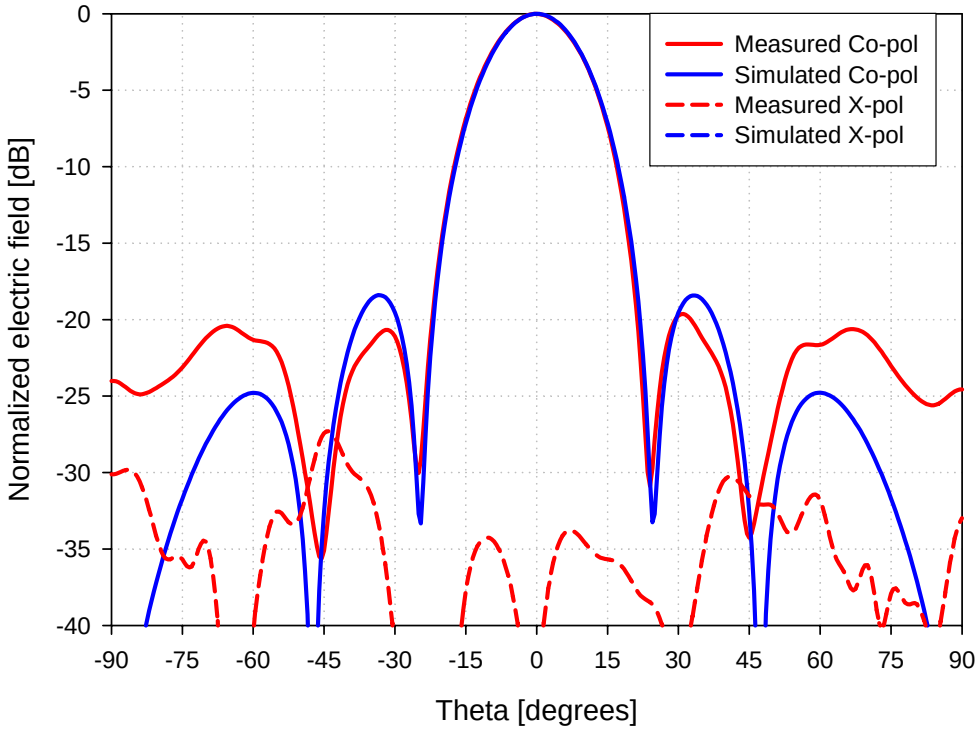

Fig. 47 Normalized electric field in the H-plane (φ = 0°), computed at the frequency *f* = 5.800 GHz. Co-pol: continuous line; X-pol: dashed line.

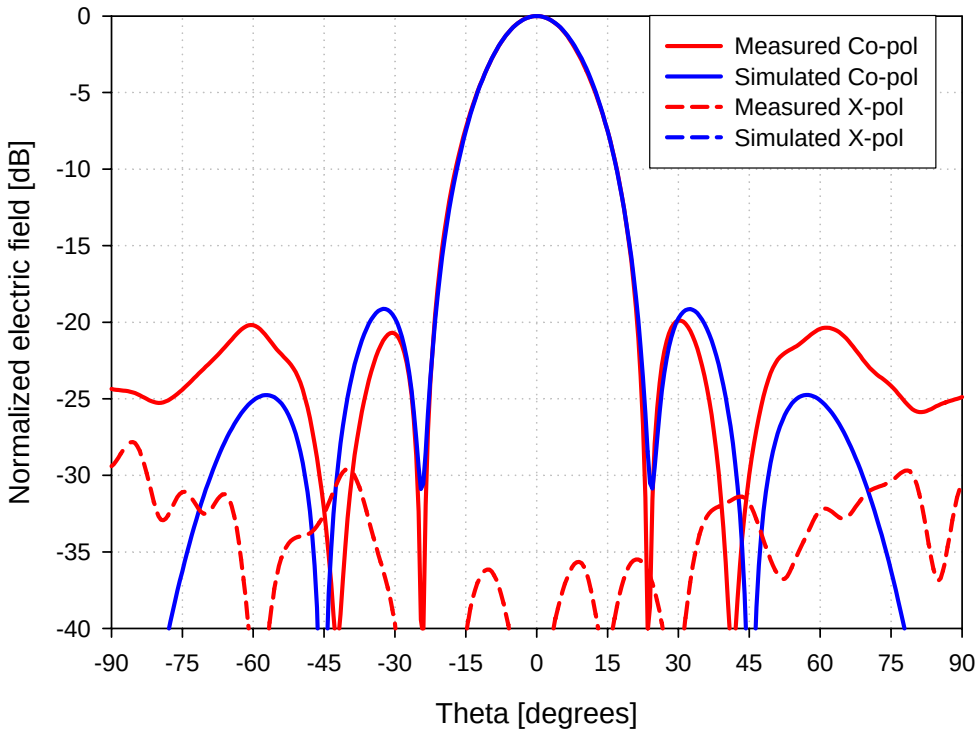

Fig. 48 Normalized electric field in the H-plane (φ = 0°), computed at the frequency *f* = 6.000 GHz. Co-pol: continuous line; X-pol: dashed line.

6- Computation resources

The simulation was performed on a desktop PC. This machine has a Pentium 4 - 3 GHz processor with an available RAM memory of 1 GB.

The simulation has been run for 61 frequencies ranging from 5GHz to 6.5GHz. Since IE3D uses a frequency interpolation scheme, it just computes the current distribution and radiation patterns at 11 frequency points. The software took 178 seconds to complete the computation of the current distribution and S parameters at 11 frequency points, while it took 306 seconds to calculate the radiation patterns. It must be noted that the antenna pattern was calculated at 37 different phi planes with 37 theta points per plane for each frequency, so it was very time-consuming. According to the program information, an amount of 29 MB of memory (1896 unknowns) was needed for the matrix solver.

Finally, note that finite dielectrics and/or ground plane have not been considered in order to reduce the computation time. Since no results of a manufactured prototype were provided, the simulation of a finite structure does not make sense.

7- Discussion

The IE3D has proved to be a powerful and efficient software to analyze any type of multilayer antennas, even including the presence of slots in an infinite ground plane. As

long as infinite layers are supposed, the computation requirements are very low, so the simulation can be carried out with rather old machines within an hour or two.

This program allows the designer to easily introduce the structure under study using its own GUI, and the simulation setup is almost immediate, since very few parameters must be changed. The common edition tools such as copy, paste, reflect, displacement, and so on, makes the definition of the structure an easy and friendly task.

With respect to the simulation results, a global good agreement is observed. The radiation patterns fit almost exactly with the results provided by UNISI in every shown plane. The VSWR frequency performance also shows a practically perfect visual agreement, but a rigorous comparison could not have been carried out due to the absence of tabulated data. However, the gain and directivity do not match to the results provided by the submitting entity, and exhibit a value difference of +1dB in the case of the gain and +2dB for the directivity. In contrast, the frequency evolution of both parameters is in agreement with the provided results.

It is the author's opinion that this tool is very well suited for the simulation of most patch antennas consisting of multilayer structures, as it provides very useful information for the antenna designer, with very little effort to introduce the structure, very low computation requirements and an straightforward simulation setup where most of the options can be kept in their default values.

12. SYNTHESIS OF RESULTS

The number of institutions which participate to the benhmarking activity is six:
UNISI (Università di Siena), Italy
EPFL (Ecole Polytechnique Federale de Lausanne), Switzerland
IETR (Institute National des Sciences Appliques de Rennes), France
KUL (Katholieke Universitet Leuven), Belgium
LIVUNI (University of Liverpool), England
UPV (Universidad Politecnica de Valencia), Spain
Three institutions participate with two softwares each. The following table contains, for each software, the applied methodology, the domain of solution, and the kind of property.

INSTITUTION	SOFTWARE	METHOD	DOMAIN	PROPERTY
UNISI	DESIGNER	MoM	F	C
EPFL	POLARIS	MoM	F	P
IETR	IMELSI	FDTD	T	P
IETR	MRFDTD	FDTD	T	P
KUL	MAGMAS	MoM	F	P
LIVUNI	CST	FI	T	C
LIVUNI	HFSS	FEM	F	C
UPV	FEKO	MoM	F	C
UPV	IE3D	MoM	F	C

Legend
MoM: method of moments
FDTD: finite difference time domain
FI: finite integration
FEM: finite element method

T: time (domain)
F: frequency (domain)

P: proprietary
C: commercial

From the table, the following conclusions can drawn:
- 5 softwares are based on a integral equation solution based on MoM. Among these, three are specifically designed for planar structures (DESIGNER, POLARIS, MAGMAS, IE3D), while one is a general-purpose MoM-based software (FEKO). All these software are frequency-domain software.
- 4 software are based on a differential equation solution, based on time-domain techniques (FDTD, FI) or frequency domain technique (FEM).

No particular difficulties have been encountered by the participants in performing the simulations.

Some of the simulated results present a certain discrepancy with respect to the measured data. In particular the level of the first side lobes in the radiation pattern at the frequencies of 5.8 and 6.0 GHz is not reproduced well by any of the software.

BENCHMARKING ACTIVITY

(WP1.1-2)

Cavity-backed microstrip antenna with dual coaxial probe feed

Proposed by
Universidad Politécnica de Madrid
-UPM-

1. STRUCTURE DESCRIPTION

1. Entity

UPM
Escuela Técnica Superior de Ingenieros de Telecomunicación
Universidad Politécnica de Madrid
Ciudad Universitaria s/n
28040-Madrid. Spain.
Phone: +34 91 5495700
Fax: +34 91 3367348
Contact persons: Miguel A. González. E-mail:mag@etc.upm.es
Juan Zapata. E-mail: jzapata@etc.upm.es

2. Name of the structure

Cavity-backed microstrip patch antenna with dual coaxial probe feed.

3. Generalities

Cavity-backed microstrip antennas have many interesting advantages with respect to the conventional configuration with patches on continuous substrates. In this configuration the patches are enclosed into metallic cavities in order to prevent surface wave modes in the dielectric substrates. The cavity enclosure provides major efficiency, improvement of radiation characteristics or small inter-element coupling in arrays, in addition to other profits; and it is often a closer modelling of the antenna in a real environment. In the case of phased arrays it allows to use thick substrates in order to increase the impedance bandwidth of the antenna without the limitation in the scanning range, or even to achieve a considerable improvement in scan performance or prevent scan blindness in large arrays.

On the other hand the use of two feed points is a common technique to obtain circular or dual polarization.

4. Structure Description

The geometry of the radiating structure proposed for benchmarking is shown in figure 1. It is a cavity-backed circular microstrip antenna with two coaxial feeds at orthogonal positions (x and y-axis). A circular patch printed on a dielectric substrate is enclosed into a circular cross-section metallic cavity recessed in an infinite metallic plane. This arrangement can be employed, for example, to accomplish low work frequencies without large patch sizes.

The coaxial feeds correspond to a 50-Ω SMA connectors. All their dimensions and the dielectric constant are proposed to be considered in the simulations.

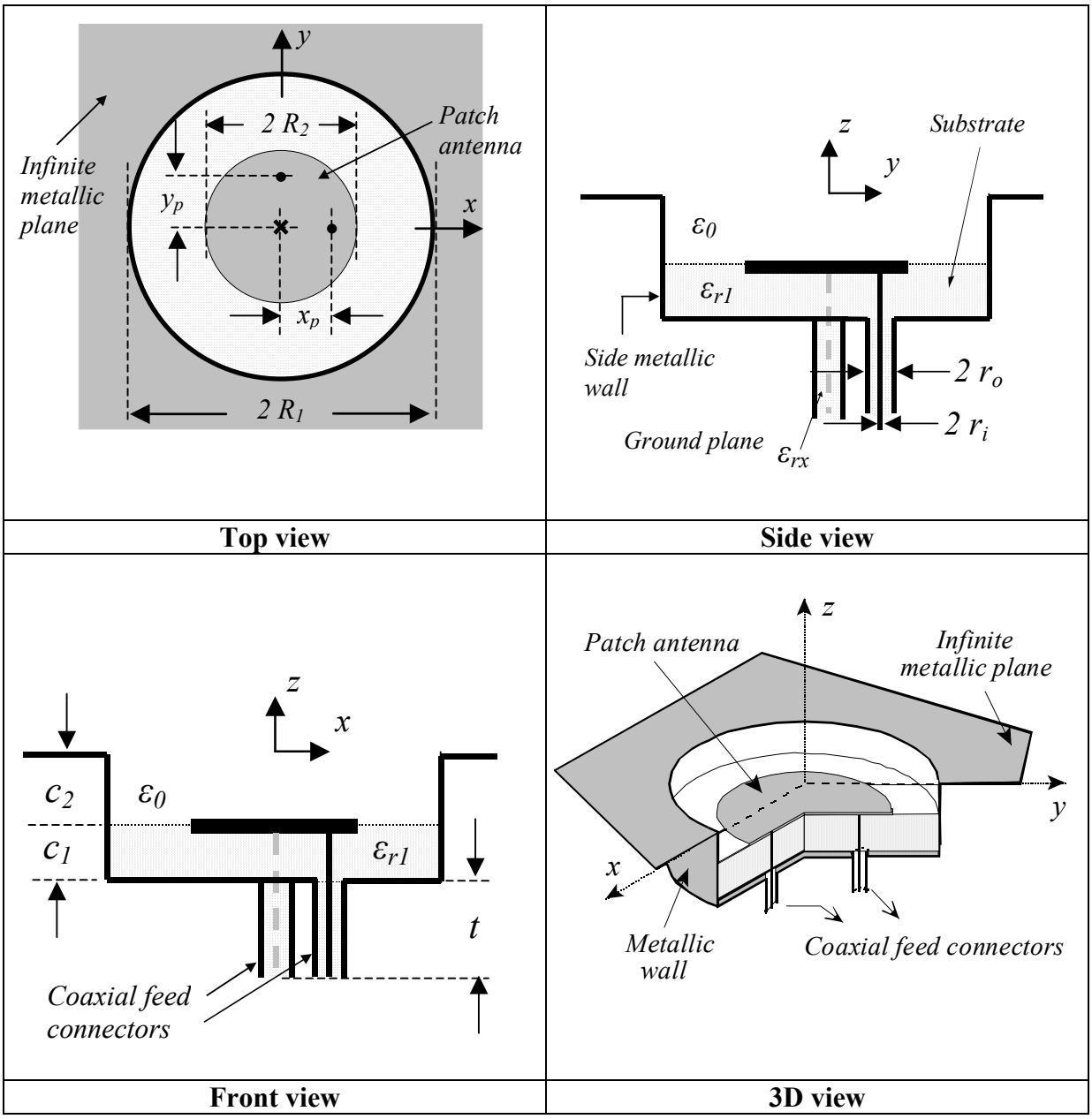

Figure 1

The dimensions and material characteristics of the proposed dual-feed cavity-backed microstrip antenna are given in the next tables:

Dimensions Table		
Object	**Variable name**	**Dimensions (mm)**
Susbtrate (GML 1032)	Radius R_1	30
	Thickness c_1	1.524 (0.06∀0.003 inches)
Cavity	Radius R_1	30
	Depth $c_1 + c_2$	5.5
Patch	Radius R_2	24.75
Probes	Radius r_i	0.65
	Location x_p	6.2
	Location y_p	6.2
Coaxial feed connectors (SMA connectors)	Inner radius r_i	0.65
	Outer radius r_o	2.05
	Length t	2.0

Materials Table	
Object	**Properties**
Susbtrate (GML 1032)	Relative dielectric constant $\varepsilon_{r1} = 3.2$ ∀0.05
	Loss tangent $tan\ \delta = 0.003$
Dielectric in the coaxial feeding	Relative dielectric constant $\varepsilon_{rx} = 1.8998$
	Loss tangent $tan\delta = 0$ (lossless)
Metallic flange	Perfect metal, infinite.
Patch, ground plane, sidewall of the cavity	Perfect metal
	No thickness (perfect 2D object)

Moreover, the same radiating structure with a finite metallic plane is also proposed for benchmarking. A finite metallic flange of aluminium circular in shape with radius R_3 and thickness e is considered. In this case the antenna is fabricated and measured. The rest of dimensions and material characteristics do not change. The geometry of the antenna with the finite metallic plane is shown in figure 2. The characteristics of this flange are given in the next table.

Dimensions Table		
Object	**Variable name**	**Dimensions (mm)**
Finite metallic flange (aluminium)	Radius R_3	150
	Thickness e	12.5

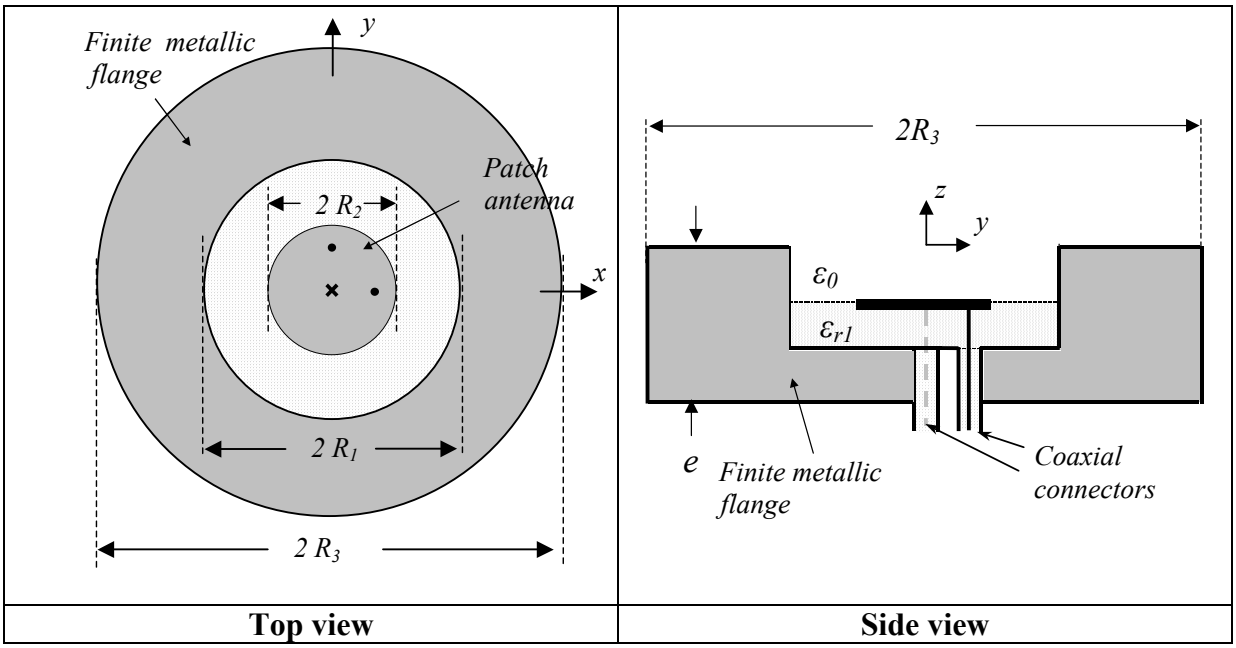

Figure 2

5. Computed and measured results

The results considered both for the case of infinite metallic plane and for the case of finite metallic plane are described next:

-. Reflection coefficient of the TEM excitation mode at the coaxial connectors versus frequency. The reference plane is located at the input port of the coaxial connectors. This is the port impedance for normalization (50Ω).

S11: Reflection coefficient at the input port located along the y-axis when the other port is terminated with a matched load.

S22: Reflection coefficient at the input port located along the x-axis when the other port is terminated with a matched load.

-. Variation of coupling coefficient, S_{12} (S_{21}) between the TEM modes at the coaxial feeds versus frequency.

-. Far field radiation patterns in different planes when the antenna is excited at both coaxial feeds.

The different simulations are detailed in the next tables.

Simulation setup 1	
Frequency range	Output results
From 1.8 GHz to 2.1 GHz	-. Reflection coefficient of the TEM excitation mode, S_{11} and S_{22} at the coaxial ports. -. Isolation or coupling coefficient, S_{12} (S_{21}), between the TEM modes at the coaxial ports.

Simulation setup 2	
Frequency	Output results
1.9575 GHz	Far field plots in amplitude of θ and φ components, A_θ (θ,φ) and A_φ (θ,φ), from θ = -90 to 90° and φ = 0, 45, 90º when the coaxial connector located along the x-axis is excited and the other port is terminated with a matched load Antenna directivity in broadside direction.

6. References

The benchmarking of this structure will consist of a comparison between numerical techniques in the case of infinite metallic plane. Simulations obtained with in-house software, SFELP, will be available. This procedure provides the Generalized Scattering Matrix of the radiating structure which relates exciting modes at the input port(s) and radiated spherical modes. From these matrices, the input impedance, and coupling and radiating characteristics, are directly deduced.

In the case of finite metallic flange measurements will be available.

7. Additional comments

2- STRUCTURE MEASUREMENTS

1. Entity

Escuela Técnica Superior de Ingenieros de Telecomunicación
Universidad Politécnica de Madrid , UPM
Ciudad Universitaria s/n
28040-Madrid. Spain.
Phone: +34 91 5495700
Fax: +34 91 3367348
Contact persons: Miguel A. González. E-mail:mag@etc.upm.es
Juan Zapata. E-mail: jzapata@etc.upm.es

2. Description of the measurement tools

- Return loss and coupling measurements are realised on a Agilent Technologies vector network analyser model E8362B
- Radiation pattern measurements and directivity are realised in anechoic chamber.

3. Generalities about measurement tools

4. Measurements Set-up

- The anechoic chamber is a spherical near-field system at the Polytechnic University of Madrid (UPM) belonging to the ACE Network , activity 1.2: 'Antenna Measurement And Facilities Sharing'. The measurements facilities are described in the VCE.

5. Measurement results

- **Return loss.**

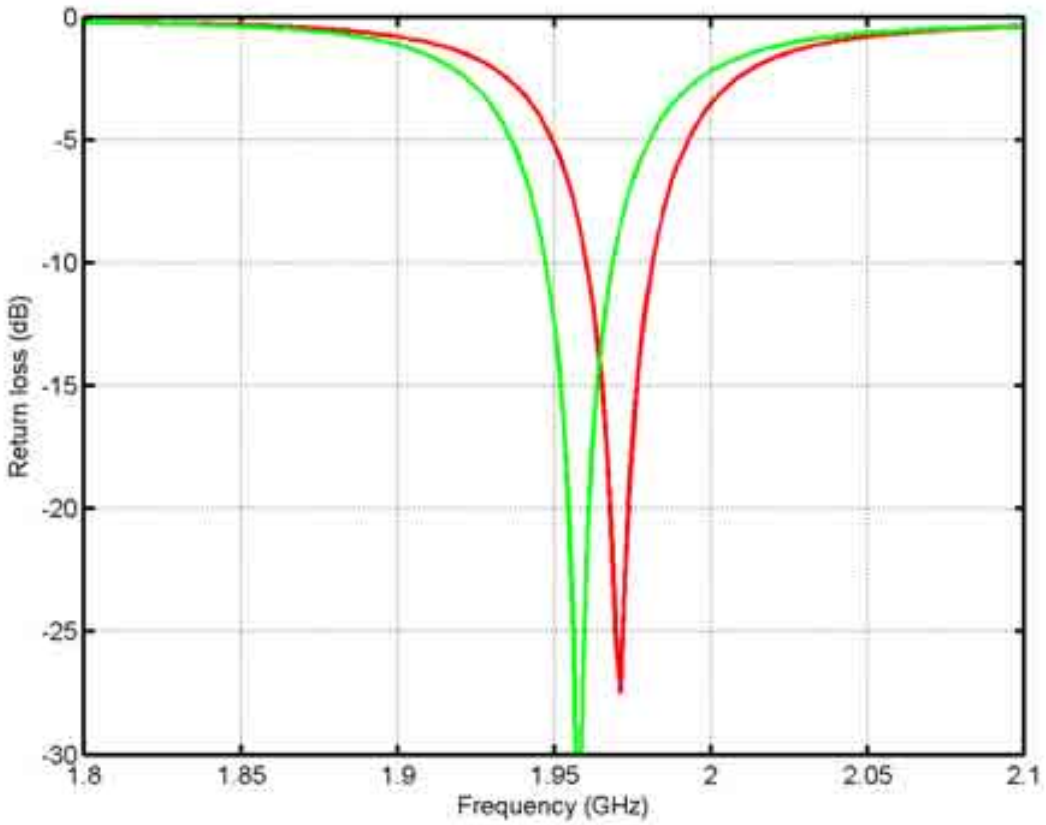

Figure 1 : Reflection coefficient magnitude versus frequency of the TEM excitation mode at the coaxial connectors.

| S_{11}| : Measured at the coaxial connector located along the y-axis (port 1) when the other port is terminated with a matched load. (Finite metallic plane)

| S_{22}| : Measured at the coaxial connector located along the x-axis (port 2) when the other port is terminated with a matched load. (Finite metallic plane)

- **Coupling magnitude.**

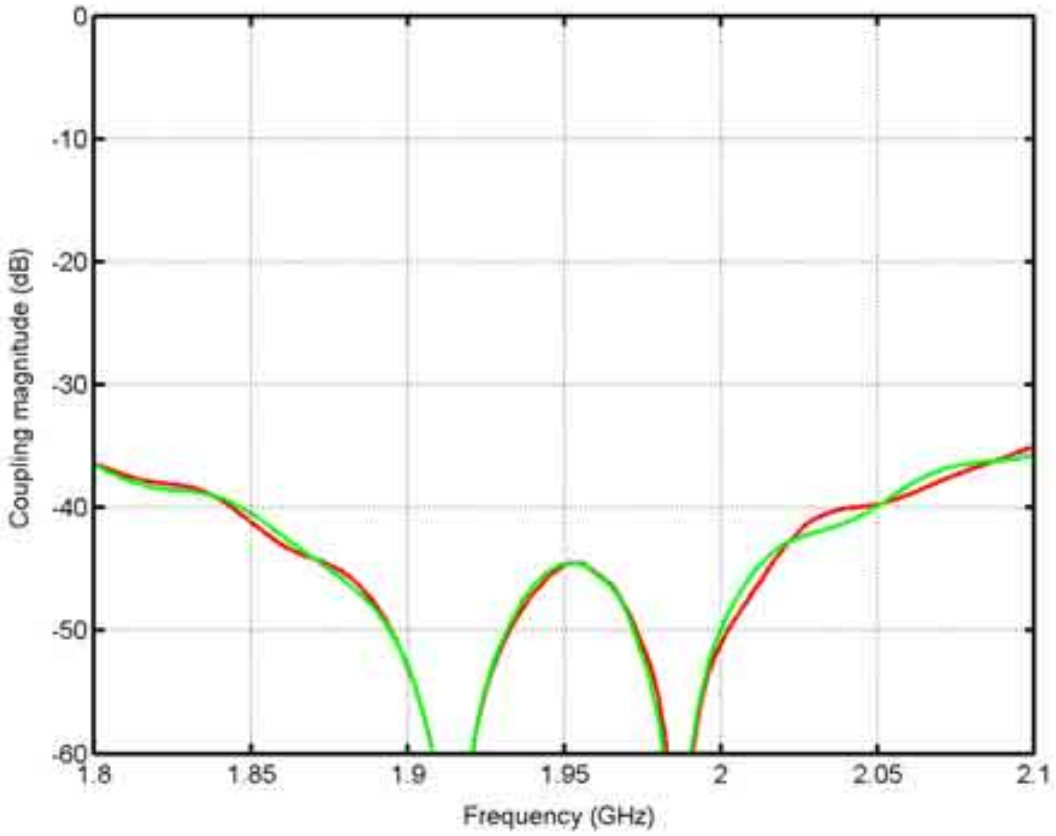

Figure 2 : Coupling coefficient magnitude versus frequency between the TEM excitation modes at the coaxial connectors.

Measured coupling magnitude $|S_{12}|$. (Finite metallic plane).

Measured coupling magnitude $|S_{21}|$. (Finite metallic plane).

- **Far-field radiation patterns.**

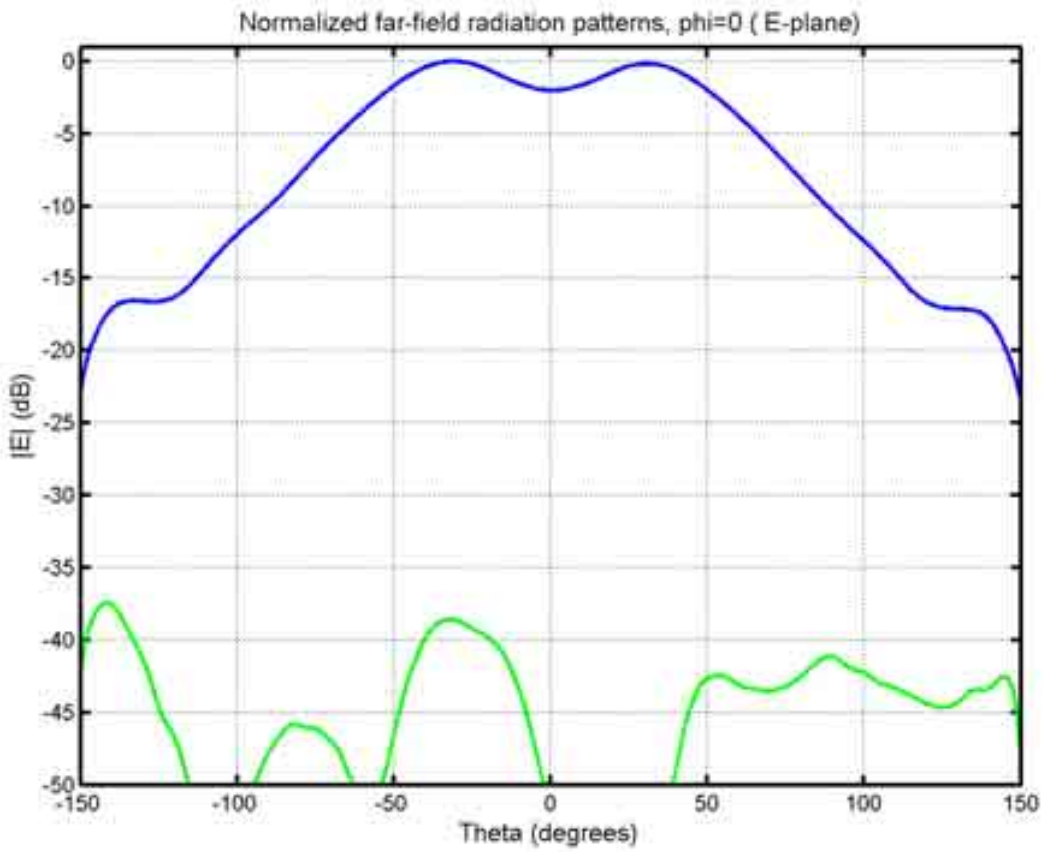

Figure 3 : E-plane radiation patterns versus theta at 1.9575 GHz when the coaxial connector located along the x-axis is excited and the other port is terminated with a matched load.

Measured co-polar component (Ephi). (Finite metallic plane).

Measured cross-polar component (Etheta). (Finite metallic plane).

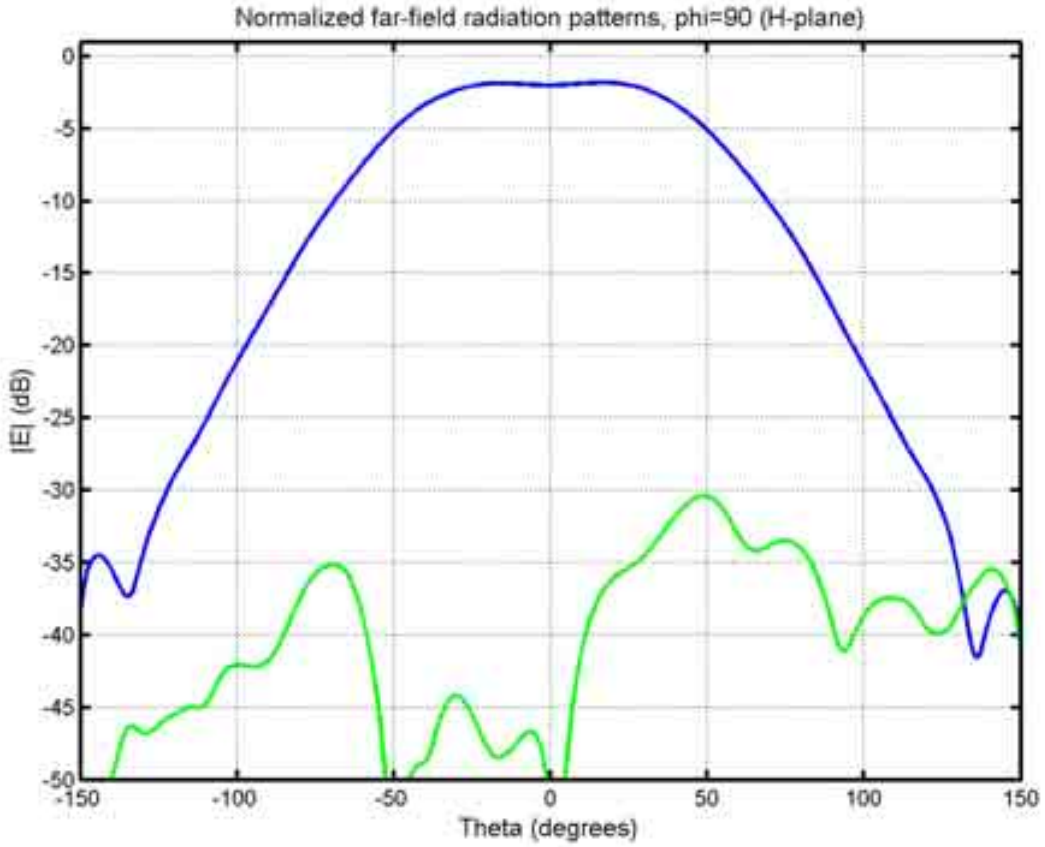

Figure 4 : H-plane radiation patterns versus theta at 1.9575 GHz when the coaxial connector located along the x-axis is excited and the other port is terminated with a matched load.

Measured co-polar component (Ephi). (Finite metallic plane).

Measured cross-polar component (Etheta). (Finite metallic plane).

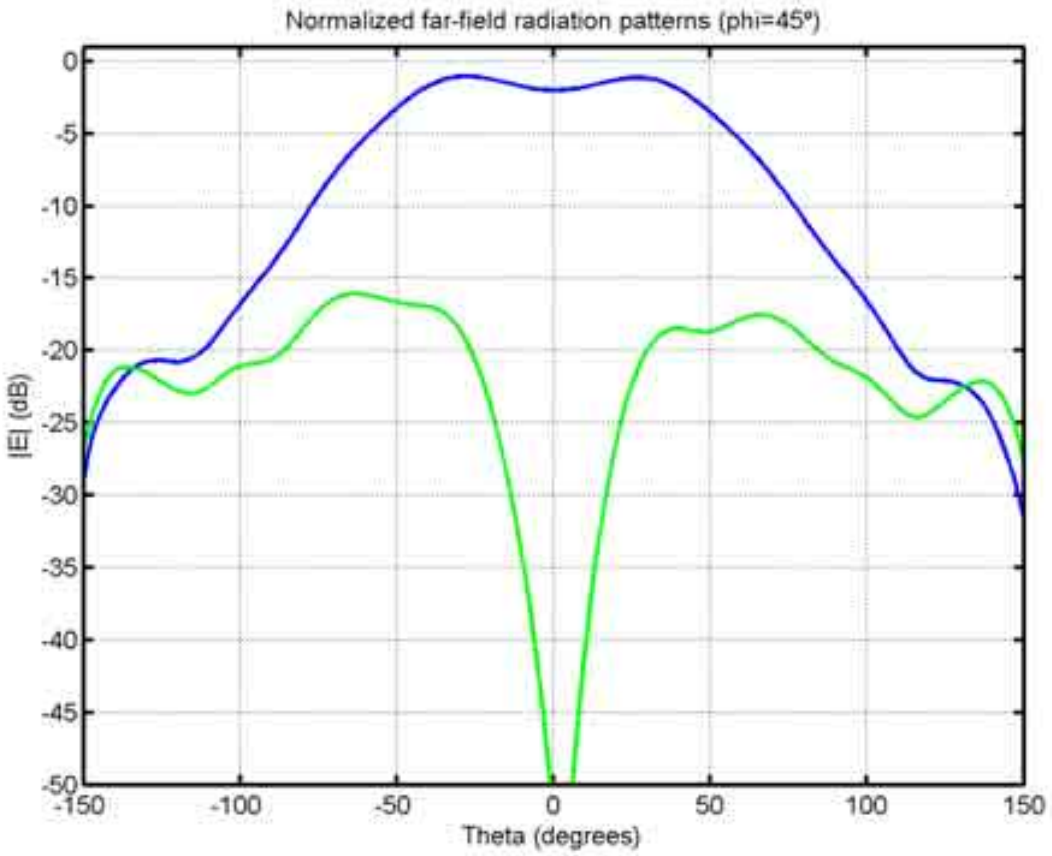

Figure 5: Radiation patterns at phi=45º versus theta at 1.9575 GHz when the coaxial connector located along the x-axis is excited and the other port is terminated with a matched load. (According to the third definition of Ludwig)

Measured co-polar component. (Finite metallic plane).

Measured cross-polar component. (Finite metallic plane).

- **Directivity.**

- Measured directivity at 1.9575 GHz when the coaxial connector located along the x-axis is excited and the other port is terminated with a matched load:

-. In Theta= 30.0 degrees and Phi= 180.0 degrees: 7.080 dBi (Maximum)

-. In Theta= 0.0 degrees and Phi= 0.0 degrees: 5.081 dBi.

- Measured directivity at 1.971 GHz when the coaxial connector located along the y-axis is excited and the other port is terminated with a matched load:

-. In Theta= 30.0 degrees and Phi= 270.0 degrees: 7.225 dBi (Maximum)

-. In Theta= 0.0 degrees and Phi= 0.0 degrees: 4.978 dBi.

6. Discussion

- Return loss measurements show two different resonances at the two coaxial connectors with a slight frequency shift displacement

7. Additional comments

3- SIMULATION RESULTS

From UPM_UPMantenna_SFELP

1. Entity

Escuela Técnica Superior de Ingenieros de Telecomunicación
Universidad Politécnica de Madrid , UPM.
Ciudad Universitaria s/n
28040-Madrid. Spain.
Tel.: +34 915495700
Contact persons: Juan Zapata. E-mail: jzapata@etc.upm.es
Miguel A. González . E-mail: mag@etc.upm.es

2. Name of the simulation tool

SFELP

3. Generalities about the simulation tool

SFELP [1,2] is a in-house software that uses a hybrid method based on the three dimensional finite element method, domain segmentation technique, modal analysis, spherical mode expansion, generalized scattering matrix and a reduced order model. This software is intended to analyse any antenna which can be embedded in a sphere in the space or in a hemisphere supported for an infinite ground plane, provided that the surface of the sphere/hemisphere is homogenous. In addition, it is able to analyse finite planar arrays of this kind of antennas.

4. Simulation Set-up (Geometry set-up, GUI, mesh, boundary conditions, excitation)

The software is divided into modules which are called sequentially by the user. Each module needs an ASCII input file, that is generated by the user by running first the module in a conversational way, and one or more binary files (data structures, DS) generated for the previous modules in the calling chain. The output of each module is, in general, a DS. The ASCII files contain a few sentences with data such as the mesh, dielectric constants, frequency range, number and kind of ports, boundary conditions etc. The DS contains intermediate results, as system matrices, description of the

boundary conditions, etc., or the final Generalized Admitance Matrix, GAM, and/or Generalized Scattering Matrix GSM of the structure.

The geometry definition and the mesh generation can be done in two different ways. The first one is with the same technique described in the previous paragraph: by defining the geometry and the degree of mesh refinement in a conversational way. This meshing tool is the same as in Modulef program, developed by the INRIA in France, from which some modules are taken. The second way for meshing generation is by using the meshing tool of a commercial program (FEMLAB). We have developed the required software interfaces to make compatible this meshing tool with our programs. This alternative approach is more flexible and powerful, since it is possible to produce a new mesh in a few minutes. The mesh generation from the first way is more costly. In both cases, the program uses vectorial tangential tetrahedral elements of degrees 2/1.

The analysis method considers the antenna as a volume with any number of ports, corresponding to the feeding waveguides and a radiation port (spheres or hemispheres). An hemisphere volume with a hemispherical port (or sphere volume with a spherical port) is employed for characterizing the radiating region. The application of the segmentation technique gives rise to a division of the overall antenna in different segments or regions. The interfaces between them are also considered as intermediate ports. Therefore, each segment is analysed separately and its individual GSM (or GAM) computed. After a connection process the overall GSM (GAM), which characterizes the antenna as a circuit, is finally obtained.

In the current version the following kind of ports have been implemented:
-. Analytical ports: Rectangular, circular , coaxial, cylindrical and spherical.
-. Numerical ports: Arbitrarily shaped homogeneous (shielded) waveguides or transmission lines and Arbitrarily shaped inhomogeneous (shielded) waveguides.

In the first group, the number and electrical symmetry of the modes can be selected automatically. In the second one, they are previously computed by 2D-FE method. Obviously, the numerical efficiency decreases with the size of the antenna. However, the antenna under analysis can be segmented, considering intermediate ports, to make the analysis more efficient.

The analysis is performed in the frequency domain. The software has two versions which have slightly different characteristics: one works on a frequency-by-frequency (FbF) basis and the other one is able to perform broadband frequency sweeps (FSW) by means of the application of a reduced order Model.

The considered circular cavity-backed microstrip antenna is segmented in two regions: on the one hand a semi-spherical region connected to a section of homogeneous circular waveguide (region 1 in figure 2), and on the other, a module which includes the coaxial feeding and cavity region of the antenna (region 2 in figure 2). The first region includes two ports, a semi-spherical surface (spherical port) and a circular port connected to the bounded domain of the antenna. The second one includes three ports, the same circular port and two coaxial ports. The next figures show the considered hemispherical region and the ports and modules used in the analysis of the antenna.

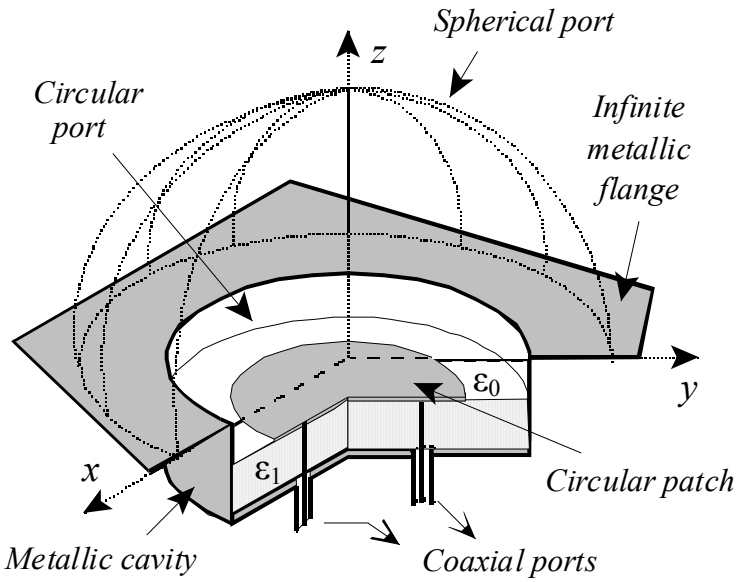

Figure 1: 3-D view of the cavity-backed patch. The ports and the hemispherical region considered in the analysis are shown.

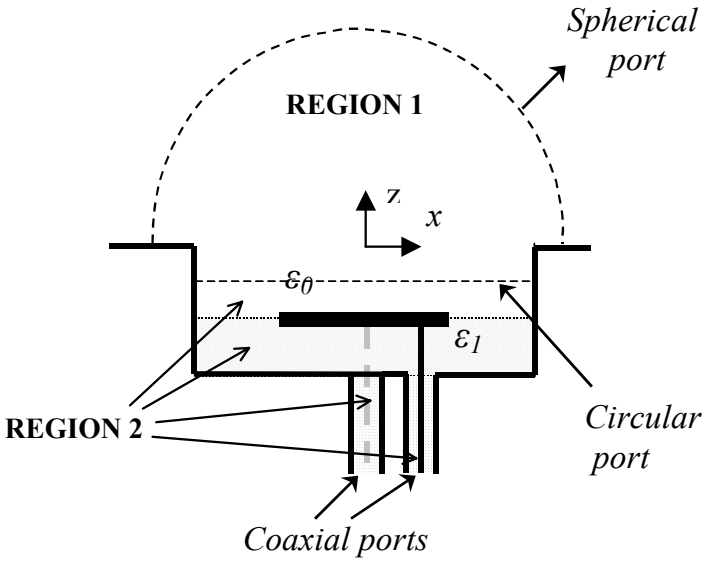

Figure 2 : front view of the cavity-backed patch. The two regions considered for the domain segmentation technique are shown.

The mesh was generated from the commercial program FEMLAB. In the simulation and for the first module, symmetry considerations make it possible to reduce the computational domain to a quarter, analysed four times with different boundary conditions. A mesh with 629 tetrahedral elements and 4862 degrees of freedom is employed. In each simulation, 35 modes were used in the spherical port and 50 modes in the circular port. Figures 3 and 4 show the geometry and the mesh of this module obtained from FEMLAB.

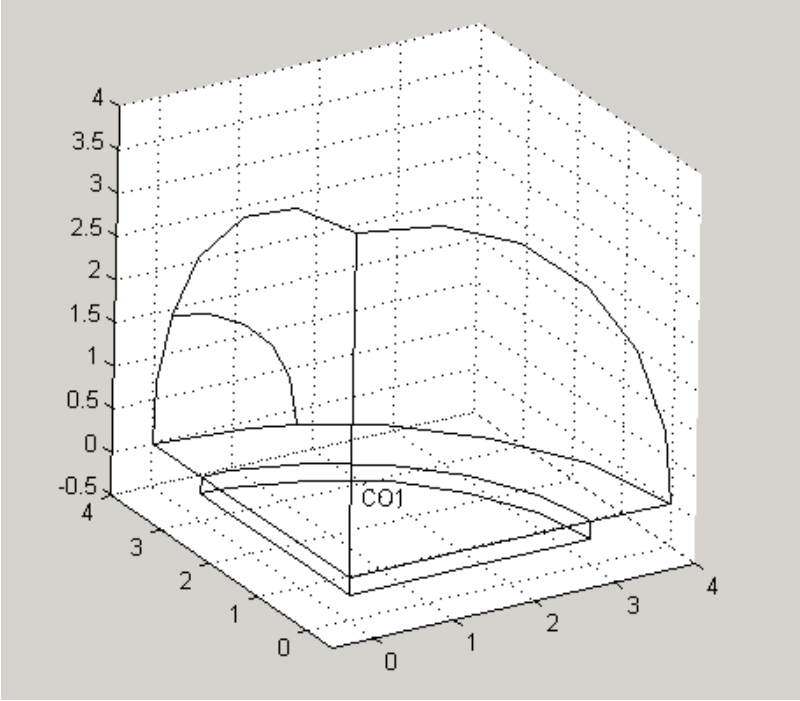

Figure 3 : Computational domain considered to analyse region 1 in Fig. 2. From symmetry considerations only a quarter of the hemispherical real region is employed in the simulations.

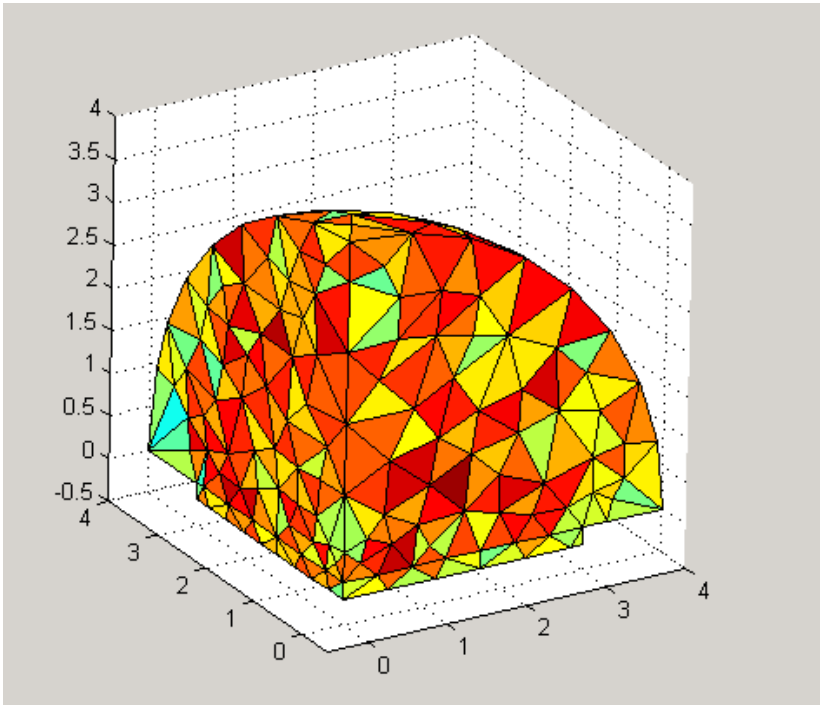

Figure 4 : Mesh of the computational domain considered for region 1.

For the second defined region, no symmetry consideration may be employed and the whole real region has to be meshed. 4133 tetrahedral elements and 32230 degrees of freedom have been employed in the mesh. In each simulation, 200 modes were used in the circular port, and 5 modes in each coaxial port. Figures 5 and 6 show the geometry and the mesh of this module obtained from FEMLAB.

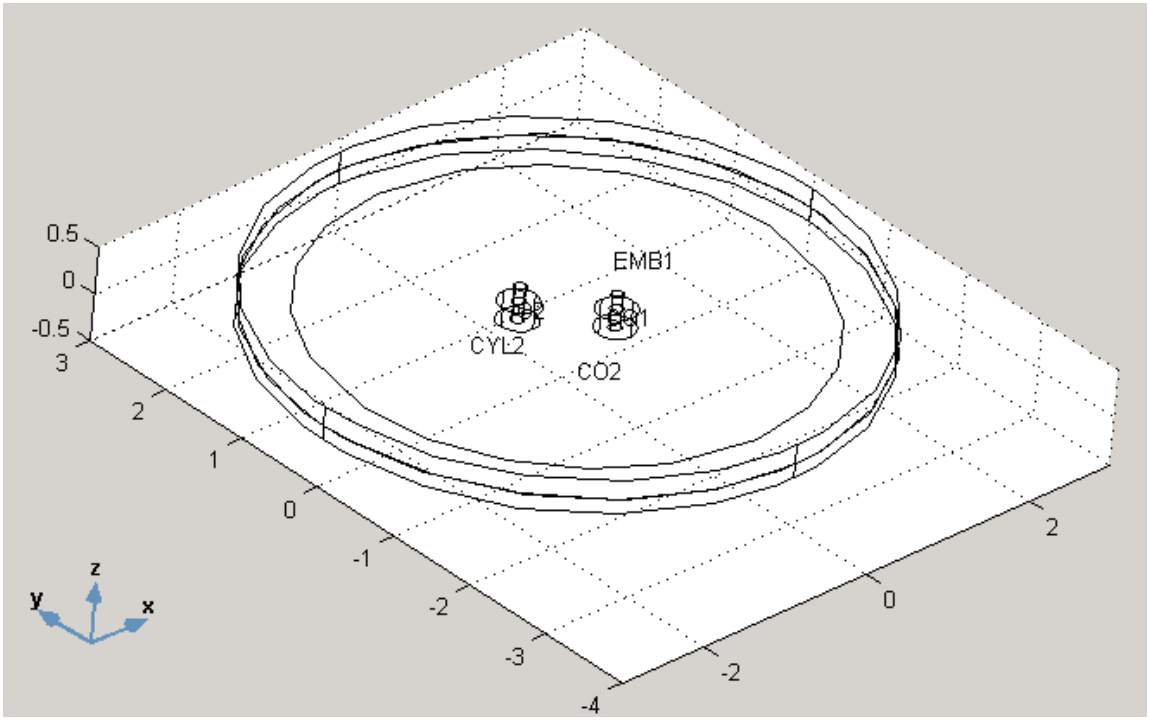

Figure 5 : Computational domain considered to analyse region 2 in Fig 2 .

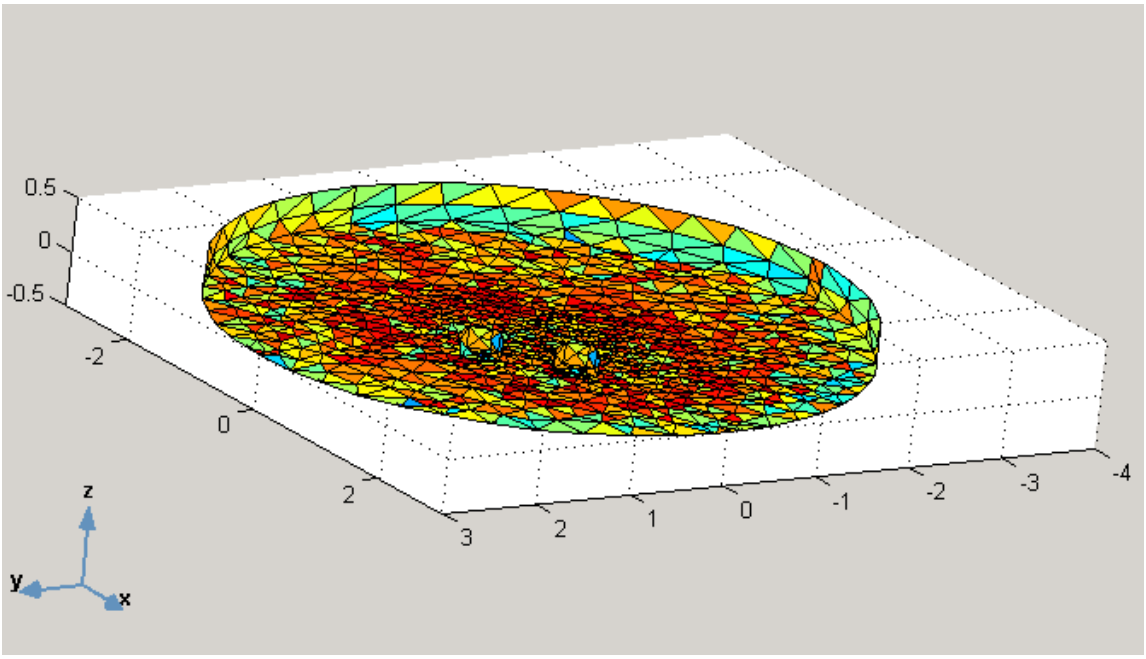

Figure 6 : Mesh of the computational domain considered for region 2.

5. Simulated and measured results

- **Return loss.**

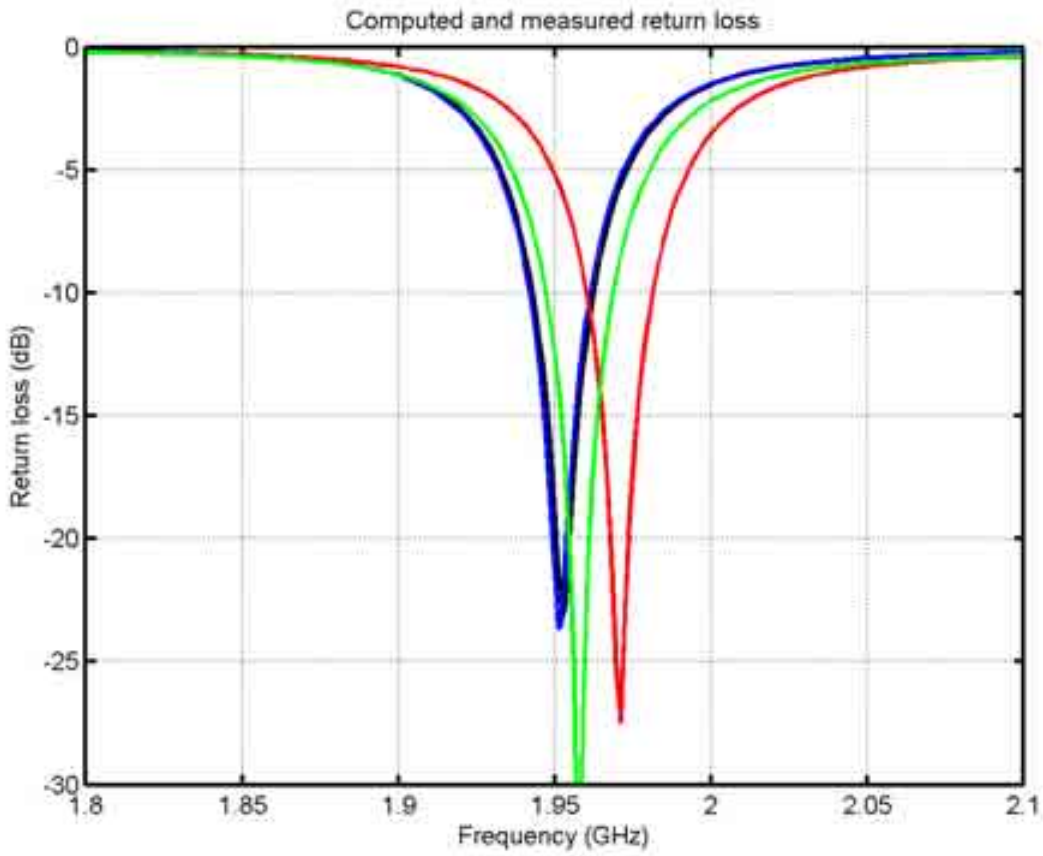

Figure 7 : Reflection coefficient magnitude versus frequency of the TEM excitation mode at the coaxial connectors.

| S_{11}| : Measured at the coaxial connector located along the y-axis (port 1) when the other port is terminated with a matched load. (Finite metallic plane)

| S_{22}| : Measured at the coaxial connector located along the x-axis (port 2) when the other port is terminated with a matched load. (Finite metallic plane)

| S_{11}| : Simulated at the coaxial connector located along the y-axis (port 1) when the other port is terminated with a matched load. (Infinite metallic plane)

| S_{22}| : Simulated at the coaxial connector located along the X-axis (port 2) when the other port is terminated with a matched load. (Infinite metallic plane)

- **Coupling magnitude.**

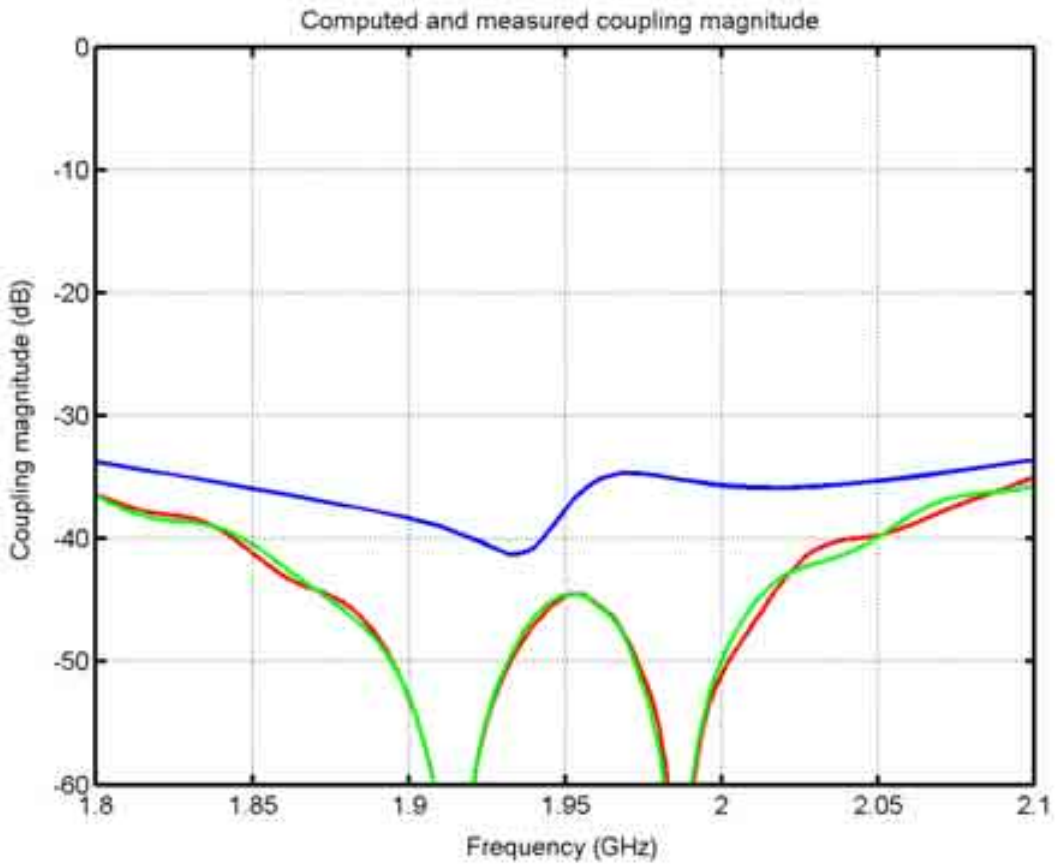

Figure 8 : Coupling coefficient magnitude versus frequency between the TEM excitation modes at the coaxial connectors.

Measured coupling magnitude $|S_{12}|$. (Finite metallic plane).

Measured coupling magnitude $|S_{21}|$. (Finite metallic plane).

Simulated coupling magnitude. ($|S_{12}|=|S_{21}|$).

- **Far-field radiation patterns.**

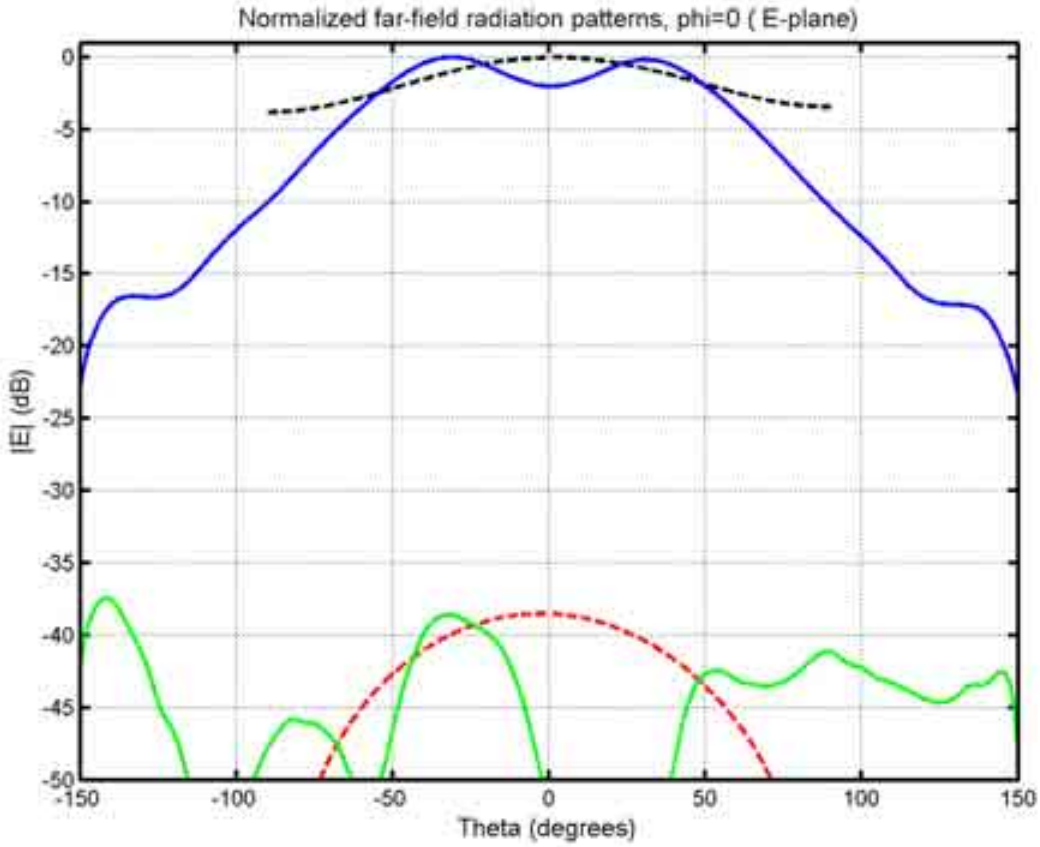

Figure 9 : E-plane radiation patterns versus theta at 1.9575 GHz when the coaxial connector located along the x-axis is excited and the other port is terminated with a matched load.

Simulated co-polar component (Ephi). (Infinite metallic plane).

Simulated cross-polar component (Etheta). (Infinite metallic plane).

Measured co-polar component. (Finite metallic plane).

Measured cross-polar component. (Finite metallic plane).

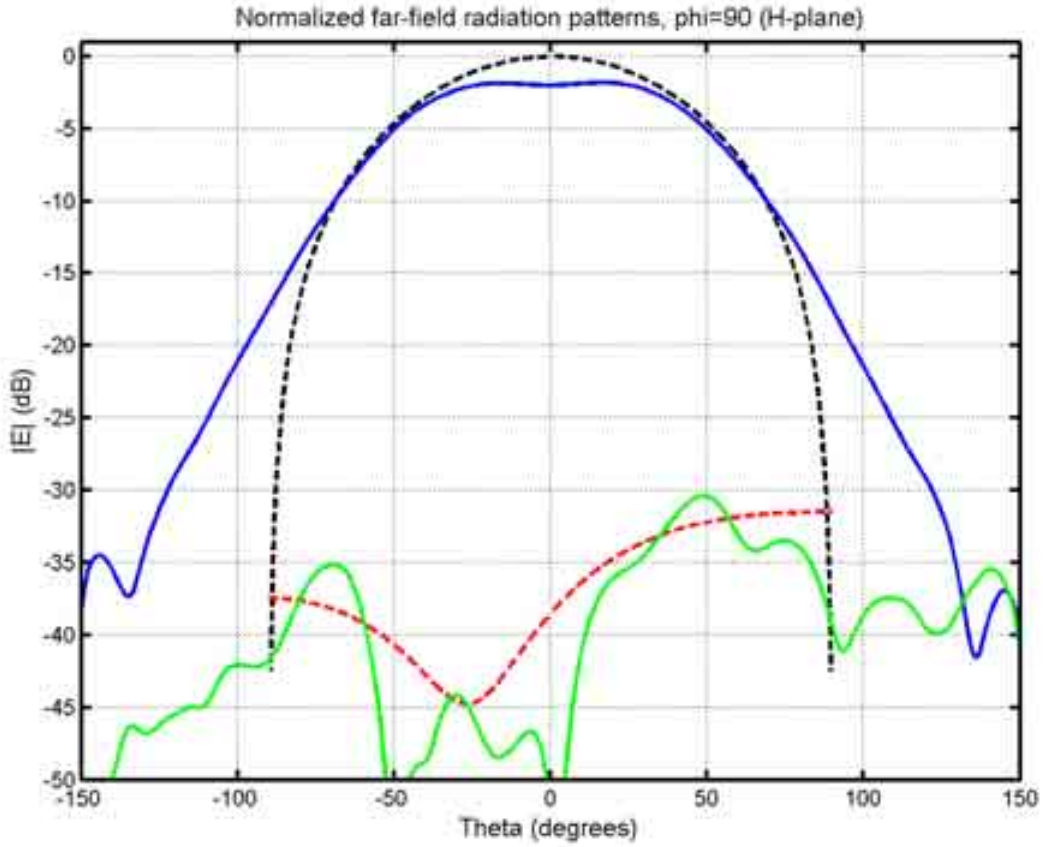

Figure 10 : H-plane radiation patterns versus theta at 1.9575 GHz when the coaxial connector located along the x-axis is excited and the other port is terminated with a matched load.

Simulated co-polar component (Ephi). (Infinite metallic plane).

Simulated cross-polar component (Etheta). (Infinite metallic plane).

Measured co-polar component. (Finite metallic plane).

Measured cross-polar component. (Finite metallic plane).

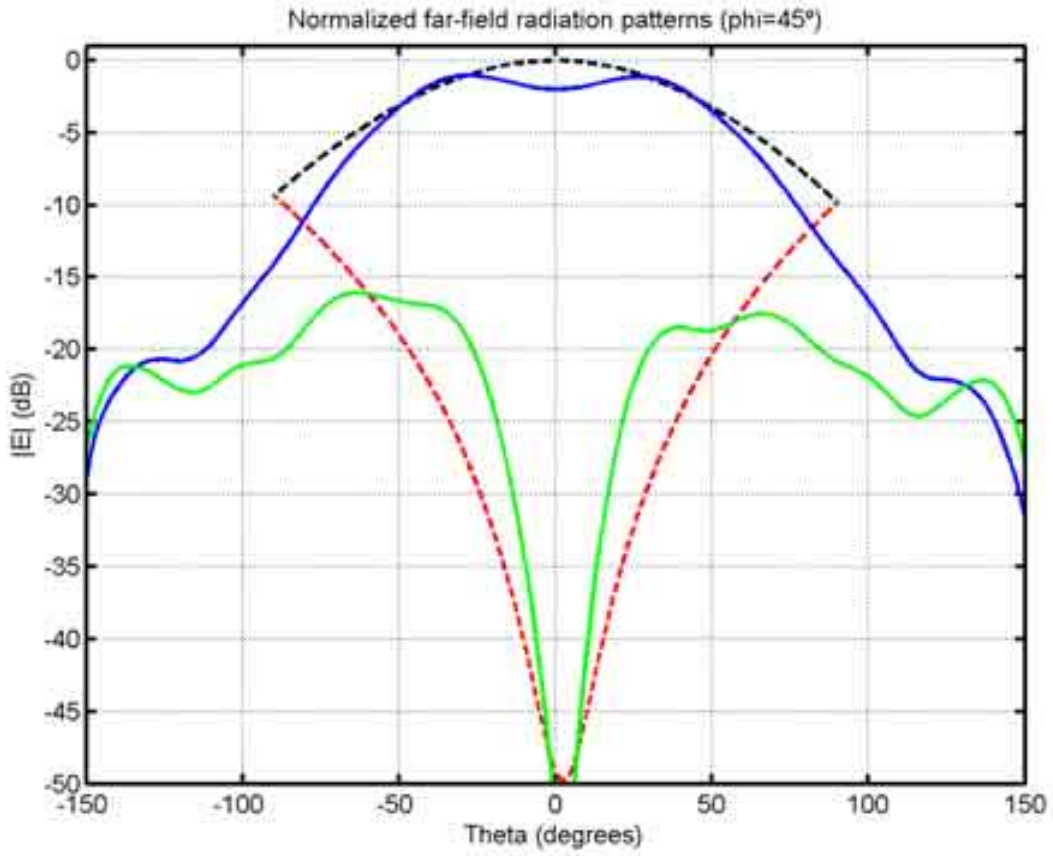

Figure 11 : Radiation patterns at phi=45º versus theta at 1.9575 GHz when the coaxial connector located along the x-axis is excited and the other port is terminated with a matched load. (According to the third definition of Ludwig)

Simulated co-polar component. (Infinite metallic plane).

Simulated cross-polar component. (Infinite metallic plane).

Measured co-polar component. (Finite metallic plane).

Measured cross-polar component. (Finite metallic plane).

6. Computation resources

The simulations has been performed on a computer with the following characteristics:

Type of machine	Desktop PC
Number of processors	*1 (Intel Pentium 4)*
Available memory	*2 GB of RAM*
CPU Speed	2.8 GHz
Operative system	Windows 2000 5.0

Simulations results are provided with the two versions of the software: the frequency-by-frequency (FbF) version and the broadband frequency sweep (FSW) version. With the FbF version, the computation of the GSM's corresponding to regions 1 a 2 takes 54 seconds and 7 minutes for each frequency point respectively. The connection of the individual GSM's to obtain the GSM of the whole antenna takes less than one second per frequency. The maximum memory required with the FbF version is 269 MB approximately.

With the FSW version, the computation of the GSM's corresponding to regions 1 a 2 for the whole considered frequency band in figures 7 and 8, requires approximately 2 and 55 minutes respectively. The connections of the individual GSM's also takes less than one second per frequency as with the previous version. If 60 frequency points are considered at the whole frequency band from 1.8 to 2.2 GHz, the average CPU time per frequency will be 58 seconds. The maximum memory required with the FSW is 700 MB approximately. From the whole GSM matrix of the antenna, the reflection and coupling coefficients in figures 7 and 8 are directly obtained.

The computation of the antenna patterns in figures 9,10 and 11 is immediate (less than a second) for a given excitation.

In the following table the principal data of the simulations are listed:

Version of the software	**FbF version**	**FSW version**
Total number of unknowns	37092	
Number of tetrahedral elements	4762	
Computation CPU time for the GSM of the whole antenna	8 min per frequency	58 min for the frequency band from 1.8 to 2.1 GHz
Average CPU time per frequency point	8 min	58 sec (60 frequency points are considered)
Computation of Antenna Pattern	< 1 second	
Max. required RAM	260 MB	700 MB

7. Discussion

The level of agreement between the measurements and the simulations is good in general. The use of the infinite ground plane approximation by SFELP gives rise to differences at particular results. For the return loss simulation (Fig. 7), a very good concordance is observed. A small resonant frequency shift in the simulations less than 10 and 20 MHz (0.5 and 1%) with respect to the measurements at the coaxial connectors located along the x and y-axes, respectively, is observed. The coupling coefficient simulations do not agree with measurements (Fig. 8), owing to the low coupling level (<24dB).

The copolar components in the radiation patterns plotted in Figs. 9, 10 and 11 show an acceptable agreement except for angles near endfire where the effect of the diffraction at the finite ground plane in the measurements becomes significant. Moreover, the ripple in the measurements due to the finite ground plane does not appear in the simulations. The level of the simulated crosspolar components concords with measurements, however the curves do not agree either owing to the infinite ground plane approximation.

The main advantages of the SFELP software come from the fact that it combines a hybrid and modular methodology for a fast frequency-sweep analysis of antennas (FSW version):
-. Capability of analyzing a complex radiating structure by its segmentation in different regions which are described by their Generalized Scattering Matrix (GSM) or the Generalized Admittance Matrix (GAM).
-. Direct computation of the GAM of each segment without post-processing.
-. Possibility to perform a frequency sweep on the GAM via a Matrix Reduced Order Model. Broadband results are obtained in a single simulation.

SFELP has demonstrated to be a very powerful software to analyse complex antennas when the infinite ground plane is good enough for the considered structure. However, several limitations should be pointed out:
-. The geometry of the structure must be segmentable, that is, the antenna is divided in different regions connected by means of ports. In particular, patches on a continuous dielectric layer cannot be analysed (as far as the hemisphere surface is not homogeneous).
-. The size of each segment of the structure to be analysed should be moderate: for segments of about three wavelengths of diameter, the required memory and computer time could become unmanageable on a PC
-. The ground plane, if it exists, must be infinite.

8. Additional comments

In addition to isolated antennas, this software is able to analyse, rigorously, finite planar arrays of antennas which can be embedded in spheres or in hemispheres supported by an infinite ground plane, for instance cavity backed microstrip antenna elements, waveguide apertures of arbitrary section or dielectric resonator antennas of arbitrary shape. This computation is rather efficient because it is based on an

analytical connection of the response of each one of the antennas considered as isolated. [3]
The possibility of analysing the quoted kind of antennas on a finite ground plane will be considered in a future.

9. References

[1] J. Rubio, J. Arroyo, J. Zapata, "SFELP: An Efficient Methodology for Microwave Circuit Analysis", IEEE Trans. Microwave Theory Tech., Vol.49, No.3, March 2001, pp.509-516.

[2] 4. Rubio J., González M. A. and Zapata J., "Analysis of cavity-backed microstrip antennas by a 3-D finite element/segmentation method and a matrix Lanczos-Padé algorithm (SFELP)," *IEEE Antennas and Wireless Propagation Letters,* vol.1, pp. 193-195, 2002.

[3] J. Rubio , M. A. González and J. Zapata , "Generalized-Scattering-Matrix Analysis of a Class of Finite Arrays of Coupled Antennas by Using 3-D FEM and Spherical Mode Expansion," *IEEE Trans. on Antennas and Propagation,* vol.53, no. 3, pp. 1133-1144, March 2005.

4- SIMULATION RESULTS

From CNRS-LEAT_UPMantenna_FPTLM

1. Entity

Laboratoire d'Electronique, Antennes et Télécommunications (LEAT)
CNRS UMR 6071
250 rue Albert Einstein, Bât. 4, 06560 Valbonne, France

Contact persons:
Jean-Lou Dubard
Phone: +33 (0)4 92 94 28 07
Fax: +33 (0)4 92 94 28 12
Email : jean-lou.dubard@unice.fr

2. Name of the simulation tool

FP-TLM

3. Generalities about the simulation tool

The Transmission Line Matrix (TLM) method is a finite-difference-time-domain technique. Although it is very similar to the FDTD method, it allows computing the six electromagnetic field components at the same location. As TLM simulation is performed in time domain, analysis in a wide frequency band is obtained with only one run by using a Fourier Transform. In FP-TLM code, the FFT operation is replaced by a Prony-Pisarenko method which performs accurate spectral analysis even with short time response. FP-TLM includes PML layers for modelling free space and is implemented on parallel computers.

4. Simulation Set-up (Geometry set-up, GUI, mesh, boundary conditions, excitation)

Since no GUI is available, the input of the geometrical structure into FP-TLM software was done manually. Also, a variable hexaedric meshing was manually performed. Perfectly matched layers (PMLs) were used to simulate free space surronding the antenna. For excitation, a lumped matched generator (occupying one cell between the ground plane and the probe connected to the radiated element) with a gaussian pulse was used. About eight hours were needed to draw the geometry and to set up the rest of the simulation.

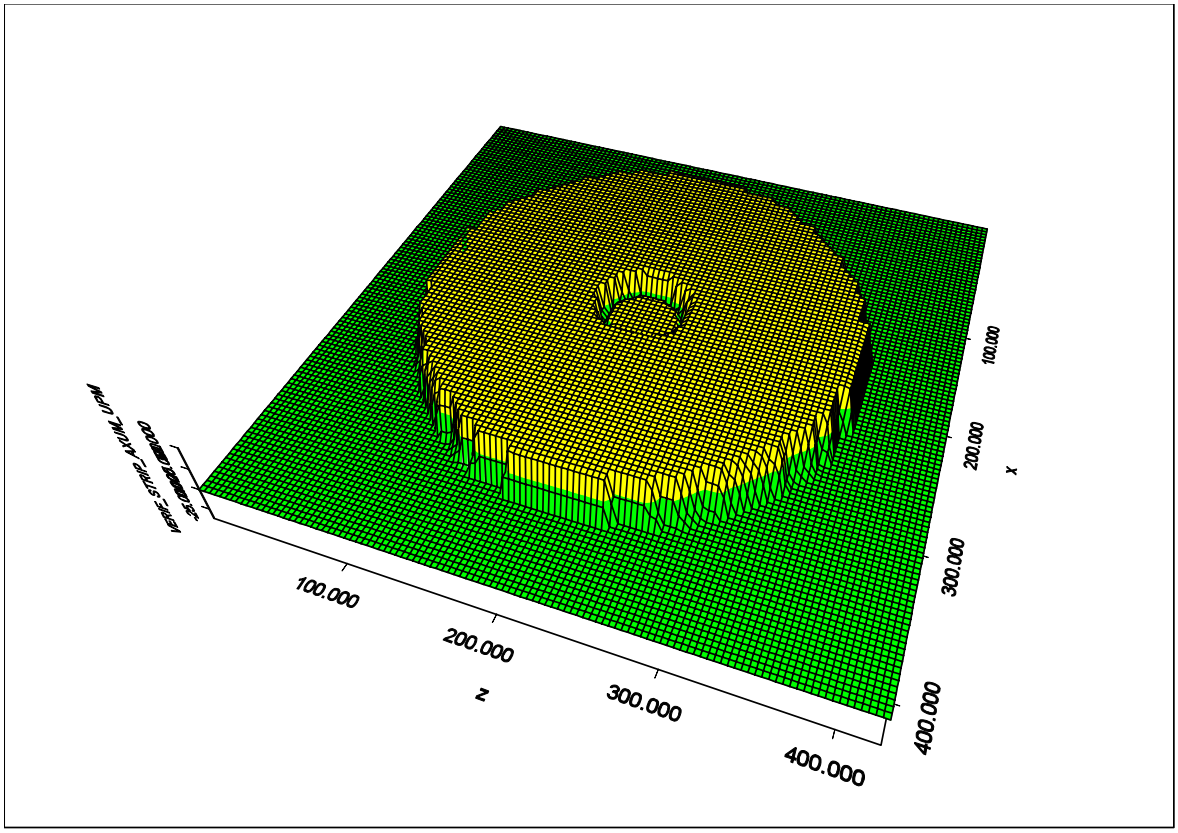

This snapshot shows the stair case approximation of the finite metallic flange used in the TLM simulation.

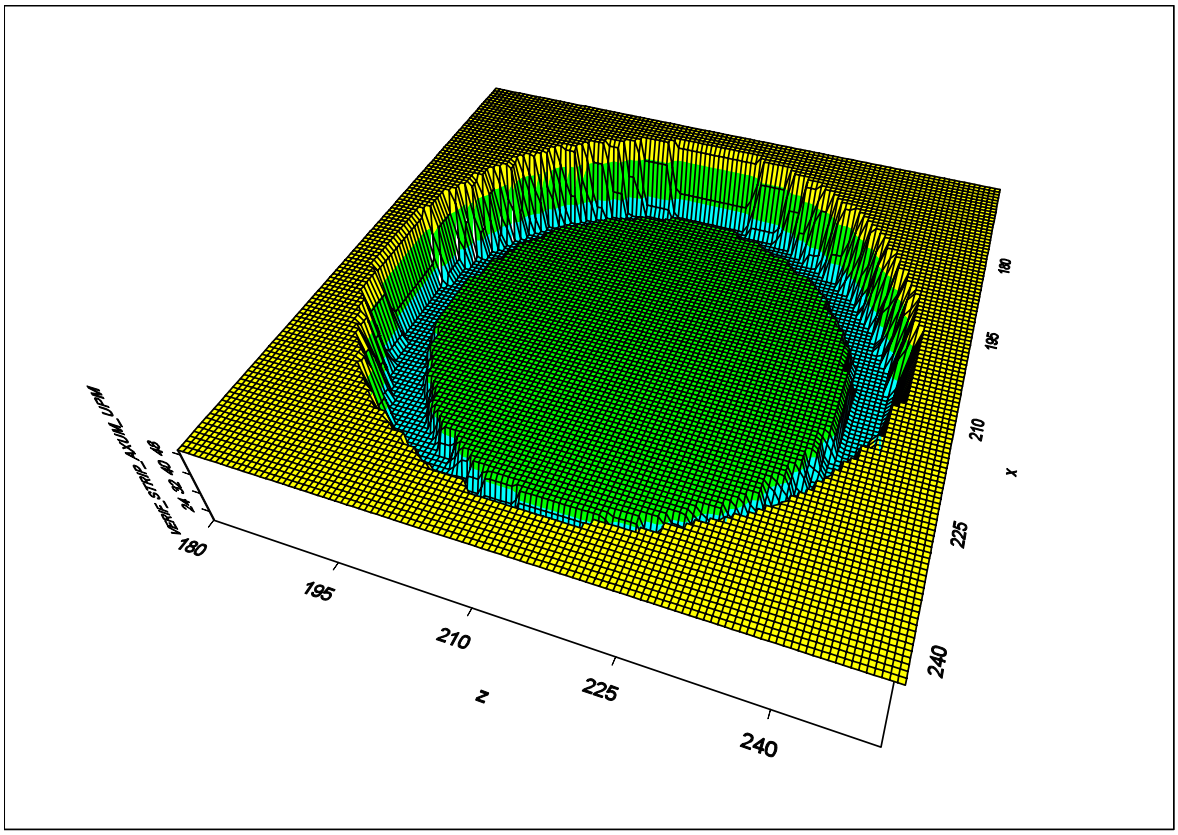

This snapshot shows the stair case approximation of the circular radiating patch inside the cavity used in the TLM simulation.

5. Simulated and measured results

- **Return loss**

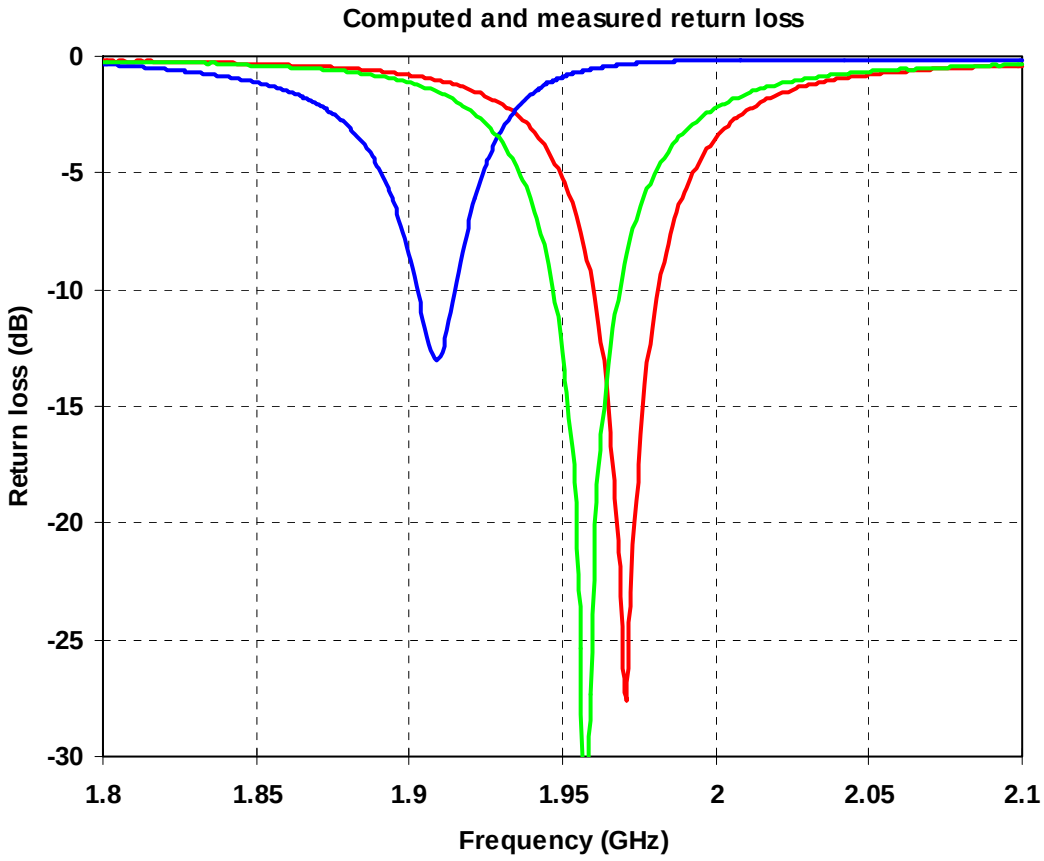

Figure 1: Reflection coefficient magnitude versus frequency of the TEM excitation mode at the coaxial connectors.

| S_{11}|: Measured at the coaxial connector located along the y-axis (port 1) when the other port is terminated with a matched load (Finite metallic plane).

| S_{22}|: Measured at the coaxial connector located along the x-axis (port 2) when the other port is terminated with a matched load (Finite metallic plane).

| S_{11}| and | S_{22}|: Simulated at both ports when the other is terminated with a matched load (Finite metallic plane).

- **Coupling magnitude**

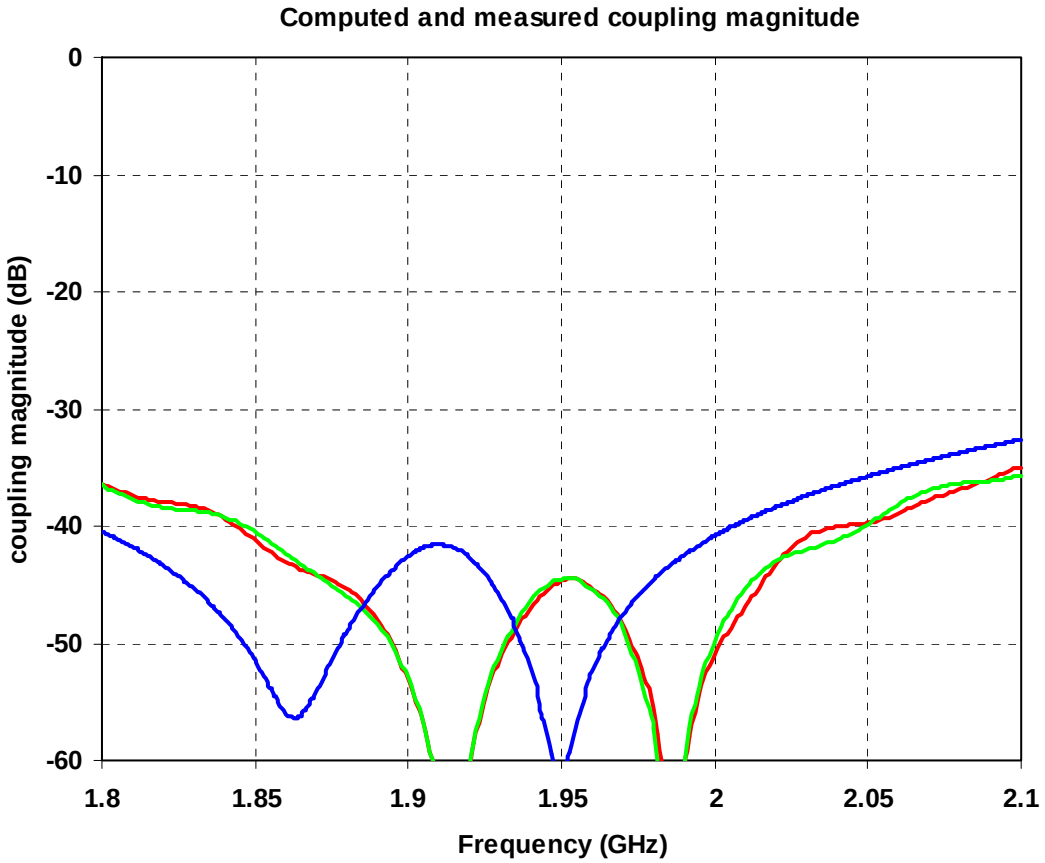

Figure 2: Coupling coefficient magnitude versus frequency between the TEM excitation modes at the coaxial connectors.

Measured coupling magnitude $|S_{12}|$ (Finite metallic plane).

Measured coupling magnitude $|S_{21}|$ (Finite metallic plane).

Simulated coupling magnitude ($|S_{12}|=|S_{21}|$) (Finite metallic plane).

- **Far-field radiation patterns**

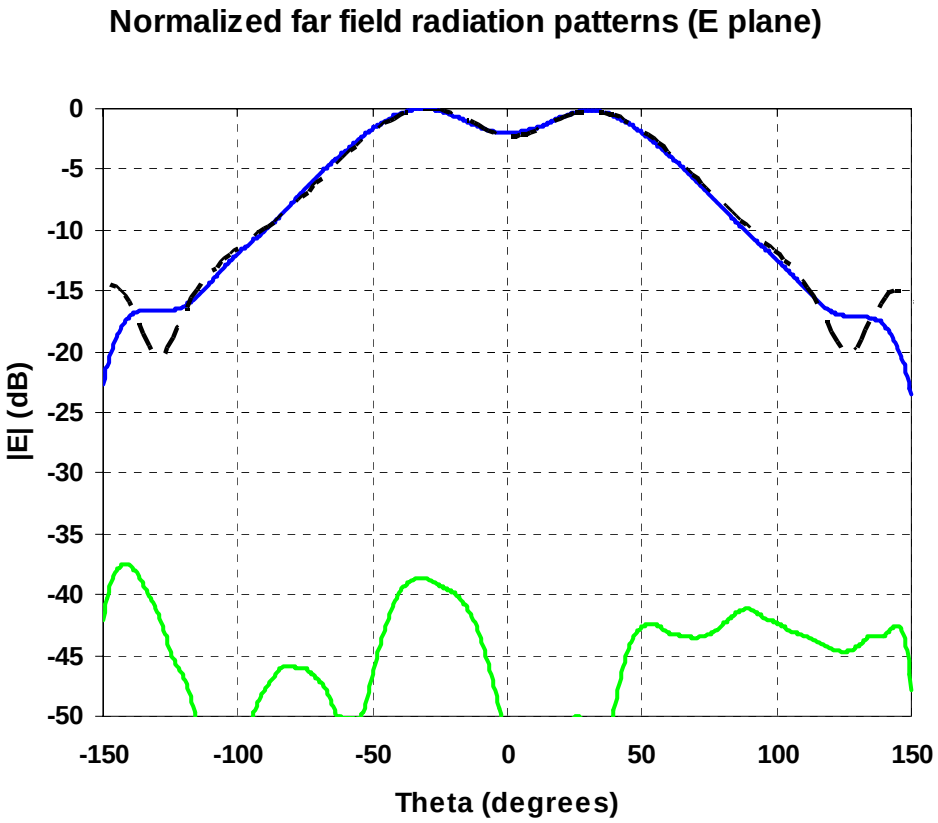

Figure 3: E-plane radiation patterns versus theta at 1.9575 GHz when the coaxial connector located along the x-axis is excited and the other port is terminated with a matched load.

Simulated co-polar component (Ephi) (Finite metallic plane).

Simulated cross-polar component (Etheta) (Finite metallic plane).

Measured co-polar component (Finite metallic plane).

Measured cross-polar component (Finite metallic plane).

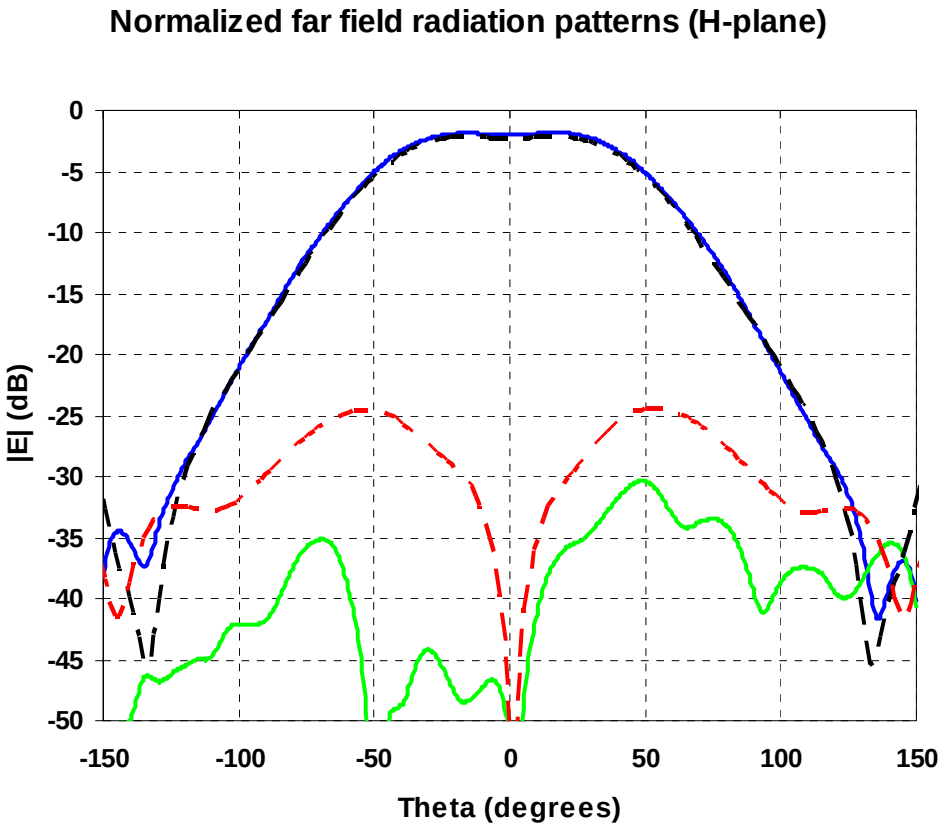

Figure 4: H-plane radiation patterns versus theta at 1.9575 GHz when the coaxial connector located along the x-axis is excited and the other port is terminated with a matched load.

Simulated co-polar component (Ephi) (Finite metallic plane).

Simulated cross-polar component (Etheta) (Finite metallic plane).

Measured co-polar component (Finite metallic plane).

Measured cross-polar component (Finite metallic plane).

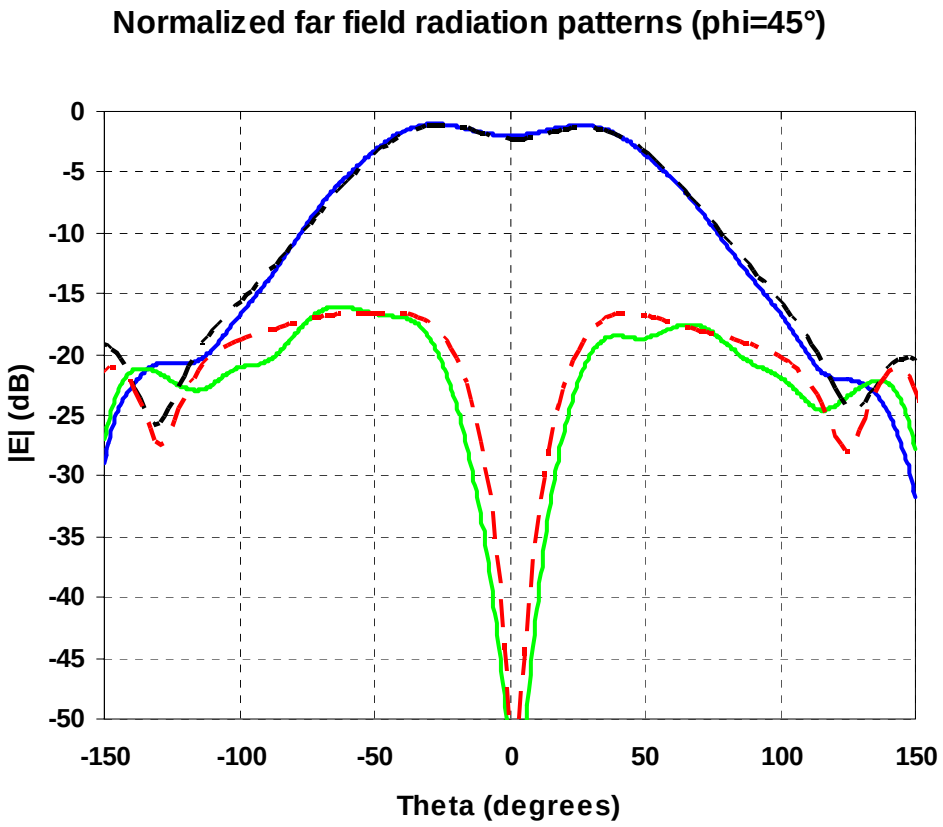

Figure 5: Radiation patterns at phi=45º versus theta at 1.9575 GHz when the coaxial connector located along the x-axis is excited and the other port is terminated with a matched load (according to the third definition of Ludwig).

Simulated co-polar component (Finite metallic plane).

Simulated cross-polar component (Finite metallic plane).

Measured co-polar component (Finite metallic plane).

Measured cross-polar component (Finite metallic plane).

- **Directivity.**

Measured directivity at 1.9575 GHz when the coaxial connector located along the x-axis is excited and the other port is terminated with a matched load:

-. In Theta= **30.0** degrees and Phi= **180.0** degrees: **7.080**dBi (Maximum)

-. In Theta= **0.0** degrees and Phi= **0.0** degrees: **5.081**dBi.

Computed directivity at 1.9575 GHz when the coaxial connector located along the x-axis is excited and the other port is terminated with a matched load:

-. In Theta= **29** degrees and Phi= **180** degrees: 7**.94**dBi (Maximum)

-. In Theta= **0** degrees and Phi= **0** degrees: **5.68**dBi.

6. Computation ressources

- *Type of machine (PC, Workstation, ...),*
  parallel computer IBM SP4
- *Number of processors,*
  16 processors
- *Maximum available memory,*
  2Gbytes/processor
- *Memory used for simulation,*
  446Mbytes/processor
- *CPU speed, ...*
  1,3GHz/processor
- *computation time*
  CPU time/proc=2880s

7. Discussion

There are no difficulties to set up the simulation and to obtain results. However, the drawing of this structure is not easy and is time consuming (no GUI).
Usually, a size step lower than $\lambda_{min}/20$ and at least 3 size steps for modelling the finest details are required in TLM simulations to obtain reliable results. For this antenna, the circular radiating patch was modelled with $41\Delta x.41\Delta z$ by using zero thickness perfect conductors although the real thickness of the finite perfect metallic flange was considered. Then, the entire computational domain was modelled using $113\Delta x.44\Delta y.113\Delta z$.

We observe a good agreement between simulation and measurements, particularly for the radiation patterns and the directivity. The simulated VSWR and coupling magnitude results look very similar to the measured results with a 2.5% frequency shift.

8. Additional comments

No comments

5- SIMULATION RESULTS

From FOI_UPMantenna_TFDTD

1. Entity

Swedish Defence Research Agency (FOI), Linköping, Sweden.

Torleif Martin
Tel. +46 13 37 82 76
email: tormar@foi.se

2. Name of the simulation tool

TFDTD

3. Generalities about the simulation tool

TFDTD is a in-house developed FDTD-program for general 3D structures. It uses a rectangular mesh. The outer boundary condition is a 6-layer PML. The structure can be placed on an infinite ground-plane, which is achieved by extending the ground-plane into the PML-region. No advanced port excitation has been implemented (yet). Discrete voltage or current sources must be used for excitation. Far-zone transformation for radiation pattern calculations can be used in both time-domain and frequency domain. Radiation pattern for structures above a PEC-ground plane and above a lossy dielectric half-space can also be calculated.

4. Simulation Set-up (Geometry set-up, GUI, mesh, boundary conditions, excitation)

The model was created in a CAD-program (Rhinoceros 2.0). The model was exported on the Wavefront file format (triangles). See Fig. 1 below.

The rectangular FDTD-mesh was created using a in-house meshing tool (CAD2TFDTD). The parameters (pulse, feeding points, output data, etc.) were set in a pre-processor program called PRETFDTD. The FDTD-cell size was set to $\Delta x=\Delta y=$ 0.5167mm and $\Delta z=$0.508mm. The size of the computational volume was 137 x 137 x 43 FDTD cells.

A small part of the coaxial structure was modelled and the inner conductor was excited using a voltage source (one FDTD-cell long). A Gaussian modulated pulse with a centre frequency of 1.9 GHz was used. The number of time-steps was 30000. Details of the FDTD-structure can be seen in Figs. 2 - 4.

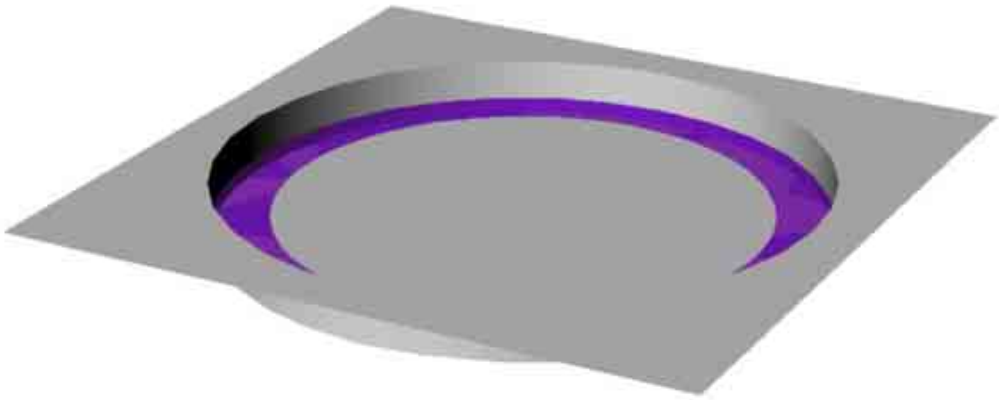

Figure 1 : CAD-model of the antenna. The ground-plane is extended into infinity in the simulation.

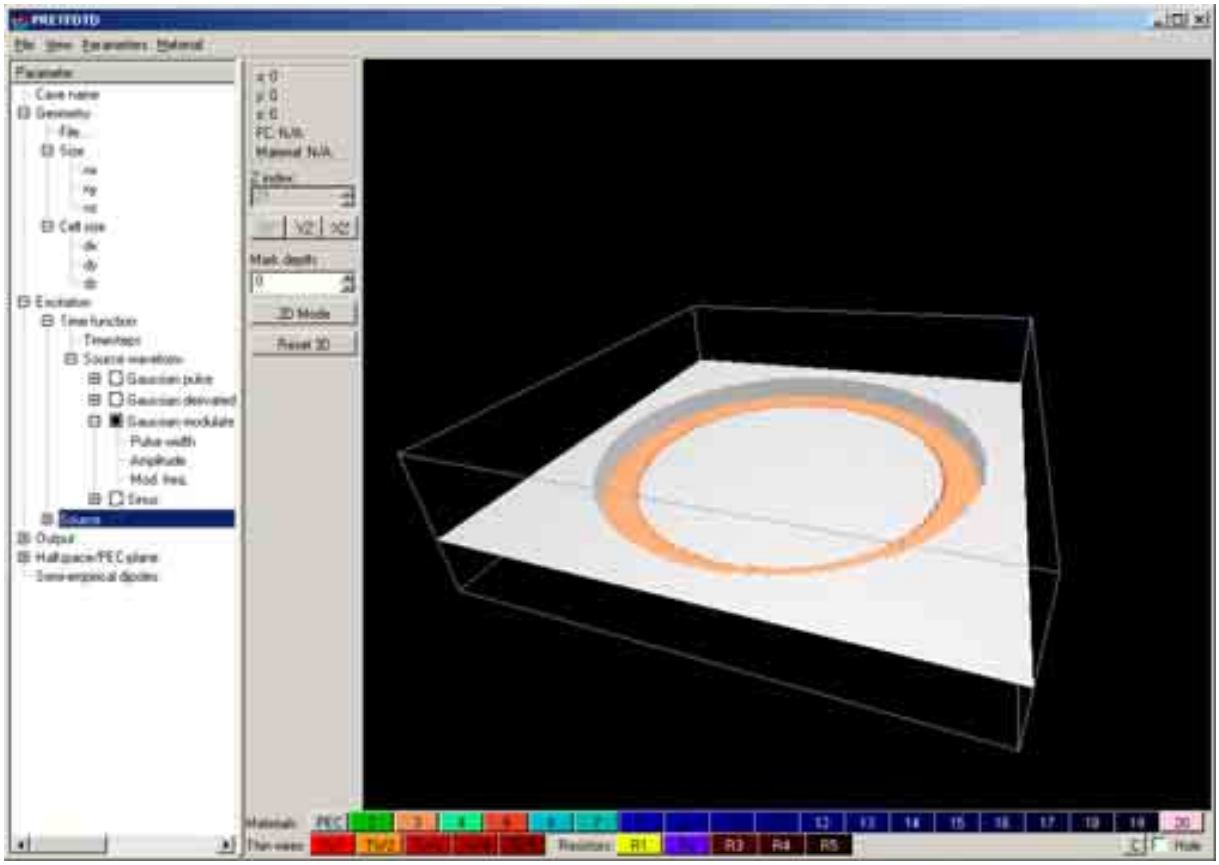

Figure 2 : FDTD-mesh seen in GUI (PRETFDTD).

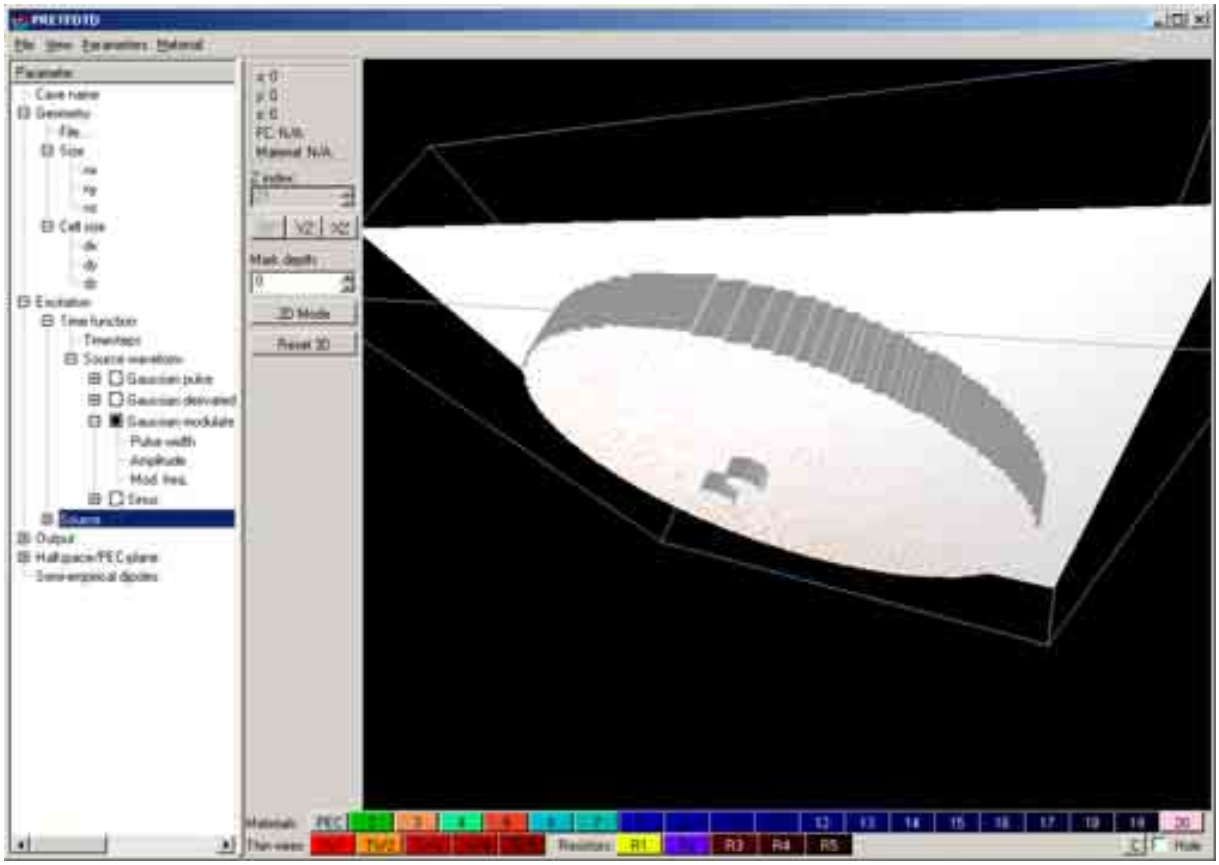

Figure 3: FDTD-mesh seen in GUI. The coaxial feeds are seen at the bottom of the cavity.

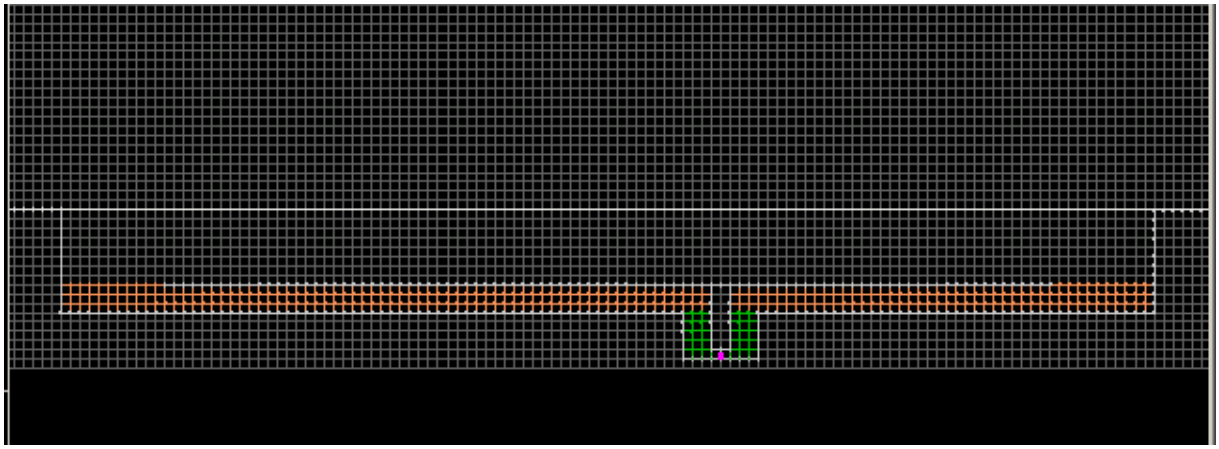

Figure 4: Through-cut in the FDTD-mesh at coaxial feed. The voltage source can be seen as a violet line.

5. Simulated and measured results

- **Return loss.**

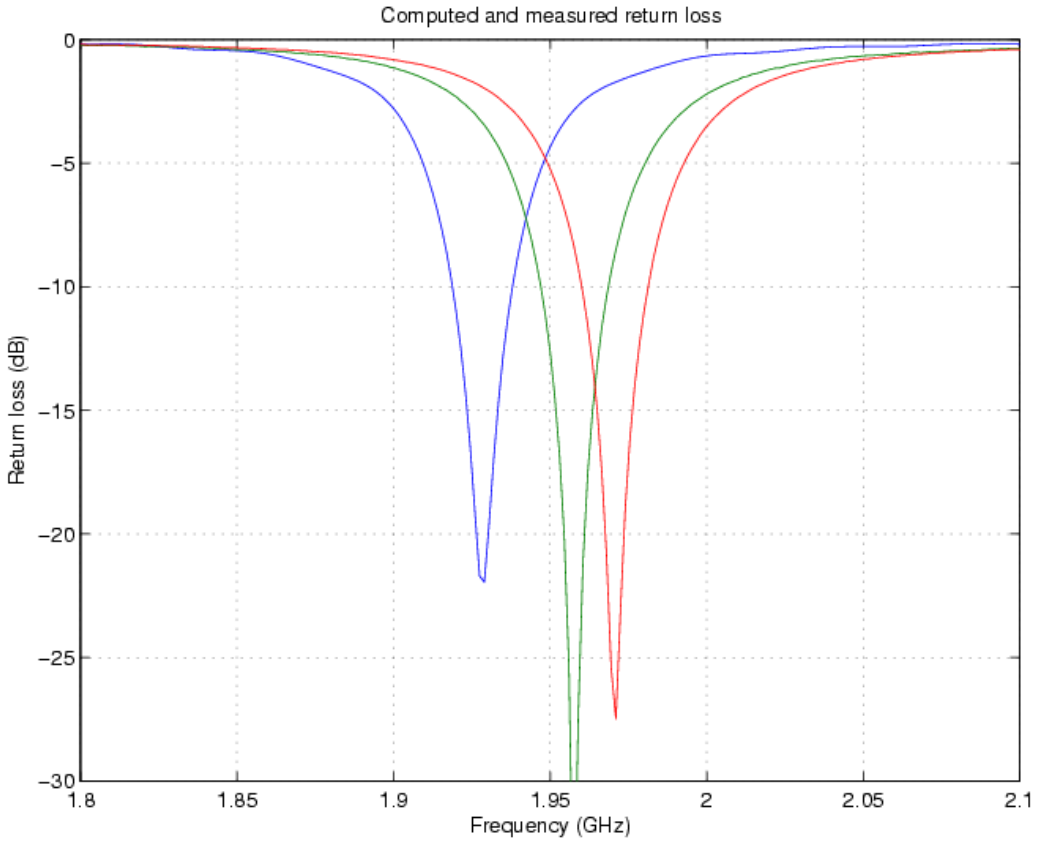

Figure 1 : Reflection coefficient magnitude versus frequency of the TEM excitation mode at the coaxial connectors.

| S_{11}| : Measured at the coaxial connector located along the y-axis (port 1) when the other port is terminated with a matched load. (Finite metallic plane)

| S_{22}| : Measured at the coaxial connector located along the x-axis (port 2) when the other port is terminated with a matched load. (Finite metallic plane)

| S_{11}| and | S_{22}| : Computed at both ports when the other is terminated with a matched load (Infinite metallic plane)

- **Coupling magnitude.**

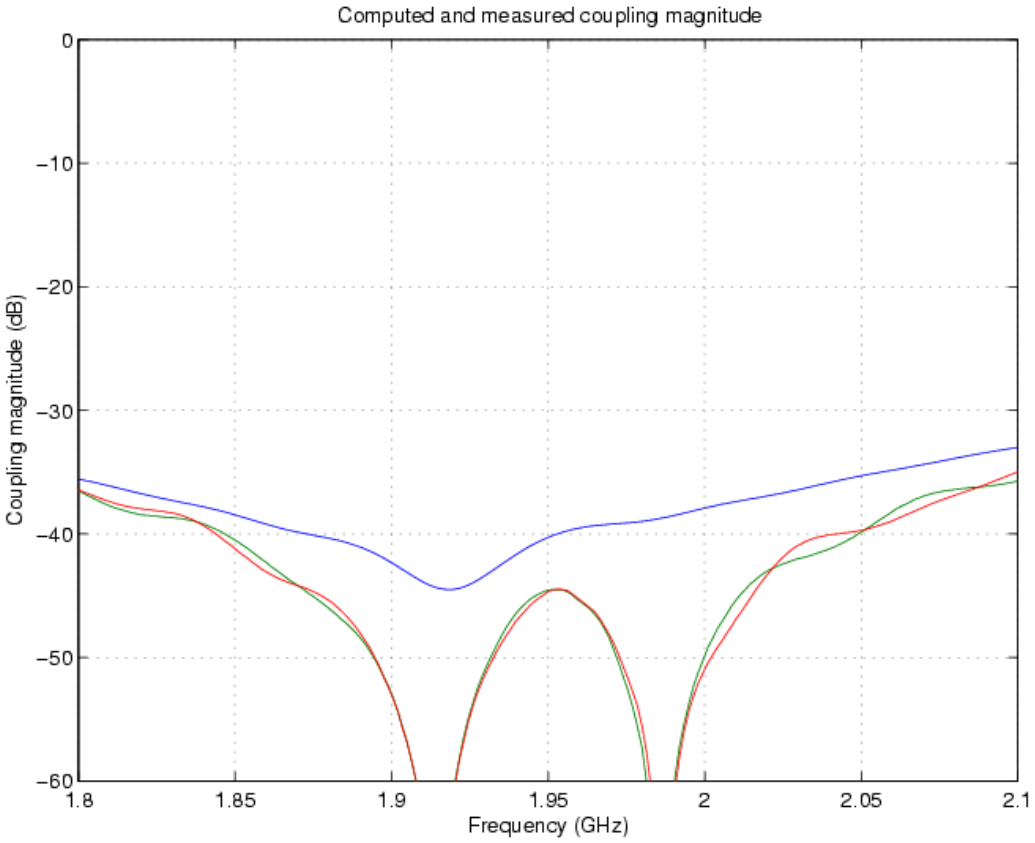

Figure 2 : Coupling coefficient magnitude versus frequency between the TEM excitation modes at the coaxial connectors.

Measured coupling magnitude $|S_{12}|$. (Finite metallic plane).

Measured coupling magnitude $|S_{21}|$. (Finite metallic plane).

Computed coupling magnitude. ($|S_{12}|=|S_{21}|$).

- **Far-field radiation patterns.**

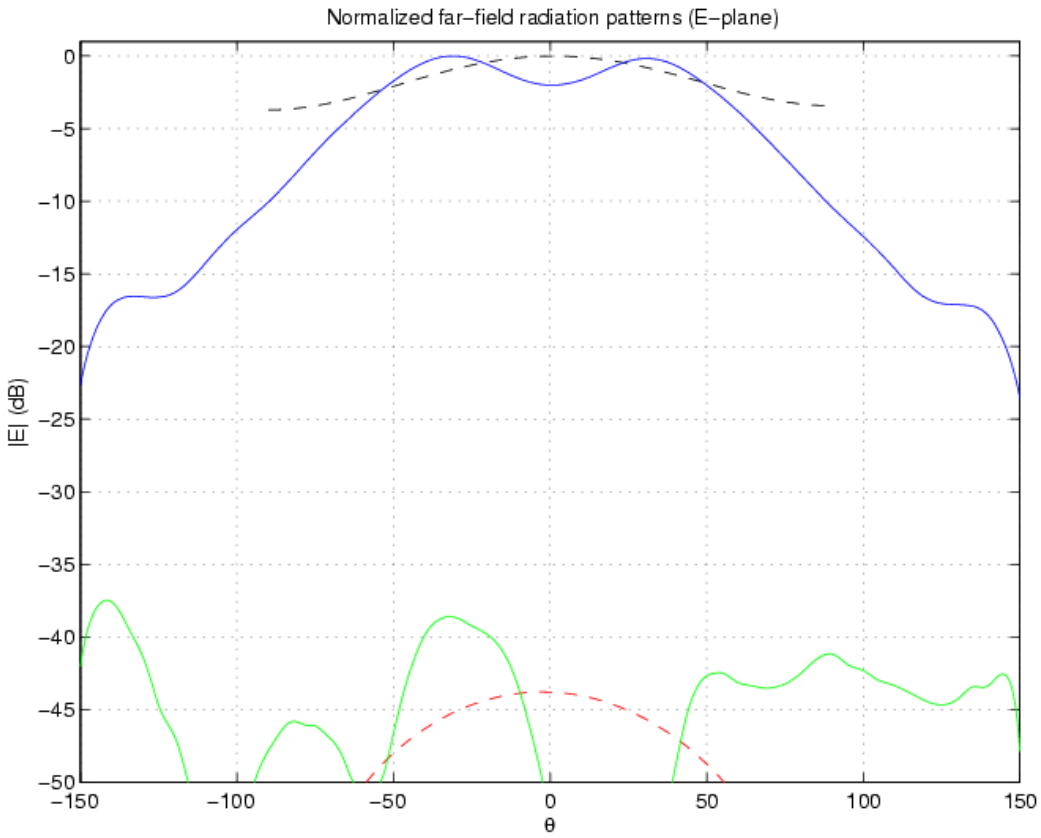

Figure 3 : E-plane radiation patterns versus theta at 1.9575 GHz when the coaxial connector located along the x-axis is excited and the other port is terminated with a matched load..

Computed co-polar component. (Infinite metallic plane).

Computed cross-polar component. (Infinite metallic plane).

Measured co-polar component. (Finite metallic plane).

Measured cross-polar component. (Finite metallic plane).

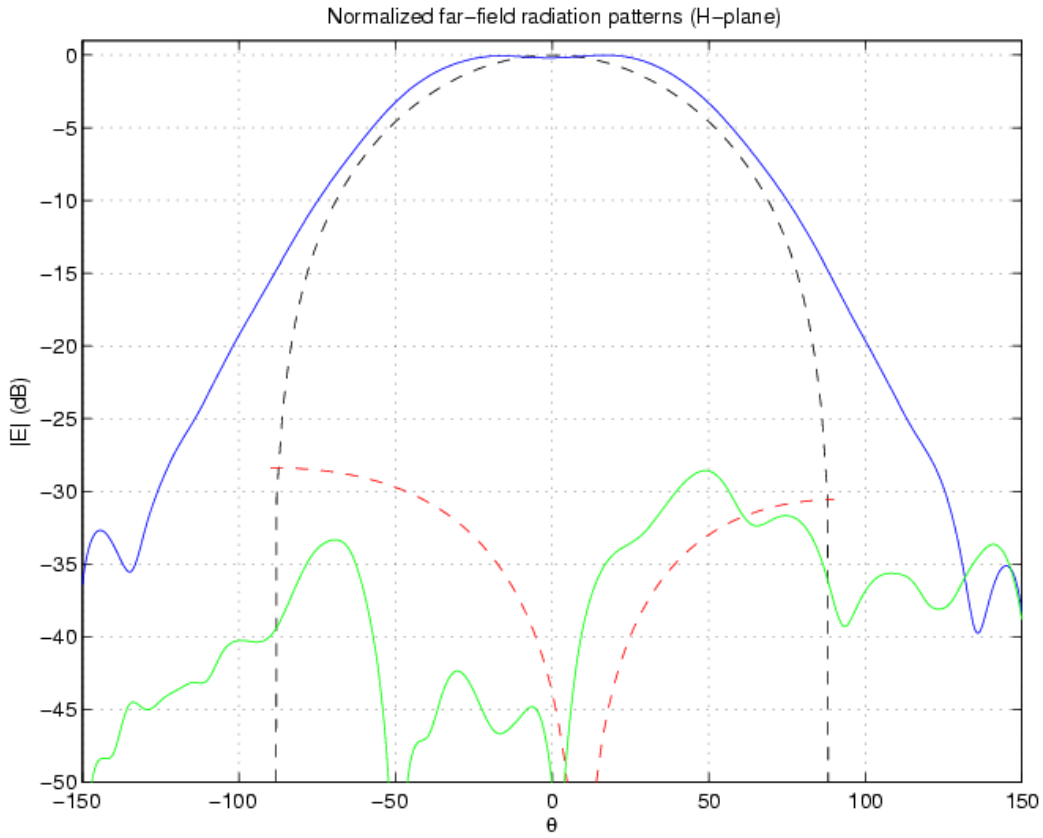

Figure 4 : H-plane radiation patterns versus theta at 1.9575 GHz when the coaxial connector located along the x-axis is excited and the other port is terminated with a matched load..

Computed co-polar component. (Infinite metallic plane).

Computed cross-polar component. (Infinite metallic plane).

Measured co-polar component. (Finite metallic plane).

Measured cross-polar component. (Finite metallic plane).

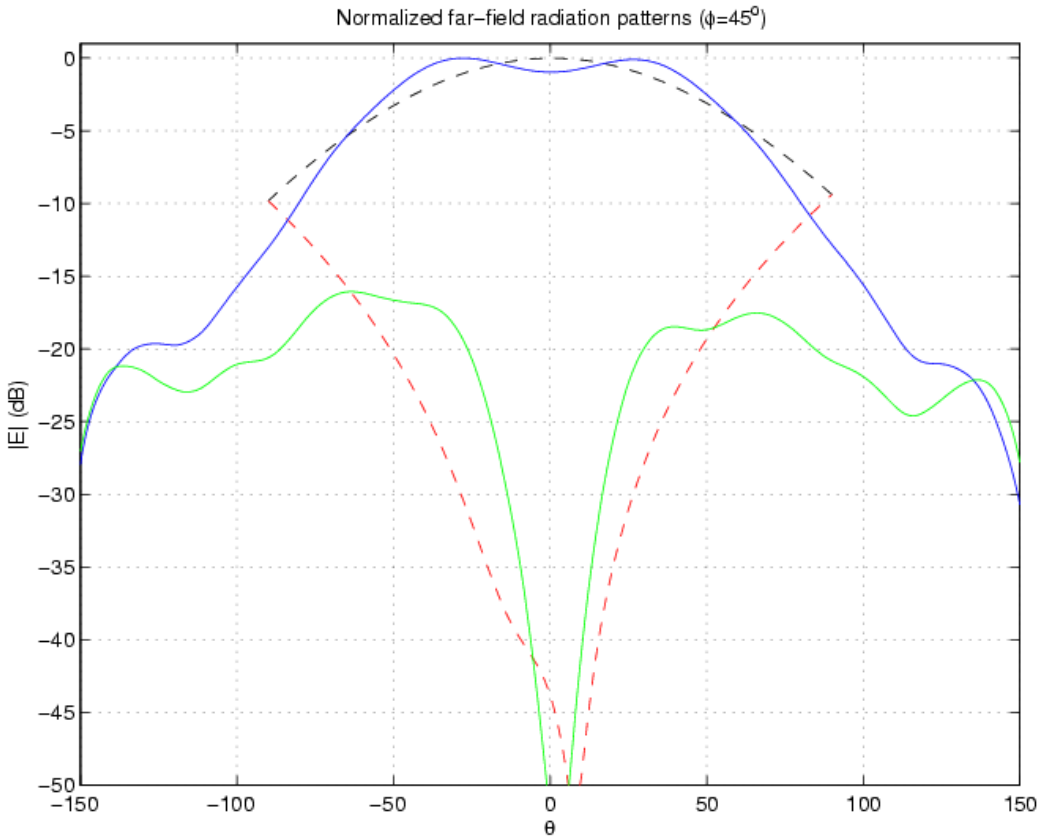

Figure 5 : Radiation patterns at phi=45º versus theta at 1.9575 GHz when the coaxial connector located along the x-axis is excited and the other port is terminated with a matched load..

Computed co-polar component. (Infinite metallic plane).

Computed cross-polar component. (Infinite metallic plane).

Measured co-polar component. (Finite metallic plane).

Measured cross-polar component. (Finite metallic plane).

- **Directivity.**

Measured directivity at 1.9575 GHz when the coaxial connector located along the x-axis is excited and the other port is terminated with a matched load:

-. In Theta= 30.0 degrees and Phi= 180.0 degrees: 7.080 dBi (Maximum)

-. In Theta= 0.0 degrees and Phi= 0.0 degrees: 5.081 dBi.

6. Computation resources

The simulation was performed on a PC (Dell Workstation PWS650, 2.4 GHz CPU) with two processors. Available memory is 1 GByte. The simulation time was about 2 hours on one processor. The required memory was 81 MByte.

The S-parameters and far-field data are written on ASCII-files, which are imported into Matlab for post-processing.

7. Discussion

The FDTD method using a rectangular lattice is not the most appropriate method for this type of problem, since the details of the feeding ports are difficult to resolve using a standard FDTD-mesh. A very fine mesh is required around the feedings. Also, the circular geometry is approximated using a rectangular mesh, which implies an additional uncertainty. However, an advantage with time-domain methods is that broadband results are obtained within a single simulation. This advantage is not fully illustrated in this problem, since it deals with a relatively narrowband antenna.

8. Additional comments

6- SIMULATION RESULTS

From UOB_UPMantenna_FDTD32

1. Entity

Computational Electromagnetics Group, Centre for Communications Research, Department of Electrical & Electronic Engineering, Merchant Venturers Building, Woodland Road, University of Bristol (UOB), Bristol BS8 1UB, United Kingdom

Dominique Lynda Paul
Tel. +44 117 954 51 23
email: d.l.paul@bristol.ac.uk

2. Name of the simulation tool

FDTD32

3. Generalities about the simulation tool

FDTD32 is an in-house 3D full-wave solver based on the Finite-Difference Time-Domain (FDTD) method. A non-uniform mesh of rectangular cells was employed and Dey-Mittra technique was utilised to account for curved metal parts of the structure. In this simulation, perfect metal conductors and lossless dielectric substrates were considered. The ground plane was modelled as infinite.

4. Simulation Set-up (Geometry set-up, GUI, mesh, boundary conditions, excitation)

The geometry was specified using our GUI Gema as displayed in Figures 1 to 3 and a dense graded mesh was created manually. A 4-cells PML layer was employed to terminate the FDTD box and simulate an open structure. A raised cosine waveform of width 120ps was applied at one of the ports together with a template excitation consisting of the snapshot of the TEM mode in the coaxial feed.

The size of the computational volume was 195x81x195 cells. At least 40ns were required to obtain the coupling coefficient with sufficient accuracy.

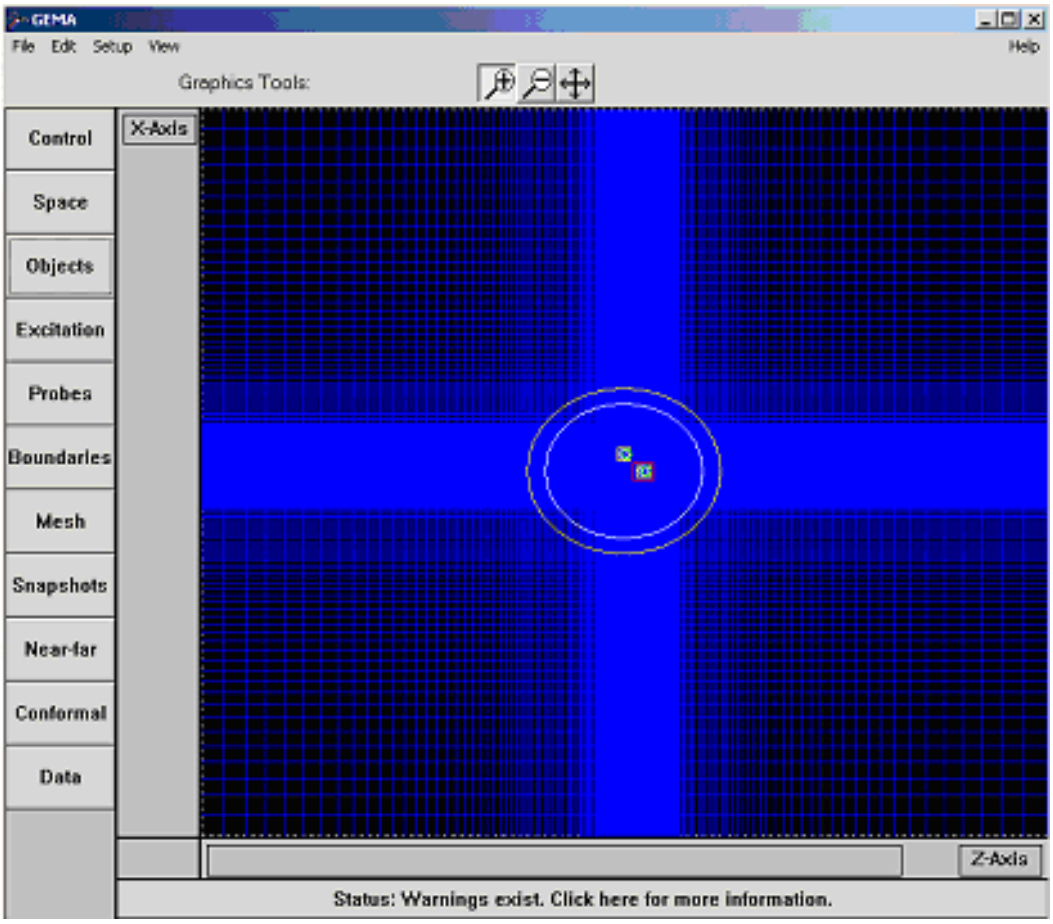

Figure 1 : Top view of antenna model in Gema GUI

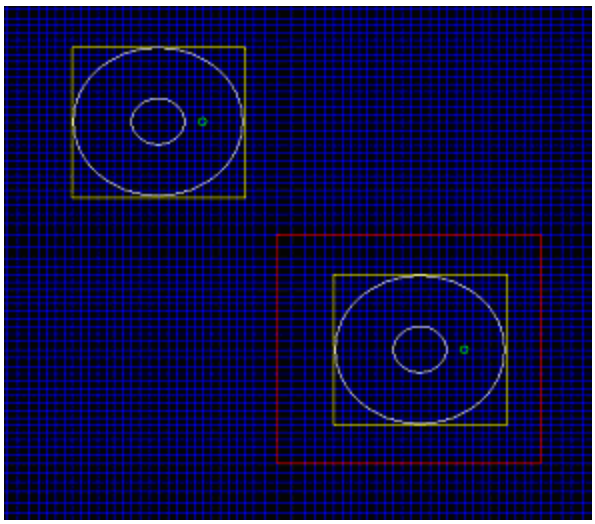

Figure 2 : Zoom of Figure 1 to show the mesh around the feeds

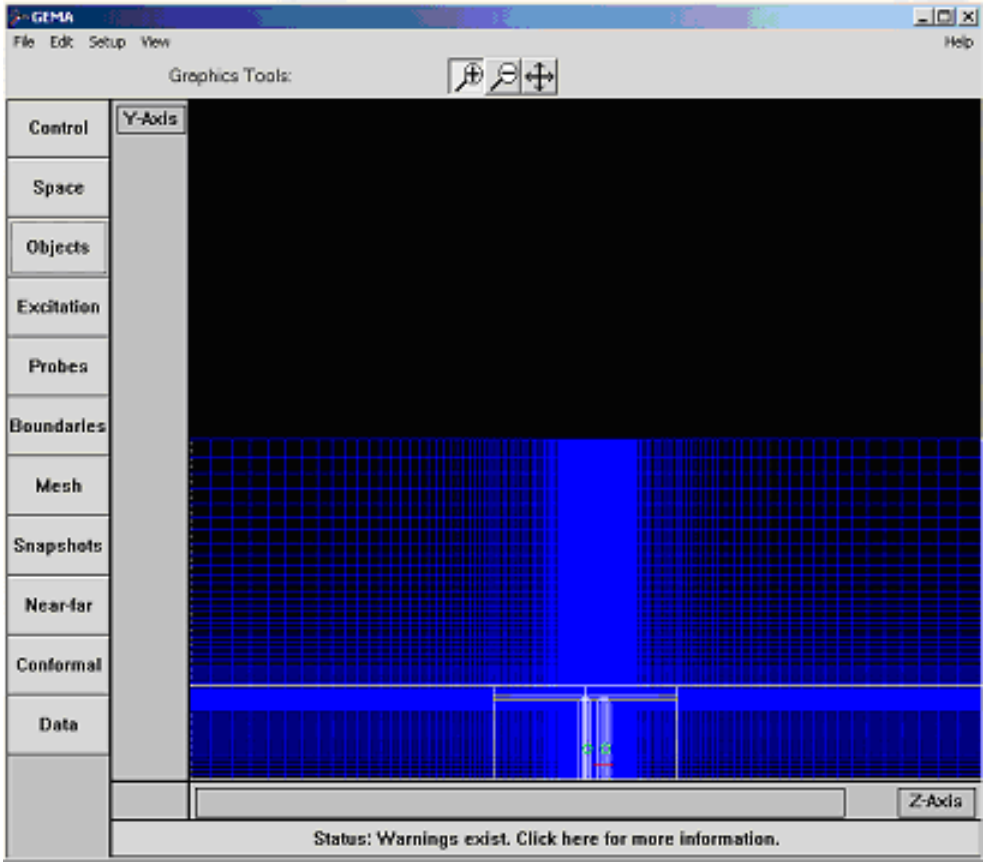

Figure 3 : Elevation view of antenna model in Gema GUI

5. Simulated and measured results

- **Return loss.**

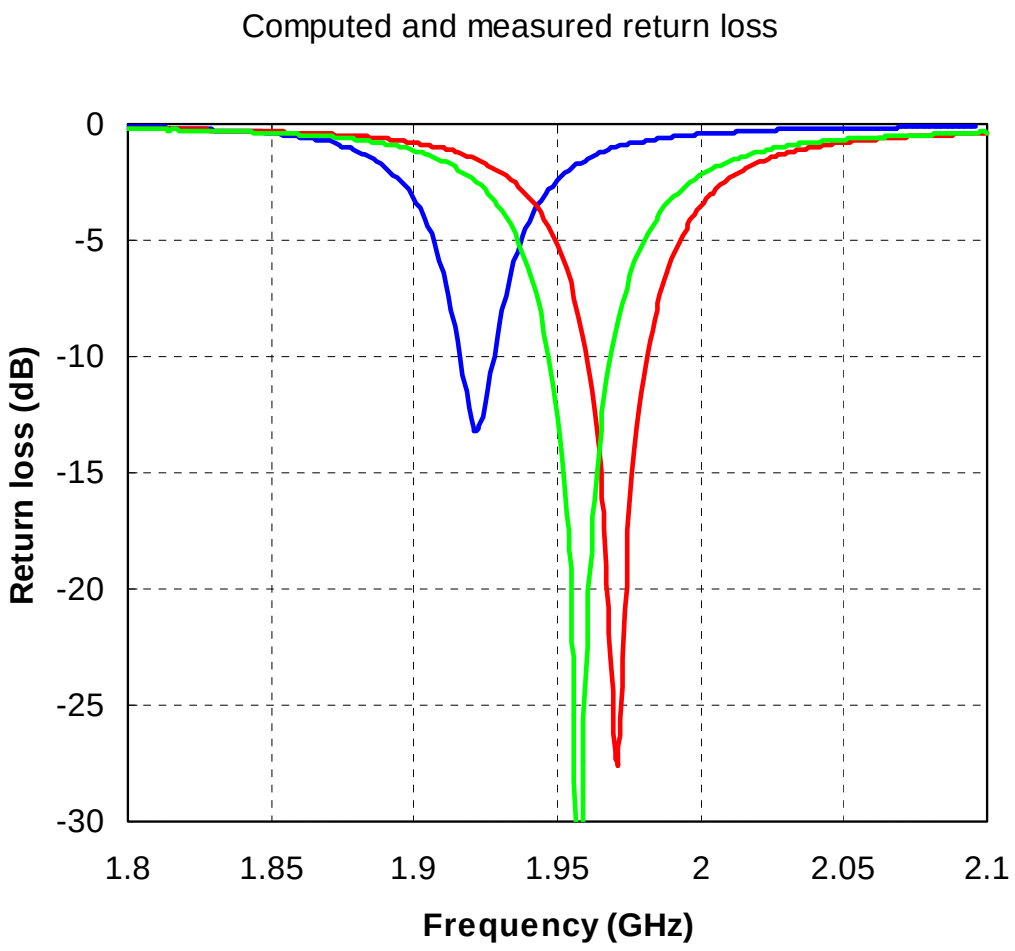

Figure 4 : Reflection coefficient magnitude versus frequency of the TEM excitation mode at the coaxial connectors.

| S_{11}| : Measured at the coaxial connector located along the y-axis (port 1) when the other port is terminated with a matched load. (Finite metallic plane)

| S_{22}| : Measured at the coaxial connector located along the x-axis (port 2) when the other port is terminated with a matched load. (Finite metallic plane)

| S_{11}| and | S_{22}| : Computed at both ports when the other is terminated with a matched load (Infinite metallic plane)

- **Coupling magnitude.**

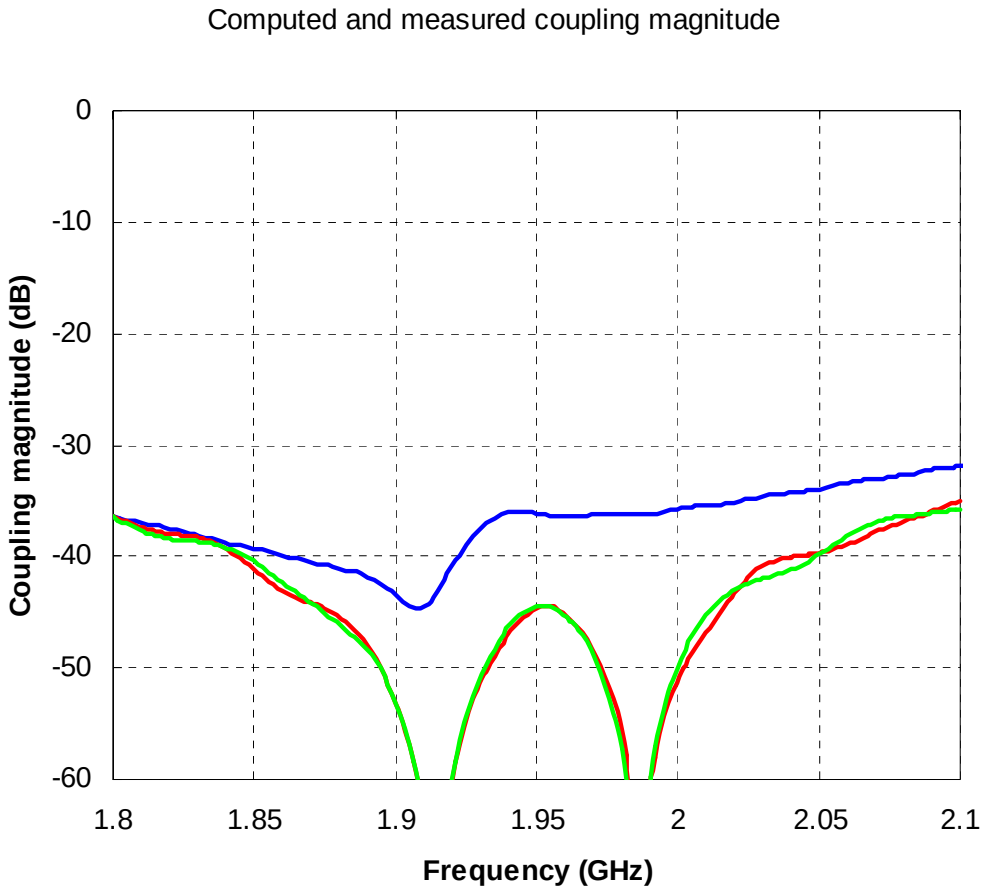

Figure 5 : Coupling coefficient magnitude versus frequency between the TEM excitation modes at the coaxial connectors.

Measured coupling magnitude $|S_{12}|$. (Finite metallic plane).

Measured coupling magnitude $|S_{21}|$. (Finite metallic plane).

Computed coupling magnitude. ($|S_{12}|=|S_{21}|$).

- **Far-field radiation patterns.**

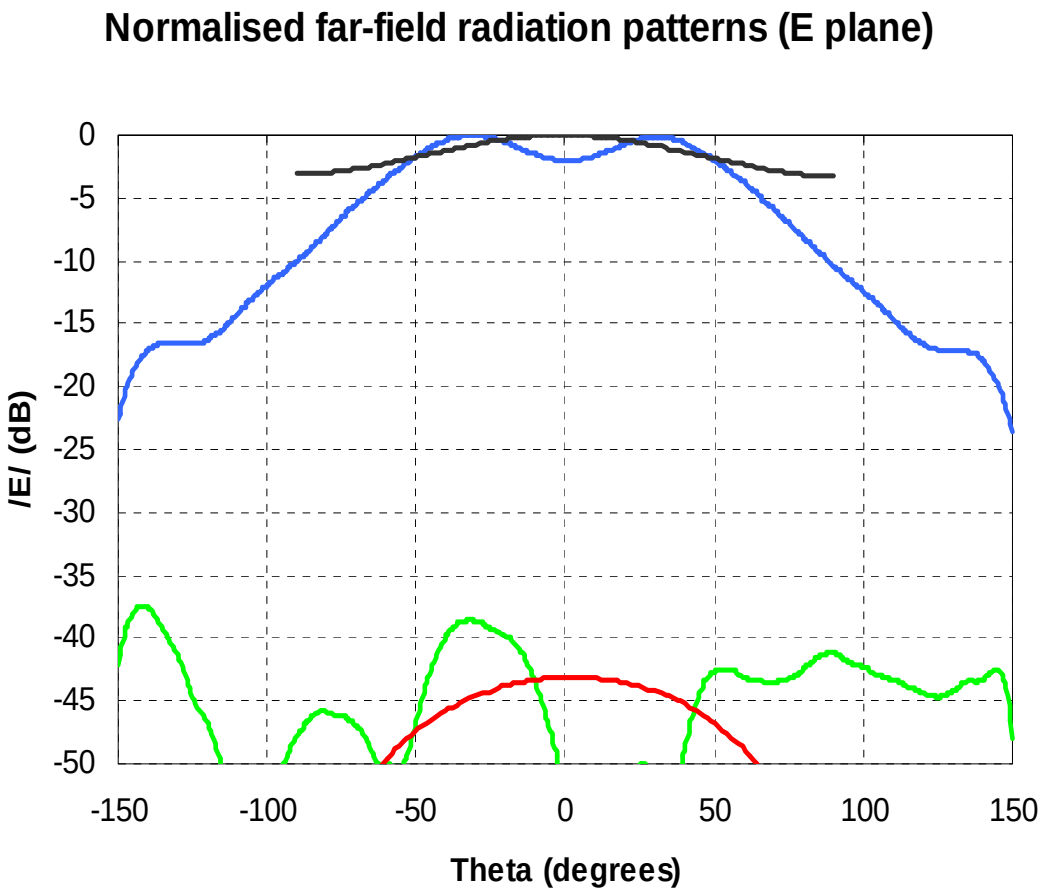

Figure 6 : E-plane radiation patterns versus theta at 1.9575 GHz when the coaxial connector located along the x-axis is excited and the other port is terminated with a matched load..

Computed co-polar component. (Infinite metallic plane).

Computed cross-polar component. (Infinite metallic plane).

Measured co-polar component. (Finite metallic plane).

Measured cross-polar component. (Finite metallic plane).

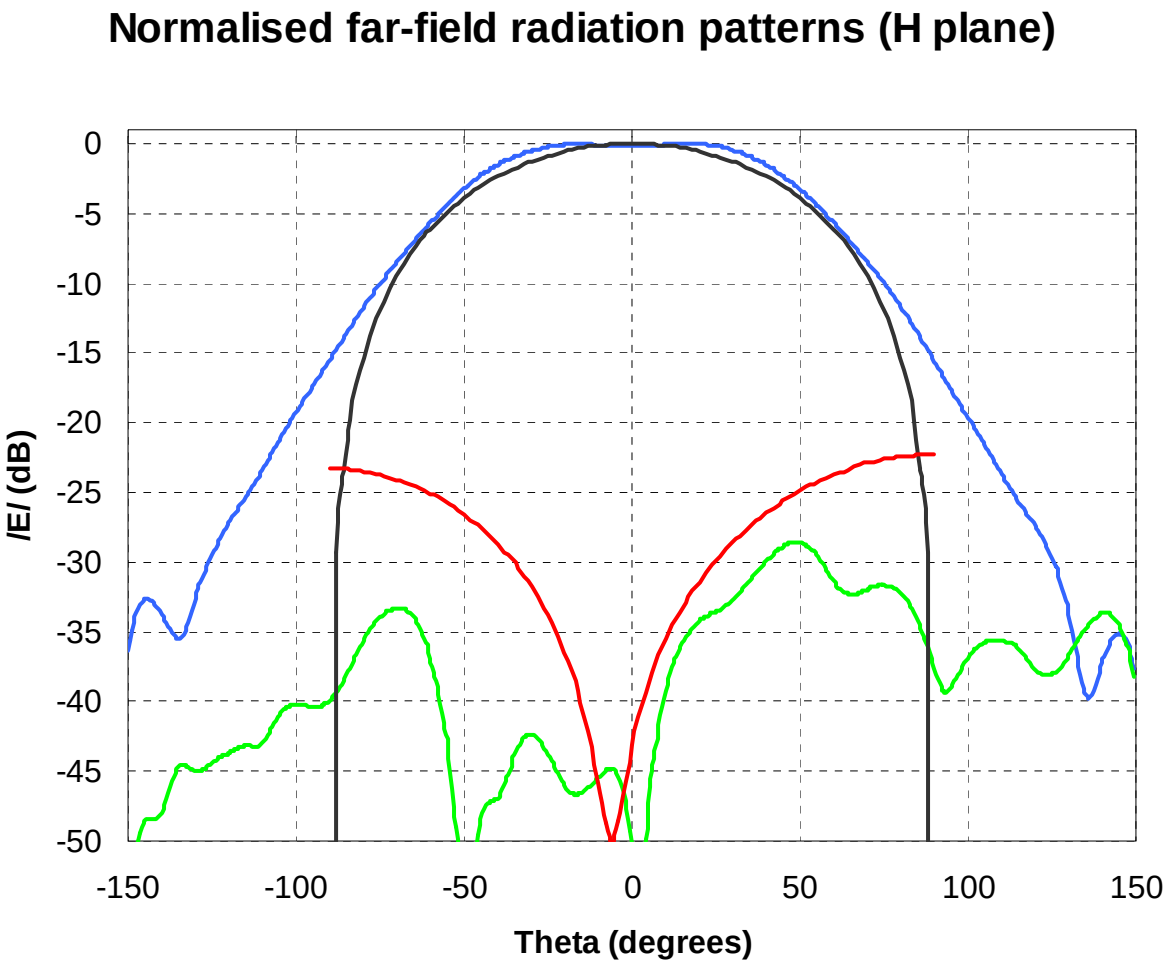

Figure 7 : H-plane radiation patterns versus theta at 1.9575 GHz when the coaxial connector located along the x-axis is excited and the other port is terminated with a matched load..

Computed co-polar component. (Infinite metallic plane).

Computed cross-polar component. (Infinite metallic plane).

Measured co-polar component. (Finite metallic plane).

Measured cross-polar component. (Finite metallic plane).

- **Directivity.**

Measured directivity at 1.9575 GHz when the coaxial connector located along the x-axis is excited and the other port is terminated with a matched load:

-. In Theta= 30.0 degrees and Phi= 180.0 degrees: 7.080 dBi (Maximum)

-. In Theta= 0.0 degrees and Phi= 0.0 degrees: 5.081 dBi.

6. Computation resources

The simulation was performed on a Viglen PC (3.2GHz, 2 GBytes RAM available). The simulation time was about 20 hours to allow the fields to vanish at the coupled port. The required memory was 560 MBytes.

7. Discussion

This cavity-backed microstrip antenna is not ideal for an FDTD simulation based on a Cartesian grid due to the difficulty to model the curved metal parts, the coaxial feed in particular. Moreover, it is a highly resonant structure with a narrow band and the CPU requirements are rather high.

As shown in Figure 4, the simulated return loss was found at a lower frequency than the measured result (with 1.8% shift).

The simulated coupling coefficient is in good agreement with the measured data as can be seen in Figure 5.

The far field patterns in the principal planes (Figures 6 and 7) are generally in good agreement with those obtained experimentally except towards endfire, due to the fact that an infinite ground plane was considered for this simulation.

8. Additional comments

7- SIMULATION RESULTS

From IETR_UPMantenna_IMELSI

1. Entity

Institut d'Electronique et Télécommunications de Rennes (IETR)
CNRS UMR 6164
Université de Rennes 1, Campus de Beaulieu, Bât 11 D
263, av. du Général Leclerc
35042 Rennes Cedex, France

Contact persons :
Sylvain Collardey
Phone : +33(0)2 23 23 56 69
Fax : +33(0)2 23 23 69 63
Email : sylvain.collardey@univ-rennes1.fr

2. Name of the simulation tool

IMELSI IMpulsionnal ELectromagnetic SImulator (FDTD)

3. Generalities about the simulation tool

IMELSI employs the finite difference in time domain method in order to generate an electromagnetic field solution. The FDTD method divides the full problem space into thousands of smaller cubic regions.

4. Simulation Set-up (Geometry set-up, GUI, mesh, boundary conditions, excitation)

Describe shortly how the geometrical structure was input into your software:

- I have drawn the structure using the GUI available with your tool

Describe shortly how the meshing operation is performed in your code:

- The mesh is manual and fixed for each simulation
- Give the mesh type: uniform cubic mesh.

Describe shortly the type of boundary conditions and excitation that were used:

Perfectly matched layers (PMLs) are available and are used to simulate open problems that allow waves to radiate infinitely far into space, such as antenna designs.
For the metallic part, I have used perfect metallic material without metallic losses.
For excitation, a lumped port (localised voltage source) associated to a metallic via is used.

Give snapshots, if available, showing the structure and its main features as described in your code, the mesh used for simulation, ...

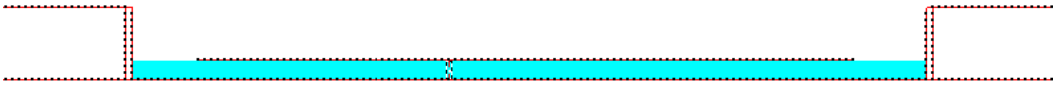

xOz plane (infinite ground plane)

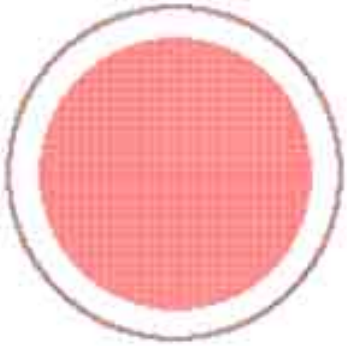

xOy plane (view of printed antenna)

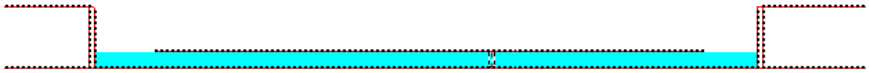

yOz plane (infinite ground plane)

How long (approximately) did it take to input the geometry? To set up the rest of the simulation?

About one hour to draw the geometry

And about 5 min to set up the rest of the simulation.

5. Simulated and measured results

- **Return loss.**

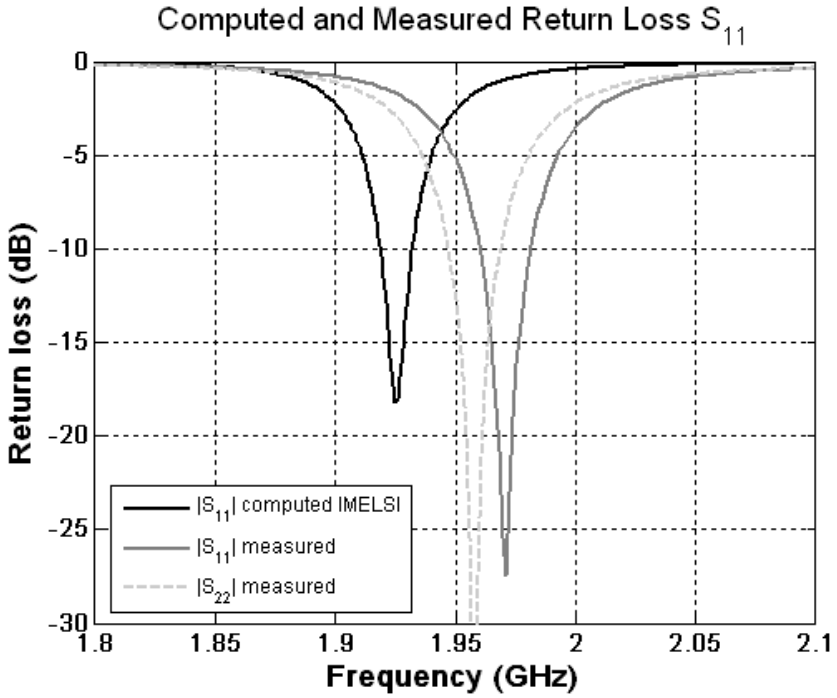

Figure 1 : Reflection coefficient magnitude versus frequency of the TEM excitation mode at the coaxial connectors.

- **Coupling magnitude.**

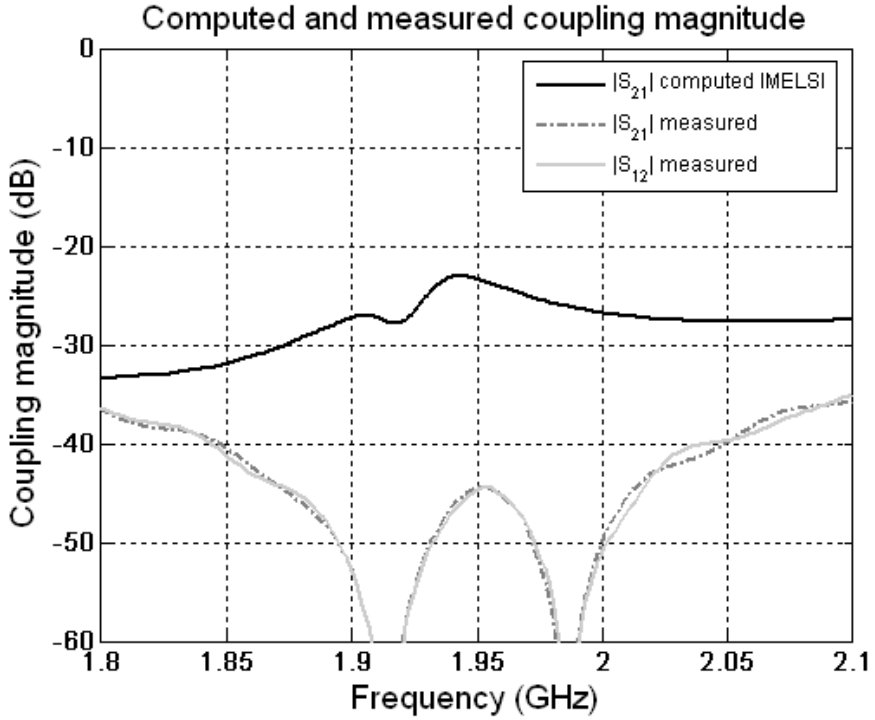

Figure 2 : Coupling coefficient magnitude versus frequency between the TEM excitation modes at the coaxial connectors.

- **Far-field radiation patterns.**

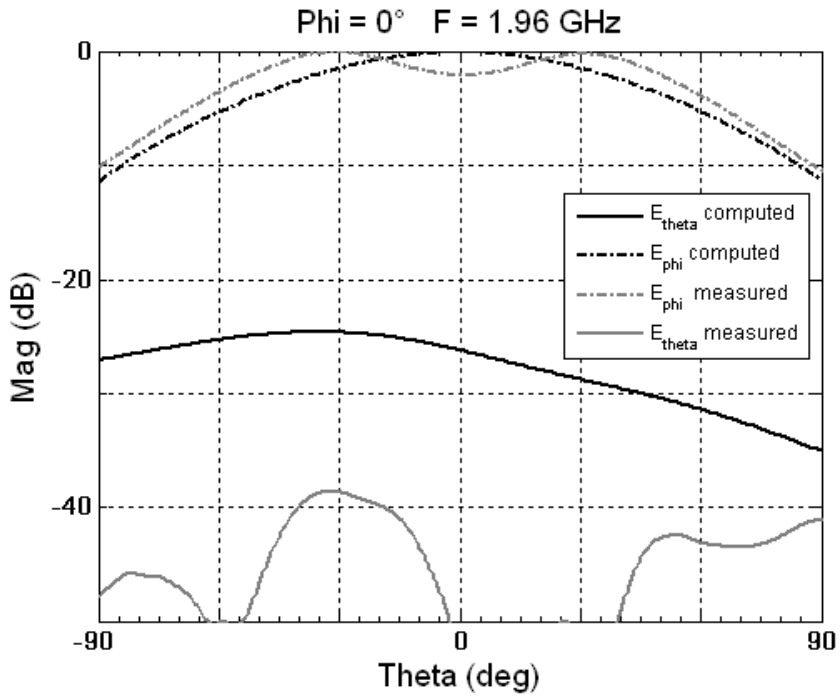

Figure 3 : Normalized E-plane radiation patterns versus theta at 1.9575 GHz when the coaxial connector located along the x-axis is excited and the other port is terminated with a matched load..

Computed co-polar component. (Infinite metallic plane).

Computed cross-polar component. (Infinite metallic plane).

Measured co-polar component. (Finite metallic plane).

Measured cross-polar component. (Finite metallic plane).

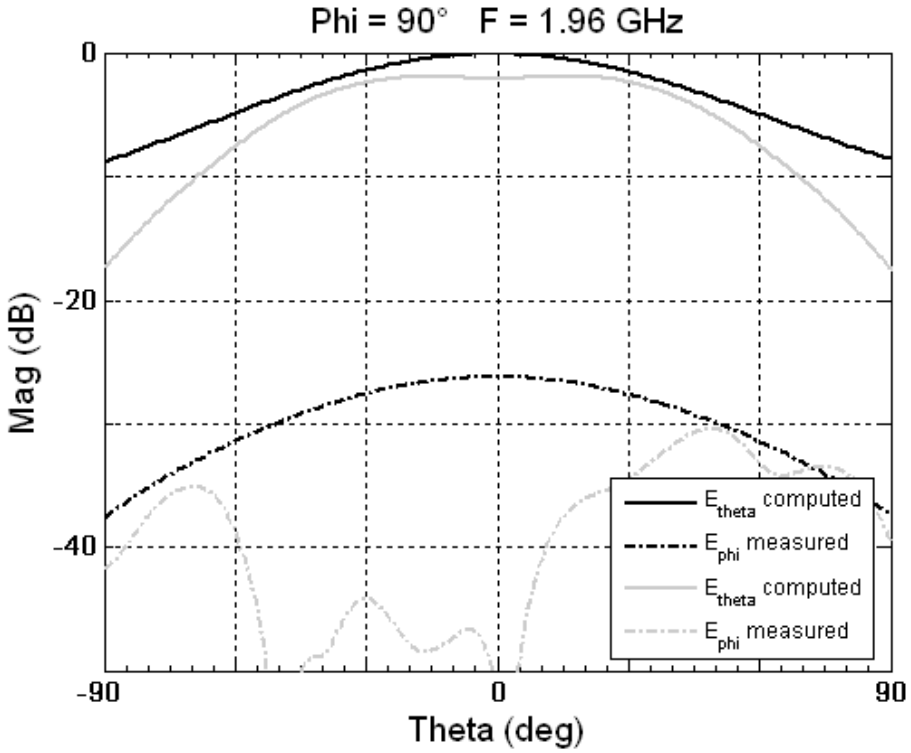

Figure 4 : Normalized H-plane radiation patterns versus theta at 1.9575 GHz when the coaxial connector located along the x-axis is excited and the other port is terminated with a matched load..

Computed cross-polar component. (Infinite metallic plane).

Computed co-polar component. (Infinite metallic plane).

Measured cross-polar component. (Finite metallic plane).

Measured co-polar component. (Finite metallic plane).

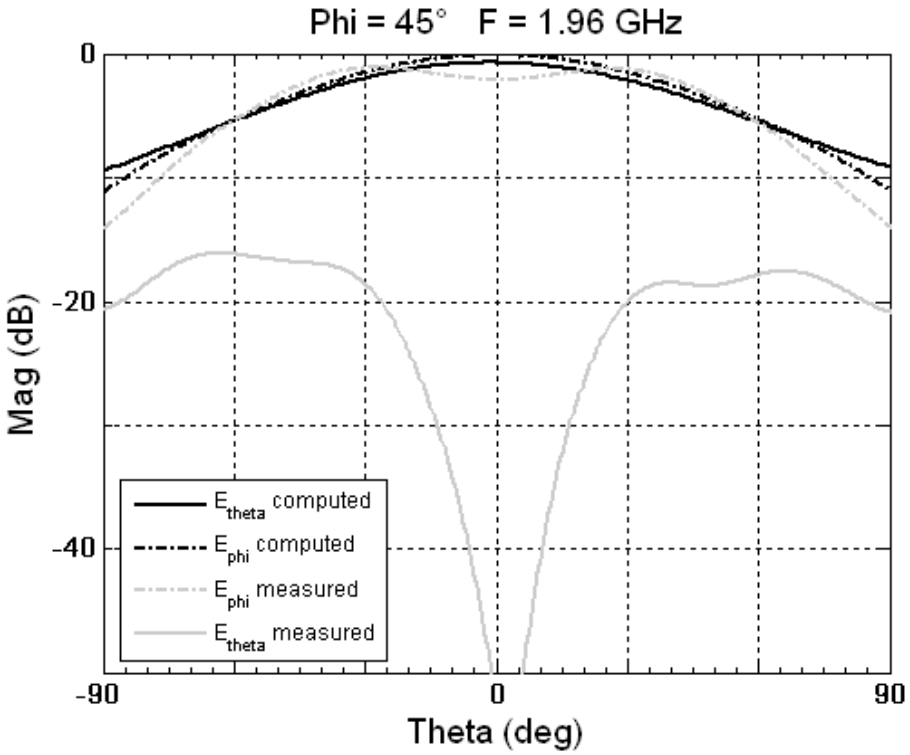

Figure 5 : Normalized radiation patterns at phi=45º versus theta at 1.9575 GHz when the coaxial connector located along the x-axis is excited and the other port is terminated with a matched load..

Computed co-polar component. (Infinite metallic plane).

Computed cross-polar component. (Infinite metallic plane).

Measured co-polar component. (Finite metallic plane).

Measured cross-polar component. (Finite metallic plane).

- **Directivity.**

The following table presents the simulated and measured maximum directivity in the E and H planes when the x axis port is excited.

	Experiments		Simulations	
	θ (°)	Max Dir (dB)	θ (°)	Max Dir (dB)
E plane (φ=180°)	30	7.08	0	5.48
H plane (φ=0°)	0	5.08	0	5.47

The following table presents the simulated and measured maximum directivity in the E and H planes when the y axis port is excited.

	Experiments		Simulations	
	θ (°)	Max Dir (dB)	θ (°)	Max Dir (dB)
E plane (φ=180°)	30	7.22	0	5.48
H plane (φ=0°)	0	4.98	0	5.47

6. Computation resources

The simulations have been performed on PC with one processor at 3GHz and 2Go of memory. The data relevant to the simulation are listed in the following table.

Simulation requirements	**Dual feed cavity patch**
Number of cells	180x180x60
Real Time per simulation	≈ 13h
Memory requirements	200Mo

7. Discussion

One simulation at 1.96 GHz has been done without loss less dielectric and with an infinite ground plane. Another one has been done with a better mesh and the results are equivalent. Even if the computed S11 is almost similar to the S11 measured with a slight shift toward low frequencies, the coupling between both ports doesn't present a good agreement with the measurement. Moreover, the computed radiation pattern (and the directivity) are not equivalent to the measured patterns. In conclusion, I don't think this software based on the FDTD method is suitable for this kind of antenna. Another simulation must be done with a finite ground plane but the memory requirement is beyond the PC memory.

8. Additional comments

8- SIMULATION RESULTS

From FT R&D_UPMantenna_SR3D

1- Entity

France Telecom, R&D Division
Fort de la tête de chien
06320 La Turbie

Philippe Ratajczak:
- tel: +33 4 92 10 65 24
- fax: +33 4 92 10 65 19
- Email: philippe.ratajczak@francetelecom.com

2- Name of the simulation tool

SR3D

3- Generalities about the simulation tool

SR3D - Structures Rayonnantes à 3 dimensions (3D Radiating Structures) - is a software which, given the geometry and the feeding of a 3D structure including homogeneous dielectrics, computes its electromagnetic characteristics The complete solution of the problem (currents densities, S matrix of the multi-port feeding, spherical expansion of the radiation pattern, ...) is obtained by a rigorous method based on integral equation formulation. The problem is numerically solved with a surface finite element method via a direct inversion of the linear system matrix.

4- Simulation Set-up (Geometry set-up, GUI, mesh, boundary conditions, excitation)

The interface between the mesh generator is achieved through an ASCII file containing the definition of:
- the 3D points,
- the lines between 2 points,
- the surfaces bounded by a closed line,
- the surfaces assembling to define the interfaces of homogeneous dielectric domains.

The triangular meshing must verify some conditions in order to obtain good results:
- each triangle must be as closed as possible to a equilateral triangle,
- the maximum size is $\lambda/5$.
- when dielectric are modelized, the mesh step depends on the dielectric wavelength.

All the objects must have finite dimensions, so we modelized a 300 mm diameter ground plane.

The mesh of cavity-backed microstrip patch is presented figure 1. There are 31 853 unknowns. The meshing of the patch and the dual coaxial probe feed is presented figure 2.

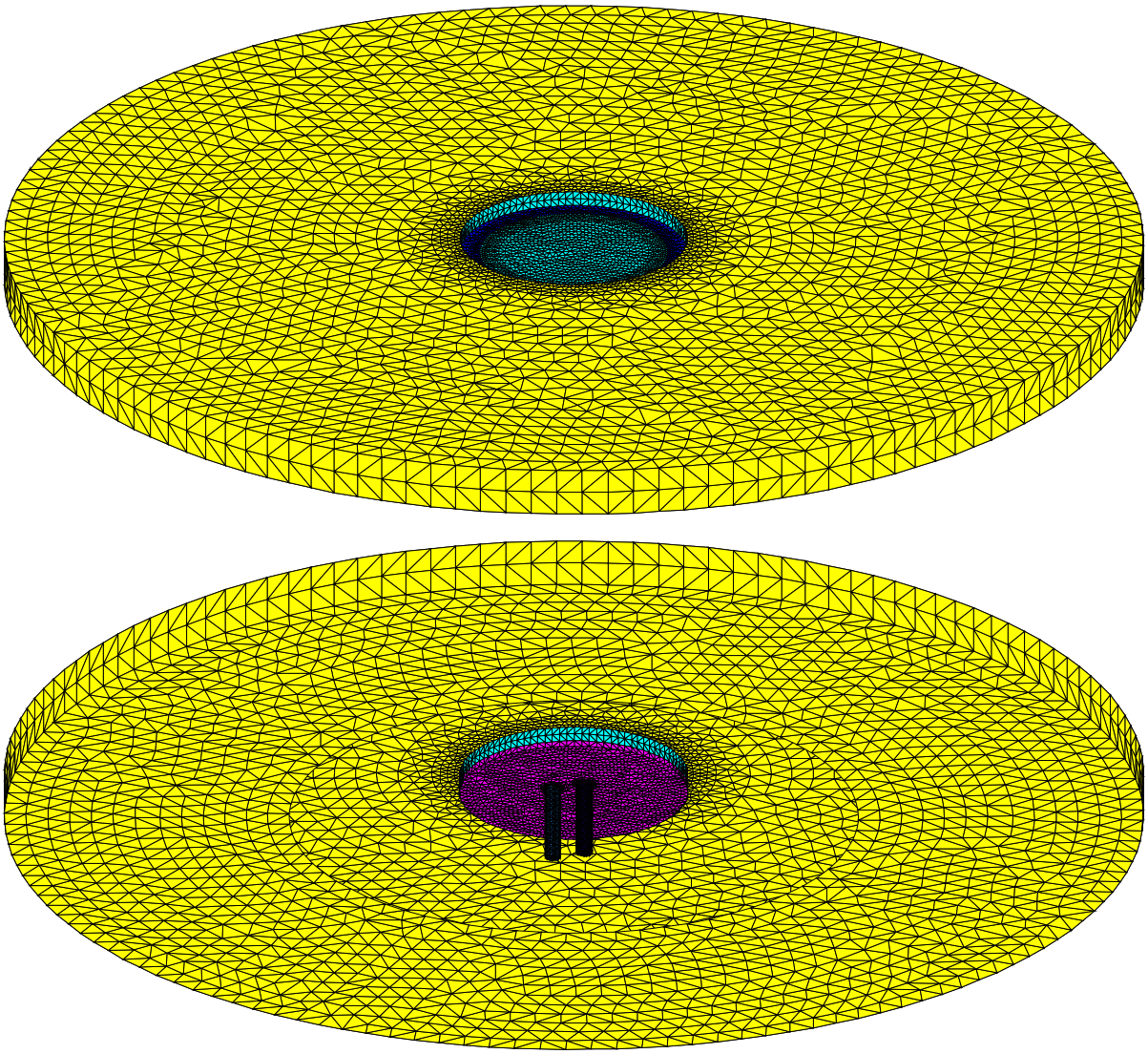

figure 1: meshing of the cavity-backed microstrip patch on finite ground plane

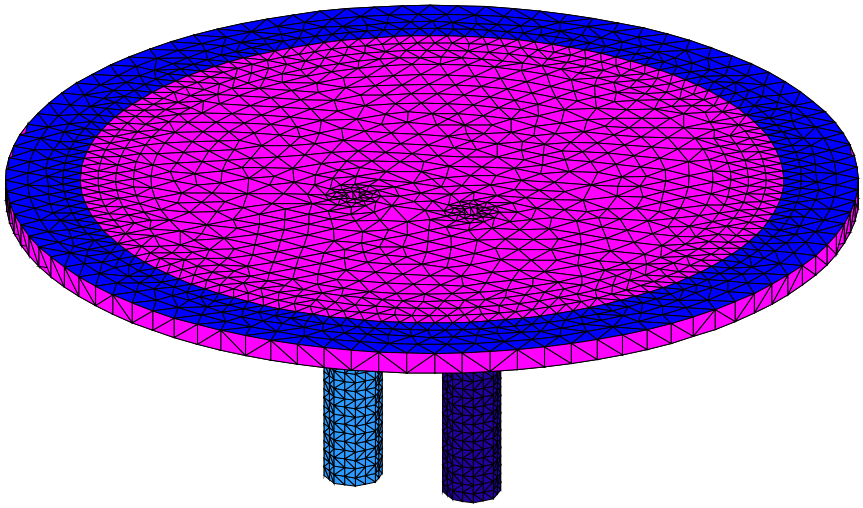

figure 2: meshing of patch with the dual coaxial feed

The structure is fed by two coaxial waveguide cross-sections equivalent to Huyghens surfaces with the fundamental mode TEM.

5- Simulation results

The figure 3 presents the comparison of the simulated and measured input impedance. The coupling coefficient comparison is presented figure 4.

For the input impedance, there is a frequency shift about 0.025 GHz on the matching frequency position. Concerning the coupling between the two ports, the simulated S_{12} and S_{21} have the same differences with the experiments as the UPM simulations.

The comparison of the simulated and measured radiation pattern at 1.95 for the x axis port excited is presented figure 5 for the E plane, figure 6 for H plane and figure 7 for the 45° plane. For the y axis port excited at 1.97 GHz, the E plane is presented figure 8, H plane figure 9 and 45° plane figure 10.

The radiation pattern is well predicted as we can see on the following figures. The simulated main and the cross polarizations are comparable to the measured ones for the two ports excited. A small difference appears in the E planes for $\theta > 110°$. In the other planes, the comparison with experiments is excellent.

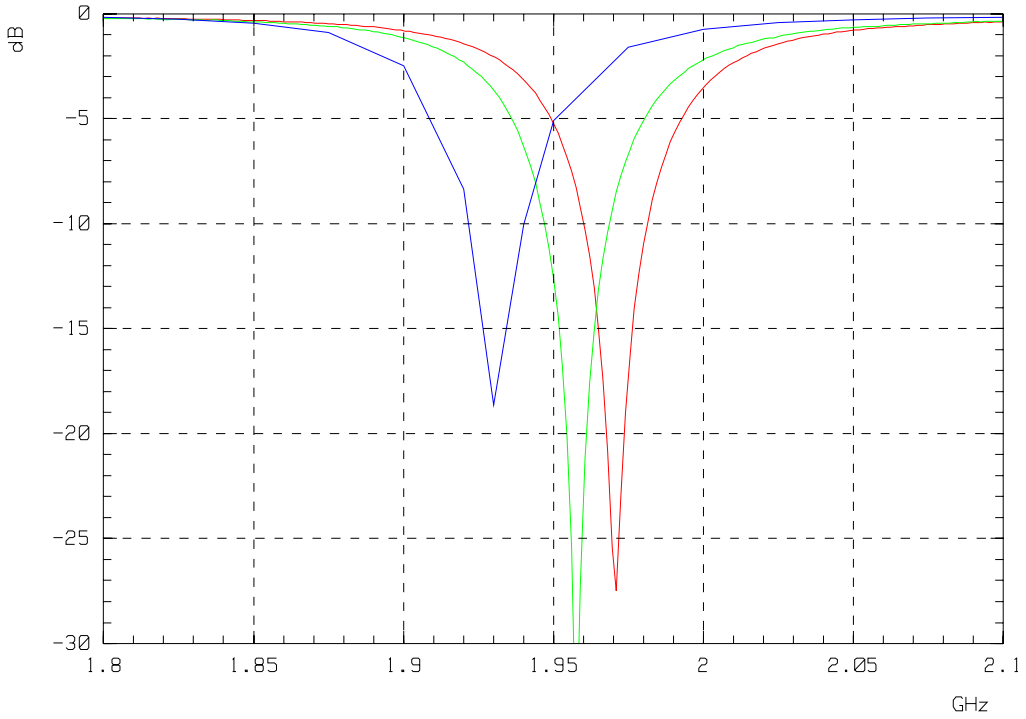

$|S_{11}|$: Measured at the coaxial connector located along the y-axis (port 1) when the other port is terminated with a matched load (finite metallic plane)

$|S_{22}|$: Measured at the coaxial connector located along the x-axis (port 2) when the other port is terminated with a matched load (finite metallic plane)

$|S_{11}|$ and $|S_{22}|$: Computed at both ports when the other is terminated with a matched load (finite metallic plane)

figure 3: Reflection coefficient magnitude versus frequency of the TEM excitation mode at the coaxial connectors.

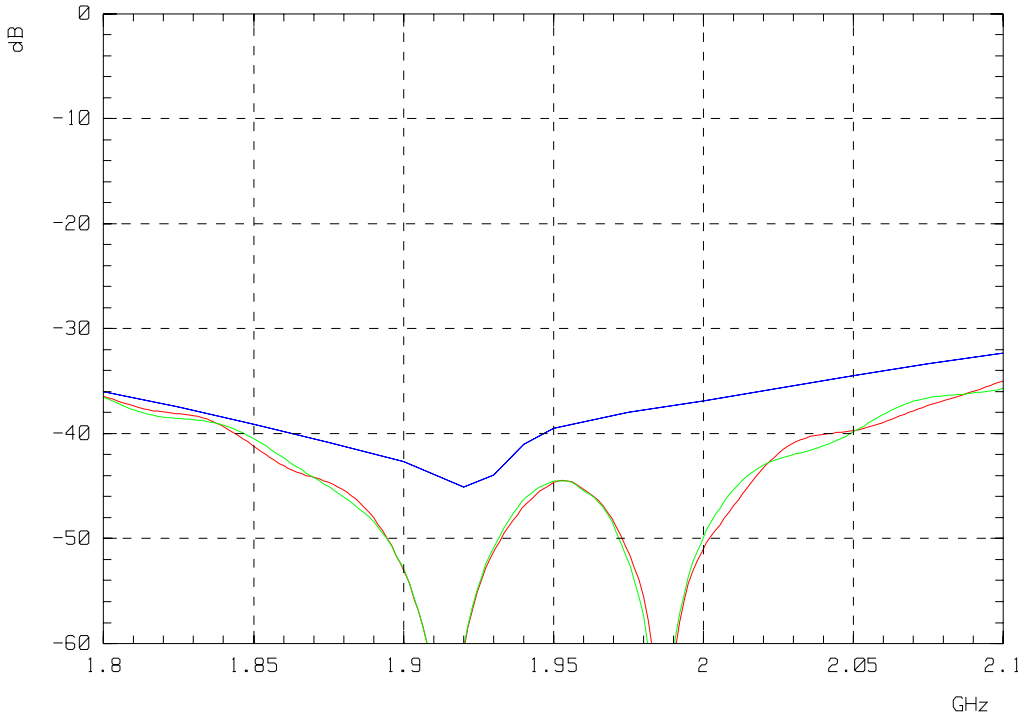

Measured coupling magnitude $|S_{12}|$ (finite metallic plane)

Measured coupling magnitude $|S_{21}|$ (finite metallic plane)

Computed coupling magnitude ($|S_{12}| = |S_{21}|$) (finite metallic plane)

figure 4: Coupling coefficient magnitude versus frequency between the TEM excitation modes at the coaxial connectors.

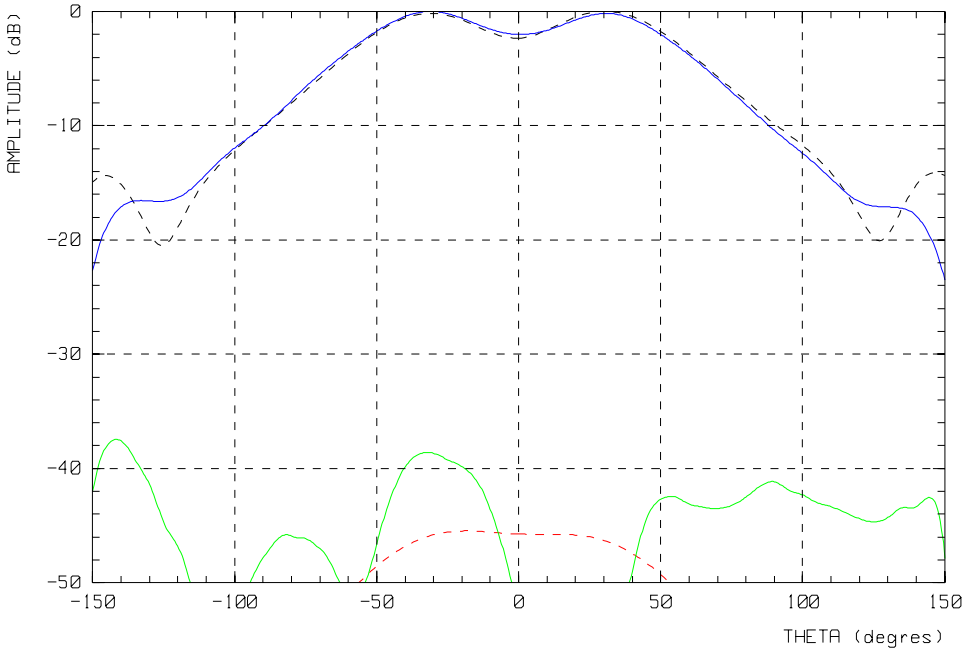

Computed co-polarization component (finite metallic plane)

Computed cross-polarization component (finite metallic plane)

Measured co-polarization component (finite metallic plane)

Measured co-polarization component (finite metallic plane)

figure 5: E-plane radiation pattern versus theta at 1.95 GHz when the coaxial connector located along x-axis is excited, the other port is terminated with a matched load.

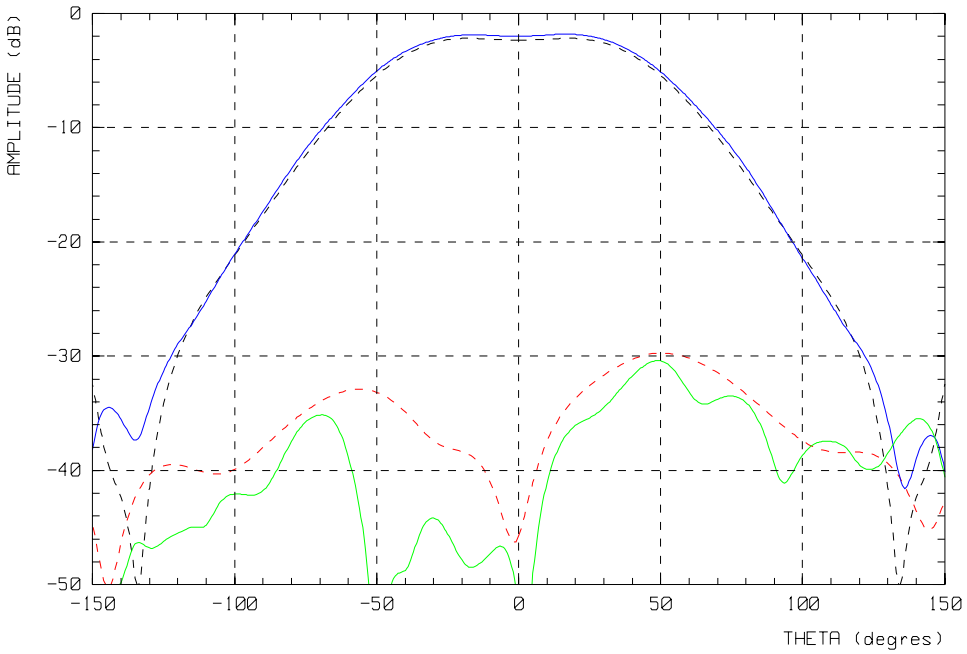

Computed co-polarization component (finite metallic plane)

Computed cross-polarization component (finite metallic plane)

Measured co-polarization component (finite metallic plane)

Measured co-polarization component (finite metallic plane)

figure 6: H-plane radiation pattern versus theta at 1.95 GHz when the coaxial connector located along x-axis is excited, the other port is terminated with a matched load.

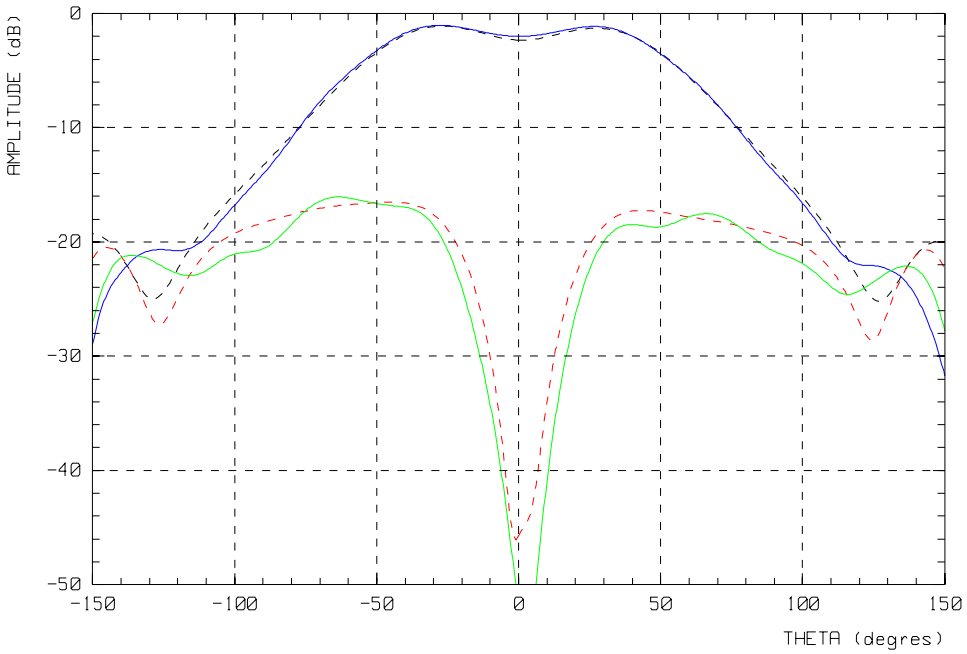

Computed co-polarization component (finite metallic plane)

Computed cross-polarization component (finite metallic plane)

Measured co-polarization component (finite metallic plane)

Measured co-polarization component (finite metallic plane)

figure 7: 45-plane radiation pattern versus theta at 1.95 GHz when the coaxial connector located along x-axis is excited, the other port is terminated with a matched load.

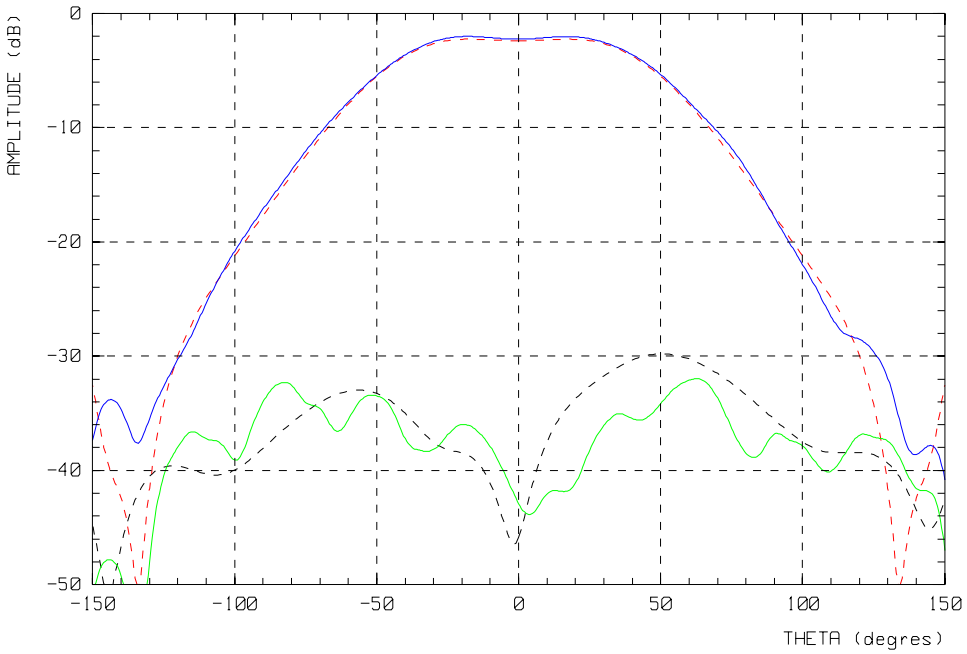

Computed co-polarization component (finite metallic plane)

Computed cross-polarization component (finite metallic plane)

Measured co-polarization component (finite metallic plane)

Measured co-polarization component (finite metallic plane)

figure 8: H-plane radiation pattern versus theta at 1.97 GHz when the coaxial connector located along y-axis is excited, the other port is terminated with a matched load.

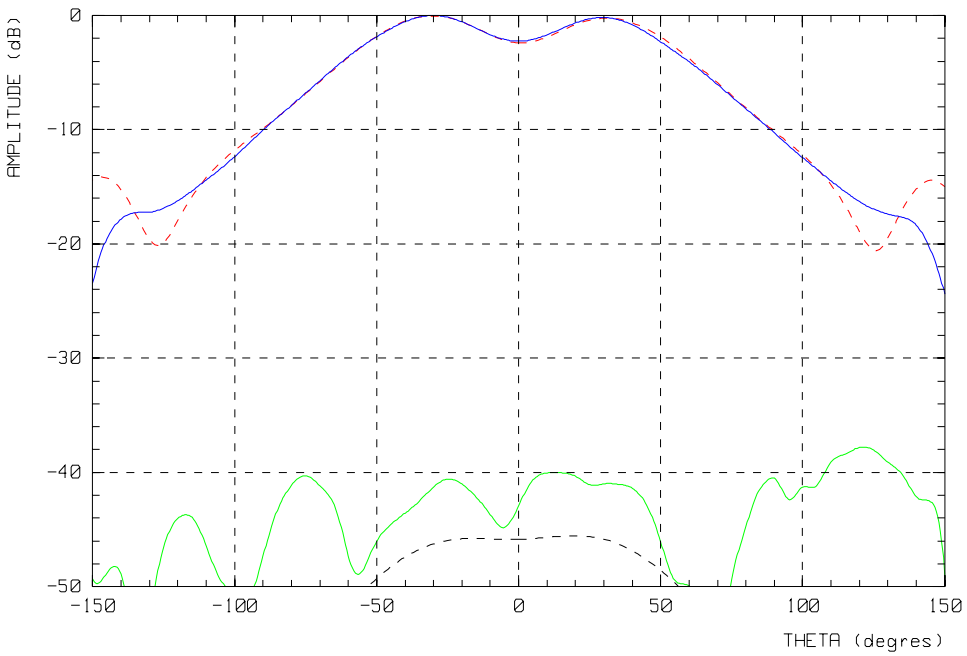

Computed co-polarization component (finite metallic plane)

Computed cross-polarization component (finite metallic plane)

Measured co-polarization component (finite metallic plane)

Measured co-polarization component (finite metallic plane)

figure 9: E-plane radiation pattern versus theta at 1.97 GHz when the coaxial connector located along y-axis is excited, the other port is terminated with a matched load.

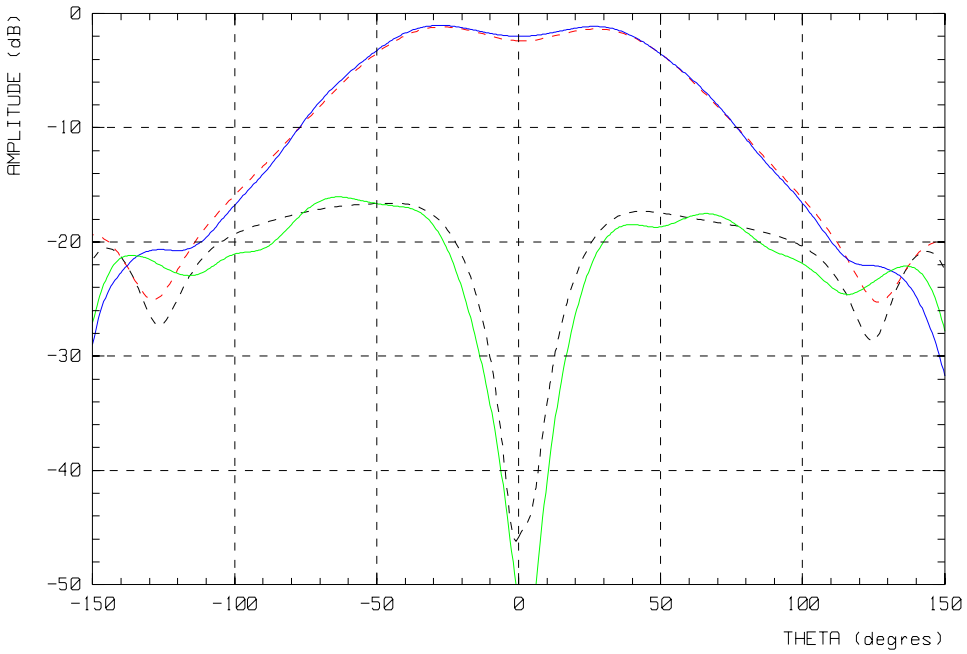

Computed co-polarization component (finite metallic plane)

Computed cross-polarization component (finite metallic plane)

Measured co-polarization component (finite metallic plane)

Measured co-polarization component (finite metallic plane)

figure 10: 45-plane radiation pattern versus theta at 1.97 GHz when the coaxial connector located along y-axis is excited, the other port is terminated with a matched load.

The following table presents the simulated and measured maximum directivity in the E and H planes when the x axis port is excited.

Tableau 1: x axis port excited

	Experiments		Simulations	
	θ (°)	Max Dir (dB)	θ (°)	Max Dir (dB)
E plane	**30.0**	**7.08**	**31.0**	**7.18**
H plane	**0.0**	**5.08**	**17.0**	**4.97**

The following table presents the simulated and measured maximum directivity in the E and H planes when the y axis port is excited.

Tableau 2: y axis port excited

	Experiments		Simulations	
	θ (°)	Max Dir (dB)	θ (°)	Max Dir (dB)
E plane	**30.0**	**7.22**	**29.0**	**7.21**
H plane	**0.0**	**4.98**	**17.0**	**5.04**

The dielectric losses at 1.95 and 1.97 GHz are about 1 dB.

6- Computation resources

The simulations have been performed on a HP RP7410 with 6 HPPA 8700 processors at 750 MHz (6 x 3.7 Gflops) (HPUX 11.00) and 4 Go of memory.

The matrix is saved out of core on disks by blocs. The data relevant to the simulation are listed in the following table.

Table 3: Simulation requirements

	Dual feed cavity patch
Number of unknowns	**31 853**
Disk space requirement	**4.27 Go**
CPU Time per frequency point	**8 h 30 min**
Real Time per frequency point	**2 h 10 min**

7- Discussion

To validate the meshing of the structure, one simulation at 1.93 GHz has been done with a loss less dielectric to verify the energy conservation test.

The quality of results obtained thanks to application of the integral equation formalism has been demonstrated. Accuracy is achieved at the cost of CPU time since for an average structure (~ 30 000 unknowns) computation time is of the order of several hours per frequency point with a calculator working at an effective rate of 22 Gflops. While the variety of cases simulated since 15 years demonstrates the flexibility of the method, their purpose is not to claim that SR3D has universal application. The formalism of integral equations should be used preferentially for external problems (i.e. essentially radiation problems) of reasonable size as we can see on the radiation pattern comparison.

The meshing quality affects directly the precision of the results and particularly the near field radiation (input impedance, ...). The validation test included in SR3D must verify the energy conservation below 3.5 % between the input energy at the feeding port and the radiated energy when no losses are included in the dielectric domains or on metallic structures. This constraint which is not sufficient but necessary, allows us to have very good agreement between simulation and experiments when we manufacture the final structure and so eliminates new simulations and modifications of the breadboard.

The main difficulty with SR3D is that we can make none approximation on the modeling of the structure, all the dimensions are finite (ground planes, wires, no attached modes between wires and planes, ...) that increases drastically the numbers of unknowns and has obliged us to make efforts on parallel processing and numerical integration in order to maintain CPU time within reasonable limits.

8- Additional comments

9- SYNTHESIS OF RESULTS

Participants and simulations tools:

-. The structure proposed by the UPM has been simulated by **five laboratories**.
-. All the simulations tools are **in house software**.

- **CNRS-LEAT** (Laboratoire d'Electronique, Antennes et Télécommunications)
  Method: **FP-TLM** (Transmission Line Matrix method)
- **FOI** (Swedish Defence Research Agency):
  Method: **TFDTD** (Finite- Difference Time Domain Method)
- **FT R&D** (France Telecom, R&D Division)
  Method: **SR3D** (Integral Equation Formulation and Finite Element Method)
- **IETR** (Institut d'Electronique et Télécommunications de Rennes) :
  Method : **IMELSI** (Finite-Difference Time Domain Method)
- **UNIBRIS** (University of Bristol):
  Method : **FDTD32** (Finite- Difference Time Domain).
- **UPM** (Universidad Politécnica de Madrid)
  Method: **SFELP** (Hybrid method based on Domain Decomposition, FEM, Modal Analysis and Reduced Order Models)

-. The simulation has been performed by **3 Finite-Difference time domain methods** (UNIBRIS,IETR,FOI). FP-TLM from CNRS-LEAT is very similar to FTDT. In all these simulations the PML is employed to simulate the open problem.

-. Two simulations have been performed with **frequency domain methods:** FT R&D employs a method based on the integral equation formulation and the finite element method. UPM uses a hybrid method based on Domain Decomposition, FEM, Modal Analysis and Reduced Order Models .

-.UNIBRIS, IETR and FOI state that a software based on the FDTD method is not suitable for this kind of antenna.

-.The simulations from UNIBRIS, IETR, FOI and UPM use an infinite ground plane approximation. FTR&D and CNRS-LEAT simulate the real finite ground plane. All the simulations except for FTR&D consider perfect metal conductors. UNIBRIS and IETR also consider lossless dielectric substrates.

-. For all return loss simulations a good agreement with simulations is observed in general except for a slight shift toward low frequencies since it is a highly resonant structure with a

narrow band. This fact may be due to the thickness and the permittivity tolerances of the substrate.

-. For all software tools (except for CNRS results that show good concordance with a shift frequency) the coupling coefficient simulations present a poor agreement with measurements although they reproduce the low coupling levels. However all these simulations show a good agreement between them.

-. A good agreement is observed between measured and simulated radiation patterns and directivity obtained from software tools that take into account the finite ground plane (FTR&D and CNRS-LEAT). With the infinite ground plane approximation the copolar component in the radiation patterns show an acceptable agreement except for angles near endfire. For this reason the simulated and measured directivity do not agree in these cases and it is not provided from some institutions. In the same way the simulated crosspolar components do not agree very well with measurements when the infinite ground plane approximation is employed.

BENCHMARKING ACTIVITY

(WP1.1-2)

Dual wideband radiating element for mobile handsets

Proposed by
Laboratoire d'Electronique, Antennes et Télécommunications
-LEAT-

1. STRUCTURE DESCRIPTION

Entity

Laboratoire d'Electronique, Antennes et Télécommunications (LEAT)
CNRS UMR 6071
250 rue Albert Einstein, Bât. 4, 06560 Valbonne, France

Contact persons:
Philippe LeThuc , Robert Staraj, Jean-Marc Ribero
Phone: +33 (0)4 92 94 28 26
Fax: +33 (0)4 92 94 28 12
email: Philippe.Lethuc@unice.fr, Robert.Staraj@unice.fr, Jean-Marc.Ribero@unice.fr

1. Name of the structure

Dual wideband radiating element for mobile handsets

2. Generalities

This structure corresponds to a realistic configuration of miniature antenna dedicated to mobile phone. The dimensions of the ground plane are close to the dimensions required in modern mobile phone handsets for the PCB supporting all electronic components and antenna. It is also a multiband structure, optimised for GSM900 (lower bandwidth) and DCS/PCS and UMTS bands (upper bandwidth).

3. Structure Description

The structure proposed for benchmarking is illustrated in the different figures below. The antenna is made up of two stacked quarter-wavelength elements short-circuited along a same plane. The patches are realized with rectangular 0.3 mm copper sheets on air substrate, to provide the largest bandwidth as possible for a total height of 11.6 mm. The originality of the structure also comes from the feed connected to the upper patch instead of the lower one (coaxial probe diameter: 1.2 mm). Each resonator includes a slot possessing a special layout and its width is 0.3mm.

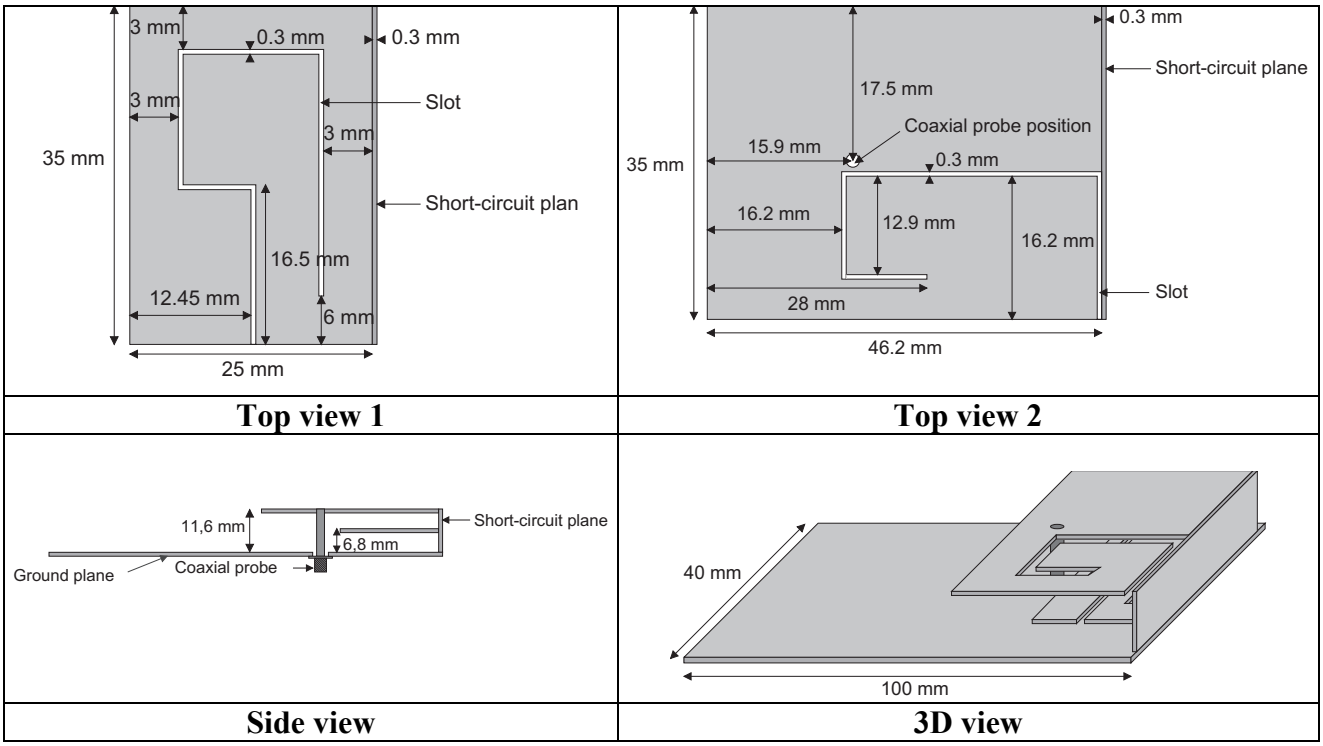

Top view 1	Top view 2
Side view	3D view

4. Computed results

Fig. 1 and 2 compare computed and measured voltage standing wave ratios (VSWR).

A generally good agreement between theory and experiment is obtained.

To obtain these good results, we have simulated our structure with a width of slot equal to 0.1mm, and a conductivity of metal $\sigma = 4.9e+7$.

The measured bandwidths are about 90 MHz (9.8% at 920 MHz) for the lower band for a VSWR ≤ 3 and about 460 MHz (23.7% at 1940 MHz) for VSWR ≤ 2.5 for the upper band.

That is enough to simultaneously cover GSM, DCS, PCS and UMTS systems.

Radiation patterns are reasonably omnidirectional (Fig. 3 and 4), that is suitable for mobile telephone applications.

For all the obtained bandwidths, these radiation patterns are very close.

Once again, we can see that simulated and measured radiation pattern results are very close too.

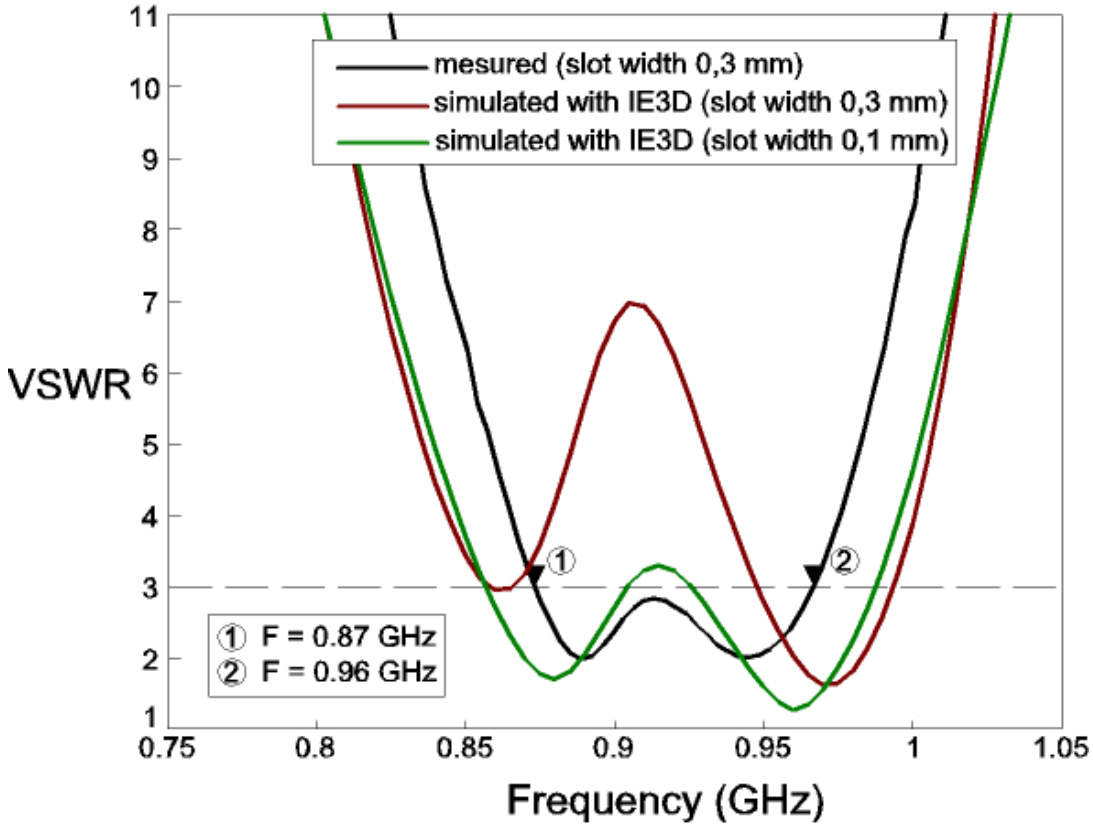

Figure 1 : VSWR in the lower band

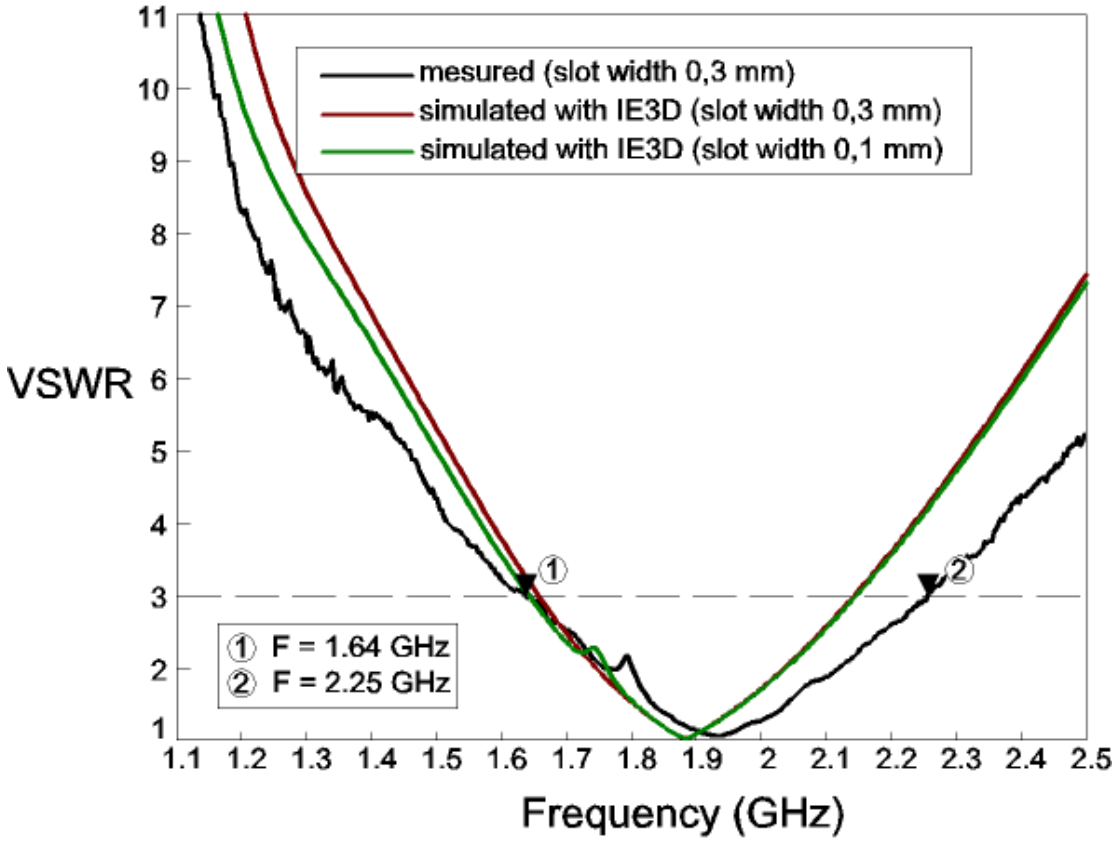

Figure 2 : VSWR in the upper band

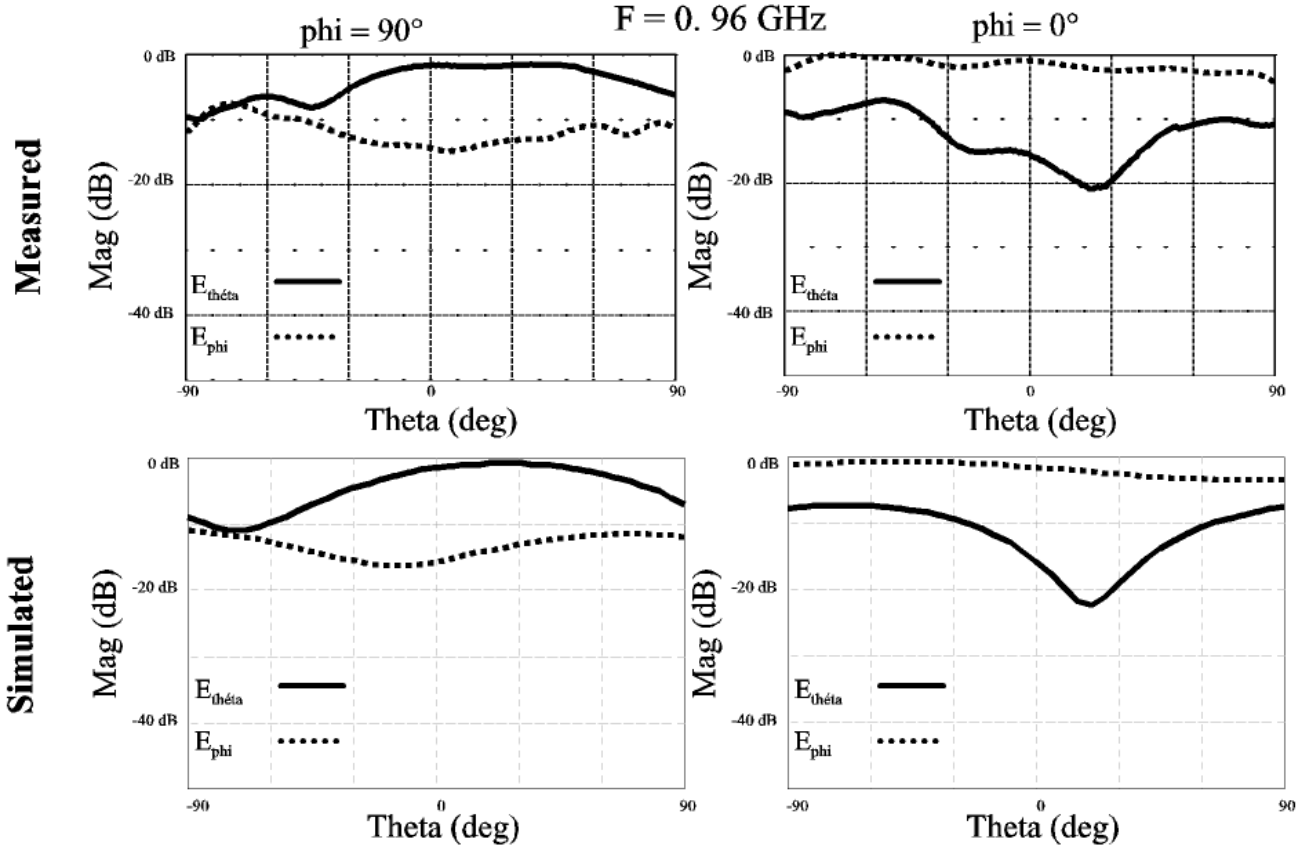

Figure 3 : Radiation pattern in the lower frequency band

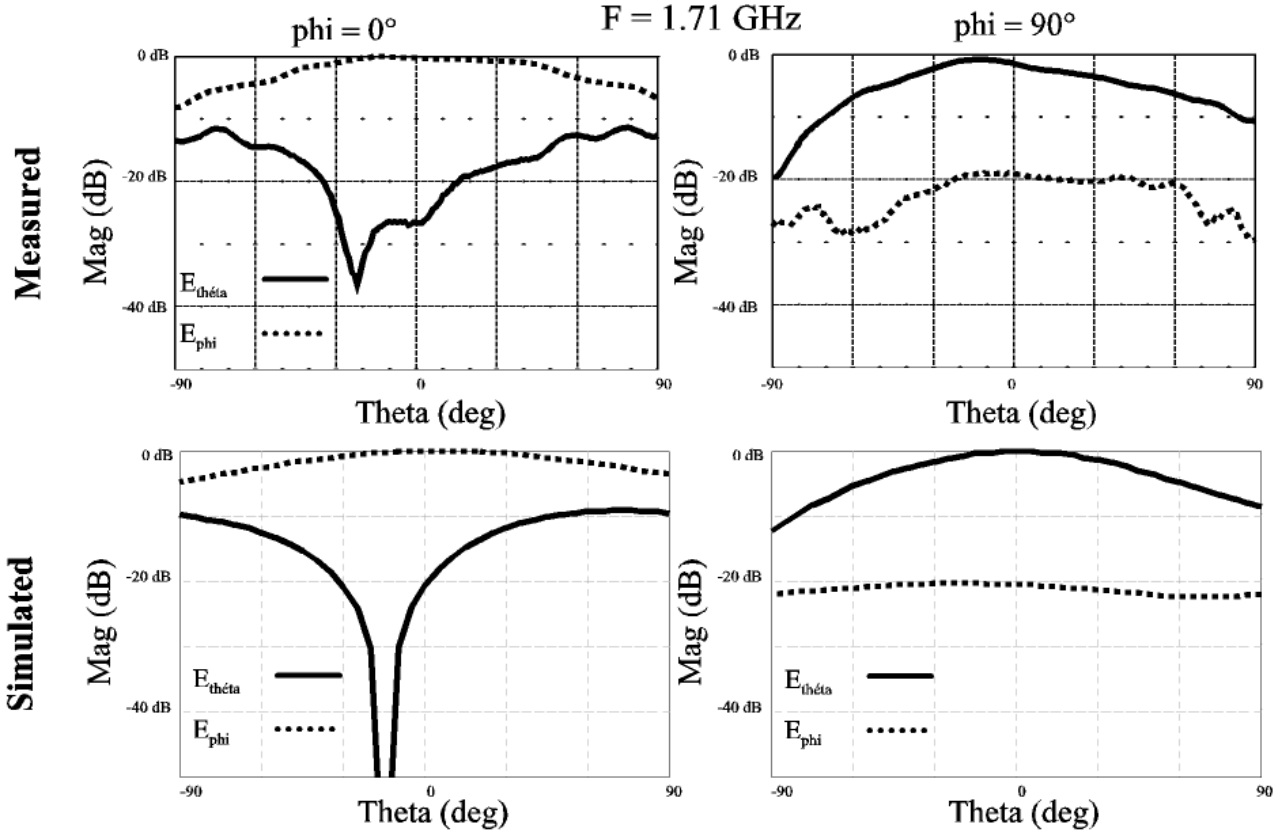

Figure 4 : Radiation pattern in the upper frequency band

5. References

The benchmarking of this structure will consist of a comparison between numerical techniques and experiment. Simulation results presented in this part are obtained with IE3D Zeland software and are given for information on the difficulty to correctly model the thin slots existing in the metallic parts. So, the proposed structure is particularly interesting for benchmarking purposes, especially due to theses thin slots. Moreover, the fact that these slots are close to the vertical metallic part of the antenna seems to create additional particular modelling difficulties.

6. Additional comments

2- STRUCTURE MEASUREMENTS

Entity

Laboratoire d'Electronique, Antennes et Télécommunications (LEAT)
CNRS UMR 6071
250 rue Albert Einstein, Bât. 4, 06560 Valbonne, France

Contact persons:
Philippe LeThuc , Robert Staraj, Jean-Marc Ribero
Phone: +33 (0)4 92 94 28 26
Fax: +33 (0)4 92 94 28 12
email: Philippe.Lethuc@unice.fr, Robert.Staraj@unice.fr, Jean-Marc.Ribero@unice.fr

1. Description of measurement tools

- ***Input impedance and Voltage Standing Wave Ratio measurements are realised using a Rohdes & Schwartz network analyser***
- ***Radiation pattern measurements are realised in anechoic chamber***
- ***Efficiency measurements are realised using Wheeler Cap Method***

2. Generalities about measurement tools

3. Measurements Set-up

- ***Annular ferrites are used on the measurement cable of the network analyser to avoid return currents and to stabilize the input impedance measurement.***
- ***The anechoic chamber is a full anechoic chamber***
- ***Two different antennas are used for lower and upper band***

4. Measurement results

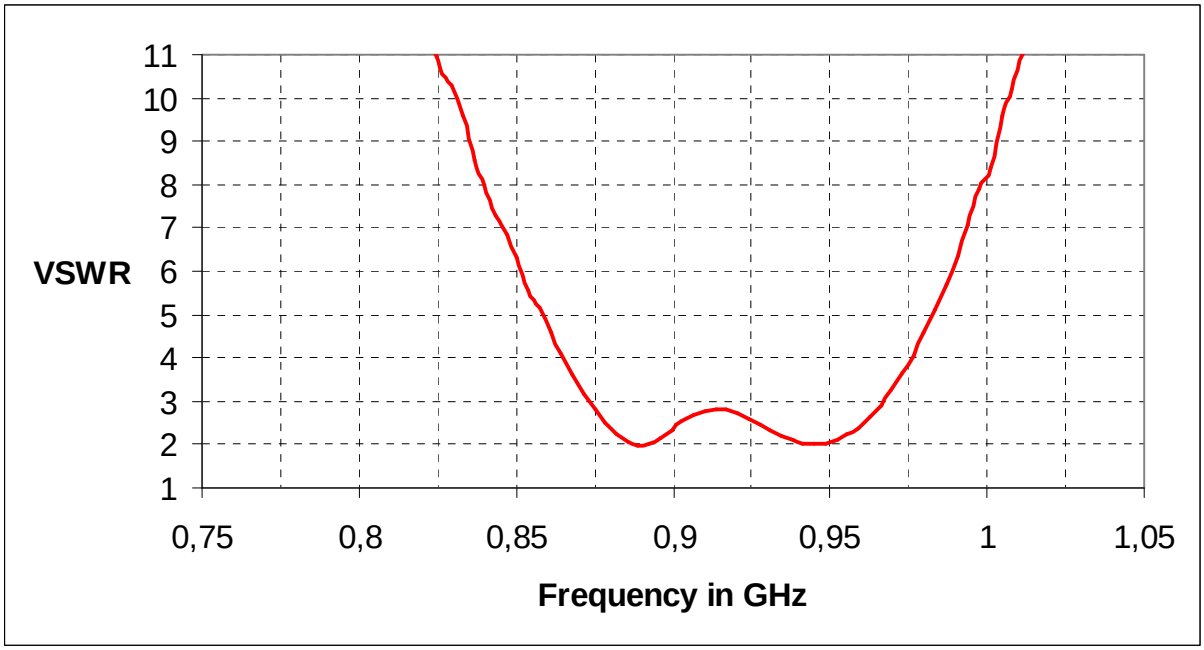

Figure 1 : VSWR versus frequency in the lower band.

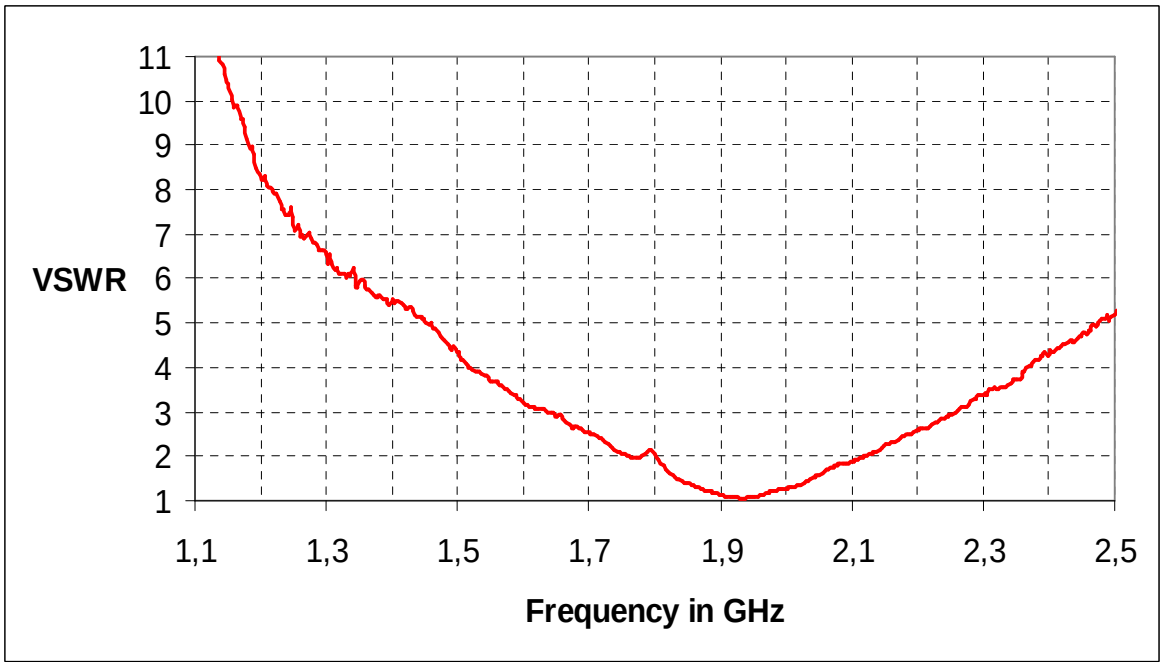

Figure 2 : VSWR versus frequency in the upper band.

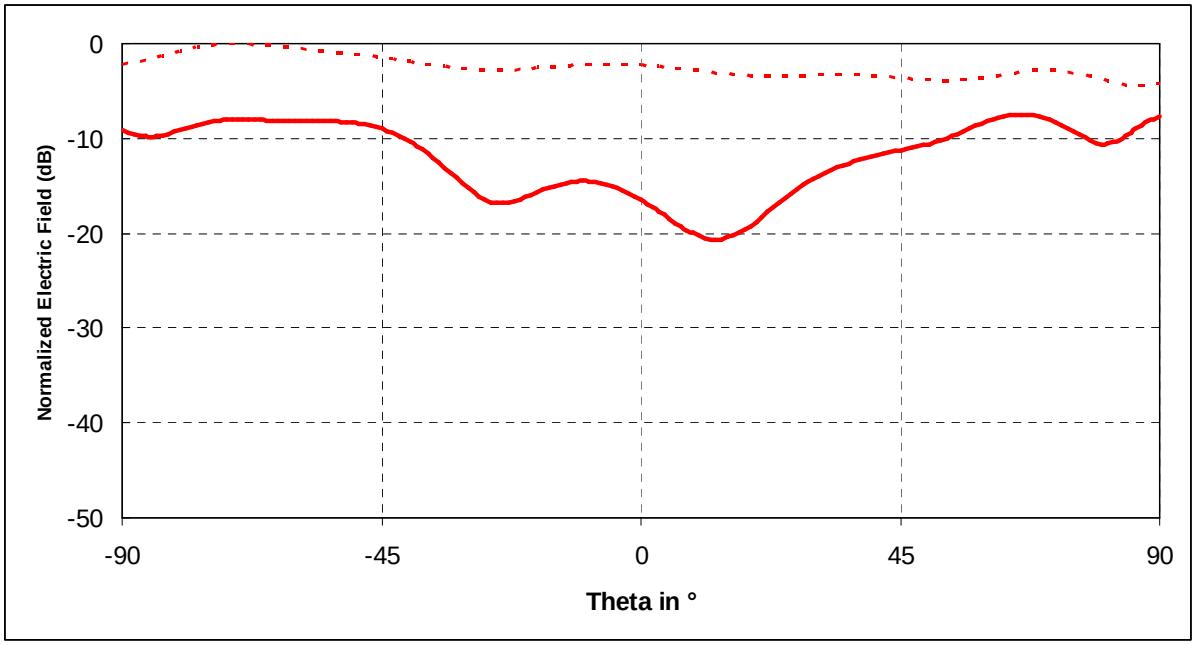

Figure 3 : E-plane radiation pattern versus theta in the lower band (f=0.96 GHz).

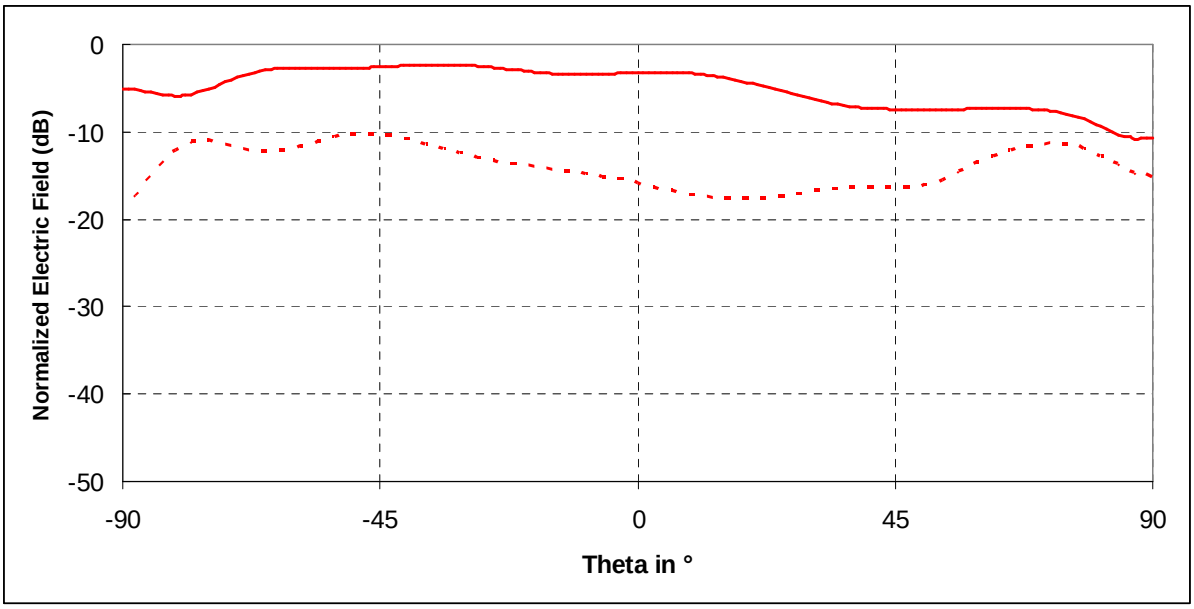

Figure 4 : H- plane radiation pattern versus theta in the lower band (f=0.96 GHz).

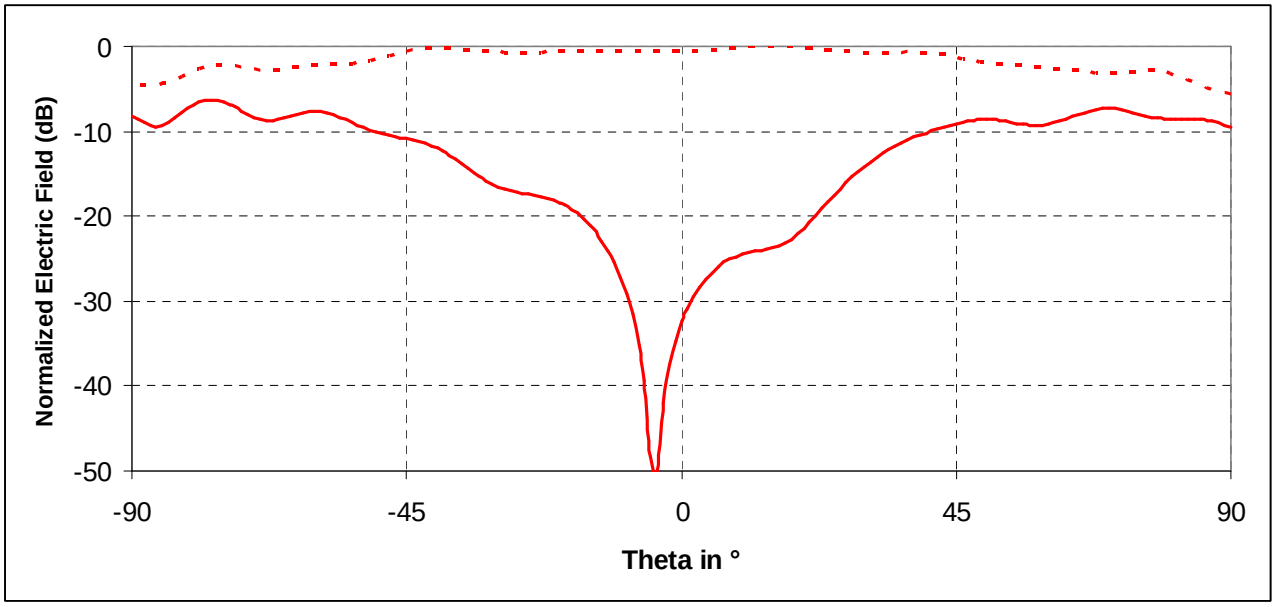

Figure 5 : E-plane radiation pattern versus theta in the upper band (f=1.71 GHz)

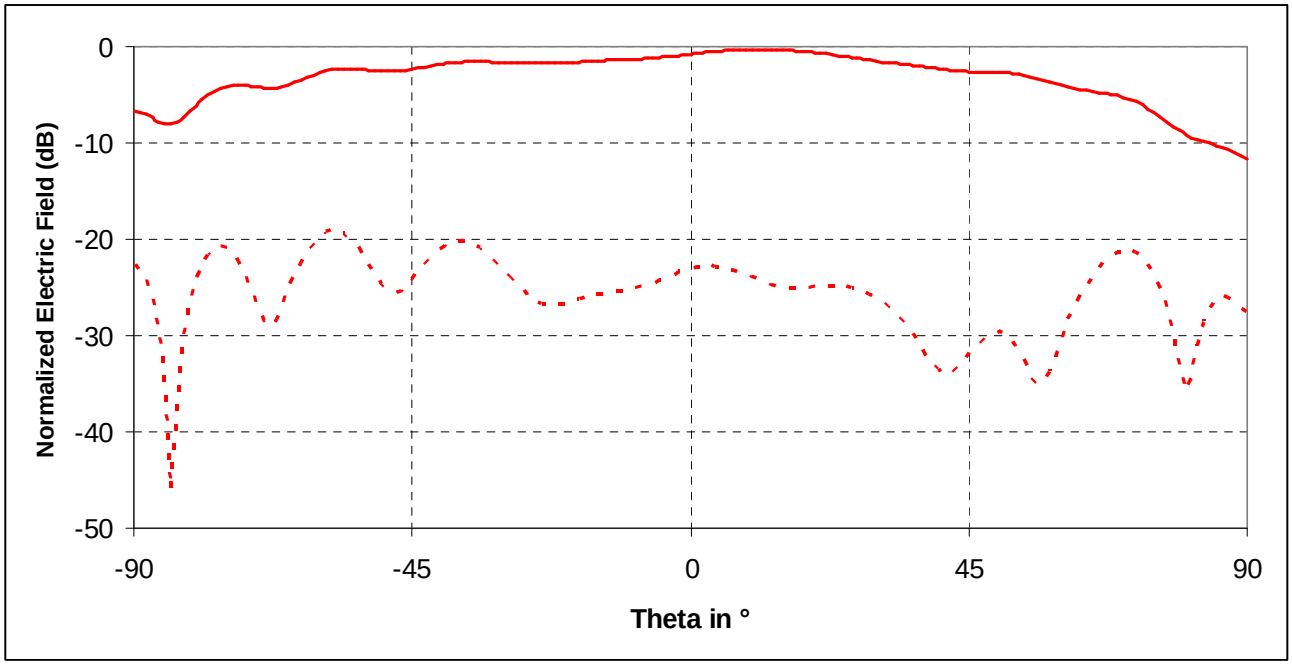

Figure 6 : H- plane radiation pattern versus theta in the upper band (f=1.71 GHz)

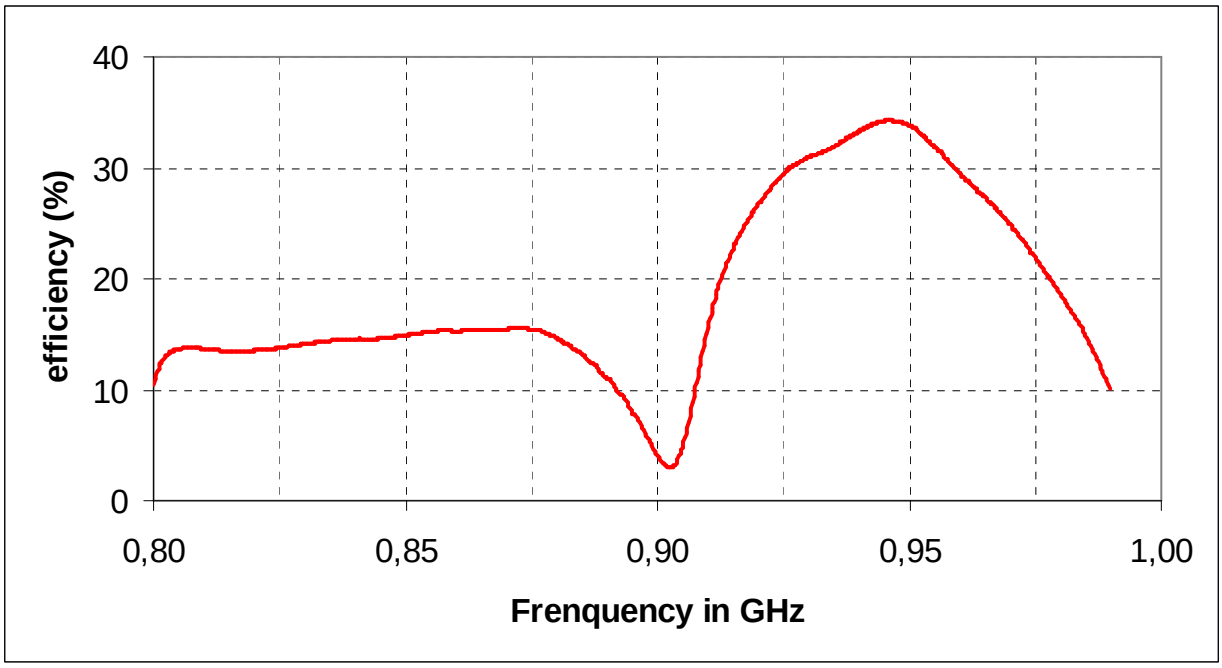

Figure 7 : Efficiency in GSM band.

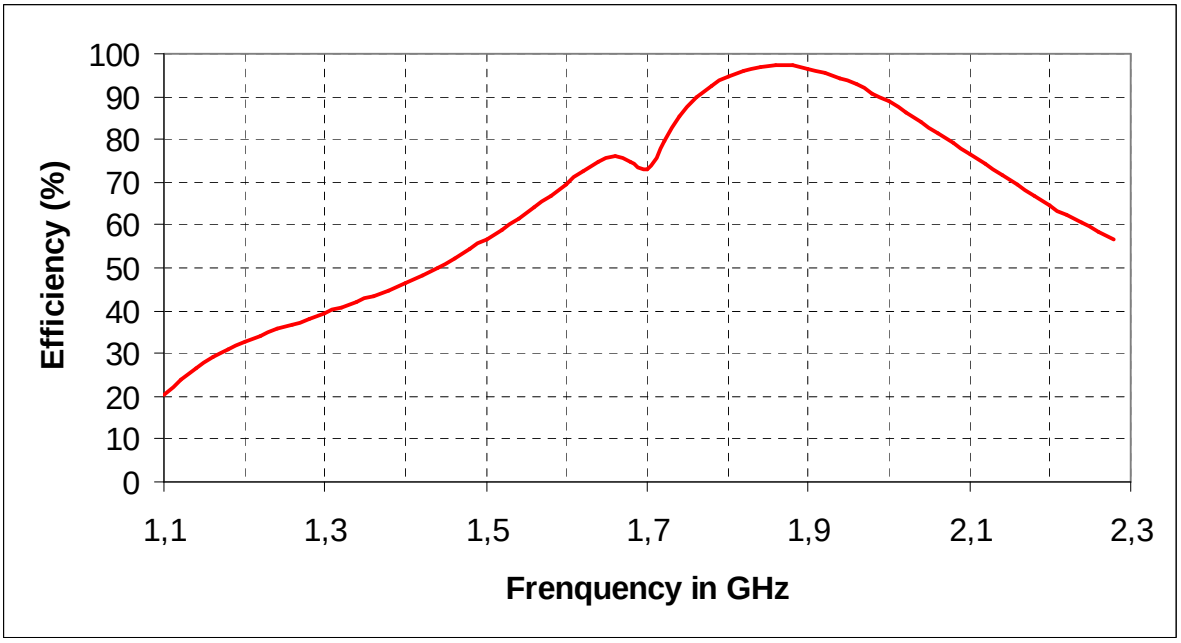

Figure 8 : Efficiency in UMTS band.

5. Discussion

- *VSWR measurements show dual-band large band behaviour*
- *Radiated measured patterns show quasi-omnidirectionnal radiating properties*
- *For special points in the lower band, efficiency seems to be very low*

6. Additional comments

3- SIMULATION RESULTS

From CNRSLEAT_LEATantenna_FPTLM

1. Entity

Laboratoire d'Electronique, Antennes et Télécommunications (LEAT)
CNRS UMR 6071
250 rue Albert Einstein, Bât. 4, 06560 Valbonne, France

Contact persons:
Jean-Lou Dubard
Phone: +33 (0)4 92 94 28 07
Fax: +33 (0)4 92 94 28 12
Email : jean-lou.dubard@unice.fr

2. Name of the simulation tool

FP-TLM

3. Generalities about the simulation tool

The Transmission Line Matrix (TLM) method is a finite-difference-time-domain technique. Although it is very similar to the FDTD method, it allows computing the six electromagnetic field components at the same location. As TLM simulation is performed in time domain, analysis in a wide frequency band is obtained with only one run by using a Fourier Transform. In FP-TLM code, the FFT operation is replaced by a Prony-Pisarenko method which performs accurate spectral analysis even with short time response. FP-TLM includes PML layers for modelling free space and is implemented on parallel computers.

4. Simulation Set-up (Geometry set-up, GUI, mesh, boundary conditions, excitation)

Since no GUI is available, the input of the geometrical structure into FP-TLM software was done manually. Also, a variable hexaedric meshing was manually performed. Perfectly matched layers (PMLs) were used to simulate free space surronding the antenna. For excitation, a lumped matched generator (occupying one cell between the ground plane and the probe connected to the radiated element) with a gaussian pulse was used. About fifteen hours were needed to draw the geometry and to set up the rest of the simulation.

5. Simulation results

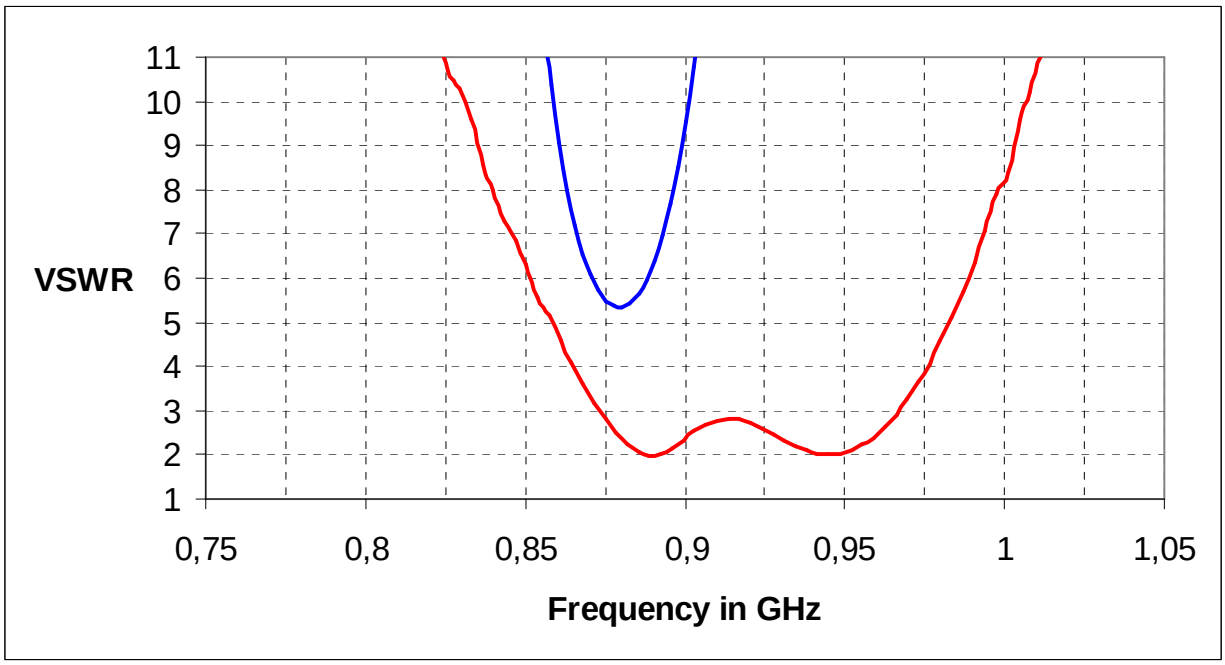

Figure 1 : VSWR in the lower band

TLM simulation

Measured results

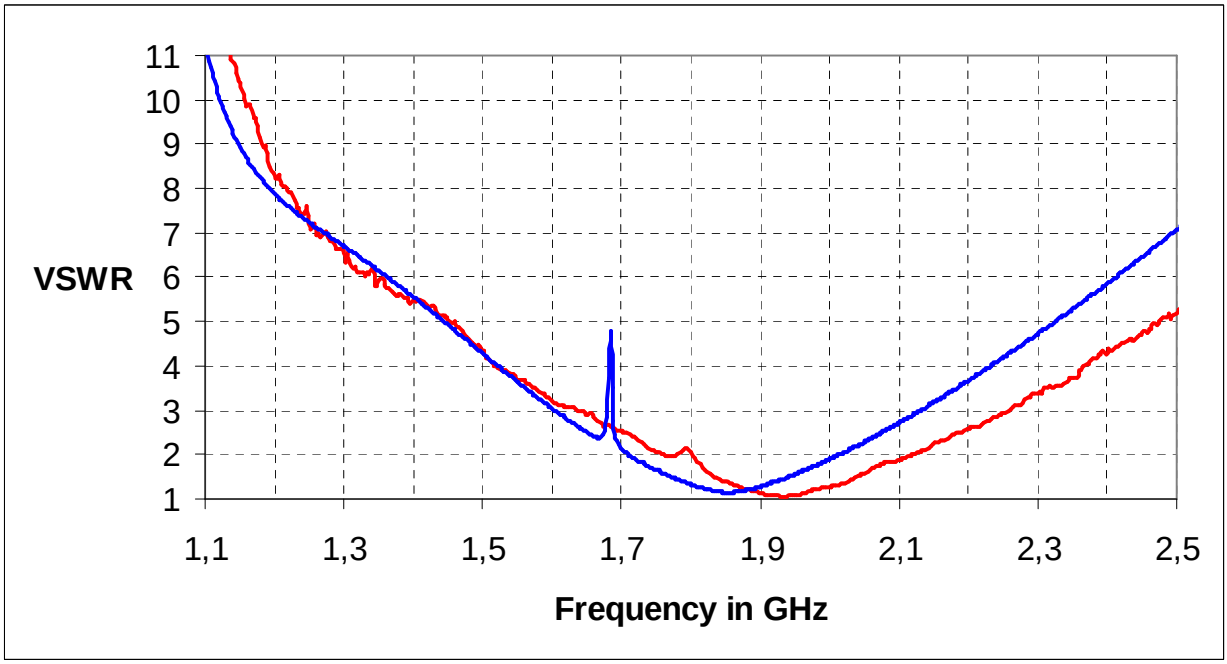

Figure 2 : VSWR of the upper band.

TLM simulation

Measured results

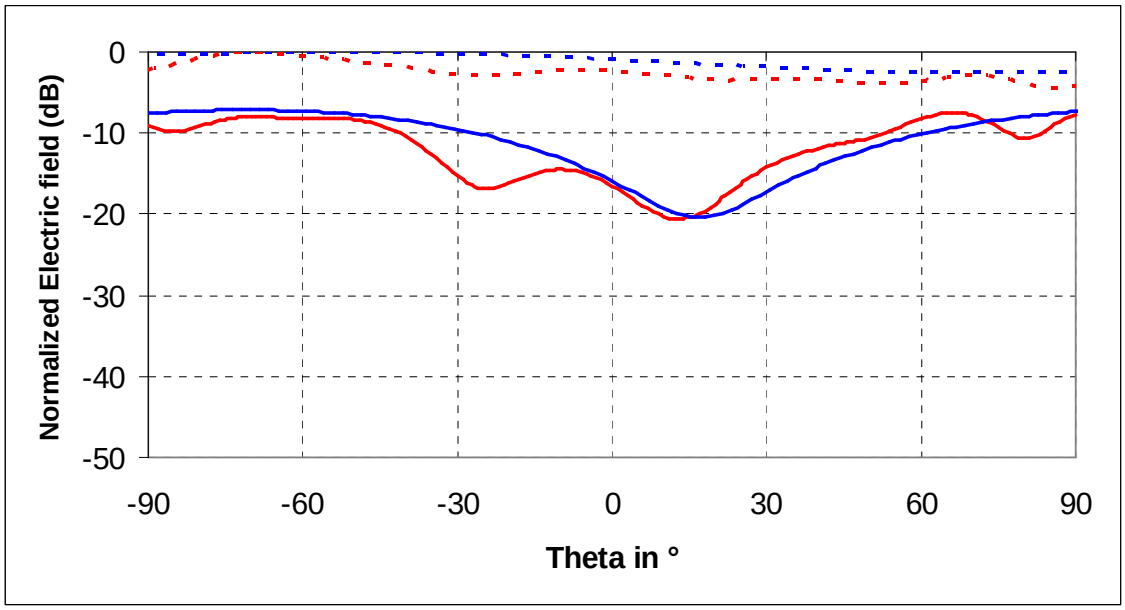

Figure 3 : E-plane radiation pattern versus theta in the lower band (f=0.96 GHz).

TLM simulation

Measured results

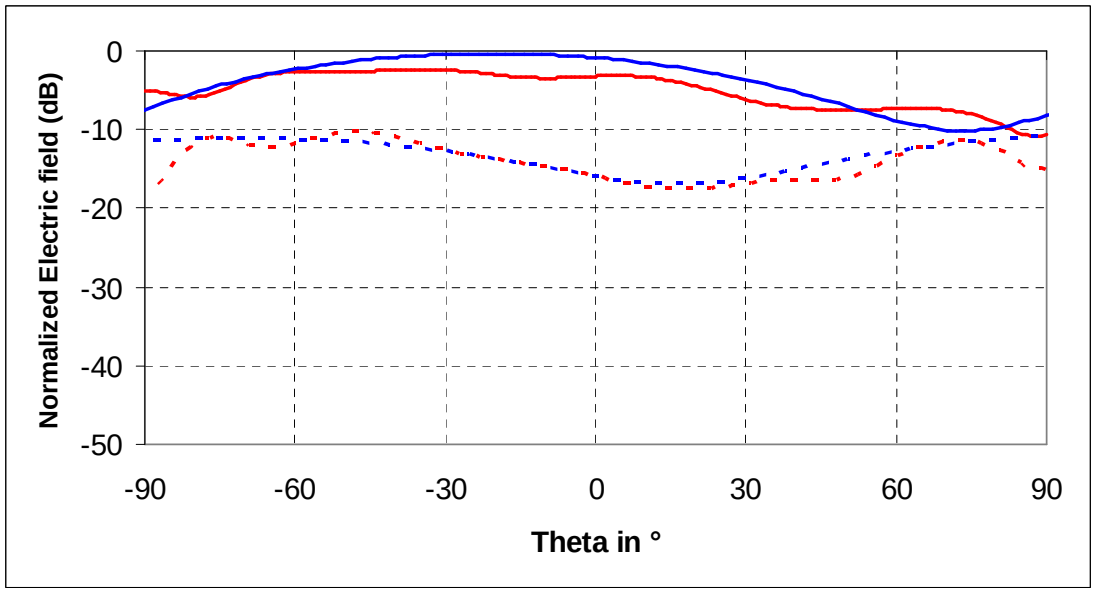

Figure 4 : H- plane radiation pattern versus theta in the lower band (f=0.96 GHz).

TLM simulation

Measured results

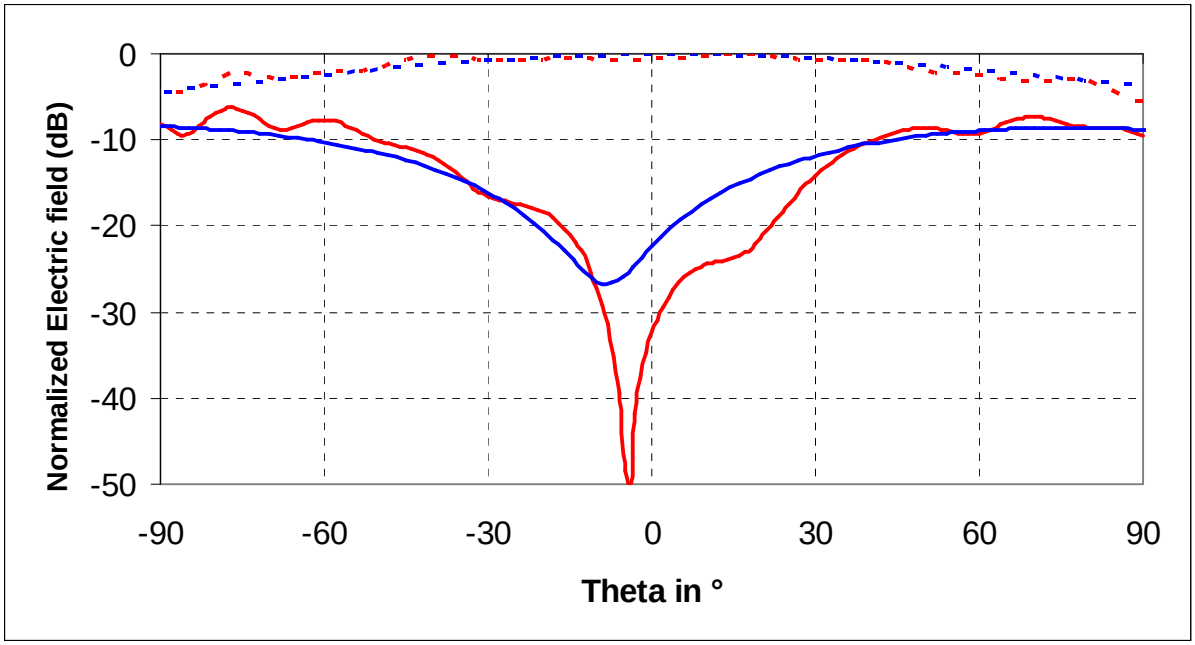

Figure 5 : E-plane radiation pattern versus theta in the upper band (f=1.71 GHz)

TLM simulation

Measured results

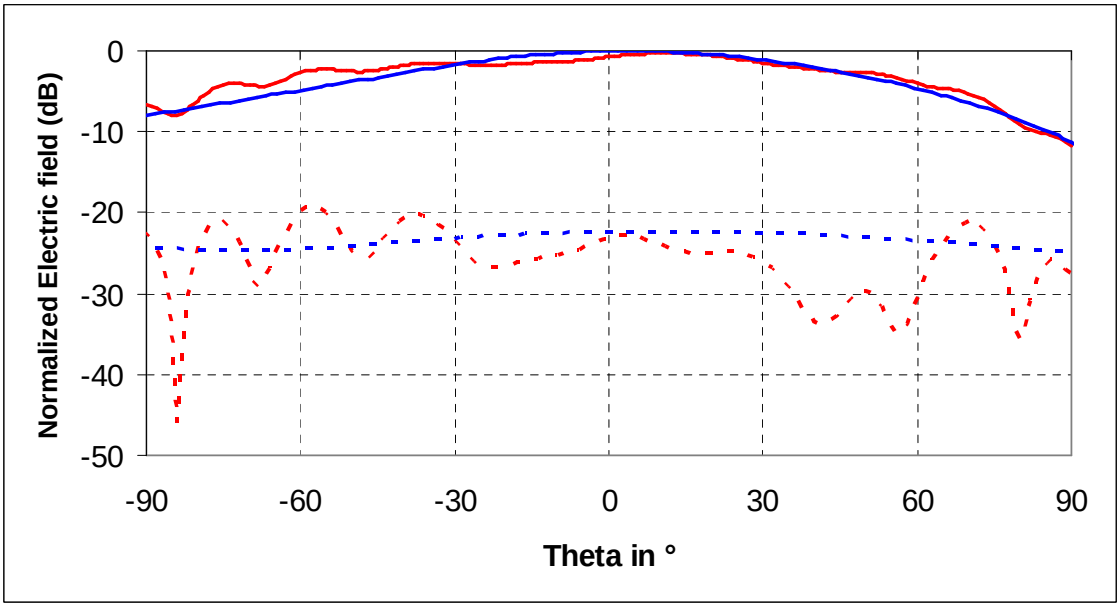

Figure 6 : H-plane radiation pattern versus theta in the upper band (f=1.71 GHz)

Note : for each plane (E, H) the far field is normalized with the maximum value of the considered cut plane.

TLM simulation

Measured results

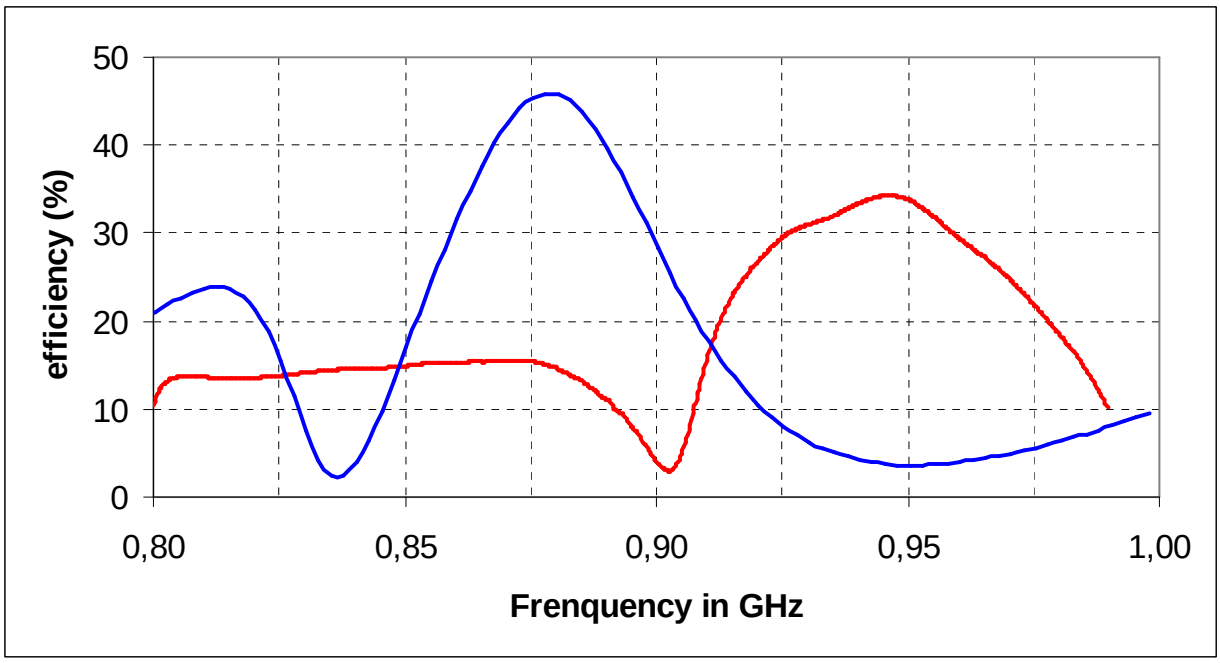

Figure 7 : Efficiency in GSM band

TLM simulation

Measured results

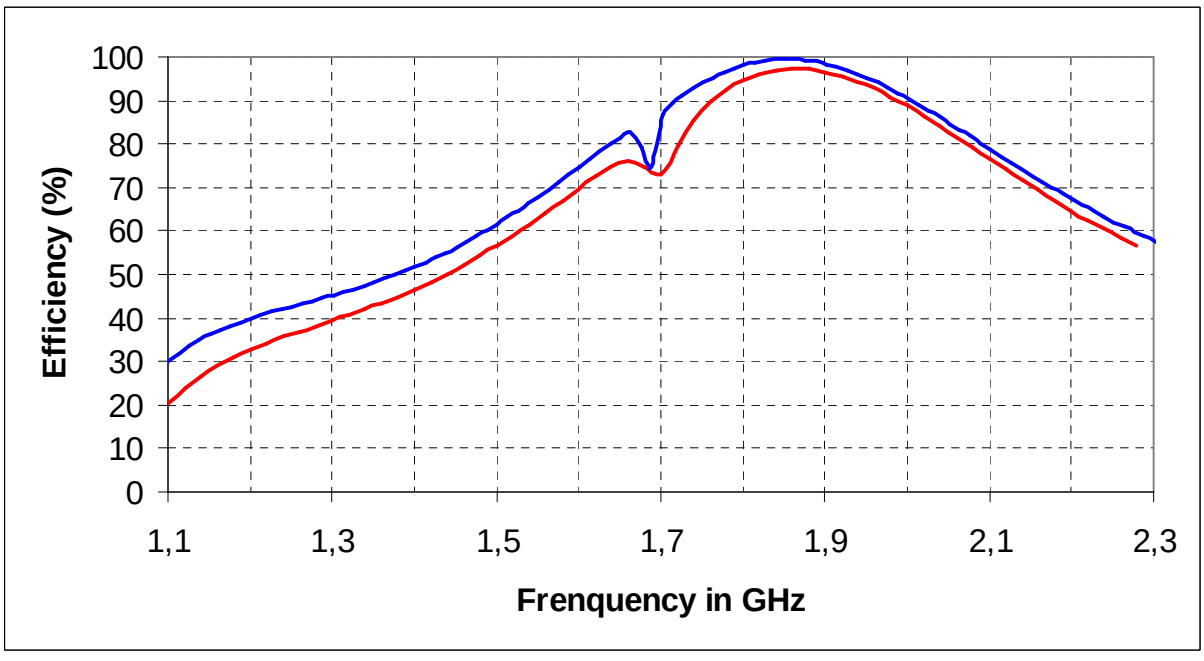

Figure 8 : Efficiency in UMTS band

TLM simulation

Measured results

6. Computation resources

- ***Type of machine (PC, Workstation, …),***
  Parallel computer SGI ORIGIN 2000
- ***Number of processors,***
  12 processors (768 available)
- ***Maximum available memory,***
  500Mbytes/processor
- ***Memory used for simulation,***
  275Mbytes/processor
- ***CPU speed, ….***
  500MHz/processor
- ***computation time***
  CPU time/proc=6720s

7. Discussion

There are no difficulties to set up the simulation and to obtain results. However, the drawing of this structure is not easy and is time consuming (no GUI).

Usually, a size step lower than $\lambda_{min}/20$ and at least 3 size steps for modelling the finest details are required in TLM simulations to obtain reliable results. For this antenna, 3 cells were used to model the slots and the thickness of the metallic parts with conductivity equal to 3.19e6 S/m. Then, the entire computational domain was modelled with a total number of cells = 70x56x106.

We observe a good agreement between simulated and measured data except for the VSWR results in GSM Band. For the efficiency, a shift in frequency between the simulated and the measured data can be observed in GSM band.

A first simulation with zero thickness perfect conductors was performed. To allow appropriate computation of efficiency, I have refined the mesh by using 3 cells to model the thickness of the metallic parts. This did not improve the results for the VSWR in GSM Band.

8. Additional comments

No

3- SIMULATION RESULTS

From IDS_LEATantenna_ADF

1. Entity

IDS - Ingegneria Dei Sistemi S.p.A.
Via Livornese, 1019
56010 Pisa
Italy
Web-site: www.ids-spa.it

Contact person
Massimiliano Marrone
E-mail: m.marrone@ids-spa.it
Phone: +39.050.3124.264
Fax: +39.050.3124.201

2. Name of the simulation tool

ADF (Antenna Design Framework)

3. Generalities about the simulation tool

ADF is a framework which contains many tools for antenna analysis, placement and design. For the present simulation we have utilized a full-wave MOM solver (MPIE formulation, RWG basis functions).

4. Simulation Set-up (Geometry set-up, GUI, mesh, boundary conditions, excitation)

The set up of the geometry is performed by a CAD tool (Bentley Microstation) available inside ADF.

The mesh is a triangular one, and it is created automatically by a proprietary 2D mesher tool, available in ADF. The meshing is performed directly on the geometry drawn by the CAD tool, the average step-size of the mesh being decided by the user. The mesher allows also to perform a local refinement of the mesh in any location.

In the early simulations we utilized step-sizes of about λ/30, to calculate and visualize the structural currents, in order to see what are the zones that need a mesh refinement.
Then other simulations have been performed with a locally refined mesh (step-sizes up to λ/100) close to the thin slots and the feeding pin.

The pin is excited at the entrance using a current generator.

The analysis is performed in the frequency domain, one simulation per frequency. In particular the main analysis, called "internal model calculation", and involving the calculation of the modal currents, is performed at each frequency of the specified range. The far field pattern and the VSWR are calculated, after that the internal model calculation has been performed, at some or all the frequencies within the specified range.
The frequency range for the lower case is [0.75-1.05] GHz with a frequency step of 0.01 GHz (31 frequency points).
The frequency range for the upper case is [1.11-2.51] GHz with a frequency step of 0.05 GHz (28 frequency points).

The meshes are conformal to the geometry shapes. The patches were assumed to be lossy (copper) and with a thickness of 0.3mm. The feeding pin was assumed to have 0.5 mm of radius.

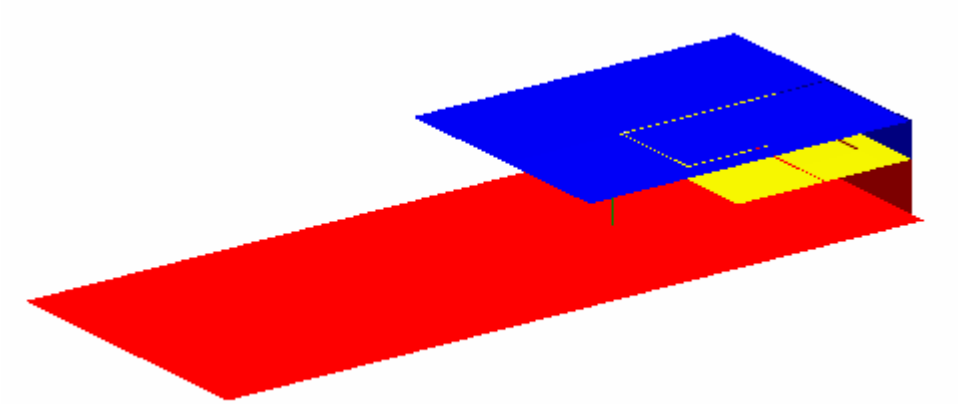

Figure 1 : Patch antenna 3D view.

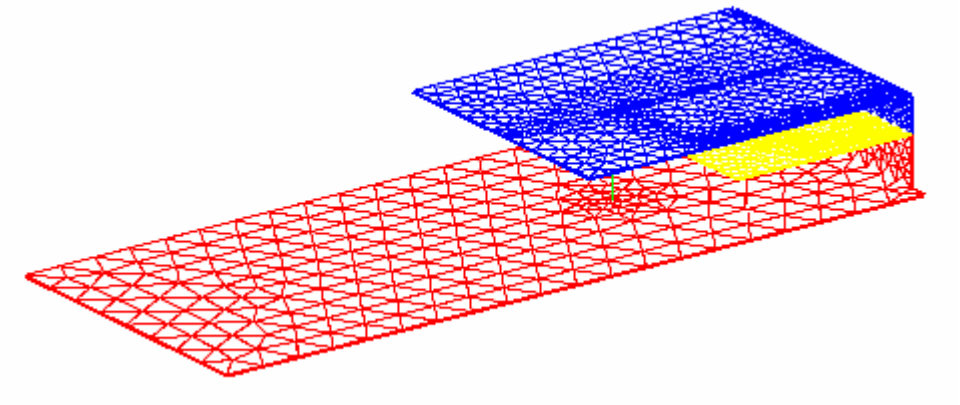

Figure 2 : Patch antenna mesh.

In order to redraw the geometry by the CAD it takes about 40 minutes. In order to set up the rest of the simulation it takes about 10 minutes.

5. Simulation results

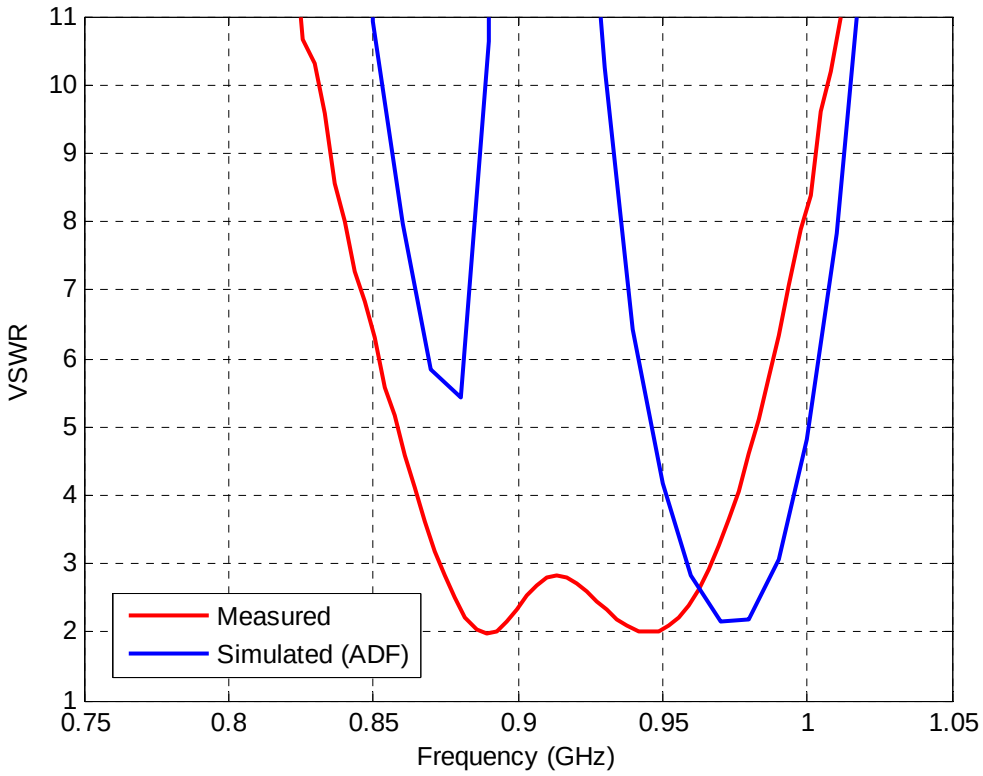

Figure 3 : VSWR versus frequency in the lower band

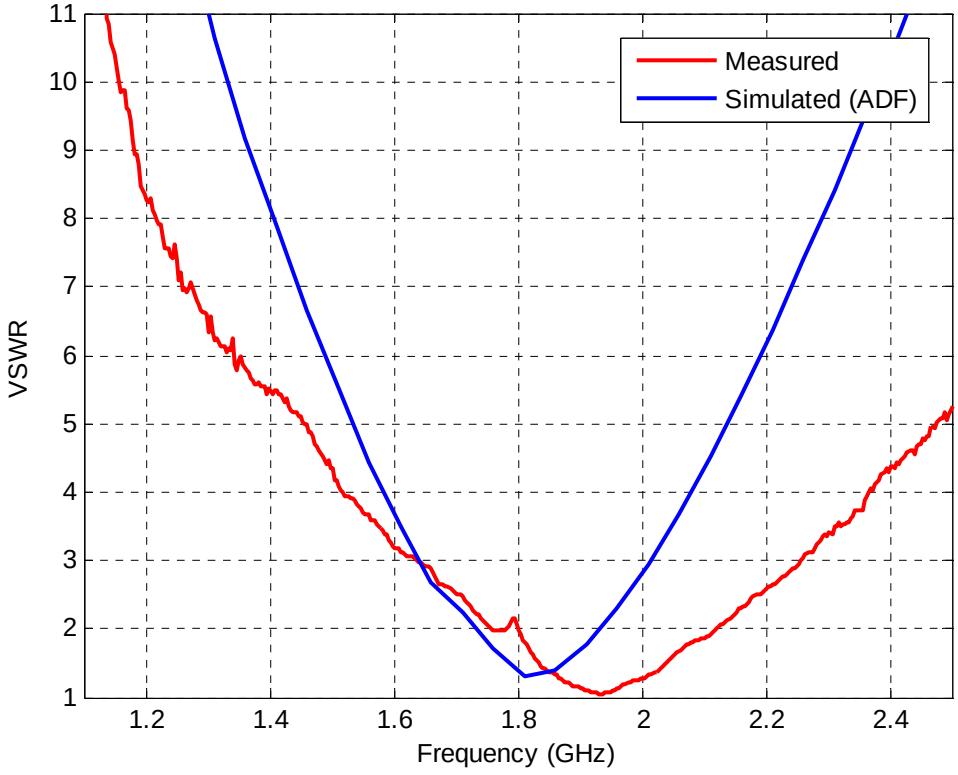

Figure 4 : VSWR versus frequency in the upper band

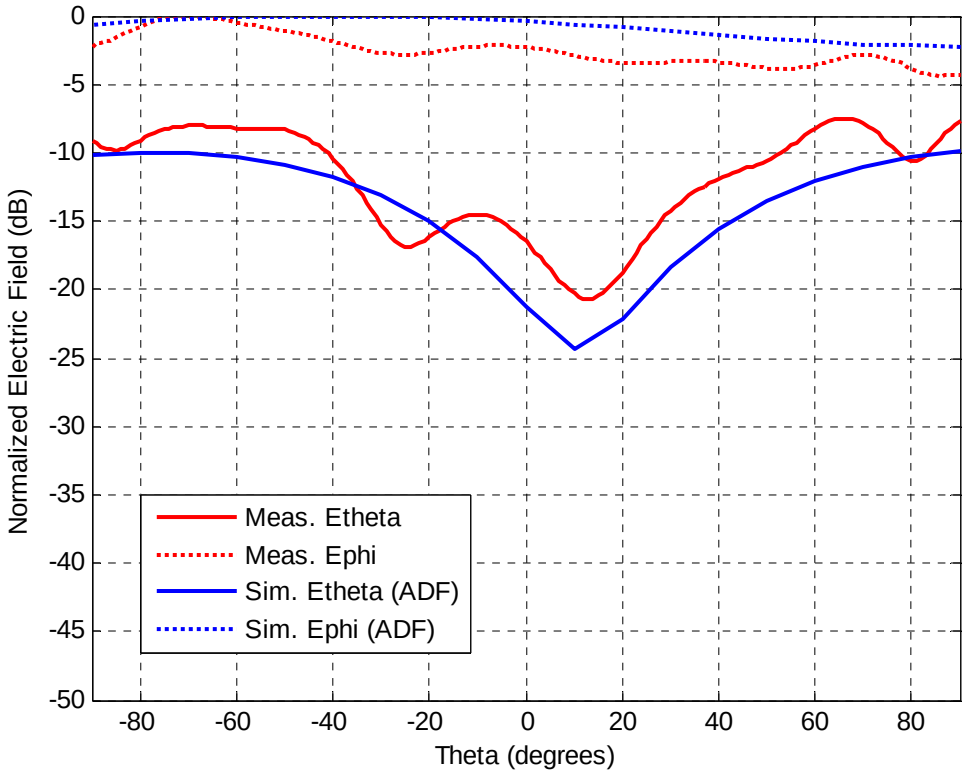

Figure 5: E-plane radiation pattern versus theta in the lower band (f=0.96 GHz)

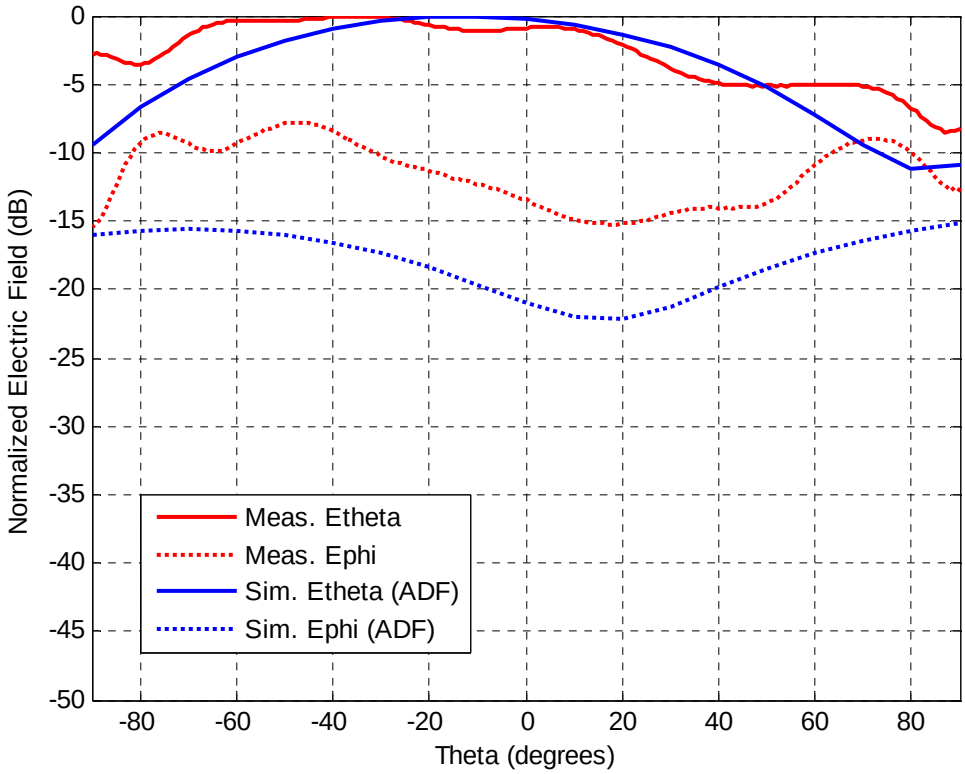

Figure 6 : H- plane radiation pattern versus theta in the lower band (f=0.96 GHz)

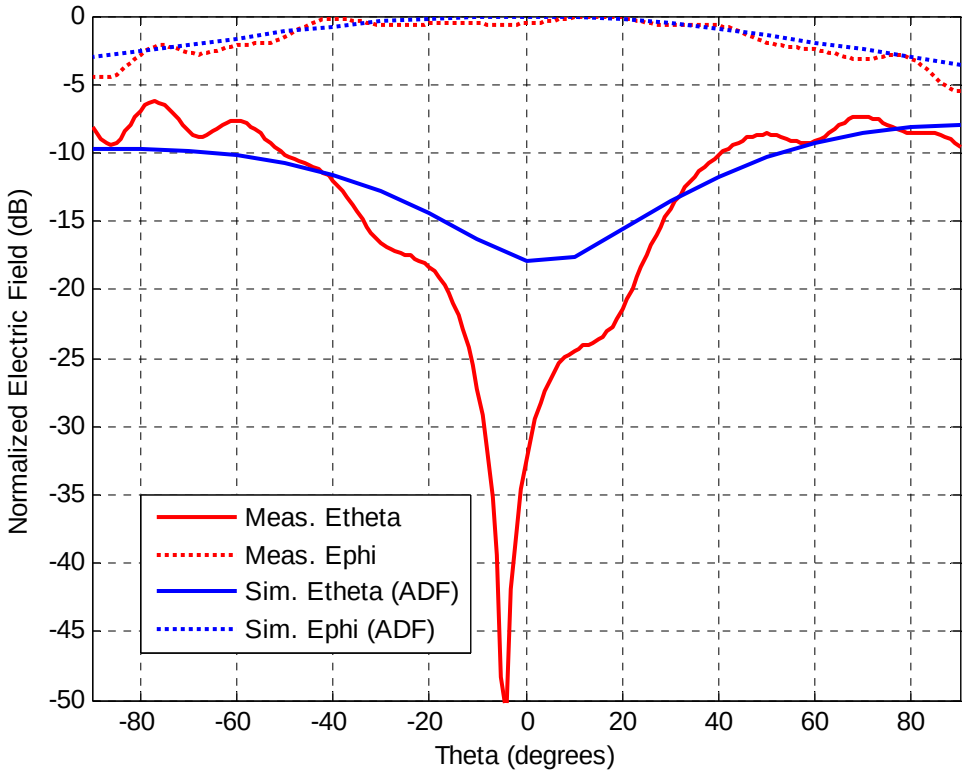

Figure 7 : E-plane radiation pattern versus theta in the upper band (f=1.71 GHz)

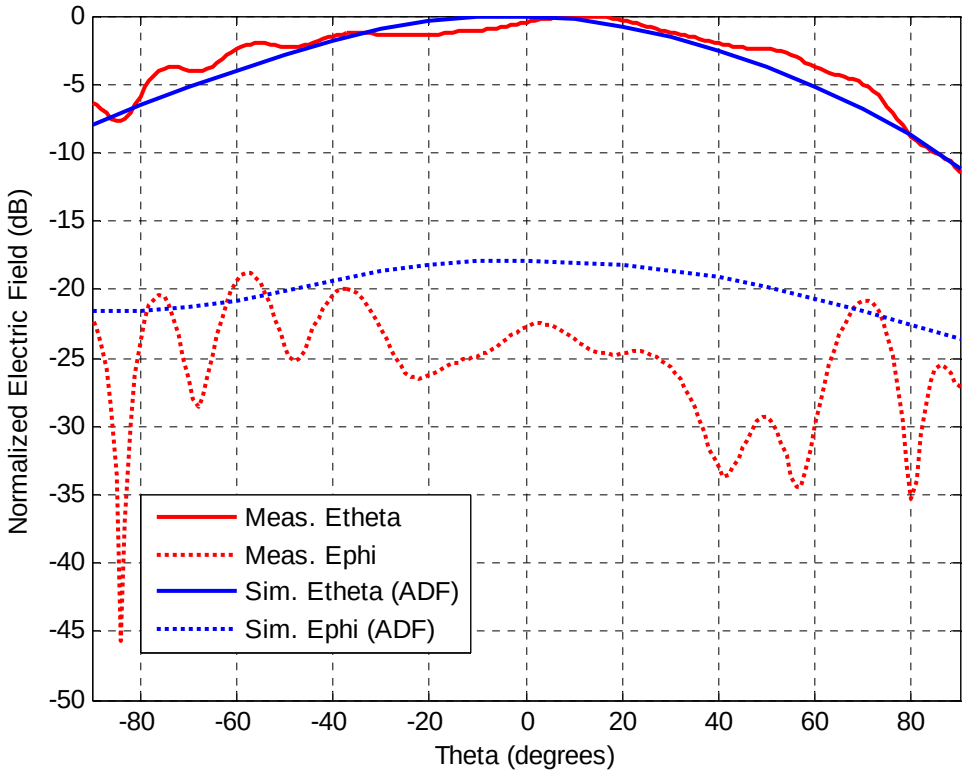

Figure 8 : H- plane radiation pattern versus theta in the upper band (f=1.71 GHz)

6. Computation resources

The simulations have been performed on a cluster of 4 PC (XEON processors running at 3.2 GHz and 4 GBytes of available memory,…). The operating system was Windows Server 2003.

	Lower band	Upper band
Number of unknowns	12570	12570
CPU time x frequency point	~ 1 h	~ 1 h
Max required RAM	~ 1 GB	~ 1 GB

7. Discussion

The geometrical structure of the patch antenna is quite easy to set up since, in the CAD environment, there are a lot of tools available to help the user in the geometry input process.
Moreover the integration of a proprietary meshing tool in the CAD environment speeds up considerably the meshing process up, and the availability of many tools for managing the mesh allows the user to refine it locally and to improve either manually or semi-automatically the quality of the mesh.
The computations were performed first using a coarse mesh and then a fine mesh. The results obtained with the fine mesh were closer to the measured ones, showing a convergence behaviour. Despite this, the lower band VSWR results are quite different from the measurements.

8. Additional comments

3- SIMULATION RESULTS

From IETR_LEATantenna_IMELSI

1. Entity

Institut d'Electronique et Télécommunications de Rennes (IETR)
CNRS UMR 6164
Université de Rennes 1, Campus de Beaulieu, Bât 11 D
263, av. du Général Leclerc
35042 Rennes Cedex, France

Contact persons :
Sylvain Collardey
Phone : +33(0)2 23 23 56 69
Fax : +33(0)2 23 23 69 63
Email : sylvain.collardey@univ-rennes1.fr

2. Name of the simulation tool

IMELSI IMpulsionnal ELectromagnetic SImulator (FDTD)

3. Generalities about the simulation tool

IMELSI employs the finite difference in time domain method in order to generate an electromagnetic field solution. The FDTD method divides the full problem space into thousands of smaller cubic regions.

4. Simulation Set-up (Geometry set-up, GUI, mesh, boundary conditions, excitation)

- I have drawn the structure using the GUI available with your tool
- The mesh is manual and fixed for each simulation
- Give the mesh type: uniform cubic mesh.

Perfectly matched layers (PMLs) are available and are used to simulate open problems that allow waves to radiate infinitely far into space, such as antenna designs.
For the metallic part, I have used perfect metallic material without metallic losses.
For excitation, a lumped port (localised voltage source) associated to a metallic via is used.

xOz plane

It takes about **one hour to draw the geometry** and about **5 min to set up the rest of the simulation**.

5. Simulation results

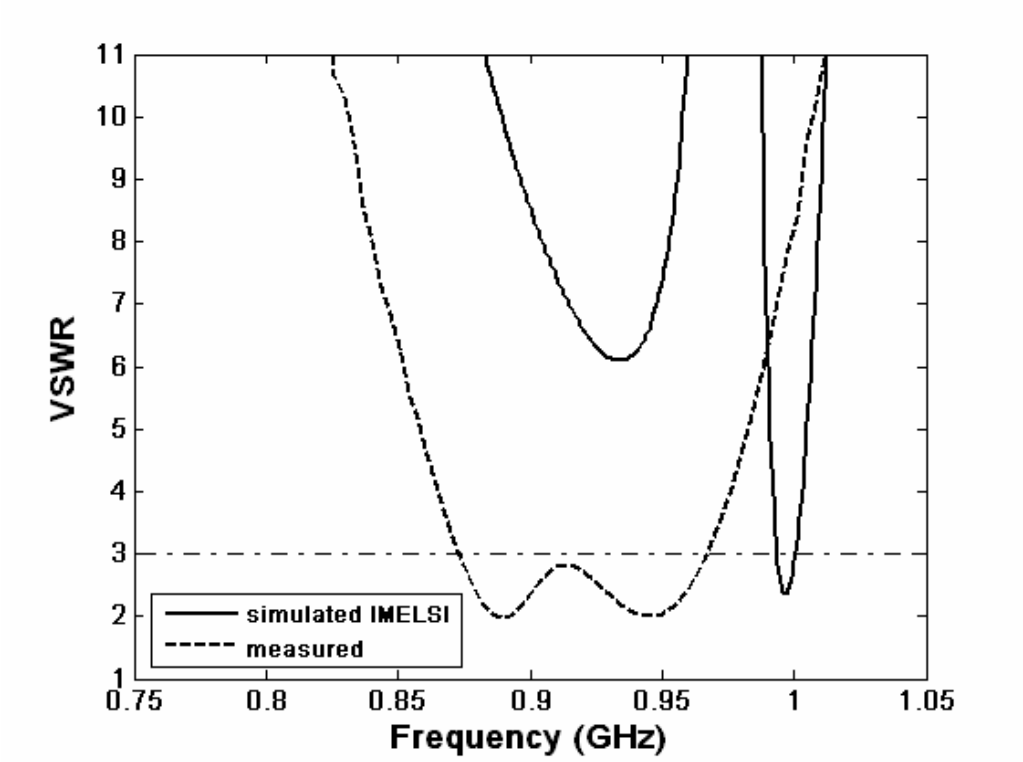

Figure 1 : VSWR versus frequency in the lower band

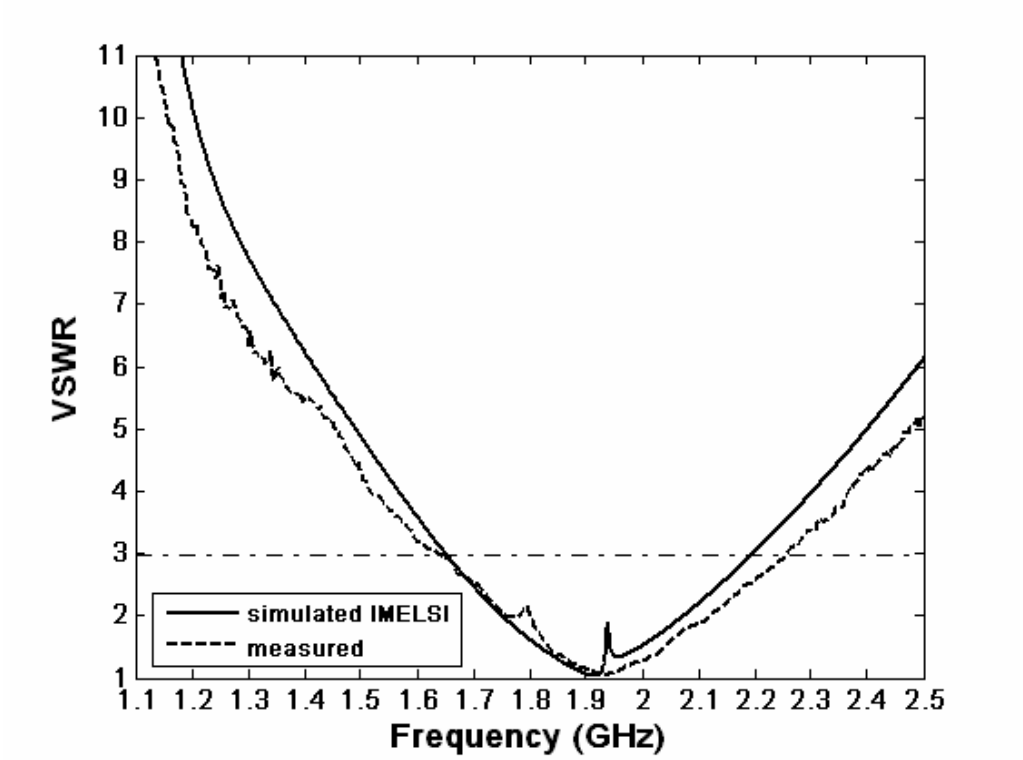

Figure 2 : VSWR versus frequency for in the upper band

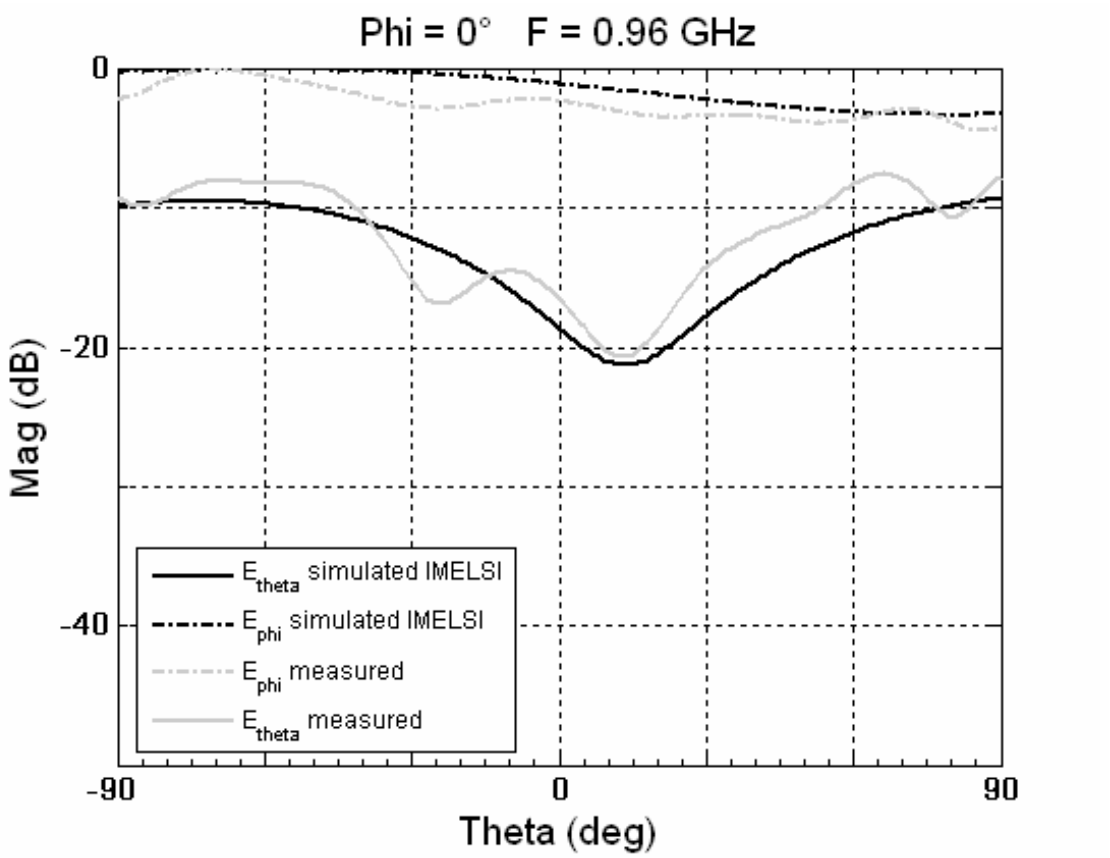

Figure 3 : E-plane radiation pattern versus theta in the lower band (f=0.96 GHz)

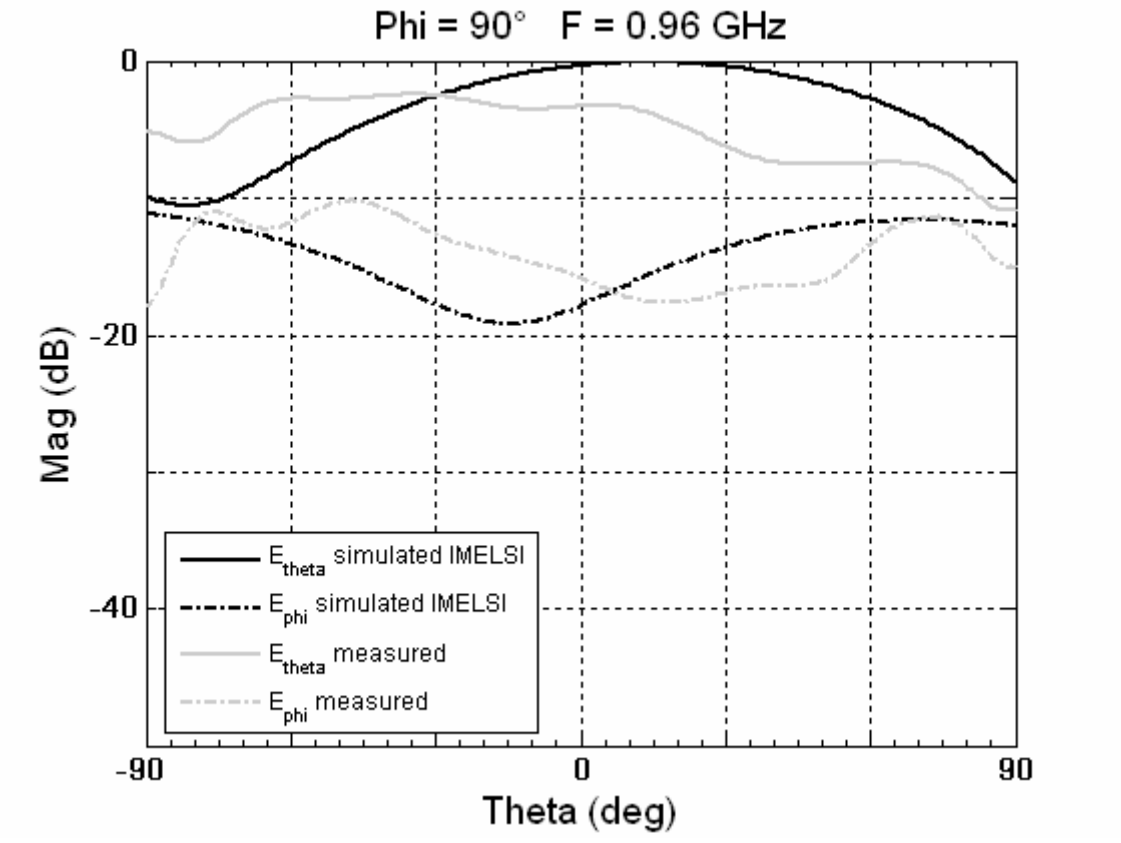

Figure 4 : H- plane radiation pattern versus theta in the lower band (f=0.96 GHz)

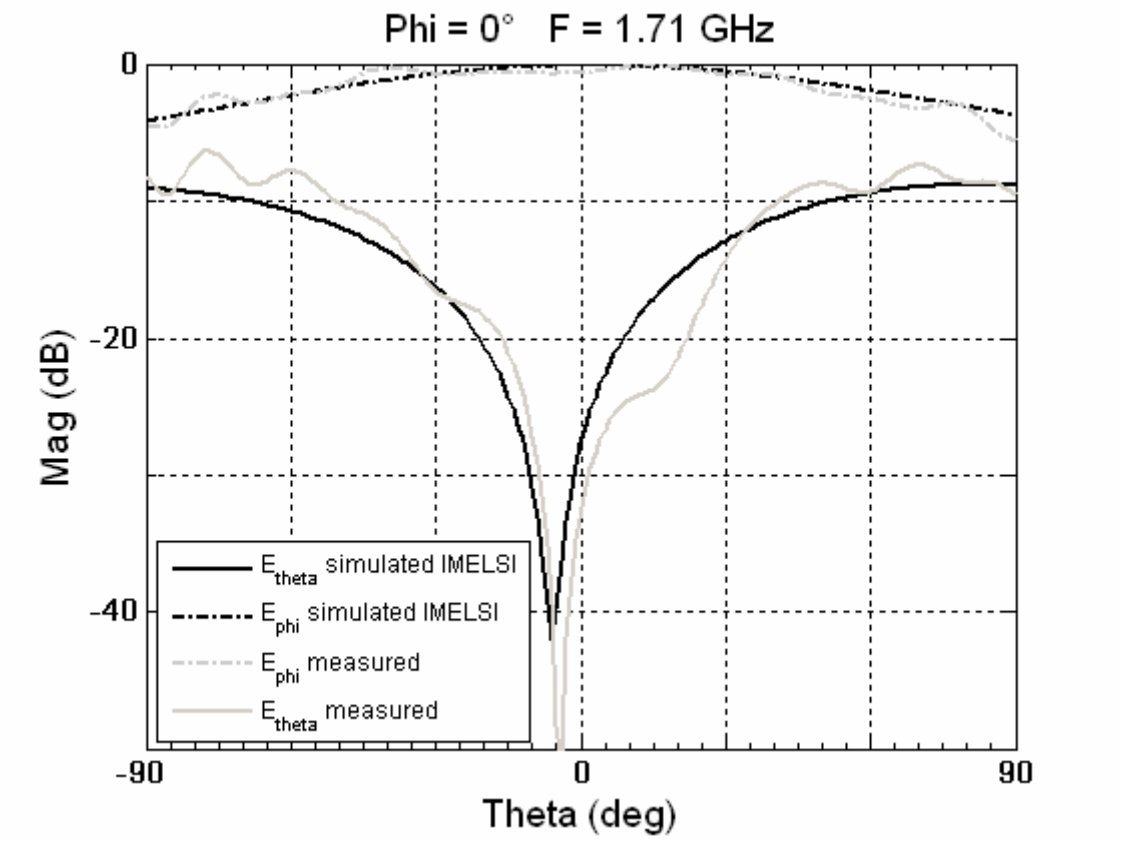

Figure 5 : E-plane radiation pattern versus theta in the upper band (f=1.71 GHz)

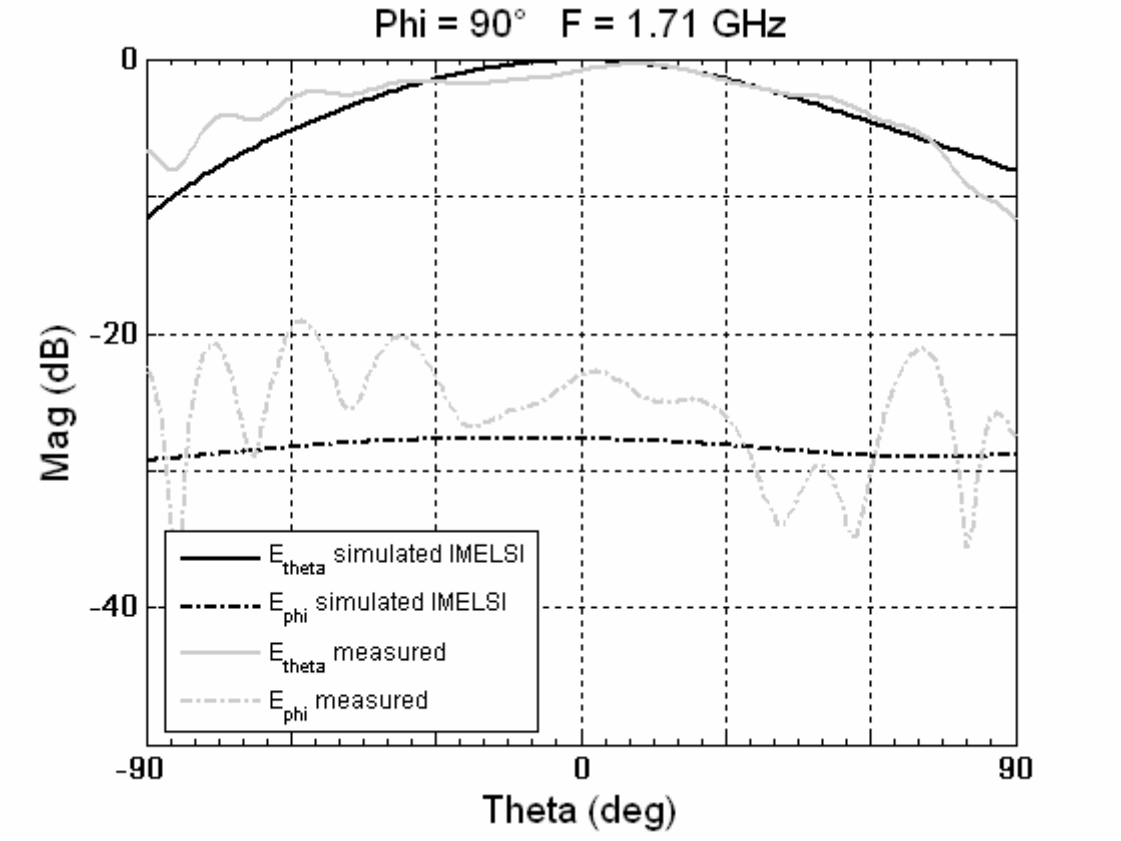

Figure 6 : H- plane radiation pattern versus theta in the upper band (f=1.71 GHz)

6. Computation resources

- ***Type of machine (PC, Workstation, …),***
  PC
- ***Number of processors,***
  1 CPU
- ***Maximum available memory,***
  2Go
- ***Memory used for simulation,***
  1.8Go
- ***CPU speed, ….***
  3GHz

Computation time and required memory for each simulation :
about 120hours

7. Discussion

- ***Easiness/difficulty to set up the simulation and output results:***
  There are no difficulties to set up the simulation and to obtain results.

- ***Computation requirements for simulation:***
  For this kind of antenna with two slots, we must mesh with an important accuracy to obtain good results, the requirement in available memory is very important.

- ***Level of agreement between your results and the reference data:***
  We observe a good agreement between simulation and measurements in the upper band. For the lower band, the results are slightly different, so the simulation requires more accurate mesh and more available memory.

I have refined the mesh up to the maximum capabilities of the PC computer. More mesh is fine, more the results are good. I have only used one cell to define the slot width. But, the FDTD code is also based on a parallelism approach to study the huge problems which need a lot of memory.

8. Additional comments

3- SIMULATION RESULTS

From UOB_LEATantenna_FDTD32

1. Entity

Computational Electromagnetics Group, Centre for Communications Research,
Department of Electrical & Electronic Engineering, Merchant Venturers Building,
Woodland Road, University of Bristol (UOB), Bristol BS8 1UB, United Kingdom

Dominique Lynda Paul
Tel. +44 117 331 51 60
email: d.l.paul@bristol.ac.uk

2. Name of the simulation tool

FDTD32

3. Generalities about the simulation tool

FDTD32 is an in-house 3D full-wave solver based on the Finite-Difference Time-Domain (FDTD) method. In this simulation, perfect metal conductors and lossless dielectric substrates were considered. The ground plane was modelled as finite. All metal parts were assumed of 0.3mm thickness.

4. Simulation Set-up (Geometry set-up, GUI, mesh, boundary conditions, excitation)

The geometry was specified using our GUI Gema as displayed in Figures 1 and 2 and a graded mesh was created manually with finer cells around edges. One FDTD cell only was used across the slots in metal. An 8-cells PML layer was employed to terminate the FDTD box and simulate an open structure. A raised cosine waveform of width 200ps was applied to the coaxial feedline.

The size of the computational volume was 104x90x75 cells for the graded mesh. A transient response of 70ns was required to allow the fields to decay in the antenna.

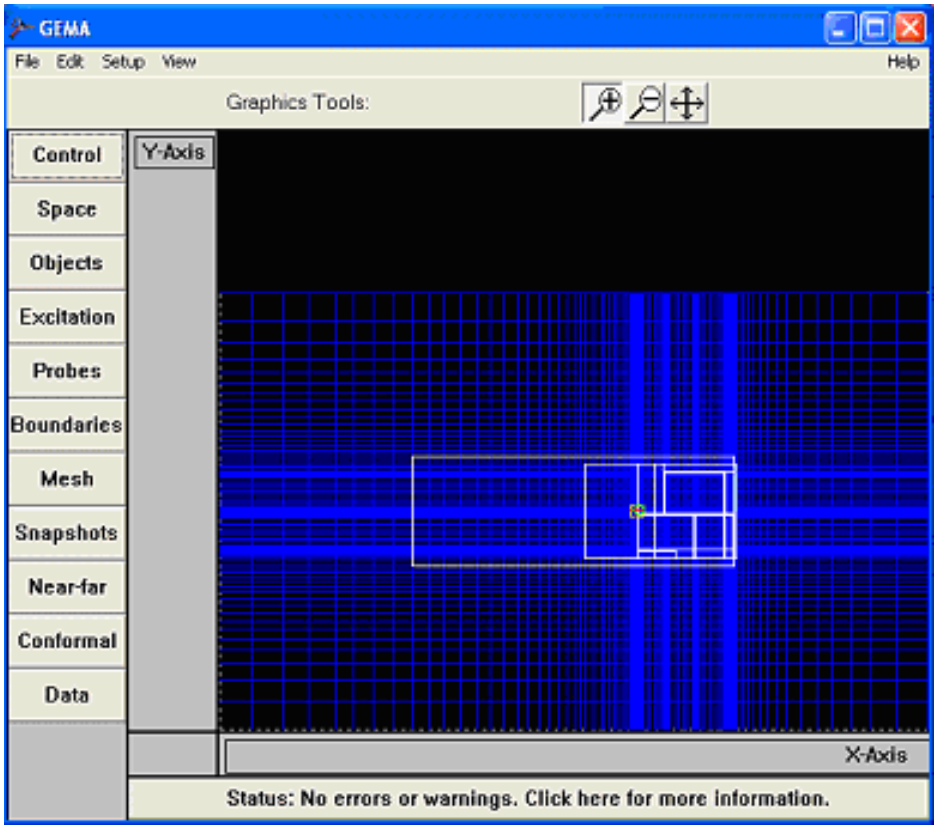

Figure 1: Top view of miniature antenna model in Gema GUI

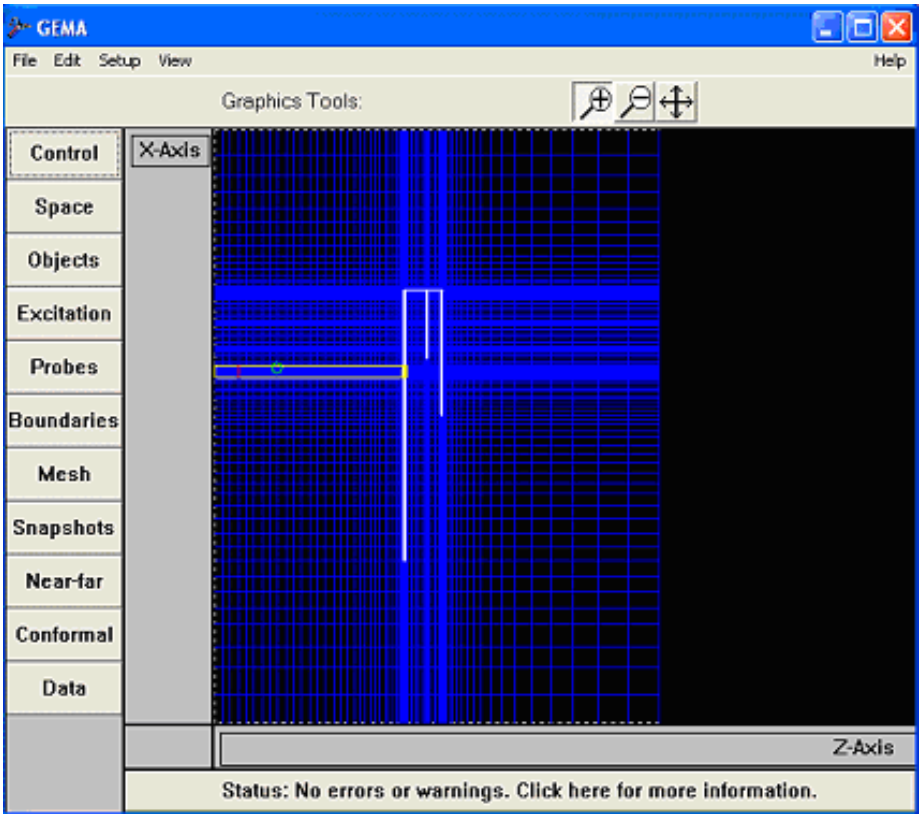

Figure 2: Elevation view of miniature antenna model in Gema GUI

5. Simulated and measured results

- **VSWR results.**

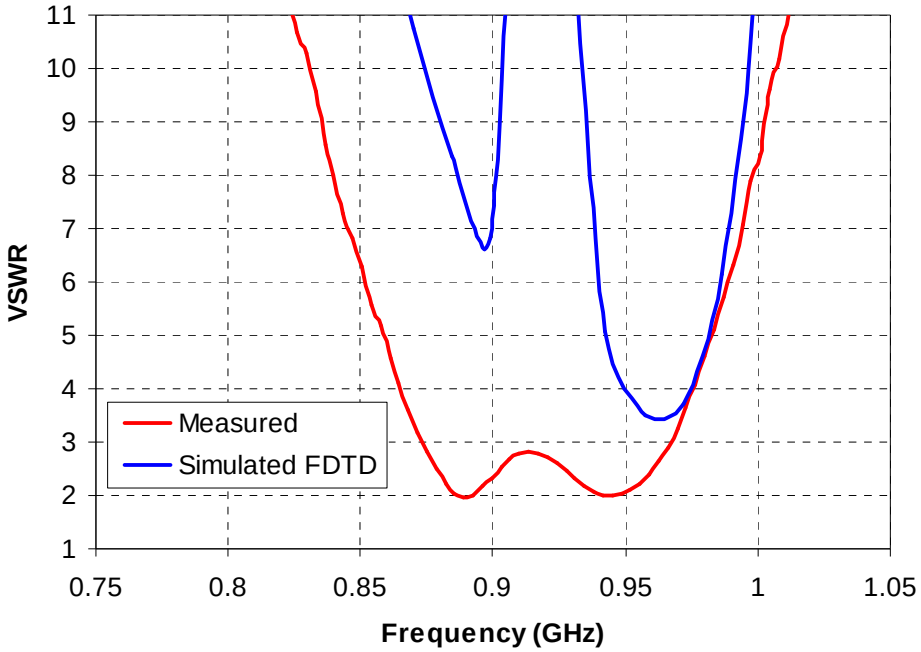

Figure 3: VSWR versus frequency for the miniature antenna in the lower band

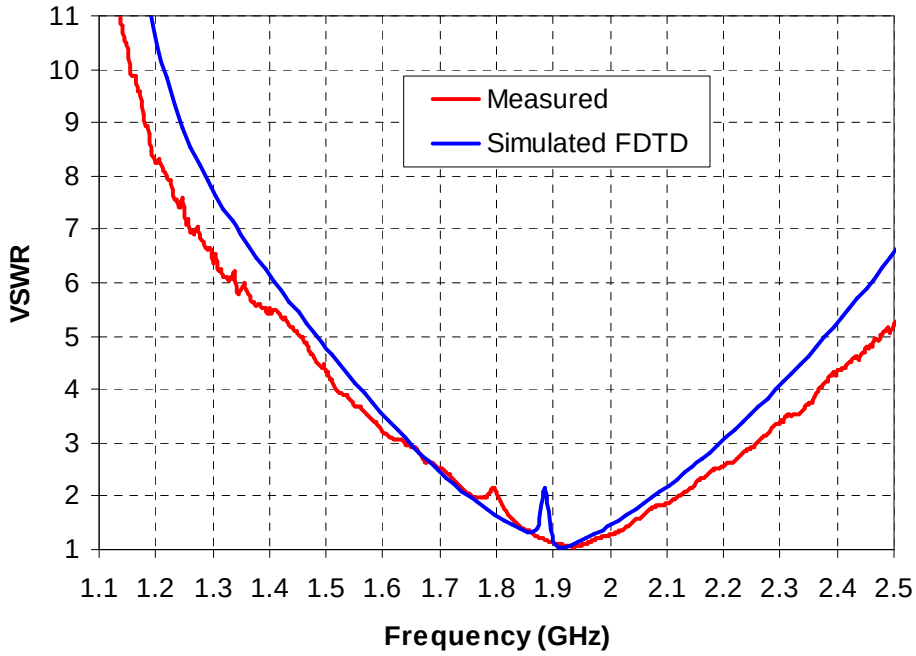

Figure 4: VSWR versus frequency for the miniature antenna in the upper band

- **Far-field radiation patterns.**

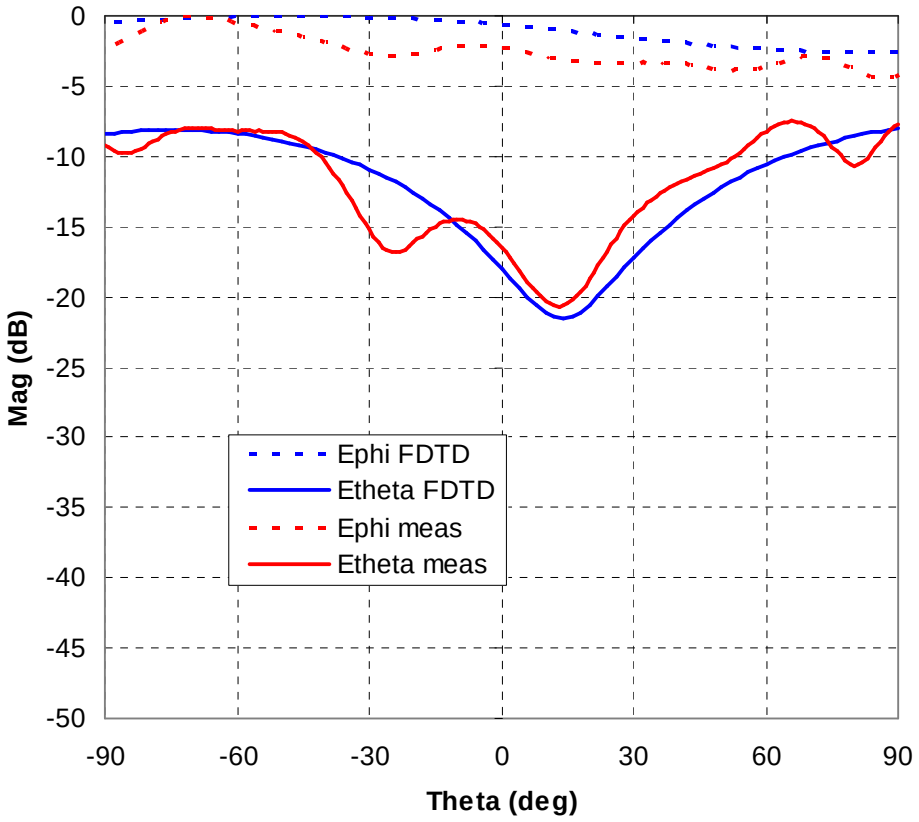

Figure 5: E-plane radiation pattern versus theta for the miniature antenna in the lower band (F=0.96GHz)

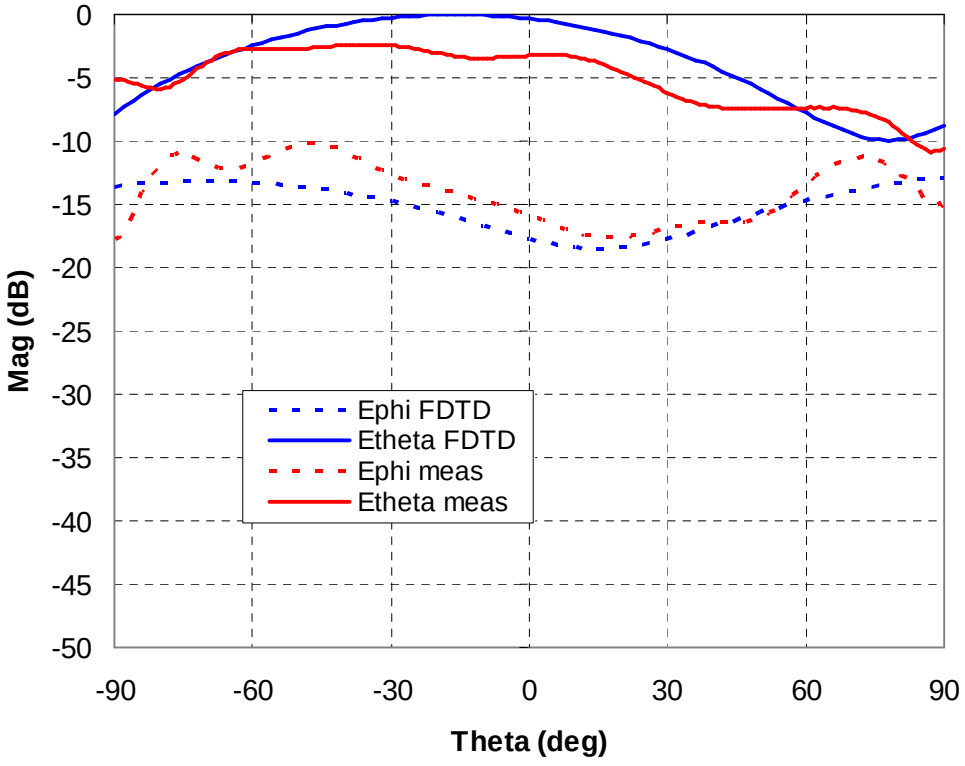

Figure 6: H-plane radiation pattern versus theta for the miniature antenna in the lower band (F=0.96GHz)

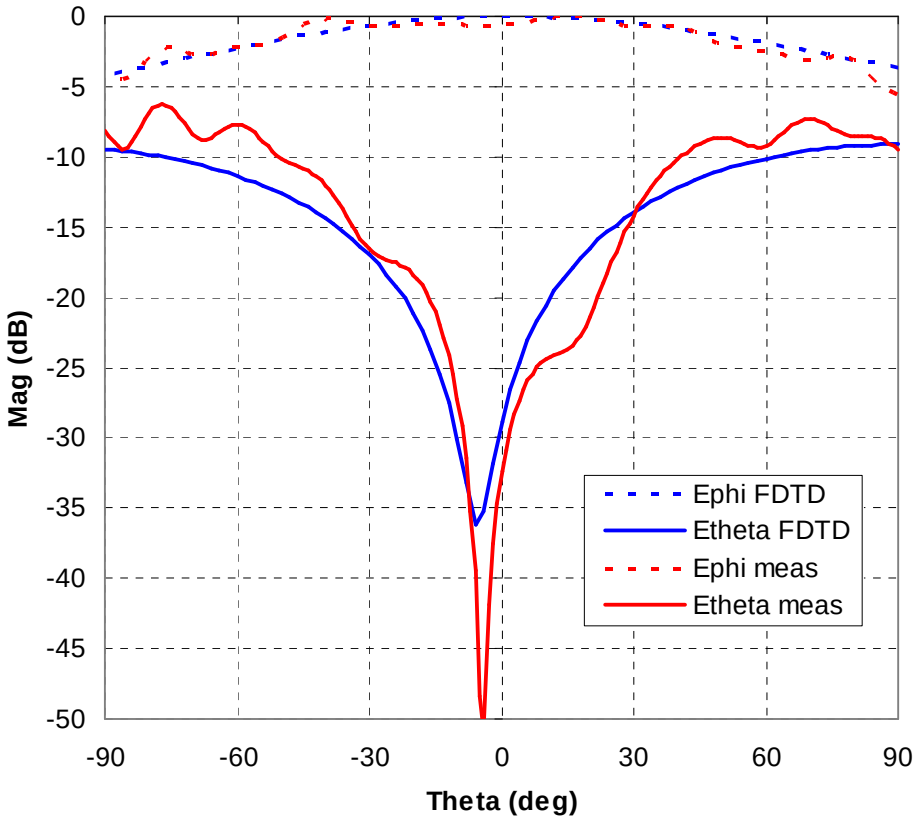

Figure 7: E-plane radiation pattern versus theta for the miniature antenna in the upper band (F=1.71GHz)

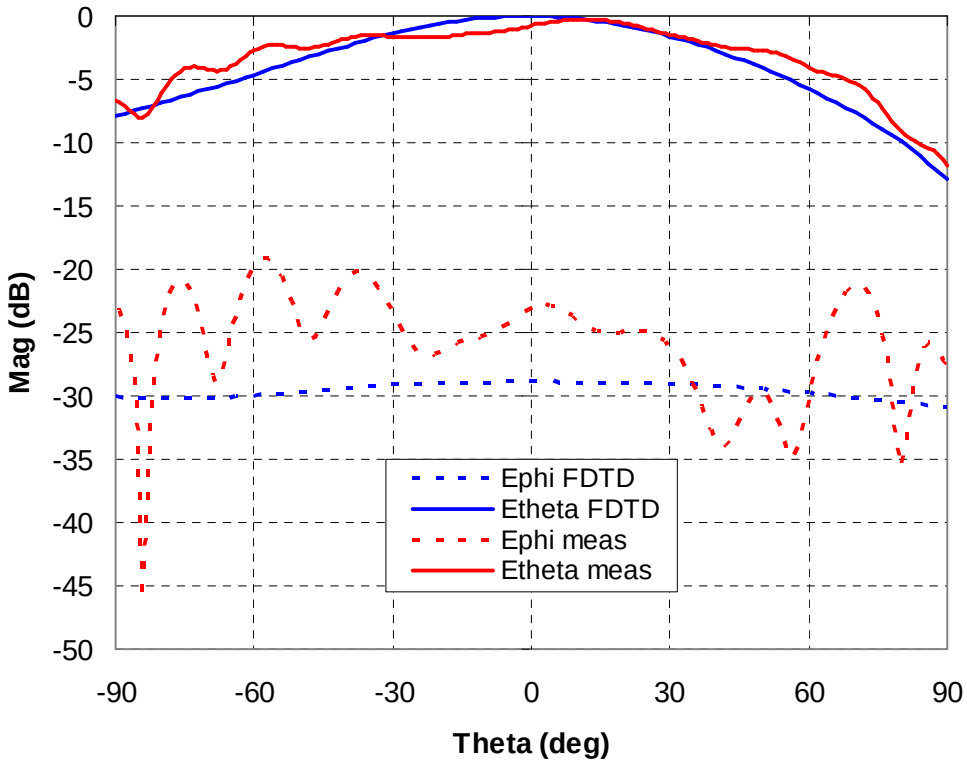

Figure 8: H-plane radiation pattern versus theta for the miniature antenna in the upper band (F=1.71GHz)

6. Computation resources

The simulation was performed on a Viglen PC (3.2GHz, 2 GBytes RAM available).

The simulation time was 11 hours with 219 Mbytes RAM to obtain VSWR and radiation patterns results.

7. Discussion

For this dual-band miniature antenna, the agreement between measured and simulated VSWR results is rather poor for the lower band (Figure 3) but very good for the upper band (Figure 4) which is surprising.

The radiation patterns in the principal planes however (Figures 5 to 8) are well predicted by FDTD32 in both bands although they appear slightly more regular than the measured ones. The levels are in good agreement both for the co- and the cross-polar components.

This type of antenna is not the best candidate for the FDTD technique as it features an electrically large structure with operation in a low frequency band and at the same time extremely fine details such as the thin slots of 0.3mm width, the finite thickness of the metal parts (0.3mm), the proximity of the coaxial feed with some of the resonant parts of the antenna and the proximity of one of the slots with the metal shorting plate. Also, the antenna has strong resonances. Therefore the transient response required is long hence demanding long computer simulation times. A more rigorous treatment of slots in the FDTD technique to take into account field singularities would probably be advantageous to improve on this result.

3- SIMULATION RESULTS

From UPV_LEATantenna_FEKO

1. Entity

Universidad Politécnica de Valencia
U.P.V.
I.T.E.A.M.
Edificio 8G
Camino de Vera S/N
Valencia 46022
Spain
Tel: 963879585

2. Name of the simulation tool

FEKO

3. Generalities about the simulation tool

FEKO is a method of moments (MoM) based, computer code for the analysis of electromagnetic problems such as: EMC, shielding, coupling, antenna design, antenna placement analysis, microstrip antennas and circuits, striplines, dielectric media, scattering analysis etc.

The MoM has been hybridised with the asymptotic high frequency techniques, physical optics (PO) and the uniform theory of diffraction (UTD). This true hybridisation reduces the computational resource requirements, enabling the analysis of very large problems.

FEKO uses a full wave formulation which enables accurate predictions of the coupling, near fields, far fields, radiation patterns, current distributions, impedances etc. Special Green's functions for planar multilayered media are used. The formulation, and the implementation thereof, enables the analysis of arbitrarily oriented metallic surfaces and wires. The metallic structures are allowed to cross multiple layers. Interpolation tables are used to speed up calculations. A surface integral formulation for multiple dielectric/magnetic volumes can also be used to model antennas with finite layers.

4. Simulation Set-up (Geometry set-up, GUI, mesh, boundary conditions, excitation)

Geometries in FEKO can either be defined using parametric geometry cards or by importing meshed CAD files. For this particular case, the structure was created using geometry cards with the interface EditFEKO. EditFEKO is a customised text editor for setting up and controlling the solution and output parameters. The resulting *.pre file is "compiled" by PreFEKO for analysis with FEKO.

The EditFEKO geometry cards allow to generate metallic plates and wires identified by a label. These labels are used to associate finite conductivity and thickness to the corresponding structures.

The meshing of the structure is done automatically by FEKO, while the mesh density can be changed by modifying some variables. To generate the mesh showed in the following figures, maximum triangle edge length of λ/30 and maximum wire segment length of λ/25 were used. The result was a mesh formed by 186 metallic triangles, and 231 unknows for MoM calculations.

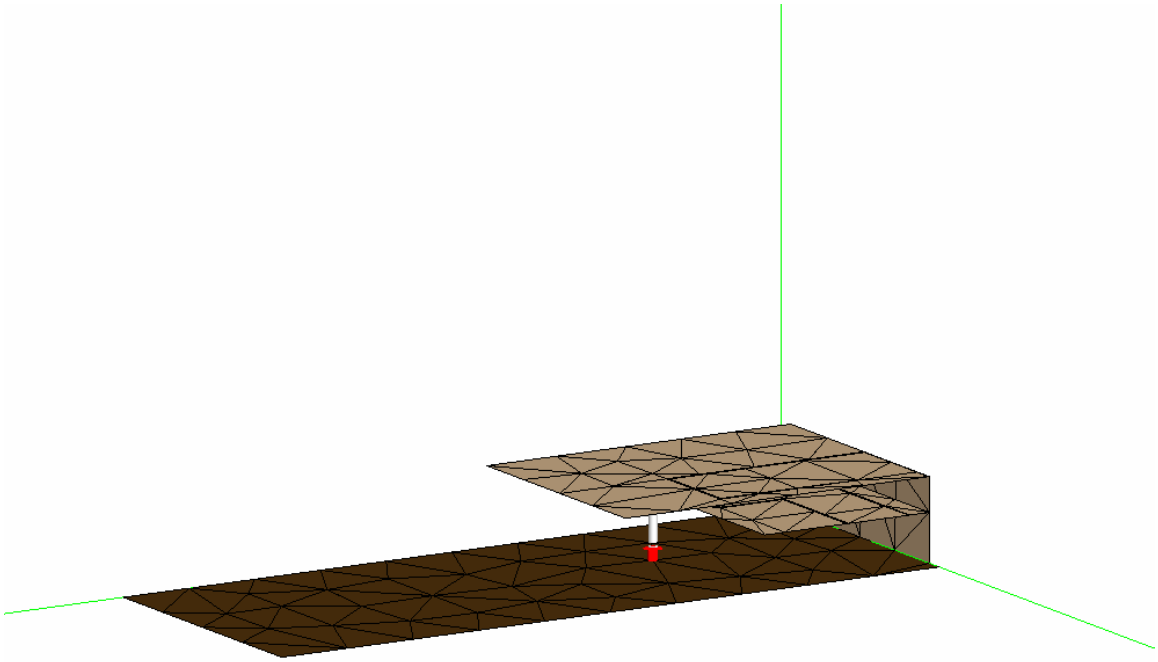

Figure 1 : Dual Wideband radiating element for mobile handsets generated with FEKO.

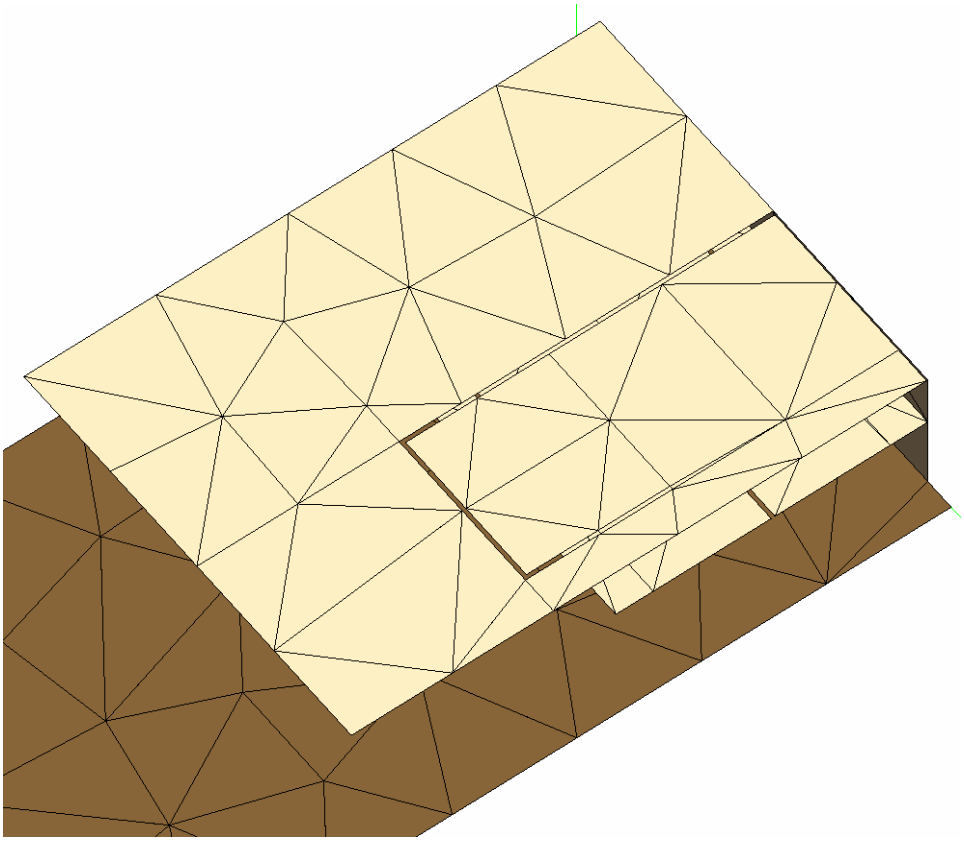

Figure 2 :Triangular meshing detail

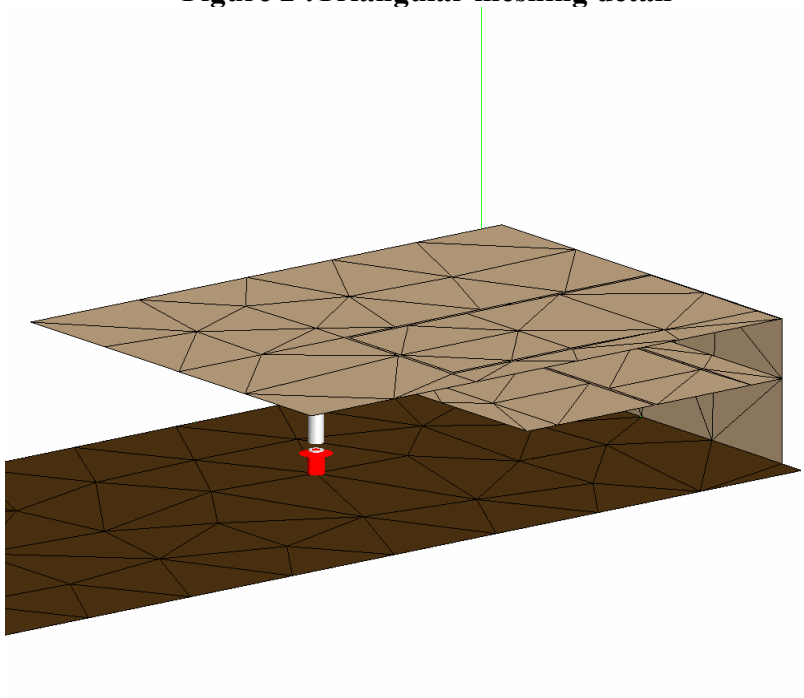

Figure 3 :Excitation detail

The excitation was modelled by using EditFEKO command A1 (Voltage source along a wire segment between triangular patches). The source was placed at a wire segment of radius 0.6mm and height 11.6mm as required. To obtain more accurate results this wire was divided in two, and the source was positioned at the lower part of the wire of length 2mm as showed in figure 3.

5. Simulation results

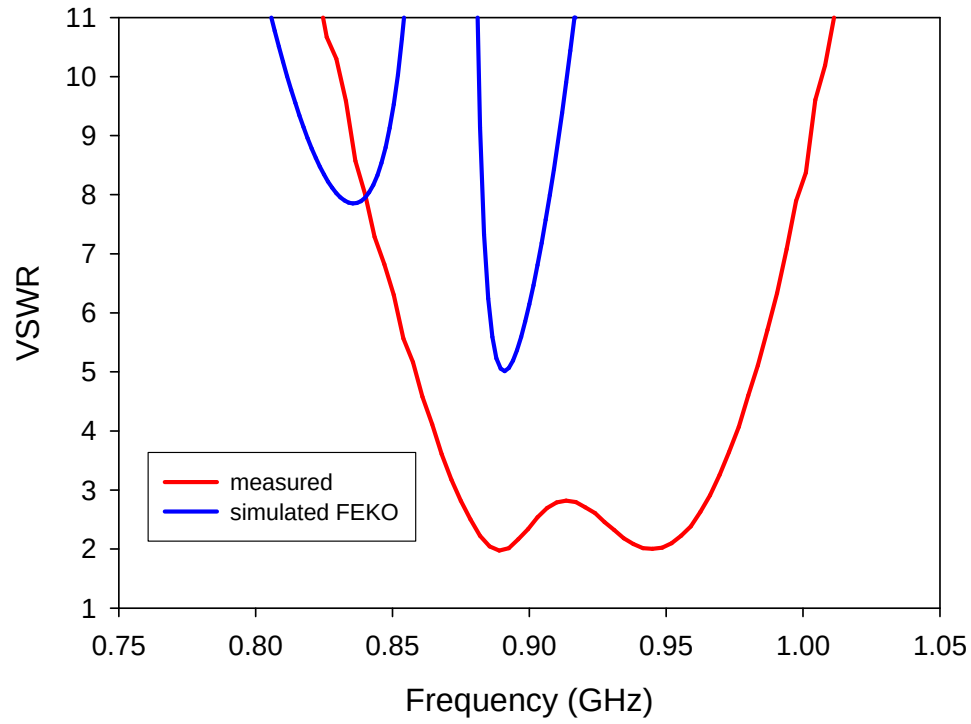

Fig. 1 : VSWR versus frequency in the lower band

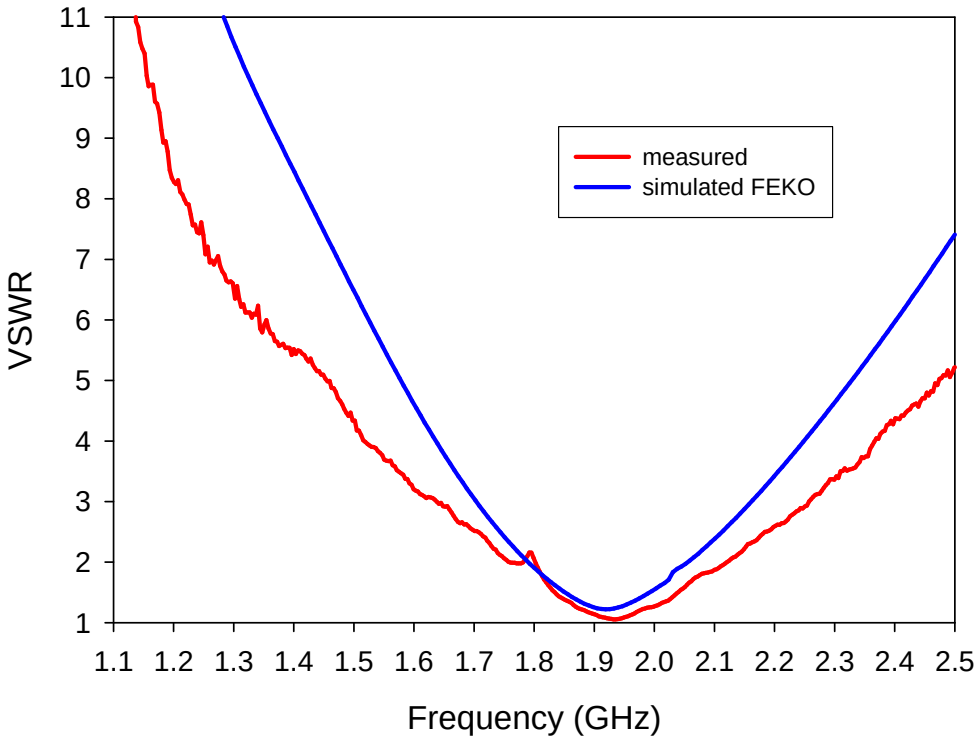

Fig. 2 : VSWR versus frequency in the upper band

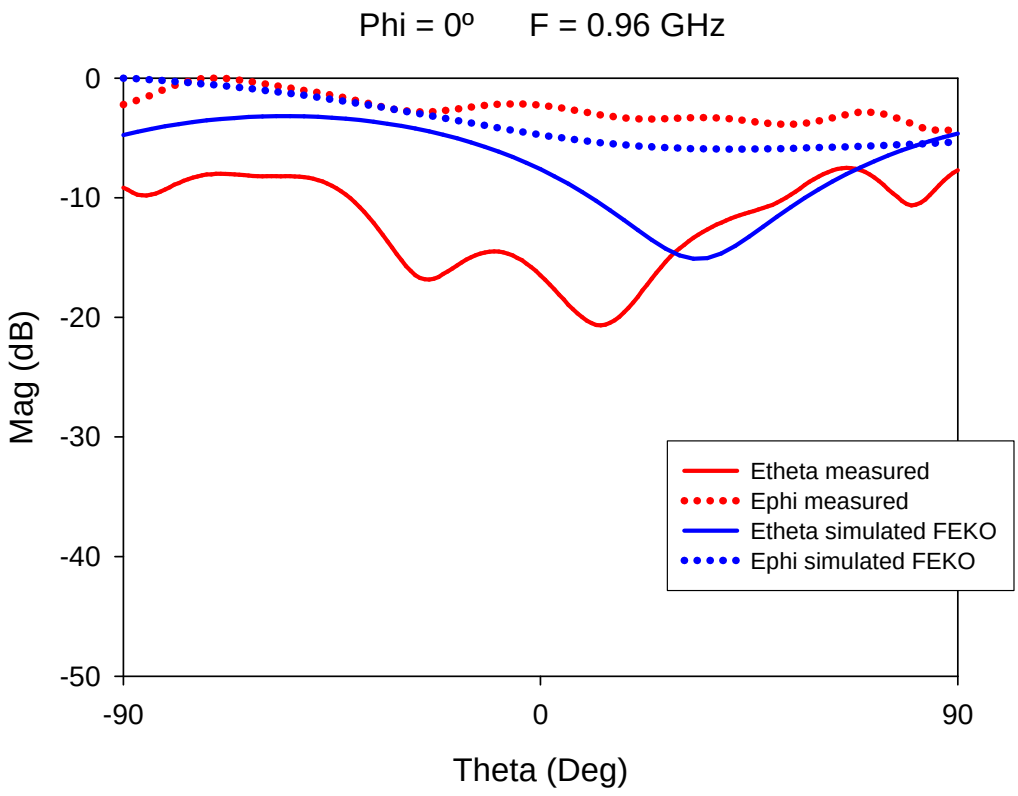

Fig. 3 : E-plane radiation pattern versus theta in the lower band (f=0.96 GHz)

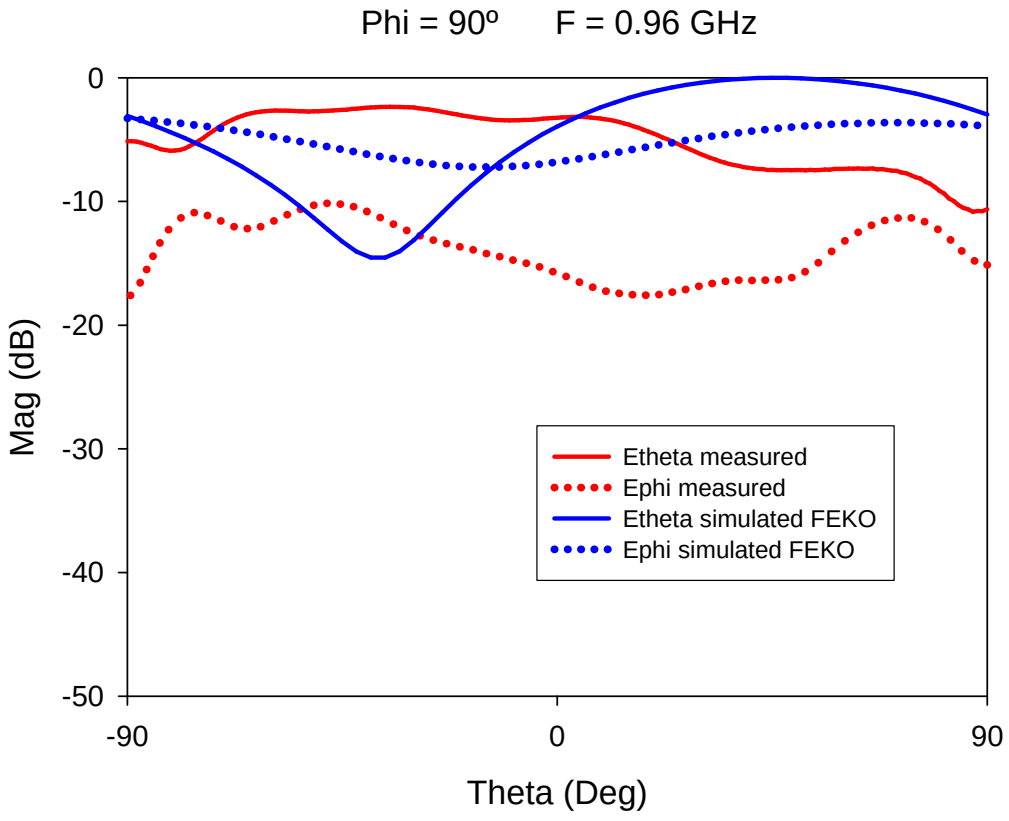

Fig. 4 : E-plane radiation pattern versus theta in the lower band (f=0.96 GHz)

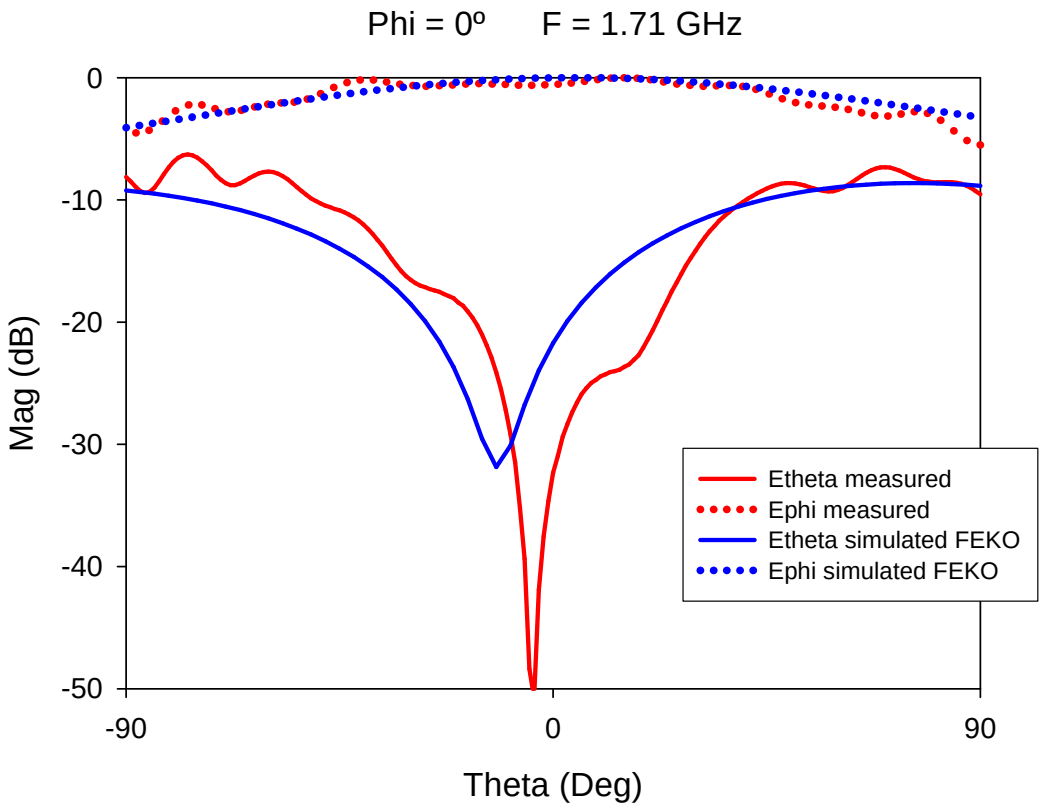

Fig. 5 : E-plane radiation pattern versus theta in the upper band (f=1.71 GHz)

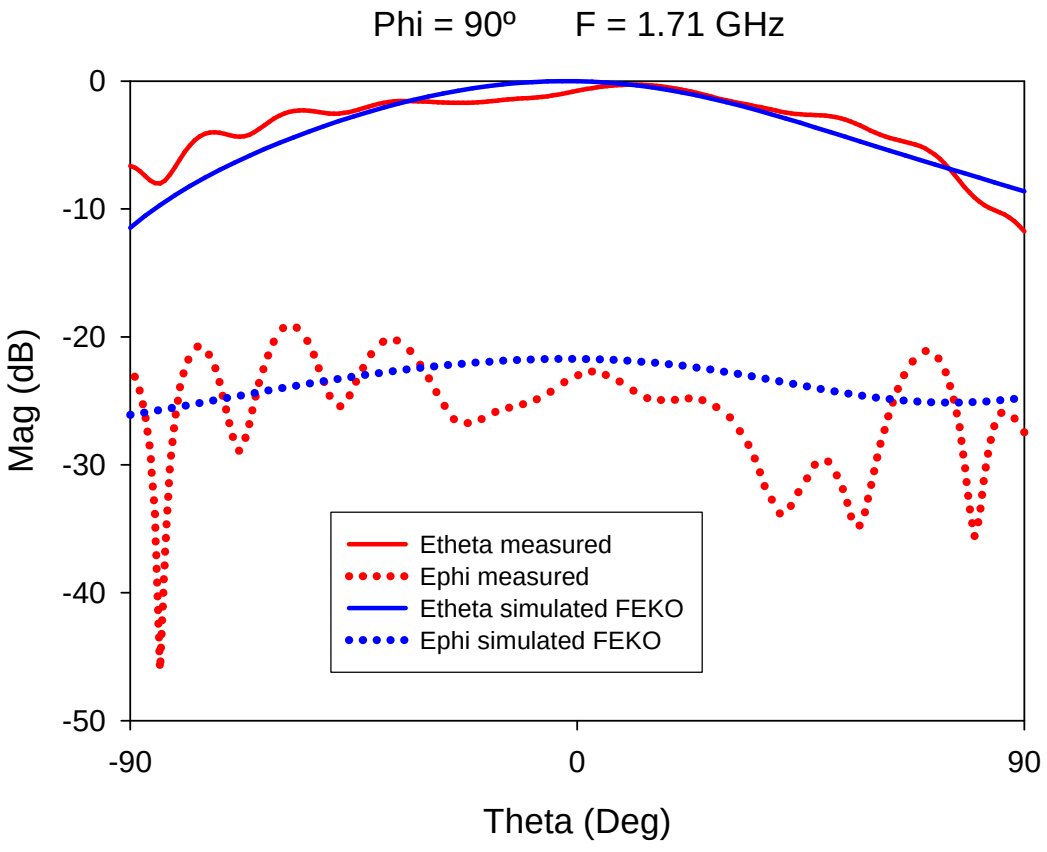

Fig. 6 : H-plane radiation pattern versus theta in the upper band (f=1.71 GHz)

6. Computation resources

The simulation was performed on a laptop PC. This machine has a Pentium processor (Centrino Mobile) at 1.6 GHz with an available RAM memory of 512 MB. It took 173.3 seconds to compute the 188 unknown currents at 402 frequencies and the radiation patterns for two frequencies. The memory usage was 986.1 kB. A finer discretisation was tested in order to check convergence. Quite similar results were obtained with triangles whose largest side was up to $\lambda/50$. That means 467 unknowns. These results were not included because no extra information can be obtained from them.

7. Discussion

Good agreement in the upper band and quite different results in the lower band, probably due to the metal thickness, which is not included in the model.

3- SIMULATION RESULTS

From UPV_LEATantenna_IE3D

1. Entity

Escuela técnica superior de ingenieros de Telecomunicación (ETSIT)
Departamento de Comunicaciones (DCOM)
Grupo de Radiación Electromagnética (GRE)
Universidad Politécnica de Valencia
Camino de Vera, s/n
46022
Valencia, España.

Contact persons:

Alejandro Valero Nogueira
Phone: 963879715
Fax: 963877309
Email: avalero@dcom.upv.es

2. Name of the simulation tool

Zeland Software, IE3D v10.23

3. Generalities about the simulation tool

IE3D is a full-wave, method-of-moments based electromagnetic simulator solving the current distribution on 3D and multilayer structures of general shape. It has been widely used in the design of MMICs, RFICs, LTCC circuits, microwave/millimeter-wave circuits, IC interconnects and packages, HTS circuits, patch antennas, wire antennas, and other RF/wireless antennas.

4. Simulation Set-up (Geometry set-up, GUI, mesh, boundary conditions, excitation)

I have redrawn the structure using the GUI available with your tool
GUI allows construction of 3D and multilayer metallic structures as a set of polygons.
You can also import the geometry from a standard format file (Autocad, …),

Automatic generation of non-uniform mesh with rectangular and triangular cells is available. Rectangular cells are used in the regular region. Triangular cells are utilized to fit the irregular boundary.

A frequency domain analysis was performed. A curve-fitting scheme is used to extract detailed frequency response of the structure by using the simulation results at a few frequency points.

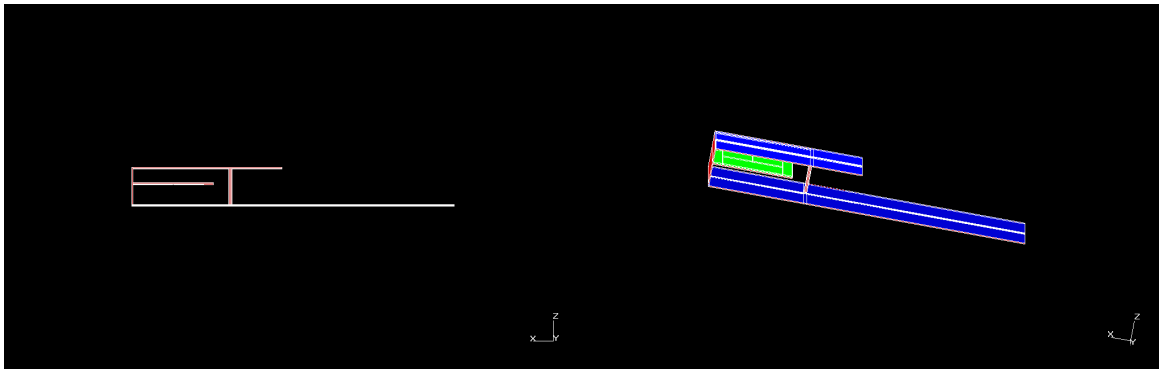

It takes about 1 hour to draw the geometry and about 10 min to set up the rest of the simulation.

5. Simulation results

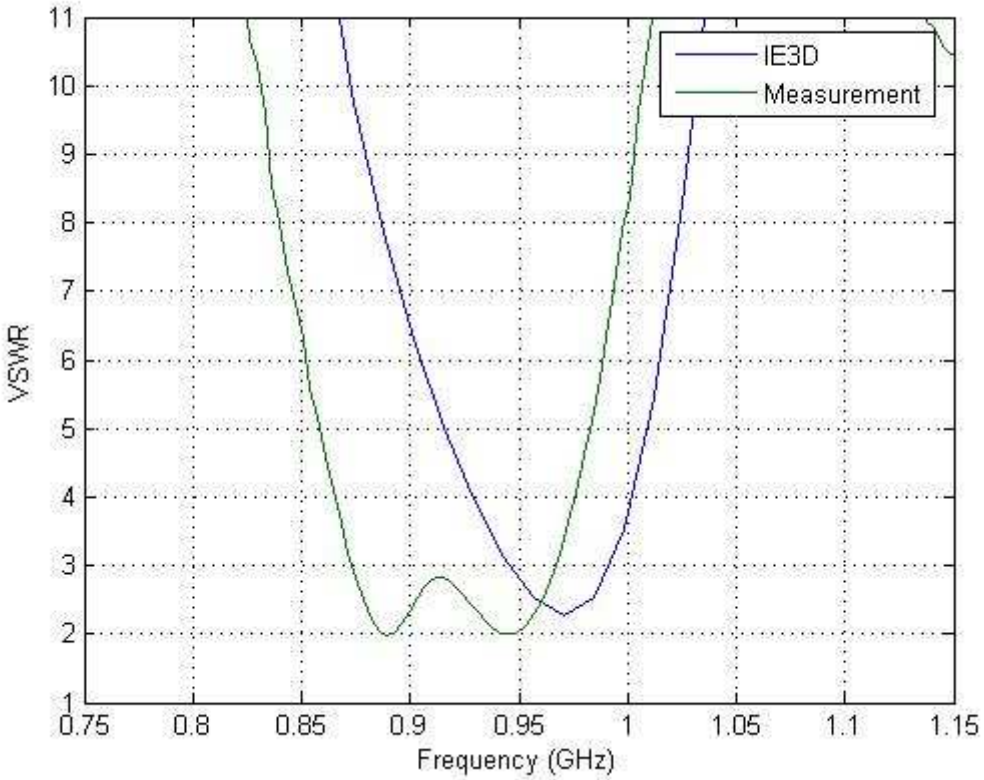

Figure 1 : VSWR versus frequency in the lower band.

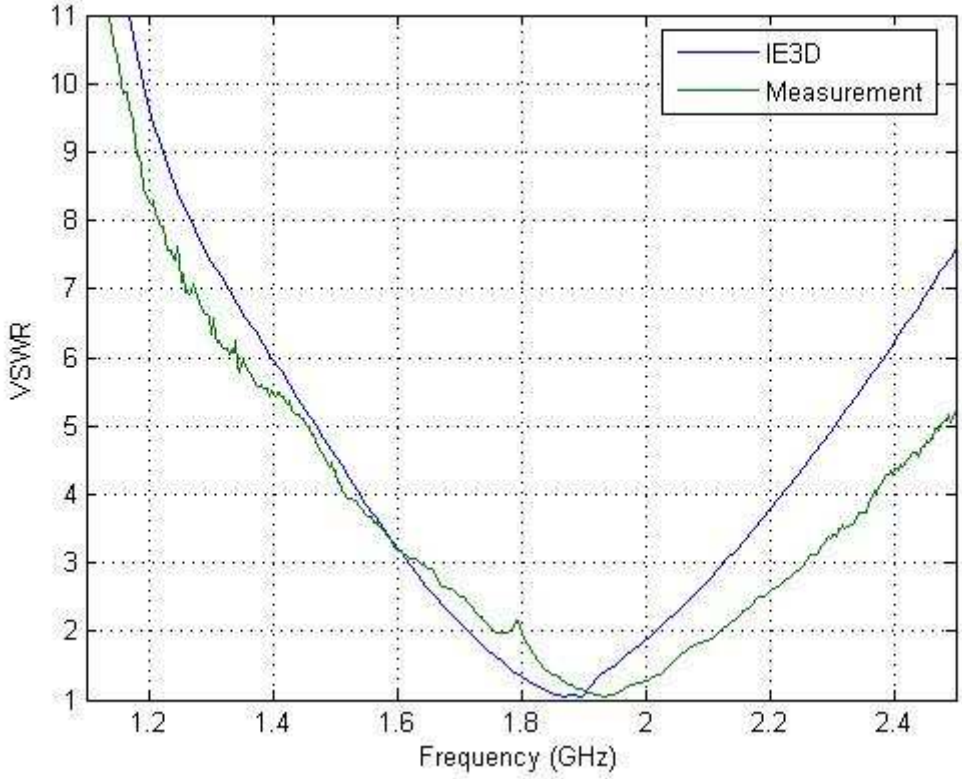

Figure 2 : VSWR versus frequency in the upper band.

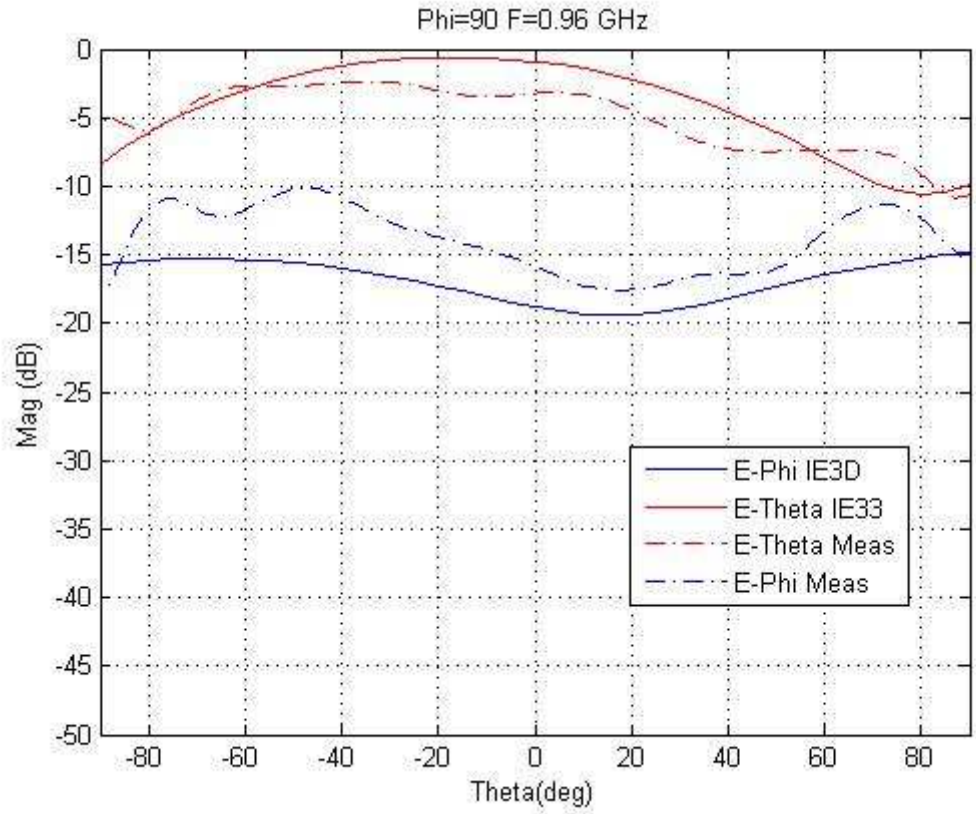

Figure 3 : E-plane radiation pattern versus theta in the lower band (f=0.96 GHz)

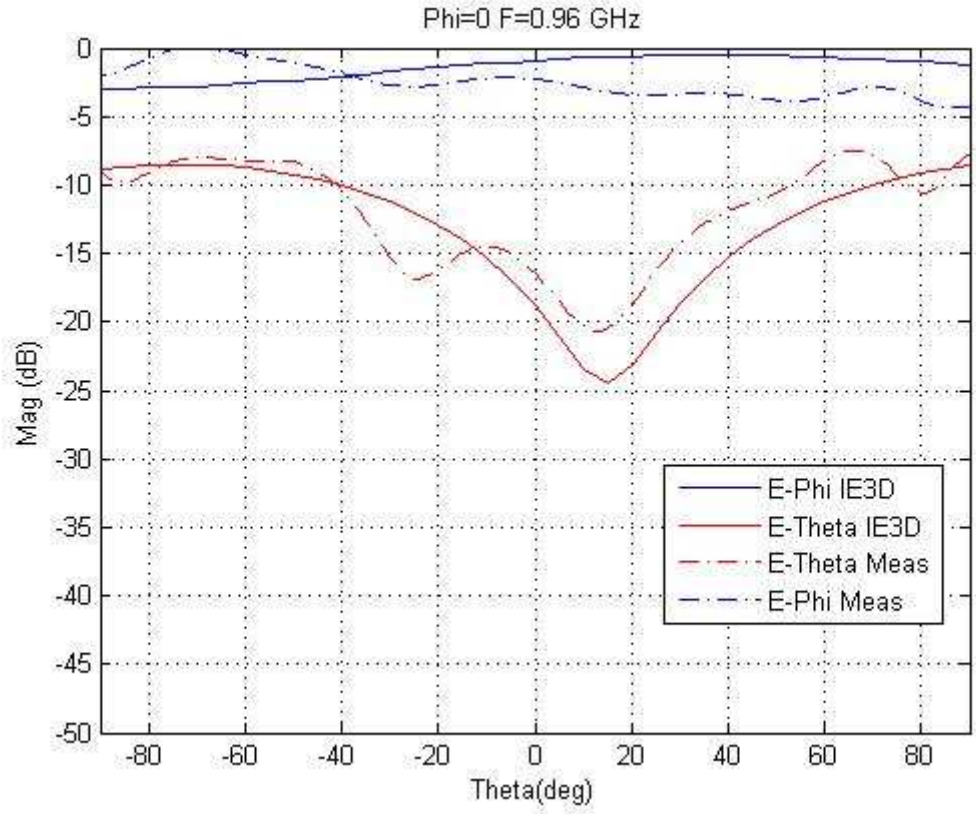

Figure 4 : H- plane radiation pattern versus theta in the lower band (f=0.96 GHz).

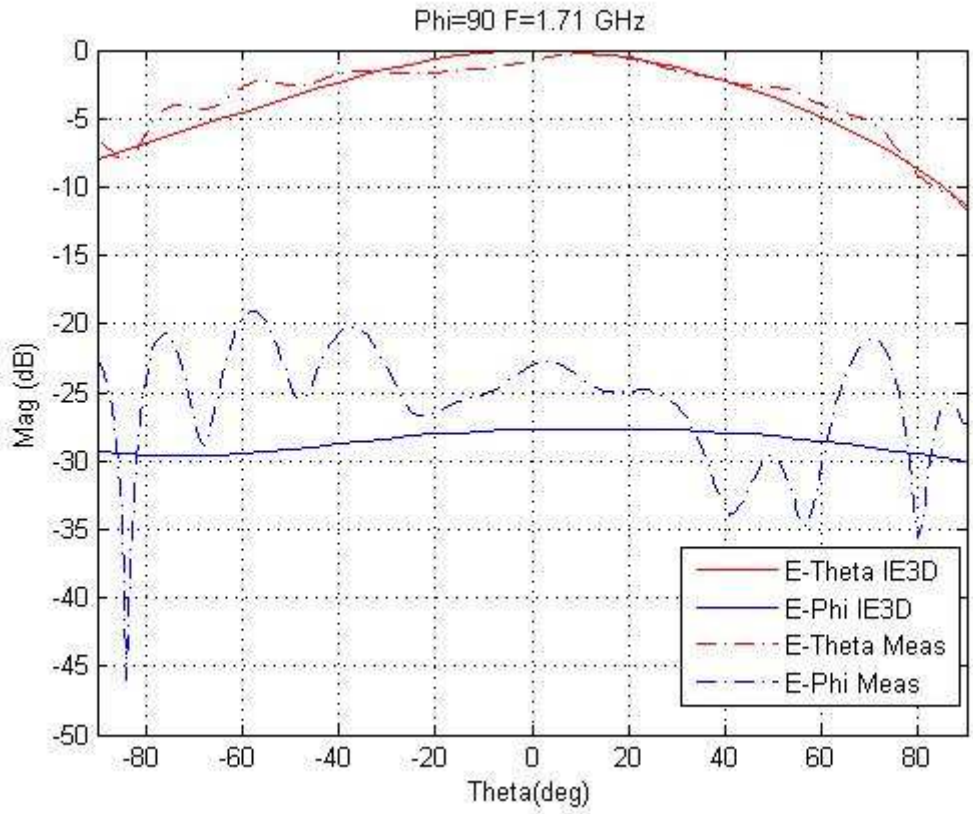

Figure 5 : E-plane radiation pattern versus theta in the upper band (f=1.71 GHz)

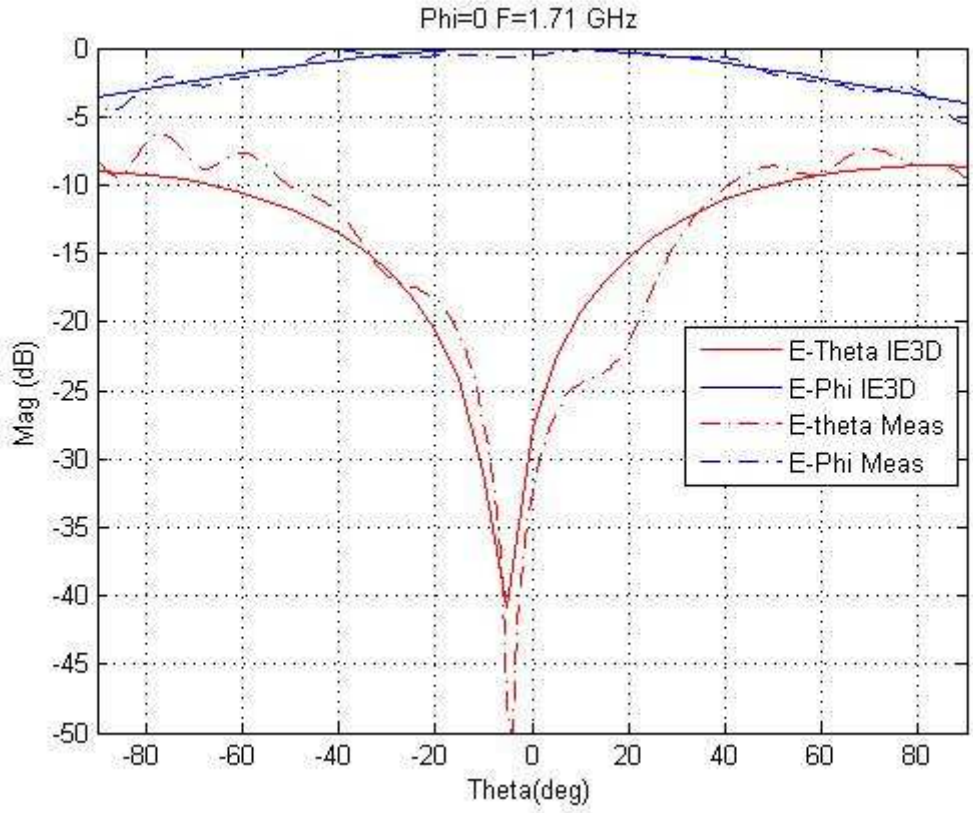

Figure 6 : H- plane radiation pattern versus theta in the upper band (f=1.71 GHz)

6. Computation resources

- ***Type of machine (PC, Workstation, …),***

PC

- ***Number of processors,***

  2

- ***Available memory,***

  1 Gb

- ***Memory used for simulation,***

  646 MB

- ***CPU speed, ….***

  3 GHz

Low band VSWR:

Total time: 331 seconds
Memory: 451 Mbytes
Time / frequency: 32 seconds
Effective processors: 1

High band VSWR:

Total time: 574 seconds
Memory: 646 Mbytes
Time / frequency: 48 seconds
Effective processors: 1

Radiation Pattern:

Total time: 129 seconds
Memory 557Mbytes
Effective processors: 1

7. Discussion

- ***Easiness/difficulty to set up the simulation and output results,***

  It is very easy to set up the simulation and obtain the results

- ***Computation requirements for your simulation,***

  The requirement in terms of memory is very important as this kind of antenna needs a thin mesh to obtain good results

- ***Level of agreement between your results and the reference data, …***

  We find an acceptable agreement between simulation and measurements.

We found these results with nominal simulation conditions that the program suggests.

8. Additional comments

3- SIMULATION RESULTS

From IETR_LEATantenna_HFSS

1. Entity

Institut d'Electronique et Télécommunications de Rennes (IETR)
CNRS UMR 6164
Université de Rennes 1, Campus de Beaulieu, Bât 11 D
263, av. du Général Leclerc
35042 Rennes Cedex, France

Contact persons :
Sylvain Collardey
Phone : +33(0)2 23 23 56 69
Fax : +33(0)2 23 23 69 63
Email : sylvain.collardey@univ-rennes1.fr

2. Name of the simulation tool

Ansoft HFSS v9.2

3. Generalities about the simulation tool

HFSS employs the finite element method in order to generate an electromagnetic field solution. The finite element method divides the full problem space into thousands of smaller regions and represents the field in each sub-region (element) with a local function. In HFSS, the geometric model is automatically divided into a large number of tetrahedra. This collection of tetrahedra is referred to as the finite element mesh.

4. Simulation Set-up (Geometry set-up, GUI, mesh, boundary conditions, excitation)

- I have redrawn the structure using the GUI available with your tool

I draw one-, two-, or three-dimensional objects. You can alter objects individually or together to create the geometry of your structure.After you draw an object in the 3D Modeler window, you can modify the object's properties, such as its position, dimensions, or color.

But you can also :

- Import the geometry from a standard format file (IGES, Autocad, …),
- Manual mesh is available, and you can choose different meshes for each part of the structure.
- An adaptative mesh based on the scattering parameters is also available after an automated mesh.
- Give the mesh type: non-uniform tetrahedral mesh.

Radiation boundaries are used to simulate open problems that allow waves to radiate infinitely far into space, such as antenna designs. HFSS absorbs the wave at the radiation boundary, essentially ballooning the boundary infinitely far away from the structure. The accuracy of the approximation depends on the distance between the boundary and the object from which the radiation emanates.

For the ground plane, I have used perfect E boundary which represents perfectly conducting surfaces in a structure. Perfectly matched layers (PMLs) are availble but they are not used.

For excitation, a lumped port associated to a metallic via is used. Lumped port is similar to traditional wave ports, but can be located internally and have a complex user-defined impedance. Lumped ports compute S-parameters directly at the port. A lumped port can be defined as a rectangle from the edge of the trace to the ground or as a traditional wave port. Describe shortly the type of analysis that was performed (frequency domain parameters, frequency range, time domain parameters, time domain range, excitation bandwidth, frequency of the mesh convergence, frequency interpolation/extrapolation for wideband response, …).

Simulator required an air box filled of vacuum with radiation boundaries to simulate open problem.

The ground plane is considered as a PEC boundary in order to speed up the simulation and decrease the requirement of memory.

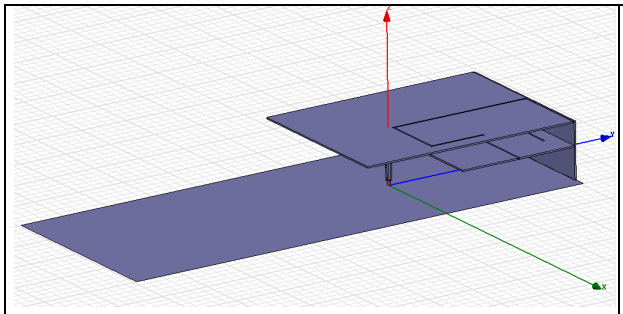

3D

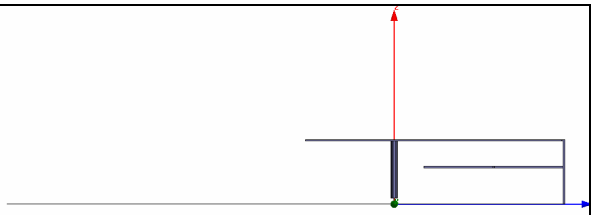

YZ-plane view

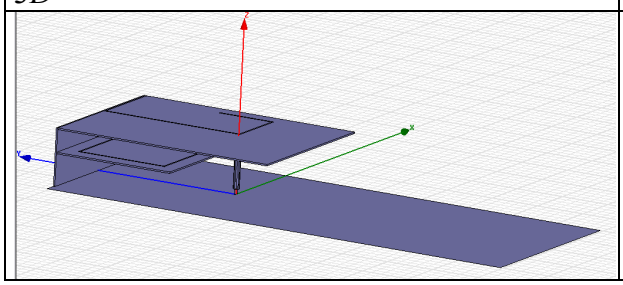

It takes about 45min to draw the geometry and about 5 min to set up the rest of the simulation.

5. Simulation results

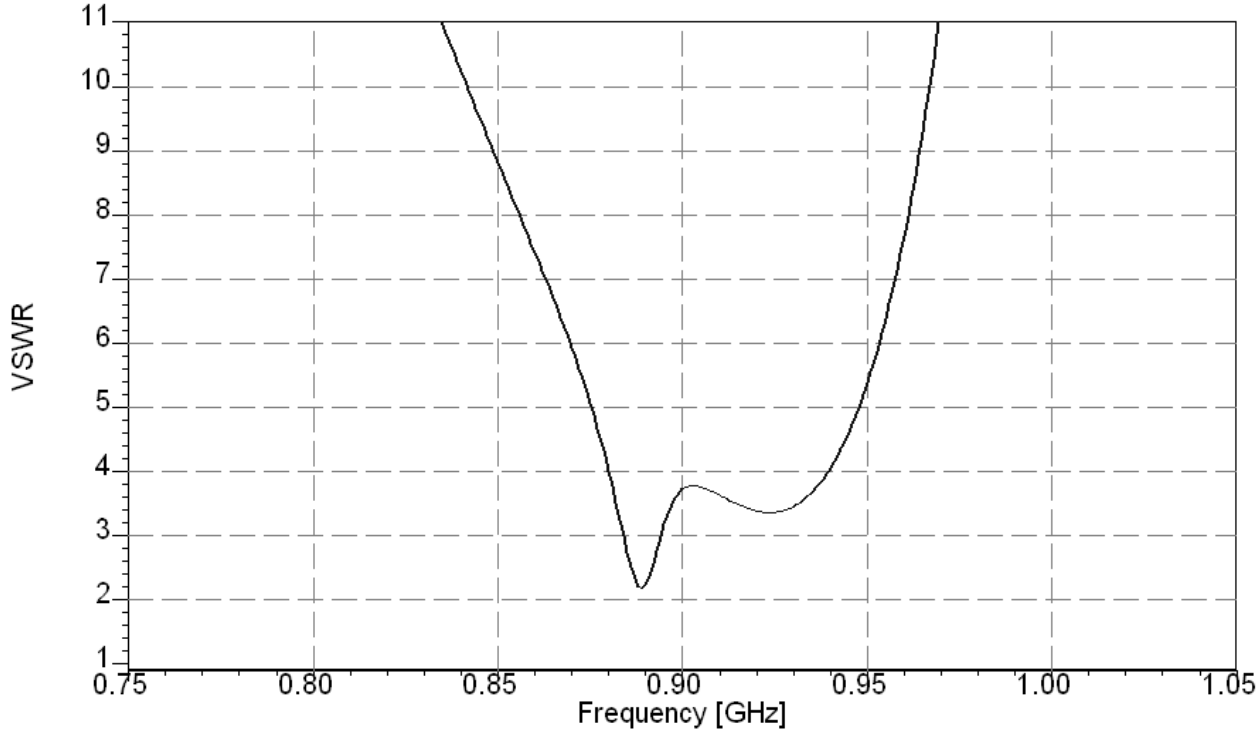

Figure 1 : VSWR versus frequency in the lower band

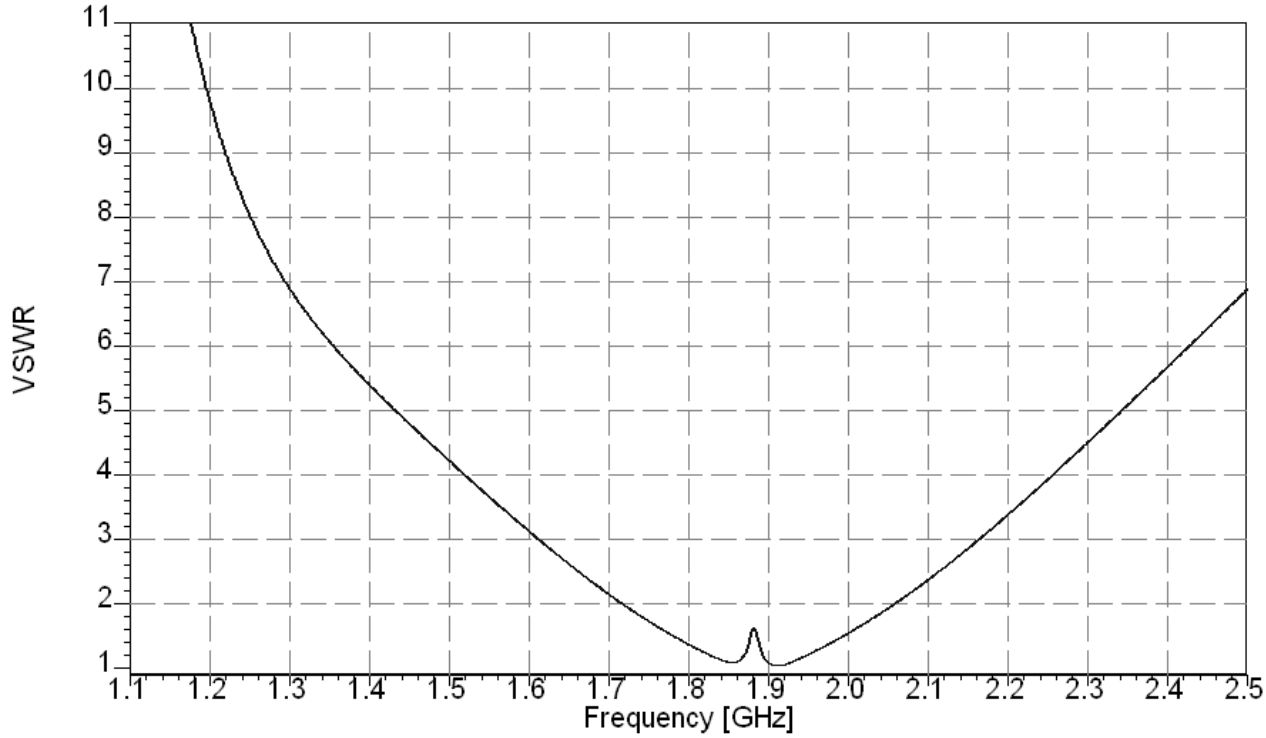

Figure 2 : VSWR versus frequency for in the upper band

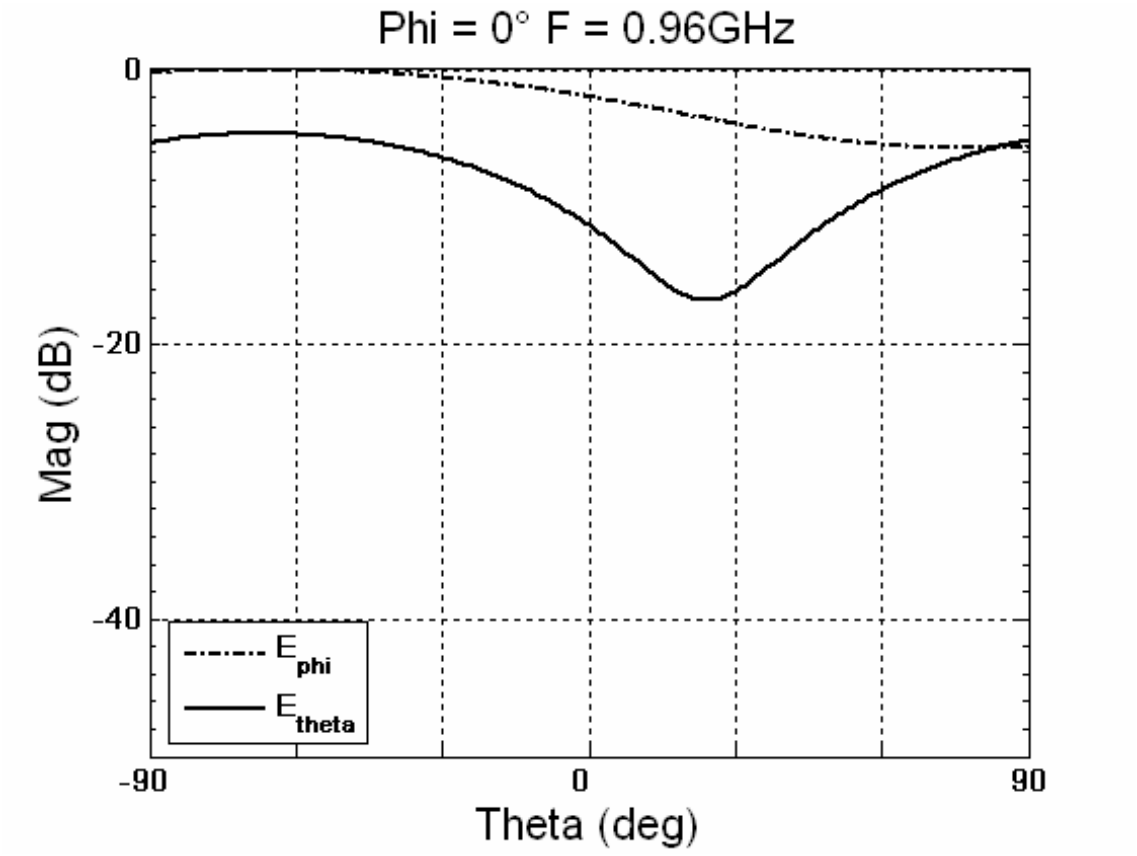

Figure 3 : E-plane radiation pattern versus theta in the lower band (f=0.96 GHz)

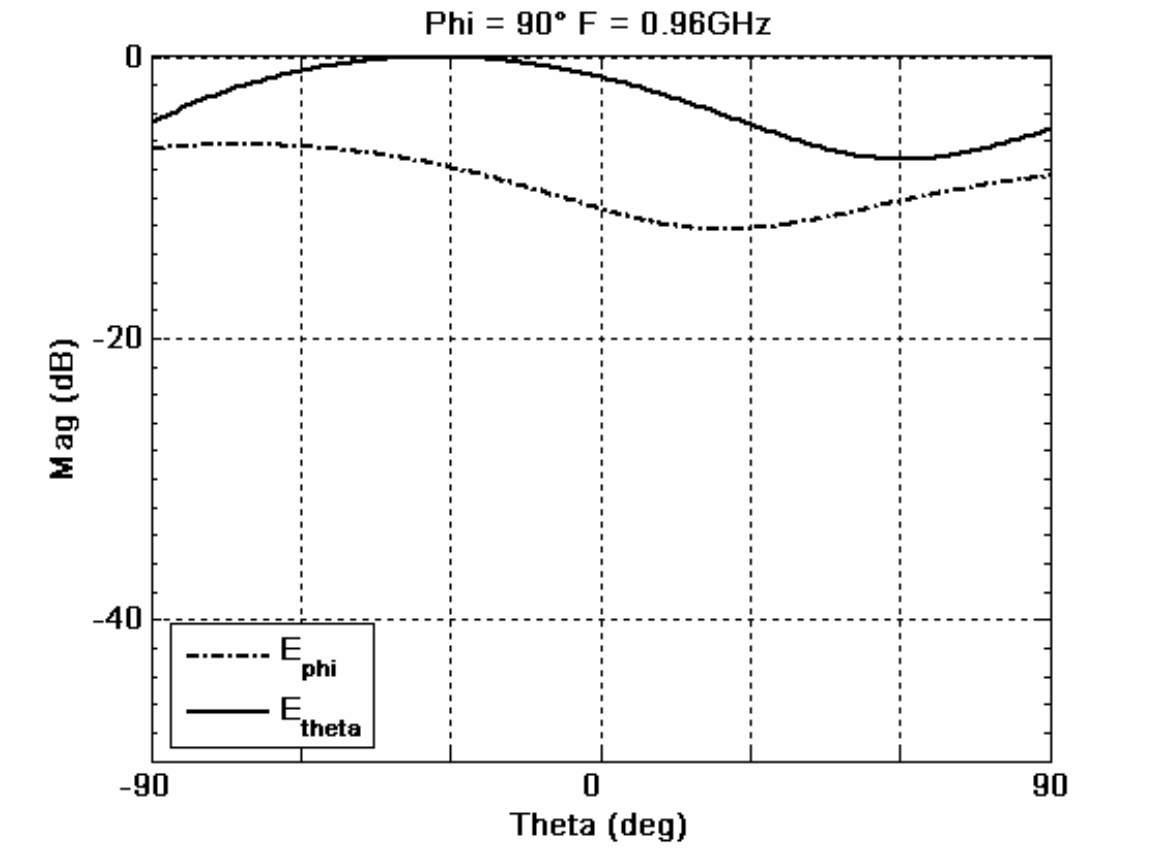

Figure 4 : H- plane radiation pattern versus theta in the lower band (f=0.96 GHz)

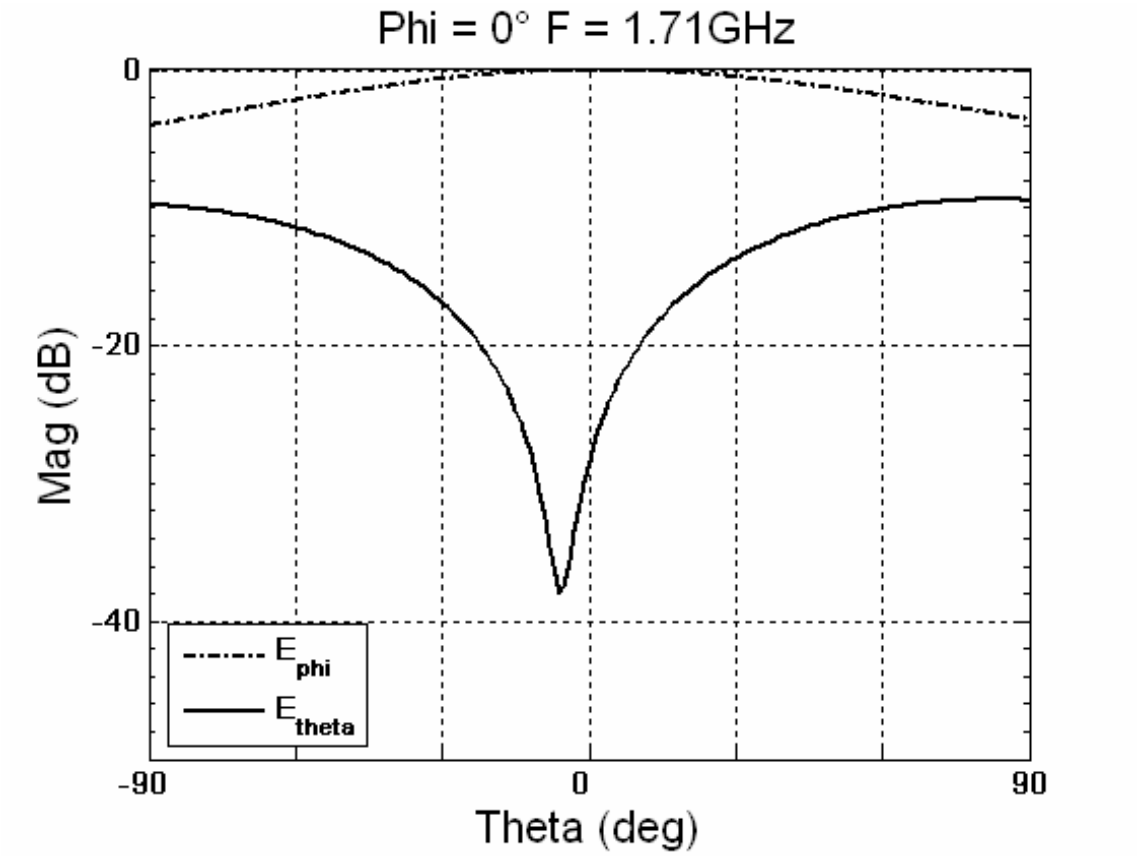

Figure 5 : E-plane radiation pattern versus theta in the upper band (f=1.71 GHz)

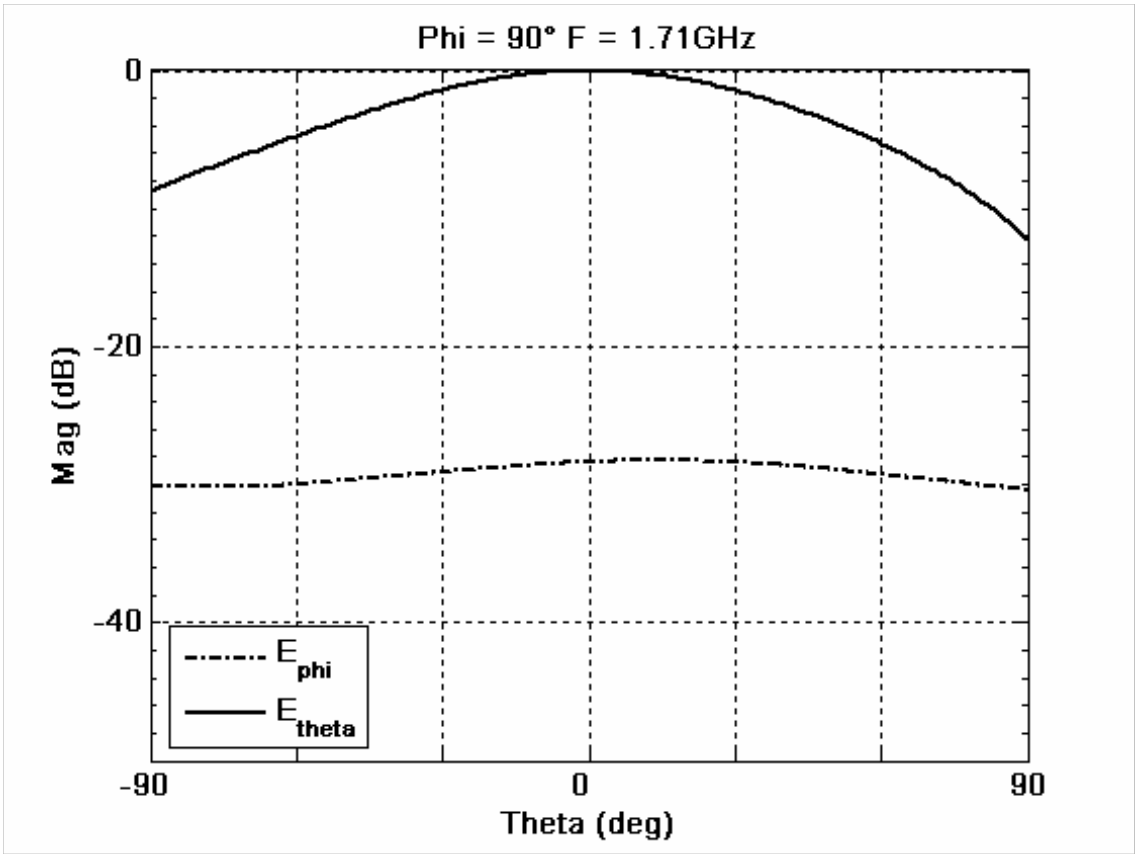

Figure 6 : H- plane radiation pattern versus theta in the upper band (f=1.71 GHz)

6. Computation resources

- ***Type of machine (PC, Workstation, …)***
  PC
- ***Number of processors,***
  1 CPU
- *Maximum available* ***memory,***
  2Go
- ***Memory used for simulation,***
  1.8Go
- ***CPU speed, ….***
  3GHz

Computation time :

About 7hours

7. Discussion

- ***Easiness/difficulty to set up the simulation and output results:***
  There are no difficulties to set up the simulation and to obtain results.

- ***Computation requirements for your simulation:***
  For this kind of antenna with two slots, we must mesh with an important accuracy to obtain good results, the requirement in available memory is very important.

- ***Level of agreement between your results and the reference data, …:***
  We observe a good agreement between simulation and measurements in the upper band. For the lower band, the results are slightly different, so the simulation requires a more accurate mesh and more available memory.

I have refined the mesh up to the maximum capabilities of the computer. More the mesh is fine, the better the results are. After 5 or 6 passes of refinement, I verify the quality of the VSWR or the radiation patterns compared to the measurements. Up to 26 passes have been used to refine the mesh of the antenna. A percentage of refinement equal to 5% has been defined between two successive passes. Better results can be achieved if we use a more powerful computer.

8. Additional comments

4- SYNTHESIS OF RESULTS

The structure proposed by the CNRS-LEAT has been simulated by **five laboratories**:

-IETR
- IDS
- LEAT
- UOB
- UPV

The simulation has been performed by **three time domain methods**:

- IETR : IMELSI
- UOB : FDTD32
- LEAT : FPTLM

And **four frequency domain methods** :

- IDS : ADF
- UPV : FEKO
- UPV : IE3D
- IETR : HFSS

- **IMELSI** and **FDTD32** are a **Finite-Difference-Time-Domain** techniques.

- Transmission Line Matrix Method (**FPTLM**) is very similar to the FDTD.

- **ADF** is a framework which contains many tools for antenna analysis, placement and design. For the present simulation, a **full-wave MOM solver** (MPIE formulation, RWG basis functions) has been used.

- FEKO, **IE3D** and **HFSS** are commercial codes.

i. **FEKO** is a method of moments (MoM) based, computer code for the analysis of electromagnetic problems.
ii. **IE3D** is a full-wave, method-of-moments based electromagnetic simulator solving the current distribution on 3D and multilayer structures of general shape.
iii. **HFSS** employs the finite element method in order to generate an electromagnetic field solution.

- For all software, there is no difficulty to set up the simulation and to obtain results.

- For all simulation tools, the agreement between measured and simulated VSWR results is rather poor for the lower band (excepted for commercials codes, which have good results) but very good for the upper band.

- The radiation patterns in the principal planes however, are well predicted by software tools in both bands although they appear slightly more regular than the measured ones. The levels are in good agreement both for the co- and the cross-polar components.

- Efficiency simulation results are only given by FPTLM

- The requirement for available memory is very important to obtain good results.

BENCHMARKING ACTIVITY

(WP1.1-2)

Pyramidal Horn with dielectric slabs

Proposed by
France Télécom R&D

1- STRUCTURE DESCRIPTION

1. Entity

France Telecom Research & Development
Fort de la tête de chien
06320 La Turbie, France

Contact Person:
Philippe Ratajczak
Phone: +33 (0)4 92 10 65 24
Fax: +33 (0)4 92 10 65 19
Email: philippe.ratajczak@francetelecom.com

2. Name of the structure

Pyramidal horn with dielectric slab fed with a rectangular to square waveguide transition

3. Generalities

The pyramidal horn is one of the standard horns used in the measurement facilities. The horn is a square pyramidal horn fed by a WR137 rectangular waveguide via a rectangular to square waveguide transition. The dielectric slabs, placed before the aperture, allow to reduce the beam width of the H plane.

4. Structure Description

The structure proposed for benchmarking is illustrated in the **Figure 1**. The geometry is symmetric with respect to (x0z) and (y0z) planes.

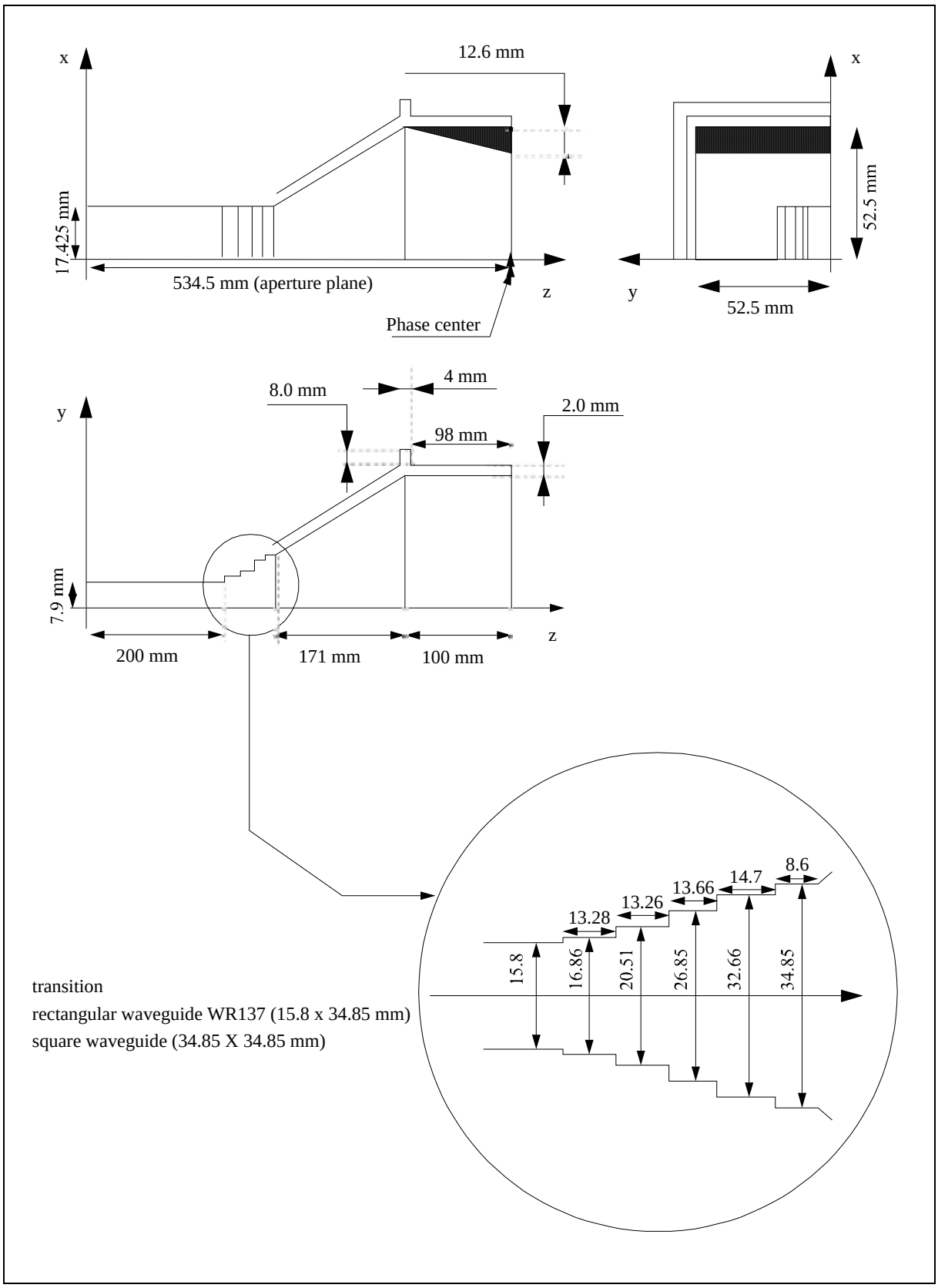

Figure 1: geometry of the pyramidal horn

The dielectric slabs are in Teflon ($\varepsilon_r = 2.2$).

The pyramidal horn is fed by the fundamental waveguide mode.
The plane (z = 0.0 mm) is the reference plane for the measurement of the S11.

The aperture plane (z = 534.5 mm) is the phase center for the measurement of the radiation patterns.

The triangular meshing presented in the **Figure 2** could be available in an ASCII file

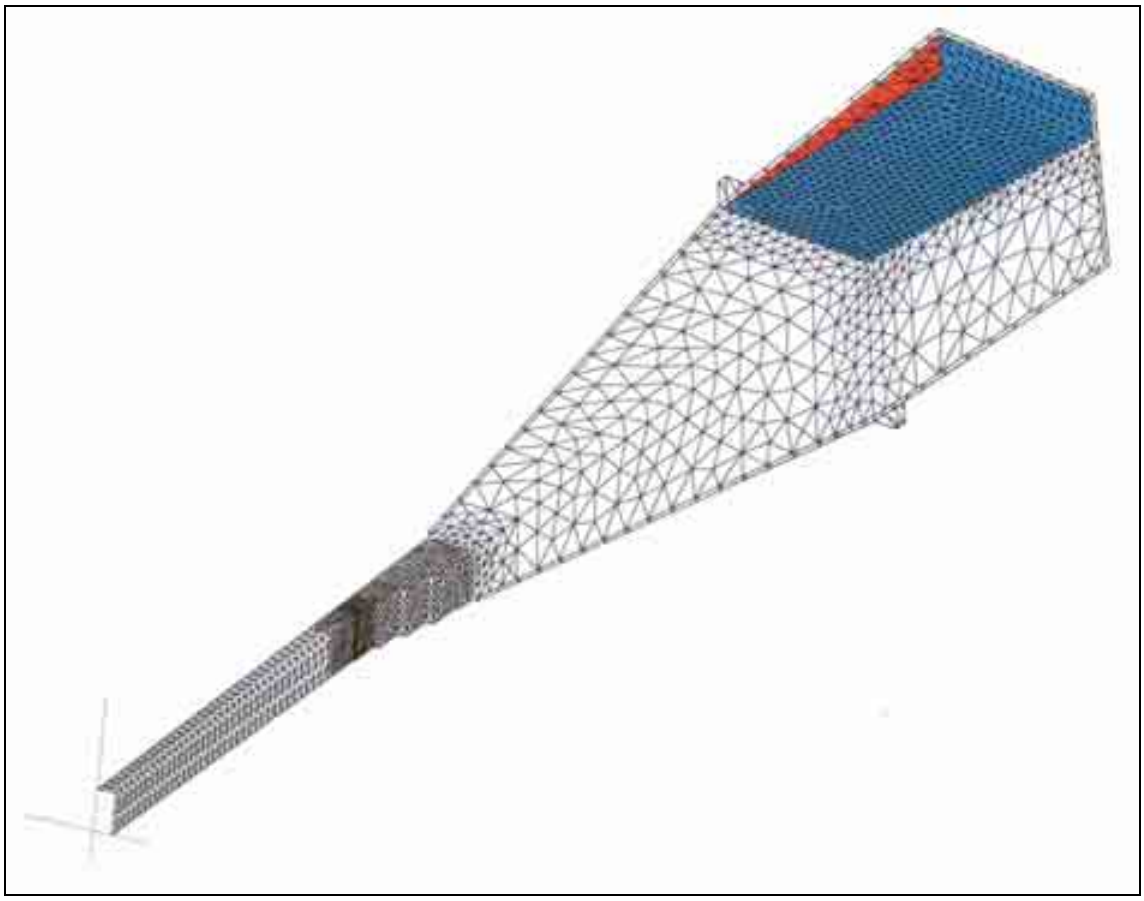

Figure 2: meshing of a quarter pyramidal horn

5. Computed results

The using frequency band of this horn is 6.0 to 6.4 GHz.

Input impedance:

The S11 parameter can be simulated from 6.0 to 6.4 GHz every 0.05 GHz with the reference plane z = 0.0 mm (200 mm before the beginning of the transition).

Radiations patterns:

The frequency range is 6.0 to 6.4 GHz every 0.05 GHz with the phase center placed in the horn aperture.
The directivity and the phase of main and cross polarization (3^{rd} definition of Ludwig) will be calculated in the main planes: $\phi = 0°$, $\phi = 45°$, $\phi = 90°$.

Some examples are presented Figure 3.

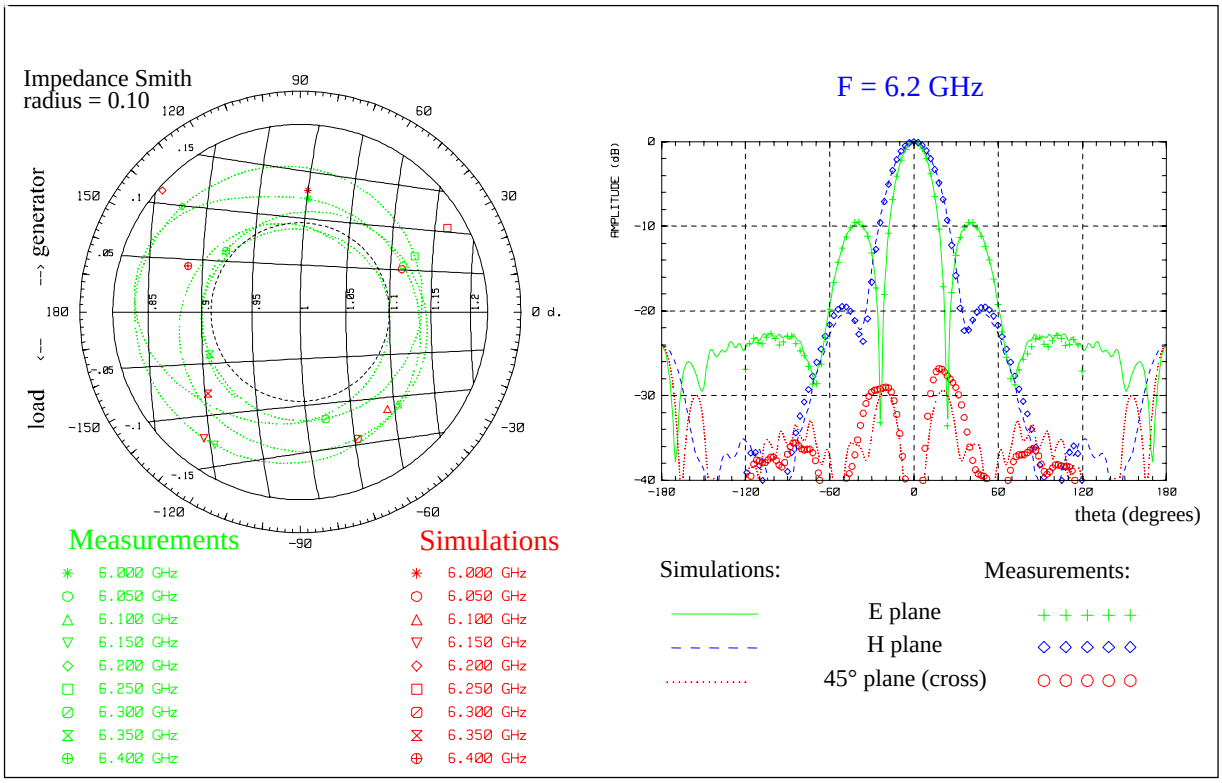

Figure 3: some results

6. References

As presented in the Figure 3, the measurements of the input impedance and the radiation patterns (6.0, 6.2 and 6.4 GHz) are available.

LUDWIG A.C.
“The definition of the cross-polarization” IEEE-AP, vol. 21, n°1, pp116-119, Jan. 1973

7. Additional comments

2 – STRUCTURE MEASUREMENTS

1. Entity

France Telecom Research & Development
Fort de la tête de chien
06320 La Turbie, France

Contact Person:
Philippe Ratajczak
Phone: +33 (0)4 92 10 65 24
Fax: +33 (0)4 92 10 65 19
Email: philippe.ratajczak@francetelecom.com

2. Measurement results

Concerning the input impedance, measurements are available in the frequency band 5.7 to 6.7 GHz with the reference plane 200 mm before the waveguide transition.
The working frequency band of the horn is 6.0 to 6.4 GHz.
Files:

- S11C76Dmes2: measured S11 between 5.7 to 6.7 GHz with 400 points
- S11C76Dmes3: measured S11 between 6.0 to 6.4 GHz every 0.05 GHz

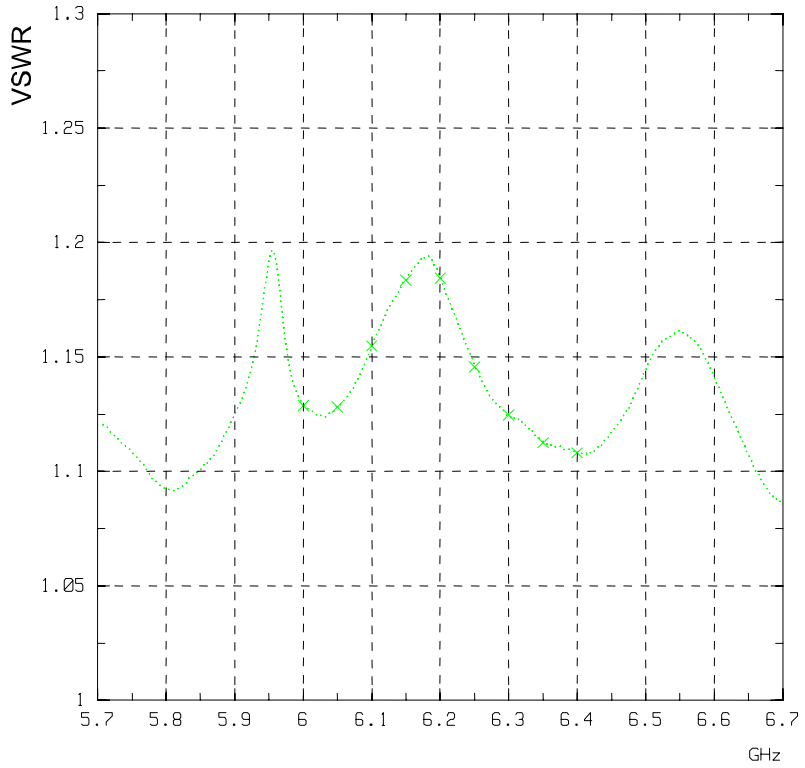

figure 1: VSWR

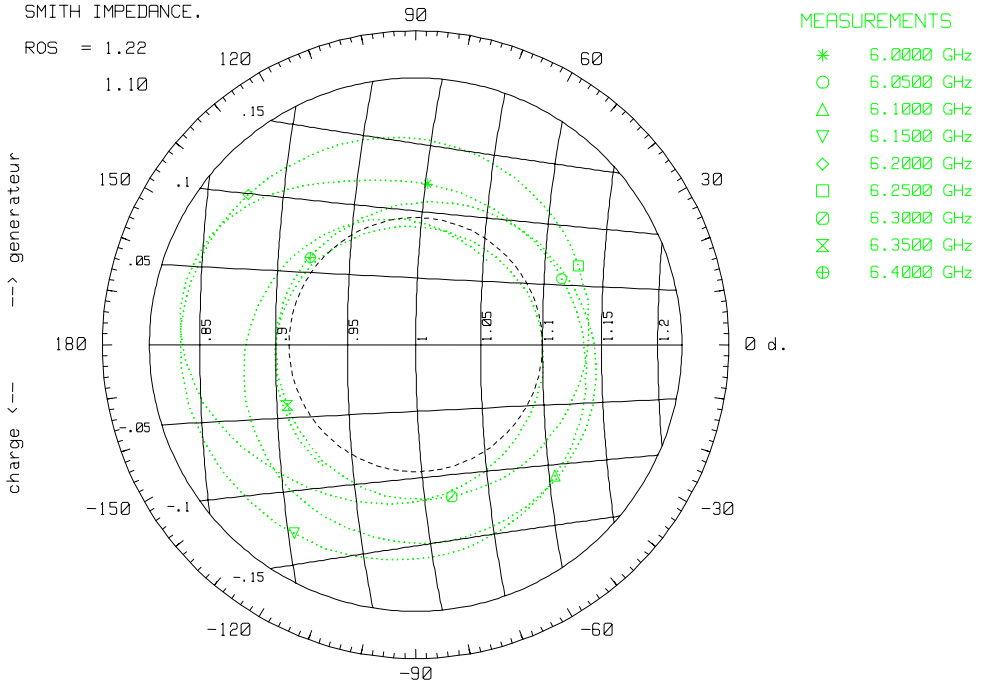

figure 2: Input impedance

Concerning the radiation patterns, measurements at 6.0, 6.2 and 6.4 GHz are available in the E, H and 45° planes in co-polarisation and cross-polarisation (3rd definition of Ludwig) for the amplitude.
The phase of the radiation pattern is available in the E and H planes for the co-polarisation with the phase center in the horn aperture.
Files:

- MES_C76D_60000: measured radiation pattern at 6.0 GHz
- MES_C76D_62000: measured radiation pattern at 6.2 GHz
- MES_C76D_64000: measured radiation pattern at 6.4 GHz

E plane is plotted in green, H plane in blue and 45° plane in red.

Simulated co-polarization is plotted in continuous line, cross-polarization in discontinuous line.

Measured co-polarization is plotted with '+' symbol and measured cross-polarization with '*' symbol.

A 180° offset must be add to the measured phase of the E plane in order to have the 0° reference at $\theta = 0°$.

For the frequencies from 6 to 6.4 GHz every 0.05 GHz, the directivity of the radiation pattern must be presented in a table:

Freq (GHz)	6.00	6.05	6.10	6.15	6.20	6.25	6.30	6.35	6.40
Directivity (dB)									

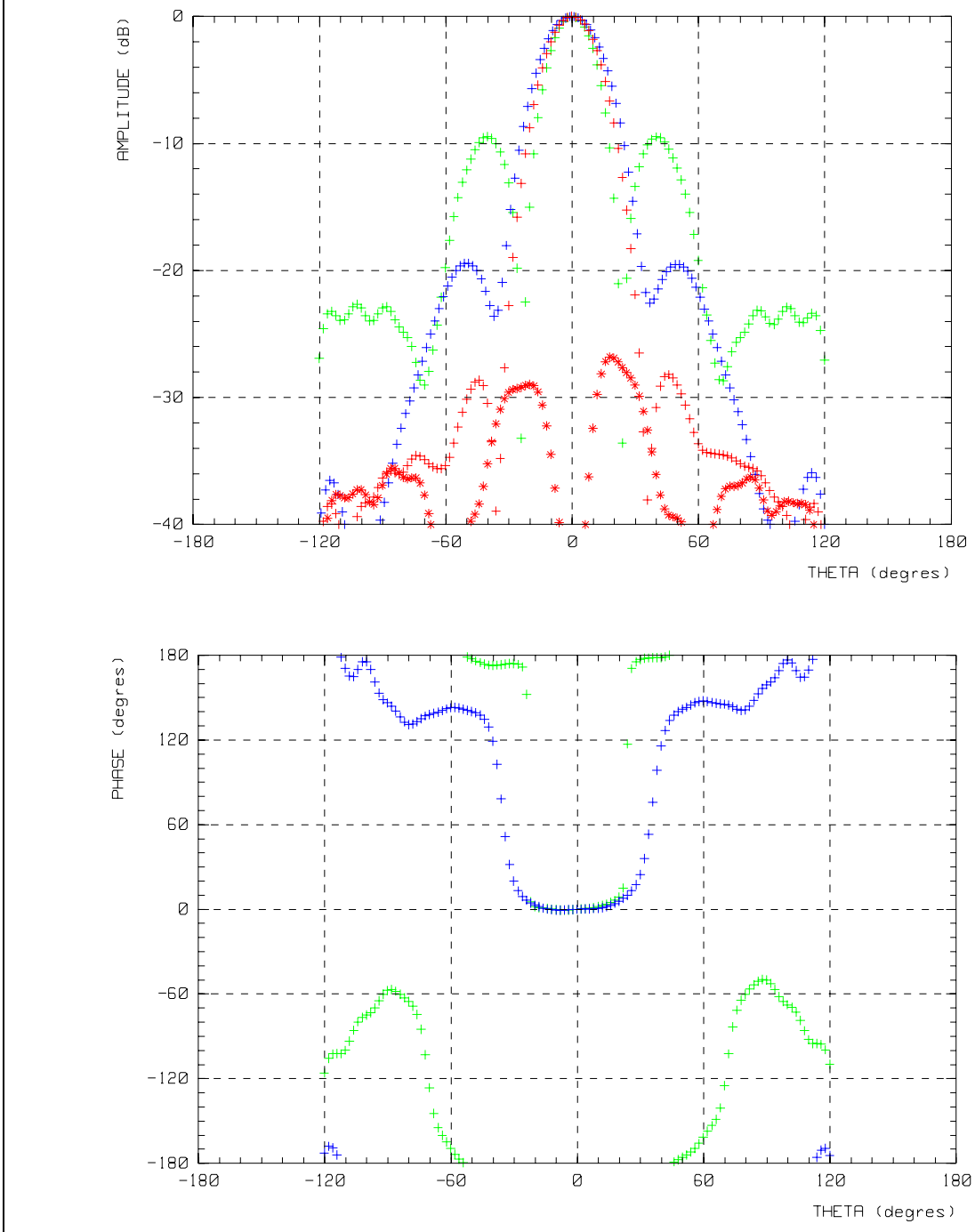

figure 4: Radiation pattern at 6.0 GHz

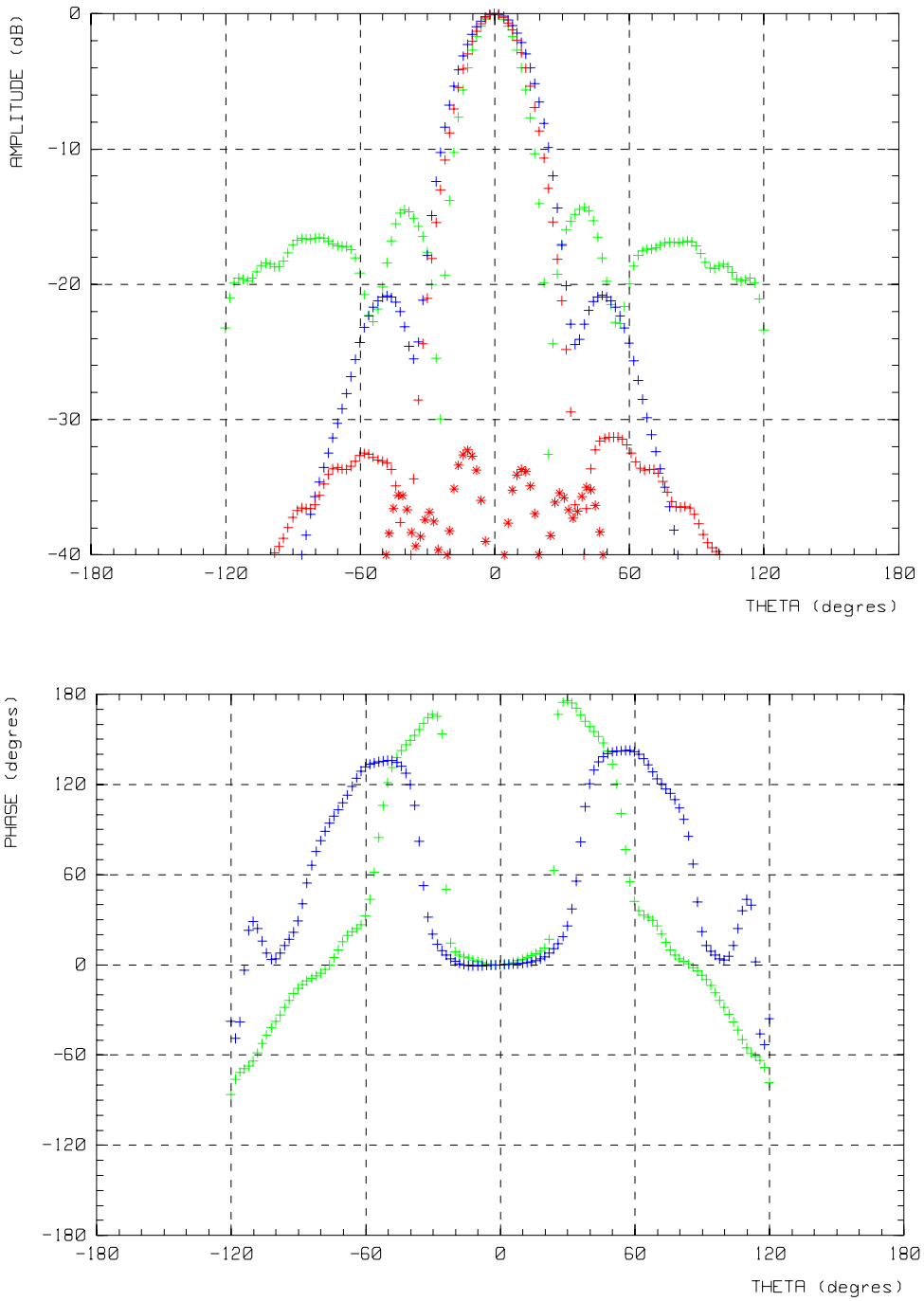

figure 5: Radiation pattern at 6.2 GHz

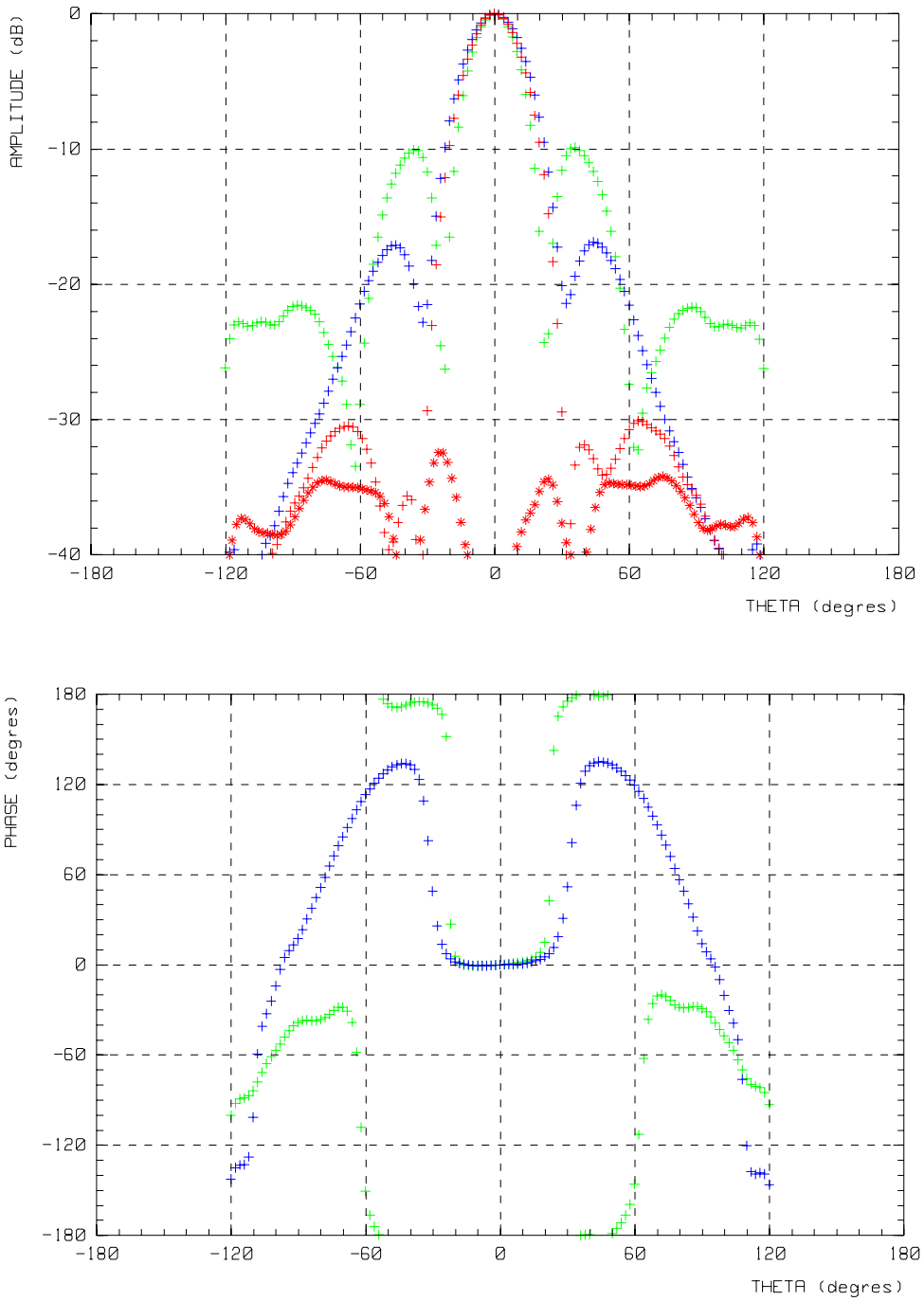

figure 6: Radiation pattern at 6.4 GHz

3- SIMULATION RESULTS

From FT_pyramidalhorn_SR3D

1. Entity

France Telecom, R&D Division
Fort de la tête de chien
06320 La Turbie

Philippe Ratajczak:
- tel: +33 4 92 10 65 24
- fax: +33 4 92 10 65 19
- Email: philippe.ratajczak@francetelecom.com

2. Name of the simulation tool

SR3D

3. Generalities about the simulations tool

SR3D - Structures Rayonnantes à 3 dimensions (3D Radiating Structures) - is a software which, given the geometry and the feeding of a 3D structure including homogeneous dielectrics, computes its electromagnetic characteristics The complete solution of the problem (currents densities, S matrix of the multi-port feeding, spherical expansion of the radiation pattern, ...) is obtained by a rigorous method based on integral equation formulation. The problem is numerically solved with a surface finite element method via a direct inversion of the linear system matrix.

4. Simulation Set-up (Geometry set-up, GUI, mesh, boundary conditions, excitation)

The geometry is symmetric with respect to (xOz) and (yOz) planes, so only a quarter of the structure is meshed. The interface between the mesh generator is achieved through an ASCII file containing the definition of:

- the 3D points,
- the lines between 2 points,
- the surfaces bounded by a closed line,
- the surfaces assembling to define the interfaces of homogeneous dielectric domains.

The triangular meshing must verify some conditions in order to obtain good results:

- each triangle must be as closed as possible to a equilateral triangle,
- The maximum size is $\lambda/5$.

So when small geometrical discontinuities must be meshed like the first step of the transition, a small mesh must be used.

The mesh is presented figure 1 with a enlargement of the transition. There are 8814 unknowns.

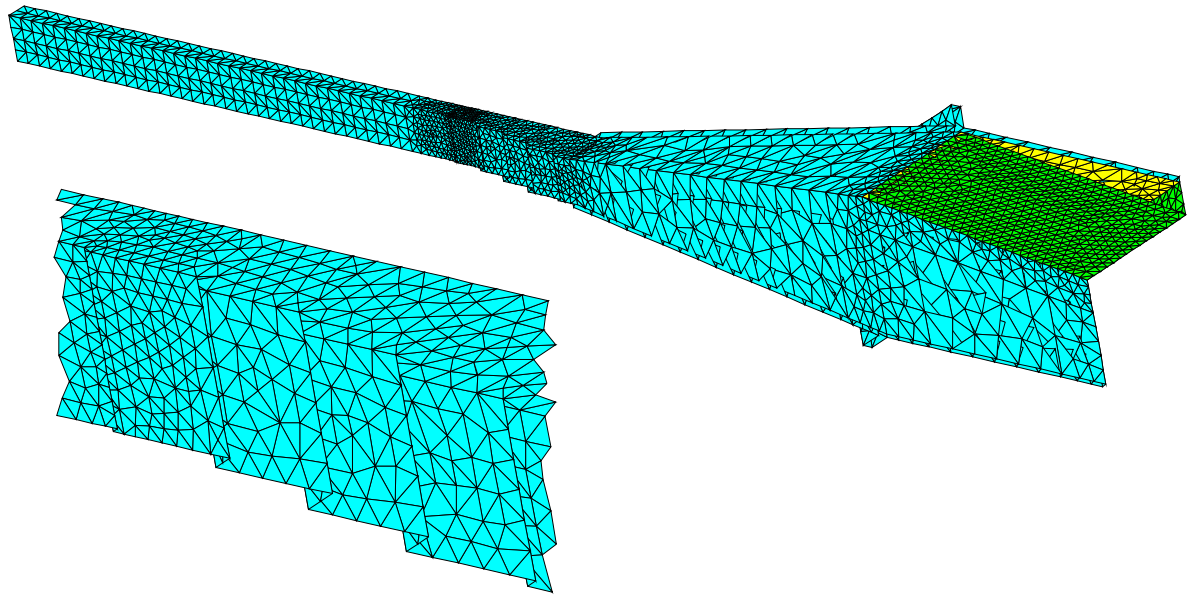

figure 1: meshing of a pyramidal horn quarter

The structure is fed by a waveguide cross-section equivalent to a Huyghens surface with the fundamental mode TE_{10}.

5. Simulation results

5.1. Input impedance

The figure 2 presents a comparison simulations/experiments of the VSWR and the figure 3 the comparison of the input impedance on a Smith chart. Very good agreement with the measurements can be observed.

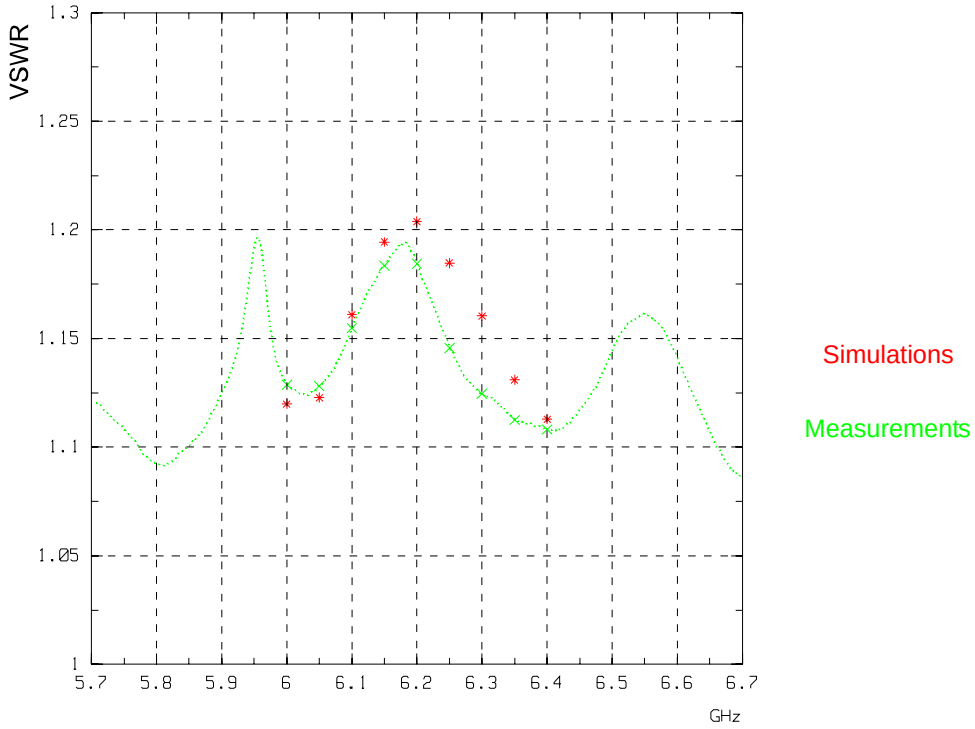

figure 2: VSWR

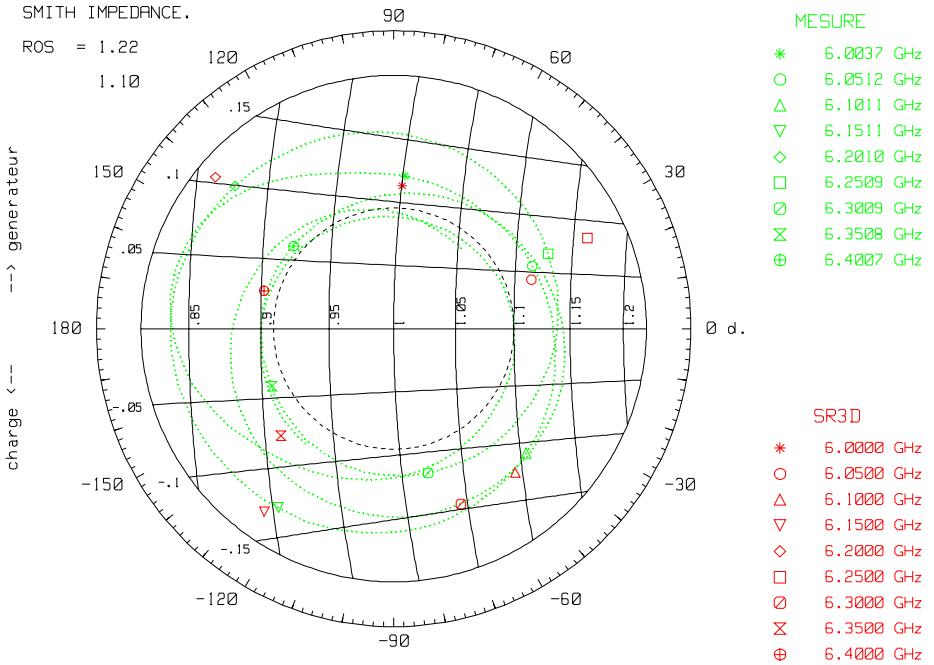

figure 3: Input impedance

5.2. Radiation pattern

The comparison of the simulated and measured radiation patterns is presented for the amplitude and phase figure 4 at 6.0 GHz, figure 5 at 6.2 GHz and figure 6 at 6.4 GHz.

The amplitude and the phase of the radiated power are well predicted with SR3D.

In the table below, the directivity of the simulated radiation pattern at the 9 simulated frequency points are presented.

Table 1: **Simulated directivity of the pyramidal horn**

freq (GHz)	**6.00**	**6.05**	**6.10**	**6.15**	**6.20**	**6.25**	**6.30**	**6.35**	**6.40**
Directivity (dB)	**16.98**	**17.01**	**17.07**	**17.27**	**17.51**	**17.41**	**17.33**	**17.49**	**17.65**

The radiation pattern at these 9 frequency points is presented in the figures 7, 8, 9, 10, 11, 12, 13, 14, 15.

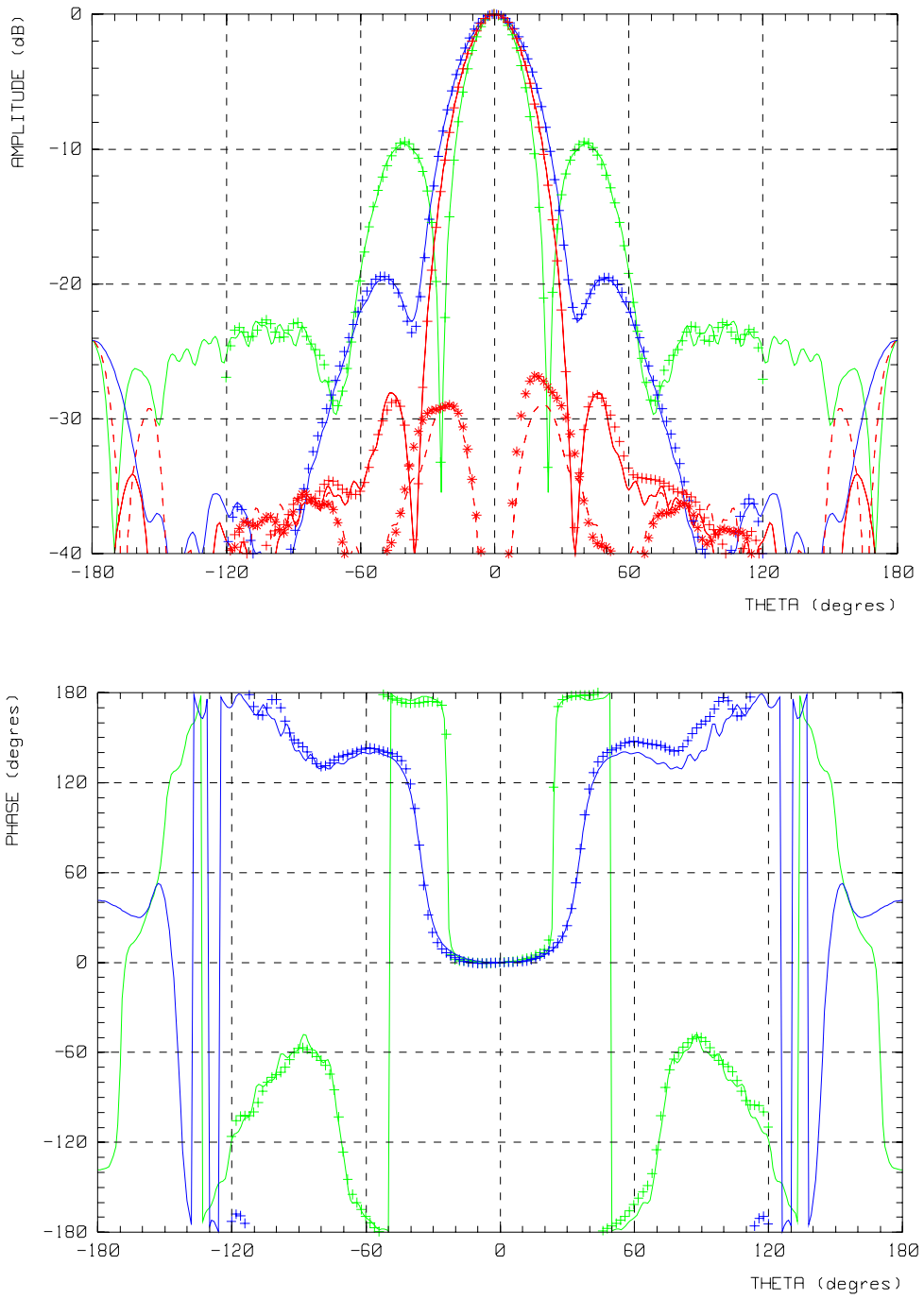

figure 4: Radiation pattern at 6.0 GHz - comparizon experiments-simulations

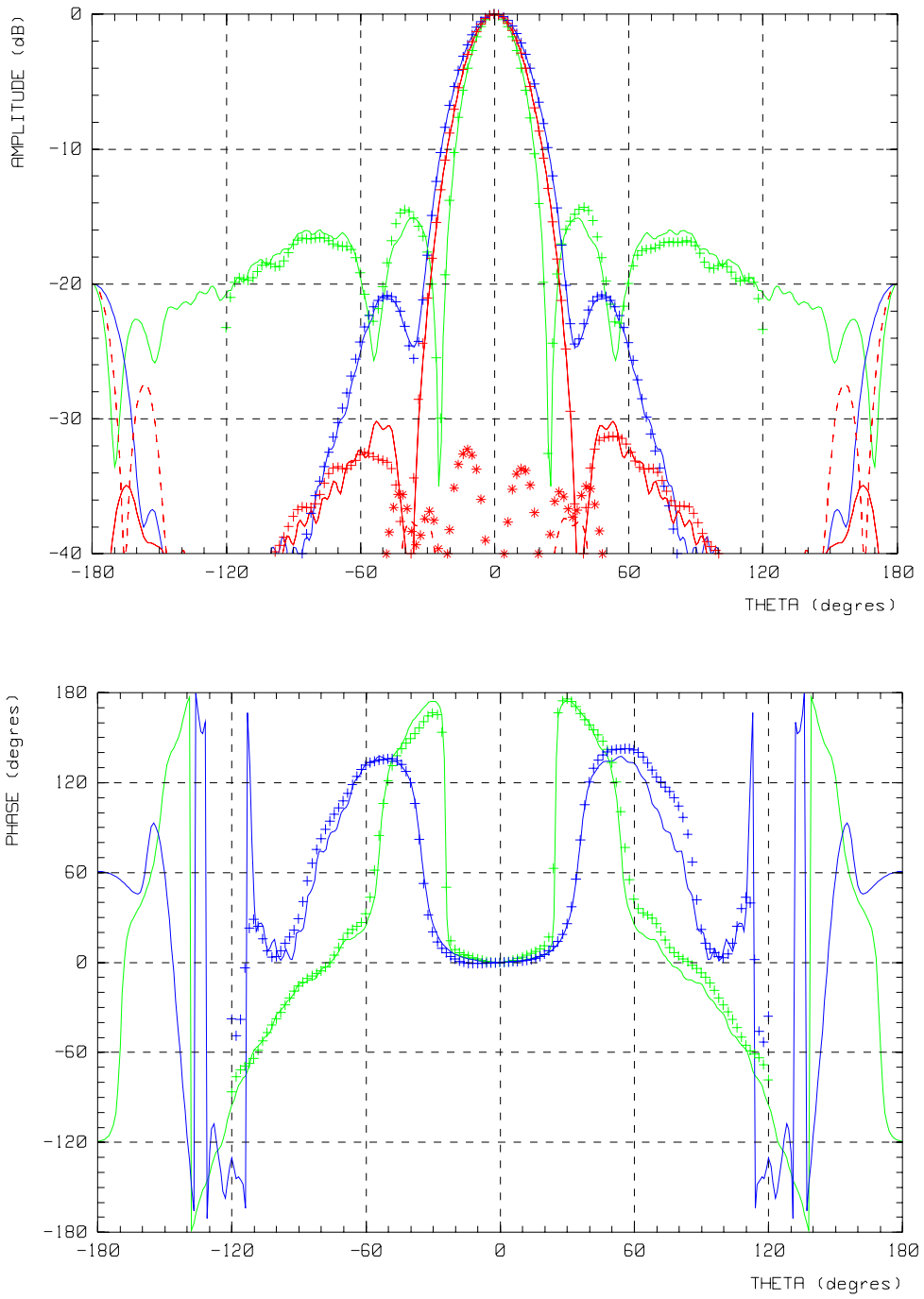

figure 5: Radiation pattern at 6.2 GHz - comparizon experiments-simulations

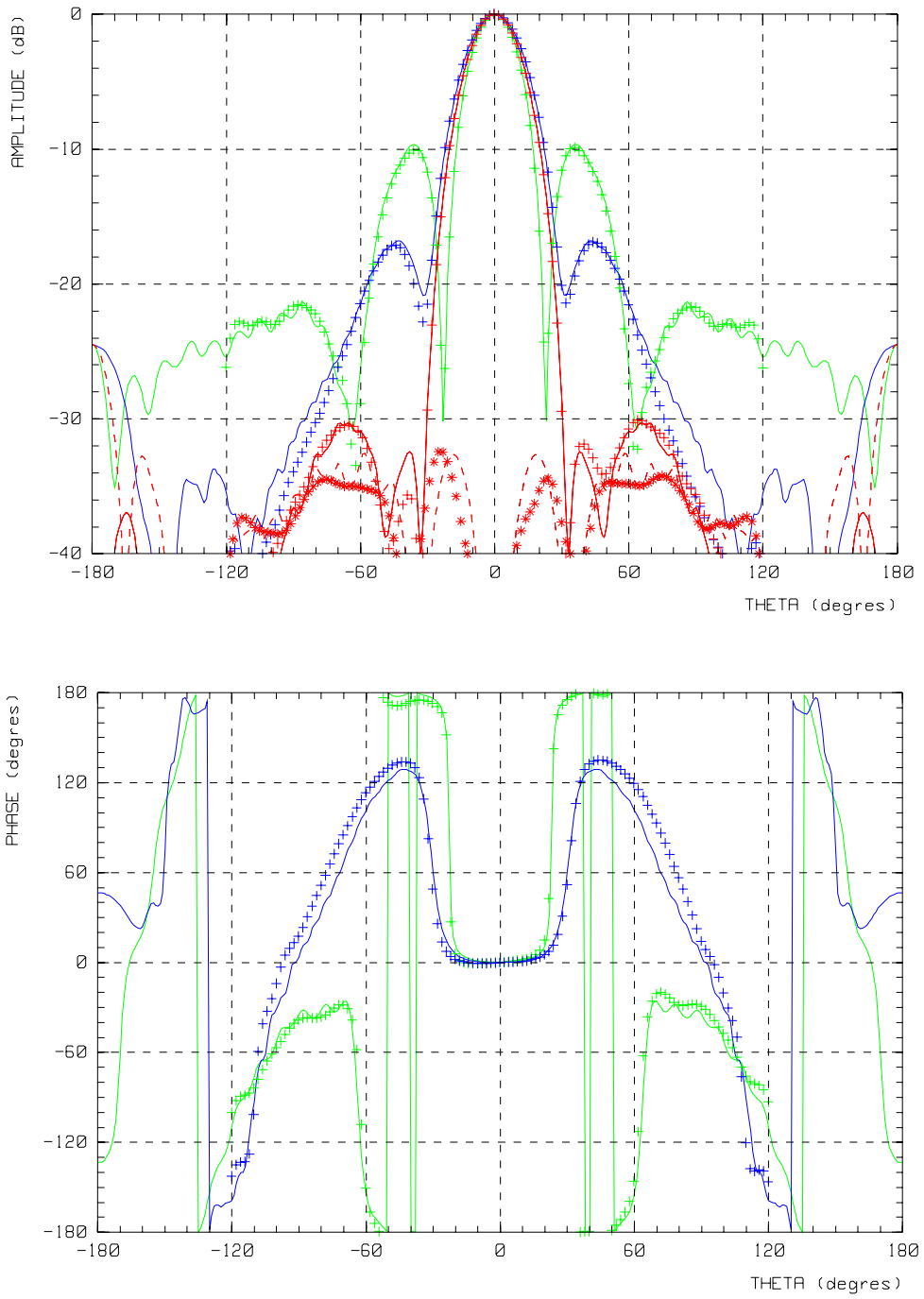

figure 6: Radiation pattern at 6.4 GHz - comparizon experiments-simulations

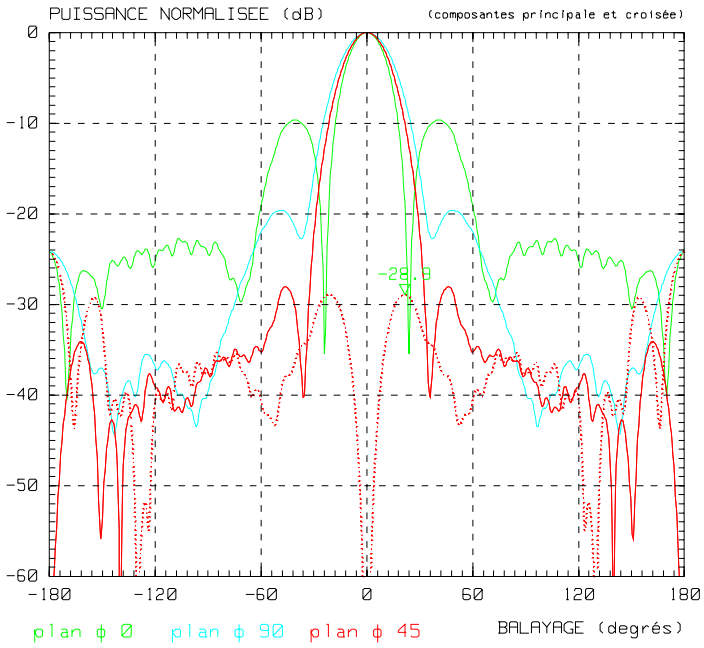

figure 7: Radiation pattern at 6.00 GHz

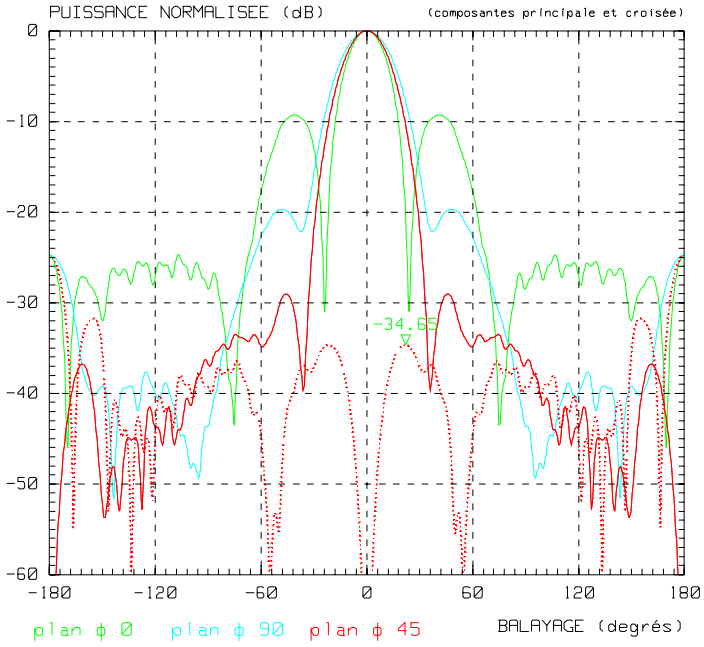

figure 8: Radiation pattern at 6.05 GHz

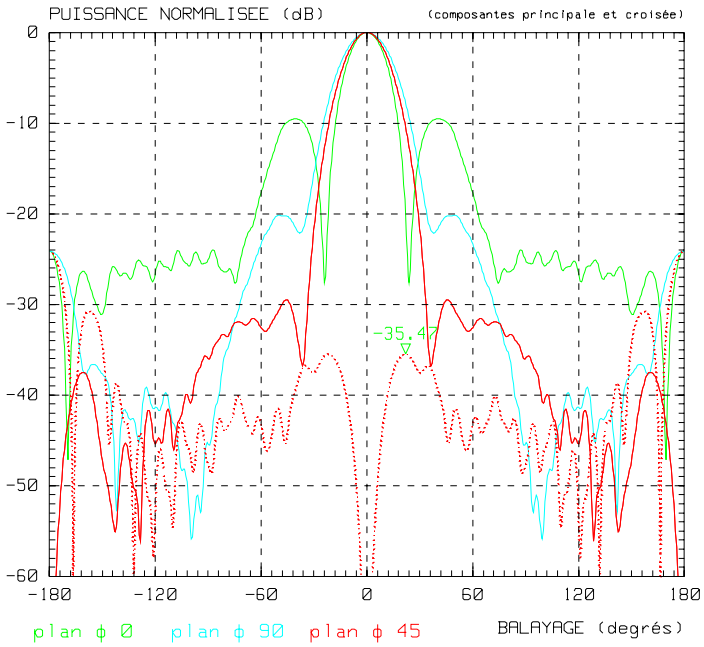

figure 9: Radiation pattern at 6.10 GHz

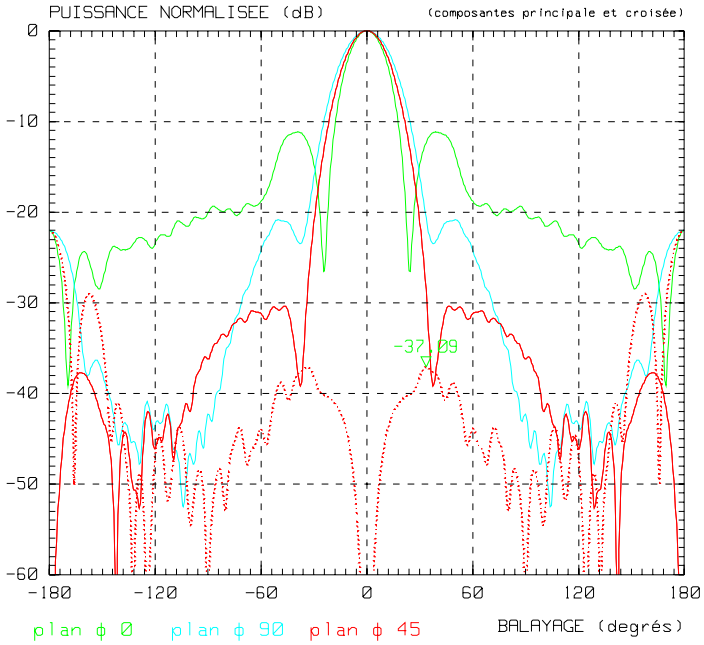

figure 10: Radiation pattern at 6.15 GHz

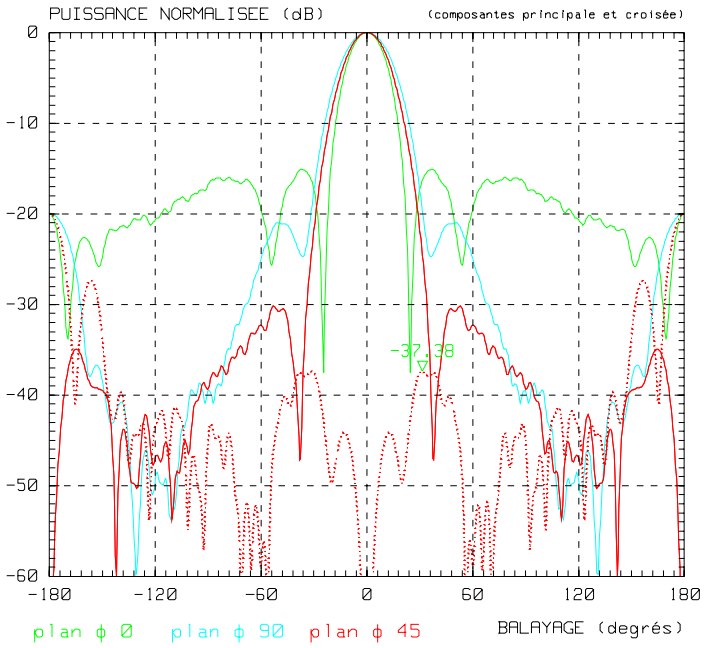

figure 11: Radiation pattern at 6.20 GHz

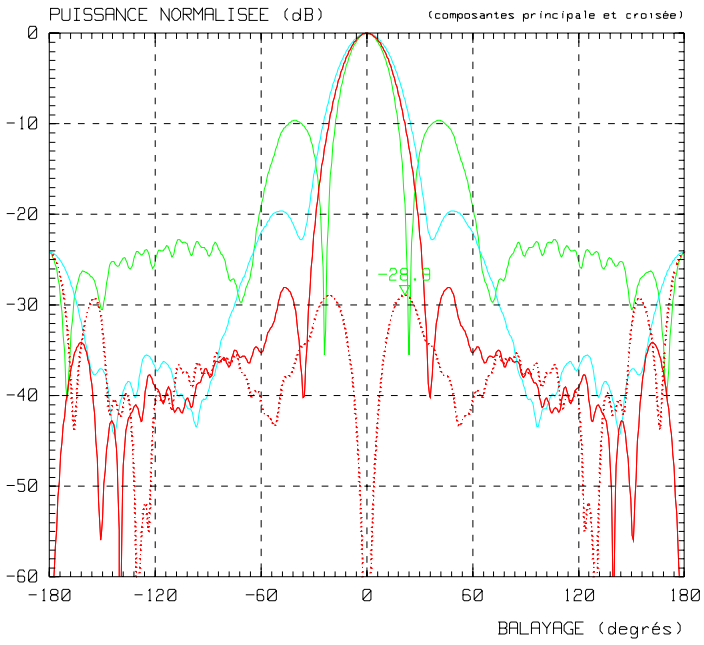

figure 12: Radiation pattern at 6.25 GHz

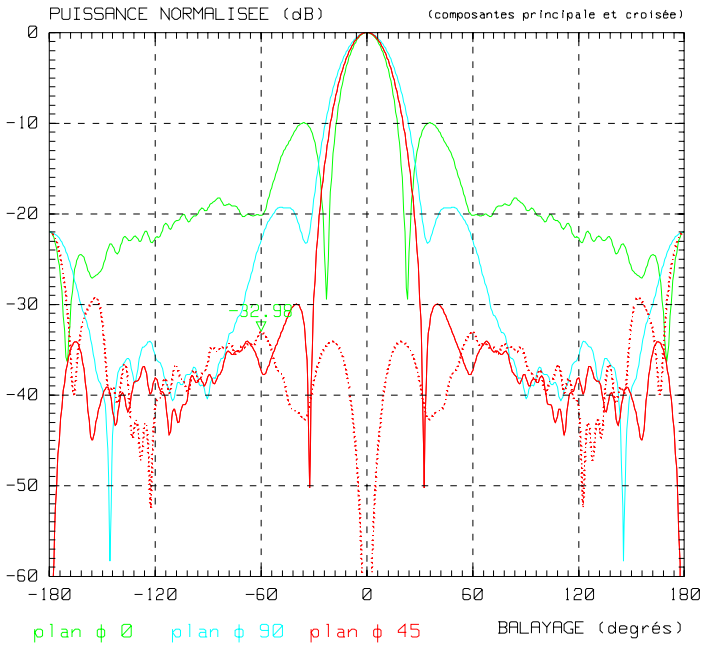

figure 13: Radiation pattern at 6.30 GHz

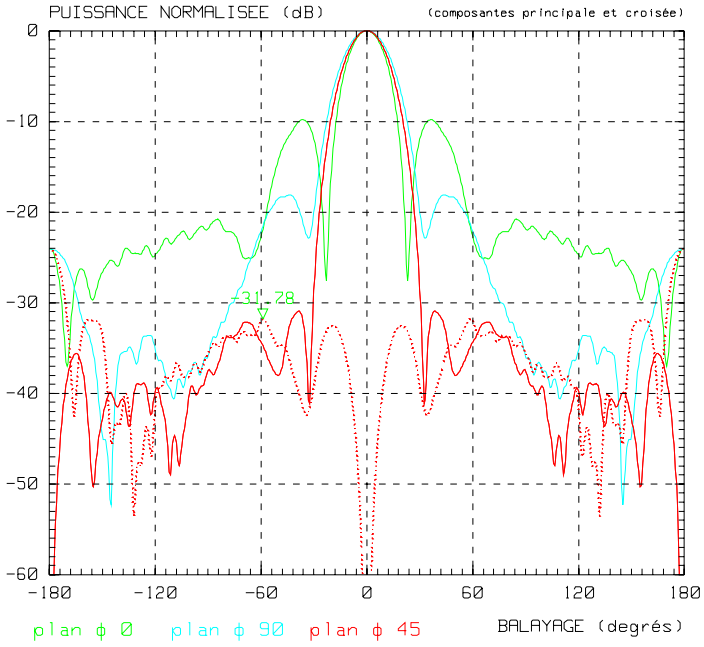

figure 14: Radiation pattern at 6.35 GHz

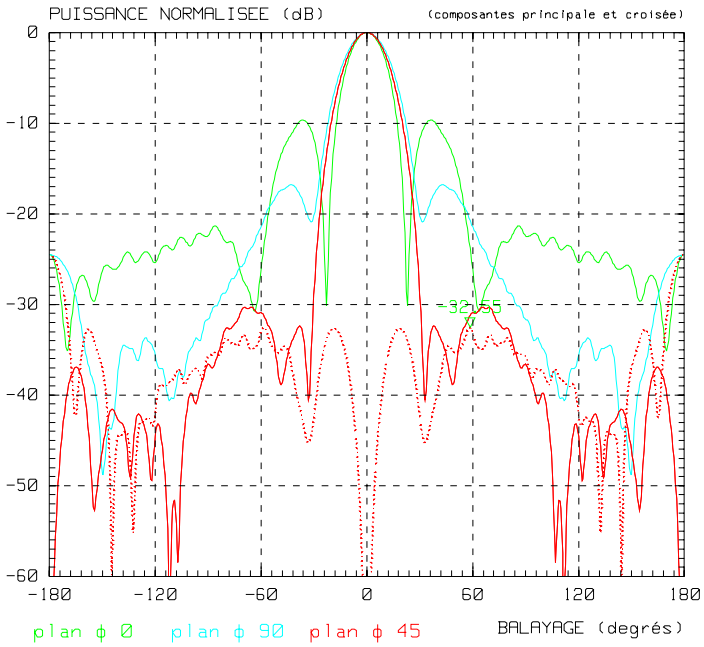

figure 15: Radiation pattern at 6.40 GHz

6. Computation resources

The simulations have been performed on a HP RP7410 with 6 HPPA 8700 processors at 750 MHz (6 x 3.7 Gflops) (HPUX 11.00) and 4 Go of memory.

The matrix is saved out of core on disks by blocs. The data relevant to the simulation are listed in the following table.

Table 2: Simulation requirements

	Pyramidal horn
Number of unknowns	**8 814**
Disk space requirement	**345 Mo**
CPU Time per frequency point	**52 min**
Real Time per frequency point	**31 min**

7. Discussion

The quality of results obtained thanks to application of the integral equation formalism has been demonstrated. Accuracy is achieved at the cost of CPU time since for an average structure (~ 30 000 unknowns) computation time is of the order of several hours per frequency point with a calculator working at an effective rate of 22 Gflops. While the variety of cases simulated since 15 years demonstrates the flexibility of the method, their purpose is not to claim that SR3D has universal application. The formalism of integral equations should be used preferentially for external problems

(i.e. essentially radiation problems) of reasonable size as we can see on the radiation pattern comparison.

The meshing quality affects directly the precision of the results and particularly the near field radiation (input impedance, ...). The validation test included in SR3D must verify the energy conservation below 3.5 % between the input energy at the feeding port and the radiated energy when no losses are included in the dielectric domains or on metallic structures. This constraint which is not sufficient but necessary, allows us to have very good agreement between simulation and experiments when we manufacture the final structure and so eliminates new simulations and modifications of the breadboard.

The main difficulty with SR3D is that we can make none approximation on the modeling of the structure, all the dimensions are finite (ground planes, wires, no attached modes between wires and planes, ...) that increases drastically the numbers of unknowns and has obliged us to make efforts on parallel processing and numerical integration in order to maintain CPU time within reasonable limits.

3- SIMULATION RESULTS

From IMST_pyramidalhorn_Empire

1. Entity

IMST GmbH
Carl-Friedrich-Gauss-Str. 2
D-47475 Kamp-Lintfort, Germany

Winfried Simon
Tel. : +49-(0)2842-981247
Fax : +49-(0)2842-981399
Email : simon@imst.de

2. Name of the simulation tool

Empire.

3. Generalities about the simulation tool

Empire: a full 3D field solver based on FDTD. It employs a Cartesian grid with adaptive discretisation in all 3 direction (X,Y,Z). It uses PML as absorbing boundary conditions and an automatic meshing. The solution obtained in time domain is transformed into frequency domain by FFT. The tool has a dedicated GIU.

4. Simulation Set-up (Geometry set-up, GUI, mesh, boundary conditions, excitation)

The model has been imported as DXF file, and firstly discretised using an automatic discretisation . This type of discretising detect all the edges of objects and whether object are metal or not. Thereafter, a fine tuning has been performed of the discretisation for some parts of the structure. The excitation is a dedicated waveguide port exciting the TE10 mode. PML (6 layers) and (8 layers) have been used as absorbing boundary conditions. The complete horn has been modelled, and enclosed by a fielddump box in order to determine the far field. The modelling of the horn itself has been performed by defining a metal block enclosing the complete horn and cutting out the horn geometry by means of extrusion. This enables a very easy & quick modelling of the horn and

significantly reduces modelling time. The distance to the PML boundaries is a couple of cells. The model is assumed to be completely lossless.

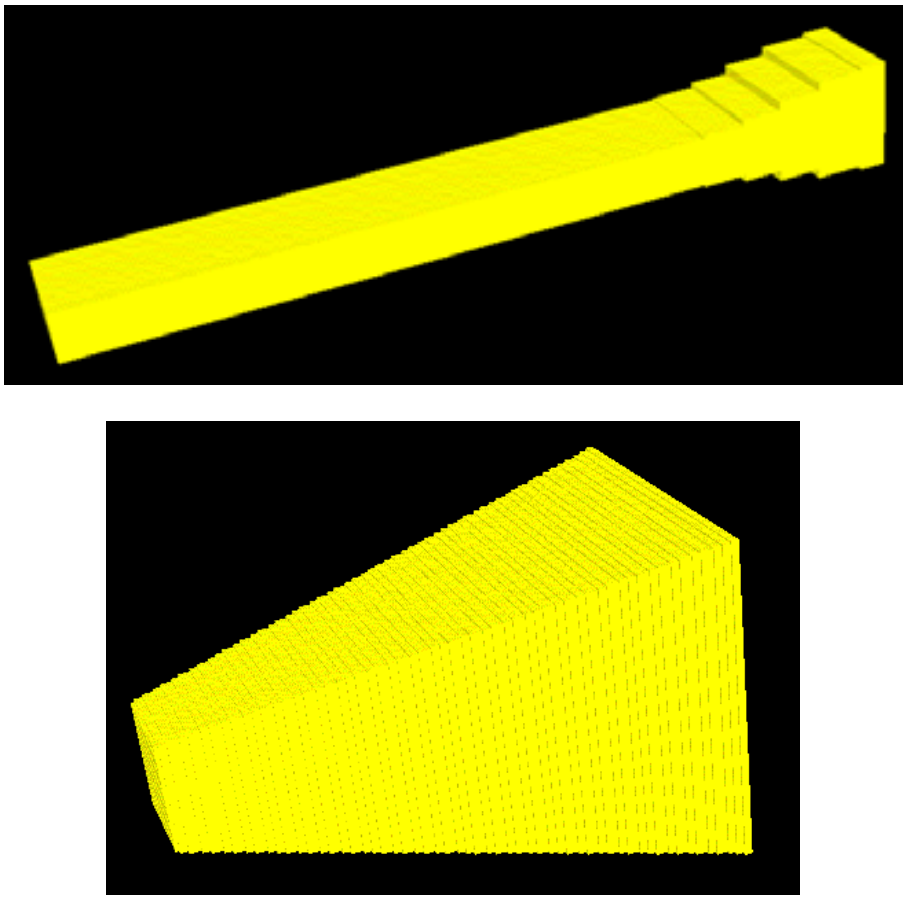

Fig. 1 **FDTD model (discretised) of the waveguide transition (upper) and horn (lower)**

5. Simulation results

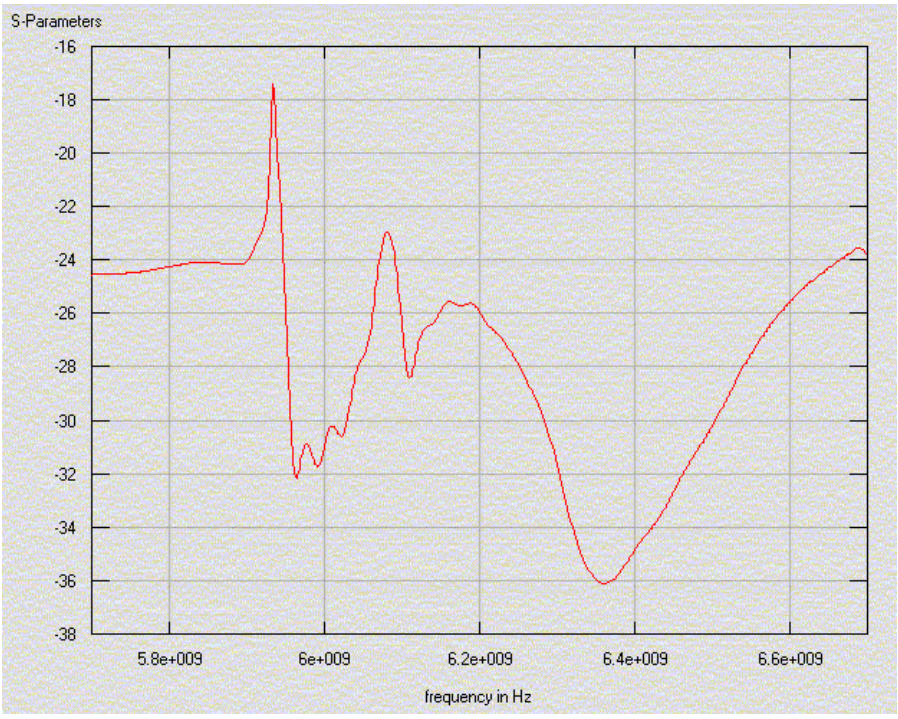

Fig. 2 **Simulated S11**

For the far fields the E- and H-plane cuts are displayed for the co-polarisation:

- E-plane: blue
- H-plane: red

All values are normalised to the maximum value and are all in dB. The cross-polarisation is not shown here because for both E- and H-cuts the far fields are all below –60 dB (normalised).

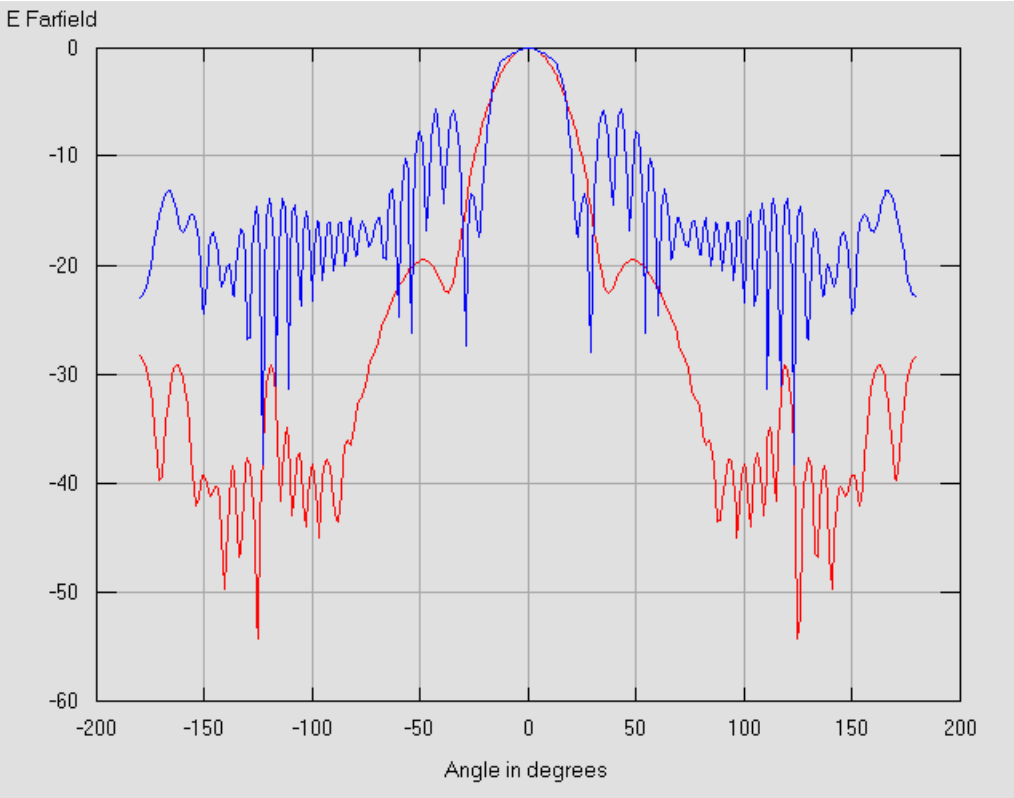

Fig. 3 **E- and H-cuts at 6.0 GHz**

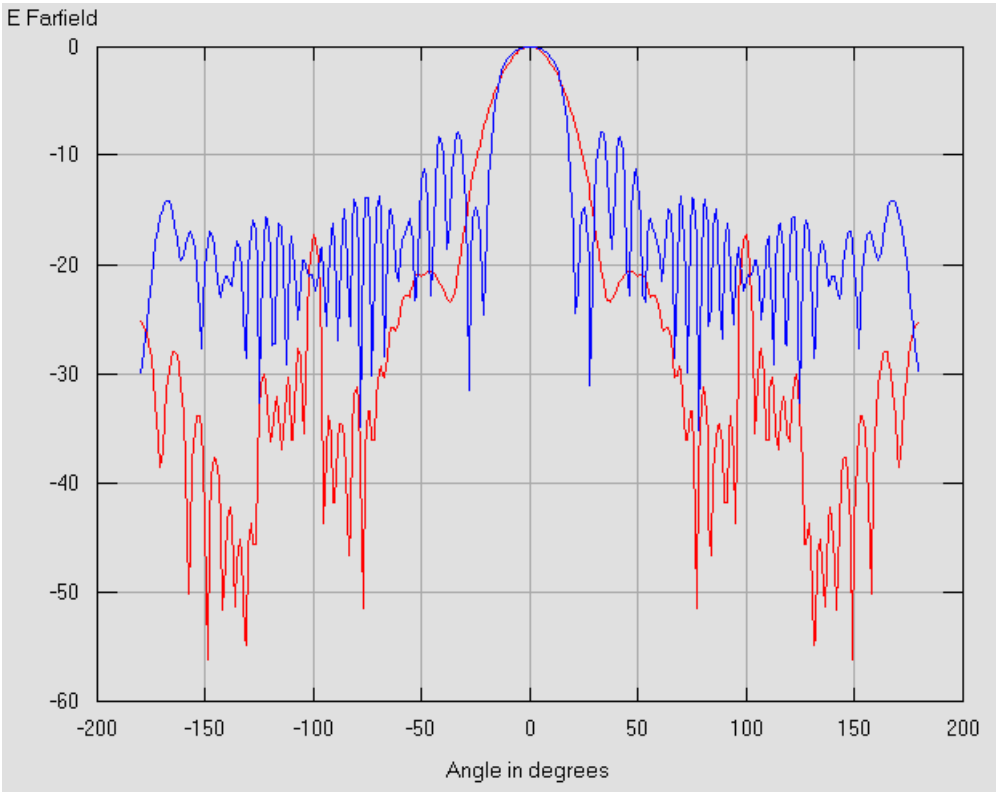

Fig. 4 **E- and H-cuts at 6.2 GHz**

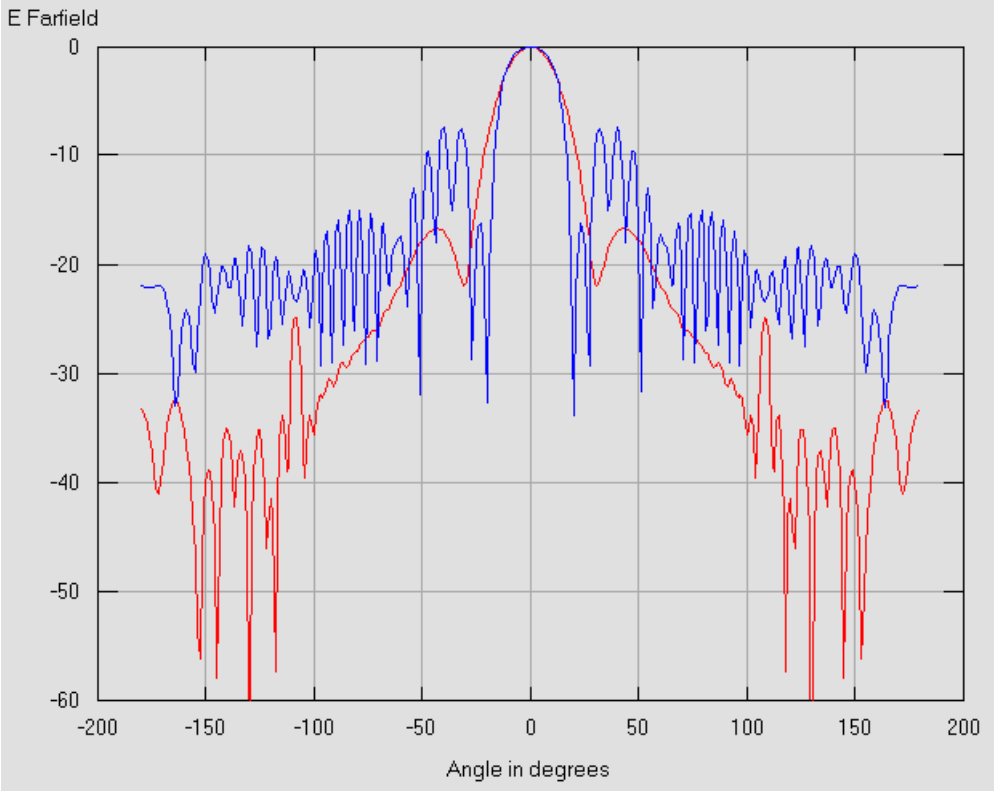

Fig. 5 **E- and H-cuts at 6.4 GHz**

The gain of the radiation pattern is presented in the table below:

Freq (GHz)	6.00	6.20	6.40
Gain (dB)	16.98	17.37	17.83

6. Computation resources

The simulations have been performed on a single-processor PC, 3.4 GHz with 4 Gb memory. All the results have been calculated in one simulation run that lasted 50 minutes. The model itself requires about 384 MB of memory.

7. Discussion

The modelling of this structure was rather easy and quick by defining extrusion blocks of air in a solid metal rectangle. The automated discretiser had little trouble with the problem, only some detailed parts like the waveguide transitions needed some extra attention and some further manual work. The structure could also be modelled using magnetic and electric walls. This would reduce the computational time. A couple of test simulation runs were necessary to find some modelling errors (in discretisation and geometry). The results are in good agreement with those provided by France Telecom.

8. Additional comments

The computed far field is not correct in the vicinity of the region around a elevation of (–)180° because the fielddump box has to cut the waveguide at its excitation. This implies that this plane of the fielddump box is not considered for the determination of the far field. This results into small errors in the far field around elevation=(-)180°.

3- SIMULATION RESULTS

From SAPIENZA_pyramidalhorn_HFSS

1. Entity

"La Sapienza" University of Rome

Contact person:

Giampiero Lovat
Department of Electrical Engineering
Via Eudossiana 18
00184 Roma, Italy
e-mail: lovat@die.uniroma1.it

2. Name of the simulation tool

Ansoft HFSS, version 9.2.

3. Generalities about the simulation tool

The adopted software is a well-known commercial software based on the finite-element method with tetrahedral elements. It is suitable for the analysis of structures with an arbitrary geometry, and especially for those derived by metallic waveguides, both closed and open (i.e., radiating).

4. Simulation Set-up (Geometry set-up, GUI, mesh, boundary conditions, excitation)

The structure was redrawn from scratch using the GUI available in Ansoft HFSS, on the basis of the specifications provided in the Structure Description form.

The meshing was done automatically by the simulation tool, following an adaptive criterion based on the input reflection coefficient of the antenna. The mesh is made of non-uniform tetrahedral elements.

The boundary conditions enforced on the outer antenna physical boundaries were those for a Perfect Conductor (PEC). A parallelepiped box was introduced to contain the whole antenna, with radiation boundary conditions enforced on its faces, with the exception of the face containing the input port. The structure was excited by means of the fundamental mode of the input rectangular waveguide, impinging on the antenna through the input port.

A frequency-domain analysis was performed at different frequencies, to obtain both the input reflection coefficient and the radiation patterns in the principal planes as well as in the 45° elevation plane.

The input of the geometry took approximately one hour. The simulation took approximately six-seven hours per frequency point.

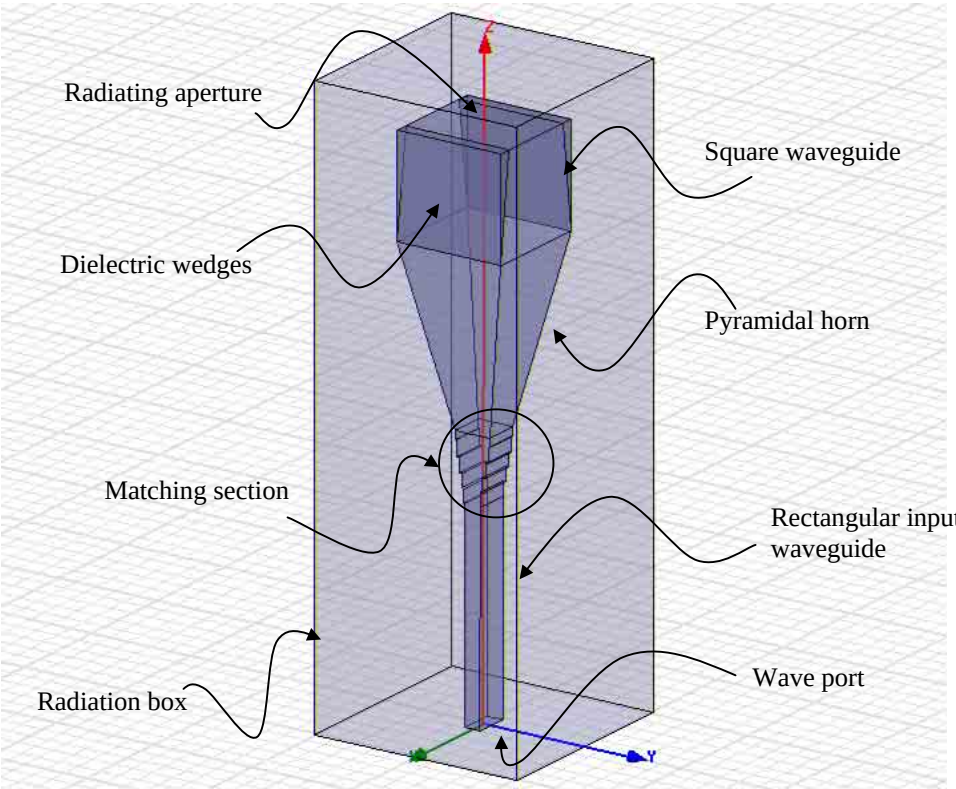

Fig. 1 – The structure as drawn in Ansoft HFSS.

5. Simulation results

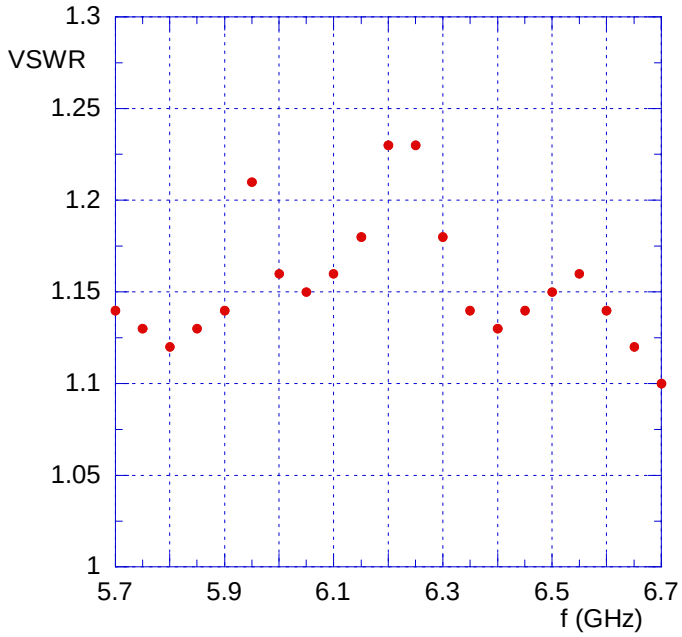

Fig. 1 – Voltage Standing-Wave Ratio (VSWR).

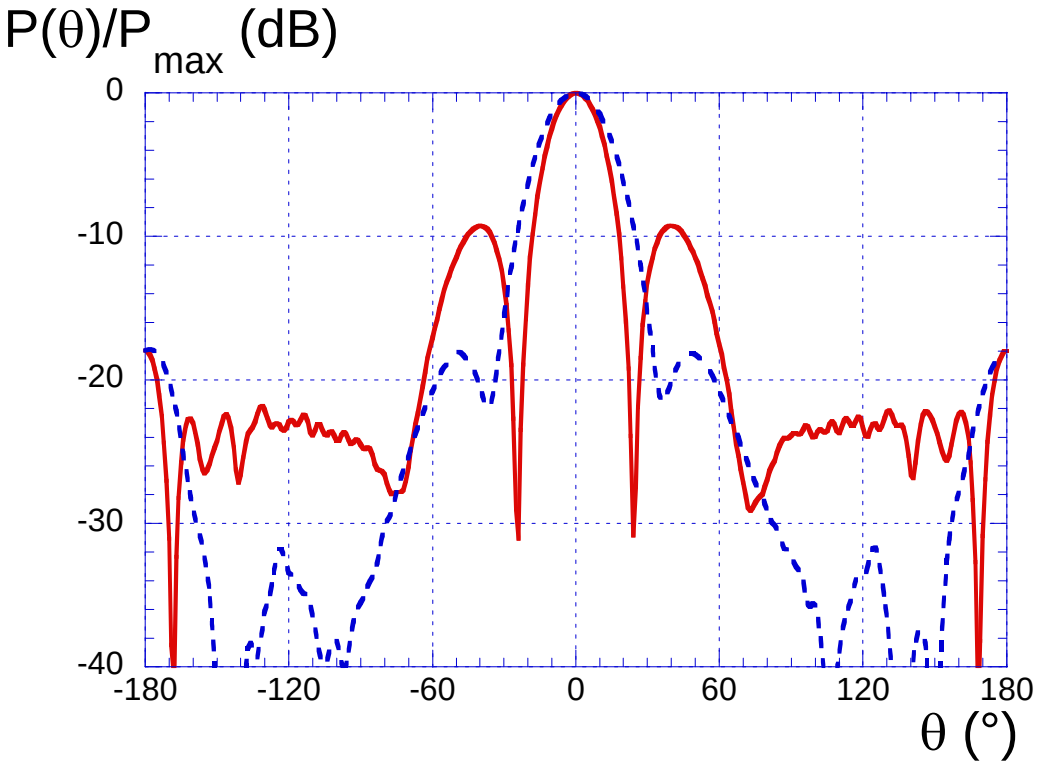

Fig. 2 - Radiation patterns in the E plane (*red curve*) and H plane (*blue curve*) at $f = 6$ GHz.

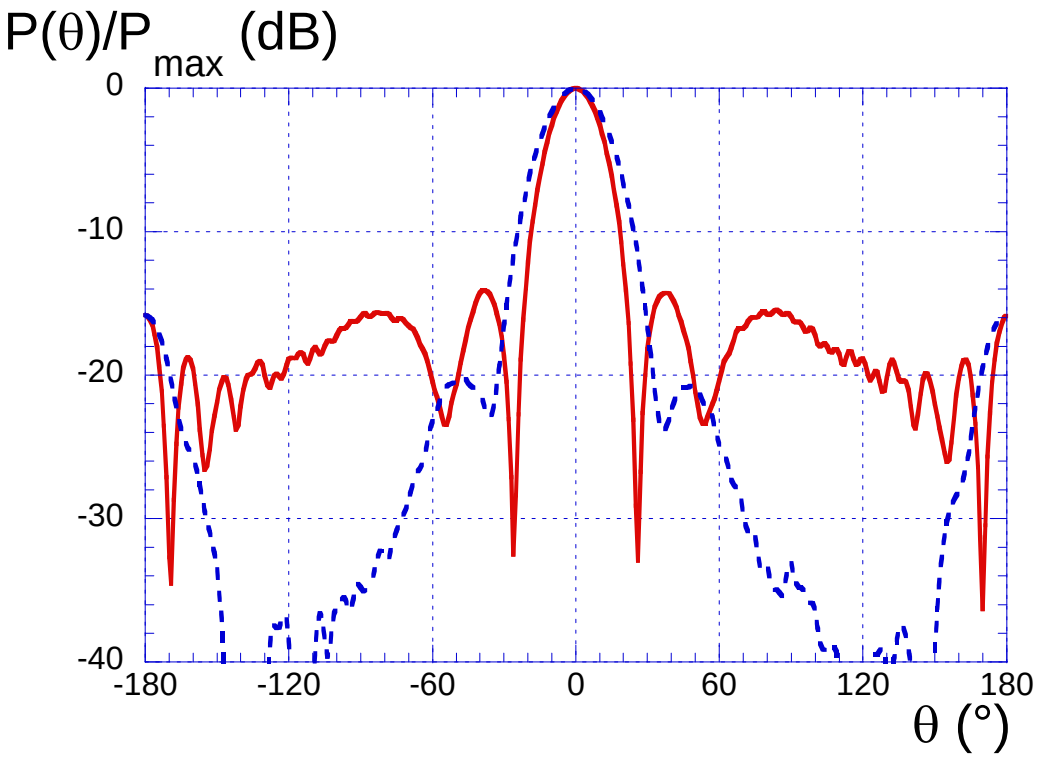

Fig. 3 - Radiation patterns in the E plane (*red curve*) and H plane (*blue curve*) at f = 6.2 GHz.

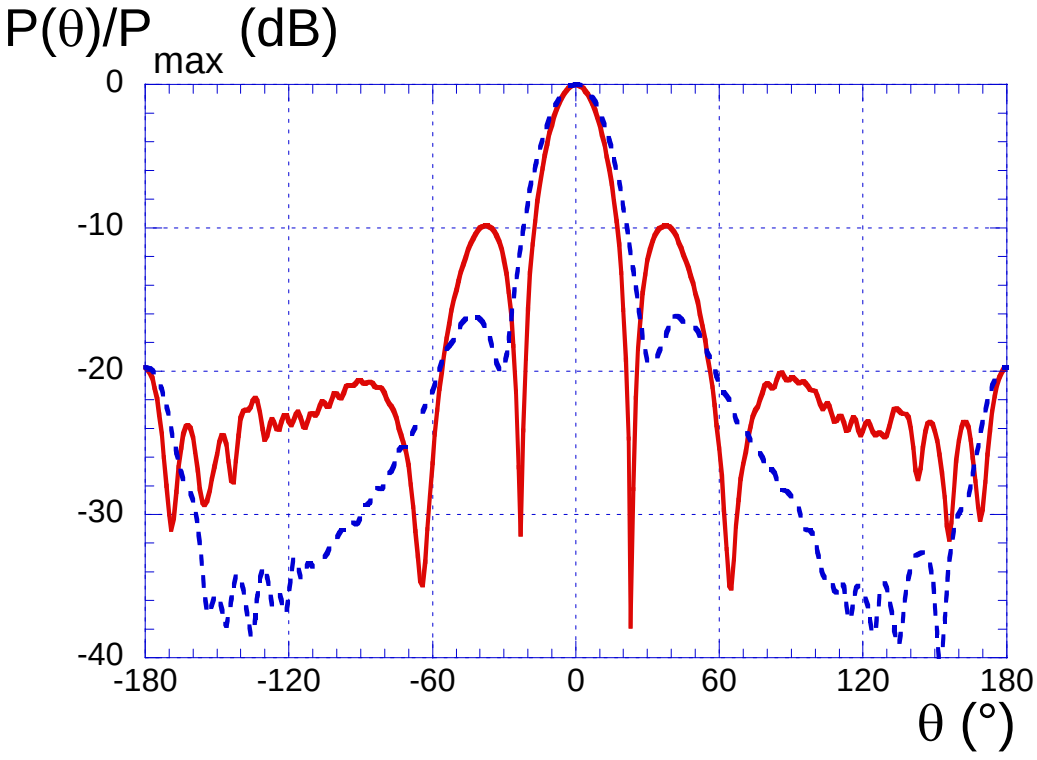

Fig. 4 - Radiation patterns in the E plane (*red curve*) and H plane (*blue curve*) at f = 6.4 GHz.

6. Computation resources

The simulation has been performed on a PC with one Pentium IV processor, with 1 GByte of RAM and a 3 GHz clock.

For each frequency point, the computation time was of the order of six-seven hours, whereas the post-processing step took from 5 to 20 minutes.

7. Discussion

The results obtained with the commercial software employed by our Unit show that a very good agreement with the available results can be obtained as far as the radiation patterns of the considered antenna in the principal planes are considered. A critical issue is the enforcement of radiation boundary conditions on the external box enclosing the antenna; it is found that satisfactory results can be obtained with a distance of the box faces from the radiating element of at least one free-space wavelength.

With reference to the input impedance, the simulations obtained so far show a good qualitative agreement with the available VSWR results. The quantitative agreement could be improved, presumably by improving the mesh fineness.

As is typical of general purpose FEM tools, the price to be paid for achieving accurate results is a very high number of unknowns (thousands), resulting in long simulation and post-processing times (hours and tens of minutes, respectively).

8. Additional comments

4- SYNTHESIS OF RESULTS

The structure proposed by the France Telecom Research and Development has been simulated by **three laboratories**:

-FTR&D
- IMST
- "La Sapienza" University of Rome

The simulation has been performed by **one time domain methods**:

- IMST : EMPIRE

And **two frequency domain methods** :

- FTR&D : SR3D
- "La Sapienza" : HFSS

- **SR3D**: .is a software base on Integral Equation solved with surface finite element method

- **EMPIRE** and **HFSS** are commercial codes.

i. **EMPIRE** is a FDTD software with adaptative discretisation in the 3 directions
ii. **HFSS** employs the finite element method in order to generate an electromagnetic field solution.

The simulation interests of the structure are:

- 3D structure including dielectric
- Waveguide feeding

For all softwares, there is no difficulty to set up the simulation and to obtain results.